

**Investigation into the molecular mechanisms underlying
invasion in the lung carcinoma cell line DLKP and its
chemotherapeutic drug resistant variants**

A thesis submitted for the degree of Ph.D.

by

Aisling Pierce, B.Sc. Hons

**The experimental work described in this thesis was carried out
under the supervision of**

Professor Martin Clynes Ph.D.

and

Dr. Niall Barron

at the

**National Institute for Cellular Biotechnology,
Dublin City University,
Glasnevin,
Dublin 9,
Republic of Ireland.**

Table of Contents

Table of Contents	i
Dedication	xii
Acknowledgements	xiii
Declaration of Ownership	xv
List of Abbreviations	xvi
Abstract	xxi

Section 1 0 Introduction

1 1 General Introduction	2
1.2 Lung Cancer	4
1 3 Pharmacology of Chemotherapeutic Drugs	7
1 3 1 The Vinca Alkaloids	7
1 3 2 The Taxanes	9
1 3 3 Chemotherapy Resistance	11
1 4 Metastasis	12
1 5 Invasion	16
1 5 1 The extracellular matrix and basement membrane	19
1 5 2 Integrins and Cancer	20
1 5 2 1 Integrin expression and function	20
1 5 2 2 Integrins and proteolytic enzymes	21
1 5 2 3 Integrins and signalling, from the outside in	22
1 5 2 4 Integrins and signalling, from the inside out	24
1 5 2 5 Survival during invasion	24
1 5 3 Proteases and Invasion	25
1 5 3 1 Cathepsin B	25
1 5 3 2 Matrix Metalloproteinases	27
1 5 3 3 Urokinase-type plasminogen activator	30
1 5 3 4 Proteases and clinical trials	32
1 5 4 Rho Proteins and Invasion	33
1 5 4 1 Rho proteins and growth factors	33

1 5 4 2	Rho and Insulin-like growth factors (IGFs)	34
1 5 4 3	Rho and Epidermal growth factor (EGF)	34
1 5 4 4	Other aspects of Rho and invasion	35
1 5 5	Chemokines	37
1.6	Microarrays	39
1 6 1	Introduction to microarray technology	39
1 6 2	Microarray analysis	41
1 6 3	Affymetrix GeneChips	44
1 6 4	Microarrays and cancer	45
1 7	RNA Interference	47
1 7 1	Introduction to siRNA technology	47
1 7 2	Applications of RNA _i	49
1 7 3	Problems associated with RNA _i	50
1 7 4	Delivery of siRNA	51
1.8	Aims of Thesis	53

Section 2 0 Materials and Methods

2 1	Water	56
2 2	Glasware	56
2.3	Sterilisation	56
2.4	Media Preparation	56
2 5	Cell Lines	57
2 5 1	Subculturing of adherent cell lines	59
2 5 2	Cell counting	59
2 5 3	Cell freezing	60
2 5 4	Cell thawing	60
2 5 5	Sterility checks	61
2.6	<i>Mycoplasma</i> analysis of cell lines	61
2 6 1	Indirect staining procedure	61
2 6 2	Direct staining procedure	62

2.7	Specialised Techniques in Cell Culture	63
2 7 1	Assessment of cell number – Acid phosphatase assay	63
2 7 2	<i>In vitro</i> invasion assay – experimental procedure	64
2 8	Immunocytochemistry	65
2 8 1	Fixation of cells	65
2 8 2	Immunofluorescence	65
2.9	Western Blot analysis	66
2 9 1	Sample preparation	66
2 9 2	Quantification of protein	66
2 9 3	Gel electrophoresis	67
2 9 4	Protein transfer and Western blotting	68
2 9 5	Enhanced chemiluminescence detection	70
2 10	RNA Extraction	71
2.11	Reverse Transcriptase Reaction	72
2 12	Polymerase chain reaction	73
2 12 1	Real Time PCR	74
2.13	Electrophoresis of PCR products	77
2 14	Densitometric Analysis	77
2 15	DNA Array Analyses	78
2 15 1	GeneChips	78
2 15 2	Sample and array processing	79
2 15 3	Microarray Data Normalisation	81
2 16	Overview of Bioinformatic Analysis	82
2 16 1	Quality Control	82
2 16 2	Generating Genelists	83
2 16 2 1	Genelist 1	83
2 16 2 2	Genelist 2	83
2 16 2 3	Genelist 3	83
2 16 2 4	Genelist 4	84
2 16 2 5	Genelist 5	84
2 16 3	Genomatix Software Suite	85

2 17	RNA interference (RNAi)	88
2 17 1	Transfection optimisation	88
2 17 2	Proliferation effects of siRNA transfection	90
2 17 3	Invasion analysis of siRNA transfected cells	91
2.18	Transfection of DLKP variants with exogenous DNA	92
2 18 1	Plasmid preparation	93
2 18 1 1	Transformation of JM109 cells	93
2 18 1 2	DNA miniprep of plasmid DNA	93
2 18 1 3	DNA maxiprep of plasmid DNA	94
2 18 1 4	Sub-cloning	95
2 18 2	Plasmid DNA sequencing	96
2 18 3	Optimisation of plasmid transient transfection	96
2 18 4	Invasion analysis of cDNA transiently transfected cells	97

Section 3.0 Results

3.1	Microarray analysis of DLKP and its invasive and chemotherapeutic resistant variants	99
3 1 1	GeneChip Quality Control	99
3 1 1 1	Scale factor	99
3 1 1 2	Noise	100
3 1 1 3	Background	100
3 1 1 4	Present Call	100
3 1 1 5	3' 5' ratio	101
3 1 1 6	Hybridisation controls	101
3 1 1 7	Visual examination	101
3 1 1 8	Quality control by unsupervised hierarchical clustering	103
3 1 2	Bioinformatic analysis – generating genelists	106
3 1 2 1	Genelist 1	106
3 1 2 2	Genelist 2	111
3 1 2 3	Genelist 3	112

3 1 2 4	Genelist 4	114
3 1 2 5	Genelist 5	117
3 1 3	Data analysis using Genomatix software suite	125
3 2	RT-PCR confirmation of array data analysis	129
3 3	Invasion assay confirmation of <i>in vitro</i> invasive capacity of DLKP variants	132
3 3 1	Graphical Representations of measurement of relative DLKP variant invasive capacity with increasing passage number	133
3 3 2	RT-PCR validation of consistent gene expression in conjunction with consistent invasion assay results	138
3 4	Investigation into role of IGF-1R in invasion in an <i>in vitro</i> cell model	139
3 4 1	Aims of experiments	139
3 4 2	RT-PCR confirmation of differential IGF-1R mRNA expression in the DLKP variants	140
3 4 3	Endogenous IGF-1R mRNA and protein levels in the DLKP cell lines	144
3 4 4	siRNA Transfection Optimisation for the DLKP cell lines	147
3 4 4 1	Summary of siRNA transfection optimisation	147
3 4 4 2	Optimisation of <i>in vitro</i> invasion analysis following siRNA transfection	149
3 4 4 3	Evaluation of siRNA transfection efficiency	152
3 4 4 4	IGF-1R- specific siRNA decrease in IGF-1R mRNA and Protein levels	154
3 4 5	Evaluation of IGF-1R siRNA effect of DLKP variant proliferation	157
3 4 6	Evaluation of IGF-1R siRNA effect on invasion	160
3 4 7	Evaluation of IGF-1R blocking antibody, α IR3 effect on invasion	167

3 5	Investigation into role of KCNJ8 in invasion in our cell model	169
3 5 1	Aims of experiments	169
3 5 2	RT-PCR investigation of KCNJ8 mRNA expression	170
3 5 3	KCNJ8 siRNA transfection in the invasive DLKP variants	174
3 5 3 1	Summary of KCNJ8 siRNA experimental plan	174
3 5 3 2	KCNJ8-specific decrease in mRNA levels	175
3 5 4	Evaluation of KCNJ8 siRNA effect on DLKP proliferation	183
3 5 5	Evaluation of KCNJ8 knockdown on DLKP variant invasion	184
3 5 6	KCNJ8 cDNA transfection in the less/non-invasive DLKP variants	188
3 5 6 1	Summary of KCNJ8 cDNA experimental plan	188
3 5 6 2	Evaluation of cDNA transient transfection efficiency using GFP	188
3 5 6 3	Western blot analysis of KCNJ8 cDNA transient transfection	191
3 5 6 4	Evaluation of KCNJ8 cDNA transient transfection on invasion	194
3 6	Investigation into role of S100A13 in invasion in the DLKP variants	197
3 6 1	Aims of S100A13 experiments	197
3 6 2	RT-PCR validation of differential S100A13 mRNA expression	198
3 6 3	S100A13 siRNA transfection in the invasive DLKP variants	201
3 6 3 1	Summary of S100A13 siRNA experimental plan	201
3 6 3 2	S100A13-specific decrease in mRNA levels	202
3 6 4	Evaluation of S100A13 siRNA effect on DLKP variant proliferation	210
3 6 5	Evaluation of S100A13 siRNA effect on DLKP variant invasion	211
3 6 6	S100A13 cDNA transfection in the non-invasive	

DLKP variants	215
3 6 6 1 Summary of S100A13 cDNA experimental plan	215
3 6 6 2 Western blot analysis of S100A13 cDNA transient transfection	215
3 6 6 3 Evaluation of S100A13 cDNA transient transfection on invasion	218
3.7 Investigation into role of SFN in invasion in the DLKP variants	221
3 7 1 Aims of SFN experiments	221
3 7 2 RT-PCR investigation of differential SFN mRNA expression	222
3 7 3 SFN siRNA transfection in the invasive DLKP variants	226
3 7 3 1 Summary of SFN siRNA experimental plan	226
3 7 3 2 SFN-specific siRNA knockdown in mRNA levels	227
3 7 4 Evaluation of SFN siRNA effect on DLKP variant invasion	232
3 7 5 SFN cDNA transfection in the non-invasive DLKP variants	235
3 7 5 1 Summary of SFN cDNA experimental plan	235
3 7 5 2 Western blot analysis of SFN cDNA transient transfection	235
3 7 6 Evaluation of SFN cDNA transient transfection on invasion	238
3.8 Investigation into role of TFPI2 in invasion in the DLKP variants	241
3 8 1 Aims of TFPI2 experiments	241
3 8 2 RT-PCR validation of differential TFPI2 mRNA expression	242
3 8 3 TFPI2 siRNA transfection in the non-invasive DLKP variants	246

3 8 3 1	Summary of TFPI2 siRNA experimental plan	246
3 8 3 2	TFPI2-specific decrease in mRNA levels	247
3 8 4	Invasion assay analysis of TFPI2 siRNA transfection	251
3 8 5	TFPI2 cDNA transfection in the invasive DLKP variants	254
3 8 5 1	Summary of TFPI2 cDNA experimental plan	254
3 8 5 2	Western blot analysis of TFPI2 cDNA transient transfection	254
3 8 5 3	Evaluation of TFPI2 cDNA transient transfection on proliferation	258
3 8 5 4	Evaluation of TFPI2 cDNA transient transfection on DLKP variant invasion	259
3 9	PCR analysis of cDNA transient transfection	263

Section 4.0 Discussion

4 1	Microarray analysis of DLKP and its invasive and chemotherapeutic drug resistant variants	271
4 1 1	Genomatix analysis	275
4 2	Confirmation of array results by RT-PCR	277
4 3	Validation of invasion status of the DLKP cell lines used in this study	279
4.4	Selection of target genes for functional analysis	281
4 4 1	Experimental design for functional analysis of array targets	282
4.5	Insulin-like growth factor –1 receptor (IGF-1R)	284
4 5 1	Endogenous IGF-1R expression in the DLKP variants	285
4 5 2	siRNA transfection optimisation for the DLKP variants	286
4 5 3	Evaluation of IGF-1R siRNA targeting on mRNA and protein levels	285
4 5 4	Evaluation of IGF-1R siRNA targeting on proliferation	288
4 5 5	Evaluation of IGF-1R knockdown on invasion	290
4.6	Inwardly rectifying potassium channel J8	294
4 6 1	KCNJ8 expression in DLKP variants	294
4 6 2	Evaluation of functional effects of KCNJ8 in DLKP variants	296
4 6 2 1	KCNJ8 siRNA transfection	296
4 6 2 2	KCNJ8 cDNA transfection	299
4 6 3	Assigning a function for KCNJ8	299
4.7	S100A13	300
4 7 1	S100A13 expression in the DLKP variants	300
4 7 2	Evaluation of functional effects of S100A13 in DLKP variants	301

4.8	Stratifin (SFN)	305
4 8 1	SFN expression in the DLKP variants	305
4 8 2	Evaluation of functional effects of SFN in DLKP variants	307
4.9	Tissue Factor Pathway Inhibitor 2 (TFPI2)	309
4 9 1	TFPI2 expression in the DLKP variants	309
4 9 2	Evaluation of functional effects of TFPI2 in DLKP variants	309
Section 5 0	Conclusions and Future work	
5 1	Conclusions	314
5 1 1	Characterisation of a panel of lung cell lines with defined behaviour in an <i>in vitro</i> invasion assay	315
5 1 2	Microarray profiling of a panel of invasive lung cancer cell lines	315
5 1 3	IGF-1R	316
5 1 4	KCNJ8	316
5 1 5	S100A13	317
5 1 6	TFPI2	317
5 1 7	SFN	318
5.2	Future Work	319
5 2 1	Microarray Analysis	319
5 2 2	IGF-1R	320
5 2 3	KCNJ8	321
5 2 4	S100A13	322
5 2 5	TFPI2	323
5 2 6	Other work	323
Section 6 0	Bibliography	324

Section 7.0	Appendices	359
7.1	Appendix 1 RT-PCR of genes with increased expression in invasive cell lines by microarray analysis	360
7.2	Appendix 2 RT-PCR of genes with decreased expression in invasive cell lines by microarray analysis	415
7.3	Appendix 3 Table of PCR primers used	437

Dedication

The work presented in this Thesis is dedicated to the memory of my Aunt Assumpta Heaney, who herself suffered from lung cancer Assumpta was always in my thoughts during my PhD and was my inspiration and driving force during the project She will, no doubt, continue in this roll for the remainder of my career in cancer research

I hope this data contributes in some way towards a better understanding of cancer mechanisms, so that we may have more appropriate and effective treatments in the future

Acknowledgements

I wish to thank, most sincerely, Prof Martin Clynes for providing me with the opportunity to carry out this research and for his guidance and advice during this project

A massive thanks has been well earned by Dr Niall Barron, my supervisor Niall, you were such a tremendous help and support to me and always knew when to be my friend and when to be the boss and kick my ass – but always in a nice way! My Dad reckons you're the best person he's ever met to get the best from me with as little drama as possible he'll be in touch for lessons soon! It was a pleasure to be you're first post-grad I couldn't have had a better mentor

Thanks to all in Molecular Biology and Bioinformatics, namely Olga, Helena, Bella, Patrick, Mohan, Jai, Paudie and Eoin I've worked with each of you at some point in this project and appreciate your help and companionship, especially on days when it seemed this work would never end! I couldn't have managed without the support of everyone in the NICB, who were always willing to help when called upon for scientific advice, job-hunting tips (thanks Norma!) or even a coffee break A big shout out also goes to Carol and Yvonne who generated order numbers at short notice (it was always an emergency!), booked printers and arranged couriers etc I am extremely appreciative to you all and will not forget your kindness

I have also made some great friends at the NICB You know who you are and I am confident that our friendship will continue despite moving on to pastures new Thank you for the laughs and support I have to mention especially, my lunch buddies, Eadaoin and Brigid, whose friendship brightened up many a dreary day Thank you girls for the moans, laughs and tears we've shared over the years long may it continue

Special gratitude is also owing to Cormac and Catherine, who are the best friends a girl could have Cormac, you were always on hand with practical "Kerryman" advice and understood where I was coming from during the mad post-grad moments. Catherine, you listened to many stories of woe and told me that it would all be ok in the end

Thank you both for being there for me I will endeavour always to be as good a friend to you both

My extended family were a great support during my college years, particularly Fran, Tom, Ciaran and Luke who welcomed me into their home when I first came to Dublin and any other time I was homeless after that Thanks Guys! Mags, Mike (aka B), Niamh and Orlaith also deserve special thanks for providing me with an alternative refuge from work, excellent company and lots of wine!! The next bottle's on me B! I also want to thank Nana and Gran for their love, friendship, prayers and support over the years Gran passed away since the completion of this thesis, but She was more excited about this achievement than I was I am so grateful that She was here to share this happy time with us and for our special friendship Meow to Marmalade ☺

My Brothers and Sister, Adrian, Eoghan and Karen were always there for me when I needed them, each in their own way Thanks to Adrian for wanting to sort out any problem I encountered, to Karen for her practical and hilarious viewpoints and to Eoghan for the limitless hugs that never failed to bring a smile to my face

I owe my parents, Richard and Mary, so much that I can never thank them enough Their faith in me never faltered and they always encouraged me to believe that I can achieve whatever I put my mind to, which is why I ended up in college for so long in the first place! Thanks Mam and Dad for your love and support, hopefully I can repay ye in some small way in the years to come

Last, but certainly not least, is Derek, who went through the highs and lows with me and never had an escape seeing as we lived in the same house Many's the time my Dad took pity on you for that and wondered how you put up with me! Thanks Derek for everything, for your love and support, for being my best friend, for the most useful birthday present ever (the laptop), feeding me and keeping the cups of tea coming and for staying up with me until I was finished working, particularly during the write up oh and for asking me to marry you! If I had to list everything I'd be here forever I hope I can make you feel as loved and cherished as you make me feel Here's to lots of good times together xxx

I hereby certify that this material, which I now submit for assessment on the programme of study leading to the award of Ph D is entirely my own work and has not been taken from the work of others save and to the extent that such work has been cited and acknowledged within the text of my work.

Signed: Asley Perce ID No.: 96453788

Date: 15/9/06

List of Abbreviations

5ac	5'aza-2'-deoxycytidine
ABC	ATP Binding Cassette
AMP	Ampicillin
ANOVA	Analysis of variance
APC	Adenomatous polyposis coli
ATCC	American Tissue Culture Collection
ATP	Adenosine-triphosphate
bFGF	Basic fibroblast growth factor
CDK	Cyclin-dependent kinases
CDNA	Complementary DNA
CTX	Charybdotoxin
DMEM	Diethyl Pyrocarbonate
DMSO	Dimethyl sulfoxide
DNA	Deoxyribonucleic Acid
DNAse	Deoxyribonuclease
dNTP	Deoxynucleotide triphosphate (N= A, C, T, G or U)
DOCK-180	Dedicator of cytokinesis 180
dsRNA	Double-stranded RNA
ECL	Enhanced chemiluminescence
ECM	Extracellular matrix
EDTA	Ethylene diamine tetracetic acid
EGFR	Epidermal growth factor receptor
EMMPRIN	Extracellular matrix metalloproteinase inducer
EST	Express sequence tags
ET-1	Endothelin-1
FAK	Focal adhesion kinase
FCS	Foetal calf serum
FGF-1	Fibroblast growth factor-1
FW score	Frame worker score
GAPDH	Glyceraldehyde-3-phosphate dehydrogenase
GAPs	GTPase-activating proteins

GDFs	GDI-dissociation factors
GDIIs	Guanine nucleotide dissociation inhibitors
GDP	Guanosine diphosphate
GE	Gel electrophoresis
GEFs	Guanine nucleotide exchange factors
GFP	Green Fluorescent Protein
GO	Gene ontology
GTP	Guanosine triphosphate
HCC	Human colon carcinoma
HDAC	Histone deacetylase
HGP	Human Genome project
ICAM	Intercellular adhesion molecule
IFN	Interferon
Ig	Immunoglobulin
IGF	Insulin growth factor
IGF-1R	Insulin like growth factor receptor 1
IL-1 α	Interleukin 1 α
IL-8	Interleukin 8
IMS	Industrial Methylated Spirits
IVT	<i>in vitro</i> transcription
IVVM	Intravital videomicroscopy
KCNJ8	Inwardly rectifying potassium channel J8
kDa	Kilo Daltons
MAb	Monoclonal Antibody
MAPK1	Mitogen-activated protein kinase 1
MAS 5.0	Microarray suite 5.0
MDR	Multidrug resistance
Mel	Melphalan
MEM	Minimum Essential Medium
MeSH	Medical subject headings
MIAME	Minimum information about a microarray experiment
miRNA	microRNA
MLCK	Myosin-light-chain kinase

MM	Mismatch
MMP	Matrix metallo proteinase
mRNA	Messenger RNA
MRP	Multidrug Resistance-associated Protein
MT1-MMP	Membrane type 1 MMP
MZF1	myleoid zinc finger 1 factors
NEAA	Non essential ammo acids
NRK	Normal Rat Kidney
NSCLC	Non-Small Cell Lung Carcinoma
OD	Optical Density
Oligos	Oligonucleotides
PAb	Polyclonal Antibody
PAI-1	Plasminogen activator inhibitor-1
PBS	Phosphate Buffered Saline
PEI	Polyethylenimine
PI3K	Phosphomositide 3-kinase
PKC	Protein Kinase C
PM	Perfect match
PMA	Phorbol 12-myristata 13-acetate
PTGS	Post translational gene silencing
QC	Quality control
qRT-PCR	Real Time Reverse Transcriptase-PCR
rAAV	Recombinant adeno viral vector
Rho	Ras homology protein
RISC	RNA-induced silencing complex
RNA	Ribonucleic Acid
RNA ₁	RNA interference
RNase	Ribonuclease
RNasin	Ribonuclease Inhibitor
rpm	Revolution(s) Per Minute
RT reaction	Reverse Transcriptase Reaction
RT	Room temperature
RTK	Receptor tyrosine kinase

RT-PCR	Reverse Transcriptase-PCR
SCLC	Small Cell Lung Carcinoma
Scrm siRNA	Scrambled siRNA
SDS	Sodium Doedecyl Sulphate
sec(s)	Second(s)
SFM	Serum-Free Medium
SFN	Stratifin
shRNA	short hairpin RNA
siRNA	Small interfering RNA
SNPs	Single nucleotide polymorphisms
SOM	Self organising map
SP1F	GC box factors SP1/GC
STAT 5A	Signal transducer of transcription 5A
SUR	Sulfonylurea receptor
TAE	Tris-acetic acid-EDTA buffer
TBE	Tris-boric acid-EDTA buffer
TBS	Tris Buffered Saline
TCF4	T Cell Factor 4/Transcription factor 4
TE	Tris-EDTA
TEMED	N, N, N', N'-Tetramethyl-Ethylenediamine
TF	Transcription factor
TFPI2	Tissue factor pathway inhibitor 2
TGF- β	Transforming growth factor β
TIMP2	Tissue inhibitor of metallopreteinase 2
TSA	Trichostatin A
TV	Trypsin/EDTA solution
TXT	Taxotere
UHP	Ultra high pure water
uPA	Urokinase type plasminogen activator
uPAR	Urokinase type plasminogen activator receptor
v/v	volume/volume
VCR	Vincristine
w/v	Weight per volume

ZBPF

zinc binding protein factor family

Investigation into the molecular mechanisms underlying invasion in the lung carcinoma cell line DLKP and its chemotherapeutic drug resistant variants

Abstract

This research described in thesis was undertaken in an attempt to increase our knowledge of mechanisms by which lung cancer cells acquire the capacity to invade. This is a critical step in cancer metastasis. To study the molecular nature of invasion, the gene-expression profiles of five lung cancer cell lines (DLKP) with differing levels of invasiveness (as determined by an *in vitro* invasion assay) were analysed using expression microarray methodology. Two invasive, non-drug exposed, variants of the DLKP cell line were used in the study along with a non-invasive Vincristine-selected (VCR) cell line, an invasive Taxotere (TXT) resistant variant and a non-invasive TXT-selected cell line that had lost its resistance to TXT. This provided us with a panel of lung cancer cell lines with various levels of invasiveness. Lists were generated from the array data containing genes that may potentially serve as transcriptional signatures for invasiveness and/or drug resistance in these cell lines. From the genelists compiled, and taking into account results from PCR-based validation and evidence from existing literature, five genes were picked as high priority targets for further investigation in the context of our invasion model. These were IGF-1R, KCNJ8, S100A13, SFN, and TFPI2.

Functional studies to investigate the role of these targets in invasion included gene over-expression and knockdown using cDNA and siRNA transfection respectively, with confirmation by semi-quantitative RT-PCR, qRT-PCR and Western blotting where possible. Most importantly any functional effect in our cell model was examined by *in vitro* invasion assay. The functional analyses identified a role for IGF-1R and TFPI2 in the invasive phenotype and also identified novel roles for the proteins KCNJ8 and S100A13 in invasion.

Section 1.0: Introduction

1.1 General Introduction

Invasion and metastasis is a major cause of death for cancer patients. The complexity of the metastatic process has forced investigators to focus on one contributing factor at a time in order to reduce the number of variables. Invasion is one of the most critical steps in metastasis. Dynamic interactions among cell adhesion molecules, extracellular matrix, proteases, cytoskeletal proteins and signalling molecules contribute to the invasive behaviour of tumour cells.

Chemotherapy is the principal therapeutic tool used to treat metastatic cancers that cannot be eradicated by surgery. Although there has been significant impact on survival of certain malignancies, the majority of human cancers are resistant to chemotherapy at presentation or become resistant after an initial response. This suggests that resistance is inherent in a tumour cell or evolves under the selection pressure of drug administration.

Drug resistance and invasion/metastasis are correlated phenomena. Highly multidrug resistant tumour cells can survive chemotherapy and escape to distant sites of the body or highly metastatic cells can escape the effect of chemotherapy. A relationship between these two phenotypes has been demonstrated by two types of experiments, firstly, in some cases, invasive/metastatic cells develop drug resistance more readily than non-invasive metastatic cells (Cillo *et al*, 1987), secondly, some tumour cells selected for resistance to chemotherapeutic drugs are more invasive/metastatic relative to non-resistant cells (Lucke-Huhle *et al*, 1994). Mechanisms underlying this relationship have not yet been elucidated. It is supposed that malignant tumours arise as a result of an accumulation of genetic mutations involving a number of oncogenes and tumour suppressor genes. Many of these genes could affect the expression of cell growth, differentiation, drug resistance, invasion and metastasis. Hence, an important goal of future research would be to determine whether a common factor exists that activates two sets of genes, those responsible for drug resistance, and those responsible for increased tumour cell invasion and metastasis.

The advent of DNA microarray technology allows the investigation of these processes either alone or in tandem depending on how the array data is mined. By using microarray technology, it is hoped in this project to identify a group of genes involved in the invasive phenotype and to understand which signals and signal transduction pathways are activated or restrained in malignant invasion.

1.2 Lung Cancer

Cancer is one of the most feared diseases of the last century in the western world. In fact, the term “cancer” includes over a hundred different forms of the disease. Cancer can develop from nearly every tissue in the body and subtypes of tumours can also be found within specific organs. Cancer cells have defects in the regulatory circuits that control cell proliferation and homeostasis (Hanahan and Weinberg, 2000). Among all types of cancer, lung cancer is the most common form. The national cancer registry (All-Ireland cancer statistics 1994-1996) reported that there are approximately 2000 lung cancer related deaths per year in Ireland. It is suggested that 87% of lung cancer cases are as a result of cigarette smoking (Hecht, 2002), but this figure may be as high as 95%. Other causes of lung cancer include exposure to chemicals such as asbestos, as well as the naturally occurring radioactive gas radon. Passive smoking of environmental tobacco smoke (ETS) has also been linked with the development of lung cancer in non-smokers.

Symptoms associated with lung cancer are cough, dyspnoea, haemoptysis and post obstructive pneumonia, (Hoffman *et al.*, 2000), although lung cancer can present with no initial symptoms. Diagnosis is achieved by invasive and non-invasive methods. Non-invasive methods for diagnosing lung cancer include sputum cytology and chest radiography. After this point, invasive techniques such as bronchoscopy and lung biopsy are performed. While the location and size of the lung tumour can be estimated from a chest x-ray or CT scan, accurate diagnosis and staging requires a biopsy, to histologically type the cells and determine if local nodes are involved.

Lung cancer is divided into 2 main groups, small cell lung cancer (SCLC) and non-small cell lung cancer (NSCLC). The World Health Organisation (WHO) compiled this histologic classification. SCLC and the subtypes of NSCLC – adenocarcinoma, squamous cell carcinoma and large cell carcinoma, account for 95% of lung cancers. SCLC presents less frequently than NSCLC and generally originates from a central location in the lung. These tumours are very aggressive, have a rapid growth rate and generally present with distant metastases at diagnosis. These tumours have the poorest prognosis of all lung cancer subtypes.

NSCLC is divided into three categories, squamous cell carcinoma (30% of all lung cancers), adenocarcinoma (40%) and large cell carcinoma (10%) Squamous cell carcinoma develops from within a central bronchus in the lung and frequently displays central cavitation from necrosis They are characterised by keratin formation Squamous cell carcinomas have slow growth rates and develop metastases at a late stage Adenocarcinomas generally develop centrally from surface epithelial cells in larger bronchi They are characterised by gland formation and mucus production These tumours tend to metastasise early and have a rapid growth rate Large cell carcinoma is characterised by large cells with large nuclei and prominent nucleoli These tumours are usually poorly differentiated and tend towards large peripheral masses

Staging of lung cancer is very important, since it will determine the type of treatment received The international staging system classifies the cancer based on the Tumour, Node, Metastasis (TNM) designation The designation T1-4 refers to the size and location of the primary tumour N0-N3 describes the extent of lymph node involvement In cases where distant metastases are present (M1), the tumour is diagnosed as stage IV lung cancer Early stage lung cancers are the most treatable, with later stage cancers such as stage IIIB and IV being virtually untreatable

Lung cancer, particularly SCLC, is characterised by rapid growth and metastatic spread (Yano *et al*, 2005) By the time of diagnosis clinically undetectable micrometastasis may already have developed within the lung Yano *et al*, (2005) injected immunodeficient mice with SCLC cell lines, SBC-3 and SBC-5 resulting in metastasis formation in liver, bone and kidney Lung cancer itself often arises as a metastasis from another site, for example, cancer of the breast (Minn *et al*, 2005)

The choice of treatment for patients with lung cancer depends strongly on the clinical stage Other details taken into account include pulmonary function and cell type Surgery is the major therapeutic option for lung cancer patients, however, approximately 75% of lung cancers are inoperable at time of diagnosis therefore surgery is only curative in patients with early stage lung cancer Radiation therapy can also be curative for a small percentage of patients To date, chemotherapy can offer improvement in short-term survival, but overall survival from lung cancer is poor The

main aim of chemotherapy is to kill the tumour cells with the least possible effect on normal cells and chemotherapy regimens are based on empirical data and clinical experience (Debatin, 2000) Chemotherapy is often used in combination with surgery or other therapies such as radiotherapy, known as adjuvant chemotherapy It is especially important for increased survival in cancer patients where these other treatments have failed Chemotherapy can increase median survival time in patients with advanced lung cancer, and prevent recurrence in resected early stage lung cancer However, the design of improved treatments for lung cancer lies in a better understanding of the disease at a molecular level

21

1.3 Pharmacology of Chemotherapy drugs

Two chemotherapeutic drugs were used to generate the drug-resistant cell lines used in this study. These are Taxotere (Docetaxol (TXT)) and Vincristine (VCR), their mechanisms of action will be discussed in the following section.

1.3.1 The Vinca Alkaloids

Vincristine (Figure 1.1) and Vinblastine are complex plant alkaloids isolated from the periwinkle plant *Catharanthus roseus*. They are members of a general class of drug that function as mitotic inhibitors which act by interfering with the function of microtubules, a class of long, tube-like cellular organelles approximately 250nm diameter (Pratt *et al*, 1994). Microtubules and microfilaments play an important role in the movement of cells relative to each other and in the movement of organelles within the cytoplasm of a single cell. The cytotoxicity of vincristine is attributed to its ability to interrupt cell division in metaphase (Bruchovsky *et al*, 1965), but other effects could also contribute to cell death. Their action is specific to the M phase of the cell cycle (Wilson *et al*, 1975).

The vinca alkaloids specifically exert their effect by binding to tubulin and preventing its polymerisation. As polymerised microtubules form the spindles that retract chromosomes into daughter cells at mitosis, their disruption results in blocked mitosis. Exposure of mitotic cells to the drug is followed by the rapid disappearance of the spindle apparatus and the maintenance of the chromosomes in the condensed state. Although the effects are seen at the time, the actual vincristine-tubulin interaction occurs during interphase.

Vincristine and vinblastine have very similar chemical structures and behave essentially the same way at the level of drug-tubulin interaction, however there are differences in the spectrum of antitumour activity of the two drugs in both experimental animal tumours and clinical cancer. The reason for these differences remains unknown. These compounds are active against a broad spectrum of cancers.

including lung, ovarian and testicular cancer (Culine *et al* , 1994, Einhorn, 1997, Schiller, 2001 and Schuette, 2001) They induce bone marrow and neural toxicities, and development of drug resistance to both agents via overproduction of P-glycoprotein (Bradley *et al* , 1989)

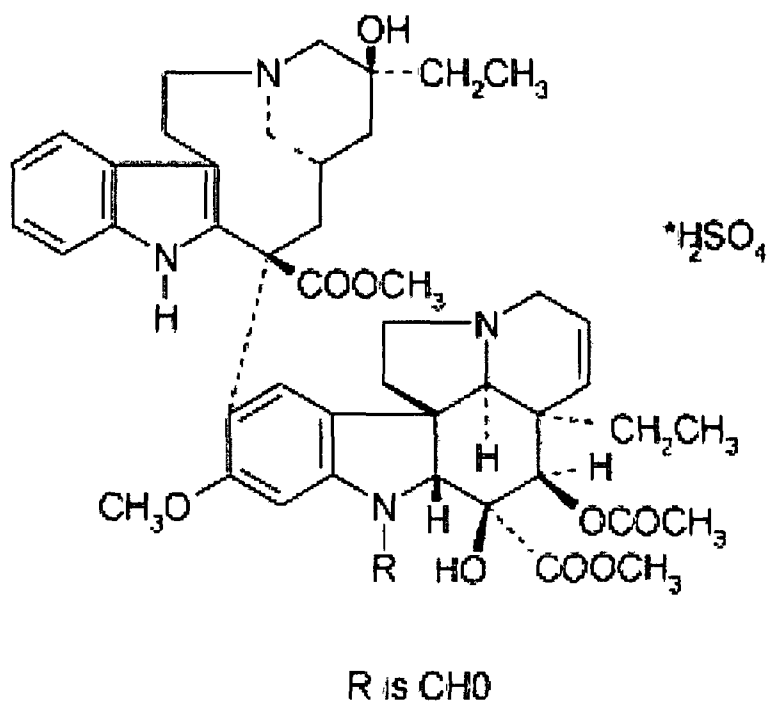


Figure 1.1: Chemical structure of Vincristine

1.3.2 The Taxanes

The taxanes are a group of drugs including paclitaxel (taxol) and docetaxol (taxotere). Taxol was originally isolated from the yew tree *Taxus brecifolia*. Despite the elucidation of its broad activity and its unique structure (Wani *et al*, 1971), it is still in the early stage of clinical development in so far as its role/potential role in the treatment of many cancer types has yet to be conclusively defined. Taxotere (docetaxol) is a semi-synthetic taxane extracted from the needles of *Taxus baccata*, and is slightly more soluble than taxol. The chemical structure of taxotere is shown in Figure 1.2. In a similar manner to the vinca alkaloids, the taxanes exert their anti-tumour effect through the disruption of mitosis. They interfere with chromosome changes during the cell cycle and are toxic to proliferating cells. They induce a shift in the physiological equilibrium between microtubules and tubulin toward polymerisation and formation of dysfunctional microtubules.

Taxol and taxotere have been shown to be active in the treatment of refractory ovarian cancer (Rowinsky *et al*, 1990). Encouraging results have been obtained in patients with metastatic breast cancer (Holmes *et al*, 1991 and Marty *et al*, 1999). Like the majority of chemotherapy drugs, the taxanes have a number of side effects. Bone marrow suppression (principally neutropenia), complete alopecia (hair loss) and hypersensitivity reactions are the most common dose limiting toxicities for the taxanes (Markman *et al*, 2003). Other side effects include, hypersensitivity reaction characterised by dyspnea, urticaria and hypotension. A variety of cardiac abnormalities have also been associated with taxol treatment (Pratt *et al*, 1994).

Resistance to taxotere arises through the mechanisms of multidrug resistance (MDR). Mechanisms of MDR include exclusion of the drug from the cell, increased detoxification of the drug, alteration in drug targets, failure to activate the drug to its active form, enhanced repair capability of the cell after injury or failure to engage an appropriate response leading to apoptosis in the damaged cells. An additional mechanism of drug resistance is the mutation of the gene coding for one of the tubulin subunits (Schibler *et al*, 1986). It is thought that, in the absence of drug, the equilibrium between free tubulin and microtubules is shifted towards disaggregation (Cabral *et al*, 1986), therefore the mutant cells have slightly greater tolerance for

taxol-induced stabilisation than that of the parent cells. Some mutants were not only resistant to taxol, but required it for growth as a result of extreme shift towards disaggregation (Pratt *et al.*, 1994).

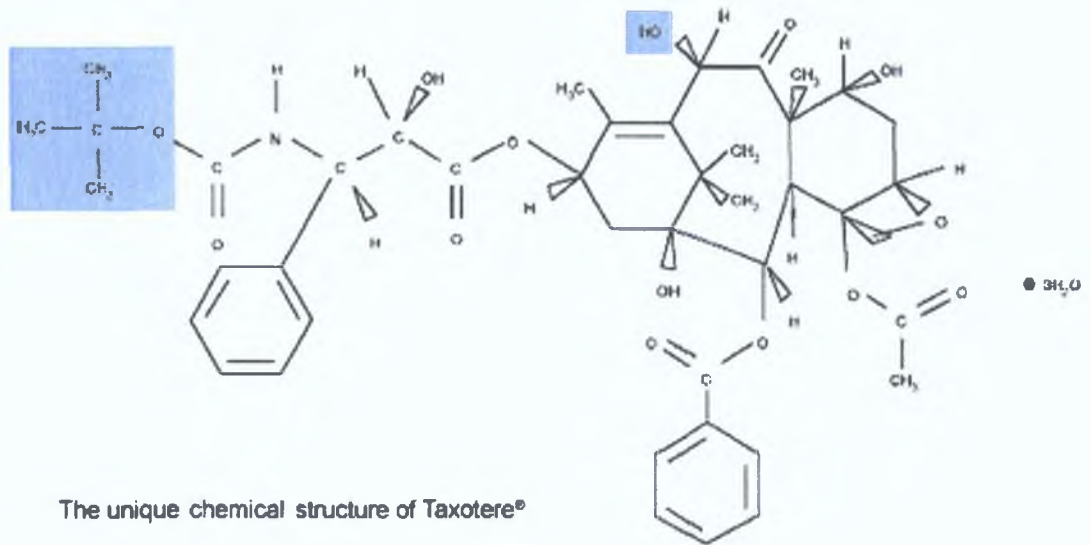


Figure 1.2 Chemical structure of Taxotere

1 3 3 Chemotherapy resistance

A major obstacle in the use of chemotherapy for cancer treatment is the development of resistance. Consequently, a better understanding of the mechanisms of drug resistance would help to overcome this obstacle. Intrinsic and acquired drug resistance are believed to cause treatment failure in over 90% of patients with metastatic cancer (Longley & Johnston, 2005). Some tumours are initially sensitive to an anticancer agent and, over time, develop a resistance to it and this is referred to as acquired resistance. Whereas, other tumours are resistant before treatment and this is known as intrinsic resistance. One of the major factors leading to drug resistance is decreased drug accumulation. This is caused by decreased drug influx or enhanced drug efflux, both of which result in the chemotherapeutic agent not exerting its effect on the tumour. Drug resistance can also be caused by modified drug activation, drug inactivation, alterations in DNA repair mechanisms and altered response to apoptosis. Treatment with one agent can often lead to associated resistance to a number of unrelated agents. The development of resistance to a variety of unrelated chemotherapeutic drugs is called multiple drug resistance (MDR). MDR is caused by a variety of changes in the cancer cells and is almost always multifactorial.

1.4 Metastasis

By the time of diagnosis, a high proportion of patients have clinically detectable metastasis. It is assumed that dissemination is impossible until invasion has occurred. For breast cancer, the period of transition from hyperproliferative but non-invasive disease to invasive cancer is estimated to average 6 years (Sprat *et al*, 1986). The time period after the invasive carcinoma grows to reach the minimum threshold size of detection (0.25cm in diameter), to establishment of the first metastasis, can be less than one year (Sprat *et al*, 1986). Thus transition of preinvasive carcinoma to invasion provides a much larger window for intervention compared to the conventional goal, which focuses on established invasive carcinoma.

Metastasis is the spread of cancer from a primary tumour to distant sites in the body. A distinguishing feature of malignant cells is their capacity to invade surrounding normal tissues and metastasise through the blood and lymphatic systems to distant organs. This process of metastasis is the most devastating aspect of cancer. It is estimated that in almost 50% of cancer patients, surgical excision of a primary tumour is not curative, as metastasis has occurred to a further site in the body (Fidler *et al*, 1994). In many patients, metastases develop some years after the resection of the primary neoplasm.

Most deaths from cancer are due to metastasis that are resistant to conventional therapies. Current therapies fail to eradicate metastasis for three major reasons. Firstly, when initially diagnosed, most tumours are well advanced and metastasis has already occurred. Secondly, specific organ environment can modify the response of a metastatic tumour cell to systemic therapy and alter the efficiency of anticancer agents. The third reason and the greatest obstacle to the success of therapy, is the heterogeneous composition of tumours, where highly metastatic cells can escape from the effect of therapeutic agents.

Cancer metastasis has been described as a complex series of sequential processes that involve (1) the initial transforming event, (2) proliferation of transformed cells, (3) the ability of cancer cells to avoid destruction by immune mechanisms, (4) nutritional supply to the tumour mass requiring the release of tumour angiogenesis factors, (5)

local invasion and destruction of extracellular matrix components and parenchymal cells, (6) migration of tumour cells away from the primary tumour mass, (7) penetration of cancer cells through the blood vessel wall, (8) embolisation of cancer cells in “clumps” to distant organs, (9) arrest of cancer cells in the lumen of small blood vessels or lymphatics, (10) reverse penetration of blood vessels, (11) repetition of the process beginning at step 2, resulting in the formation of a secondary tumour (metastases) (Fidler *et al* , 1994)

Metastasis is thought to be an inefficient process. Large numbers of cells can be shed into the circulation from a primary tumour but only a small fraction of the cells will succeed in forming metastases. Results from a series of experiments using intravital videomicroscopy (IVVM), a technique which permits direct observation of the microcirculation *in vivo*, suggest that early steps in metastasis, including destruction of cells in circulation and extravasion, contribute less to metastatic inefficiency than previously assumed. Rather, regulation of growth of individual extravasated cells in target tissue appears to be the rate-limiting step (Chambers *et al* , 1995)

Some metastases will arise on the basis of circulatory anatomy. The lungs are a common site of metastasis. Similarly, metastases from the colon often arise in the liver as the liver receives direct drainage from the large intestine. Metastases also arise in other organs due to “Seed and soil” theory. In 1889, Paget concluded that metastasis occurred only when certain favoured tumour cells (the “seed”) had a special affinity for certain specific organs (the “soil”). The formation of metastases required the interaction of the right cells with the compatible organ environment. Metastasis favours the survival and growth of a few subpopulations of cells that pre-exist within the parent neoplasm (Fidler and Kripke, 1977). Thus, metastases can have a clonal origin, and different metastases can originate from the proliferation of different single cells (Talmadge *et al* , 1982)

In the past our inability to accurately diagnose patients at high risk for the development of metastasis has precluded the possibility of tailored treatment, increased monitoring, or preventive action. However, advances in gene expression profiling have allowed many researchers including van't Veer *et al* , (2002) to distinguish metastatic primary tumours from non-metastatic primary tumours. These results have led to much debate

as to the mechanisms of metastatic development. The ability to identify metastatic tumours using transcriptional signatures from bulk tumour tissues suggests that primary oncogenic mutations determine the metastatic potential of a tumour. This idea may be viewed as incompatible with the conventional theory of tumour progression which predicts that only a small number of cells from the primary tumour achieve metastatic potential. Both seemingly contradictory models have a variety of supporting data suggesting that both are correct to some extent (Hunter, 2006)

Organ microenvironment can influence the biology of cancer growth and metastasis in several different ways. During the interaction of metastatic cells with host tissues, signals from autocrine, paracrine or endocrine pathway can influence tumour cell growth and proliferation, due to the different concentrations of hormones in particular organs, local factors that are differentially expressed or paracrine growth factors concentrated in different tissues. In this way metastatic tumour cells can respond to physiological signals produced when homeostasis is disturbed. Tumour cells can also originate from or have an affinity for growth in a particular organ by responding to these physiological signals (Fidler, 2002). For example, human colon carcinoma (HCC) cells implanted subcutaneously (ectopic site) into nude mice produce low levels of secreted type IV collagenase, whereas the same cells growing in the wall of the colon (orthotopic site) produce high levels of type IV collagenase (Nakajima *et al*, 1990). In another study highly metastatic clones of human prostate cancer were implanted into the prostate (orthotopic site) and subcutis (ectopic site). Tumours growing in the prostate exhibited higher levels of epidermal growth factor receptor (EGF-R), basic fibroblast growth factor (bFGF), interleukin 8 (IL-8), type IV collagenase and the multidrug resistance (mdr-1) gene than those growing in the subcutis. This data indicates that the expression level of metastasis-regulating genes by metastatic cells can be induced by factors in the organ microenvironment (Fidler, 2002)

Metastasis is the final stage in tumour progression from a normal cell to a fully malignant cell in some cases. The best-developed example is the characterisation of the molecular progression in colon cancer, in which specific changes (e.g. loss of tumour-suppressor genes and mutation of oncogenes) are preferentially associated with specific changes of progression (Fearon and Vogelstein, 1990, Kinzler and Vogelstein, 1996). However, the final stage in tumour progression to a metastatic phenotype remains to be elucidated at a molecular genetic level in colon and other cancers. Transfection with a variety of oncogenes (e.g. *ras* and *src*) has been shown to produce metastatic cells (Chambers and Tuck, 1993). For example, metastatic H-*ras* transfected NIH-3T3 cells had increased levels of a variety of gene products including proteinase and adhesive proteins (Tuck *et al* , 1991a and 1991b). Loss of tumour-suppressor gene function has also been implicated in the conversion to metastatic ability in specific tumour types, e.g. *nm23* (MacDonald *et al* , 1995), *KAI1* (Dong *et al* , 1995), *KISS-1* (Lee *et al* , 1996), although none is likely to be universally implicated in all tumour types. It appears more likely that regulation of expression of genes that contribute functionally to metastasis can occur in a tissue-specific manner. The development of gene expression profiling may help to elucidate the genes that contribute to metastatic development in many cancer types.

1.5 Invasion

Invasion is the active translocation of neoplastic cells across tissue boundaries and through host cellular and extracellular matrix barriers. Invasion is not only due to growth pressure but is attributed to additional genetic deregulation over and above those molecular events that cause uncontrolled proliferation. At the biochemical level, the mechanism of invasion used by tumour cells may be similar to that used by non-malignant cells which traverse tissue boundaries under normal physiological conditions. Examples of physiological invasion are smooth muscle cell migration from the tunica media (which contains smooth muscle fibres and elastic and collagenous tissues) to the intima (which is composed of the endothelial cell layer) of blood vessels, angiogenesis, embryogenesis, morphogenesis, nerve growth cone extension and homing, and trophoblast implantation. In contrast to malignant invasion, physiological invasion is tightly regulated and ceases when the stimulus is removed. Invading tumour cells appear to have lost the control mechanisms that which prevents normal cells from invading neighbouring tissue at inappropriate times and places. Thus, the fundamental difference between normal and malignant cells is regulation. The difference must lie in the proteins that start, stop or maintain the invasion programme at times and places that are inappropriate for non-malignant cells. A major goal is to understand what signals and signal transduction pathways are perpetually activated or deregulated in malignant invasion (Kohn and Liotta, 1997).

Liotta *et al*, (1977) has proposed a simplified three step theory of invasion (1) tumour cell attachment *via* cell surface receptors which specifically bind to the components of the extracellular matrix (ECM), (2) the anchored tumour cell secretes hydrolytic enzymes, such as matrix metalloproteinases, to degrade the extracellular matrix, (3) tumour cell locomotion into the region of the matrix modified by the proteolysis. Thus, regulation of the molecular events necessary for invasion requires spatial and temporal coordination at an individual cell level.

For cells migrating within a three dimensional extracellular matrix, such as penetrating a basement membrane, protrusion of a cylindrical pseudopod occurs prior to translocation of the whole cell body (Condeelis, 1993). A number of observations

support the central role of the cytoskeleton-driven pseudopodia as organs of motility and invasion. Pseudopodia aggregate or concentrate cell surface degradative enzymes and adhesion receptors (Guirguis *et al* , 1987). A balance must switch from proteolysis to adhesion in order for the advancing pseudopod to grip the matrix and pull the cell forward. General unregulated proteolysis alone cannot be responsible for the entire invasion cascade. When the cell moves into the zone of lysis, adhesion is required and proteolysis must be shut down. At the rear of the cell, dissociation from adjacent cells, and detachment from previous attachment sites are necessary to release the cell. This type of motility is described as mesenchymal motility (Sahi, 2005).

The basement membrane and interstitial stroma also have important regulatory roles in invasion. They serve as a storage depot for latent proteinases, cytokines and growth factors, which can be activated or released by the invading cells. The critical pathological turning point is in the initiation of local invasion leading to the dissemination of tumour cells. Tumour-induced neovascularisation occurs in parallel with invasion and provides vascular entry necessary for dissemination. A positive correlation between tumour aggressiveness and protease levels has been documented for all four classes of proteases including serine, aspartyl, cysteinyl and matrix metalloproteinase (MMP). It has been established that the integrity of the basement membrane can be regulated by the balance between MMPs and their inhibitors (Talhok *et al* , 1992).

Altered signalling pathways are also associated with invasion. In 1986, Pozzatti *et al* , transfected activated H-ras into primary rat embryo fibroblast cells. This resulted in the generation of a malignant and invasive phenotype that was characterised by the production of gelatinase B and marked pulmonary colonisation after tail vein inoculation of transfected cells. Similar effects have been observed with the expression of other oncogenes including Her-2/neu (Yu *et al* , 1993). These studies demonstrate the overlap between oncogene-induced tumour development and dissemination but highlight the fact that distinct signals must be in place for the functional separation of transforming activity and metastasis to occur. Signal transduction pathways that are further downstream of activated oncogenes may regulate the invasive phenotype.

The molecular characterisation of invasion has led to the identification of two categories of checkpoints that constitute possible intervention targets. The first category includes cell surface and secreted proteins e.g. adhesion receptors, degradative enzymes and their inhibitors and motility stimulating cytokines. The second checkpoint category includes regulatory proteins and pathways such as calcium-mediated signalling, G-protein activation and tyrosine phosphorylation events. It is the molecular examination of these checkpoint molecules that may provide the basis for the development of therapeutics that can potentially block tumour invasion or growth (Kohn and Liotta, 1997)

Mechanisms of invasion are known to involve a complex array of genetic and epigenetic changes many of which are specific for different types of tumours and different sites of metastasis. The roles of adhesion molecules such as integrins and cadherins in invasion have undergone a major transition over the past decade. It is now apparent that these molecules have a critical role in signalling from the outside to inside a cell thus controlling how a cell can interact with and sense its local environment. It has also become clear that proteolytic enzymes and their inhibitors not only degrade the ECM, but are involved in the release of factors that can positively or negatively affect the growth of tumour cells. In more recent years, the importance of the post-extravasational stages of invasion was highlighted, where adhesion and proteolysis are now known to play a role along with other processes including apoptosis, dormancy, growth factor-receptor interactions and signal transduction. It has also been found that it is not only the immediate cellular microenvironment, but also the extended cellular microenvironment that can modify cellular gene expression and enhance metastasis. Our improved understanding of the expanded roles of the individual molecules involved has resulted in a mechanistic blurring of the previously described discrete stages of the metastatic process (Cairns et al , 2003)

1.5.1 The extracellular matrix and basement membrane

The extracellular matrix is a complex structure of carbohydrate- and protein-containing components that comprise the basement membrane underlying epithelial tissues and that surround structural tissues such as bone and muscle (Yurcheno and Schittny, 1990). Almost all multicellular organisms have basement membranes. They are the first extracellular matrices that are produced during embryogenesis. Epithelial, endothelial and many mesenchymal cells are supported by this thin sheet-like ECM structure. The membrane acts as a solid regulator of cell attachment, differentiation and growth, as well as a passive barrier that segregates tissue compartments. Metastatic cancer cells have to penetrate the tumour's own basement membrane, that of the vasculature and target tissue in order to establish secondary disease sites (Hood and Cheresch, 2002).

The basement membrane has a complex molecular architecture that consists of laminins, type IV collagen, entactin and heparan sulphate proteoglycans. Laminins are flexible four-armed, 850kDa glycoproteins. Laminin monomers polymerise into 3D structures in a time- and concentration- dependent manner. As an initial step in metastasis, many epithelial tumours exhibit altered localisation or expression of laminin-binding integrins (e.g. $\alpha6\beta4$). This promotes invasion through the basement membrane and increases motility in the stroma, where tumour cells can remodel the matrix by depositing laminin (Hood and Cheresch, 2002). The most prevalent protein in the basement membrane is type IV collagen. Type IV collagen is a thread-like flexible molecule that can itself form a heterotrimer involving hydrophobic and disulphide bonds. The covalent binding of collagen provides mechanical stability to the basement membrane. Proteins such as entactin, which forms connections between networks of collagen and laminin, further stabilise the membrane. Many of the proteases with increased expression in metastatic tumours exhibit high enzymatic activity against type IV collagen. The basement membrane also contains heparan sulphate proteoglycans – a class of molecules that contain a protein core covalently linked to heparan sulphate chains. These molecules are linked to the membrane through interactions with laminin and may influence tumour biology by acting as a repository for growth factors including fibroblast growth factor.

1.5.2 Integrins and cancer

The integrins are composed of a large family of heterodimeric integral cell surface receptors that mediate cell-to-ECM and cell-to-cell interactions (Hynes, 1992). Derangement of integrin expression may be responsible for many aberrant cellular activities during tumour onset, progression and metastasis. The integrins, composed of α and β chain heterocomplexes act as integral cell membrane receptors that form focal adhesion contacts with ECM ligands e.g. fibronectin, laminin, entactin, intercellular adhesion molecule (ICAM) and the collagens to name but a few. Integrins also interact with cytoplasmic cytoskeletal filament-associated proteins e.g. actin, paxillin and talin. The family can form at least 25 distinct pairings of its 18 α and 8 β subunits, with each integrin consisting of a noncovalently linked α - and β -subunit, with each subunit having a large extracellular domain, a single membrane-spanning domain and a short, non-catalytic cytoplasmic tail (Mizejewski, 1999). In addition to regulating cell adhesion to the ECM, integrins relay molecular cues regarding the cellular environment that influence cell shape, proliferation, survival, migration and gene transcription.

1.5.2.1 Integrin expression and function

Invasive cells undergo changes in integrin expression levels and integrin affinity for ECM substrates. Many studies have reported significant differences in the surface expression and distribution of integrins in malignant tumours when compared with pre-neoplastic tumours of the same type. For example, $\alpha 5 \beta 3$ integrin is strongly expressed at the invasive front of melanoma cells and angiogenic blood vessels, but weakly expressed on pre-neoplastic melanomas and blood vessels (Brooks *et al.*, 1994). While the expression of some integrins is increased during tumorigenesis, the expression of others decreases. Cells can also assume a more migratory and invasive phenotype by altering their adhesive and signalling profile by increasing the affinity of integrins for their ligand (Hood and Cheresch, 2002).

1.5.2.2 Integrins and proteolytic enzymes

Epithelial to mesenchymal transformation (EMT) is the process by which epithelial cells lose their strong intracellular adhesion and their basolateral polarity to gain front-end to back-end polarity, and the ability to migrate through the ECM (Savagner, 2001). As cells lose cell-cell contact, new cell-ECM interactions are generated. Thus, many cell surface-associated adhesion molecules change function and are the source of signals that activate growth, ECM degradation and metastasis (DeClerck *et al* , 2004). Important changes in integrin interaction occur during EMT. For example, contact of integrins $\alpha6\beta4$ and $\alpha3\beta1$ with the ECM decreases the expression of cell-cell adhesion molecules such as E-cadherin and promotes the expression of proteases and their receptors and growth factors. The co-localisation of urokinase plasminogen activator receptor (uPAR) and integrin allows a physical interaction between the $\alpha3$ subunit and uPAR which downregulates E-cadherin and further promotes EMT. Together, these changes alter the interactions that occur at the cell surface from cell-cell to cell-ECM thereby promoting ECM degradation, invasion and motility (DeClerck *et al* , 2004).

Integrins are also involved in regulating the activities of proteolytic enzymes that degrade the basement membrane. The activation of these enzymes and cellular invasion are correlated under many pathophysiological settings. In human melanomas and metastatic breast tumours, for example, stromal cells close to the invasive front have increased levels of MMP activity compared with non-malignant control cells (Monteagudo, *et al* , 1990). Integrins may also be involved in activating specific MMPs. For instance, MMP2 is activated on the cell surface by a multimeric complex that is composed of MMP2, membrane type 1 MMP (MT1-MMP) and tissue inhibitor of metalloproteinase 2 (TIMP2). Studies on melanomas, gliomas and angiogenic endothelial indicate that this MMP2 activating complex also includes $\alpha5\beta3$ integrin (Hood and Cheresch, 2002). Thus, during invasion, $\alpha5\beta3$ integrin functions as an adhesion/migration receptor and in activating and localising proteases that are required to degrade the ECM. Negative-feedback regulation of integrin/protease binding is needed to prevent excessive degradation of the ECM. Proteolysis is negatively regulated by MMP2-dependent generation of hemopexin fragments, called PEX, which inhibits protease activation by competing with MMP2 for binding to $\alpha5\beta3$ integrin (Brooks *et al* , 1998).

1.5.2.3 Integrins and signalling; from the outside in

A further function of integrins is in the regulation of the intracellular signalling pathways that control cytoskeletal organisation, force generation and survival. Depending on ECM composition, integrins can activate one or more intracellular signalling pathways. These pathways involve phosphorylation of focal adhesion kinase (FAK), the recruitment of adaptor proteins, activation of small GTPases and the activation of downstream effector molecules. These signals, along with growth factor signals, regulate cell behaviour in a complex tissue microenvironment.

Integrin binding of ECM ligands induce integrin clustering and FAK activation. FAK is a cytoplasmic protein kinase that colocalises with integrins at focal adhesion structures. Activated FAK binds to many signalling molecules which promote cell proliferation through activation of the Ras-extracellular-signal-regulated-kinase (REK) pathway. FAK activation also promotes integrin-or growth factor-induced cell survival and migration (Hood and Cheresch, 2002).

Activated FAK also associates with the adaptor protein CAS. FAK and Src both phosphorylate CAS at multiple tyrosine kinase residues which results in the association of CAS with another adaptor protein, CRK, and localise to membrane ruffles. The CAS-CRK complex is part of the molecular migration machinery found at the leading edge of motile cells (Klemke *et al*, 1998). This complex acts as a molecular switch that induces cell motility by activating dedicator of cytokinesis 180 (DOCK-180), which in turn activates the small GTP-binding protein RAC (Hood and Cheresch, 2002).

The SHC family is a group of adaptor proteins that are recruited to activated tyrosine kinase in response to ligation of certain integrins and extracellular receptors in response to growth factor binding. This leads to SHC-dependent cell cycle progression, migration, survival and ERK activation (Wary *et al*, 1996).

In highly motile cells, initiation of migration is characterised by the reorganisation of actin to the cell edge, the protrusion of a leading lamellipodium and membrane ruffling at the advancing front of the lamellipodium. The RHO family of small GTPases can regulate these changes. Family members include RHO, CDC42 and RAC. RHO activation is dependent on integrins, syndecan-6 and other cell surface receptors,

whereas RAC and CDC42 are activated by ligation of integrins (Ren *et al*, 1999) Activation of RHO leads to the formation of actin stress fibres and the assembly of focal adhesions Activation of CDC42 is involved in the formation of filopodia and activation of RAC leads to membrane ruffling and cell migration (Hood and Cheresch, 2002) The expression of active RAC and CDC42 can depolarise differentiated mammary epithelial cells and induce integrin-mediated invasion through a 3D collagen matrix (Kealy *et al*, 1997)

During cell migration, the formation of new integrin contacts provides the cell with molecular signals that activate ERK signalling Integrins regulate ERK activity through several FAK-dependent and independent pathways and also by modulating growth factor-stimulated ERK activity ERK activation influences gene transcription cell survival and cell motility (Hood and Cheresch, 2002) During cell migration, the ERK signal decreases integrin-mediated adhesion and phosphorylates myosin-light-chain kinase (MLCK), which regulates the contractile force within the cell MLCK phosphorylates and activates myosin II, an ATPase found in leading lamellae and posterior regions of motile cells that generates force by promoting translational movement along actin cables Activated myosin then generates contractile forces that pull the cell forward towards the new integrin contacts and breaks the contacts at the trailing edge of the cell (Klemke *et al*, 1997) Phosphatidylinositol 3-kinase (PI3K) regulates integrin dependent cell movement by modulating integrin responses in normal and neoplastic tissue PI3K activity is needed for CDC42 and RAC-induced cell motility and invasiveness in mammary epithelial cells (Kealy, *et al*, 1997)

The Protein Kinase C (PKC) family of serine/threonine kinases are important in regulating integrin function and signalling For instance, ligation of fibronectin by integrins and syndecan-4 recruits PKC to membrane adhesions where it is required for focal adhesion formation, phosphorylation of FAK, cell spreading, migration and SHC-dependent ERK activation (Hood and Cheresch, 2002)

1.5.2.4 Integrins and signalling; from the inside out

For cells to acquire the traction needed for movement, adhesion to ECM through integrin heterodimers is critical. Maximum cell movement occurs at intermediate levels of adhesion where the cells can generate enough traction to move efficiently at the cell front while releasing contacts at the rear. Thus, integrins respond to intracellular clues and modify the way in which they act with the extracellular environment by modulating their affinity and avidity for their ECM ligands thereby regulating invasion and migration (Hood and Cheresh, 2002)

1.5.2.5 Survival during invasion

Invading cells must be able to activate survival mechanisms and escape apoptosis. Indeed, integrin-binding to ECM ligands initiates pro-survival mechanisms. Many anti-apoptotic pathways are the same as those that are involved in regulating migration. Many targets of FAK signalling such as RAS, RAC, PI3K and ERK have also been implicated in cell survival (Hood and Cheresh, 2002)

1.5.3 Proteases and Invasion

Tumour cell invasion involves attachment of tumour cells to the basement membrane, local proteolysis and migration of tumour cells through the proteolytically modified region (Liotta *et al* , 1983) Localised proteolysis is carried out by proteases outside the tumour cell that may be bound to the cell surface or secreted from the tumour cell Proteases inside the tumour cell also partake in local proteolysis by digesting phagocytosed ECM Most investigations to date have focused on the role of proteases in invasion and metastasis More recent studies have demonstrated that proteases are also involved in tumour growth at both primary and metastatic sites (Koop *et al* , 1994, Sympson *et al* , 1995 and Wilson *et al* , 1997)

Endopeptidases are categorised into five major classes cysteine (e.g. cathepsins B, L, S, K, Q, caspases, bleomycin hydrolase), aspartic (e.g. urokinase-type plasminogen activator, plasmin, chymase) metallo- (e.g. gelatinases A and B, meprin), threonine (e.g. proteasome) and serine proteases This introduction will focus on cathepsin B and the MMPs as examples of the involvement of proteases in tumour progression, invasion and metastasis

1.5.3.1 Cathepsin B

Increased cathepsin B expression, activity and changes in localisation have been observed in many different tumours including breast (Poole *et al* , 1978), colorectal (Campo *et al* , 1994) and lung (Sukoh *et al* , 1994) The increased expression of cathepsin B at mRNA level is associated with gene amplification, increased transcription, the possible use of multiple promoters and alternatively spliced transcripts Changes in the localisation of cathepsin B seem to precede the increase in protein levels, which suggests that alterations in trafficking of cathepsin B are independent of increased expression (Koblinski *et al* , 2000)

Proteases can interact, leading to the activation of proteolytic cascades that can degrade ECM components For example, Procathepsin B can be activated by cathepsin D, tPA, uPA, cathepsin G and elastases Active cathepsin B in turn activates pro-uPA, which converts plasminogen to plasmin, which can degrade several ECM components and activate MMP-1, -3, -9, -12 and -13 The MMPs can then degrade other ECM

components e.g. collagen -I and -IV, gelatins and activate further MMPs (Koblinski *et al*, 2000) Cathepsin B can activate MMPs indirectly via the plasminogen activator cascade and directly activate MMP-1 and -3 Thus, cathepsin B may be an important regulator of the activation of pro-uPA/ plasminogen and pro-MMPs

Both direct and indirect interactions between tumour and stromal cells can increase the expression of proteases For example the expression of gelatinases A and B are increased in fibroblasts upon contact with tumour cells These fibroblasts then partake in further degradation of the ECM Expression of cathepsin B and D can also be regulated by diffusible factors such as basic fibroblast growth factor (bFGF), insulin growth factor-1 (IGF-1) and epidermal growth factor (EGF) Paracrine factors secreted from tumour and stromal cells can thus regulate the expression of proteases (Koblinski *et al*, 2000)

There is an inverse correlation between cathepsin B and basement membrane staining in many cancers including lung (Sukoh *et al*, 1994) This result is consistent with a role for cathepsin B in ECM degradation *in vivo* Sameni and Slaone developed an assay that allows the visualisation of matrix proteolysis by living cells during invasion through a 3D gelatin matrix The matrix contains a quenched fluorescent substrate that fluoresces when cleaved by proteases By using this assay they have observed cathepsin B involvement in matrix degradation (Koblinski *et al*, 2000) Furthermore, the proteolytically active cells facilitate invasion by other cells by attracting them to cleared tracks in the matrix (Kramer *et al*, 1986)

Cathepsin B may increase cell proliferation by activating growth factors e.g. bFGF, EGF, IGF, vascular endothelial growth factor (VEGF) and transforming growth factor β (TGF- β) by freeing them from the ECM where they are sequestered Oursler *et al*, (1993) found that dexamethasone treatment of normal human osteoblast-like cells simultaneously increased cathepsin B and TGF- β expression

1.5.3.2 Matrix Metalloproteinases (MMPs)

MMPs are a zinc dependent family of endopeptidases that have a pro-domain a catalytic domain and a highly conserved active site domain. MMPs are synthesised and secreted in inactive zymogen form and depends on the presence of zinc and calcium ions. The production of active enzymes requires that proteolytic removal of the pro-domain. Over twenty MMP family members are known to exist (Polette *et al* , 2004). Most MMPs can cleave at least one component of the ECM, as listed in Table 1.1. MMPs are subdivided into collagenases, stromelysins, gelatinases and MT-MMPs based on their substrate preference. MMPs are physiologically expressed during various stages of development in processes requiring cell migration, tissue remodelling, wound healing, placentation or tumour progression. Many external stimuli can induce the expression of many MMPs.

Table 1.1 MMPs and their substrates.

Group	MMPs	Preferred Substrate
Collagenases	MMP1, MMP18 & MMP13	Collagen I-III Collagen IV
Gealtinases	MMP 2 & MMP9 (type IV collagenases)	Type IV collagen Laminin
Stromelysins	MMP3 (stromelysin 1), MMP10 (stromelysin 2), MMP19 (collagenase 4) & MMP11 MMP 7 & MMP26 (Matrilysins) MMP12 (metallo-elastase)	Type IV, V, IX & X collagen Fibronectin, laminin, elastin, gelatin & proteoglycn core proteins
MT-MMPs	MMP14, MMP15, MMP16, MMP24 & MMP25	Activators of pro-MMP2 Type I-III collagenases Fibronectin, laminin, gelatin, nidogen & cartilage proteoglycan core protein

Plasmin has been described to proteolytically activate some latent MMPs (Mignatti *et al* , 1996) and the cooperation between MMPs and the plasminogen activator/ plasmin cascade have an important role in the regulation of tumour invasion *in vivo* MMPs can autoactivate in some cases and can also effect mutual activation For example, MMP1 can activate latent MMP2 (Nagase, 1996) The proteolytic activity of MMPS is controlled by tissue inhibitors of MMPs (TIMPs), which specifically block activity of active MMPs by binding to the conserved zinc-binding site (Polette *et al* , 2004) Four TIMPs are currently known TIMP-1 and -2 inhibit most MMP activity, while TIMP-2 and -3 inhibit MT1-MMP TIMP-3 inhibits MMP-1, -2, -3, -7, -9 and -13 TIMP-4 inhibits MMP-2 and-7 (Knauper *et al* , 1996, and Liu *et al* , 1997)

It was originally thought that tumour cells were implicated in the invasion process via secreted proteolytic enzymes However, *in vivo* in situ hybridisation studies demonstrated that stromal cells were the source of MMPs In 1990, Basset *et al* , demonstrated that MMP11 was expressed specifically by fibroblasts in breast carcinomas and not by their benign counterparts Thus, host cells have an important role in the production of MMPs and tumour invasion due to the cooperation of stromal and tumour cells Extracellular matrix metalloproteinase inducer (EMMPRIN) is produced by tumour cells and can stimulate MMP-1 -2 and -3 by fibroblasts (Biswas *et al* , 1995) EMMPRIN mRNA is overexpressed in many carcinomas compared to benign and normal tissues, which suggests a role in invasion (Polette *et al* , 1996)

A complex interplay exists between cell adhesion molecule organisation and MMP expression that can also be involved in the development of an invasive phenotype by tumour cells β -catenin is an intracellular attachment protein that can attach cytoplasmic actin bundles to cadherin transmembrane adhesion molecules at the site of cell-cell junctions Since tumour cells detach from neighbouring cells in invasion abnormalities in the β -catenin/E-cadherin complex are likely to be involved (Curran and Murry, 2000) β -catenin and the DNA binding protein T Cell Factor 4/Transcription factor 4 (TCF4) also acts a transcriptional regulator of specific genes Normally, the protein product of tumour suppressor gene adenomatous polyposis coli (APC) binds to cytoplasmic β -catenin and causes its degradation In most colorectal cancers APC is mutated, so β -catenin accumulates and complexes with TCF which activates the transcription of target genes including cyclin D1 and c-myc Brabletz *et*

al, (1999) report that MMP-7 is also a target of β -catenin/ TCF Brooks *et al*, (1996) demonstrated that melanoma cells expressing integrin $\alpha v \beta 3$ had the ability to bind active MMP-2 facilitating collagen degradation Thus, a cell surface receptor known to be involved in directed cellular motility can also bind an enzyme that can degrade a major component of the basement membrane Furthermore, the cell surface receptor determinant CD44 which is known to promote growth and metastasis of tumour cells, has been shown by Yu and Stamenkovic (2000) to associate with active MMP-9 at the cell surface of human melanoma cells Disruption of MMP-9/CD44 aggregates decreases the invasiveness of tumour cells *in vivo*

Cytokines have also been shown to regulate MMPs For example, interleukin -1 (IL-1) induces the transcription of MMP-1 and -3 (Borghaei *et al*, 1998) In a study by Bar-Eli (1999) transfection of human melanoma cells with IL-8 increased the activity of MMP-2 and the invasiveness of the cells

MMPs can also regulate cell growth, either directly through the release of growth factors or indirectly by changes in cell adhesion as described above MMPs can degrade insulin-like growth factor (IGF) binding protein 3, which regulates the bioavailability and activity of IGF-II (Fowlkes *et al*, 1995) Powell *et al*, (1999) demonstrated that MMP-7 proteolytically generates active soluble Fas ligand and potentiates epithelial cell apoptosis These different effects of MMPs and their inhibitors depend on the balance between them in the local microenvironment

1.5.3.3 Urokinase-type plasminogen activator

Urokinase-type plasminogen activator (uPA) is a serine protease that is involved in the progression of cancer particularly in invasion and metastasis. Many studies of breast cancer patients whose primary cancers have high uPA levels have significantly poorer outcome than those with low uPA levels. Paradoxically, high levels of plasminogen activator inhibitor-1 (PAI-1) a uPA inhibitor, is also predictive of poorer patient outcome (Duffy, 2002).

The human uPA gene encodes a 53kDa protein that is initially synthesised as a catalytically inactive single chain peptide. Conversion to active form is brought about by a number of proteases including plasmin, cathepsin-B and -L. uPA is a multifunctional protein involved in both proteolysis and signal transduction. As a protease, uPA catalyses the conversion of plasminogen to active plasmin. Plasmin can then promote the degradation of ECM substrates that include fibrin, fibronectin and laminin. It can also activate MMPs and activate or release specific growth factors such as FGF-2 and TGF- β . uPA-catalysed proteolysis occurs *in vivo* while the protease is attached to a membrane anchored protein receptor, uPAR (Andreasen *et al.*, 1997). Binding of uPA to its receptor enhances proteolysis and also results in signal transduction, including activation of mitogen-activated protein kinase (MAPK), extracellular signal-regulated kinases 1 and 2 and other signalling pathways that activate Fos and Jun (Ossowski and Aguirre-Ghiso, 2000). uPA activity can be neutralised *in vivo* by two inhibitors called as plasminogen activator inhibitors 1 and 2 (PAI-1 and PAI-2), which belong to the serpin family of protease inhibitors and inhibit apoptosis. PAI-1 can also modulate adhesion and migration independently of its role as a protease inhibitor (Duffy, 2002).

Positive correlations between uPA levels and metastasis have been found in both cell lines and animal tumours. Transfecting cell lines with uPA cDNA enhances the metastasis of the transfected cells. Inhibition of uPA activity or expression reduced metastasis in model systems. Blocking uPA:uPAR binding also decreases metastasis in systems studied. Tumours in uPA null mice exhibit less progression than those in mice expressing uPA (Andreasen *et al.*, 1997). Since metastasis is the main cause of death

in cancer patients, and since uPA is an important mediator of this process, uPA is an ideal candidate for use as a marker to predict the likely formation of metastasis. Indeed, as a predictor of outcome for breast cancer patients, uPA acts as a potent biological marker. High levels of uPA are also correlated with poorer patient outcome in patients with stomach, colorectal, bladder, ovary, endometrium and brain cancers (Duffy, 2002b, Schmidt *et al* , 1997). High levels of PAI-1 are also associated with aggressive disease and poorer patient outcome. Although the reason for this is not clear, there are many possible explanations. For example, a critical PAI-1 concentration may be needed to prevent excessive ECM degradation by uPA during cancer invasion, where excessive ECM degradation could leave insufficient substrate on which cancer cells could migrate. PAI-1 is also needed for angiogenesis to occur and can modulate both cell adhesion and migration and thus metastasis and can inhibit apoptosis, hence increased PAI-1 expression is a poor prognostic factor (Duffy, 2002, Duffy, 2002b). Both uPA and PAI-1 are possible targets for cancer therapeutics, specifically with applications in the prevention of metastases.

1.5.3.4 Proteases and clinical trials

The detection of high expression of MMPs in many cancers and their association with poor prognosis make them ideal candidates for therapeutic targets. Therapeutic approaches using anti-MMP agents in conjunction with conventional chemotherapy have been developed over the last decade (Baker *et al* , 2002, Coussens *et al* , 2002). However, these new treatments have not provided any significant results due to the side effects caused. Also, since the matrix metalloproteinase inhibitors are cytostatic rather than cytotoxic, traditional endpoints used in anticancer drug trials, such as a decrease in tumour size, may not be appropriate in assessing the inhibitor effectiveness. Indeed, the conversion of tumours from an aggressive type to a more dormant state may be an acceptable therapeutic outcome and one will need to be able to document their biological activity on angiogenesis or tumour proliferation using non-invasive imaging technologies *in vivo*. If tumour dormancy is the aim, a drug would have to be administered long term therefore the issue of toxicity would have to be addressed.

Pre-clinical models that more closely mimic the interaction between neoplastic and stromal cells in cancer progression are needed. A consortium of several investigators including Carl Blovel (Sloan-Kettering), Lisa Coussens (UCSF) and Ching Tung (Harvard) to name but a few was recently created to determine the exact role that proteases play in tumour growth and invasion. The consortium determined that an optimal assortment of model systems would need to be evaluated based on the following criteria: (1) examination of multiple stages of tumour progression, (2) an orthotopic environment for tumour cells, (3) tumours are grown at organ sites of the most prevalent sites of human cancers, (4) multiple classes of proteases are expressed. They hope to identify causal role in malignant progression, validate proteases as therapeutic targets, develop functional assays for imaging proteolytic activity to analyse interactions among the cell types comprising a solid tumour, and develop functional assays for non-invasive imaging of the activity of the proteases that are validated as potential targets (Curran and Murry, 2000, Koblinski *et al* , 2000, and DeClerck *et al* , 2004).

1.5.4 Rho proteins and invasion

1.5.4.1 Rho proteins and growth factors

The Rho (Ras homology) GTPases are a subfamily of small GTP-binding proteins that are related to the Ras oncogene. All aspects of motility and invasion are regulated by the Rho GTPases and are closely linked to signals from the extracellular environment, particularly in response to growth factors. Most Rho GTPases act as molecular switches that cycle between an inactive GDP-bound conformation and an active GTP-bound conformation. To be effective in achieving the invasive phenotype, the Rho proteins need to complete a full GTPase cycle, alternating between an active and inactive state (Ren *et al.*, 1999; Lin *et al.*, 1999 and Symons and Settleman, 2000). Rho proteins are activated via extracellular signals which result in the binding and hydrolyses of GTP and the induction of downstream effector molecules generating a cellular response (Kjoller *et al.*, 1999). It is the activation state of Rho proteins and not their expression levels that dictate cellular response. Rho activation by growth factors occurs through interactions with Rho regulatory proteins. These include; GTPase-activating proteins (GAPs); guanine nucleotide dissociation inhibitors (GDIs); GDI-dissociation factors (GDFs) and guanine nucleotide exchange factors (GEFs) (Geyer and Wittnghofer, 1997). The cycle is balanced by GDIs, which prevent guanosine diphosphate (GDP) dissociation and sequester Rho in the cytoplasm.

During the progression of cancer, early dysregulation of growth factor signalling such as EGFR amplification may have a mitogenic effect needed for tumour cell growth and survival. However, later in cancer progression these same growth factor signals may activate Rho GTPases and drive metastasis. The ability to migrate is critical for tumourogenic cells and requires cellular depolarisation and turnover of focal adhesions, which contain integrins, cytoskeletal and signalling proteins such as α -actinin and focal adhesion kinase (FAK). FAK expression in FAK null mice leads to a transient inhibition of RhoA and RhoC activity, ROCK activation, restoration of focal adhesion turnover and cell migration. Loss of FAK expression activates Rho/ROCK and decreased migration (Ren *et al.*, 2000).

1.5.4.2 Rho and Insulin-like growth factors (IGFs)

Treatment of IGF-1R overexpressing MCF-7 breast cancer cells with IGF-1 leads to actin filament disassembly, cellular depolarisation and the formation of fascin microspikes associated with lamellipodia (Guvakova and Surmacz, 1999). These changes involve the activation of the phosphatidylinositol 3-kinase (PI3K) pathway and transient dephosphorylation of FAK and Crk-associated substrate and paxillin (Guvakova *et al*, 2002) causing Rho activation, actin depolymerisation, focal adhesion turnover and loss of cellular polarity. Phosphorylation of FAK inhibits Rho activity, stabilises focal adhesions and activates Rac and Cdc42 needed for fascin microspike formation and lamellipodial formation. This demonstrates how Rho GTPases must work together to induce cell motility. A study by Pennisi *et al*, (2002) demonstrated that decreased IGF-1R levels increased motility and invasiveness in MCF-7 cells by increasing the activity of Rac and Cdc42 and decreasing Rho activity and E-cadherin expression. This implies that activation of IGF-1R stabilised the E-cadherin/ β -catenin complex and potentially activates RhoA, promoting cellular aggregation. In RIP1-Tag2 murine model of pancreatic tumorigenesis by Lopez and Hanahan (2002) IGF-1R is increased in invasive tumours. Here, IGF-II activates IGF-1R in hyperproliferative, oncogene-expressing β cells and is uniformly expressed in invasive tumours. Thus, overexpression of IGF-1R accelerates tumour progression and enhances invasive and metastatic capabilities of the cells, possibly mediated by Rac and Rho.

1.5.4.2 Rho and Epidermal growth factor (EGF)

EGF-induced cellular motility and invasion by Rho proteins is well documented. *In vivo* invasive properties of the MTLn3 rat mammary carcinoma cell line are significantly decreased when transfected with dominant negative forms of RhoA, Rac1, and Cdc42 (Bouzahzah *et al*, 2001). Kusama *et al*, (2001) demonstrated a dose-dependent increase of RhoA-mediated *in vitro* cellular invasion in Panc-1 human pancreatic cancer cell line stimulated with EGF. Treatment of the cells with statins, inhibitors of 3-hydroxy-3-methylglutaryl-coenzyme A, abrogates EGF-induced

invasion, possibly by preventing Rho-A from localising in the inner plasma membrane, where it can be activated by RhoGEFs.

1.5.4.4 Other aspects of Rho and invasion

There is also evidence that Rho proteins can change the expression of genes encoding proteins that degrade the ECM. Rac stimulates activation of the kinase JNK and subsequent phosphorylation of the transcription factor Jun. Jun is a component of AP1 transcription factors, which induce MMP expression (Ozanne *et al.*, 2000). Cell cycle progression involves the sequential activation of various cyclin-dependent kinases (CDKs). The expression of cyclins and other CDK regulators vary during the progression of the cell cycle and are frequently deregulated in cancers. Rho, Rac and Cdc42 have been reported to effect the expression of CDK regulators in cultured cells (Ridley, 2004). RhoH is the only Rho family member known to be genetically altered in human cancers. Its rearrangement leads to the expression of a fusion protein that expresses the full RhoH protein. It remains to be seen if RhoH can contribute to the development of cancer in animal models (Ridley, 2004). Tiam1 is a Rac specific guanine nucleotide exchange factor (GEF) originally identified by Price and Collard, (2001) for its ability to promote T lymphoma invasion *in vitro*. Studies of human cancer and animal cancer models indicate that Tiam1 has an effect on cancer development.

Altered Rho family expressions have been revealed in many human cancer studies. Indeed, there is often isoform-specific upregulation i.e. RhoA, RhoB, RhoC, Rac1, Rac2 and Rac3. The expression of RhoC mRNA is selectively increased in metastatic melanomas, and is sufficient to stimulate melanoma cell metastasis in a murine model (Clark *et al.*, 2000). Regulators of Rho GTPases whose expression is increased in human tumours include the GEFs β -PIX in breast cancers (Ahn *et al.*, 2003) and Vav1 in glioblastomas (Hornstein *et al.*, 2003).

A key question arising from gene expression profiling is whether increased expression of a particular gene is important for the development of cancer or whether it is an

indirect result of the change in state of the cancer cell compared to the normal cell. A study by Wang *et al*, (2002) where the gene expression in a metastatic breast cancer cell line was compared to its non-metastatic counterpart revealed that many genes encoding actin-regulatory proteins were more highly expressed in the metastatic cells. The fact that Rac and Rho family members and their regulators are also upregulated in various cancers may simply reflect a higher migration capacity in these cells. While this may be diagnostically informative, it remains to be seen if Rho and Rac pathways are good targets for cancer therapy. To determine this will require testing the effects of inhibiting or deletion of these genes on cancer development in animal models.

1.5.5 Chemokines

Chemokines are a family of low molecular weight pro-inflammatory cytokines that bind to G-protein coupled receptors. More than forty different chemokines have been isolated. Their main function is chemoattraction and activation of specific leucocytes in immuno-inflammatory responses. Chemokines have been shown to be involved in all stages of tumour development. There are four groups of chemokines, which are defined by the arrangement of cysteine residues of mature proteins (Baggiolini *et al* , 1997). The first three classes all have four conserved cysteines whereas the fourth has only two. The chemokine receptors are part of a larger family of G-protein-coupled receptors, including receptors for hormones, neurotransmitters and inflammatory mediators. Each receptor binds ligands from only one of the four-chemokine structural groups giving four receptor groups (Arya *et al* , 2003).

Growth factors induce cells to enter and proceed through the cell cycle (Gospodarowicz, 1983). Schadendorf *et al* , (1993) found IL-8 (CXCL8) to be an essential autocrine growth factor for some human melanoma cell lines. This chemokine binds to CXCR1 or CXCR2 receptors. In a further study by Metzner *et al* , (1999) showed that proliferation of human epidermoid carcinoma cells A431 and KB could be induced by IL-8 and inhibited by antibodies against IL-8 or its receptor. This indicated an autocrine growth mechanism in these cells. CXCL1 is also thought to act as an autocrine growth factor for human adenocarcinoma cell lines from the lung, stomach and pancreas (Arya *et al* , 2003).

Angiogenesis occurs during embryonic development and wound healing. It is also required for tumours to develop beyond 2mm in diameter (Folkman, 1995). Studies have shown that CXCL4 has angiostatic properties, it prevents endothelial cell proliferation and thus angiogenesis and tumour growth in immunodeficient mice (Maione *et al* , 1990). The ELR+ CXCL8 was the first chemokine shown to stimulate angiogenesis and tumour growth (Koch *et al* , 1992). By substituting the ELR motif in CXCL8 with the amino acids TVR (Thr-Val-Arg) or DLQ (Asp-Leu-Gln), Strieter *et al* , (1995) demonstrated that the ELR motif is critical for determining the effect of the CXCL8 chemokine has on angiogenesis. CXCL10 was also shown to inhibit angiogenesis stimulated by bFGF *in vivo* (Angiolillo *et al* , 1995). It is thought that

CXC chemokines form a balanced network of angiogenic and angiostatic regulators that are deregulated in cancer. Indeed, the balance of ELR+ and ELR- chemokines produced by a tumour and its stroma may determine the extent of angiogenesis and hence the invasiveness of the tumour.

Chemokines are also important in the induction of proteases during invasion. CXCL8 expression in human melanoma cells has been found to transcriptionally activate MMP-2, which increases invasiveness through the ECM (Bar-Eli, 1999). Muller *et al*, (2001) looked into the mechanisms involved in the metastasis of breast cancer to specific organs. They found the expression of the receptor genes CXCR4 and CXCR7 was increased in human breast cancer cell lines, malignant breast tumours and metastasis relative to the levels in normal mammary epithelial cells. A panel of normal human organs were screened for the ligands of these receptors, CXCL12 and CXCL21. Peak levels of expression of these ligands were found in organs preferred for breast cancer metastasis. These ligands stimulated pseudopodia formation and directional migration and local invasion through the ECM and basement membrane in breast cancer cell lines. These findings support the theory that certain chemokine ligands and their receptors are involved in the homing of metastatic tumour cells to specific organs.

Since chemokines function as immunostimulatory molecules, they may have great potential in cancer therapy. Vicari *et al*, (2000) demonstrated that mouse CCL21 had a strong antitumour effect by inducing angiostatic and T lymphocyte-mediated tumour resistance mechanisms. Also, injection of recombinant CCL21 directly into the tumour site induced potent antitumour responses and led to the complete eradication of alveolar carcinoma and Lewis lung carcinoma (Sharma *et al*, 2000).

1.6 Microarrays

Each cell in the body contains a full set of chromosomes containing identical genes but only a fraction of these genes are expressed at any given time. It is this group of expressed genes that makes each cell type unique. Aberrant gene expression profiles are responsible for many diseases. The completion of the Human Genome project (HGP) has led to a vast amount of information becoming available about almost all genes in the genome, and is necessary to understand the functions of these gene products. The development of full genome expression microarrays, have allowed researchers to study the expression of almost every gene simultaneously. It is important to note, however, that we may not yet have identified all genes correctly from the sequence data and our knowledge of the range of splice variants remains incomplete to date.

1.6.1 Introduction to microarray technology

Microarrays are artificially constructed grids of DNA where each element of the grid contains a specific oligodeoxynucleotide probe. This enables researchers to simultaneously measure the expression of thousands of genes in a given sample. Microarray experiments rely on the ability of RNA to bind specifically to a corresponding sequence-complementary probe. DNA microarrays are classified based on the DNA molecule that is immobilised on the slide. There are two basic types either oligodeoxynucleotide or cDNA arrays. Oligodeoxynucleotide arrays are typically made up of 25-80 mer oligodeoxynucleotides while cDNA arrays are printed with 500-5000 base pair PCR products.

Microarray technology can be used to detect specific gene changes in, for example diseased tissue compared to normal healthy tissue or the changing gene expression profiles of developing tissues over a defined time period. These types of experiments have the potential to help explain why a disease occurs and also how best to overcome it by improving our understanding of the molecular mechanisms attributing to disease development and progression.

The steps of a microarray experiment are shown in Figure 1.3. This is an example of an Affymetrix GeneChip experimental workflow.

- 1 Total RNA is isolated from the cells being studied.
- 2 The RNA is enzymatically converted into a double stranded DNA copy known as a complementary DNA (cDNA). This is done through reverse transcription (RT).
- 3 The cDNA is allowed to go through *in vitro* transcription (IVT) to RNA (now known as cRNA). This RNA is labelled with Biotin by incorporating a biotin-labelled ribonucleotide during the IVT reaction.
- 4 This labelled cRNA is then fragmented into pieces anywhere from 30 to 200 base pairs in length by metal-induced hydrolysis.
- 5 The fragmented, Biotin-labelled cRNA is then hybridized to the array for 16 hours.
- 6 The array is then washed to remove any unhybridized cRNA and then stained with a fluorescent molecule streptavidin phycoerythrin (SAPE), which sticks to Biotin.
- 7 Lastly, the entire array is scanned with a laser and the information is automatically transferred to a computer for analysis of what genes were expressed and at what approximate level.

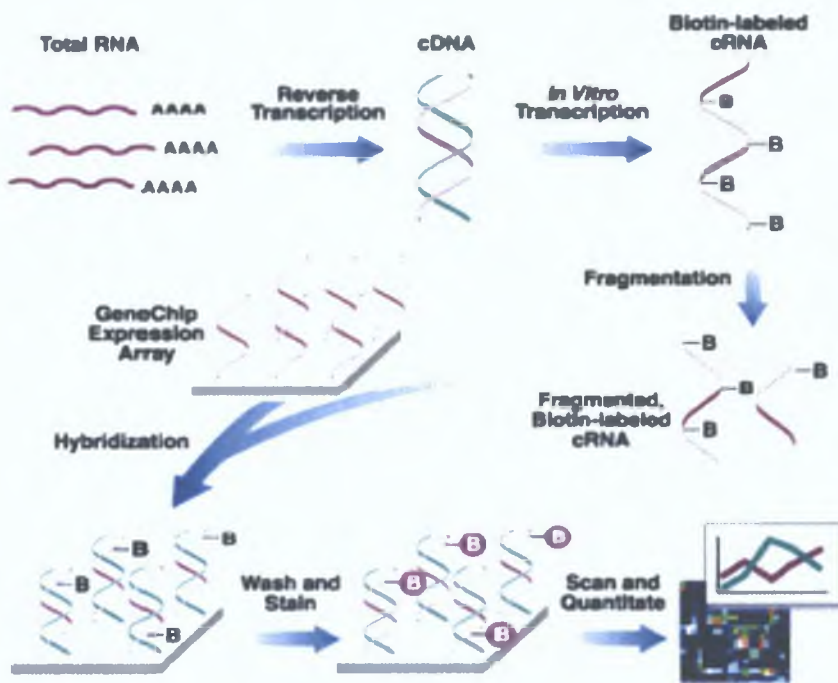


Figure 1.3 Steps in a microarray experiment (www.affymetrix.com)

1.6.2 Microarray analysis

Microarray experiments generate vast amounts of data in a short period of time. For the results of a microarray experiment to be acceptable, the raw data from the experiment must be validated. Good experimental design is the first step. It is important that the proper controls and replicates are included in each experiment. Replicates are particularly important since the methods used to identify differentially expressed genes are predominantly statistical. Microarray data is normalised to measure real biological changes by minimising processing variation. This process standardises the data so that the gene expression levels are comparable.

Quality control checks must also be included at all stages of the experiment. These checks would usually include quality checks on the initially isolated RNA and processed sample at regular intervals, e.g. Agilent Bioanalyser. The Agilent Bioanalyser analyses sample RNA in order to determine quality. Detailed information about the condition of RNA samples is displayed in the form of highly sensitive electropherograms. Post-experimental quality control checks include the chip controls shown in Table 1.2.

Table 1.2 Array quality control measures

QC measure	Result
Background	Measure of non-specific binding
3'/5' Ratio	Indicates how well IVT reaction has proceeded
Hybridisation controls	Checks spike controls added to each sample
Percentage present	All samples should have comparable % genes present
Noise	The electrical noise from scanner
Scale factor	Measures the brightness of array- All chips in an experiment should have scale factors within 3-fold of each other

The format for reporting microarray data was described by Brazma *et al.*, (2001), and is called the "minimum information about a microarray experiment" (MIAME). MIAME has two general principles. The first is that there should be sufficient information recorded about each experiment to allow interpretation of the experiment, allow for comparison to similar experiments and enable replication of the experiment. The second principle is that the data be presented in a structured manner to allow automated data analysis and mining.

Bioinformatics is the application of software to large biological data sets for interpretation and analysis of molecular biological information. In this case, the large spreadsheets of Gene Expression data from the microarray experiments were manipulated using the Affymetrix MAS and GeneSpring software packages (Section 2.16). These software packages enable the selection of potentially important genes in

the biological system under investigation by statistically comparing experimental conditions

Although statistics are used to generate lists of potentially interesting genes from the microarray data, many of the filtering choices (e.g. to include genes above a certain level in an analysis) are subjective and influence the resulting gene lists. For this work, several alternative analyses were performed and genes that were highlighted from multiple approaches were prioritised for further investigation.

1.6.3 Affymetrix GeneChips

The microarray experiments performed in these studies employed the Affymetrix Genechip system, which are oligodeoxynucleotide microarrays. Affymetrix probes are designed using publicly available information (NCBI database). The probes are manufactured on the chip using photolithography. Each genechip contains approximately 1,000,000 features. Each probe is spotted as a pair, one being a perfect match (PM), the other with a mismatch at the centre (MM). Each gene transcript is represented on the genechip by 11 probe pairs (PM+MM). This can be seen in Figure 1.4. Each transcript has 22 different probes in total to ensure that the microarray is detecting the correct piece of RNA while also helping to estimate and eliminate background. The amount of light emitted at 570nm from stained chip is proportional to the quantity of labelled RNA bound to each probe. Therefore, after scanning, the initial computer file generated (.DAT) contains a numerical value for every probe on the array.

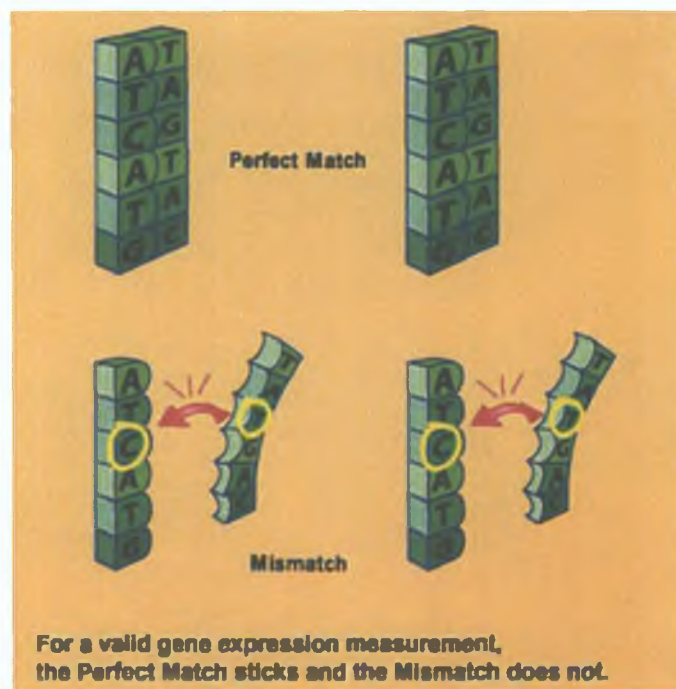


Figure 1.4 Perfect match and mismatch probe pairs on Affymetrix GeneChips
(www.affymetrix.com)

1.6.4 Microarrays and cancer

Microarray technology is and has been used intensively to better understand the development of a metastatic phenotype and cancer progression, both *in vivo* and *in vitro*. In 2002, van't Veer *et al* , used DNA microarray technology to compare the gene expression profiles of 117 primary breast tumours from young patients. They applied supervised classification to identify a 70-gene expression signature that would strongly predict the development of distant metastasis in lymph node negative patients in a short time frame. This study also reported a signature identifying BRCA1 tumours. In all, these signatures were suitable to select patients who would benefit from adjuvant therapy.

Ramaswamy *et al* , (2003) compared the gene expression profiles of twelve metastatic adenocarcinoma nodules of diverse origin with 64 primary adenocarcinomas representing the same spectrum of tumour types. The group identified a 17-gene signature associated with the development of metastasis in multiple tumour types, indicating that a molecular program of metastasis may exist that is shared by many solid tumour types, suggesting the possible existence of therapeutic targets common to many cancer types.

More recently, and in a study more similar in nature to the one described in this thesis, in that the expression profiles of closely related cell lines were compared, Orián-Rousseau (2005) used suppression subtractive hybridisation and cDNA array analysis to compare to closely related colon cancer lines, the invasive HT29p and the non-invasive HT29-MTX. The expression of fifty-eight genes was increased in metastatic cells, the majority were previously undescribed relevant to the development of metastasis.

cDNA microarray analyses were also used to distinguish squamous non-small lung cancers from normal bronchial tissue (Rommelink *et al* , 2005). In this way 19 genes were differentially expressed between normal and cancer tissue. Rickardson *et al* , (2005) profiled ten human tumour cell lines including parental and drug resistant subtypes using array methodology. Hierarchical clustering based on drug-gene correlations yielded drug clusters with similar modes of action. The analysis also generated

gene lists correlating with both drug resistance and drug sensitivity respectively, which may be useful in the development of new therapeutic drugs

This study used Affymetrix U133A expression microarrays to compare the expression profiles of five closely related variants of a lung cancer cell line (DLKP), some of which are resistant to chemotherapeutic drugs and which differ in their capacity to invade as measured using an *in vitro* invasion assay

1.7 RNA Interference

RNA interference is the biological mechanism by which double-stranded RNA (dsRNA) induces gene silencing at the level of translation by targeting complementary mRNA for degradation. RNAi has the potential to help elucidate the complex issues involved in eukaryotic development, to aid in dissecting cellular pathways, and to identify targets for therapeutic intervention that otherwise would remain unidentified.

1.7.1 Introduction to siRNA technology

The phenomenon of post translational gene silencing (PTGS) was first discovered in plant studies. A major study into the silencing of specific genes in *C. elegans* by the introduction of dsRNA by Fire and Mello in 1998 demonstrated that the presence of a small number of molecules of dsRNA was sufficient to almost completely abolish the expression of a gene that was homologous to the dsRNA (McManus and Sharp, 2002).

Experiments conducted in *Drosophila* have indicated a four-step mechanism for the RNAi pathway. Briefly, long dsRNA is cleaved into 21-25nt double stranded fragments, termed small interfering RNAs (siRNAs). This step is ATP-dependent. These siRNAs are incorporated into a protein complex. ATP-dependent unwinding of the siRNA duplex leads to activation of the complex to an RNA-induced silencing complex (RISC). The RISC can recognise and cleave a target RNA complementary to the guide strand of the siRNA (Hutvagner and Zamore, 2002). A schematic diagram of the mechanism of RNAi can be seen in Figure 1.5. A member of the RNase III family of endonucleases termed Dicer is responsible for the production of siRNAs. Certain structural features are important for entry of siRNAs into the RNAi pathway, such as a 5' phosphate and 3' hydroxyl termini and two single-stranded nucleotides on the 3' ends.

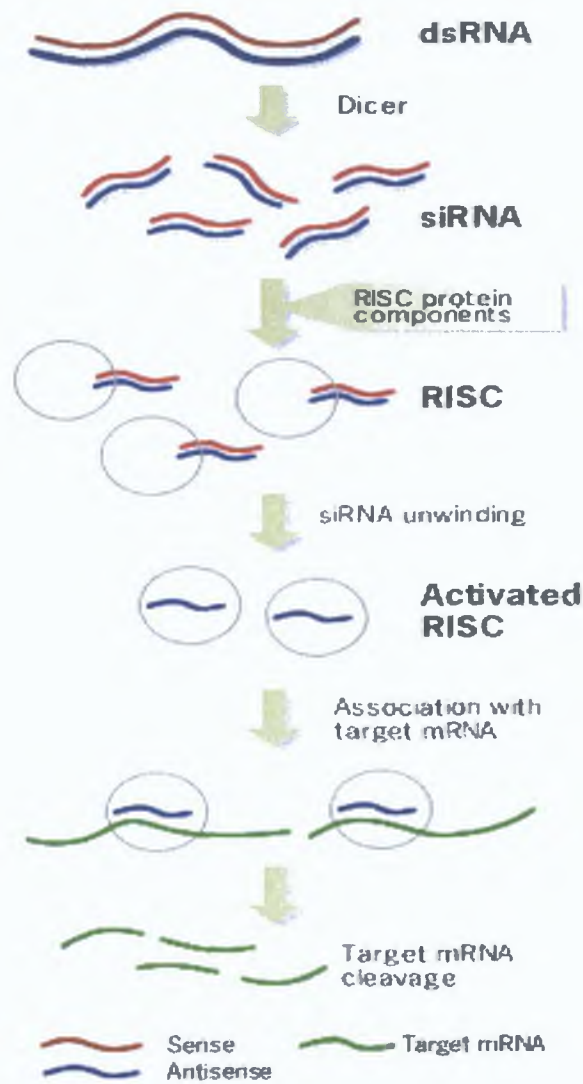


Figure 1.5 The mechanism of RNAi (www.ambion.com)

The enzymatic machinery for generating siRNA sequences is also used for the production of an additional class of endogenously encoded small RNA molecules termed microRNAs. These miRNAs are a newly identified, large family of RNAs with highly conserved expression patterns. Hundreds of miRNAs have been found in *C. elegans*, plants and mammals. A common feature of miRNAs, not seen in siRNAs, is that the miRNA sequences are found in the stem of a stem-loop structure (Kim, 2003). A large number of the miRNA targets identified to date are proteins involved in cell growth and development or transcription factors (Ke *et al.*, 2003). The binding specificity of miRNA sequences and speed at which miRNAs can be generated (when compared to the time taken to synthesise regulatory proteins), result in regulatory molecules that are ideally suited for the precise temporal control required during development. miRNAs may also help to explain the diversity of phenotypes among higher organisms with a limited number of protein coding genes.

The PTGS mechanisms of siRNA and miRNA are largely identical, as indicated by the fact that endogenously encoded human miRNAs can cleave exogenously added RNA substrates with fully complementary target sites while siRNAs can repress translation without RNA cleavage when there are slight central mismatches (Zeng *et al.*, 2003).

1.7.2 Applications of RNAi

Gene silencing using siRNA is quickly becoming the most common method to study the function of these genes whose functions are unknown. The use of antisense and ribozymes to decrease gene expression are laborious and time-consuming. Libraries of siRNAs and automatic screening systems are now available which make it possible to screen large sections of the human genome simultaneously.

It is clear that siRNA may have multiple applications in disease therapy. Diseases that may potentially benefit therapeutically from RNAi technology include viral infections, cancer and genetic disorders (Kim, 2003). The concentration of siRNA used is of paramount importance for therapeutic applications considering that siRNAs applied at 100nM nonspecifically induced the expression of a number of genes involved in apoptosis and cellular stress responses. Reduction of the dosage to 20nM eliminated this effect however (Semizarov *et al.*, 2003).

Tumour invasion and metastasis rely on the mobility of tumour cells and their interaction with the host microenvironment. Thus, RNAi targeting of molecules important for tumour invasion or metastasis may have therapeutic potential (Pai *et al.*, 2006). For example, insulin-like growth factor-binding protein 2 (IGFBP2) is frequently overexpressed in ovarian carcinomas, particularly in serous carcinoma (Lee *et al.*, 2005). These IGFBP2-overexpressing cells were more invasive than control cells as measured by *in vitro* matrigel invasion assay. Furthermore, silencing of IGFBP2 expression by RNAi technology in an ovarian cancer cell line (PA-1) decreases its invasiveness. An additional study by Zheng *et al.*, (2005) saw the application of siRNA technology to decrease E-cadherin expression in gastric cancer cells. Invasion was increased in siRNA transfected cells. In fact siRNAs could be used to target any of the molecules that regulate tumour cell invasion and metastasis in an effort to control cancer spread. In order for siRNA to become a potential therapy, problems with delivery must be overcome.

1.7.3 Problems associated with RNAi

Long dsRNA has been found to induce an immune response when introduced into mammals (Bridge *et al.*, 2003; Sledz *et al.*, 2003), leading to induction of the interferon (IFN) response. In mammalian systems this can be overcome by introduction of synthetic siRNAs.

In early studies using RNAi, there were questions regarding siRNA specificity. In a study by Jackson and colleagues (2003), using gene expression profiling, it was revealed that there was direct silencing of non-targeted genes (some containing as little

as 11 contiguous nucleotides homologous to the siRNA) This is in agreement with the finding that siRNAs can suppress expression of off-target proteins even with 3-4 base mismatches and additional G-U mismatches (Saxena *et al* , 2003) These results are disputed however in a study by Chi *et al* (2003), where DNA microarray analysis demonstrated the precise sequence specificity of siRNA constructs In general, it is recognised that well designed siRNA sequences will not elicit “off-target” effects, and that many failures in RNAi experiments may have been caused by lack of experiment optimisation

1 7.4 Delivery of siRNA

The most widely used delivery technique for RNAi is siRNA transfection Design of siRNAs is critical for experimental success Choice of target site, transfection method and protein turnover rate must be taken into consideration There are certain guidelines available for siRNA design Secondary structures and mRNA binding proteins can influence the ability of an siRNA to bind its target Companies such as Ambion create siRNAs using algorithms that overcome these issues The choice of transfection reagent and conditions, such as cell density, also important in the success of an siRNA transfection Transfection of synthetic siRNA duplexes at low concentration can help to prevent the IFN response of cells (Kim *et al* , 2004) This method of siRNA delivery is transient and protein inhibition is lost after a number of days, depending on its turnover rate To allow the expression of short hairpin RNAs (shRNAs, these undergo post-transcriptional processing into 21nt duplex siRNAs by Dicer), plasmids have been designed using promoters based on RNA polymerase II or III e g Sui *et al* , 2002 The plasmids can contain a selectable marker so that sub- populations of cells with permanently silenced target genes can be isolated Viruses are excellent vehicles for siRNA delivery, especially retroviruses (Devroe & Silver, 2004) Other viral delivery vehicles include HIV based, lentivirus based vectors (Stewart *et al* , 2003) or adenoviruses (Shen *et al* , 2003) although these may trigger an immune response over time A lentiviral vector capable of expressing a siRNA against GFP was used to silence GFP in a transgenic mouse that had stable expression of GFP (Tiscornia *et al* , 2003)

Successful silencing in the lung has been achieved by intranasal or intratracheal administration of siRNAs. Remarkably, siRNA specific effects on pulmonary epithelial cells have even been elicited *in vivo* by siRNAs used without transfection reagents or other delivery molecules (Bitko *et al* , 2005, and Zhang *et al* , 2004). This indicates that the lung (and possibly other tissues) may have a means for siRNA uptake. The transformed cell lines commonly used for *in vitro* RNAi experiments require a transfection reagent or other mechanism for siRNA uptake and knockdown to occur. The first therapeutic benefit in the lung was demonstrated for influenza A infection. siRNAs against conserved influenza sequences when complexed with the polycation polyethyleneimine (PEI) were delivered to the lung by intravenous low pressure injection and reduced viral titers by 1–2 logs (Hagstrom *et al* , 2004). A concurrent study to that of Hagstrom *et al* , which combined injection of the same siRNAs and intranasal instillation of siRNA complexed to oligofectamine protected mice from lethal challenge with several highly pathogenic strains of influenza A (Tompkins *et al* , 2004). These studies did not observe evidence of interferon induction induced by the siRNA treatment *in vivo*. These experiments established the proof of principle for treating pulmonary infections with siRNAs, although the injection method is may not be suitable for clinical use and the PEI carrier may also have unacceptable toxicity (Dykxhoorn *et al* , 2006).

Delivery of siRNAs to effect treatment is a surmountable hurdle. Preclinical studies such as those by Hagstrom *et al* , (2004) and Tompkins *et al* , (2004) have demonstrated successful delivery of siRNA by inhalation and intravenous injection however delivery can be local, systemic, and cell selective. Whether conjugations that enhance delivery interfere with siRNA incorporation into RISC will need to be explored. Despite this, rapid advances in knowledge of siRNA design foretell that this theoretical concern will be solved too (Aronin, 2006).

1.8 Aims of Thesis

Metastasis is a major cause of mortality in cancer (Fidler *et al.*, 1994). This phenomenon occurs when cells detach from the primary tumour and invade through the surrounding extracellular matrix, eventually finding their way into the blood stream. They then travel to a distant site, re-attach to and invade through the capillary wall and into surrounding tissues. Some of the mechanisms that these metastatic tumour cells utilise in order to undertake this journey are better understood than others. However, on the whole, this process remains poorly understood, particularly in terms of the underlying molecular mechanisms that drive the switch to a metastatic phenotype. Our laboratory has an ongoing interest in this aspect of cancer biology, and this particular project was designed to utilise one of the model cell systems developed here, in combination with advanced transcriptional profiling methods, to further our understanding of the metastatic process.

The specific aims of the project were as follows:

1. To establish the degree of invasiveness of the individual cell lines within a panel in an *in vitro* invasion assay. In order for this model to be of use we needed to establish that the relative invasiveness of the sub-lines (compared to each other) remained constant over a reasonable number of passages and under specific culturing conditions. Defining these parameters at the outset would give greater confidence in any of the observed changes subsequent to deliberate experimental manipulation, once the established assay protocol and boundaries were adhered to.
2. To generate gene lists from the array data that may potentially serve as a molecular signature for invasiveness and/or drug resistance in these cell lines.
3. To validate the results of the array-based differential expression analyses by RT-PCR. Microarray data is generally quite accurate in terms of quantifying changes in mRNA abundance, however we felt it was important to confirm the trends observed, in a small panel of target genes, by an alternative

quantification method. This would not only give greater confidence in the significance of gene lists generated from array data mining but also function as a validation step before choosing particular target genes for further investigation.

- 4 To choose a small group of high priority target genes for follow-on study in the laboratory. These targets were chosen based on a number of criteria including being consistently associated with or correlating (either negatively or positively) with invasion during bioinformatic analysis. PCR validation should confirm array data trends and, in addition, review of published data should either demonstrate previous recognised association with cancer/metastasis or alternatively, complete novelty in this regard.
- 5 To investigate the role of these targets in invasion by knocking down endogenous mRNA levels using siRNA technology. This technology is still relatively new but has quickly become the first choice in molecular and cell biology labs when attempting to identify molecular function. Confirmation of knockdown by RT-PCR, qRT-PCR and/or Western blotting was undertaken where possible. In most cases an investigation into a functional effect on proliferation was also included. Most importantly any functional effect was examined by invasion assay using our *in vitro* cell model.
- 6 To complement the knockdown studies by over expression of the same target genes by transient cDNA transfection in the cell line panel. Where a target gene was chosen on the basis that its endogenous expression levels were very low in invasive cells only or vice-versa, it was of interest to discover whether this phenotype could be reversed by artificially elevating transcript expression. Again RT-PCR and/or western blotting confirmed overexpression where possible. Effect on proliferation was also investigated and most importantly any functional effect of the cells was examined by invasion assay.

Section 2.0: Materials and Methods

2.1 Water

Ultrapure water was used in the preparation of all media and solutions. This water was purified by a reverse osmosis system (Millipore Milli-RO 10 Plus, Elgastat UHP) to a standard of 12-18M Ω /cm resistance.

2.2 Glassware

Solutions pertaining to all cell culture and maintenance were prepared and stored in sterile glass bottles. Bottles and lids and all other glassware used for any cell related work were prepared as follows - all glassware lids were soaked in a 2% (v/v) solution of RBS-25 (AGB Scientific) for at least 1 hour. Following scrubbing and several rinses in tap water, the bottles were then washed by machine using Neodisher detergent, an organic, phosphate-based acid detergent. The bottles were then washed with distilled water, followed by a rinse with ultrapure water and were sterilised by autoclaving.

2.3 Sterilisation

Water, glassware and all thermostable solutions were sterilised by autoclaving at 121°C for 20 minutes (min) under a pressure of 1bar. Thermolabile solutions were filtered through a 0.22 μ m sterile filter (Millipore, millex-gv, SLGV-025BS). Low protein-binding filters were used for all protein containing solutions.

2.4 Media Preparation

Medium was routinely prepared and sterility checked by our technician (Joe Carey). The basal media used during routine cell culture were prepared according to formulations shown in Table 2.4.1. 10x media were added to sterile ultrapure water, buffered with HEPES and NaHCO₃ and adjusted to a pH of 7.45-7.55 using sterile 1.5M NaOH and 1.5M HCl. The media were then filtered through sterile 0.22 μ m bell filters (Gelman, 121-58) and stored in 500ml sterile bottles at 4°C. Sterility checks were carried out on each 500ml bottle of medium as described in section 2.5.6.

The basal media were stored at 4°C up to their expiry dates as specified on each individual 10x medium container. Prior to use, 100ml aliquots were supplemented with 5% foetal calf serum and this was used as routine culture medium. This was stored for up to 2 weeks at 4°C, after which time, fresh culture media was prepared. For all DLKP cell lines ATCC (Hams F12/DMEM (1:1) supplemented with 5% FCS) was routinely used. For the RPMI cell lines Minimum Essential Medium (MEM) supplemented with 5% FCS, 1% Sodium pyruvate, 1% Non essential amino acids (NEAA) and 1% L-glutamine was used.

2.5 Cell Lines

All cell work was carried out in a class II down-flow re-circulating laminar flow cabinet (Nuair Biological Cabinet) and any work that involved toxic compounds was carried out in a cytogard (Gelman). Strict aseptic technique was adhered to at all times. The laminar flow cabinet was swabbed with 70% industrial methylated spirits (IMS) before and after use, as were all items used in the cabinet. Each cell line was assigned specific media and waste bottles. Only one cell line was worked with at a time in the cabinet, which was allowed to clear for 15min between different cell lines. The cabinet itself was cleaned each week with industrial detergents (Virkon, Antec International, TEGO, TH Goldschmidt Ltd), as were the incubators. The cell lines used during the course of this study, their sources and their basal media requirements are listed in Table 2.1.1. Lines were maintained in 25cm² flasks (Costar, 3050), 75cm² (Costar, 3075) or 175cm² flasks (Corning, 431079) at 37°C and fed every two to three days.

Table 2.1 1 Cell lines used during the course of this study

Cell Line	Basal Medium	Cell Type	Invasive Status	Source
DLKP-1	ATCC (5% FCS)	Human poorly-differentiated lung carcinoma	Invasive	Dr Yizheng Liang, NCTCC
DLKP-2	ATCC (5% FCS)	Human poorly-differentiated lung carcinoma	Invasive	Dr Rasha Linehan, NCTCC
DLKP-Taxotere 1 (TXT-1)	ATCC (5% FCS)	Human poorly-differentiated Taxotere treated lung carcinoma	Mildly invasive	Dr Yizheng Liang, NCTCC
DLKP-Taxotere 2 (TXT-2)	ATCC (5% FCS)	Human poorly-differentiated Taxotere treated lung carcinoma	Highly Invasive	Dr Rasha Linehan, NCTCC
DLKP-Vincristine (VCR)	ATCC (5% FCS)	Human poorly-differentiated Vincristine treated lung carcinoma	Almost Non-invasive	Dr Rasha Linehan, NCTCC
RPMI-2650	MEM (5%FCS, 1%L-glut, 1%NEAA, 1& Sodium Puruvate)	Human nasal squamous carcinoma cell line	Non-invasive	NCTCC culture collection (originally from ATCC)
RPMI-Melphalan (RPMI-Mel)	MEM (5%FCS, 1%L-glut, 1%NEAA, 1& Sodium Puruvate)	Human nasal squamous carcinoma cell line treated with Melphalan	Highly Invasive	Dr Yizheng Liang, NCTCC

2.5.1 Subculture of Adherent Lines

During routine subculturing or harvesting of adherent lines, cells were removed from their flasks by enzymatic detachment

Waste medium was removed from the flasks and the cells were rinsed with a pre-warmed (to 37°C) trypsin/EDTA (TV) solution (0.25% trypsin (Gibco, 5090-028), 0.01% EDTA (Sigma, EDS) solution in PBS A (Oxoid BR14a)) The purpose of this was to remove any naturally occurring trypsin inhibitor that could be present in the residual serum Fresh TV was then placed on the cells (2ml/25cm² flask, 5ml/25cm² or 75cm² flask) and the flask incubated at 37°C until the cells were seen to have detached (5-10min) The trypsin was then deactivated by addition of an equal volume of complete (*i.e.* containing 5% FCS) growth medium The entire solution was transferred to a 30ml sterile universal tube (Sterilin, 128a) and centrifuged at 1,000rpm for 5 min The resulting cell pellet was resuspended in pre-warmed fresh complete growth medium, counted (Section 2.5.2) and used to re-seed a flask at the required cell density or to set up an assay

2.5.2 Cell Counting

Cell counting and viability determinations were carried out using a trypan blue (Gibco, 15250-012) dye exclusion technique

An aliquot of trypan blue was added to a sample from a single cell suspension in a ratio of 1:5 After 3 min incubation at room temperature, a sample of this mixture was applied to the chamber of a haemocytometer over which a glass coverslip had been placed Cells in the 16 squares of the four outer corner grids of the chamber were counted microscopically, an average per corner grid was calculated with the dilution factor being taken into account, and final cell numbers were multiplied by 10⁴ to determine the number of cells per ml The volume occupied by the chamber is 0.1cm x 0.1cm x 0.1cm *i.e.* 0.0001cm³ Therefore cell number x 10⁴ is equivalent to cells per ml Non-viable cells were those that stained blue while viable cells excluded the trypan blue dye and remained unstained

2.5.3 Cell Freezing

To allow long-term storage of cell stocks, cells were frozen and cryo-preserved in liquid nitrogen at temperatures below -180°C . Once frozen properly, such stocks should survive indefinitely.

Cells to be frozen were harvested in the log phase of growth (*i.e.* actively growing and approximately 60-70% confluent) and counted as described in Section 2.5.2. Pelleted cells were resuspended in serum. An equal volume of a DMSO/serum (1:9, v/v) was slowly added dropwise to the cell suspension to give a final concentration of at least 5×10^6 cells/ml. This step was very important, as DMSO is toxic to cells. When added slowly the cells had a period of time to adapt to the presence of the DMSO, otherwise cell lysis can occur. The suspension was then aliquoted in cryovials (Greiner, 122278), which were then quickly placed in the vapour phase of liquid nitrogen containers (approximately -80°C). After 2.5 to 3.5 hours, the cryovials were lowered down into the liquid nitrogen where they were stored until required.

2.5.4 Cell Thawing

Immediately prior to the removal of a cryovial from the liquid nitrogen stores for thawing, a sterile universal tube containing pre-warmed complete growth medium was prepared for the rapid transfer and dilution of thawed cells to reduce their exposure time to DMSO freezing solution which is toxic at room temperature. The suspension was centrifuged at 1,000rpm for 5 min, the DMSO-containing supernatant removed and the pellet resuspended in fresh growth medium. A viability count was carried out (Section 2.5.2) to determine the efficiency of the freezing/thawing procedures. Thawed cells were placed into tissue culture flasks with an appropriate volume of medium (5ml/25cm² flask and 10ml/75cm² flask) and allowed to attach overnight. After 24 hours, the cells were re-fed with fresh medium to remove any residual traces of DMSO.

2.5.5 Sterility Checks

Sterility checks were routinely carried out on all media, supplements and trypsin used for cell culture. Samples of basal media were inoculated into Columbia (Oxoid, CM331) blood agar plates, Sabouraud (Oxoid, CM217) dextrose and Thioglycollate (Oxoid, CM173) broths, which detect most contaminants including bacteria, fungus and yeast. Complete growth media were sterility checked at least two days prior to use by incubating samples at 37°C, which were subsequently examined for turbidity and other indications of contamination.

2.6 *Mycoplasma* Analysis

Mycoplasma examinations were performed routinely (at least every 3 months) on all cell lines used in this study. NICB staff members, Aine Adams and Michael Henry performed these analyses.

2.6.1 Indirect Staining Procedure

In this procedure, *Mycoplasma*-negative NRK cells (a normal rat kidney fibroblast line) were used as indicator cells. These cells were incubated with supernatant from test cell lines and then examined for *Mycoplasma* contamination. NRK cells were used for this procedure because cell integrity is well maintained during fixation. A fluorescent Hoechst stain was utilised which binds specifically to DNA and so will stain the nucleus of the cell in addition to any *Mycoplasma* DNA present. A *Mycoplasma* infection would thus be seen as small fluorescent bodies in the cytoplasm of the NRK cells and sometimes outside the cells.

NRK cells were seeded onto sterile coverslips in sterile Petri dishes at a cell density of 2×10^3 cells/ml and allowed to attach over night at 37°C in a 5% CO₂, humidified incubator. 1ml of cell-free (cleared by centrifugation at 1,000 rpm for 5 min) supernatant from each test cell line was then inoculated onto a NRK Petri dish and incubated as before until the cells reached 20-50% confluency (4-5 days). After this time, the waste medium was removed from the Petri dishes, the coverslips washed twice with sterile PBS A, once with a cold PBS/Carnoy's (50/50) solution and fixed

with 2ml of Carnoy's solution (acetic acid : methanol – 1 : 3) for 10 min. The fixative was then removed and after air-drying, the coverslips were washed twice in deionised water and stained with 2ml of Hoechst 33258 stain (BDH) (50ng/ml) for 10 min. From this point on, work was carried out in the dark to limit quenching of the fluorescent stain.

The coverslips were rinsed three times in PBS. They were then mounted in 50% (v/v) glycerol in 0.05M citric acid and 0.1M disodium phosphate and examined using a fluorescent microscope with a UV filter.

2.6.2 Direct Staining

The direct stain for *Mycoplasma* involved a culture method where test samples were inoculated onto an enriched *Mycoplasma* culture broth (Oxoid, CM403) – supplemented with 16% serum, 0.002% DNA (BDH, 42026), 2mg/ml fungizone (Gibco, 15290-026), 2×10^3 units penicillin (Sigma, Pen-3) and 10ml of a 25% (w/v) yeast extract solution – to optimise growth of any contaminants and incubated at 37°C for 48 hours. Samples of this broth were then streaked onto plates of *Mycoplasma* agar base (Oxoid, CM401) which had also been supplemented as above and the plates incubated for 3 weeks at 37°C in a CO₂ environment. The plates were viewed microscopically at least every 7 days, the appearance of small “fried egg”-shaped colonies is indicative of a *Mycoplasma* infection.

2.7 Specialised Techniques in Cell Culture

2.7.1 Assessment of cell number –Acid Phosphatase Assay

A Acid Phosphatase in 96-well plate format

- 1 Following an incubation period of 72 hours, media was removed from the plates
- 2 Each well on the plate was washed with 100µl PBS This was removed and 100µl of freshly prepared phosphatase substrate (10mM *p*-nitrophenol phosphate (Sigma 104-0) in 0.1M sodium acetate (Sigma, S8625), 0.1% triton X-100 (BDH, 30632), pH 5.5) was added to each well The plates were wrapped in tinfoil and incubated in the dark at 37°C for 2 hours
- 3 The enzymatic reaction was stopped by the addition of 50µl of 1M NaOH to each well

B Acid Phosphatase in 6-well plate format

- 1 Following an incubation period of 72 hours, media was removed from the plates
- 2 Each well on the plate was washed with 1ml PBS This was removed and 2ml of freshly prepared phosphatase substrate (10mM *p*-nitrophenol phosphate (Sigma 104-0) in 0.1M sodium acetate (Sigma, S8625), 0.1% triton X-100 (BDH, 30632), pH 5.5) was added to each well The plates were wrapped in tinfoil and incubated in the dark at 37°C for 2 hours
- 3 The enzymatic reaction was stopped by the addition of 1ml of 1M NaOH to each well

Plates were read in a dual beam plate reader at 405 nm with a reference wavelength of 620 nm

2.7.2 Invasion Assay experimental procedure

Invasion assays were performed using the method of Albini (1998) using commercial invasion assay kits (Beckton Dickinson, Cat no 354480) that were pre-coated with matrigel. The invasion assay kits were allowed to come to room temperature before use, were rehydrated on the top and bottom of the insert with 0.5ml pre-warmed serum-free media for 2 hours at 37°C. Following this incubation, the media underneath the insert was replaced with pre-warmed media containing 5% FCS. The cells were trypsinised, counted and resuspended in pre-warmed media containing 1% FCS at a density of 1×10^6 cells/ml. 100µl of the cell suspension was added to each insert. The cells were incubated at 37°C for 24 hours. After this time, the inside of the insert was wiped with a wet cotton swab and the underside of the insert stained with 0.25% crystal violet for 10 minutes, followed by washing with UHP and allowed to air dry. The inserts were then viewed under the microscope and photographed. The percentage of invasive cells was determined by microscopically counting 10 representative fields at 20X.

2.8 Immunocytochemistry

2.8.1 Fixation of cells

For fixation, medium was removed from 6-well plates, cells were rinsed 3 times with prechilled sterile PBS. The cells were fixed with the addition of prechilled methanol placed in -20°C for 5-7 minutes. The methanol was removed and the cells allowed to air dry for approximately 20 min at room temperature (RT). The plates were then wrapped in tinfoil and stored at -20°C until required, or used immediately.

2.8.2 Immunofluorescence

Fixed cells on 6 well plates were taken from storage at -20°C and allowed to come to RT for 30 min. A DAKO pen was used to generate small wells within the centre of each well for staining. The cells were rehydrated for 5 mins with 50 μl tris buffered saline (TBS) per well and then blocked with 5% swine serum for 20 mins at RT. Following removal of the blocker the cells were incubated with rabbit anti-IGF-1R (Santa Cruz, sc-713) diluted 1/500 overnight at 4°C . The next day the primary antibody was removed and the cells were washed three times with TBS allowing 5 min per wash. Working in conditions of reduced light, swine anti-rabbit secondary antibody (DakoCytomation, P0164) was diluted 1/40 in TBS and added to the wells (50 μl /well) for 30 mins. This was removed and the cells were washed three times with TBS. The cells were then mounted with fluorescent mounting medium containing DAPI (Vectashield, Vector Labs) and coverslips were placed over the stained area taking care to avoid bubbles. The fluorescence was visualised using a Leica Confocal microscope. Negative controls whereby primary antibody was replaced with TBS were included in each experiment to validate the specificity of staining.

2.9 Western Blot Analysis

Proteins for western blot analysis were separated by SDS-polyacrylamide gel electrophoresis (SDS-PAGE).

2.9.1 Sample Preparation

Cells were scraped directly on culture dishes using NP40 lysis buffer (20mM Tris pH 7.4, 50mM NaCl, 50mM NaF, 1% NP40) supplemented with 1mM PMSF, 1mM protease inhibitor cocktail (Roche, 1 873 580) and 1mM Na₃VO₄. Lysis was carried out over twenty min on ice and following vortexing, the lysate was spun at 4°C for 15min at maximum speed to remove any insoluble debris. The protein was quantified using the method of Bradford (Bio-Rad; 500-0006) and the protein samples were supplemented with 2X Lamelli sample buffer (contains loading dye, Sigma-Aldrich S3401) and water to a final stock concentration. The samples were then boiled for 2min and stored at -20°C until required.

2.9.2 Quantification of Protein

Protein levels were determined using the Bio-Rad protein assay kit (Bio-Rad; 500-0006) with a series of bovine serum albumin (BSA) (Sigma, A9543) solutions as standards. A stock solution of 25mg/ml BSA was used to make a standard curve. 10µl samples were diluted into eppendorfs in a stepwise fashion from 0 – 2mg/ml BSA. The Biorad solution was first filtered through 3MM filter paper (Schleicher and Schuell, 311647) and then diluted 1/5 with UHP as it was supplied as a 5-fold concentrate. The diluted dye reagent (490µl) was added to each standard and sample eppendorf and the mixtures vortexed. The 500µl samples were divided out in 100µl aliquots onto a 96-well plate (Costar, 3599). After a period of 5min to 1hr, the OD₅₇₀ was measured, against a reagent blank. From the plot of the OD₅₇₀ of BSA standards versus their concentrations, the concentration of protein in the test samples was determined. From this, a relative volume for each protein sample was determined for loading onto the gels. Usually 10-20µg protein per lane was loaded.

2.9.3 Gel Electrophoresis

Resolving and stacking gels were prepared as outlined in Table 2.9.1 and poured into clean 10cm x 8cm gel cassettes that consisted of 2 glass plates separated by a plastic spacer. The resolving gel was poured first and allowed to set. The stacking gel was then poured and a comb placed in the stacking gel in order to create wells for sample loading. Once set, the gels could be used immediately or wrapped in aluminium foil and stored at 4°C for 24 hours.

Samples containing an equal amount of protein were loaded onto the stacking gels, alongside molecular weight markers (Invitrogen, LC5725). The gels were run at 0.04 Amps for approximately 2 hours in an Atto gel rig (until the protein was run at least half way into the gel as judged by the migration of colour markers during the electrophoretic process). All gels were made from a stock of Acrylamide (Sigma, 148660). Sample calculations for an 8% resolving gel and a 5% stacking gel are shown in Table 2.1.3.

Table 2.1.2 Preparation of gels for protein electrophoresis

Components	Resolving gel (8%)	Stacking Gel (5%)
UHP	3.22ml	1.4ml
30% Acrylamide	1.82ml	330µl
1.5mM Tris (pH 8.8)	1.82ml	250µl
10% SDS (Sigma, L-4509)	70µl	20µl
10% APS (Sigma, A-1433)	70µl	20µl
TEMED (Sigma, T-8133)	4.2µl	2µl

2.9.4 Protein Transfer and Western Blotting

Following electrophoresis, the acrylamide gels were equilibrated in transfer buffer (25mM Tris, 192mM glycine (Sigma, G-7126) pH 8.3-8.5 without adjusting) for 20min. Proteins in gels were transferred onto Hybond ECL nitrocellulose membrane (Amersham, RPN 2020D) using a semi-dry transfer cell (Biorad). Eight sheets of Whatman 3mm filter paper (Whatman, 1001824) were soaked in transfer buffer and placed on the cathode plate of a semi-dry transfer cell. Excess air was removed from between the filters by moving a glass pipette over the filter paper. Nitrocellulose membrane, cut to the same size of the gel, was soaked in transfer buffer and placed over the filter paper, ensuring that there were no air bubbles. The acrylamide gel was placed over the nitrocellulose and four more sheets of presoaked filter paper were placed on top of the gel. Excess air was again removed by rolling the pipette over the filter paper. The proteins were transferred from the gel to the nitrocellulose membrane at 0.34 Amps (15 Volts) for 30min.

From this point on, all further steps were carried out on a revolving apparatus to ensure even exposure of the membrane blot to all reagents. Following transfer, the membranes were blocked in fresh filtered 5% non-fat dried milk (Cadburys; Marvel skimmed milk) in TBS (20mM Tris, 0.15M NaCl)/0.1% Tween 20 (Sigma, P1379), pH 7.4 for 2 hours. After blocking, the membranes were rinsed with TBS/0.1% Tween and incubated with primary antibody overnight at 4°C. Primary antibodies used are listed in Table 2.1.4. The following day the primary antibody was removed and the membranes rinsed three times with TBS/0.1% Tween. The membranes were then incubated in 1/1000 dilution of suitable HRP-labelled secondary antibody rabbit anti-Mouse (DakoCytomation, P0260), goat anti-Rabbit (DakoCytomation, P0448) or goat anti-chicken (Abcam. Ab68771) in 1% marvel for 1 hour at room temperature (R.T.). The secondary antibody was then removed and blots were washed three times for 15min in TBS/0.1% Tween. Bound antibody was detected using enhanced chemiluminescence (ECL) (Section 2.9.4).

Table 2.1.3 Antibodies used for western blot analysis

Antibody	Dilution/Concentration	Supplier	Catalogue no.
IGF-1R (C-20) (R)	1/1000	Santa Cruz	Sc-713
CAF-1 (anti Kir-6.1/KCNJ8)	1/200	Gift Prof. Willian Coetzee	N/A
14-3-3- σ (SFN) (M)	1/250	US Biological	0014-19
S100A13 (R)	1/500	Gift Prof. Claus Heizmann	N/A
TFPI2 (R)	1/500	Gift Prof. Walt Kiesel	N/A
α -Tubulin (M)	1/2000	Sigma	T5168
GAPDH (M)	1/5000	Abcam	Ab9484
β -actin (M)	1/10000	Sigma	A5441

Nomenclature

(M) = Mouse anti-human IgG.

(R) = Rabbit anti-human IgG.

(C) = Chicken anti-human IgG.

2.9.5 Enhanced Chemiluminescence detection

Protein bands were developed using the enhanced chemiluminescence kit (ECL) (Amersham, RPN2109) according to the manufacturer's instructions.

After blots were washed in TBS/0.1% Tween three times for 5min, a sheet of parafilm was flattened over a smooth surface, *e.g.* a glass plate, ensuring all air bubbles were removed. 1.5ml of ECL detection reagent 1 and 1.5ml of reagent 2 were mixed and covered over the membrane. Charges on the parafilm ensured the fluid remained on the membrane. The reagent was removed after one min and the membrane wrapped in cling film. The membrane was exposed to autoradiographic film (Kodak; X-OMAT S, 500 9907) in an autoradiographic cassette for various lengths of time, depending on the strength of signal obtained. The autoradiographic film was then developed for 5min in developer (Kodak, LX24), diluted 1:6.5 in water. The film was briefly immersed in water and transferred to a Fixer solution (Kodak, FX-40) diluted 1:5 in water, for 5min. The film was transferred to water for 5min and then air-dried.

2.10 RNA Extraction

RNA extraction was achieved using the Qiagen RNeasy mini kit (Qiagen, 74104). This extraction is based on the guanidine thiocyanate method of extraction and yields high quality RNA. The procedure was performed as follows:

1. To harvest RNA, culture media was removed from cells in culture and the cells were washed with PBS.
2. Cells were then lysed directly in the culture dish by the addition an appropriate volume of buffer RLT containing 10 μ l β -mercaptoethanol per ml of buffer RLT. 350 μ l RLT was used to lyse less than 5×10^6 cells, while 600 μ l RLT was used to lyse between 5×10^6 and 1×10^7 cells.
3. This suspension was then homogenised by passing it through a 20-gauge needle fitted to an RNase free syringe at least five times.
4. One volume of 70% ethanol was then added to the homogenised sample and mixed well by pipetting. This sample was then applied to an RNeasy mini column placed in a 2ml collection tube and centrifuged for 15s at 10,000rpm. The flow through was discarded.
5. 700 μ l of buffer RW1 was applied to the RNeasy column. The tube was closed and centrifuged for 15s at 10,000rpm to wash the column. The flow through and the collection tube were discarded at this point and the RNeasy column transferred to a new collection tube.
6. 500 μ l of buffer RPE was applied to the column, the lid closed and the tube centrifuged for 15s at 10,000 rpm to wash the column. The flow through was discarded and a further 500 μ l of buffer RPE applied to the RNeasy column. The tube was then closed and spun for 2 min at 10,000rpm to dry the silica-gel membrane.
7. The RNA was then eluted in a new 1.5ml collection tube using 20 μ l RNase-free water. The tube was closed and allowed to stand for 1min and then spun for 1 min at 10,000rpm.
8. The RNA was then quantified and diluted as appropriate.

RNA concentrations were calculated by measuring OD at 260nm and 280nm and using the following formula:

$$\text{OD}_{260\text{nm}} \times \text{Dilution Factor} \times 40 = \mu\text{g}/\mu\text{l RNA}$$

The purity of the RNA extraction was determined by calculating the $A_{260}:A_{280}$ ratio. An $A_{260}:A_{280}$ ratio of 2 is indicative of pure RNA. Only those samples with ratios between 1.7 and 2.1 were used in this study.

2.11 Reverse Transcriptase Reaction

Reverse transcriptase (RT) reactions were set up in laminar flow cabinets using micropipettes which were specifically allocated to this work.

To form cDNA, the following reagents were mixed in a 0.5ml eppendorf (Eppendorf, 0030 121.023) heated to 72°C for 10 min and then cooled to 37°C.

1.2µl 25mM MgCl₂ (Sigma, M-8787)

2µl 10x PCR Buffer (Sigma, P-2317)

2µl Oligo dT18 (0.5µg/µl) (MWG/Sigma)

0.4µl 10mM dNTP's (10mM of each dNTP; Sigma, D 5038)

0.5µl RNAsin (40U/µl) (Sigma, R-2520)

2µl total RNA (0.5µg/µl)

6.9µl DEPC water

Added directly to this mixture was, 4µl DEPC water and 1µl Moloney murine leukaemia virus reverse transcriptase (MMLV-RT) (40,000U/µl) (Sigma, M-1302). The RT reaction was carried out by incubating the eppendorfs at 37°C for 1 hour. The MMLV-RT enzyme was inactivated by heating to 95°C for 5 min. The cDNA was stored at -20°C until required for PCR reactions as outlined in Section 2.12.

2.12 Polymerase Chain Reaction

A standardised polymerase chain reaction (PCR) procedure was followed in this study. The reactions were carried out in 0.5ml safe-lock eppendorf tubes (Eppendorf, 0030 121.023). All reagents had been aliquoted and stored at -20°C and all reactions were performed in a laminar flow cabinet. Primers and annealing temperatures are detailed in the appendices.

A typical PCR tube contained the following:

1.5 μl 25mM MgCl_2 (Sigma, M-8787)

2.5 μl 10x PCR Buffer (Sigma, P-2317)

1 μl each of the forward and reverse strand target primers (10 μM)

0.5 μl each of the forward and reverse strand endogenous control primer (15ng/ μl)

5.5 μl UHP

2.5 μl cDNA

10 μl *Taq*/dNTP mixture*

*= 0.5 μl 10mM dNTP's (10mM of each dNTP; Sigma, D 5038)

0.25 μl of 5U/ μl *Taq* DNA Polymerase enzyme (Sigma, D-4545)

9.25 μl of UHP

DNA was amplified by PCR as follows:

95 $^{\circ}\text{C}$ – 5 min –denature

35* Cycles: 95 $^{\circ}\text{C}$ – 30sec - denature

X $^{\circ}\text{C}$ – 30sec – anneal

72 $^{\circ}\text{C}$ – 30sec – extend

And finally, 72 $^{\circ}\text{C}$ – 5min – extend

*The cycle number varied with primers used but was generally 35 cycles.

X = the annealing temperature varied with primer set used.

The reaction tubes were then stored at 4 $^{\circ}\text{C}$ for analysis by gel electrophoresis.

2.12.1 Real-Time PCR

RNA was extracted (Section 2.10) and cDNA synthesised as per Section 2.11. The Taqman® Real Time PCR analysis was performed using the Applied Biosystems Assays on Demand PCR kits, and experiments were performed in triplicate as follows:

- 22.5µl of qPCR master mix was added to was added to the relevant wells of a 96-well PCR plate (cat no. 4366932).
- 2.5µl of each cDNA sample was added to give a final reaction volume of 25µl. Each cDNA sample was analysed in triplicate for the separate measurement of target gene expression and endogenous control (β -actin).

The components of the master mix were as follows:

Table 2.1.4 Components of Real Time PCR master mix

Reaction Component	Volume/well per 25µl reaction	Final Concentration
TaqMan universal PCR mastermix, (2X) (Cat no. 4318157)	12.5µl	1X
20X assays on demand gene expression assay mix (primers)	1.25µl	1X
RNase-free water	8.75µl	-
cDNA	2.5µl	-

Table 2.1.5 TaqMan assays used in this study.

Gene	TaqMan assay catalog number
IGF-1R	Hs001385_m1
KCNJ8	Hs00270663_m1
S100A13	Hs00195583_m1
SFN	Hs00602835_s1
TFPI2	Hs00197918_m1
β -actin	4326315E

- The plate was then covered with an optical adhesive cover and placed in the ABI 7500 Real Time PCR instrument.
- The thermal cycling conditions were set using the following default settings;
 1. 2 min at 50°C (default for optimal AmpErase UNG activity. Not required when UNG is not added to reaction).
 2. 10mins at 95°C
 3. 40 cycles of 15s at 95°C denaturation and 1min at 60°C annealing.
 4. The sample volume was changed to 25 μ l and the run started.

Each real time PCR run was analysed as follows:

1. The file detailing the qPCR run for analysis was opened in the 7500 system software under Relative Quantification ddCt study.
2. A calibrator sample was selected and set to a value of one, allowing for the comparison of all other samples in relation to the calibrator.
3. For the analysis of target gene or endogenous control amplification, the baseline was set to average, normalised fluorescent signal before detectable increase (usually 3-15 cycles) and the cycle threshold was set in the exponential part of the curve.
4. The well information was then analysed. The Ct standard error was ideally less than +/-0.161. Ct errors with values greater than this were removed as outliers.
5. The endogenous control was used automatically to normalise the data.
6. When this was achieved for both the target and endogenous control, the relative quantity values for the run were generated and plotted relative to the calibrator sample.

2.13 Electrophoresis of PCR Products

A 2% agarose gel (Sigma, A-9539) was prepared in 1X TBE buffer (10.8g Tris base, 5.5g Boric acid, 4ml 0.5M EDTA, 996ml UHP) and melted in a microwave oven. After allowing to cool, 0.003% (v/v) of a 10mg/ml ethidium bromide solution was added to the gel which was then poured into an electrophoresis apparatus (BioRad). Combs were placed in the gel to form wells and the gel allowed to set.

5 μ l loading buffer (50% glycerol, 1mg/ml xylene cyanol, 1mg/ml bromophenol blue, 1mM EDTA) was added to 25 μ l PCR samples and 10 μ l was run on the gel at 80-90mV for approximately 2 hours. When the dye front was seen to have migrated the required distance, the gel was removed from the apparatus and examined on a UV-transilluminator and photographed.

2.14 Densitometric Analysis

Densitometric analysis was carried out using the MS Windows 3.1 compatible Molecular Analyst software/PC image analysis software available for use on the 670 Imaging Densitometer (Bio-Rad, CA) Version 1.3. In each gel photograph, a standard area was selected and scanned. The amount of light blocked by the DNA band was in direct proportion to the intensity of the DNA present. The software calculated a value for the Optical Density (O.D.) of each individual pixel on the screen. The average value of this O.D. (within a set area, usually 1cm²) was corrected for background of an identical set area. The corrected reading, for a given amplified band of interest was then normalised by dividing with a normalised reading obtained from an endogenous control band (usually β -actin). No comparator was set; as a result, these O.D. readings have arbitrary units.

2.15 DNA Array Analyses

2.15.1 GeneChips

The microarray gene expression experiments that were carried out in this body of work were performed using Affymetrix™ Human Genome U133A GeneChips™. Affymetrix GeneChip probe microarrays are manufactured using photolithography and combinatorial chemistry. Tens to hundreds of thousands of different oligonucleotide probes are synthesised and located in a specific area on the microarray slide, called a probe cell. Each probe cell contains millions of copies of a given oligonucleotide and each feature size on the Affymetrix U133A GeneChip is 10 microns.

The most important aspect in efficient probe design is the quality of the sequence information used. Probe selection and array design are two major factors in reliability, sensitivity, specificity and versatility of expression probe arrays. Probes selected for arrays by Affymetrix are generated from sequence and annotation data obtained from multiple databases including GenBank, RefSeq and dbEST. Sequences from these databases are collected and clustered into groups of similar sequences. Using clusters provided by the Unigene database as a starting point, sequences are further subdivided into subclusters representing distinct transcripts.

This categorisation process involves alignment to the human genome, which reveals splicing and polyadenylation variants. The alignment also extends the annotation information supplied by the databases pinpointing low quality sequences. These areas are usually trimmed for subsequent generation of high quality consensus sequences or alternatively Affymetrix employ quality ranking to select representative sequences, called exemplars, for probe design.

Generally, Affymetrix use 11 to 16 probes which are 25 bases in length for each transcript. The probe selection method used by Affymetrix for their U133A GeneChips takes into account probe uniqueness and the hybridisation characteristics of the probes, which allow probes to be selected, based on probe behaviour. Affymetrix use a multiple linear regression (MLR) model in the probe design that was derived from a

thermodynamic model of nucleic acid duplex formation. This model predicts probe binding affinity and linearity of signal changes in response to varying target concentrations. A further probe selection criterion used by Affymetrix for quantitative expression analysis is that the hybridisation intensities of the selected probes must be linearly related to target concentrations.

A core element of Affymetrix microarray design is the Perfect/Mismatch probe strategy. For each probe that is designed to be perfectly complementary to a given target sequence, a partner probe is also generated that is identical except for a single base mismatch in its centre. These probe pairs, called the Perfect Match Probe (PM) and the Mismatch probes (MM), allow the quantitation and subtraction of signals caused by non-specific cross-hybridisation. These differences in hybridisation signals between the partners, as well as their intensity ratios, serve as indicators of specific target abundance.

2.15.2 Sample and Array Processing

After RNA isolation, quantification and purification using the Qiagen RNeasy isolation method, cDNA was synthesised using the GeneChip T7-Oligo (dT) Promoter Primer Kit (Affymetrix; 900375) from 10µg total RNA. First strand cDNA synthesis was performed using the SuperScript Choice Kit (BioSciences; 11917-010). First strand cDNA synthesis involved “primer hybridisation” where the T7-Oligo (dT) primer was incubated with the RNA and DEPC-treated water at 70°C for 10mins, followed by a short incubation on ice; “temperature adjustment” where 5X first strand buffer, DTT and dNTP mix were added to the RNA mix and incubated at 42°C for 2mins; and “first strand synthesis” where superscript II RT was added to the mix and incubated at 42°C for 1 hour. The second strand mastermix was assembled containing: 91µl RNase-free water; 30µl 5X 2nd strand reaction mix; 3µl dNTP(10mM); 1µl *E.coli* DNA ligase; 4µl *E.coli* DNA polymerase I and 1µl RNase H. To each first strand synthesis sample, 130µl of second-strand mastermix was added. The tubes were mixed and centrifuged briefly and incubated for 2 hours at 16°C. After incubation, 2µl of T4 DNA Polymerase was added to each sample, and incubated for 5 minutes at 16°C. To stop any further reaction, 10µl of EDTA (0.5M) was then added to each tube.

cRNA was then synthesised and biotin-labelled using the ENZO BioArray HighYield RNA Transcript Labelling Kit (Affymetrix; 900182). For the IVT reaction the following reagents were added to the cDNA: 14µl RNase-free water; 4µl 10X IVT labelling buffer; 12µl labelling NTP mix and 4µl IVT labelling enzyme mix. These reagents were mixed carefully and centrifuged briefly. The reaction tubes were then incubated for 16 hours at 37°C. Biotin-labelled cRNA was purified using the GeneChip Cleanup module Kit (Affymetrix; 900371) and quantified. A sample of biotin-labelled cRNA was taken for gel electrophoresis analysis. The labelled cRNA was then fragmented before hybridisation onto the Affymetrix GeneChip probe microarrays. The aliquot of fragmented sample RNA as stored at -20°C until ready to perform the hybridisation step.

Hybridisation of fragmented cRNA onto the Affymetrix GeneChip human microarrays HU133A was performed in the Conway Institute, University College Dublin, where the Affymetrix Hybridisation Oven and Fluidics Station is set up along with the Affymetrix GeneChip Scanner, which exported the data directly into the Affymetrix analysis software, MicroArray Suite 5.0 (MAS 5.0).

An initial microarray experiment on the two invasive DLKP parents (DLKP-1 and DLKP-2), the invasive TXT-2, the mildly invasive TXT-1 and the almost non-invasive VCR was carried out in this institute by Dr. Rasha Linehan as single samples for analysis. Further duplicate sets of the above samples were then prepared for microarray analysis, for this thesis. This generated a triplicate data set for the analysis of the DLKP invasive variants.

2.15.3 Microarray Data Normalisation

The purpose of data normalisation is to minimise the effects of experimental and technical variation between microarray experiments so that meaningful biological comparisons can be drawn from the data sets and that real biological changes can be identified among multiple microarray experiments. Several approaches have been demonstrated to be effective and beneficial. However, most biologists use data scaling as the method of choice despite the presence of other alternatives. In order to compare gene expression results from experiments using microarrays, it is necessary to normalise the data obtained following the microarray chip scanning process. There are two main ways in which this type of normalisation is performed, the first of which is “per-chip” normalisation. This type of normalisation helps to reduce minor differences in probe preparation and hybridisation conditions which may potentially result in the high intensity of certain probe sets. These adjustments in probe intensity are made to set the average fluorescence intensity to some standard value, so that all the intensities on a given microarray chip increase or decrease to a similar degree. However, this type of normalisation should only be performed on microarrays using similar cell or tissue types. One drawback of this normalisation is that some aspects of the microarray data may potentially be obscured, such as whether the RNA samples or the probe preparation steps were equal for each sample. All data in this study were scaled to a value of 100.

The second way in which most biologists normalise their data sets is by using the “per gene” normalisation method. The aim of microarray experiments is to identify genes whose expression changes in different conditions, be that tracking gene changes across a temporal experiment or when comparing gene expression between an invasive and non-invasive sample. Therefore, it is necessary to normalise microarray data sets using “per gene” normalisation to find genes that have a similar expression pattern across an experiment. Analysis of raw data from microarray experiments is useful for identifying genes that are expressed at the same level, for example, genes that are highly abundant in the samples. In contrast to a time course investigation, there was no clear “control” sample to be used as a baseline in this experiment, so the median value for each gene was calculated and given a normalized value of one. This is known as normalisation to median.

2.16 Overview of Bioinformatic Analysis

2.16.1 Quality Control

Scanned images of the Affymetrix™ U133A arrays were loaded into Affymetrix™ MAS software. Here, they were checked for damage and then analysed. The chips were scaled in MAS to make them comparable. Scaling is a linear process that adjusts all the values on an array so that all the arrays in the experiment have the same trimmed mean, 100 Affymetrix units.

QC output for the array data is graphed (Figure 3.1.1). Overall, the quality metrics should be looked at as a whole. These Quality Control Metrics graphs are an important part of the experimental record. To simplify visualisation of all the metrics on the same graph, some of the values are divided by constants to get the values in the same region of the graph.

Hierarchical clustering is used as an internal QC step within the Centre. Since the chips are scaled, no further normalisations were required for this QC step. This clustering allows the direct comparison of the different chips based on the profile of altered genes on each chip. The hierarchical clustering generated for this experiment is presented in Figures 3.1.2 and 3.1.3.

Since the array data was scaled in MAS, “per chip” normalization was not required in GeneSpring. A per gene normalization was then carried out. In contrast to a time course investigation, there is no clear “control” sample to be used as a baseline in this experiment, so the median value for each gene was calculated and given a normalized value of one. This is known as normalisation to median.

2.16.2 Generating Genelists

2.16.2.1 Genelist 1

Initially the single 5 chips were analysed alone. In this case statistics were not used as the data was generated by one set of samples. For this analysis, multiple experiments were set up in GeneSpringTM with all possible pairs of samples. A filter was applied to remove any genes that were consistently flagged as absent. These “pairwise” comparisons were used to identify genes that were up and down regulated (using an arbitrary two fold cut off) between the five cell lines. These lists (which contained hundreds of genes each) were overlapped (using the Venn diagram function in GeneSpringTM) to find genes that were consistently up or down regulated in invasive samples relative to non-invasive samples. Using this single data set, 31 genes came through the above analysis (Tables 3.1.1 and 3.1.2). A literature search was carried out on the 31 genes with 19 genes subsequently picked as candidates for RT-PCR to confirm array analysis.

2.16.2.2 Genelist 2

The second analysis was carried out using the same method as above except that the analysis was performed on the duplicate chips prepared subsequently to the initial single set, that is duplicate chips of the five cell lines (Table 3.1.3). Again, statistics were not used in this analysis. Using the same method as analysis 1, only nine genes came through and all were selected for confirmatory RT-PCR.

2.16.2.3 Genelist 3

The third analysis was the analysis of the 15 chips (that is the 5 cell lines in triplicate). The same method as analysis 1 and 2 was used to determine if any genes came through all of the 3 analyses. 40 genes came through this analysis (Table 3.1.4). RT-PCRs were not carried out on all 40 genes.

2.16.2.4 Genelist 4

A further analysis was carried out, this time using a different approach on all fifteen chips. Genes that did not cross a two-fold threshold above or below the median in at least one cell line were removed from the analysis, as were genes that were consistently called absent by the Affymetrix software. A Welch ANOVA (analysis of variance) statistical test was used to find genes that were reliably differentially expressed between the five different cell lines. Subsequently, a further Welch ANOVA test was used to find genes in this list that were useful in discriminating between invasive and poorly invasive samples. This generated a gene list containing 45 genes, whose expression patterns (see heatmap Figure 3.1.4) were analysed visually to identify 18 possible invasion related genes (Table 3.1.5).

2.16.2.5 Genelist 5

Rather than grouping the samples into invasive and non-invasive, an arbitrary scale of invasion was applied to reflect the intermediate degrees of invasion displayed by the cell lines in the *in vitro* invasion assay. This arbitrary scale of invasiveness was put into the GeneSpring™ cell information, which allowed for analysis of the data based on relative invasiveness of the. The scale was as follows:

DLKP-1	5
TXT-2	5
DLKP-2	3.5
DLKP-TXT-1	1
DLKP-VCR	0

To analyse the data using the information above on the 15 chips, a ratio interpretation by analysis name was used. A filter was applied that included genes that were present or marginal in three out of 15 samples and also genes whose expression were 1.5 fold increased or decreased in three out of 15 samples. A genelist was made of the genes that passed these stipulations. A Welch ANOVA (settings: P-value; 0.01, no multiple testing correlation) was applied to this list using the invasion parameter (scale)

mentioned above. 531 genes came through this statistical test and were referred to as consistently changing genes.

These 531 consistently changing genes were put into Self Organising Maps (SOMs). SOMs group together genes with similar expression pattern in clusters. The user defines the number of clusters into which the genes should be organised. The SOMs for the 531 changing genes related to invasiveness but a similar approach could be used to group genes related to drug resistance. A 7x6 SOM (log scale) was used to organize the 531 changing genes into clusters with similar expression patterns (Figure 3.1.5).

2.16.3 Genomatix Software Suite

Genomatix provide software that allows users to explore published studies as well as combine sequence analysis, and genome annotation in order to help researchers to get a complete overview of their biological data (www.genomtix.de) The software offered by Genomatix is designed to help researchers gain a better understanding of gene regulation at the molecular level. The Genomatix software suite is comprised of six main tools: ElDorado, Gene2Promoter, BiblioSphere, GEMS Launcher, MatInspector and PromoterInspector. ElDorado is a gene orientated genome search engine which provides the user with information about functional genomic elements within a specific region of the genome. This piece of software compiles and integrates information on gene function and regulatory pathway. In addition, information on mRNAs, their exon/intron structure and coding sequences, single nucleotide polymorphisms (SNPs) and potential promoter regions may be retrieved using ElDorado. The hypothesis underlying this type of analysis is that genes with similar expression patterns may be co-regulated and therefore may be activated by the same transcriptional signals.

BiblioSphere is a data-mining solution for extracting and studying gene relationships from literature databases and genome-wide promoter analysis. Based on PubMed (www.ncbi.nlm.nih.gov), BiblioSphere currently searches over 14 million abstracts. The unique data-mining strategy allows you to find direct gene-gene co-citations and

even yet unknown gene relations via interlinks. BiblioSphere data is displayed as 3D interactive view of gene relationships (Figure 3.1.6). Results can be classified by tissue, Gene Ontology and Medical Subject Headings (MeSH). Statistical rating by z-scores indicate over- and under-representation of genes in the various biological categories. BiblioSphere can be applied to single gene analysis, gene cluster analysis and analysis of gene regulatory mechanisms.

The 104 probe sets as selected from SOMs were pasted into BiblioSphere™ (Genomatix™ software) and a BiblioSphere was generated (Figure 3.1.6). A MeSH disease filter called “Neoplasm Invasiveness” (z-score = 19.2) (other filters could have been chosen) was applied to the BiblioSphere cluster and 11 genes from the cluster were related to this parameter.

Transcription factors were excluded assuming that an over-expressed TF may also be on a superior position in a regulative network and the identifiers for nine genes (excluding transcription factors) were copied into Gene2Promoter to retrieve the promoter sequences for these transcripts.

Since co-regulation of gene transcription often originates from common promoter elements the identification and characterisation of these elements provides a more in-depth analysis for the expression of microarray genelists. Gene2Promoter allows users to automatically extract groups of promoters for genes that may be of interest. This piece of Genomatix software provides access to promoter sequences of all genes annotated in available genomes.

MatInspector is a tool that employs a library of matrix descriptions for transcription factor binding sites on a given promoter sequence. Graphical display of transcription factor binding sites common to a set of inputted promoters is obtained following MatInspector analysis. These promoter sequences were then subjected to “FrameWorker” analysis. FrameWorker allows users to extract a common *framework* of elements from a set of DNA sequences. These elements are usually transcription factor binding sites since this tool is designed for the comparative analysis of promoter sequences. FrameWorker returns the most complex models that are common to the input sequences (and satisfying the user parameters). These are all elements that occur

in the same order and in a certain distance range in all (or a subset of) the input sequences. The settings used for the framework analysis were as follows;

- A limit of 30% of nine input promoter sequences was used (denotes that only models are considered that occur in at least three of the nine sequences). Other percentage constraints were used but did not generate promoter models with more than two elements. (For a mixed set of input data (e.g. if it is not known if and how many of the promoter sequences share a common transcription model) this parameter should be lowered from 80% as above).
- Distance constraints of 5 and 50 (default settings, were used).

Once a model of transcription factor binding sites was generated using FrameWorker software, sequence databases were scanned for regulatory units that match the models, which were generated using ModelInspector. ModelInspector provides a library of experimentally verified promoter models against which transcription factor models may be scanned. The promoter models generated in this analysis were scanned against a library of experimentally verified human promoter models using ModelInspector. This generated a list of genes with the same promoter models from an experimentally verified human promoter database.

2.17 RNA interference (RNAi)

RNAi using small interfering RNAs (siRNAs) was performed to silence specific genes. The siRNAs used were purchased from Ambion Inc. These siRNAs were 21-23 bps in length and were introduced to the cells via reverse transfection with the transfection agent siPORTTM NeoFXTM (Ambion Inc., 4511).

2.17.1 Transfection optimisation

There were a number of different parameters that had to be determined to establish an optimised protocol for the siRNA transfection of DLKP and its variants. Initially, the transfection protocol itself was considered. In order to determine the optimal conditions for siRNA transfection, an optimisation with a siRNA for kinesin (Ambion Inc., 16704) was carried out for each cell line. Cell suspensions were prepared at 1×10^5 ; 3×10^5 and 7×10^5 cells per ml. Solutions of negative control and kinesin siRNAs at a final concentration of 30nM were prepared in optiMEM (GibcoTM, 31985). NeoFX solutions at a range of concentrations were prepared in optiMEM in duplicate and incubated at room temperature for 10min. After incubation, either negative control or kinesin siRNA solution was added to each NeoFX concentration. These solutions were mixed well and incubated for a further 10 minutes at room temperature. 100 μ l of the siRNA/neoFX solutions were added to each well of a 6-well plate. 1ml of the relevant cell suspensions were added to each well. The plates were mixed gently and incubated at 37°C for 24 hours. After 24hr, the transfection mixture was removed from the cells and the plates were fed with fresh medium. The plates were assayed for changes in proliferation at 72hr using the acid phosphatase assay (Section 2.7.1b). Optimal conditions for transfection were determined as the combination of conditions which gave the greatest reduction in cell number after kinesin siRNA transfection and also the least cell kill in the presence of transfection reagent. The optimised conditions for the cell lines were 2 μ l NeoFx to transfect 30nM siRNA in a cell density of 3×10^5 per well of a 6-well plate.

qPCR analysis of these early transfections demonstrated that mRNA knockdown was not being achieved, which led to the examination of cell line handling during the transfection process. It transpired that cell handling during the transfection protocol is particularly important. The following procedures were optimised for siRNA transfection in these cell lines:

- Cells should be in log/growth phase and in a healthy condition when used to seed siRNA transfections and should be fed with fresh medium 24h prior to transfection.
- The cell suspensions should be prepared in serum containing medium i.e. normal growth medium (as opposed to medium with reduced serum e.g. Optimem).
- Cells should be in suspension for as short a time as possible and maintained at 37°C to avoid heat shock while the siRNA complex is being prepared.

Five cell lines were too many cell lines to transfect with siRNA in any one transfection. The reasons for this are twofold; the cells are in suspension for longer time periods than if you were working with fewer cell lines. It was found that cells in suspension should be dispensed onto complexed siRNA/NeoFx solutions immediately following the complex incubation period (i.e. reverse transfection). Extended time periods lead to poor transfection efficiency and thereby poor target knockdown. We determined that three cell lines are the maximum number suitable in any single transfection experiment.

2.17.2 Proliferation effects of siRNA transfection

Solutions of siRNA at a final concentration of 30nM were prepared in optiMEM (Gibco, 31985). NeoFX solution was prepared in optiMEM and incubated at room temperature for 10 minutes. After incubation, an equal volume of NeoFX solution was added to each siRNA solution. These solutions were mixed well and incubated for 10 minutes at room temperature. Replicates of 100µl of the siRNA/NeoFX solutions were added to a 6-well plate. 1ml of each cell suspension was added to at a concentration of 3×10^5 per well. The plates were mixed gently and incubated at 37°C for 24 hours. After 24 hours, the transfection mixture was removed from the cells and the plates were fed with fresh medium. The plates were assayed for changes in proliferation at 72 hours using the acid phosphatase assay (Section 2.7.1b).

Table 2.1.6 List of siRNAs used

Target name	Ambion IDs
Scrambled	Negative control #2
IGF-1R	74 (validated)
KCNJ8	7346, 7252
S100A13	42125, 263271, 263272
SFN	17396
TFPI2	17988

An additional assay format was used to investigate proliferation. Kinesin siRNA was included as a positive control for the transfection. Solutions of siRNA at a final concentration of 30nM were prepared in optiMEM (Gibco, 31985). NeoFX solution was prepared in optiMEM and incubated at room temperature for 10min. After incubation, an equal volume of NeoFX solution was added to each siRNA solution. These solutions were mixed well and incubated for a further 10min at room temperature. Replicates of 10 μ l of the siRNA/NeoFX solutions were added to a 96-well plate. Cell suspensions were overlaid to each well at densities of 2.5x10³ and 5x10³ per well. The plates were mixed gently and incubated at 37°C for 24hr. After 24 hr, the transfection mixture was removed from the cells and the plates were fed with fresh medium. The plates were assayed for changes in proliferation at 72hr using the acid phosphatase assay (Section 2.7.1a).

2.17.3 Invasion analysis of siRNA transfected cells

To assay for changes in invasive capacity, siRNA experiments in 6-well plates were set up using 2 μ l NeoFx to transfect 30nM siRNA in a cell density of 3x10⁵ per well of a 6-well plate. Transfection medium was removed after 24hr and replaced with fresh growth medium. The transfected cells were assayed for changes in invasion capacity at 72hr using the optimised *in vitro* invasion assay described in Section 2.7.2.

2.18 Transfection of DLKP variants with Exogenous DNA

In order to understand the role of target genes more clearly, a vector, pSport6, containing the target cDNA sequence was transiently transfected into host cells to exogenously increase the level of expression of the target genes. Plasmids containing each target were purchased from OpenBiosystems in destination vectors and were sub-cloned into the expression vector pSport6. Stock plasmid was produced by transforming competent JM109, growing up a large stock of these cells and isolating the plasmid from them. This isolated plasmid was then transfected into the chosen cell line. The plasmids used in this study are detailed in Table 2.1.7.

Table 2.1.7 Plasmids used in this study

Name	Resistance to	Catalogue no.	Supplied Vector	Expression Vector
KCNJ8	CAM	MHS1011-59229	pOTB7	pCMV-SPORT6
SFN	CAM	MHS1011-61174	pOTB7	pCMV-SPORT6
S100A13	CAM	MHS1011-59294	pOTB7	pCMV-SPORT6
TFPI2	CAM	EHS1011-4411426	pDNR-LIB	pCMV-SPORT6
GFP	AMP	-	pEGFP-C1	pEGFP-C1

2 18 1 Plasmid Preparation

2 18 1 1 Transformation of JM109 Cells

A bacterial cell suspension (100µl) of competent JM109 (Promega, L2001) was mixed with 20ng DNA and placed on ice for 40min after which the mixture was heat-shocked at 42°C for 90s and then placed on ice for 3min LB broth (1ml) ((10g Tryptone (Oxoid, L42), 5g Yeast Extract (Oxoid, L21) 5g NaCl (Merck, K1880814))/litre LB, autoclaved before use) was added to the competent cell suspension and incubated at 37°C for 1hr Different volumes of this suspension was spread on a selecting agar plates (LB agar containing appropriate antibiotic concentration of ampicillin or chloramphenicol) and incubated overnight at 37°C Single colonies that grew on these selecting plates were incubated into 5ml LB broth containing appropriate selection antibiotic

Single colonies inoculated into 5ml LB broth (10g Tryptone (Oxoid, L42), 5g Yeast Extract (Oxoid, L21), 5g NaCl (Merk, K1880814) per litre of LB, autoclaved before use) containing appropriate selection antibiotic and were grown for 8hr with shaking at 37°C and were subject to a DNA mini preparation (Section 2 18 1 2) or Large Scale Preparation (Section 2 18 1 3) For a large scale DNA preparation this culture was then inoculated into 270ml LB broth containing 0.3ml ampicillin (100mg/ml) in 1L baffled flask with shaking overnight at 37°C

2.18 1 2 DNA Miniprep of Plasmid DNA

Plasmid DNA was isolated from a 5ml culture grown in LB broth containing selection antibiotic overnight with shaking at 37°C using the Qiagen Plasmid DNA Extraction Mini Kit (Qiagen, 12143) To determine and select the colonies containing the inserted DNA sequence, a miniprep of the plasmid DNA was carried out Single colonies were selected off the selection plates and incubated in universals containing 5mls LB/Amp shaking at 180rpm at 37°C overnight After incubation, the cells were centrifuged at

8,500rpm for 3 min Pelleted cells were resuspended in 250µl of buffer P1 and the cell suspension was transferred to a microcentrifuge tube To this solution, 250µl buffer P2 was added and mixed gently A volume of 350µl buffer N3 was added to the solution and the tube was mixed immediately This mixture was centrifuged for 10min at 13,000 rpm The supernatant was applied to a QIAprep spin column and centrifuged for 60s The flow-through was discarded The column was washed by adding 500µl buffer PB and centrifuging for 60s The flow through was discarded This step was repeated with 750µl buffer PB The column was centrifuged for a further 60s to remove the entire wash buffer The column was then placed in a clean microcentrifuge tube To elute the DNA, 50µl of buffer EB was added to the column The column was let stand for 60s and then centrifuged for 60s The DNA concentration was determined by measuring the OD_{260nm} Plasmid was stored at -20°C until required

2 18 1.3 DNA Maxiprep of Plasmid DNA

Plasmid DNA was purified using an endofree plasmid maxi kit (Qiagen, 12362) Following growth of plasmid culture in into 270ml LB broth containing 0.3ml ampicillin (100mg/ml) in 1L baffled flask with shaking overnight at 37°C, the culture was split into 2 x 250ml centrifuge bottles and spun at 3,500rpm for 15min at 4°C Pellets were weighed and either frozen at -80°C until required or processed further

The bacterial pellet was resuspended in 10ml buffer P1 To this, 10 ml buffer P2 was added, mixed gently and incubated at room temperature for 5min A volume of 10ml chilled buffer P3 was added to the lysate and mixed immediately and gently The lysate was poured into the barrel of the QIAfilter cartridge and incubated at room temperature for 10min The cap from the QIA filter outlet nozzle was removed and the plunger was gently inserted in to the cartridge The cell lysate was filtered into a 50ml tube To the lysate, 2.5ml buffer ER was added and mixed by inverting repeatedly This was incubated on ice for 30min A qiagen-tip 500 was equilibrated by applying 10ml buffer QBT and the column was allowed to empty by gravity flow The filtered lysate was then applied to the qiagen-tip and allowed to enter the resin by gravity flow The qiagen-tip was washed twice with 30ml buffer QC The DNA was eluted by

addition of 15ml buffer QN and the eluate was collected in a 30ml tube. The DNA was precipitated by adding 10.5ml isopropanol to the eluated DNA. This was mixed and centrifuged at ~10,000rpm for 30min at 4°C. The DNA pellet was washed with 5ml of 70% ethanol and this was centrifuged at ~10,000rpm for 10min. The pellet was air-dried and dissolved in 500µl buffer TE. The DNA concentration was determined by measuring the OD_{260nm}.

2.18.1.4 Sub-cloning

5µg of each plasmid from OpenBiosystems were digested with the appropriate restriction endonucleases (see table 2.1.8) for 1hr at 37°C to remove the gene coding sequence for insertion into pSport6 expression vector.

Table 2.1.8 Restriction Digestions of plasmids in their supplied vectors.

Target	Restriction Enzymes used	Fragment size
KCNJ8	EcoRI/XhoI	1.7kb
S100A13	EcoRI/XhoI	0.5kb
SFN	EcoRI/XhoI	1.3kb
TFPI2	XbaI/SalI	1.2kb

These restriction digests were analysed by TAE low melt 1% gel electrophoresis and the relevant fragment size excised from the gel using a fresh clean blade for each excision. The DNA was purified from the gel by the addition of PB buffer (Qiagen Gel Purification Kit) to each gel slice, this was melted at 55°C for 10min and applied under vacuum to a gel purification column. The DNA was column was washed with 750µl of PE buffer under vacuum and centrifuged at 13,000rpm for 1min to dry. The pellet was

re-dissolved in 15µl EB buffer and a portion of this run out on a 1% TAE agarose gel. This ensured that the cDNA fragment was not contaminated and thus suitable for ligation.

Each insert was ligated with pSport6 (digested with matching REs) at 15°C overnight in a mastermix typically containing expression vector (100ng), target insert cDNA (300ng), water, 10X ligation buffer and T4 ligase (2.5U) in a total volume of 10µl. Half of this ligation reaction was then transformed into JM109 competent cells as described above (2.18.1.1). Single colonies that grew on the relevant selection plates were incubated into 5ml LB broth containing appropriate selection antibiotic and used for a DNA mini-preparation, a small volume was then digested and analysed by 1% TAE gel electrophoresis to ensure clean DNA preparations and confirm that bands obtained corresponded to the expected sizes of the expression vector and target fragments. Once this was confirmed the plasmids were then sent for sequencing and used for maxi preparation of DNA stocks (2.18.1.3).

2.18.2 Plasmid DNA Sequencing

In order to fully confirm the orientation and the origin of the inserted DNA in the plasmids, each plasmid was sent to MWG-Biotech (Germany) for sequencing. Once these parameters had been confirmed, transfection could be carried out.

2.18.3 Optimisation of plasmid transient transfection protocol

The transient transfection protocol was optimised for each of the five DLKP cell lines used in the study. To this end a cell suspension was generated at a concentration of 4×10^5 cells/ml in complete growth medium and seeded 24hr before transfection. Lipofectamine 2000 (Invitrogen, 11668019) and Green Fluorescent Protein (GFP) plasmid DNA was prepared with the volumes of Lipofectamine 2000 and cDNA being varied. The conditions investigated to ascertain the most efficient transfection conditions were as follows,

- 2µg GFP cDNA 5µl Lipofectamine 2000
- 4µg GFP cDNA 10µl Lipofectamine 2000

Briefly, the plasmid and optiMEM were incubated at room temperature for 5min. During this time the Lipofectamine 2000 and optiMEM were also incubating at room temperature. Both incubations were combined, mixed gently and formed complexes over 20min at room temperature. 1ml of this complex was added per well and mixed gently. The cells were viewed using a fluorescent microscope after 24hr and the optimum transfection efficiency determined for each cell line by comparing the number of cells that fluoresced green with the number of cells in a particular field (Section 3.5.6.2). The Lipofectamine 2000 had a toxic effect on the cells, thus the lowest volume of transfection reagent was used while maintaining high transfection efficiencies. To this end 5µl Lipofectamine 2000 was used to transfect 2µg plasmid cDNA in all transient cDNA transfections in this study.

2.18.4 Invasion analysis of cDNA transiently transfected cells

To assay for changes in invasive capacity, cDNA experiments in 6-well plates were set up using 5µl Lipofectamine 2000 to transfect 2µg plasmid cDNA in a cell density of 4×10^5 per well of a 6-well plate. Transfection medium was removed after 24hr and replaced with fresh growth medium. The transfected cells were assayed for changes in invasion capacity at 72hr using the optimised *in vitro* invasion assay described in Section 2.7.2).

Section 3.0: Results

3.1 Microarray analysis of DLKP and its invasive and chemotherapeutic resistant variants

The gene-expression profiles of five human lung cancer cell lines with differing levels of invasion (as determined by an *in vitro* invasion assay) were analysed using expression microarray methodology. Two invasive parental DLKP cell lines (DLKP-1 and DLKP-2) were used along with an invasive Taxotere (TXT) resistant DLKP variant (DLKP-TXT-2) and a non-invasive TXT selected DLKP cell line that had lost its resistance to TXT (DLKP-TXT-1). This provided us with an *in vitro* model of invasion. The aim of this microarray study was to identify genes involved in the development of an invasive phenotype in lung cancer cell lines. These cell lines with differing levels of invasiveness (derived from the same parent) offered a unique opportunity to study the less-well characterised mechanisms of invasion.

An important point to remember when considering this analysis is that there are potentially two ways to approach this data in that one could look at drug resistance and/or invasion. The main focus in this thesis was to analyse differences between the invasive and poorly invasive cell lines. Theoretically however, any differentially expressed genes identified by the microarray analysis could relate to drug resistance and/or invasion.

3.1.1 GeneChip Quality Control

This section details the quality control measures were used in these microarray experiments before gene expression analysis began.

3.1.1.1 Scale factor

Each array had varying image intensity, and this intensity, or brightness, was measured by the “scaling factor”. In order to make an accurate comparison of multiple sets of array data the mean intensities of the arrays were brought to the same arbitrary set point, typically 100. This algorithm was performed using Microarray Suite 5.0 (MAS 5.0) with a mathematical technique known as ‘scaling’. Scaling worked by calculating the overall intensity of an array and averaging every probe set on the array (with the exception of the top and bottom 2% of the probe set intensities). The average intensity

of the array was then multiplied by the scaling factor to ensure that all of the intensities on the given array went up or down to a similar degree. Therefore very dim chips typically have large scale factors. Scaling allowed normalisation of several experiments to one target intensity. For the experiments to be comparable, there must be no more than 3 fold difference between the scaling factors for each chip.

3 1 1 2 Noise

“Noise” measured the pixel-to-pixel variation of probe cells on the array and is caused by small variations in the digital signal observed by the scanner as it sampled the array surface. As each scanner has a unique electrical noise associated with its operation, noise values among scanners vary. Therefore arrays that were scanned on the same scanner were expected to have similar noise values.

3 1 1 3 Background

Affymetrix have found that typical background values range from 20 to 100 and that arrays being compared should have similar background. The background values ranged from 47 to 66 for this set of arrays, which is acceptable. High background can result from ethanol carryover during sample processing and result in a reduced percentage present call.

3 1 1 4 Present call

The percentage of genes present relates to the number of probe sets present relative to the total number of probe sets on the array. Replicate samples should have similar percentage present calls that typically vary between 40-60%, but this may be cell line dependent.

3 1 1 5 3':5' ratio

All of the arrays used β actin and GAPDH to assess RNA sample and assay quality by having probes specific for the 3', middle and 5' end of these genes. The ratio of signal intensity from 3' probes to 5' probes was a measure of the number of cDNA synthesis reactions that went to completion. A ratio of 1 indicated full-length transcript and was considered ideal. A cut-off value of 3 was applied, values above 3 indicated that either the in vitro transcription (IVT) reaction was not complete or that the RNA was degraded. Values of less than 1 are also possible and indicate preferential binding of 5' probes.

3 1 1 6 Hybridisation controls

Spiked cRNAs were used as hybridization controls. BioB, bioC and bioD represent genes in the biotin synthesis family of *E. coli*, and Cre is the recombinase gene from the P1 bacteriophage. They were spiked in increasing concentrations and the average difference values were expected to be present in increasing amounts, bioB being the least and Cre the most. Chips passed QC if MAS 5.0 deemed the BioB control "present".

3.1 1 7 Visual examination

After scanning the array, chips were inspected for the presence of image artefacts. These include spots or regions on the chip with unusually high or low intensity, scratches or overall background. All of the chips used passed visual inspection.

The overall quality control for the duplicate array samples are visualised in Figure 3 1 1. In order to visualise each quality control metric on one graph, values for background and percent present calls were divided by ten, and raw values were divided by 25.

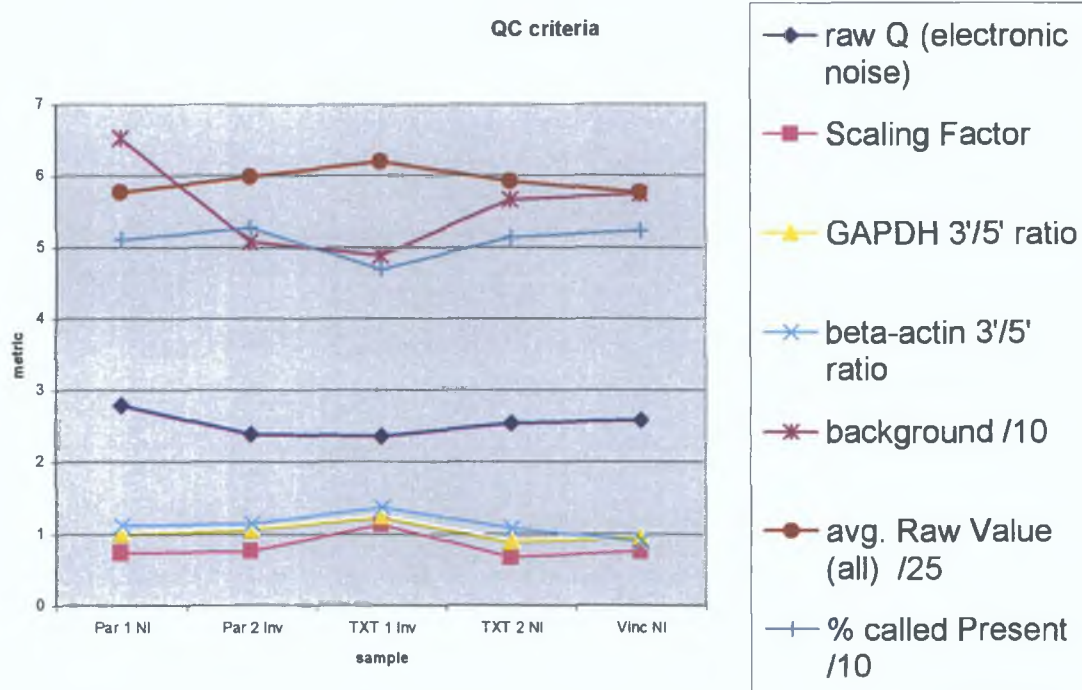


Fig 3.1.1 Quality Control for the duplicate Affymetrix Chips

This graph demonstrates that the U133A duplicate array chips used for the duplicate analysis of the five DLKP variants were within the required quality control parameters recommended by Affymetrix.

Hierarchical clustering is used as an internal QC measure taken within the NICB when the chip run is deemed satisfactory. Since the chips were scaled, no further normalisations were required for this QC step. Unsupervised Hierarchical clustering grouped samples together based on similar expression levels of the genes analysed by the microarrays and identifies any bias in the system. This clustering allowed the direct comparison of the different chips based on the profile of altered genes on each chip. One would expect that chips used to analyse biological replicates should resemble each other more than chips used to analyse unrelated samples and would be grouped separately.

The hierarchical cluster generated by GeneSpring for this experiment can be seen in Figure 3 1 2. Ideally, the five cell lines would group together in triplicates. In this case however, the DLKP parents that were put on the array in duplicate clustered together but the single DLKP parent did not align beside them in the cluster. Duplicate VCR samples also clustered together but did not align beside the single VCR sample. The three TXT non-invasive samples did not cluster together at all and likewise for the TXT invasive samples. This is not the optimal result for a hierarchical cluster. However, the result is unsurprising since the initial sample generation and array processing on the two invasive DLKP parents, the invasive DLKP-TXT-2, and the poorly invasive DLKP-TXT-1 and DLKP-VCR was carried out by a different researcher, Dr Rasha Linehan in 2003 as single samples for analysis. Further duplicate sets of the above samples were then prepared for microarray analysis, for this thesis. This generated an overall triplicate data set for the statistical analysis of the DLKP invasive variants. This is reflected in a further hierarchical cluster, where the samples cluster by researcher or by date of processing (Figure 3 1 3). Despite these anomalies in the hierarchical clustering, the results of this study indicate a useful microarray data set in terms of identifying genes involved in invasion and/or drug resistance, although it is likely that some data was lost due to the reduced reproducibility.

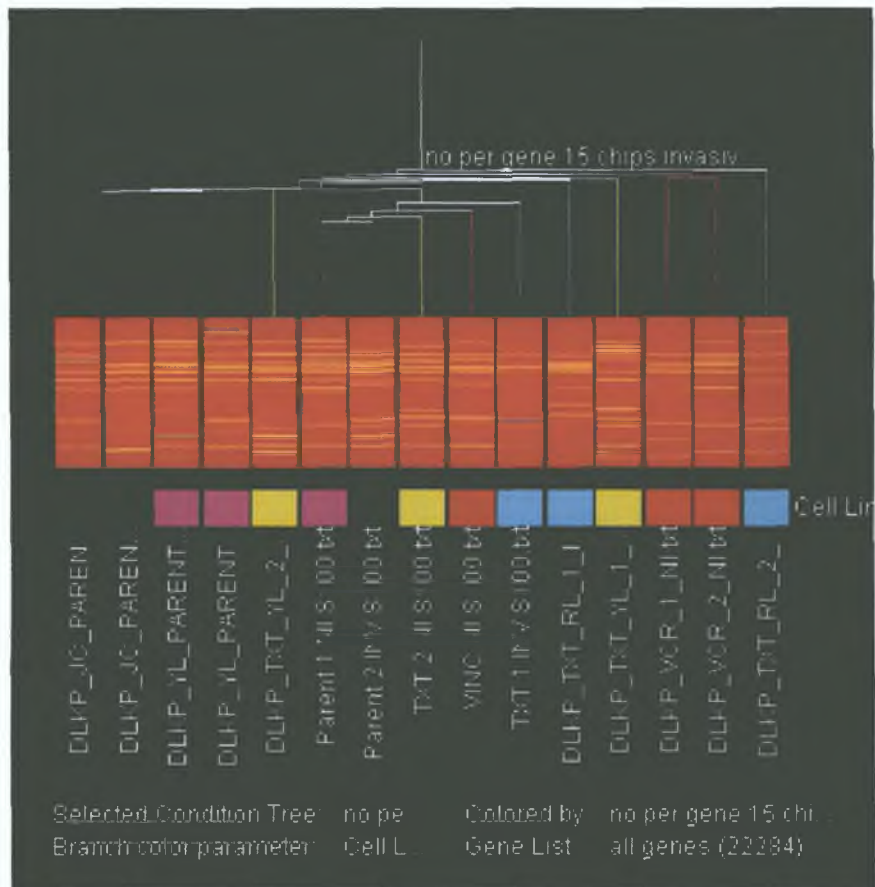


Figure 3.1.2 Hierarchical Cluster of DLKP and the variant samples in triplicate
 Ideally, the five cell lines would group together into their biological triplicates. Coloured boxes represent replicate samples. Red/yellow bars indicate expression levels of genes used in generating cluster.

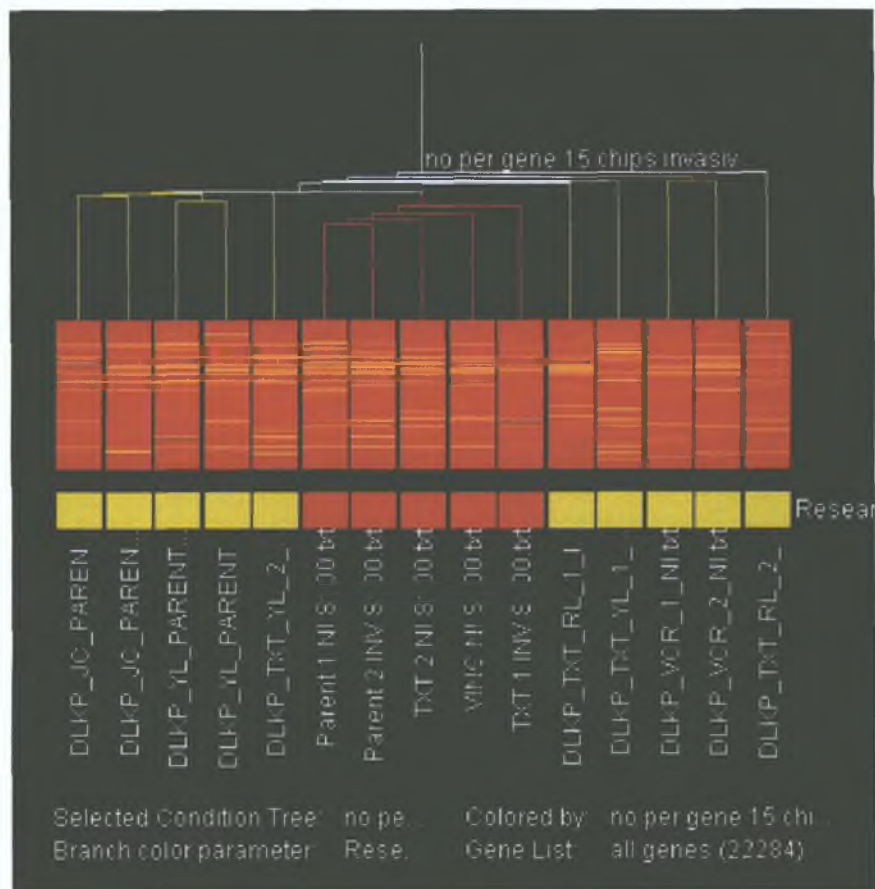


Figure 3.1.3 Hierarchical Cluster of DLKP and the variant samples in triplicate

The samples cluster by researcher/date of sample processing. The red boxes are indicative of samples prepared by Dr. Rasha Linehan in 2003. The yellow boxes are indicative of samples processed in 2004 to generate an overall triplicate data set for the statistical analysis of the DLKP variants.

3.1.2 Bioinformatic analysis – generating genelists

A major aim of this work was to generate gene-lists from the raw array data that may potentially serve as a genotypic signature for invasiveness and/or drug resistance in the DLKP variants. Various methods were employed including using software such as GeneSpring, Bibliosphere (Genomatix), and promoter analysis using Gene2promoter, FrameWorker and ModelInspector (also from Genomatix). This is detailed in section 2.16. Various analyses were used to compile the different genelists detailed in this section to increase confidence in the identification and selection of targets for further analysis. For example, the GeneSpring™ software was used to generate genelists one to five in this study. This allowed for the identification of genes that would otherwise have been missed had the data been interpreted in only one way, while identifying targets that consistently appeared on each genelist.

3.1.2.1 Genelist 1

For the generation of genelist 1 (Tables 3.1.1 and 3.1.2), multiple experiments were created in GeneSpring with all possible pairs of samples. A filter was applied to remove any genes that were consistently flagged as absent. These “pairwise” comparisons were used to identify genes that were up and down regulated (using an arbitrary two fold cut off) between the five cell lines. These lists (which contained hundreds of genes each) were overlapped (using the Venn diagram function in GeneSpring) to find genes that were consistently up or down regulated in invasive samples relative to poorly invasive samples. Using this single data set, 31 genes came through the above analysis. Genes emboldened were analysed by semi quantitative RT-PCR to confirm that the array results were reflective of gene expression across the DLKP cell model.

Table 3.1.1 Genes 2X down-regulated on genelist 1

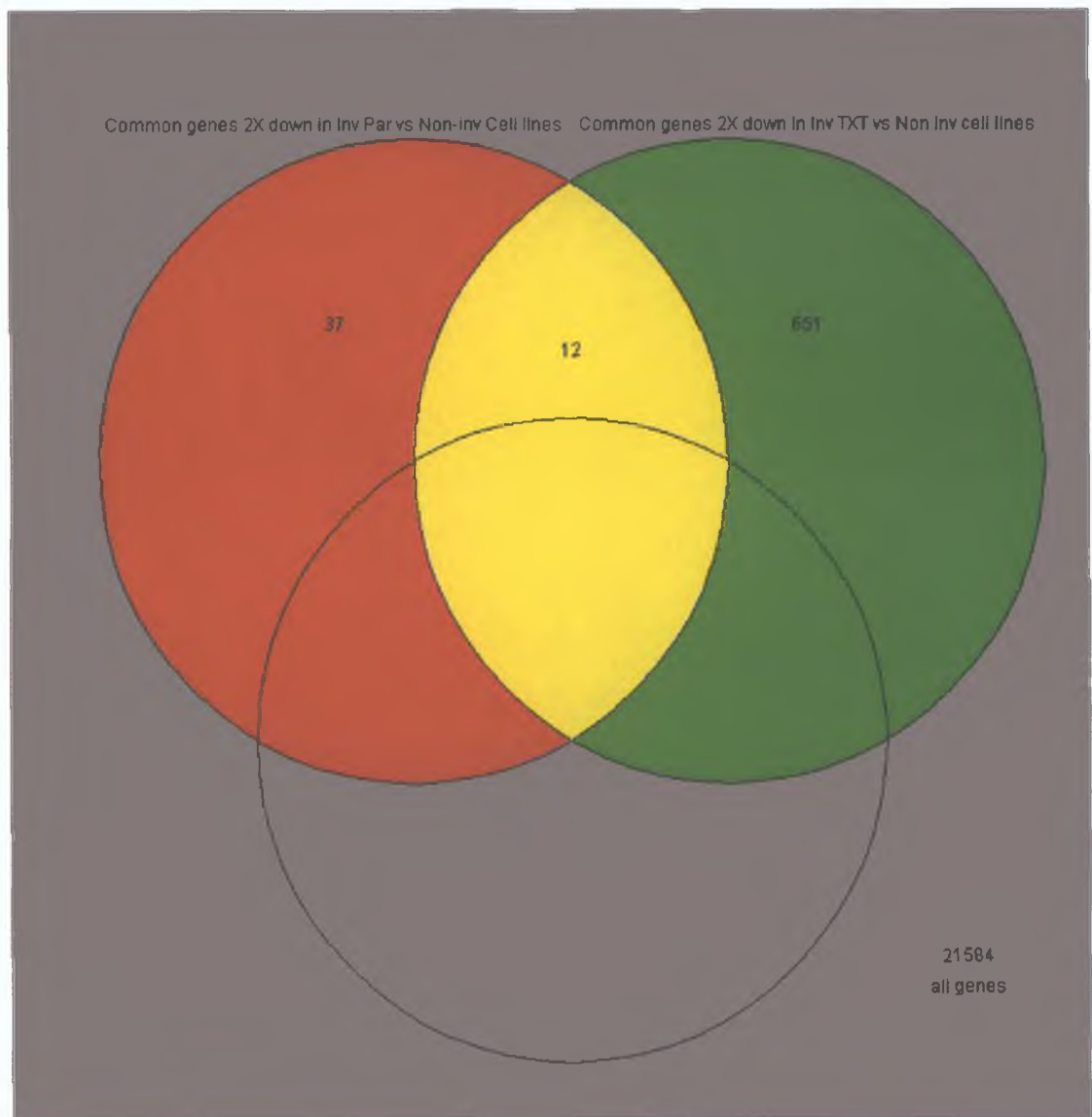


Figure 3.1.4 Genes Downregulated with respect to invasion from Pairwise analysis.

Pairwise comparisons were used to identify genes whose expression was different (using an arbitrary two fold cut off) between the five cell lines. These lists, containing hundreds of genes each, were overlapped using the Venn diagram function in GeneSpring to identify genes that were consistently down regulated in invasive samples relative to poorly invasive samples. Eleven genes were identified as having decreased expression in the invasive cell lines (there was two different probe sets reported for one of the genes).

Symbol	Gene Name	Function (if known)
VAMP4	vesicle-associated membrane protein 4	Vesicle associated protein trafficking
HLA-DRB1	Major Histocompatibility Complex, Class II, Dr β -1	MHC class II antigen
NRG1	neuregulin 1	Neurogenesis embryonic development cell differentiation
SLC4A7	solute carrier family 4, sodium bicarbonate cotransporter, member 7	Anion transport bicarbonate transport
SPP1	secreted phosphoprotein 1 (osteopontin, bone sialoprotein I, early T-lymphocyte activation 1)	anti-apoptosis cell-matrix adhesion, cell-cell signalling negative regulation of bone mineralization immune cell chemotaxis
TEM6/TENS1	tensin-like SH2 domain containing 1	protein amino acid dephosphorylation intracellular signaling cascade
RANBP2	RAN binding protein 2	protein folding protein-nucleus import transport
GLI	glioma-associated oncogene homolog 1 (zinc finger protein)	regulation of transcription from Pol II promoter signal transduction development regulation of smoothed signaling pathway
SCHIP1	schwannomin interacting protein 1	unknown
ATP9A	ATPase, Class II, type 9A	cation transport metabolism
TFPI2	tissue factor pathway inhibitor 2	serine-type endopeptidase inhibitor activity extracellular matrix structural constituent protease inhibitor activity

Table 3.1.2 Genes 2X up-regulated on genelist 1

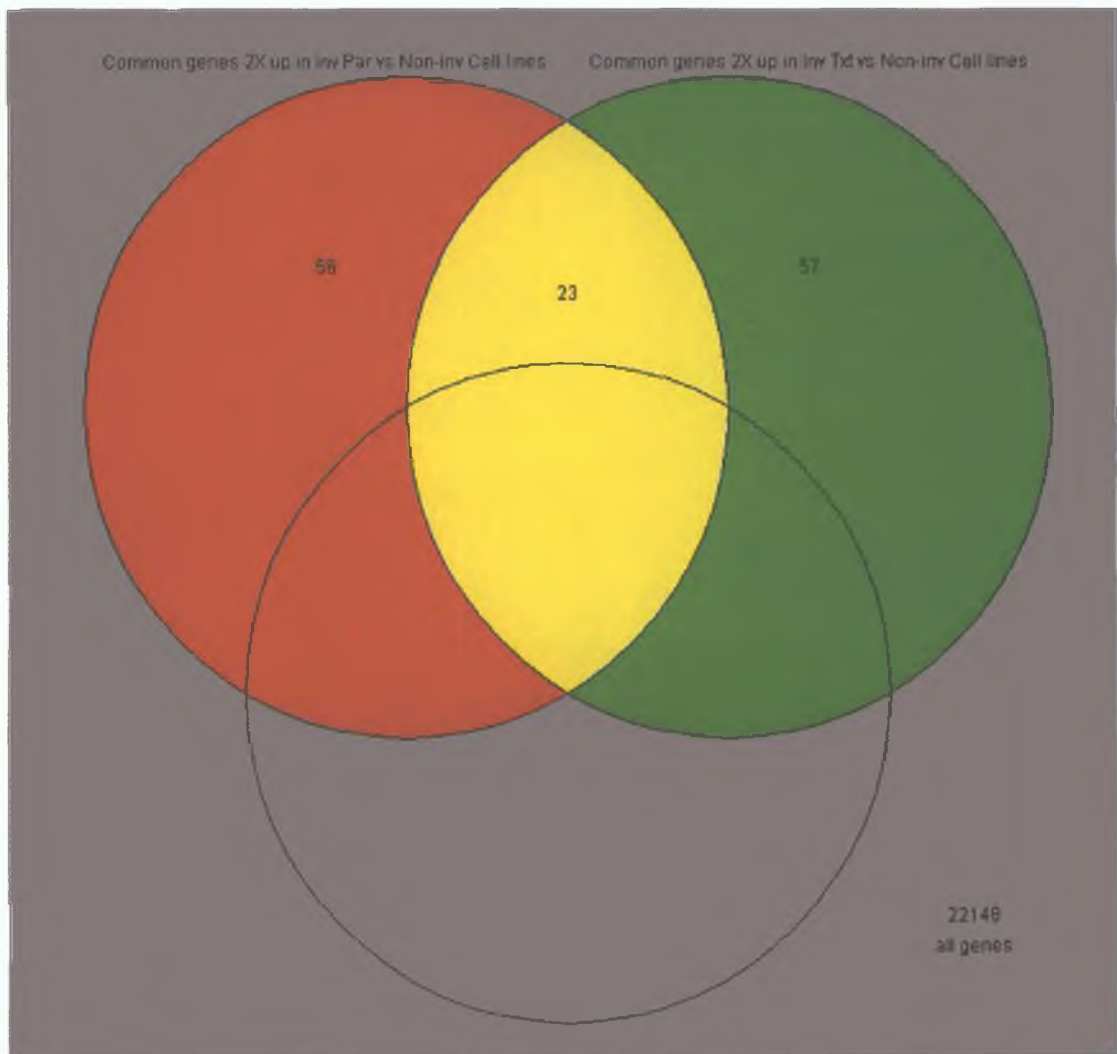


Figure 3.1.5 Genes Upregulated with respect to invasion from Pairwise analysis. Pairwise comparisons were used to identify genes whose expression was changing (using an arbitrary two fold cut off) between the five cell lines. These lists, containing hundreds of genes each, were overlapped using the Venn diagram function in GeneSpring to identify genes whose expression were consistently up regulated in invasive samples relative to poorly invasive samples. 23 genes were identified as having decreased expression in the invasive cell lines (Some of these 23 probe sets identified, reported increased expression for the same gene).

Symbol	Gene Name	Function (if known)
PRLR	prolactin receptor	anti-apoptosis, cell surface receptor linked signal transduction, transmembrane receptor protein, tyrosine kinase activation (dimerization)
GLP1R	glucagon-like peptide 1 receptor	generation of precursor metabolites and energy G-protein coupled receptor protein, signaling pathway, adenylate cyclase activation
BCHE	butyrylcholinesterase	beta-amyloid binding cholinesterase activity, serine esterase activity, hydrolase activity, enzyme binding
TLX1	T-cell leukemia, homeobox 1	unknown
loc51159	colon carcinoma related protein	unknown
KCNJ8	potassium inwardly-rectifying channel, subfamily J, member 8	voltage-gated ion channel activity, potassium channel activity, ATP-activated inward rectifier potassium channel activity
TEM7 PLXDC1	plexin domain containing 1	Angiogenesis development
CYB5R2	cytochrome b5 reductase b5R.2	electron transport
DSCR6	Down syndrome critical region gene 6	unknown
MFAP2	microfibrillar-associated protein 2	extracellular matrix structural constituent
ICAM1	intercellular adhesion molecule 1 (CD54), human rhinovirus receptor	cell-cell adhesion, transmembrane receptor activity, protein binding
SOX13	SRY (sex determining region Y)-box 13	regulation of transcription, DNA dependent morphogenesis
SFN	stratifin	regulation of cell cycle, negative regulation of protein kinase activity, signal transduction, cell proliferation
IGF-1R	Insulin-like growth factor 1 receptor	regulation of cell cycle, protein amino acid phosphorylation, anti apoptosis, signal transduction, positive regulation of cell proliferation, insulin receptor signaling pathway
AKAP11	A kinase (PRKA) anchor protein 11	protein kinase cascade

3.1.2.2 Genelist 2

Genelist 2 (Table 3.1.3) was generated in a similar manner to genelist 1, except the raw data from the duplicate DLKP variant sample set was analysed. Again, pairwise comparisons were used to identify genes that were up and down regulated (using an arbitrary two fold cut off) between the five DLKP variants. These lists were compared using the Venn diagram function in GeneSpring and genes that were consistently up or down regulated in invasive samples relative to poorly invasive samples were identified. Genes emboldened were subject to RT-PCR confirmation of differential expression.

Table 3.1.3 Genelist 2

Symbol	Gene Name	Function (if known)
DHRS1	dehydrogenase/reductase (SDR family) member 1	metabolism
S100A13	S100 calcium binding protein A13	cell differentiation, calcium ion binding
EFNB2	ephrin-B2	cell-cell signalling, neurogenesis, morphogenesis
TFPI2	tissue factor pathway inhibitor 2	serine-type endopeptidase inhibitor activity, extracellular matrix structural constituent, protease inhibitor activity
VEGF-C	vascular endothelial growth factor C	regulation of cell cycle, angiogenesis, substrate-bound cell migration, signal transduction, cell proliferation, positive regulation of cell proliferation
MAP3K12		Signal transduction
MGC39900	hypothetical protein MGC39900	cytoskeleton organization and biogenesis, actin binding
SFN	stratifin	regulation of cell cycle, negative regulation of protein kinase activity, signal transduction, cell proliferation

3.1.2.3 Genelist 3

Pairwise comparisons were also used to generate Genelist 3 (Table 3.1.4) in a manner similar to that used to generate gnelists 1 and 2, except that the triplicate DLKP variant microarray data set was included for analysis. RT-PCR was employed to investigate the expression of genes in bold to confirm the trends indicated by the array data. Genelist 3 contained genes that were potentially differentially expressed in the invasive cell lines DLKP-1, DLKP-2 and DLKP-TXT-2, compared with the poorly invasive DLKP-TXT-1 and DLKP-VCR.

Table 3.1.4 Genelist 3

Symbol	Gene Name	Function (if known)
ABCG5	ATP-binding cassette, sub-family G (WHITE), member 5 (sterolin 1)	Transport cholesterol absorption
ADAM7	a disintegrin and metalloproteinase domain 7	proteolysis and peptidolysis metalloendopeptidase activity
ARHGAP8	Rho GTPase activating protein 8	GTPase activator activity
CACNALc	Calcium channel, voltage-dependent, L type, alpha 1C subunit	voltage-gated calcium channel activity, cation channel activity, calcium ion binding
CORO2B	coronin, actin binding protein, 2B	actin cytoskeleton organization and biogenesis
CXCL13	chemokine (C-X-C motif) ligand 13 (B-cell chemoattractant)	Chemotaxis, inflammatory response, positive regulation of cytosolic calcium ion concentration, cell-cell signaling
CYLC1	cylicin, basic protein of sperm head cytoskeleton 1	structural molecule activity
DLG5	discs, large homolog 5 (Drosophila)	regulation of cell cycle, intracellular signaling cascade, cell-cell adhesion
flj11467	Hypothetical protein FLJ11467	unknown
flj22639	hypothetical protein FLJ22639	unknown
GAD1	glutamate decarboxylase 1	glutamate decarboxylase activity, protein binding lyase activity
GATA6	GATA binding protein 6	transcription factor activity, zinc ion binding, transcriptional activator activity
GLI	glioma-associated oncogene homolog 1 (zinc finger protein)	regulation of transcription from Pol II promoter, signal transduction,

		development, regulation of smoothed signaling pathway
GPT	glutamic-pyruvate transaminase (alanine aminotransferase)	Gluconeogenesis, nitrogen compound metabolism, biosynthesis
HEMK	HemK methyltransferase family member 1	DNA methylation, protein amino acid methylation
KCNK13	potassium channel, subfamily K, member 13	voltage-gated ion channel activity, potassium channel activity
KRT18	keratin 18	structural constituent of cytoskeleton
KRTAP1-1	keratin associated protein 1-1	structural constituent of epidermis
LAPTM5	lysosomal associated multispinning membrane protein 5	unknown
LY6G6E	lymphocyte antigen 6 complex, locus G6E	unknown
MBLL39	muscleblind-like 2	nucleic acid binding
MRPS6	Mitochondrial ribosomal protein S6	protein biosynthesis
ORM1	orosomucoid 1	transporter activity
PHF3	PHD finger protein 3	Transcription, regulation of transcription, DNA-dependent development
PIB5PA	phosphatidylinositol (4,5) biphosphate 5-phosphatase, A	inositol or phosphatidylinositol phosphatase activity inositol-polyphosphate 5 phosphatase activity hydrolase activity
PIK3R4	Phosphoinositide-3-kinase, regulatory subunit 4, p150	protein serine/threonine kinase activity, binding ATP binding, transferase activity
PLA2G2E	phospholipase A2, group IIE	phospholipase A2 activity, calcium ion binding, hydrolase activity
PTK6	PTK6 protein tyrosine kinase 6	non-membrane spanning protein tyrosine kinase activity, ATP binding, transferase activity
PXR1	peroxisomal biogenesis factor 1	protein transport
TACSTD2	tumor-associated calcium signal transducer 2	cell surface receptor linked signal transduction, visual perception, cell proliferation
TFPI2	tissue factor pathway inhibitor 2	serine-type endopeptidase inhibitor activity, extracellular matrix structural constituent, protease inhibitor activity
TNS	Tensin	intracellular signaling cascade

3.1.2.4 Genelist 4

The data was further analysed to generate genelist 4 (Table 3.1.5), this time using a different approach on all fifteen chips. Genes that did not cross a two-fold threshold above or below the median in at least one cell line were removed from the analysis, as were genes that were consistently called absent by the Affymetrix software. A Welch ANOVA statistical test was used to find genes that were reliably differentially expressed between the five different cell lines. Subsequently, a further Welch ANOVA test was used to find genes in this list that were useful in discriminating between invasive and non-invasive samples. This generated a gene list containing 45 genes, whose expression patterns (see heatmap Figure 3.1.6) were analysed visually to identify 18 possible invasion related genes i.e. genelist 4.

Table 3.1.5 Genelist 4

Symbol	Gene Name	Function (if known)
ATP9A	ATPase, Class II, type 9A	cation transport metabolism
CD34	Cd34 antigen	Adhesion molecule
DPEP3		unknown
EFNB2	ephrin-B2	cell-cell signalling, neurogenesis, morphogenesis
flj23033	Hypothetical protein	unknown
flj23091	Hypothetical protein	unknown
GDAP1L1	Ganglioside-induced differentiation-associated protein 1-like 1	GST-like protein
GLI	glioma-associated oncogene homolog 1 (zinc finger protein)	regulation of transcription from Pol II promoter, signal transduction, development, regulation of smoothed signaling pathway
HGF	Hepatocyte growth factor	regulation of cell cycle, substrate-bound cell migration, signal transduction, cell proliferation, positive regulation of cell proliferation
ICAM1	intercellular adhesion molecule 1 (CD54), human rhinovirus receptor	cell-cell adhesion, transmembrane receptor activity, protein binding
JAG2	Jagged 2	Cell signalling

mgc39900	hypothetical protein MGC39900	cytoskeleton organization and biogenesis, actin binding
PLXDC1 (tem7)	plexin domain containing 1	Angiogenesis development
S100A13	S100 calcium binding protein A13	cell differentiation, calcium ion binding
SCHIP1	schwannomin interacting protein 1	unknown
SFN	stratifin	regulation of cell cycle, negative regulation of protein kinase activity, signal transduction, cell proliferation
TLX1	T-cell leukemia, homeobox 1	unknown

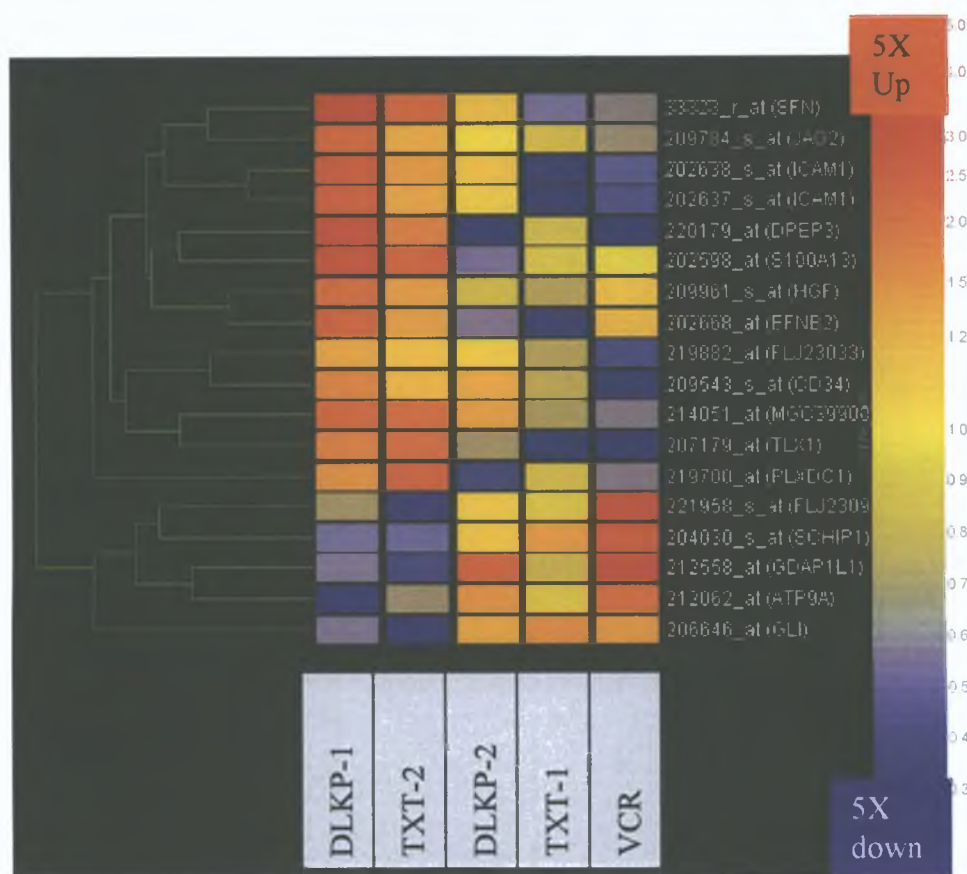


Fig 3.1.6 Heatmap of Gene-expression.

In this expression heatmap there is a gene on each row and the five columns represent our five cell lines. Genes are coloured red if they are upregulated relative to the median for that gene. A blue colour indicates downregulation. The gene tree to the left of the heatmap (in green) shows groups of genes with similar expression patterns (as grouped by the Pearson correlation). The genes on this heatmap are differentially expressed the in invasive versus poorly invasive DLKP variants and are detailed in Table 3.1.5 above.

3.1.2.5 Genelist 5

Rather than grouping the samples into invasive and non-invasive, an arbitrary scale of invasion was applied to reflect the intermediate degrees of invasion displayed by the cell lines in the *in vitro* invasion assay. The scale was as follows:

DLKP-1 = 5

DLKP-2 = 3.5

DLKP-TXT-1 = 1

DLKP-TXT-2 = 5

DLKP-VCR = 0

To analyse the data using this scale, a filter was applied that included genes that were present or marginal in three out of 15 samples and also genes whose expression were 1.5 fold increased or decreased in three out of 15 samples. A genelist was made of the genes that passed these stipulations. A Welch ANOVA (settings: P-value; 0.01, no multiple testing correlation) was applied to this list using the invasion scale mentioned above. 531 genes came through this statistical test and are referred to as consistently changing genes.

These 531 consistently changing genes were put into Self Organising Maps (SOMs) (Figure 3.1.7). SOMs group together genes with similar expression pattern in clusters. The user defines the number of clusters into which the genes should be organised. The SOMs for the 531 changing genes relate to invasiveness only but a similar approach could be used to group genes related to drug resistance. A 7x6 SOM (log scale) was used to organise the 531 changing genes into clusters with similar expression patterns. Interesting expression patterns that may relate to invasion were chosen visually. The clusters picked for further analysis were (2,1), (5,1), (6,1), (3,7), (4,7), (5,7), (6,7) (where the 1st number relates to the cluster and the second number relates to the row the cluster is on). These reflect genes which either generally increase or generally decrease with invasion i.e. genelist 5 (Tables 3.1.6 and 3.1.7).

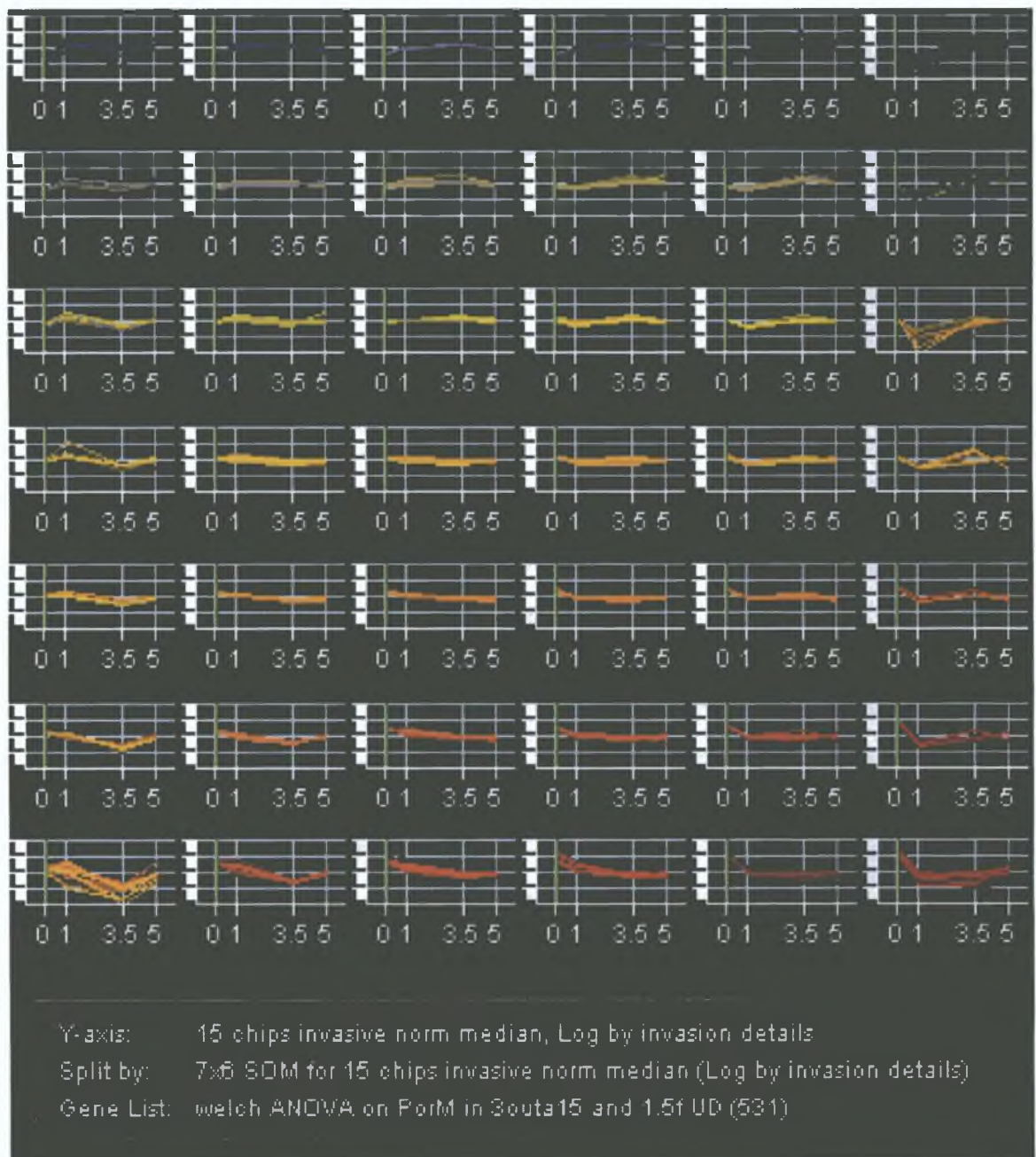


Figure 3.1.7 7x6 SOMs for the 531 changing genes based on the invasion scale derived from invasion assay.

Interesting expression patterns that may relate to invasion were chosen visually. The clusters picked for further analysis were (2,1), (5,1), (6,1), (3,7), (4,7), (5,7), (6,7) (where the 1st number relates to the cluster and the second number relates to the row the cluster is on). These reflect genes that either generally increase or generally decrease with invasion.

Table 3.1.6 Genelist 5; Genes with negative correlation to invasion from SOMs

Symbol	Gene Name	Function (if known)
ARK5	AMP-activated protein kinase family member 5	protein kinase activity, protein serine/threonine kinase activity, ATP binding transferase activity
BEX1	brain expressed, X-linked 1	unknown
CD24	CD24 antigen (small cell lung carcinoma cluster 4 antigen)	humoral immune response
CRYAB	crystallin, alpha B	protein folding, muscle contraction, visual perception
CSRP2	cysteine and glycine-rich protein 2	muscle development, cell proliferation, cell growth, cell differentiation
ENC1	ectodermal-neural cortex (with BTB-like domain)	actin binding, protein binding, development, neurogenesis
flj10097	Hypothetical protein	unknown
FN1	fibronectin 1	acute-phase response, cell adhesion, metabolism, response to wounding, cell migration
FSTL1	follistatin-like 1	calcium ion binding, heparin binding
GAS1	growth arrest-specific 1	cell cycle arrest, negative regulation of cell proliferation, negative regulation of S phase of mitotic cell cycle
GPC3	glypican 3	morphogenesis
HIST1H2BK	histone 1, H2bk	nucleosome assembly, chromosome organization and biogenesis
IFIT1	interferon-induced protein with tetratricopeptide repeats 1	immune response
IGFBP7	insulin-like growth factor binding protein 7	regulation of cell growth, negative regulation of cell proliferation, insulin-like growth factor binding
ISL1	ISL1 transcription factor, LIM/homeodomain, (islet-1)	regulation of transcription, DNA-dependent
KCTD12	potassium channel tetramerisation domain containing 12	voltage-gated potassium channel activity
kiaa0992	palladin	unknown
LAMB1	laminin, beta 1	cell adhesion, structural molecule activity, protein binding
LRRN3	leucine rich repeat neuronal 3	unknown

MDM1	Mdm4, transformed 3T3 cell double minute 1, p53 binding protein	unknown
MT1F	metallothionein 1F	copper ion binding, zinc ion binding, cadmium ion binding, metal ion binding
MT1H	metallothionein 1H	metal ion binding
MT1X	metallothionein 1X	metal ion binding
NELL2	NEL-like 2	cell adhesion, structural molecule activity, calcium ion binding
OASL	2'-5'-oligoadenylate synthetase-like	protein modification, immune response
OIP106	OGT(O-Glc-NAc transferase)-interacting protein 106 KDa	protein binding
PCDH7	BH-protocadherin	cell adhesion, homophilic cell adhesion
PHLDA1	pleckstrin homology-like domain, family A, member 1	unknown
PI15	protease inhibitor 15	peptidase activity, trypsin inhibitor activityF
PPM1D	protein phosphatase 1D magnesium-dependent, delta isoform	regulation of cell cycle, protein amino acid dephosphorylation, negative regulation of cell proliferation, response to radiation
PRSS12	protease, serine, 12	proteolysis and peptidolysis
RAP1B	RAP1B, member of RAS oncogene family	intracellular protein transport, small GTPase mediated signal transduction
SFRP4	secreted frizzled-related protein 4	signal transduction, embryo implantation, Wnt receptor signaling pathway
SGK	serum/glucocorticoid regulated kinase	protein serine/threonine kinase activity, ATP binding, transferase activity
SPP1	secreted phosphoprotein 1	cytokine activity, integrin binding, protein binding, growth factor activity
TBX2	T-box 2	regulation of transcription, DNA-dependent, development
TITF1	thyroid transcription factor 1	regulation of transcription, DNA-dependent
TNFSF10	tumor necrosis factor (ligand) superfamily, member 10	Apoptosis, induction of apoptosis, immune response, signal transduction, cell-cell signalling, positive regulation of I-kappaB kinase/NF-kappaB cascade
TNNC1	troponin C, slow	calcium ion binding
ZFPM2	zinc finger protein, multitype 2	regulation of transcription, DNA-dependent
ARK5	AMP-activated protein kinase	protein kinase activity, protein

	family member 5	serine/threonine kinase activity, ATP binding, transferase activity
BEX1	brain expressed, X-linked 1	unknown
CRYAB	crystallin, alpha B	protein folding, muscle contraction, visual perception
CSRP2	cysteine and glycine-rich protein 2	muscle development, cell proliferation, cell growth, cell differentiation
DAB2	disabled homolog 2, mitogen-responsive phosphoprotein	cell proliferation
dkfzp586a0522	DKFZP586A0522 protein	S-adenosylmethionine-dependent methyltransferase activity, transferase activity
EGF	epidermal growth factor	epidermal growth factor receptor activating ligand activity, calcium ion binding, growth factor activity

Table 3.1.7 Genelist 5; Genes with positive correlation to invasion from SOMs

Symbol	Gene Name	Function (if known)
ARHGAP4	Rho GTPase activating protein 4	cytoskeleton organization and biogenesis, Rho protein signal transduction SH3/SH2 adaptor protein activity, Rho GTPase activator activity
CAMK1	calcium/calmodulin-dependent protein kinase I	protein serine/threonine kinase activity, calcium- and calmodulin-dependent protein kinase activity, calmodulin binding, ATP binding, transferase activity
CD34	CD34 antigen	cell adhesion, protein binding
CDH10	cadherin 10, type 2 (T2-cadherin)	homophilic cell adhesion, calcium ion binding, protein binding
CDH2	cadherin 2, type 1, N-cadherin	cell adhesion calcium ion binding, protein binding
CUGBP2	CUG triplet repeat, RNA binding protein 2	RNA binding
EFHC1	EF-hand domain (C-terminal) containing 1	calcium ion binding
HOXA10	homeo box A10	regulation of transcription, DNA-dependent, development
HOXA2	homeo box A2	regulation of transcription, DNA-dependent, development
HOXA9	homeo box A9	Transcription, regulation of transcription, DNA-dependent, development
IGF-1R	Insulin-like growth factor 1 receptor	regulation of cell cycle, protein amino acid phosphorylation, anti-apoptosis, signal transduction, positive regulation of cell proliferation, insulin receptor signaling pathway
IGFBP3	insulin-like growth factor binding protein 3	regulation of cell growth, negative regulation of signal transduction, positive regulation of apoptosis, positive regulation of myoblast differentiation, insulin-like growth factor binding, protein tyrosine phosphatase activator activity, metal ion binding
IRS1	insulin receptor substrate 1	signal transduction from IGF-1R

KCNJ8	potassium inwardly-rectifying channel, subfamily J, member 8	voltage-gated ion channel activity, potassium channel activity, ATP-activated inward rectifier potassium channel activity
MMP3	matrix metalloproteinase 3 (stromelysin 1, progelatinase)	stromelysin 1 activity, calcium ion binding, zinc ion binding hydrolase activity
MRPS10	mitochondrial ribosomal protein S10	protein biosynthesis
NRG1	neuregulin 1	receptor binding, growth factor activity, transmembrane receptor protein tyrosine kinase activator activity, receptor tyrosine kinase binding
PDE4B	phosphodiesterase 4B, cAMP-specific	signal transduction
PLCB4	phospholipase C, beta 4	phosphoinositide phospholipase C activity, signal transducer activity, calcium ion binding, hydrolase activity
PLXNC1	Plexin C1	cell adhesion, development
PROCR	protein C receptor, endothelial (EPCR)	receptor activity
RGC32	response gene to complement 32	regulation of cyclin dependent protein kinase activity
SCG2	secretogranin II	calcium ion binding
SMS	spermine synthase	spermidine synthase activity, transferase activity, spermine synthase activity
SSX1	synovial sarcoma, X breakpoint 1	regulation of transcription, DNA-dependent
SSX2	synovial sarcoma, X breakpoint 2	regulation of transcription, DNA-dependent, G-protein coupled receptor protein signaling pathway,
SSX4	synovial sarcoma, X breakpoint 4	regulation of transcription, DNA-dependent
TACSTD1	tumor-associated calcium signal transducer 1	unknown
TCF4	transcription factor 4	regulation of transcription from Pol II promoter
TLE4	transducin-like enhancer of split 4 (E(sp1) homolog, Drosophila)	regulation of transcription, DNA-dependent, frizzled signaling pathway
TLX1	T cell homeobox 1	unknown
VEGF	vascular endothelial growth factor	regulation of cell cycle, angiogenesis, vasculogenesis, response to stress, signal

		transduction, neurogenesis, cell proliferation, positive regulation of cell proliferation, cell migration, positive regulation of vascular endothelial growth factor receptor signaling pathway, negative regulation of apoptosis, induction of positive chemotaxis
--	--	---

3.1.3 Data analysis using Genomatix software suite

Genomatix provide software that allows users to explore published studies as well as combine sequence analysis, and genome annotation in order to help researchers to get a complete overview of their biological data (www.genomtix.de) The software offered by Genomatix is designed to help researchers gain a better understanding of gene regulation at the molecular level. The Genomatix software suite is comprised of six main tools: ElDorado, Gene2Promoter, BiblioSphere, GEMS Launcher, MatInspector and PromoterInspector. ElDorado is a gene orientated genome search engine that provides the user with information about functional genomic elements within a specific region of the genome. This piece of software compiles and integrates information on gene function and regulatory pathway. In addition, information on mRNAs, their exon/intron structure and coding sequences, single nucleotide polymorphisms (SNPs) and potential promoter regions may be retrieved using ElDorado. The hypothesis underlying this type of analysis is that genes with similar expression patterns may be co-regulated and therefore may be activated by the same transcriptional signals.

BiblioSphere is a data-mining solution for extracting and studying gene relationships from literature databases and genome-wide promoter analysis. Based on PubMed (www.ncbi.nlm.nih.gov), BiblioSphere currently searches over 14 million abstracts. The unique data-mining strategy allows direct gene-gene co-citations and even yet unknown gene relations to be found via interlinks. BiblioSphere data is displayed as 3D interactive view of gene relationships (Figure 3.1.8). Results can be classified by tissue, Gene Ontology and Medical Subject Headings (MeSH). Statistical ratings by z-scores indicate over- and under-representation of genes in the various biological categories. BiblioSphere can be applied to single gene analysis, gene cluster analysis and analysis of gene regulatory mechanisms.

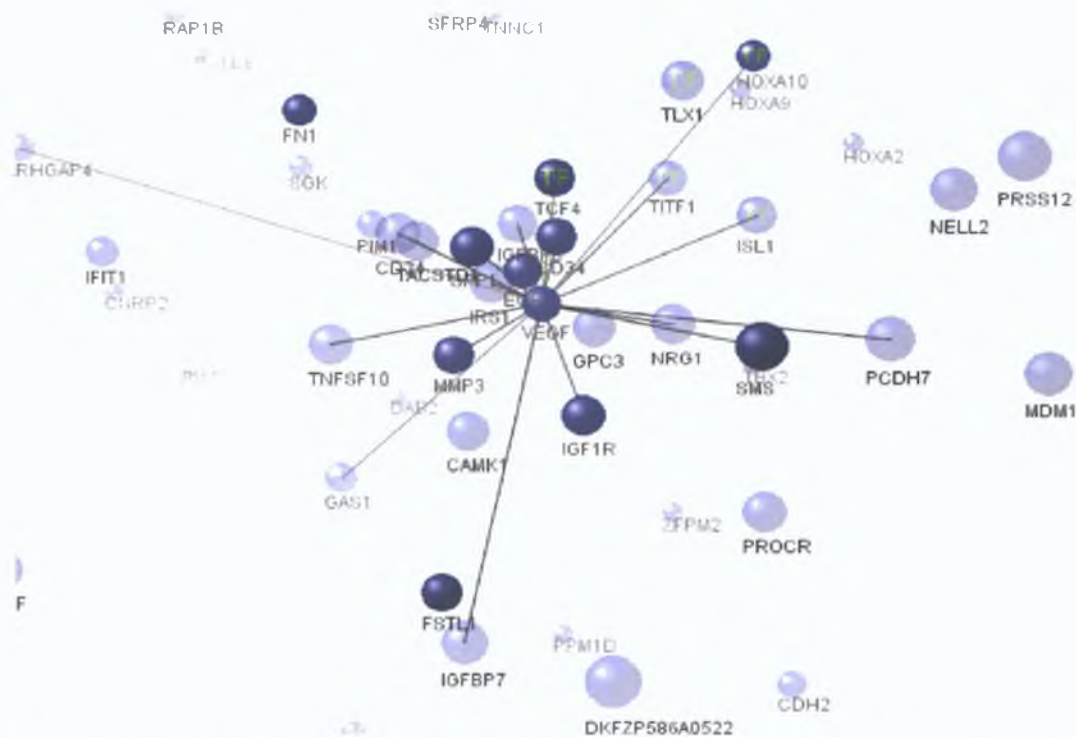


Figure 3.1.8 BiblioSphere analysis of the genes identified as potentially related to invasion from the SOM expression clusters.

The cluster contains all input genes. The dark blue spheres relate to the neoplasm invasiveness MeSH filter. The faded blue spheres represent genes that do not relate to this disease filter. Genes that have a grey line linking them are co-cited genes in relation to this filter. A green line from a sphere labelled “TF” signifies a transcription factor-binding site in the promoter of that gene.

The Genomatix analysis generated (as described in section 2.16.3) two promoter models each containing 5 elements involving three genes, VEGF, FSTL1 and FN1 (Figures 3.1.9 and 3.1.10). Since co-regulation of gene transcription often originates from common promoter elements the identification and characterisation of these elements provides a more in-depth analysis for the expression of microarray genelists. Gene2Promoter allows users to automatically extract groups of promoters for genes that may be of interest. The FW score for these models is 0.75. These scores allow to assess the quality of a model generated by FrameWorker: The higher the scores, the more specific is the extracted model. A very low FW-score (<0.5) indicates a model that is likely to match very often in random DNA sequences. The promoter models generated suggest possible co-regulation of these three genes, VEGF, FSTL1 and FN1. These promoter models are comprised of the zinc binding protein factor family (ZBPF), the myeloid zinc finger 1 factors (MZF1) and the GC-box factors SP1/GC (SP1F). Searches were made for genes to which any of these family members bind to in the genelist of the 531 consistently changing genes. Only the SP1F transcription factors KLF5 and TIEG2 were found in this data set. Both transcription factors appear to be downregulated with increasing invasiveness based on the values for the genes in the array data.

To determine if VEGF, FSTL1 and FN1 might be co-regulated, RT-PCR analysis was performed in our cell model for those gene. The RT-PCR results did not demonstrate differential expression of these genes with invasion and were therefore not subject to further investigation.

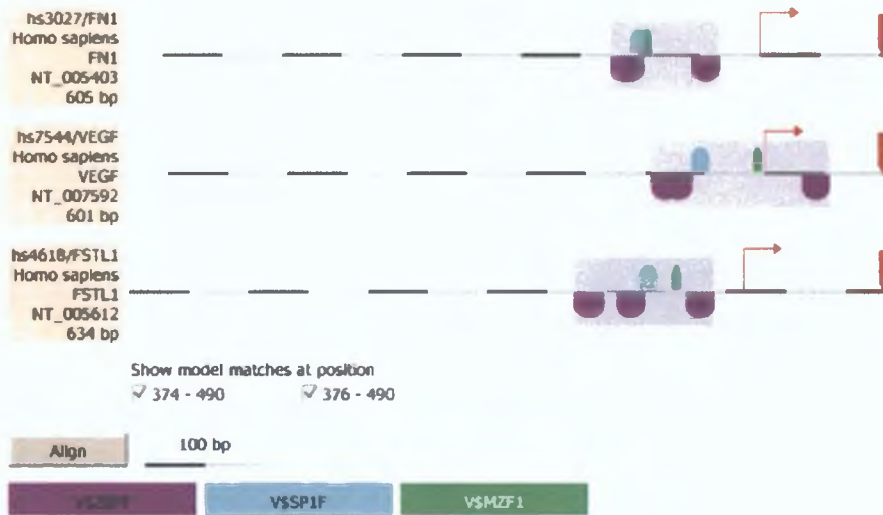


Figure 3.1.9 Promoter model 1 from Genomatix analysis.

Dashed lines signify genomic region upstream of gene sequence. Angled arrows denote transcriptional start sites; thick arrows indicate start of coding region. Coloured shapes signify TF binding sites with putative promoter modules shaded.

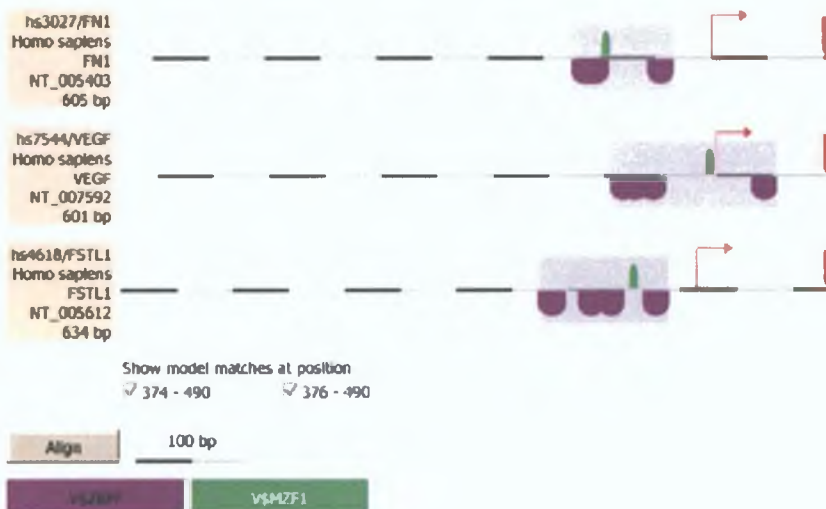


Figure 3.1.10 Promoter model 2 from Genomatix analysis.

3.2 RT-PCR confirmation of array data analysis

The genelists generated from the various bioinformatic analyses of the microarray data were subject to further scrutiny before final targets for functional analysis were chosen. In Section 3.1.2, genes highlighted in bold were subject to RT-PCR analysis in the five DLKP cell lines comprising our cell model to confirm the trends indicated by the array data.

Twenty-eight genes were selected, based on literature searches and on proposed functions for a given gene, for RT-PCR analysis across the five cell lines. The PCR was performed on the following RNA samples,

- 1 RNA used for the original single array experiment.
- 2 RNA used for the subsequent duplicate experiment.
- 3 RNA from a fresh culture of the five cell lines that were not analysed by microarray. This was to ensure that results from the array data were not an anomaly and reflected gene expression in an independent batch of the cell lines, separate to those harvested for microarray analysis.
- 4 RNA from the five DLKP cell lines over increasing passage number. This was to ensure that results from the array data were true for cells over a specific time period i.e. ten passages.

An overview of the results from the RT-PCR study is detailed in Tables 3.2.1 and 3.2.2. The actual gels representing each PCR are available for examination in the Appendices.

Table 3.2.1 Summary of RT-PCR results for genes with increased expression in invasive cell lines

Gene Symbol	Band Size (kb)	Agrees with array data	Pick as Target
AKAP11	233	No obvious expression differences in PCR	No
BCHE	180	Trend agrees with array data	Yes
CYB5R2	172	Decreased expression in VCR only, not TXT-1	No
EFNB2	220	Fluctuations in different sample sets,	No
GLP1R	228	Initial trend matches, check other samples	
ICAM1	245	Trend agrees with array data	Yes
IGF1R	241	Trend agrees with array data	Yes
KCNJ8	210	Trend agrees with array data	Yes
LOC5119	249	Not increased in invasive cell lines	No
MFAP2	422	check in other samples.	
MGC3900	219	No clear-cut expression differences in PCR	No
MMP3	214	Trend agrees with array data, need to rpt some samples	Yes
S100A13	219	Trend agrees with array data, check passaged samples.	Yes
SFN	195	Trend agrees with array data	Yes
TCF4	204	Trend agrees with array data, very. low expression in VCR samples	Yes
TEM7	239	Trend fluctuating in sets of PCR samples	No
TLX1	201	Trend agrees with array data	Yes
VEGFA	186	Optimised, No clear-cut expression differences in PCR	No
VEGFC	249	Trend agrees with array data	Yes

Table 3.2.2 Summary of RT-PCR results for genes with decreased expression in invasive cell lines

Gene Symbol	Band Size (kb)	Agrees with array data	Pick as Target
FN1	230	Consistently high expression in VCR compared to other cell lines	Yes
FSTL1	242	Slight expression differences in PCR can rpt.	No
MAP3K12	240	No obvious expression differences in PCR	No
NRG1	190	No expression differences in PCR	No
RANBP2	218	No clear-cut expression differences in PCR	No
SCHIP1	355	Trend fluctuating in sets of PCR samples	No
SPP1	244	Consistently high expression in VCR compared to other cell lines	Yes
TEM6	199	No obvious expression differences in PCR	No
TFPI2	183	Trend agrees with array data	Yes

3.3 Invasion assay confirmation of *in vitro* invasive capacity of DLKP variants

The invasion assay used to monitor *in vitro* invasion was optimised for use within this cell model. Commercial invasion assay kits containing inserts pre-coated with matrigel were used for analysis. This eliminated the risk of batch-to-batch variation possible when manually coating inserts with matrigel.

The inserts were placed in medium containing 5% serum. Cell suspensions were prepared in medium containing 1% serum and 100 μ l of a 1 \times 10⁶ cells/ml suspension was added to each insert. This provided serum gradient in the assay. The cells were incubated at 37°C for 24hr. After this time, the underside of the insert stained with crystal violet and allowed to air dry.

The invasion assay was validated by analysing fresh cultures of the DLKP variants using the optimised conditions outlined above over increasing passage number. This confirmed that the trend of invasive capacity for each cell line was consistent over ten passages (Figures 3.3.1-3.3.1.5). In order to verify that that batch-to-batch variation was negligible between the commercial kits, cells with the same passage number and from the same cell suspension were applied to two different kits with different batch and lot numbers (Figure 3.3.1.2). RT-PCR was also used for a number of selected genes to determine if gene expression patterns were consistent with the invasive capacities of the cell lines as determined using the invasion assay.

The overall trend for the DLKP cell lines is as follows, starting from the most to least invasive; TXT-2 > DLKP-1 > DLKP-2 > TXT-1 > VCR. This validation study demonstrated reproducible results over ten passages for the cell lines and confirmed the suitability of the cell lines in conjunction with the optimised invasion assay as a model system suitable for use in subsequent investigations into the molecular mechanisms of invasion. For the purposes of simplicity in subsequent Results and Discussion sections, these five cell lines will be split into two groups broadly referred to as “invasive” (TXT-2, DLKP-1, DLKP-2) and less or non-invasive lines (TXT-1 and VCR).

3.3.1 Graphical Representations of measurement of relative DLKP variant invasive capacity with increasing passage number

Fresh stocks of the DLKP variants were thawed and analysed by invasion assay over increasing passage number using commercial invasion assay kits, a serum gradient and equal cell number over 24hr. The underside of each insert was stained and the cells counted. Averaging counts from 10 fields of view with 20X magnification generated final counts, which were included in each graphical representation of the invasion assay results. Each condition was analysed using at least two inserts. The overall trend is as follows, starting from the most to least invasive; $\text{TXT-2} > \text{DLKP-1} > \text{DLKP-2} > \text{TXT-1} > \text{VCR}$. This set of experiments demonstrate reproducible trends of DLKP variant invasion capacity and verify the suitability of these cell lines for use as a cell model to study invasion using these defined parameters over ten passages

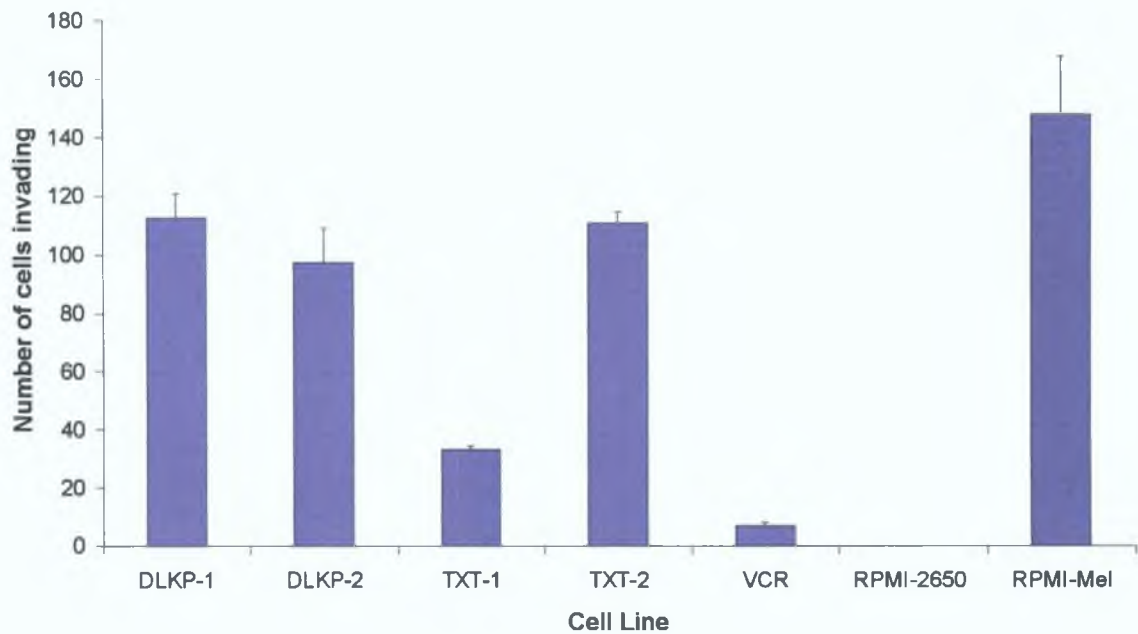


Figure 3.3.1 Measurement of relative invasion using 24hr Boyden chamber assay.

The DLKP variants are compared by invasion assay over 24hr. Counts from ten fields of view at 20X magnification per insert were averaged. At least two inserts per condition were included in each analysis and counted and the average of each insert calculated. This generated figures for the number of cells invading and allowed graphical representation of relative invasion. Counts for RPMI-2650 (non-invasive parental) and RPMI-Melphalan (RPMI-Mel) selected human nasal carcinoma cell line are included as negative and positive invasion assay controls in this study.

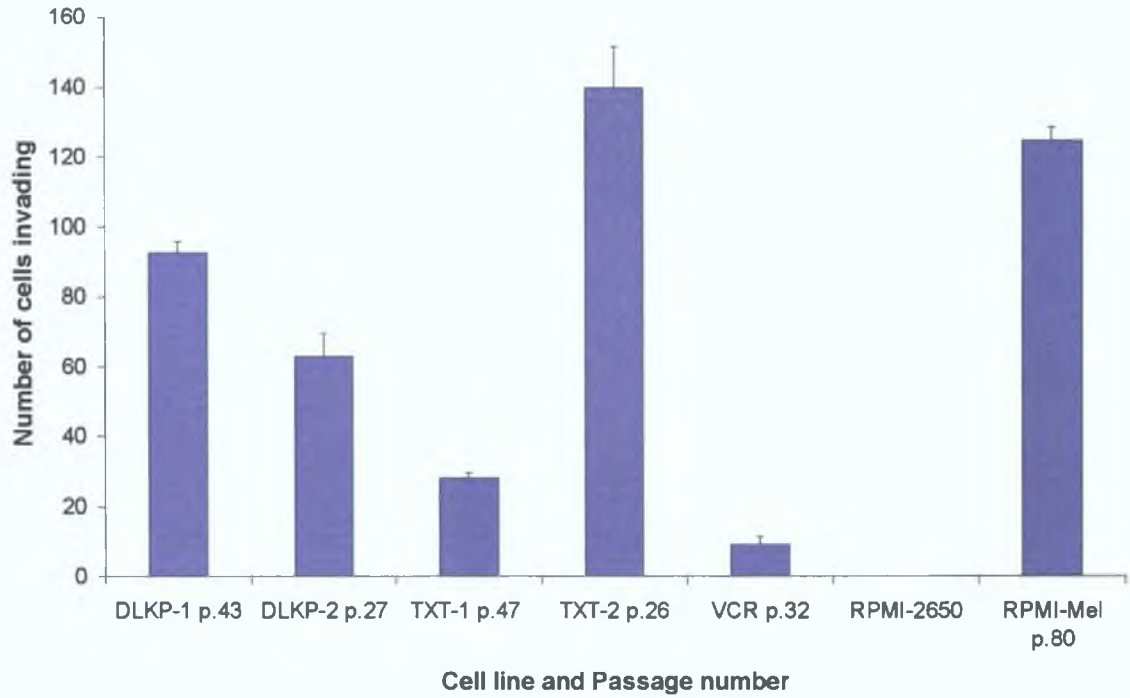


Figure 3.3.1.1 Measurement of relative DLKP invasive capacity from early passage in culture (i.e. the cells are at passage 1 in culture).

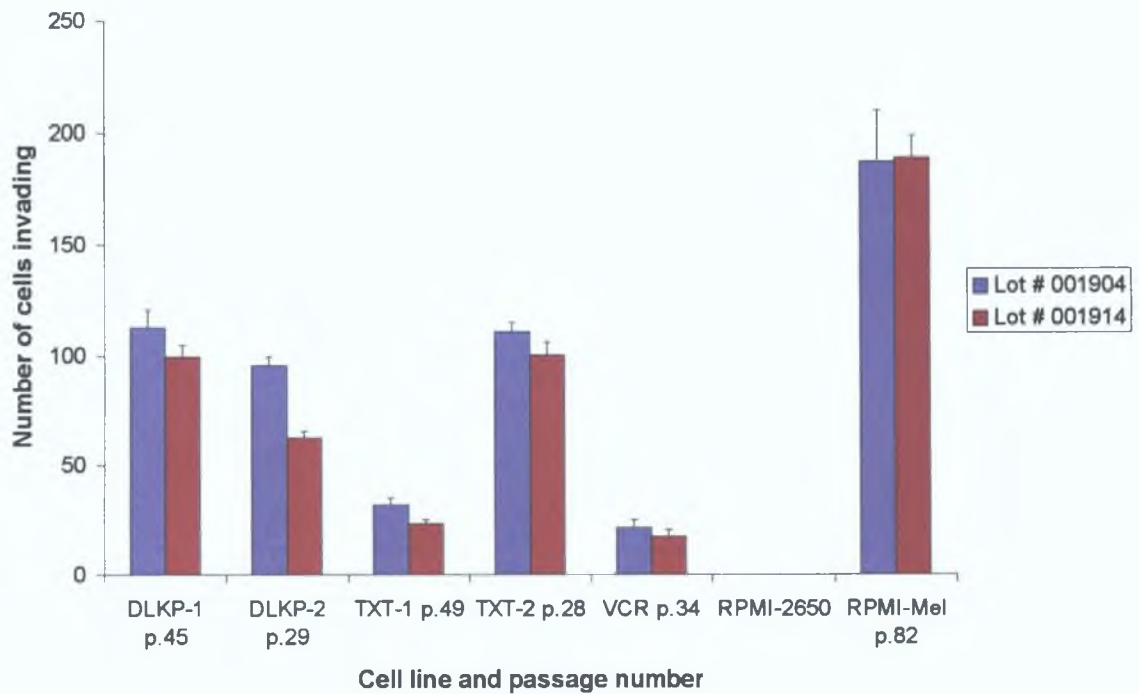


Figure 3.3.1.2 Measurement of relative DLKP invasive capacity from passage 2 in culture and comparing different invasion assay kit lot numbers to ensure consistent results.

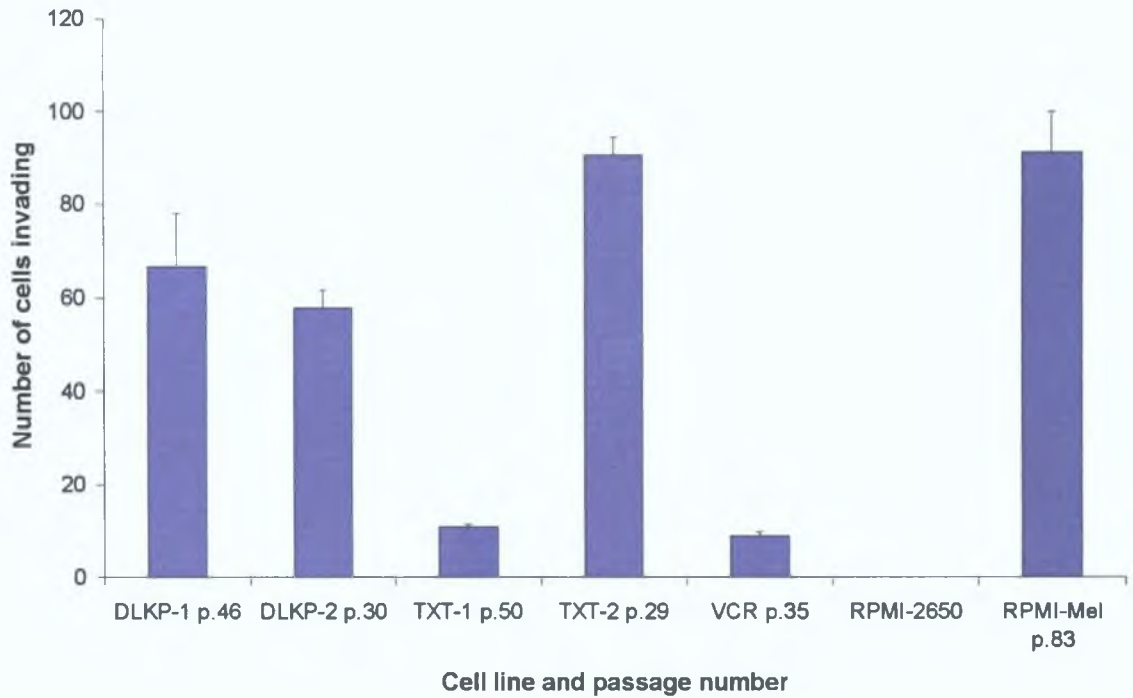


Figure 3.3.1.3 Measurement of relative DLKP invasive capacity from passage 3 in culture

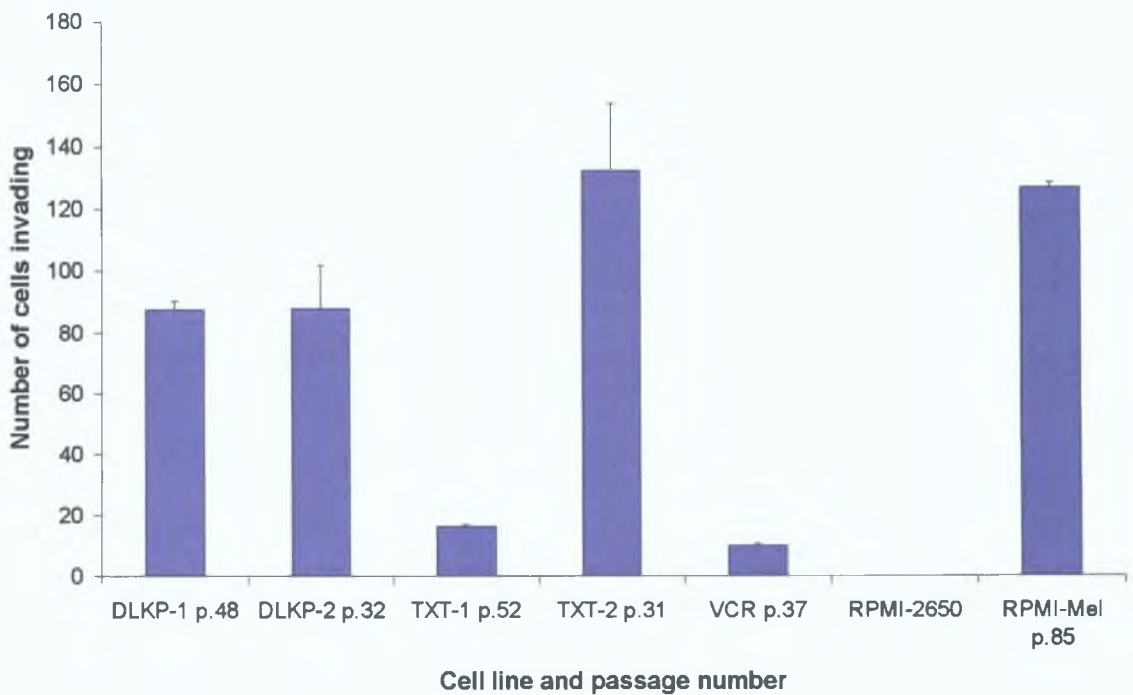


Figure 3.3.1.4 Measurement of relative DLKP invasive capacity from passage 5 in culture

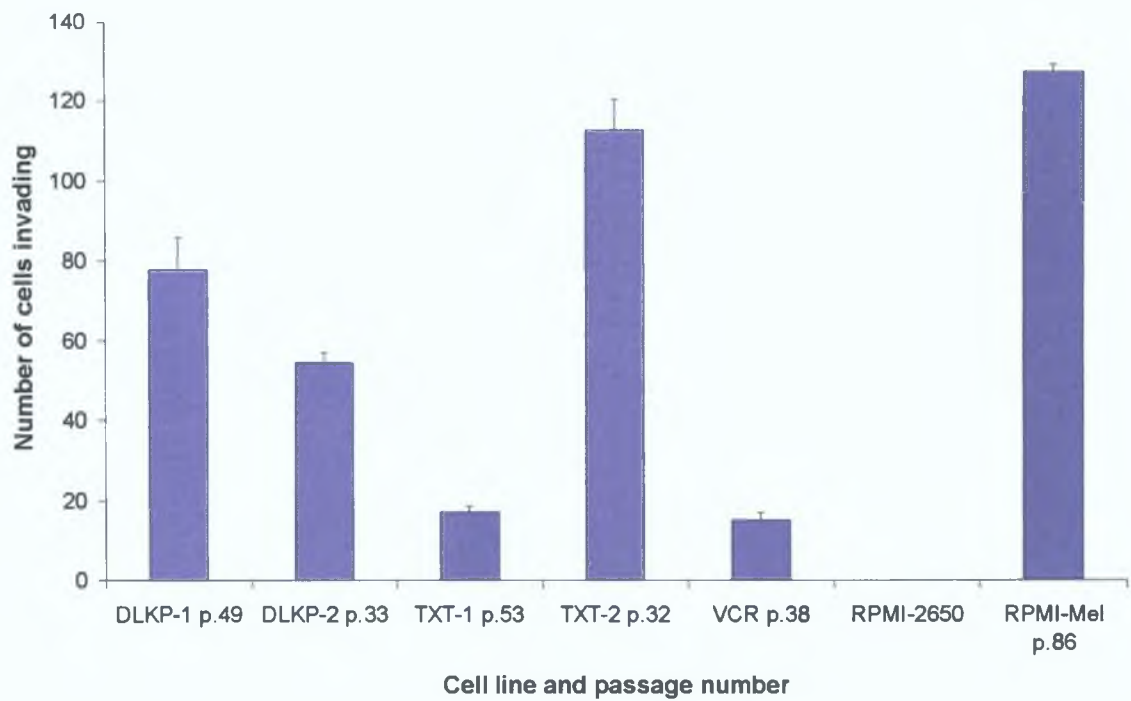


Figure 3.3.1.5 Measurement of relative DLKP invasive capacity from passage 6 in culture

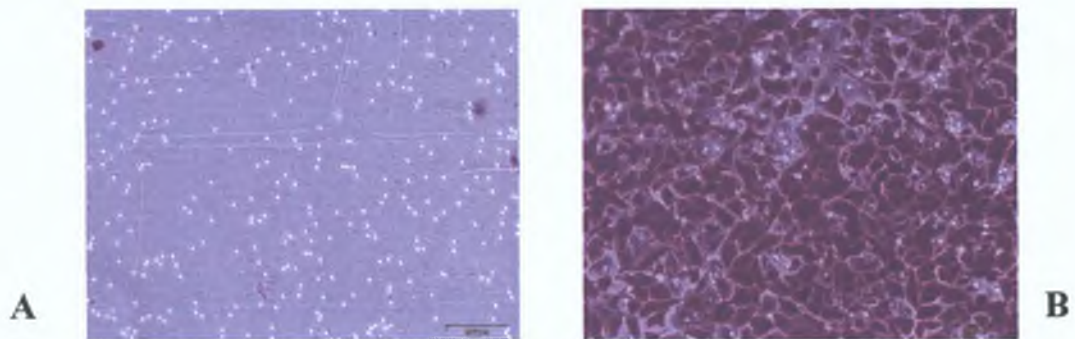


Figure 3.3.1.6 Invasion assay controls.

Photographic representation of the negative invasion control RPMI-2650 (A) and the positive invasion control RPMI-Melphalan (Mel) (B) at 10X.

3.3.2 RT-PCR validation of consistent gene expression in conjunction with consistent invasion assay results.

The mRNA expression of a number of selected genes was analysed by RT-PCR to determine if relative gene expression patterns remained consistent in parallel with the relative invasive capacities of the cell lines over a number of passages. The genes selected for RT-PCR analysis to investigate if the invasive capacities of the cell lines correlated with differential gene expression (i.e. increased/decreased mRNA expression in the invasive cell lines compared with the non-invasive cell lines) were consistent as the cell lines were cultured are detailed in Table 3.3.1. The results demonstrated that mRNA was not differentially expressed between the invasive and non-invasive cell lines for EFNB2, VEGF-C, FN1 and FSTL1. These genes were not selected for further functional analysis as a result. The trends in mRNA expression for the remaining genes were consistently differentially expressed between the invasive and non-invasive cell lines as the cell lines were cultured.

Table 3.3.1 Genes selected for RT-PCR analysis to ensure that mRNA expression correlated with invasion assay results over time.

Gene Symbol
IGF-1R
TLX-1
SFN
KCNJ8
ICAM1
EFNB2
VEGF-C
TCF4
MMP3
FN1
FSTL1
TFPI2

3.4 Investigation into role of IGF-1R in invasion in an *in vitro* cell model

3.4.1 Aims of experiments

IGF-1R was identified as a gene potentially involved in invasion in our microarray study. The microarray data analysis revealed that IGF-1R expression was increased in the more invasive cell lines compared to the lesser invasive cell lines. The aims of this set of experiments was as follows:

1. To confirm by PCR that IGF-1R was differentially expressed between the DLKP cell lines.
2. To quantify endogenous IGF-1R levels in the cell model by qRT-PCR and western blot.
3. To demonstrate transfection efficiency of the siRNA sequence immunofluorescence.
4. To decrease IGF-1R expression by transfecting a validated siRNA to the IGF-1R sequence using optimised transfection conditions.
5. To demonstrate IGF-1R-specific siRNA knockdown at mRNA and protein level.
6. To evaluate the effect of IGF-1R knockdown on proliferation.
7. To evaluate the effect of IGF-1R knockdown on invasion.
8. To compare the effect of treatment using an IGF-1R blocking antibody (α IR3) on invasion, with the effect of IGF-1R siRNA knockdown on invasion.

To summarise the results detailed in this section, it was found that IGF-1R was differentially expressed in the panel of cell lines studied, correlating with array data. Conditions for the transfection of siRNA sequences were optimised for these cell lines. Decreasing IGF-1R expression had no effect on proliferation, but did decrease invasion substantially, as determined by *in vitro* invasion assays. Treatment of the cells with a blocking antibody to IGF-1R, α IR3, also decreased invasion.

3.4.2 RT-PCR confirmation of differential IGF-1R mRNA expression in the DLKP variants

RT-PCR was utilised to confirm that IGF-1R expression changes in the array data were reflected in the cell lines studied.

RNA samples from the preliminary Affymetrix array study by Dr. Rasha Linehan in 2003 (Figure 3.4.2.1), RNA from the duplicate array samples 2004 (Figure 3.4.2.2), RNA from a fresh set of cultures harvested separately to those for array analysis including RNA from three samples analysed on the Agilent array platform (Figure 3.4.2.3) were included in this analysis. The Agilent data was not analysed for inclusion in this work due to limitations in data analysis capabilities at the time. This was to ensure that results from the array study matched to independent analysis of the cell lines.

In all of the Figures in this section β -actin was used as an endogenous control to normalise for RNA quantities added to each reaction. The reactions were analysed by gel electrophoresis (GE) on a 2% agarose gel. The band size for IGF-1R is 241bp. PCR negative controls consisted of PCR master mix to which no cDNA template was added. cDNA negative control (cDNA neg) consisted of PCR master mix with cDNA but without addition of Taq enzyme. Densitometric analysis was performed and Figures were generated by dividing IGF-1R intensity values by β -actin intensity values and were plotted for each sample. The gels included in this section are representative of at least two independent repeats.

This analysis by semi quantitative PCR demonstrates a trend of increased IGF-1R expression in the more invasive cell lines DLKP-1, DLKP-2 and TXT-2, compared to the lesser invasive cell lines TXT-1 and VCR. This correlates with the array IGF-1R data.

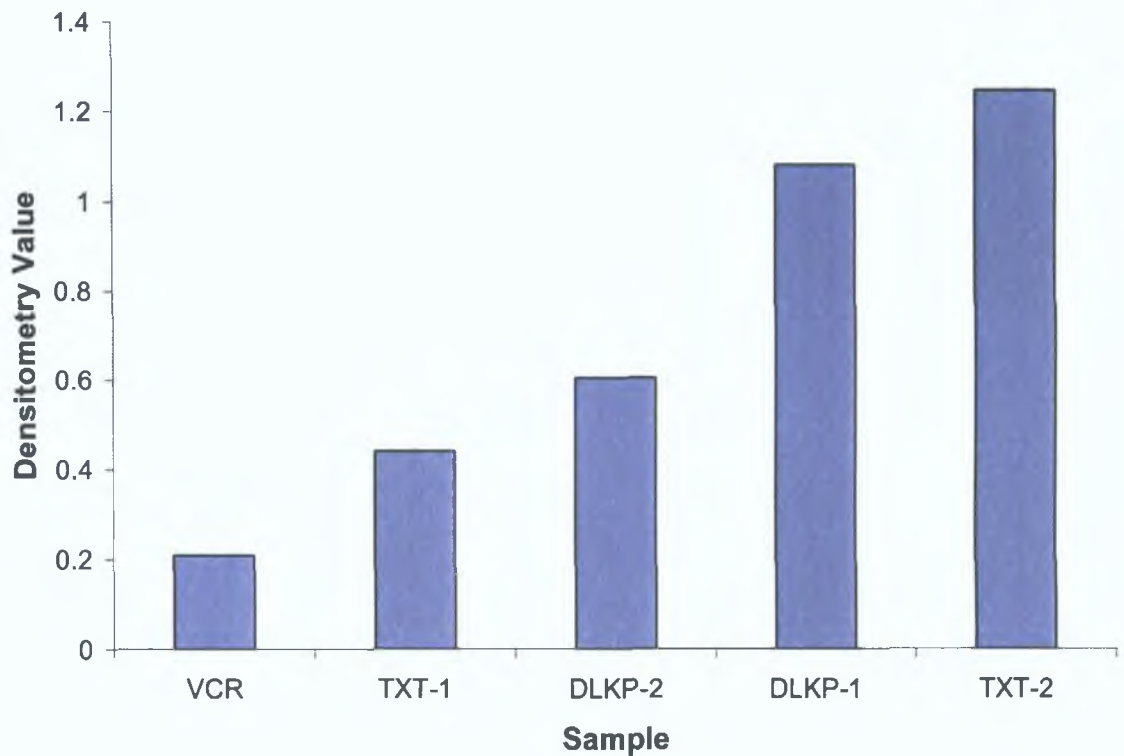


Figure 3.4.2.1 RT-PCR of IGF-1R mRNA expression from RNA used in array samples 2003.

RNA used for this PCR was analysed on the 2003 arrays. β -actin was used as an endogenous control to normalise for RNA quantities added to each reaction. The reaction was analysed by gel electrophoresis (GE) on a 2% agarose gel. A PCR Negative (PCR Neg) control was included in the analysis and consisted of PCR master mix to which no cDNA template was added. Figures for the densitometry values were generated by dividing IGF-1R intensity values by β -actin intensity values and were graphed for each sample. The trend indicates decreased IGF-1R mRNA expression in the poorly invasive cell lines compared to invasive cell lines.

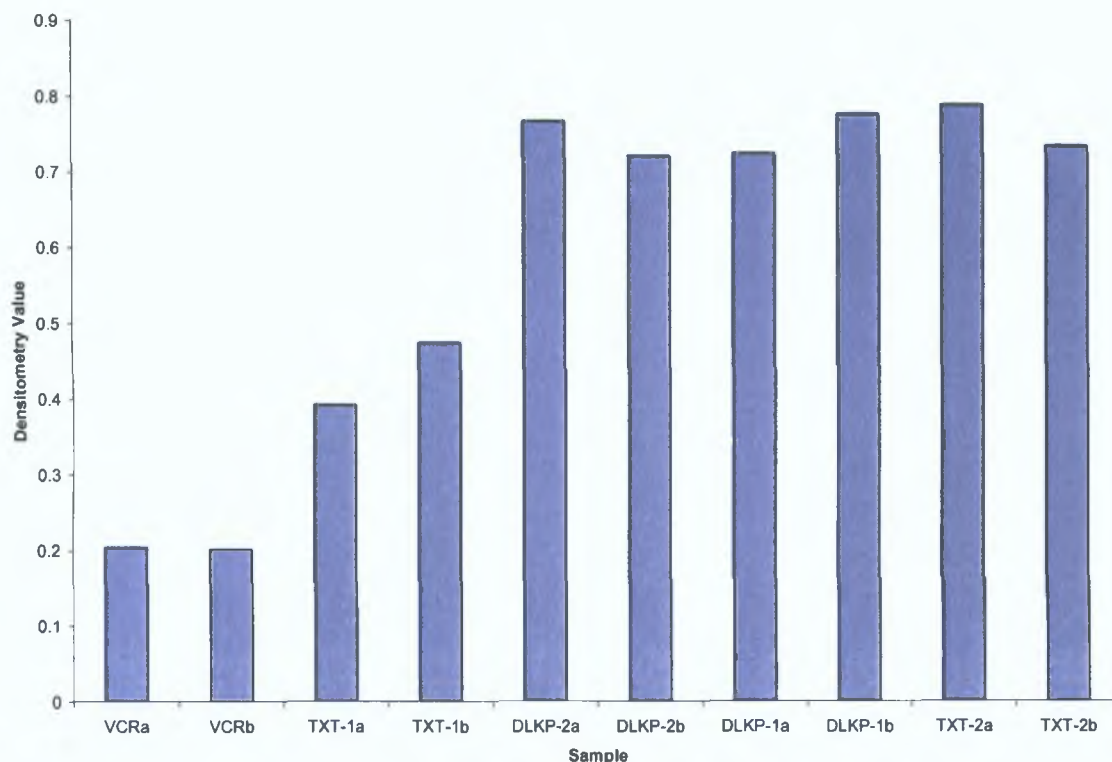


Figure 3.4.2.2 RT-PCR of IGF-1R mRNA expression from RNA used in duplicate array samples 2004.

RNA for this PCR was analysed in the duplicate array analysis of the DLKP cell lines in 2004. β -actin was used as an endogenous control. The reaction was analysed by GE on a 2% agarose gel. PCR negative (PCR Neg) and cDNA negative controls were included in the analysis. Densitometry values were generated by dividing IGF-1R intensity values by β -actin intensity values and were graphed for each sample. IGF-1R mRNA expression is decreased in the poorly invasive cell lines compared to invasive cell lines.

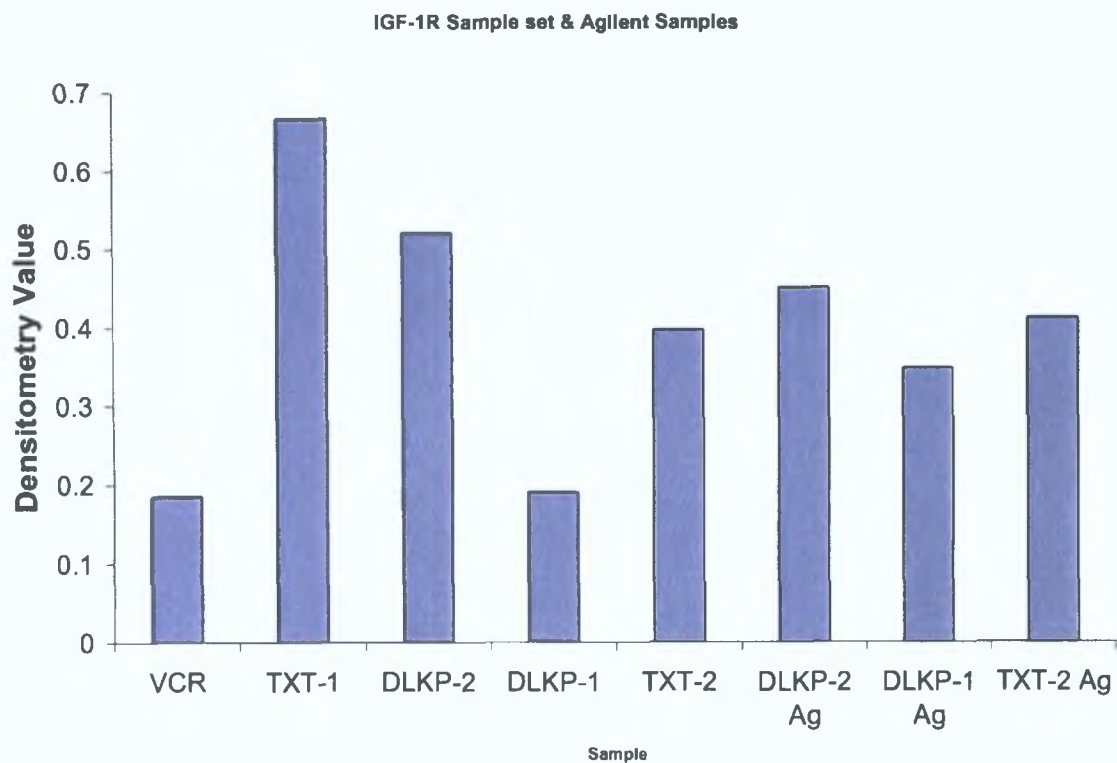


Figure 3.4.2.3 RT-PCR of IGF-1R mRNA in a separate sample set and Agilent samples.

RNA for this analysis was from a separate batch of DLKP variant cultures not harvested or processed for Affymetrix array analysis. Also included were three samples analysed on the Agilent array platform but which were not investigated further. β -actin was used as an endogenous control. The reaction was analysed by GE on a 2% agarose gel. Densitometry values were generated by dividing IGF-1R intensity values by β -actin intensity values and were graphed for each sample.

This PCR demonstrates high IGF-1R expression in TXT-1, which is one of the poorly invasive cell lines and is an unexpected result. However, the endogenous levels on IGF-1R were subsequently determined by qPCR and confirm the array results.

3.4.3 Endogenous IGF-1R mRNA and protein levels in the DLKP cell lines

Quantitative real time PCR (qPCR) gives a more accurate measurement of mRNA expression than the trends identified by semi-quantitative RT-PCR. qPCR was used to determine endogenous IGF-1R mRNA expression using a commercial TaqMan IGF-1R probe and normalised using β -actin as an endogenous control (Figure 3.4.3.1). Forty cycles of 15s at 95°C were used in the reaction.

Endogenous IGF-1R protein expression in the DLKP variants was determined by western blot. α -tubulin and GAPDH antibodies were used to demonstrate even loading between the samples (Figure 3.4.3.2).

These results correlate with the array results and demonstrate differential IGF-1R expression, where there is higher expression in the invasive cell lines, DLKP-2 and TXT-2 and lower expression in the lowly invasive cell line VCR. DLKP-1 and TXT-1, unexpectedly, have similar IGF-1R protein levels despite DLKP-1 being more invasive than TXT-1.

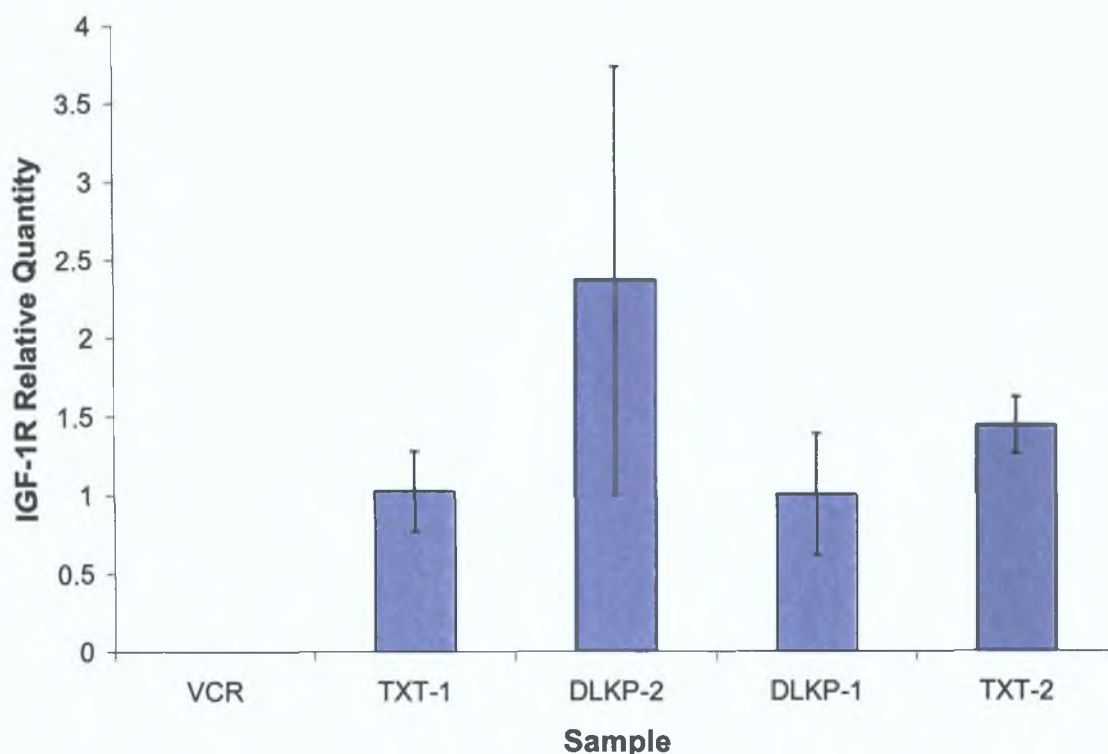


Figure 3.4.3.1 qRT-PCR of endogenous IGF-1R mRNA levels.

Endogenous IGF-1R mRNA expression in the DLKP variants was examined by qRT-PCR using a commercial TaqMan IGF-1R probe and normalised for RNA content using β -actin as an endogenous control. The data represents IGF-1R expression relative to DLKP-1, which was set to 1 for the analysis. This result demonstrates higher expression in the invasive cell lines, DLKP-2 and TXT-2 and lower expression in the poorly invasive cell line VCR. DLKP-1 and TXT-1, unexpectedly, have similar IGF-1R mRNA levels despite DLKP-1 being more invasive than TXT-1.

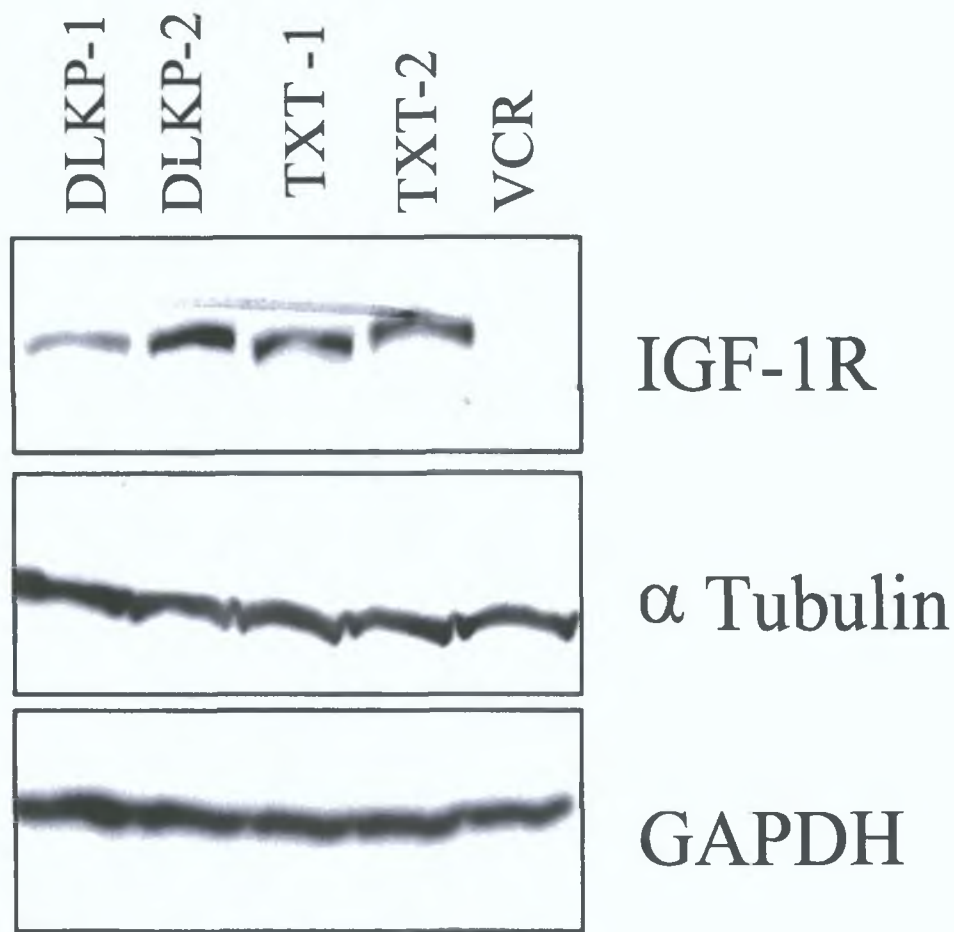


Figure 3.4.3.2 Western blot analysis of endogenous IGF-1R protein levels.

Endogenous IGF-1R protein expression in the DLKP variants was determined by western blot. α -tubulin and GAPDH antibodies were used to demonstrate even loading between the samples. This result correlates with the endogenous qPCR results above, and demonstrate differential IGF-1R expression, where there is higher expression in the invasive cell lines, DLKP-2 and TXT-2 and lower expression in the mildly invasive cell line VCR. DLKP-1 and TXT-1, unexpectedly, have similar IGF-1R protein levels despite DLKP-1 being more invasive than TXT-1. This is a representative picture of at least 3 independent analyses.

3.4.4 siRNA Transfection Optimisation for the DLKP cell lines

3.4.4.1 Summary of siRNA transfection optimisation

There were a number of different parameters that had to be determined to establish an optimised protocol for the siRNA transfection of DLKP and its variants. Initially, only the transfection protocol itself was considered. 2µl of NeoFx transfection reagent per well of a 6-well plate was used to transfect 30nM of target siRNA into the cells. These were amounts recommended by Ambion. qPCR analysis of these early transfections demonstrated that mRNA knockdown was not being achieved, which led to the examination of cell line handling during the transfection process. It transpired that cell handling during the transfection protocol is particularly important. The following procedures were optimised for siRNA transfection in these cell lines:

- Cells should be in log/growth phase and in a healthy condition when used to seed siRNA transfections and should be fed with fresh medium 24h prior to transfection.
- The cell suspensions should be prepared in serum containing medium i.e. normal growth medium (as opposed to medium with reduced serum e.g. OptiMEM).
- Cells should be in suspension for as short a time as possible and maintained at 37°C to avoid heat shock while the siRNA complex is being prepared.
- Five cell lines are too many cell lines to transfect with siRNA in any one transfection. The reasons for this are twofold; the cells are in suspension for longer time periods than if you were working with fewer cell lines. It was found that cells in suspension should be dispensed onto complexed siRNA/NeoFx solutions immediately following the complex incubation period (i.e. reverse transfection). Extended time periods lead to poor transfection efficiency and thereby poor target knockdown. We determined that three cell lines are the maximum number suitable in any single transfection experiment.

- A protocol was also optimised for the analysis of a target siRNA specific effect on invasion. This was of particular importance since the transfection agent itself, NeoFx, caused a decrease in invasion as determined by *in vitro* invasion assay. In addition, it was found that allowing the transfected cells more time to recover following siRNA transfection minimised the non-specific effect of the transfection on invasion. To this end, siRNA transfected cells were analysed by *in vitro* invasion assay 72h post-transfection.

3.4.4.2 Optimisation of *in vitro* invasion analysis following siRNA transfection

A validated IGF-1R siRNA sequence was transfected into the DLKP variants. The effect on invasion was determined by invasion assay 48h post-siRNA transfection (Figure 3.4.4.1). Non treated and scrambled siRNA transfected cell lines were the controls for this experiment. RPMI-Mel and RPMI-2650 are included as positive and negative invasion assay controls respectively. Each condition was examined using at least two invasion kit inserts. Ten random fields per insert were counted at 20X and average and the average of the inserts per condition calculated. While a specific decrease in invasion could be attributed to the IGF-1R siRNA for DLKP-1, there was no related decrease in invasion in the other four samples. Also, there was a considerable non-specific decrease in invasion in the scrambled siRNA treated cells compared with the non-treated cells. This was most likely due to the transfection process and not the scrambled siRNA, since the scrambled siRNA was one of only three sequences that Ambion sells as a transfection control as they do not target any RNA sequence.

It was decided to allow the cells to recover from the transfection for as long as possible before invasion analysis, in order to minimise the non-specific transfection effect on invasion. To this end the invasion assay was performed 48 and 72h post-transfection (Figure 3.4.4.2). From these results, it appeared that performing the invasion assay 72h post siRNA transfection allowed more recovery time for the cells and decreased the non-specific transfection effect on invasion. This was the time point at which all-further invasion analysis of siRNA transfected samples were performed. Fig 3.4.4.3 and 3.4.4.7 demonstrate that IGF-1R expression was eliminated in IGF-1R siRNA transfected samples.

Invasion assay analysis 48h post-IGF-1R siRNA transfection

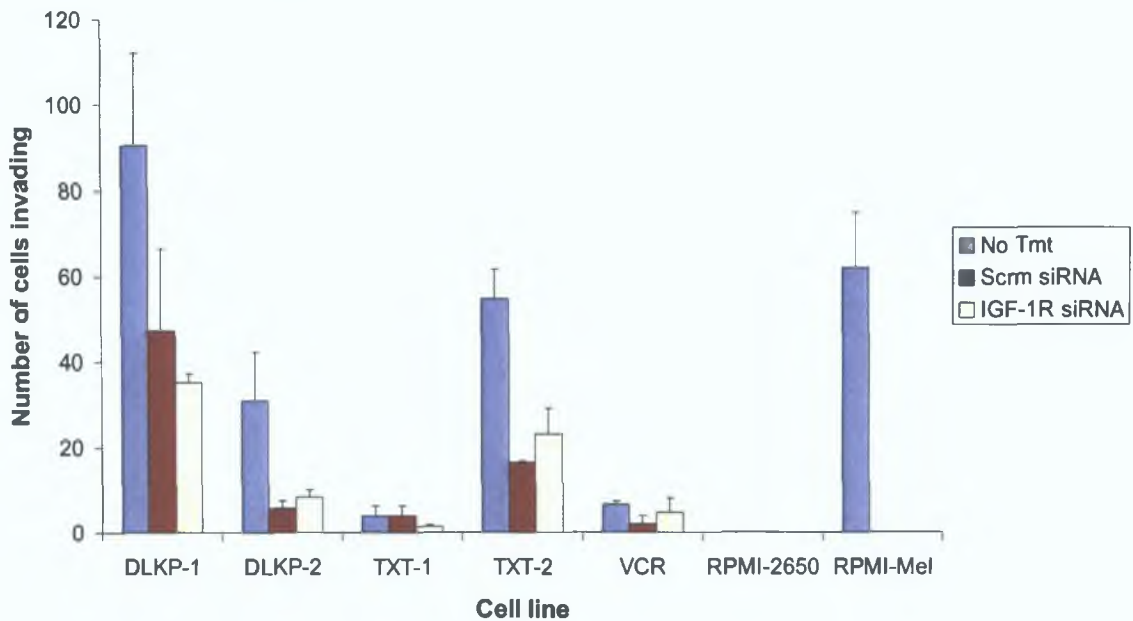


Figure 3.4.4.1 Determination of the effect of IGF-1R siRNA transfection on invasion.

The invasion assay was performed 48h post-siRNA transfection. Non treated and scrambled siRNA transfected cell lines are the controls for this experiment. RPMI-Mel and RPMI-2650 are included as positive and negative invasion assay controls respectively. Ten random fields per insert were counted at 20X. Each condition was examined using at least two invasion kit inserts and the counts averaged. Only a slight IGF-1R-specific siRNA related decrease in invasion was observed for the DLKP-1 sample, with no related decrease in the other four DLKP cell lines. There was also a considerable non-specific decrease in invasion in the scrambled siRNA treated cells compared with the non-treated cells. This was probably due to the transfection process and not the scrambled siRNA, since the scrambled siRNA is one of only three sequences that Ambion markets as a transfection control as they do not target any RNA sequence.

Minimisation of non-specific effect of transfection reagent on invasion assay analysis

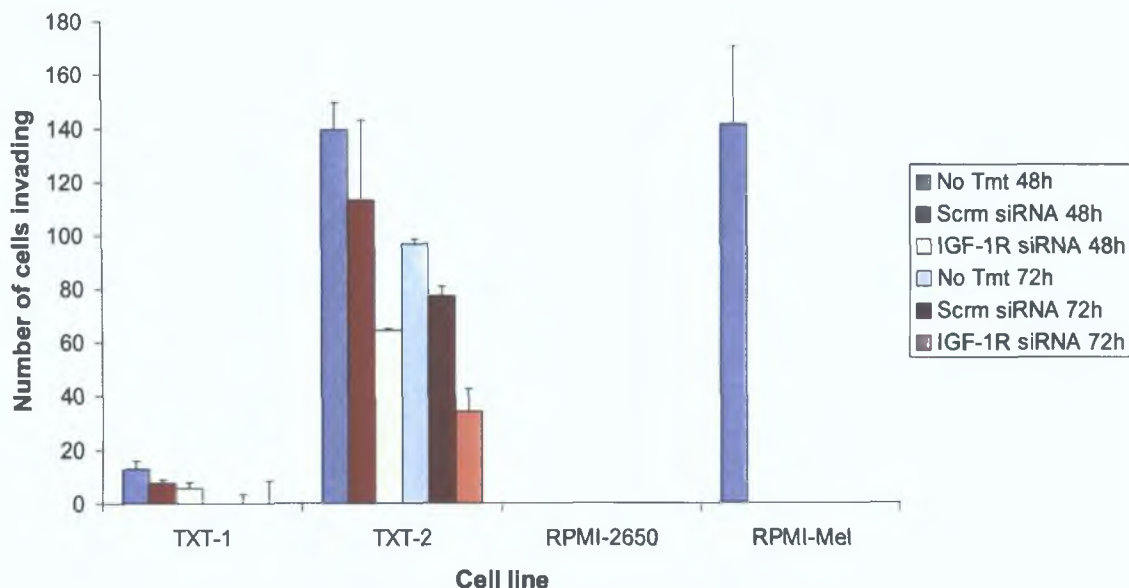


Figure 3.4.4.2 Minimisation of non-specific transfection effect on invasion.

An additional IGF-1R siRNA transfection was performed and analysed by invasion assay at 48 and 72h post-transfection. Non treated and scrambled siRNA transfected cell lines are the controls for this experiment. RPMI-Mel and RPMI-2650 are included as positive and negative invasion assay controls respectively. Ten random fields per insert were counted at 20X. Each condition was examined using at least two invasion kit inserts and the counts averaged and graphed. These results suggest that performing the invasion assay 72h post siRNA transfection allows more recovery time for the cells and decreases the non-specific transfection effect on invasion. This was the time point at which all-further invasion analysis of siRNA transfected samples were performed.

3.4.4.3 Evaluation of siRNA transfection efficiency

siRNA transfection efficiency was evaluated using immunofluorescence and confocal microscopy (Figure 3.4.4.3) and was also visualised photographically in Figure 3.4.4.4.

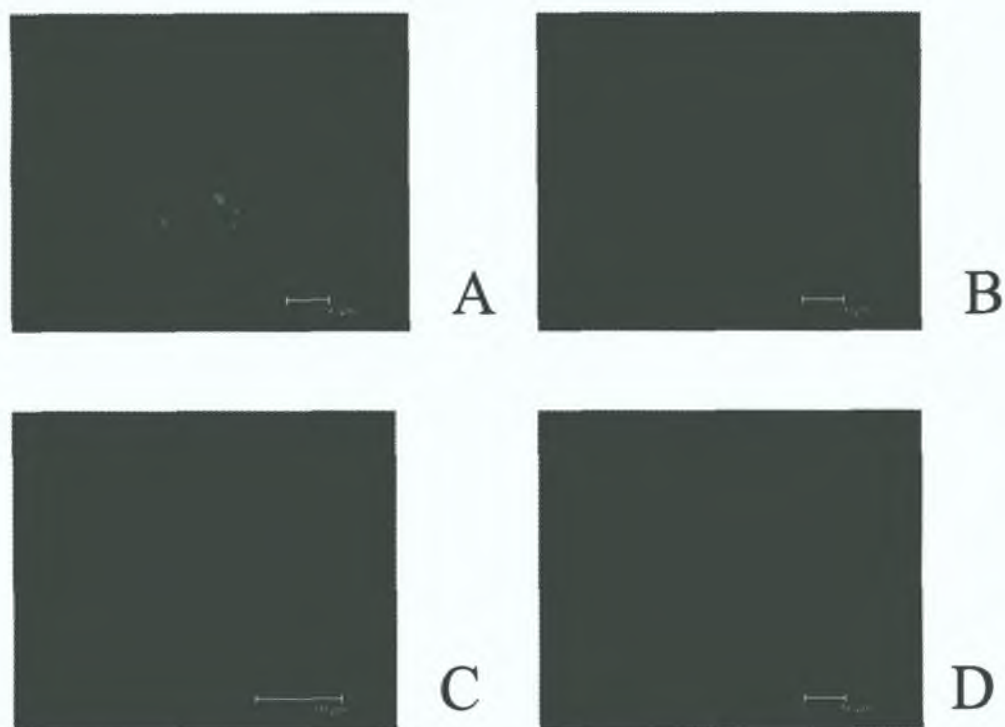


Figure 3.4.4.3 Evaluation of transfection efficiency using immunofluorescence and confocal microscopy.

Immunofluorescent localisation of IGF-1R expression in the invasive TXT-2 cell line (A), and following siRNA knockdown (B). FAM labelled IGF-1R siRNA can be seen as punctuate fluorescence in the cytoplasm of transfected TXT-2 (C). Untransfected cells (D) are presented as a control. The nuclei were stained with DAPI in all cases.

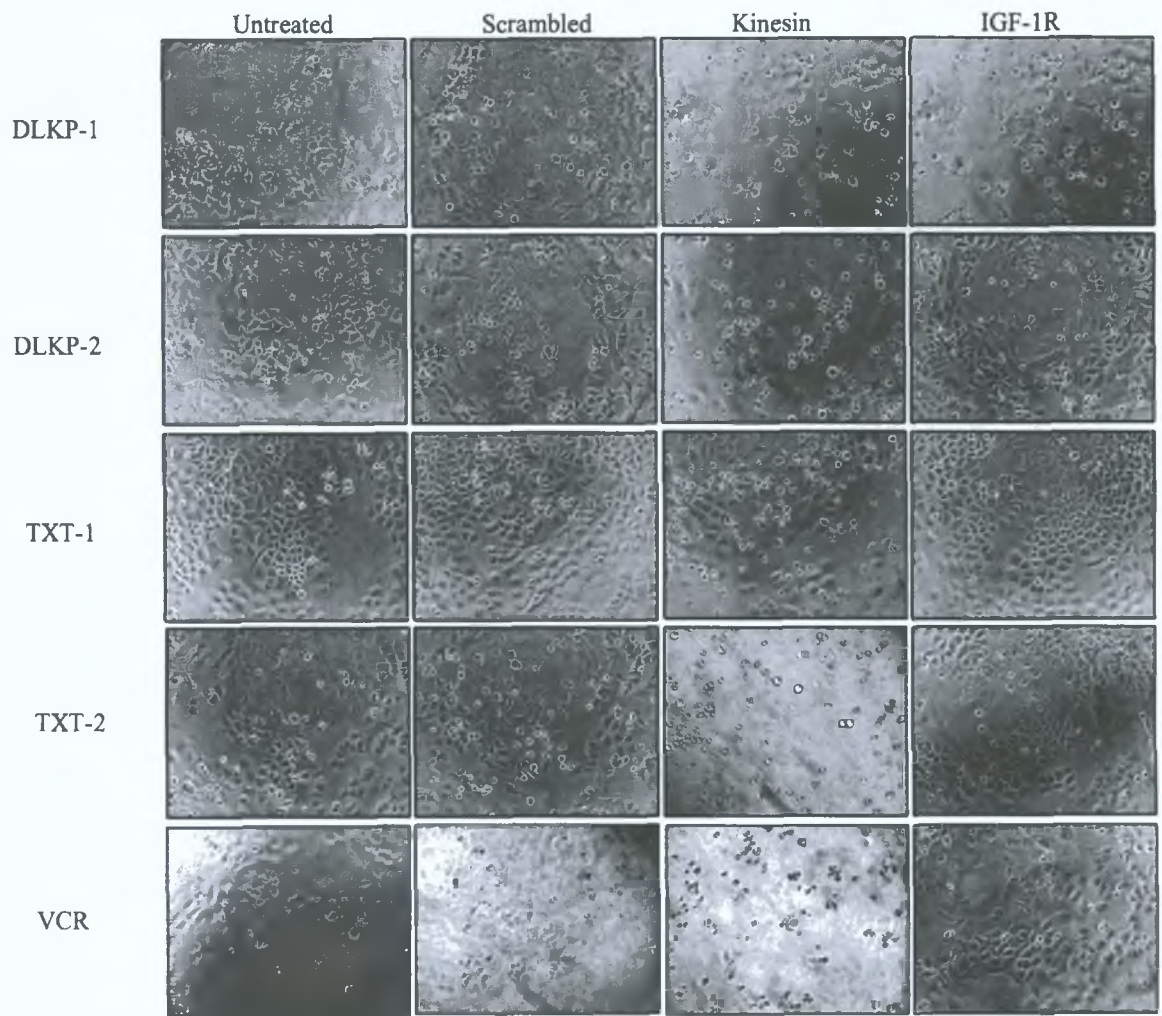


Figure 3.4.4.4 Photographic representation of effect of siRNA targeting IGF-1R and Kinesin on DLKP variant cell growth.

Scrambled siRNA transfection has a slight toxic effect on the cells. This was also observed in our invasion analysis optimisation. However, from the pictures above it is clear that an siRNA targeting IGF-1R does not induce additional toxic effects on the cells than caused by the transfection process itself. The effect of an efficient kinesin transfection is visualised above as the typical rounded morphology associated with cells arrested in mid cell division.

3.4.4.4 IGF-1R- specific siRNA decrease in IGF-1R mRNA and Protein levels

A validated IGF-1R specific siRNA sequence was transfected into the DLKP variants and a decrease in IGF-1R mRNA and protein expression was confirmed by qPCR and western blot respectively.

Relative IGF-1R mRNA expression was measured using a commercial TaqMan IGF-1R probe and normalised using β -actin as an endogenous control (Figure 3.4.4.5).

IGF-1R protein expression in the DLKP variants and their IGF-1R siRNA transfected counterparts was determined by western blot. Cells were transfected with a scrambled siRNA sequence as a control to ensure that the transfection process did not affect target protein expression. An α -tubulin antibody was used to demonstrate even loading between the samples (Figure 3.4.4.6).

These qPCR results do not show a substantial decrease in IGF-1R mRNA expression in response to IGF-1R siRNA transfection. However, the western blots demonstrate close to 100% decrease in IGF-1R protein expression in IGF-1R siRNA transfected cells compared to the non-treated and scrambled siRNA transfected cells. This indicates that the siRNA might be acting like a microRNA (miRNA) and blocking translation rather than directing target mRNA degradation.

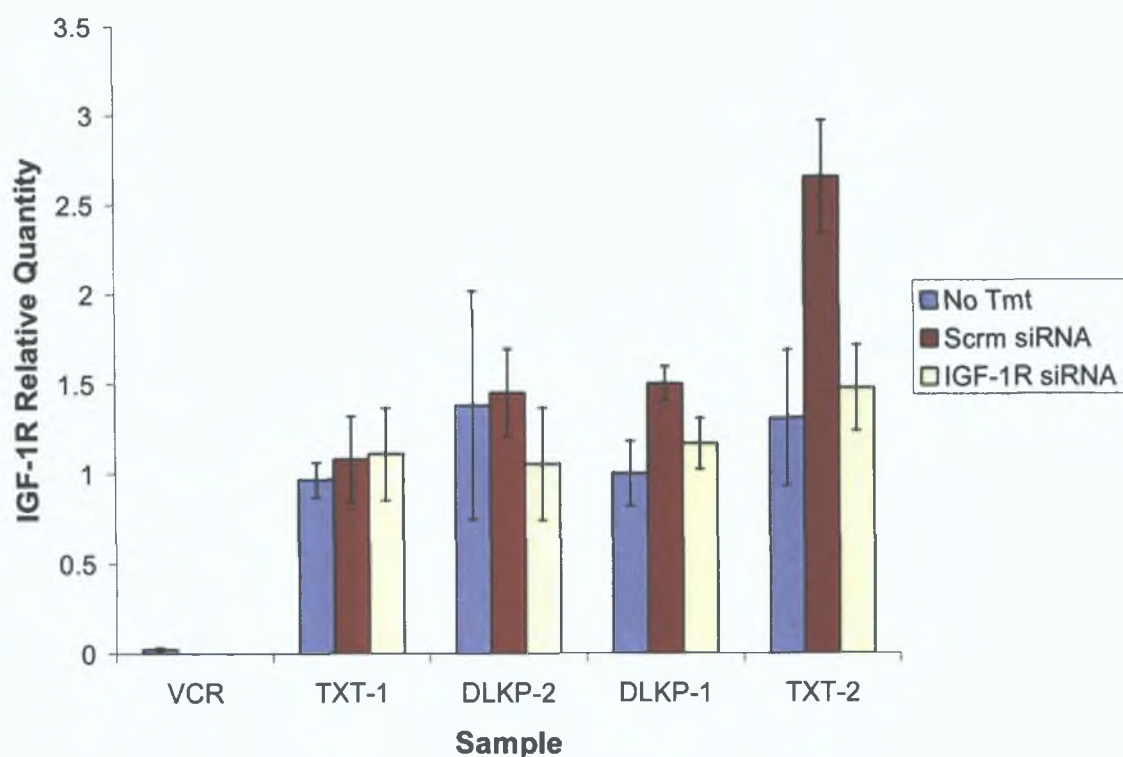


Figure 3.4.4.5 qRT-PCR of IGF-1R 48h post siRNA transfection.

IGF-1R mRNA expression was examined by qRT-PCR using a commercial TaqMan IGF-1R probe and normalised for RNA content using β -actin as an endogenous control. The data represents IGF-1R expression relative to DLKP-1, which was set to 1 for the analysis. A slight decrease in IGF-1R mRNA expression was observed in the IGF-1R siRNA treated samples 48h post-transfection compared to the scrambled control, except for TXT-1. IGF-1R mRNA expression was increased in scrambled siRNA transfected cells compared with the non-treated cells.

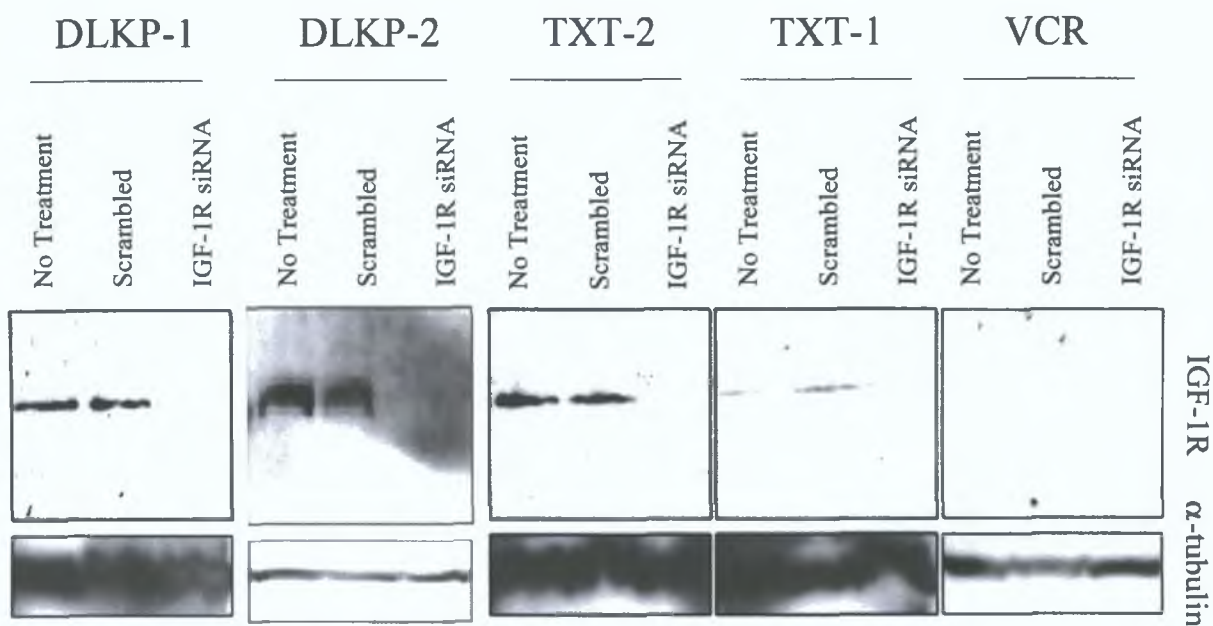


Figure 3.4.4.6 Western blot of IGF-1R 72h post siRNA transfection.

Protein was harvested 72h post-transfection and used to determine an IGF-1R-siRNA specific decrease at protein level in response to siRNA transfection by western blot. An α -tubulin antibody was used to demonstrate even loading between the samples. The above figure demonstrates an IGF-1R siRNA specific decrease close to 100% in IGF-1R protein levels compared with scrambled and non-treated samples. This is a representative picture of at least 3 independent analyses.

3.4.5 Evaluation of IGF-1R siRNA effect of DLKP variant proliferation

The effect of IGF-1R siRNA transfection on proliferation was examined using two cell densities a “low density” of 2.5×10^3 cells/well of a 96-well plate (Figure 3.4.4.7), and a “high density” of 5×10^3 cells/well of a 96-well plate (Figure 3.4.4.8). Cell number was determined using the acid phosphatase assay. An siRNA sequence to Kinesin was transfected as a positive control and acts by preventing cell doubling thus kinesin siRNA transfected cells do not increase in number compared with the non-treated, scrambled siRNA- and IGF-1R siRNA- transfected cells.

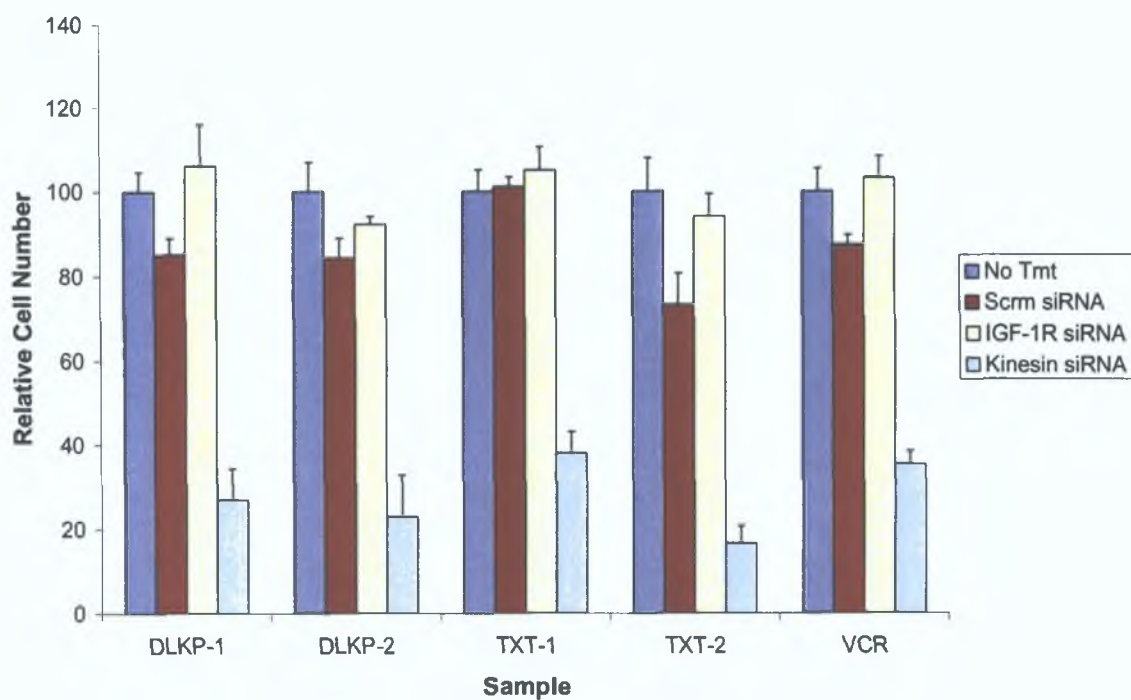


Figure 3.4.4.7 Effect of siRNA targeting IGF-1R and Kinesin on DLKP variant cell number at lower seeding density.

The cells were seeded at a “low density” of 2.5×10^3 cells/well of a 96-well plate. Relative cell number was measured using the acid phosphatase assay. IGF-1R siRNA treatment does not appear to affect proliferation compared with the scrambled siRNA and non-treated cells. The kinesin results indicate effective siRNA transfection.

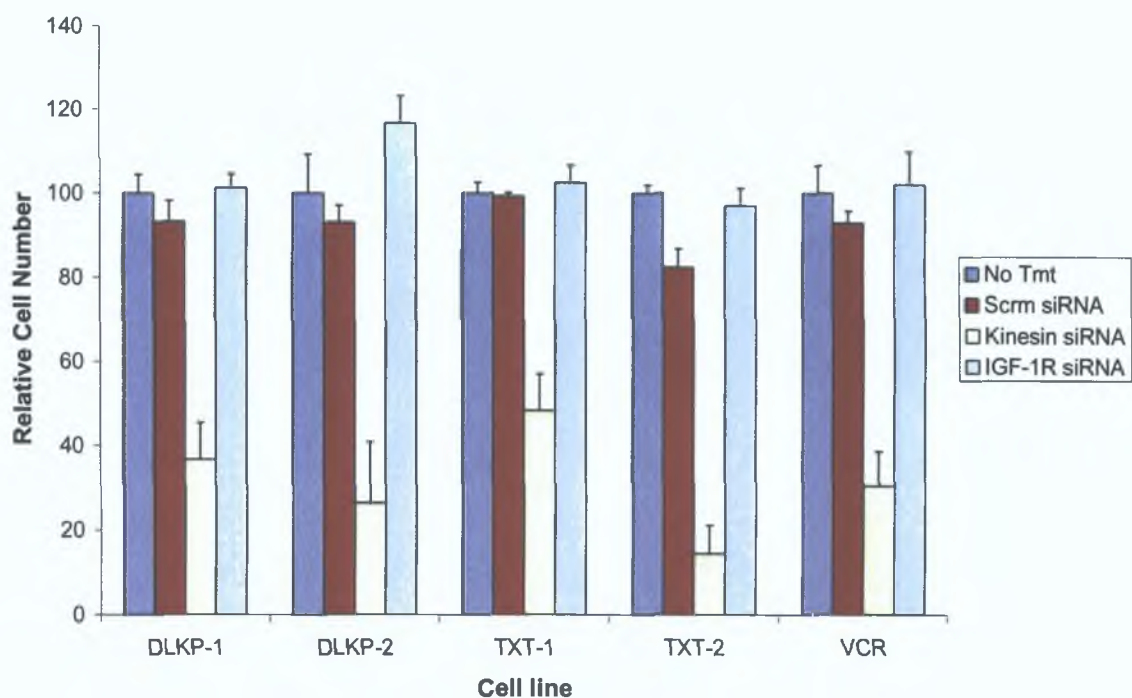


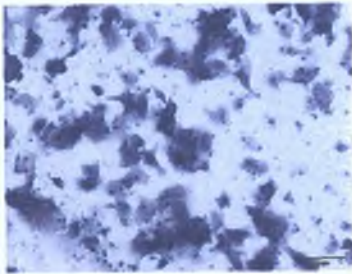
Figure 3.4.4.8 Effect of siRNA targeting IGF-1R and Kinesin on DLKP variant cell number at higher seeding density.

The cells were seeded at a “high density” of 5×10^3 cells/well of a 96-well plate. A decrease in cell number for the kinesin treated cells demonstrates act as a positive control for the siRNA transfection. IGF-1R siRNA treatment does not affect proliferation compared with the scrambled siRNA and non-treated cells when seeded at a high cell density.

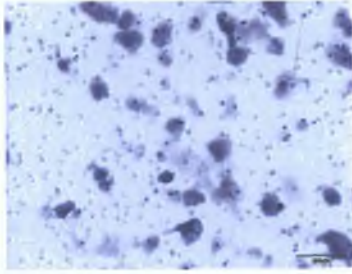
3.4.6 Evaluation of IGF-1R siRNA effect on invasion

The effect of IGF-1R knockdown on DLKP variant invasive capacity was examined. Invasion assay analysis was performed 72h post transfection. Commercial invasion assay kits containing inserts pre-coated with matrigel were used for analysis and a serum gradient was used in the assay. The cells were incubated at 37°C for 24h. After this time, the underside of the insert stained with crystal violet and allowed to air dry. The inserts were then photographed using 10X magnification. Ten fields of view were counted per insert at 20X magnification and averaged. At least two inserts were used for the analysis of each condition. The counts per number of inserts used were then also averaged and this figure used to generate graphs of relative invasive capacity per cell line per condition.

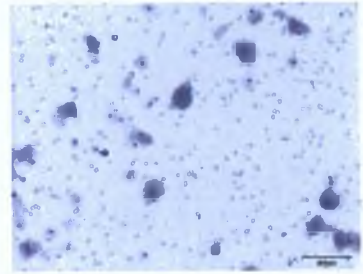
Two sets of representative photographs were included (Figure 3.4.4.9 and 3.4.4.11) in this section and clearly show a decrease in invasion in IGF-1R siRNA transfected cells. Invasion assay results are also presented graphically (Figures 3.4.4.10 and 3.4.4.12) as percentage invasion normalised to the scrambled siRNA for each cell line..



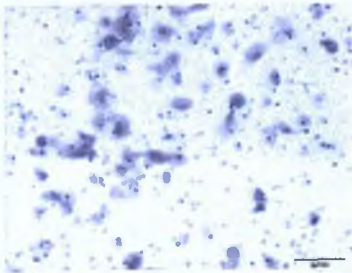
DLKP-1 10X



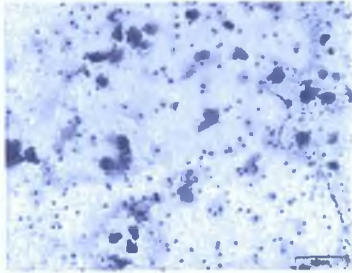
DLKP-1 Scrm siRNA 10X



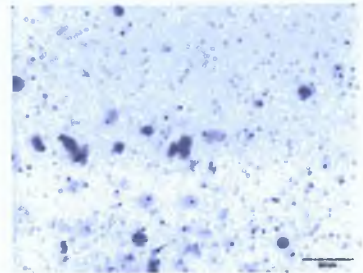
DLKP-1 IGF-1R siRNA 10X



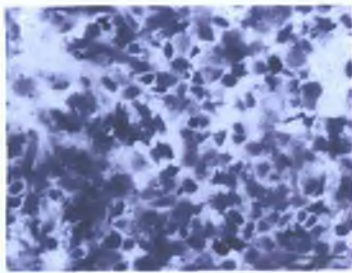
DLKP-2 10X



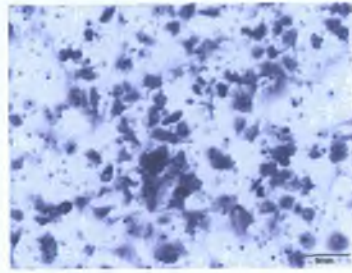
DLKP-2 Scrm siRNA 10X



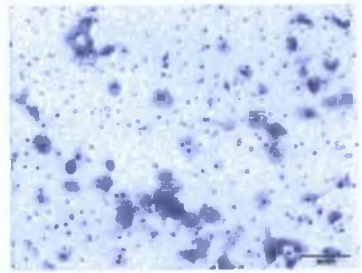
DLKP-2 IGF-1R siRNA 10X



DLKP TXT-2 10X



TXT-2 Scrm siRNA 10X



TXT-2 IGF-1R siRNA 10X

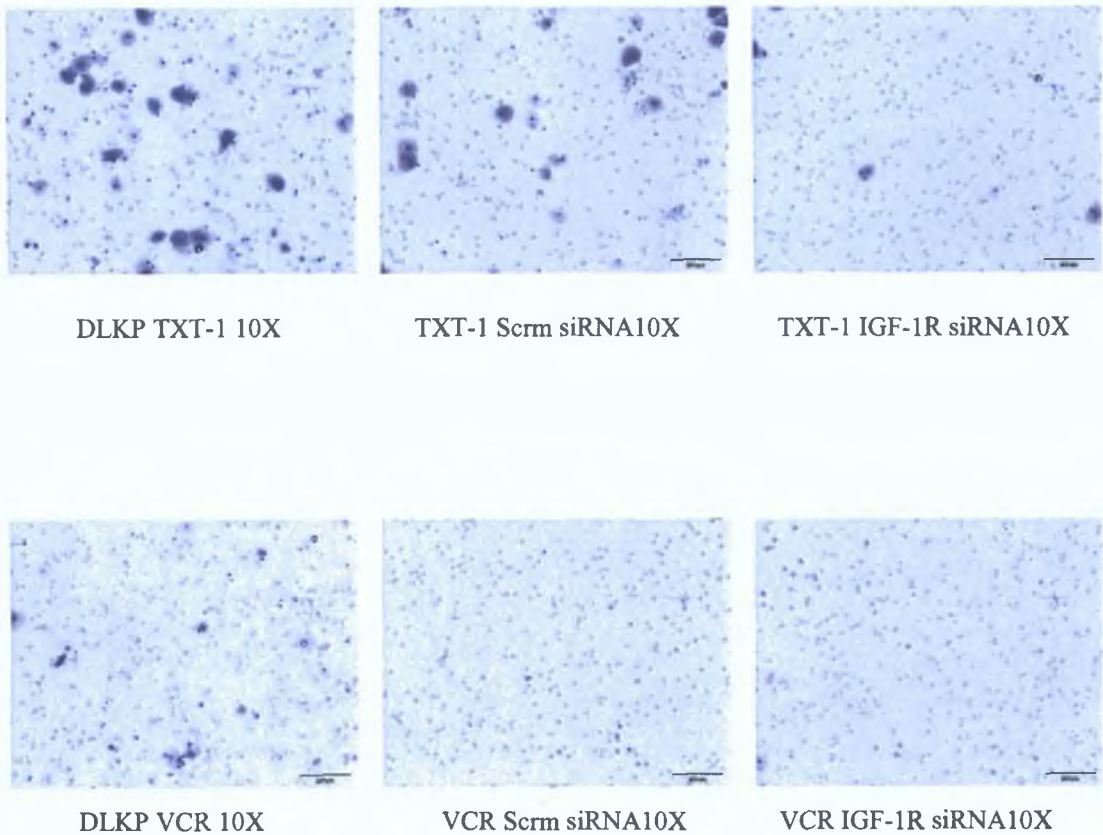


Figure 3.4.4.9 Photographic representation of invasion assay results 72h post IGF-1R siRNA transfection I.

The invasion assay was performed 72h post-transfection. Untransfected- and scrambled siRNA transfected- cell lines were the controls for this experiment. Representative photographs at 10X are shown above. Invasion was decreased in IGF-1R siRNA transfected cells compared with the scrambled siRNA and non-treated cells.

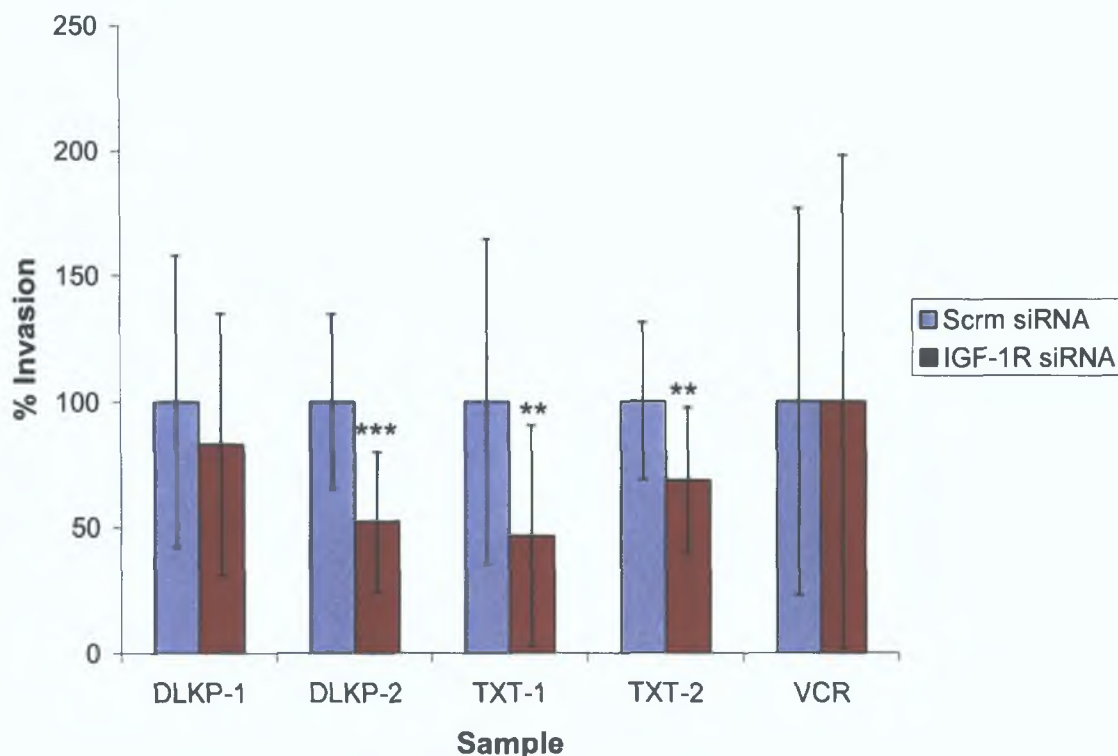
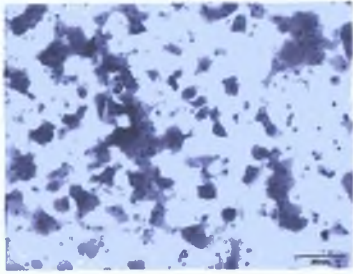


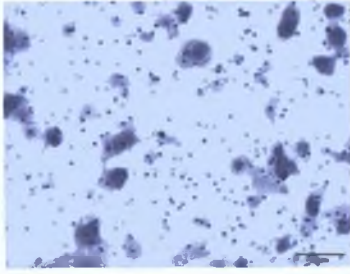
Figure 3.4.4.10 Graphic representation of invasion assay results 72h post IGF-1R siRNA transfection I.

The invasion assay was performed 72h post-transfection. Scrambled siRNA transfected- cell lines are the controls for this experiment. Ten random fields were counted at 20X. Each condition was examined using at least two invasion kit inserts. Counts per insert were averaged and plotted as percentage invasion normalised to the scrambled siRNA for each cell line. Invasion was decreased in IGF-1R siRNA transfected DLKP-2 ($P < 0.001$), TXT-1 and TXT-2 ($P < 0.005$) compared with the scrambled siRNA control. There was a decrease in invasion in DLKP-1 IGF-1R siRNA transfected cells also, albeit insignificant. This may be attributed to poor transfection efficiency in this cell line.

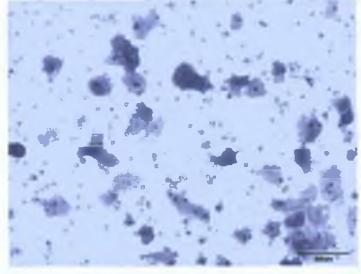
Scale: $P < 0.01 = *$, $P < 0.005 = **$, $P < 0.001 = ***$



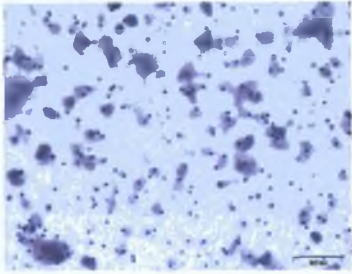
DLKP-1 10X



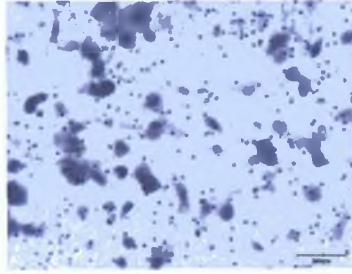
DLKP-1 Scrm siRNA 10X



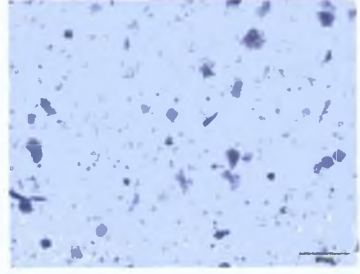
DLKP-1 IGF-1R siRNA 10X



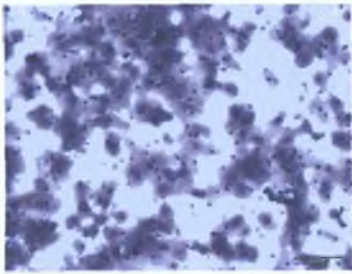
DLKP-2 10X



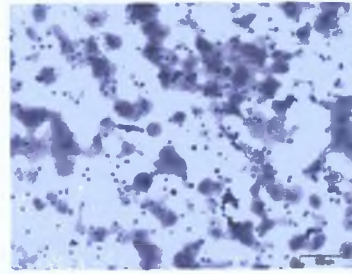
DLKP-2 Scrm siRNA 10X



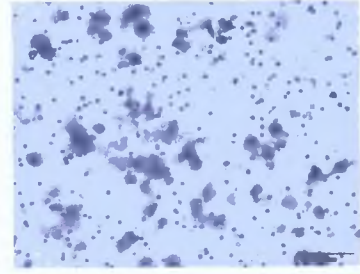
DLKP-2 IGF-1R siRNA 10X



DLKP TXT-2 10X



TXT-2 Scrm siRNA 10X



TXT-2 IGF-1R siRNA 10X

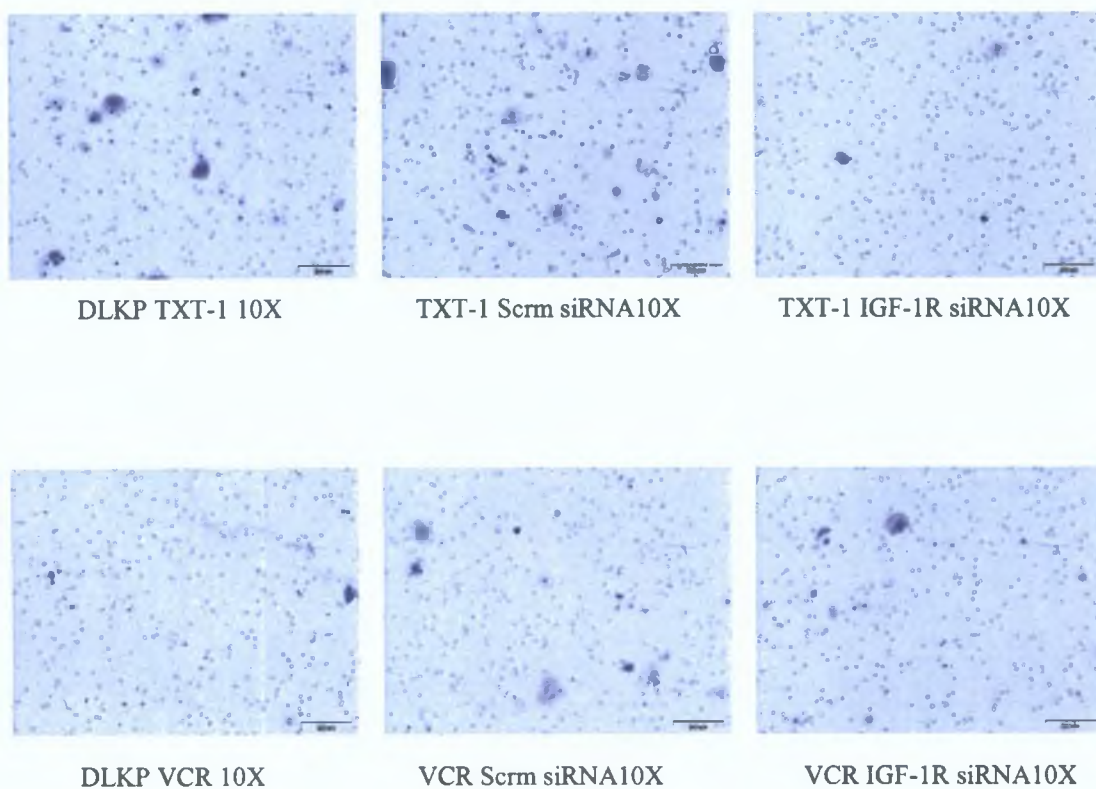


Figure 3.4.4.11 Photographic representation of invasion assay results 72hr post IGF-1R siRNA transfection II.

The invasion assay was performed 72h post-transfection. Untransfected- and scrambled siRNA transfected- cell lines are the controls for this experiment. Representative photographs at 10X are shown above. Invasion was decreased in IGF-1R siRNA transfected cells compared with the scrambled siRNA and non-treated cells.

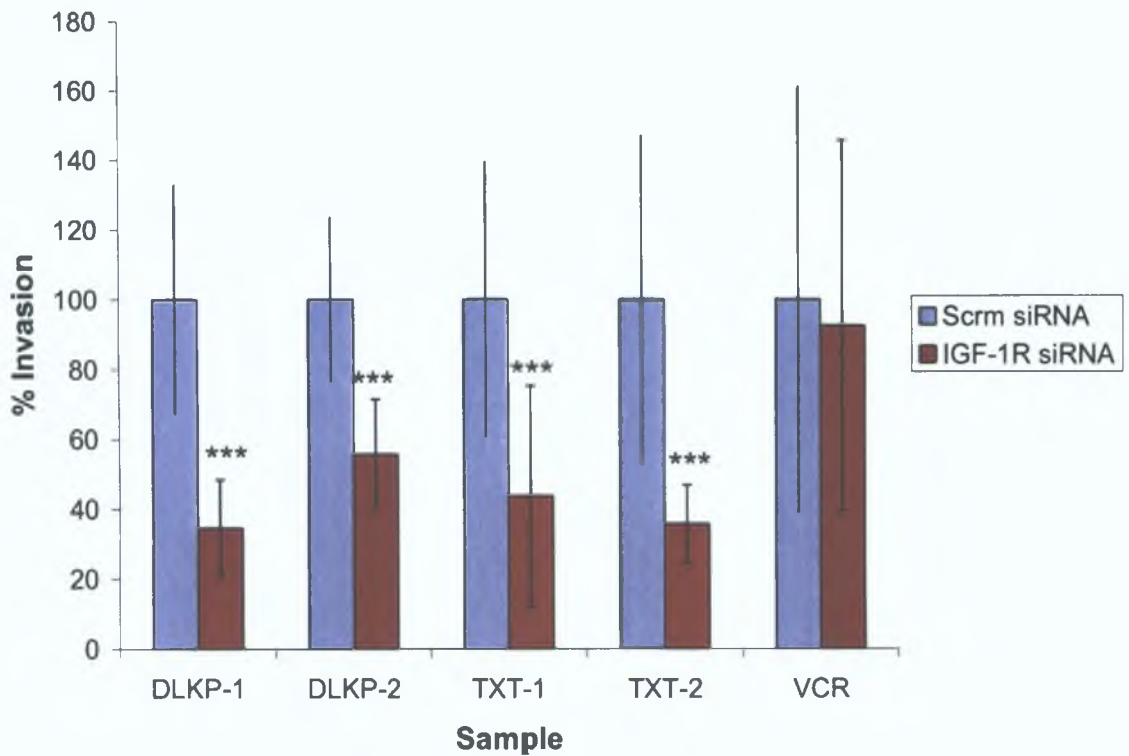


Figure 3.4.4.12 Graphic representation of invasion assay results 72hr post IGF-1R siRNA transfection II.

The invasion assay was performed 72h post-transfection. Untransfected- and scrambled siRNA transfected- cell lines are the controls for this experiment. Ten random fields were counted at 20X. Each condition was examined using at least two invasion kit inserts. Counts per insert were averaged and plotted as percentage invasion normalised to the scrambled siRNA for each cell line. Invasion was decreased in IGF-1R siRNA transfected cells ($P < 0.001$), compared with the scrambled siRNA control. Invasion was unaffected in VCR IGF-1R siRNA transfected cells, however this cell line is considered non-invasive in the first instance and does not express endogenous IGF-1R.

Scale: $P < 0.01 = *$, $P < 0.005 = **$, $P < 0.001 = ***$

3.4.7 Evaluation of IGF-1R blocking antibody, α IR3 effect on invasion

The effect of an additional method of preventing IGF-1R expression on invasion was investigated (Figure 3.4.4.13). To this end, only the invasive DLKP variants DLKP-1, DLKP-2 and TXT-2 were treated with 1000ng/ml of α IR3 monoclonal antibody for 24h.

The cell lines were seeded from 80% confluency for invasion analysis with or without the addition of 1000ng/ml α IR3 monoclonal antibody. After 24h incubation, the invading cells on the underside of the insert were stained with crystal violet and allowed to air dry. Each condition was examined using at least two invasion kit inserts. Ten random fields per insert were counted at 20X. Counts per insert were averaged and graphed above. RPMI-Mel and RPMI-2650 are included as positive and negative invasion assay controls respectively.

A shortcoming in this experiment was the lack of a control antibody to confirm the specificity of the α IR3 antibody on IGF-1R activity and its subsequent effect on the invasive capacity of the DLKP variants. This would be included in future experiments. It would also have been interesting to evaluate the amount of IGF-1R being blocked by the antibody. This could have been achieved by taking a sample of α IR3 treated and non-treated cells and using protein G sepharose to pull down the IGF-1R and compare the treated versus non-treated IGF-1R quantities in each sample. The decrease in IGF-1R amounts could then be correlated with the effect on invasion. Nevertheless, invasion was decreased in α IR3 treated cells compared with the non-treated cells at similar levels to those achieved using an siRNA strategy to decrease IGF-1R expression.

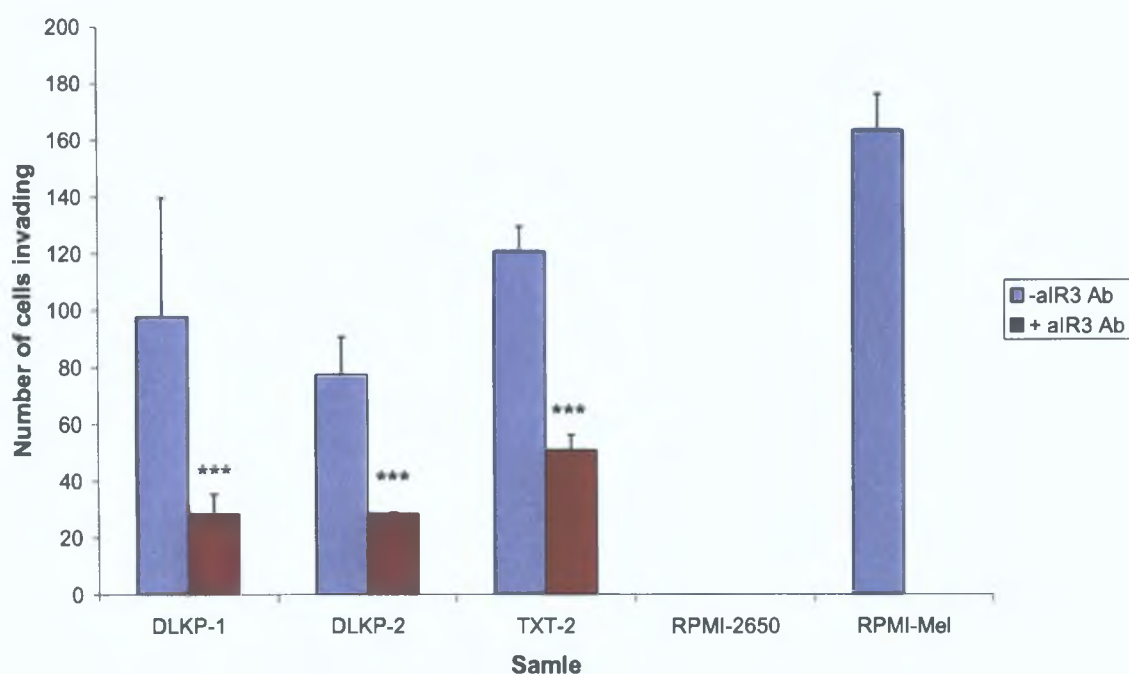


Figure 3.4.4.13 Graphic representation of IGF-1R blocking antibody, α IR3, treatment on DLKP variant invasion.

The above cell lines were seeded for invasion analysis with or without the addition of 1000ng/ml α IR3 monoclonal antibody. After 24h incubation, the invading cells on the underside of the insert were stained with crystal violet and allowed to air dry. Each condition was examined using at least two invasion kit inserts. Ten random fields per insert were counted at 20X. Counts per insert were averaged and graphed above. RPMI-Mel and RPMI-2650 are included as positive and negative invasion assay controls respectively. Invasion was decreased in α IR3 treated cells compared with the non-treated cells ($P < 0.001$).

Scale: $P < 0.01 = *$, $P < 0.005 = **$, $P < 0.001 = ***$

3.5 Investigation into role of KCNJ8 in invasion in our cell model

3.5.1 Aims of KCNJ8 experiments

KCNJ8 was identified as a gene potentially involved in invasion in the microarray study. The data indicated that KCNJ8 expression was higher in the more invasive cell lines compared to the lesser invasive cell lines. The aims of this set of experiments were as follows:

1. To confirm by PCR that KCNJ8 was differentially expressed across the DLKP cell line panel.
2. To decrease KCNJ8 expression by transfecting two independent siRNA sequences to KCNJ8 into the invasive cell lines DLKP-1, DLKP-2 and TXT-2.
3. To demonstrate KCNJ8 siRNA-specific knockdown at mRNA level.
4. To evaluate the effect of KCNJ8 knockdown on proliferation.
5. To evaluate the effect of decreased KCNJ8 expression on invasion.
6. To determine cDNA transfection efficiency using Green Fluorescent Protein (GFP).
7. To increase KCNJ8 expression by transfecting a pSport6 plasmid containing the KCNJ8 sequence into the lesser or poorly invasive cell lines TXT-1 and VCR.
8. To confirm an increase in KCNJ8 cDNA transfected cells at protein level.
9. To evaluate the effect of increasing KCNJ8 expression on invasion.

To summarise the results detailed in this section, it was found that KCNJ8 was differentially expressed in the panel of cell lines studied, in agreement with array data. Decreasing KCNJ8 expression had no effect on proliferation, but did increase invasion. This was an unexpected result. Increasing KCNJ8 expression had no effect on invasion in the non-invasive cell lines. However, western blots for KCNJ8 overexpression were not conclusive.

3.5.2 RT-PCR investigation of KCNJ8 mRNA expression

Semi quantitative RT-PCR was used to confirm that KCNJ8 expression changes in the array data were reflected in the cell lines studied.

To ensure that results from the array study matched to independent analysis of the cell lines, RNA samples from the preliminary Affymetrix array study by Dr. Rasha Linehan in 2003 (Figure 3.5.2.1), RNA from the duplicate array samples 2004 (Figure 3.5.2.2), RNA from a fresh set of cultures harvested separately to those for array analysis including RNA from three samples analysed on the Agilent array platform (Figure 3.5.2.3) were included in this analysis. The Agilent data was not analysed further in this work.

In all of the PCRs in this section β -actin was used as an endogenous control to normalise for RNA quantities added to each reaction. The reactions were analysed by gel electrophoresis (GE) on a 2% agarose gel. The band size for KCNJ8 was 210bp. cDNA negative control (cDNA neg) consisted of PCR master mix with cDNA but without addition of Taq enzyme. PCR negative controls consisted of PCR master mix to which no cDNA template was added. Densitometric values were normalised by dividing KCNJ8 intensity values by β -actin intensity values and were graphed for each sample. The gels included in this section are representative of at least two independent repeats.

This analysis by semi quantitative PCR demonstrates a trend of increased KCNJ8 expression in the more invasive cell lines DLKP-1, DLKP-2 and TXT-2, compared to the poorly invasive cell lines TXT-1 and VCR. This correlates with the array KCNJ8 data.

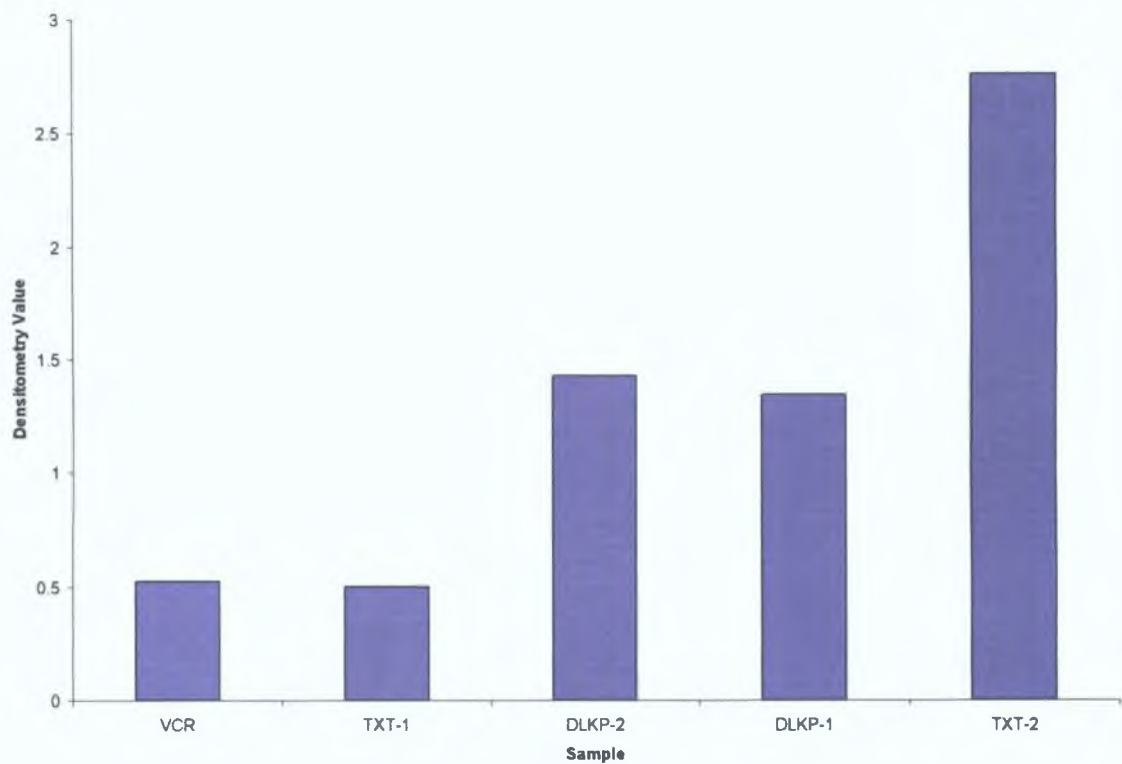


Figure 3.5.2.1 RT-PCR of KCNJ8 expression from RNA used in array samples 2003.

RNA used for this PCR was analysed on the 2003 arrays. β -actin was used as an endogenous control to normalise for RNA content in each reaction. The PCR was analysed by gel electrophoresis (GE) on a 2% agarose gel. A PCR Negative (PCR Neg) control was included in the analysis and consisted of PCR master mix to which no cDNA template was added. The trend indicates lower KCNJ8 mRNA expression in the poorly invasive cell lines TXT-1 and VCR compared to invasive cell lines.

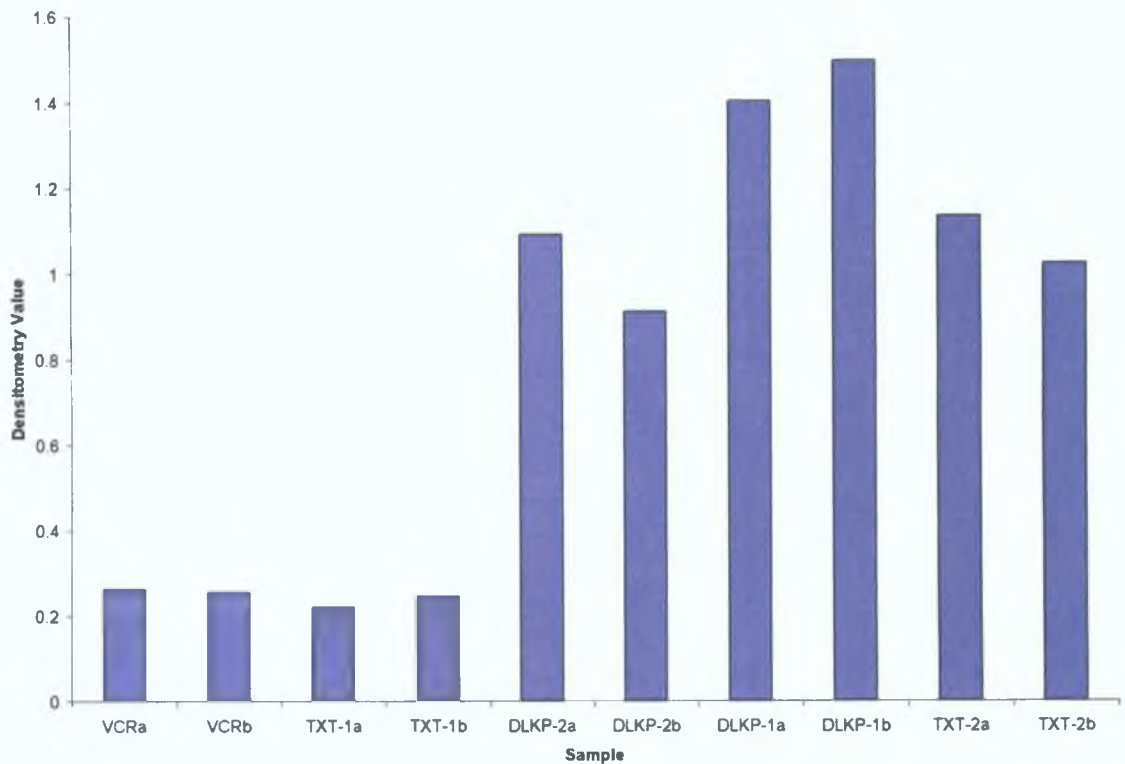


Figure 3.5.2.2 RT-PCR of KCNJ8 mRNA expression from RNA used in duplicate array samples 2004.

RNA for this reaction was analysed in the duplicate array analysis of the DLKP cell lines in 2004. β -actin was used as an endogenous control. The reaction was analysed by GE on a 2% agarose gel. PCR negative (PCR Neg) and cDNA negative controls (cDNA neg consisted of PCR master mix with cDNA but without addition of Taq enzyme) were included in the analysis. KCNJ8 mRNA expression is decreased in the poorly invasive cell lines compared to invasive cell lines.

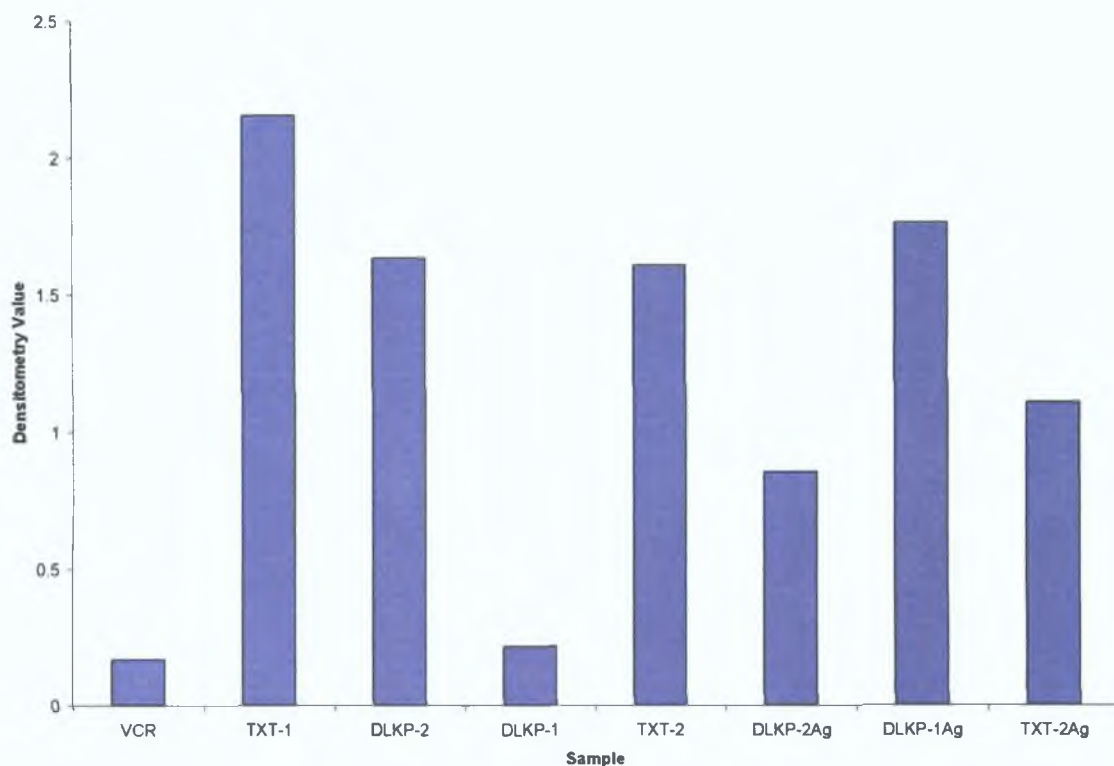


Figure 3.5.2.3 RT-PCR of KCNJ8 mRNA in a separate sample set and Agilent samples.

RNA for this analysis was from a separate batch of DLKP variant cultures not harvested or processed for Affymetrix array analysis. Also included were three samples analysed on the Agilent array platform but which were not investigated further. β -actin was used as an endogenous control. The reaction was analysed by GE on a 2% agarose gel. Densitometry values were normalised by dividing KCNJ8 intensity values by β -actin intensity values and were graphed for each sample.

This PCR demonstrates elevated KCNJ8 expression in TXT-1, which is one of the less invasive cell lines and lower KCNJ8 mRNA expression in DLKP-1. This is an unexpected result. However, KCNJ8 levels in VCR remain low.

3.5.3 KCNJ8 siRNA transfection in the invasive DLKP variants

3.5.3.1 Summary of KCNJ8 siRNA experimental plan

Since array data and RT-PCR results indicated that KCNJ8 mRNA expression was higher in the invasive compared with the mildly invasive DLKP lines, it was decided to decrease KCNJ8 expression using two independent siRNA sequences in the invasive cell lines DLKP-1, DLKP-2 and TXT-2 to investigate any impact on an invasive phenotype. Initial experiments were performed using KCNJ8 siRNA 1. A repeat was then performed using KCNJ8 siRNA 1 and the additional KCNJ8 siRNA 2 sequence. 2 μ l of NeoFx transfection reagent per well of a 6-well plate was used to transfect 30nM of target siRNA into the cells. Transfections were performed using the optimum procedures identified in Section 3.4.4.1. KCNJ8 siRNA specific knockdown was confirmed by PCR and the effect of this knockdown on proliferation and invasion investigated. Counter to what was expected; KCNJ8 knockdown appeared to enhance the invasive nature of the cell lines.

3.5.3.2 KCNJ8-specific siRNA decrease in mRNA levels

KCNJ8-specific siRNA sequences were transfected into the invasive DLKP cell lines and a decrease in mRNA expression examined by semi quantitative RT-PCR and qPCR respectively.

Timecourse analysis of KCNJ8 knockdown was investigated using RT-PCR (Figures 3.5.3.2 to 3.5.3.4). β -actin was included as an endogenous control to normalise for RNA quantities added to each reaction. The PCRs were analysed by gel electrophoresis (GE) on a 2% agarose gel. The band size for KCNJ8 was 210bp. cDNA negative control (cDNA neg) consisted of PCR master mix with cDNA but without addition of Taq enzyme. PCR negative controls consisted of PCR master mix to which no cDNA template was added. Densitometric values were calculated by dividing KCNJ8 intensity values by β -actin intensity values and were graphed for each sample. The gels included in this timecourse study are representative of at least two independent repeats. These results suggest that RT-PCR is not sensitive enough to accurately monitor KCNJ8 expression but indicates an overall trend from the data that KCNJ8 siRNA transfection did not deplete KCNJ8 mRNA expression. There is a possibility that the KCNJ8 siRNA 1 is acting like a miRNA.

Relative KCNJ8 mRNA expression was measured using a commercial TaqMan KCNJ8 probe and was normalised using β -actin as an endogenous control (Figure 3.5.3.1). An investigation into the timecourse of mRNA expression in KCNJ8 siRNA transfected samples was measured by qPCR (Figures 3.5.3.5 to 3.5.3.7). The results show that KCNJ8 knockdown was achieved at mRNA level, although the decrease was not striking in some case. There is the possibility that the KCNJ8 siRNA sequences act in a manner similar to that observed with the IGF-1R siRNA, whereby the changes in mRNA expression in response to siRNA transfection were small but expression of the IGF-1R protein was almost entirely diminished. However, this theory remains inconclusive due to the lack of a suitable KCNJ8 antibody to detect changes at the protein level.

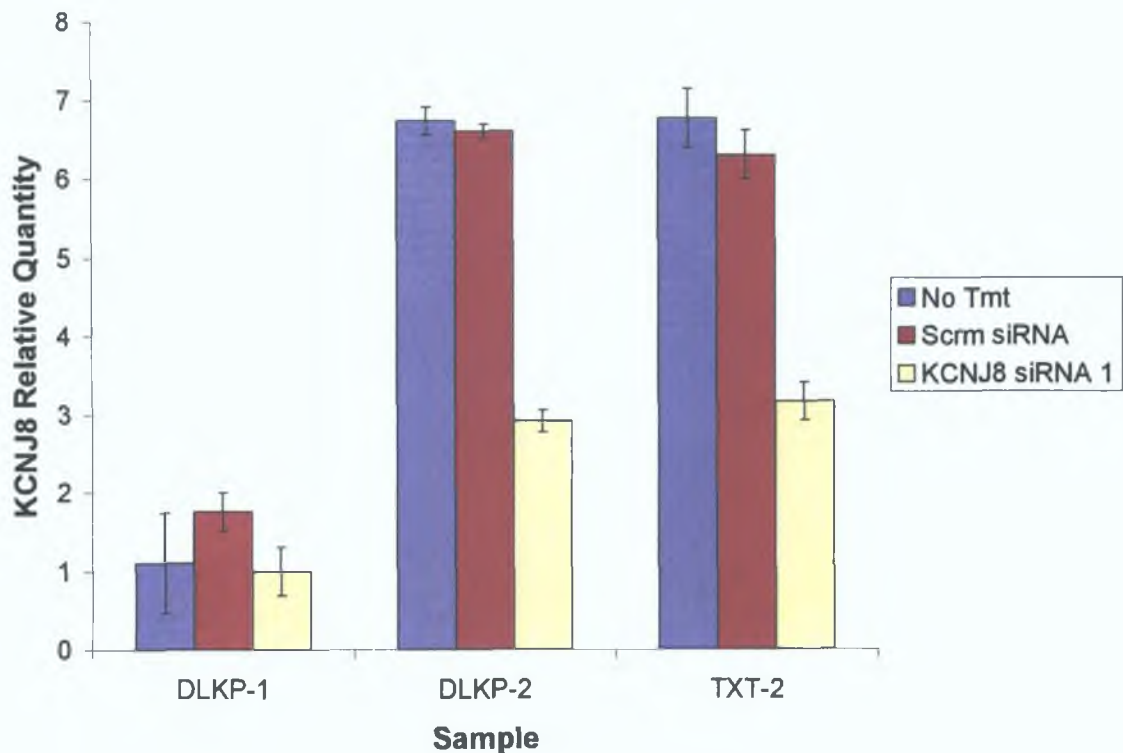
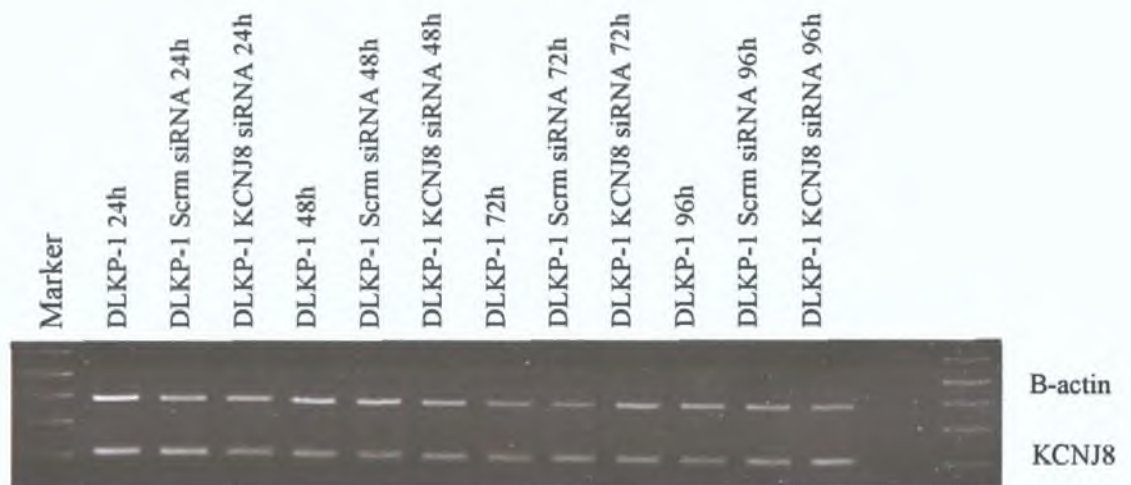


Figure 3.5.3.1 qPCR analysis of KCNJ8 siRNA experiment (I) at 24h.

KCNJ8 mRNA expression was examined by qRT-PCR using a commercial TaqMan KCNJ8 probe and normalised for RNA content using β -actin as an endogenous control. RNA was harvested 24h post-transfection and used to determine a KCNJ8-siRNA specific decrease in mRNA in response to siRNA transfection. This graph is a composite of three biological repeats. The data represents KCNJ8 expression relative to DLKP-1 KCNJ8 siRNA, which was set to 1 for the analysis and was the lowest expresser in the qPCR data set. A decrease in KCNJ8 mRNA expression was observed in the DLKP-2 and TXT-2 KCNJ8 siRNA treated samples. KCNJ8 expression in DLKP-1 was not decreased compared to untreated cells although this may be due to noise in the data.



Densitometry showing timecourse of KCNJ8 mRNA knockdown in DLKP-1 (YL)

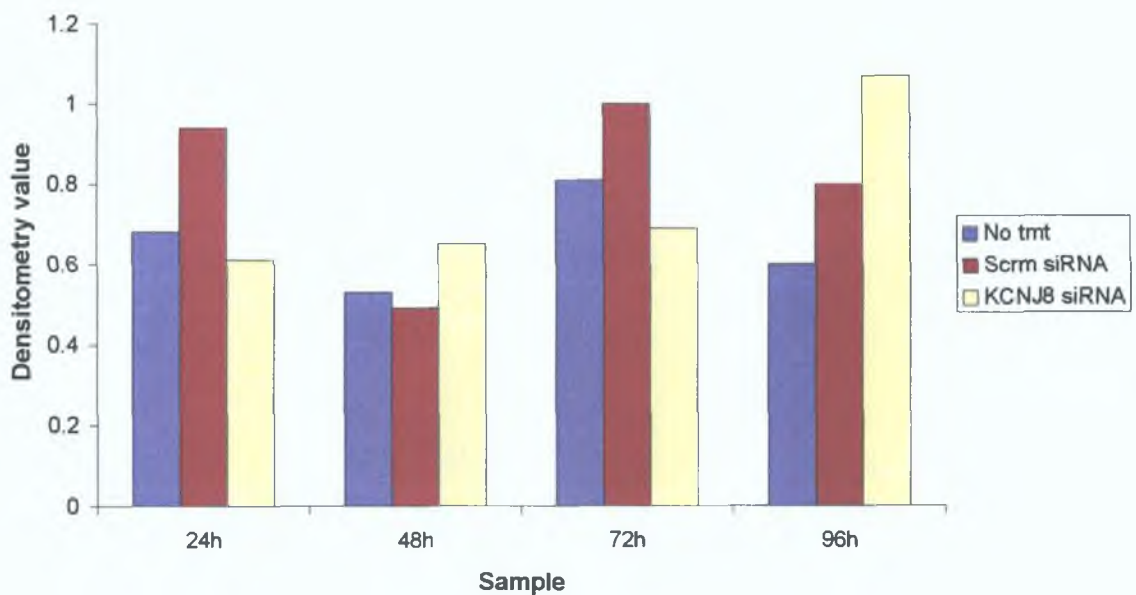


Figure 3.5.3.2 Timecourse analysis of KCNJ8 mRNA knockdown (I) by semi-quantitative RT-PCR in DLKP-1.

KCNJ8 siRNA was transfected into DLKP-1. RNA for the analysis of KCNJ8 mRNA was harvested at 24, 48, 72 and 96h. β -actin was used as an endogenous control to normalise for RNA content in each PCR. Figures for the densitometry values were normalised by dividing KCNJ8 intensity values by β -actin intensity values and were graphed for each sample. KCNJ8 mRNA expression was only slightly affected at certain time points by KCNJ8 siRNA transfection.



Densitometry showing timecourse of KCNJ8 mRNA knockdown in DLKP-2 (JC)

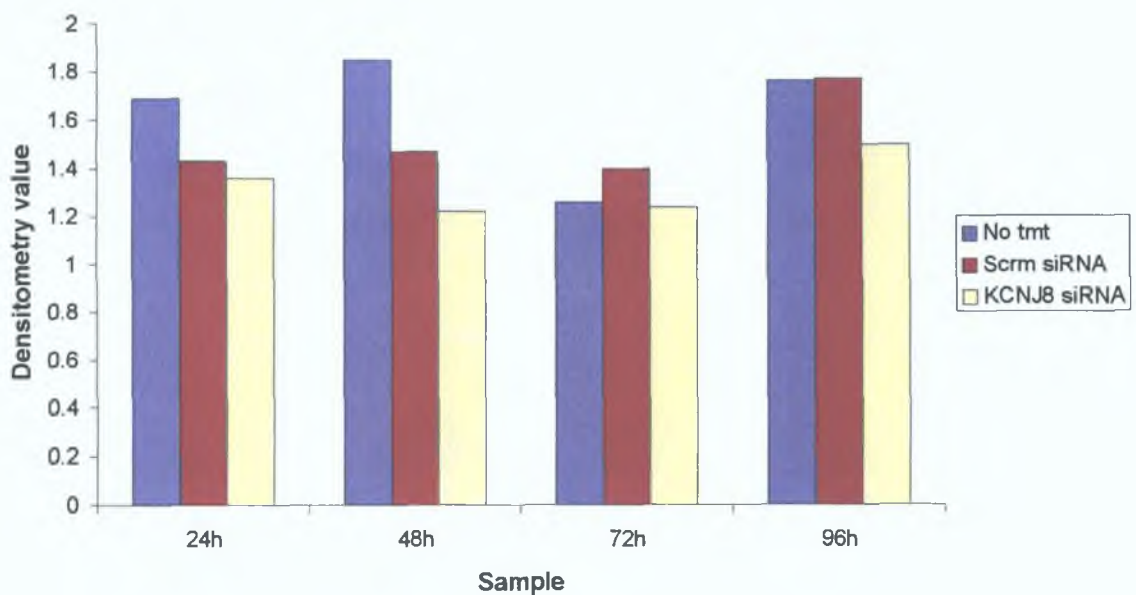


Figure 3.5.3.3 Timecourse analysis of KCNJ8 mRNA knockdown (I) by semi-quantitative RT-PCR in DLKP-2.

KCNJ8 siRNA was transfected into DLKP-2 and KCNJ8 mRNA analysed at 24, 48, 72 and 96h. β -actin was used as an endogenous control to normalise for RNA content in each PCR. cDNA negative control (cDNA neg) consisted of PCR master mix with cDNA but without addition of Taq enzyme. KCNJ8 mRNA expression was only slightly affected at certain time points by KCNJ8 siRNA transfection in DLKP-2.



Densitometry showing timecourse of KCNJ8 mRNA knockdown in TXT-2 (RL)

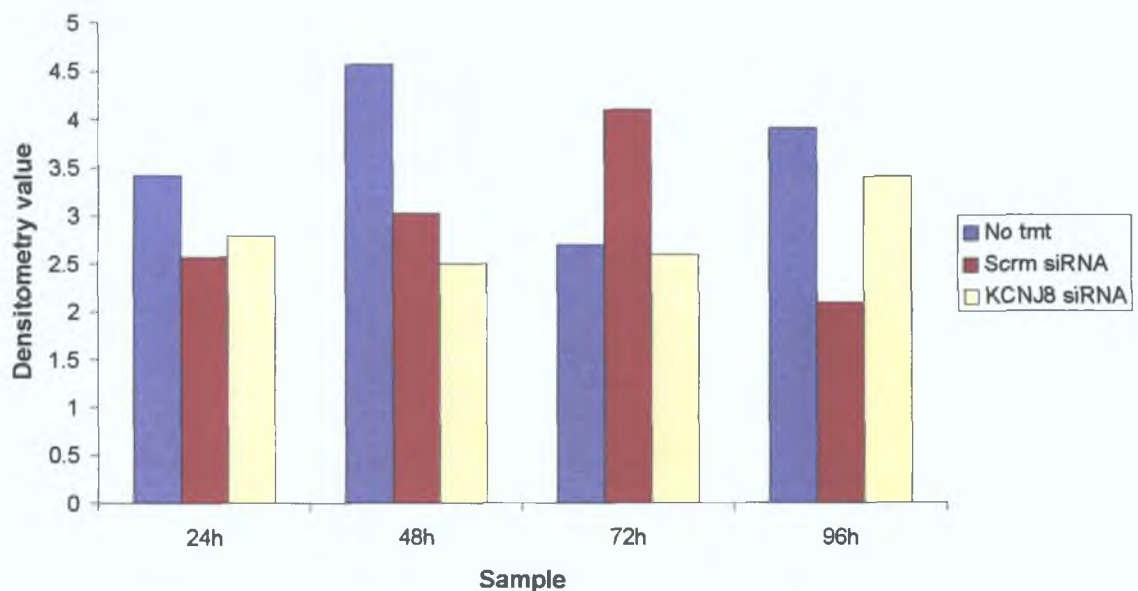


Figure 3.5.3.4 Timecourse analysis of KCNJ8 mRNA knockdown (I) by semi-quantitative RT-PCR in TXT-2.

KCNJ8 siRNA was transfected into TXT-2 and KCNJ8 mRNA measured at 24, 48, 72 and 96h. β -actin was used as an endogenous control to normalise for RNA content in each PCR. PCR negative control contained PCR master mix without addition of cDNA. Figures for the densitometry values were normalised by dividing KCNJ8 intensity values by β -actin intensity values and were graphed for each sample. KCNJ8 mRNA expression was only slightly affected by KCNJ8 siRNA transfection in TXT-2.

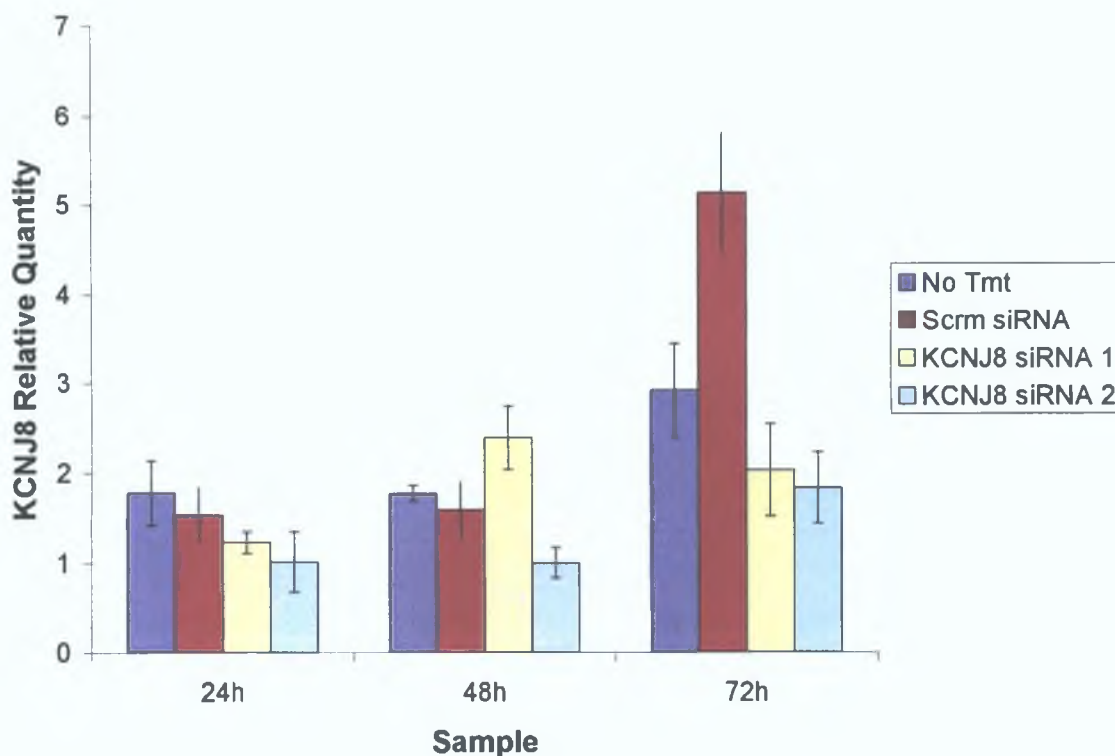


Figure 3.5.3.5 Timecourse analysis of KCNJ8 mRNA knockdown (II) in DLKP-1 by qPCR.

Two independent KCNJ8 siRNA sequences were transfected into DLKP-1. KCNJ8 mRNA expression in these samples was analysed by qPCR at 24, 48 and 72h using a commercial TaqMan KCNJ8 probe and normalised for RNA content using β -actin as an endogenous control. The data represents KCNJ8 expression relative to the lowest KCNJ8 expresser in this data set, DLKP-1 KCNJ8 siRNA 2 48h sample, which was set to 1 for the analysis. KCNJ8 mRNA expression was reduced by KCNJ8 siRNA transfection in all siRNA transfected samples with the exception of the DLKP-1 KCNJ8 siRNA 1 48h sample.

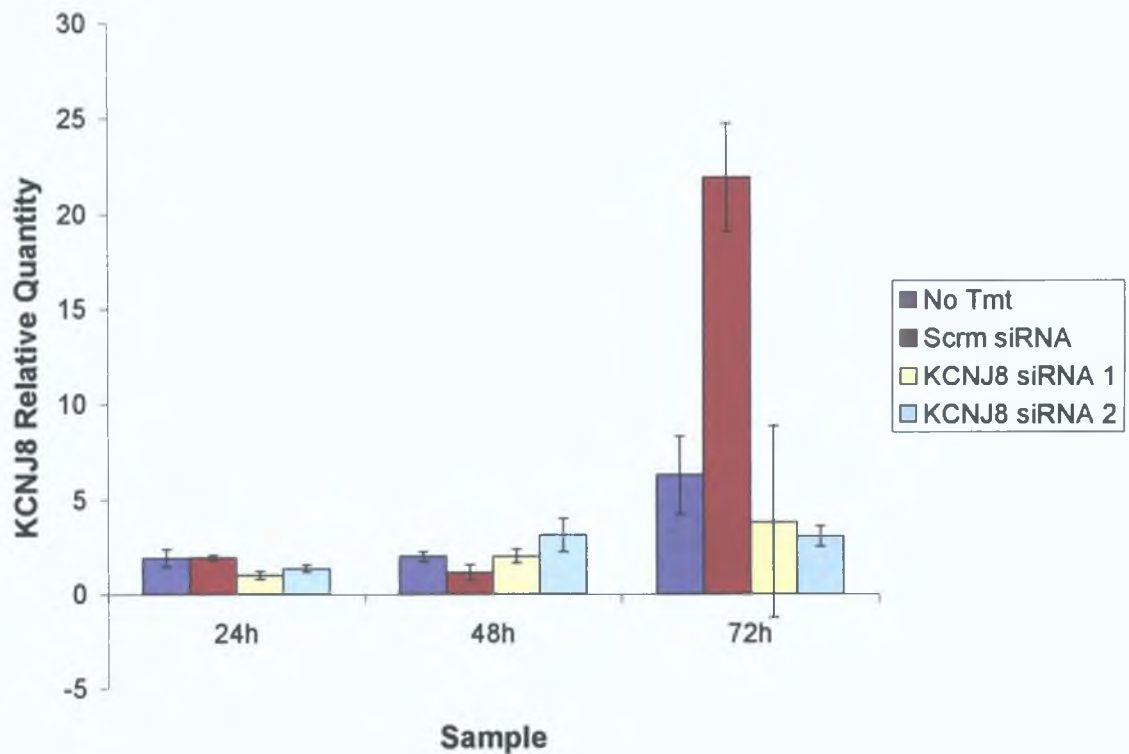


Figure 3.5.3.6 Timecourse analysis of KCNJ8 mRNA knockdown (II) in DLKP-2 by qPCR.

Two independent KCNJ8 siRNA sequences were transfected into DLKP-2. KCNJ8 mRNA expression in these samples was analysed by qPCR at 24, 48 and 72h using a commercial TaqMan probe. β -actin was used as an endogenous control. The data represents KCNJ8 expression relative to the lowest KCNJ8 expresser in this data set, DLKP-2 KCNJ8 siRNA 1 24h sample, which was set to 1 for the analysis. KCNJ8 knockdown using the KCNJ8 siRNA sequences was not achieved at mRNA level in DLKP-2 but was achieved for the 24 and 72h transfected samples. It is possible that the efficiency of the 48h transfected samples were poor than those achieved for the 24 and 72h cells.

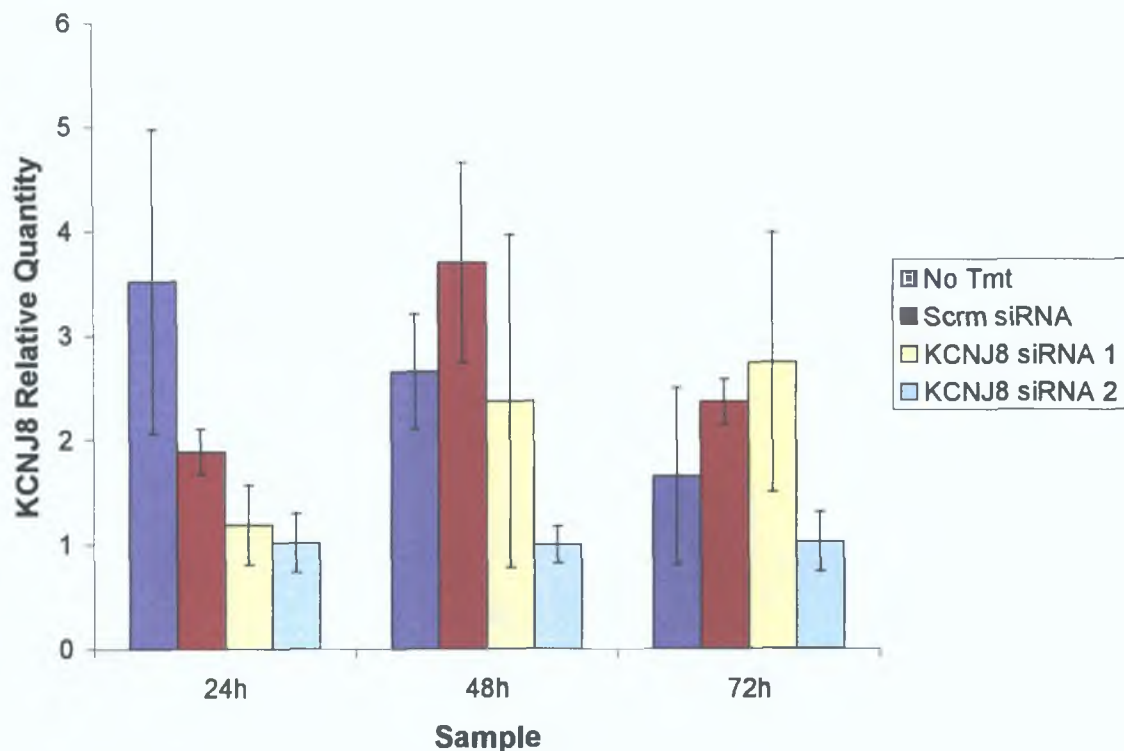


Figure 3.5.3.7 Timecourse analysis of KCNJ8 mRNA knockdown (II) in TXT-2 by qPCR.

Two independent KCNJ8 siRNA sequences were used to target KCNJ8 in TXT-2. KCNJ8 mRNA expression in these samples was analysed by qPCR at 24, 48 and 72h using a commercial TaqMan KCNJ8 probe and normalised for RNA content using β -actin as an endogenous control. The data represents KCNJ8 expression relative to the lowest KCNJ8 expresser in this data set, TXT-2 KCNJ8 siRNA 2 48h sample, which was set to 1 for the analysis. A decrease in KCNJ8 mRNA expression was attained in all KCNJ8 siRNA transfected samples with the exception of TXT-2 KCNJ8 siRNA 1 72h.

3.5.4 Evaluation of KCNJ8 siRNA effect on DLKP variant proliferation

The effect of KCNJ8 siRNA transfection on proliferation was investigated by transfecting cells seeded at 3×10^5 cells/well of a 6-well plate (Figure 3.5.4.1). Relative cell number was determined using the acid phosphatase assay at 72h post transfection. Cell numbers were measured to determine what functional effect, if any, a decrease in KCNJ8 expression was having on proliferation.

Transfection with KCNJ8 siRNA sequences did not affect proliferation compared with non-treated and scrambled siRNA transfected cells.

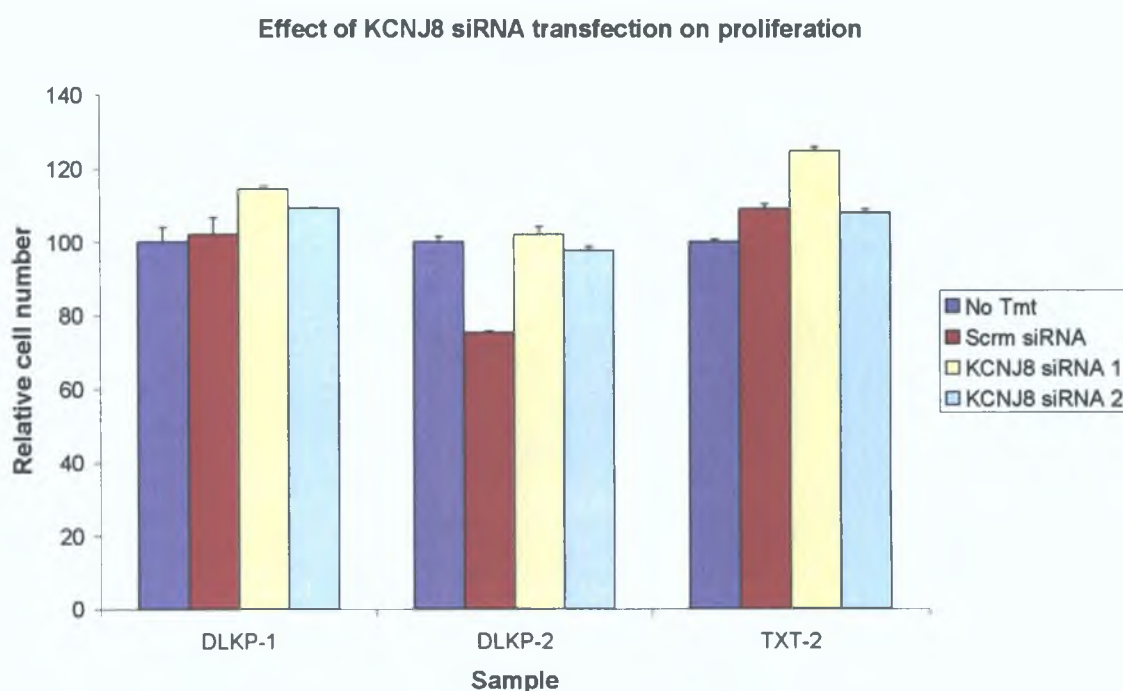


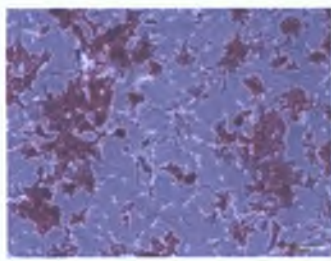
Figure 3.5.4.1 Effect of siRNA targeting KCNJ8 on DLKP variant cell number.

The cells were seeded at a 3×10^5 cells/well of a 6-well plate. Cell number was measured using the acid phosphatase assay at 72h post transfection. KCNJ8 siRNA transfection does not appear to significantly affect proliferation compared with the scrambled siRNA and non-treated cells.

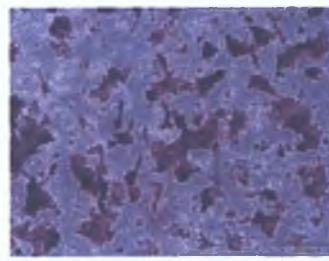
3.5.5 Evaluation of KCNJ8 knockdown on DLKP variant invasion

The effect of KCNJ8 knockdown on DLKP variant invasion was investigated. Invasion assay analysis was performed 72h post transfection, using commercial invasion assay kits containing inserts pre-coated with matrigel in conjunction with a serum gradient. The cells were incubated at 37°C for 24h after which, the underside of the inserts were stained with crystal violet and allowed to air dry. The inserts were then photographed using 10X magnification. Ten fields of view were counted per insert at 20X magnification and averaged. At least two inserts were used for the analysis of each condition. The counts per number of inserts used were then also averaged and this figure was used to generate graphs of relative invasive capacity per cell line per condition.

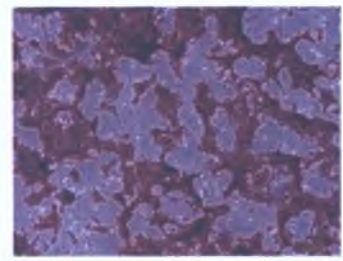
One set of representative photographs was included (Figure 3.5.5.1) in this section and clearly shows an increase in invasion in KCNJ8 siRNA transfected cells. Invasion assay results are also presented graphically (Figures 3.5.5.2 and 3.5.5.3).



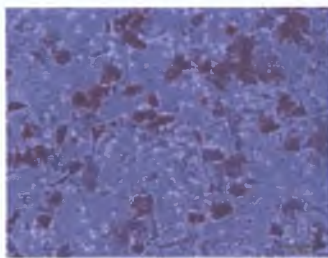
DLKP-1 10x No tmt



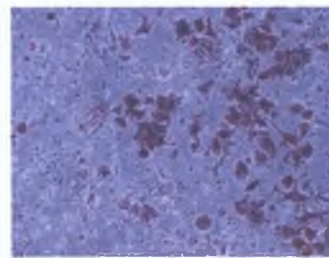
DLKP-1 10x Scrm siRNA



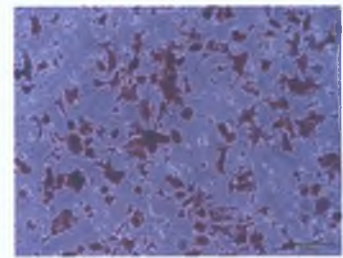
DLKP-1 10x KCNJ8 siRNA 1



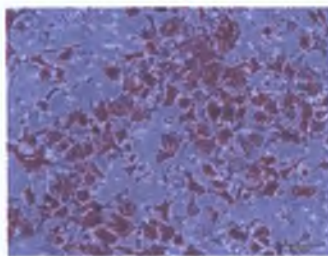
DLKP-2 10x No tmt



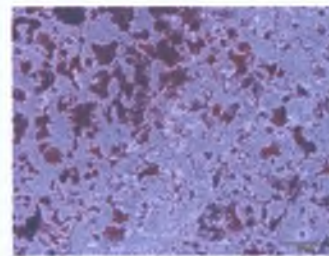
DLKP-2 10x Scrm siRNA



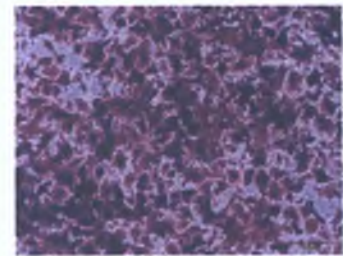
DLKP-2 10x KCNJ8 siRNA 1



TXT-2 10x No tmt



TXT-2 10x Scrm siRNA



TXT-2 10x KCNJ8 siRNA 1

Figure 3.5.5.1 Photographic representation of invasion assay results 72h post KCNJ8 siRNA transfection (I).

The invasion assay was performed 72h post-transfection. Untransfected- and scrambled siRNA transfected- cell lines were the controls for this experiment. Representative photographs at 10X are shown above. Invasion was increased in KCNJ8 siRNA transfected cells compared with the scrambled siRNA and non-treated cells.

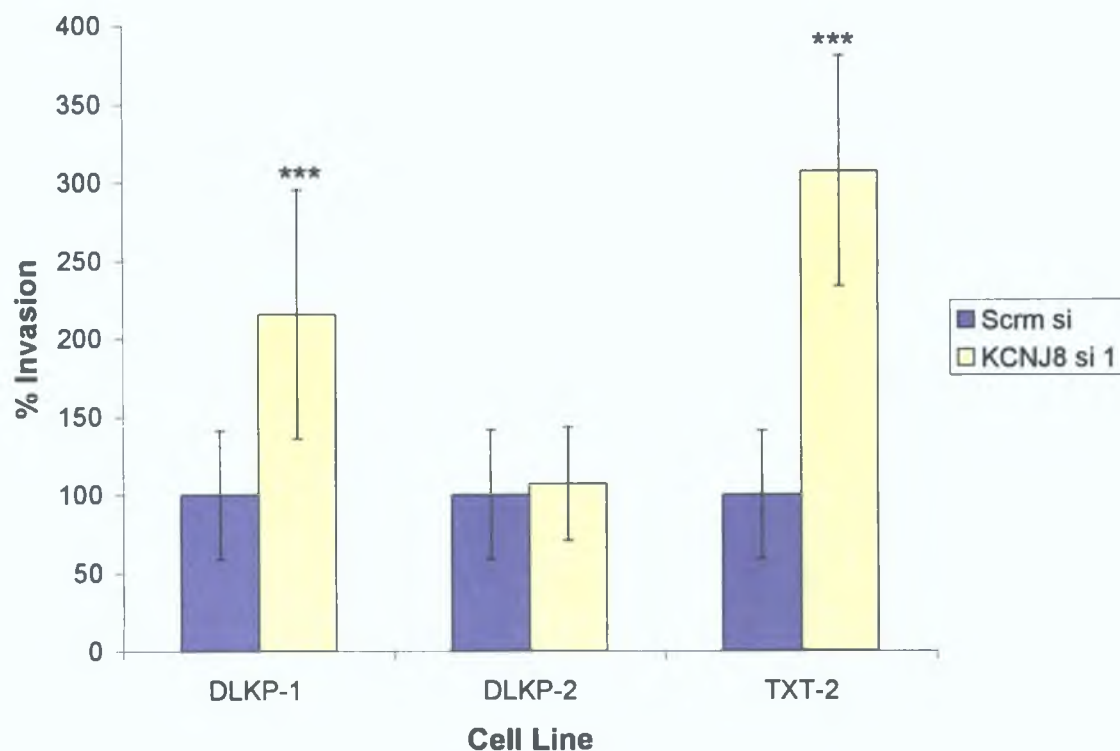


Figure 3.5.5.2 Graphic representation of invasion assay results 72h post KCNJ8 siRNA transfection (I).

The invasion assay was performed 72 hours post-transfection. Untransfected- and scrambled siRNA transfected- cell lines were the controls for this experiment. Ten random fields were counted at 20X. Each condition was examined using at least two invasion kit inserts. Counts per insert were averaged and plotted as percentage invasion normalised to the scrambled siRNA for each cell line. Invasion was increased in KCNJ8 siRNA transfected cells compared with the scrambled siRNA control ($P < 0.001$), except in the case of DLKP-2, which may be due to poor transfection efficiency in this cell line.

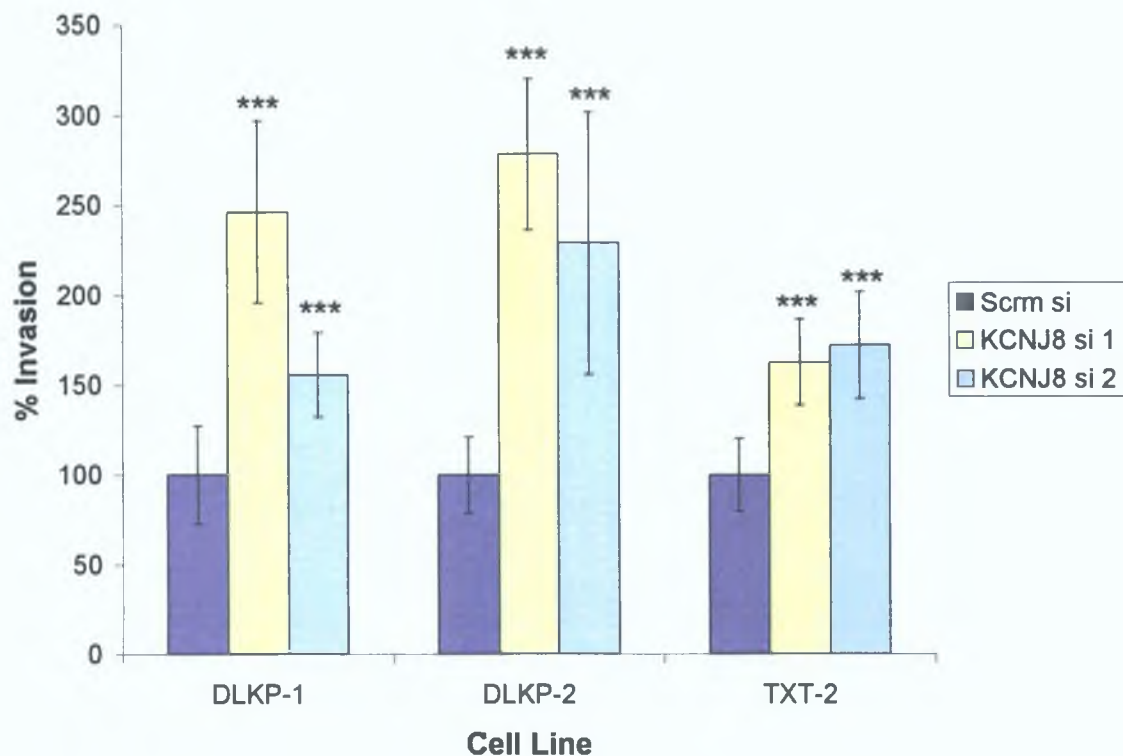


Figure 3.5.5.3 Graphic representation of invasion assay results 72h post KCNJ8 siRNA transfection (II).

The invasive cell lines DLKP-1, DLKP-2 and TXT-2 were transfected with scrambled siRNA and two independent siRNA sequences to KCNJ8. The effect of decreasing KCNJ8 expression on invasion was examined 72h post transfection. Ten random fields were counted at 20X. Each condition was examined using at least two invasion kit inserts. Counts per insert were averaged and plotted as percentage invasion normalised to the scrambled siRNA for each cell line. An increase was observed in invasion in both of the KCNJ8 siRNA transfected samples compared with the scrambled siRNA control ($P < 0.001$).

3.5.6 KCNJ8 cDNA transfection in the less- or non-invasive DLKP variants

3.5.6.1 Summary of KCNJ8 cDNA experimental plan

Since array data and RT-PCR results indicated that KCNJ8 mRNA expression was higher in the invasive compared with the less invasive DLKP lines, it was decided to increase KCNJ8 expression by transfecting the expression vector pSport6 containing the cDNA sequence to KCNJ8 into the mildly/non-invasive cell lines TXT-1 and VCR. This would help determine whether increasing KCNJ8 expression in poorly invasive cell lines could induce an invasive phenotype. Western blot (not fully optimised) was used to examine KCNJ8 expression in the cDNA transfected samples.

3.5.6.2 Evaluation of cDNA transient transfection efficiency using GFP

Two cell lines, TXT-1 and VCR, were transiently transfected with Green Fluorescent Protein (GFP) expression plasmid using different conditions in order to achieve optimal transfection efficiency (Figures 3.5.6.1 to 3.5.6.4). Cells were seeded at 5×10^5 cells/well of a six-well plate and transfected using 2 or 4 μg GFP plasmid with 5 or 10 μl of Lipofectamine 2000, transfection reagent. Transfection efficiency was evaluated by estimating the number of green fluorescent cells per field of vision.

Using 2 μg GFP with 5 μl Lipofectamine 2000, approximately 80% efficiency was achieved for TXT-1, while approximately 60% was achieved for VCR. There was a toxic effect attributed to the use of Lipofectamine 2000, so 2 μg plasmid DNA, 5 μl Lipofectamine 2000 were the conditions chosen for all cDNA transient transfections used in this study.



Figure 3.5.6.1 Evaluation of cDNA transfection efficiency I.

TXT-1 transfected using 2 μ g GFP with 5 μ l Lipofectamine 2000 and viewed under normal and fluorescent view. Transfection efficiency here is approximately 80%.

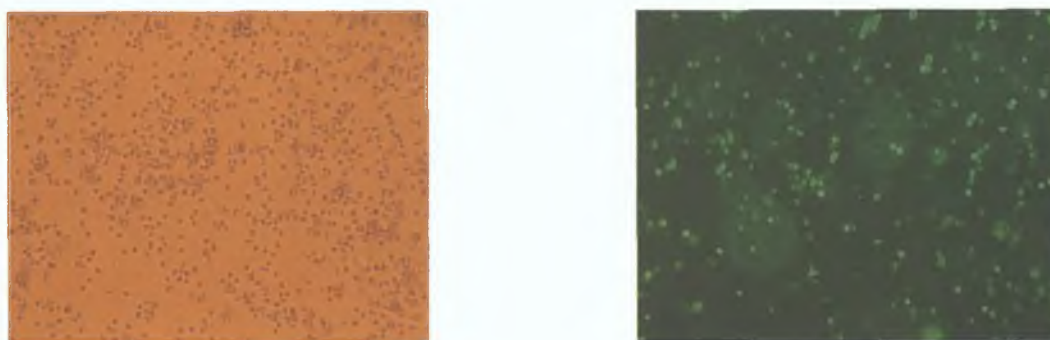


Figure 3.5.6.2 Evaluation of cDNA transfection efficiency II.

TXT-1 transfected using 4 μ g GFP with 10 μ l Lipofectamine 2000 and viewed under normal and fluorescent view. Transfection efficiency here is approximately 60%.

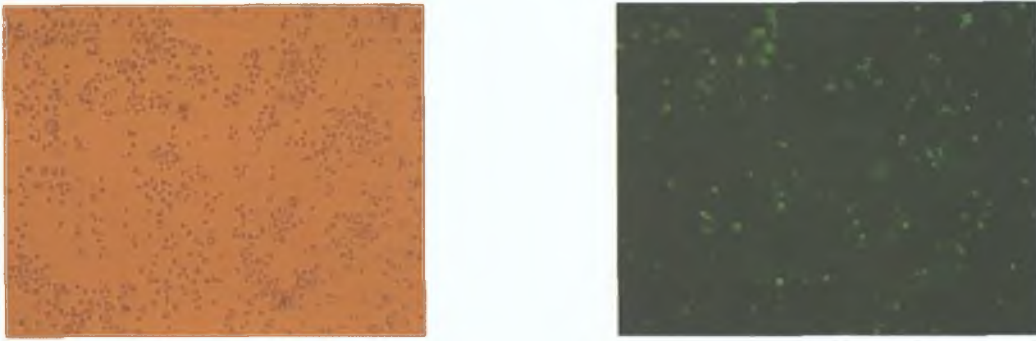


Figure 3.5.6.3 Evaluation of cDNA transfection efficiency III.

VCR transfected using 2 μ g GFP with 5 μ l Lipofectamine 2000 and viewed under normal and fluorescent view. Transfection efficiency here is approximately 60%.

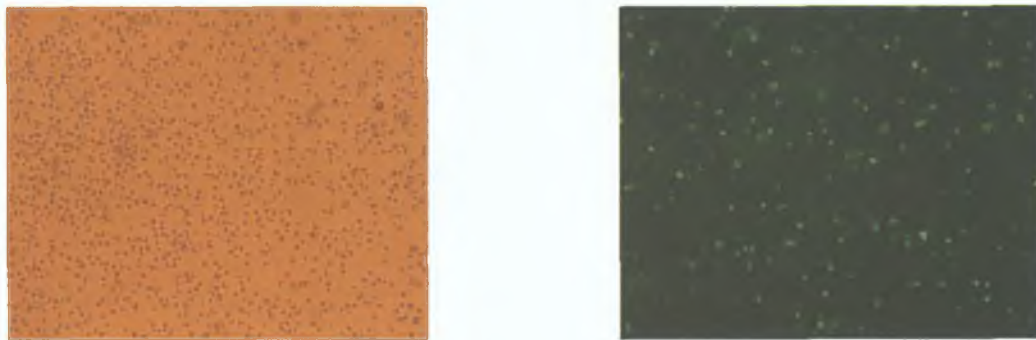


Figure 3.5.6.4 Evaluation of cDNA transfection efficiency IV.

TXT-1 transfected using 4 μ g GFP with 10 μ l Lipofectamine 2000 and viewed under normal and fluorescent view. Transfection efficiency here is approximately 40%.

3.5.6.3 Western blot analysis of KCNJ8 cDNA transient transfection

Considerable effort was made to determine KCNJ8 protein expression in the poorly invasive DLKP variants and their KCNJ8 cDNA transfected counterparts by western blot. Cells transfected with a pSport6 empty vector were used as a control to ensure that the transfection process did not affect target protein expression (Figures 3.5.6.5 and 3.5.6.6)

The polyclonal anti-kir6.1 (KCNJ8) CAF-1 antibody used in these experiments was a gift from Prof. William A. Coetzee (NYU School of Medicine) and was raised in chickens. Blots were incubated using a 1/200 dilution of this antibody which reportedly generates a 44kDa band specific to KCNJ8 as well as other non-specific bands. The western blot was not fully optimised and one cannot draw any conclusions, as there was no obvious increase at the 44kDa size or any clearly identifiable band. One strategy to overcome this limitation could include the utilisation of HA tags to quantify the KCNJ8 protein. Alternatively, an in-house antibody to KCNJ8 could be developed to aid more sensitive KCNJ8 protein detection, although previous studies by Yoshida *et al.*, (2004) demonstrate the difficulties in developing a specific and sensitive antibody to this protein.

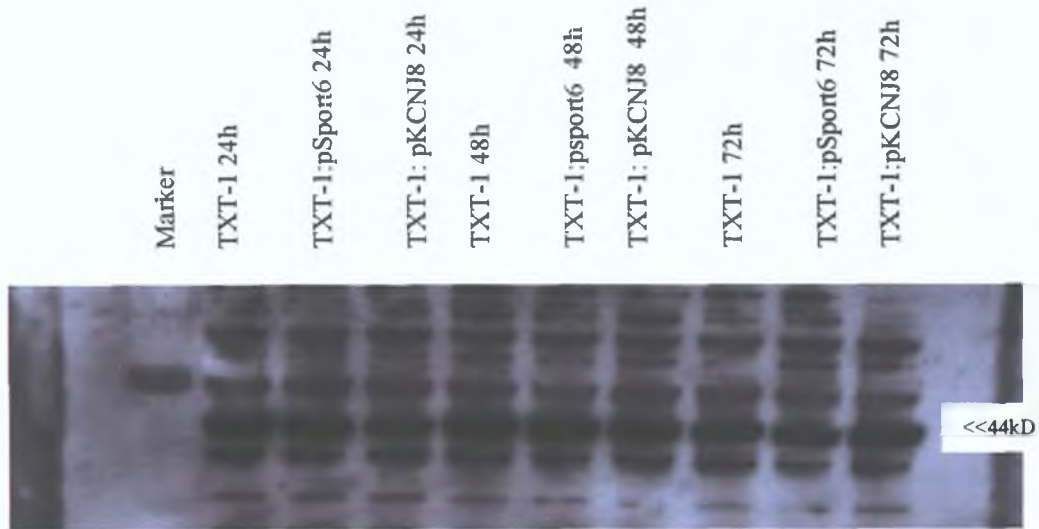


Figure 3.5.6.5 Western blot analysis of KCNJ8 cDNA transient transfection in TXT-1.

The polyclonal anti-kir6.1 (KCNJ8) CAF-1 antibody used in this experiment was a gift from Prof. William A. Coetzee (NYU School of Medicine) and was raised in chickens. Blots were incubated using a 1/200 dilution of this antibody and generates a 44kDa band specific to KCNJ8. Due to the number of non-specific bands on the blot it is one cannot conclude if KCNJ8 cDNA transfection increased protein expression in TXT-1 or not. Ideally, this protocol would be optimised further.

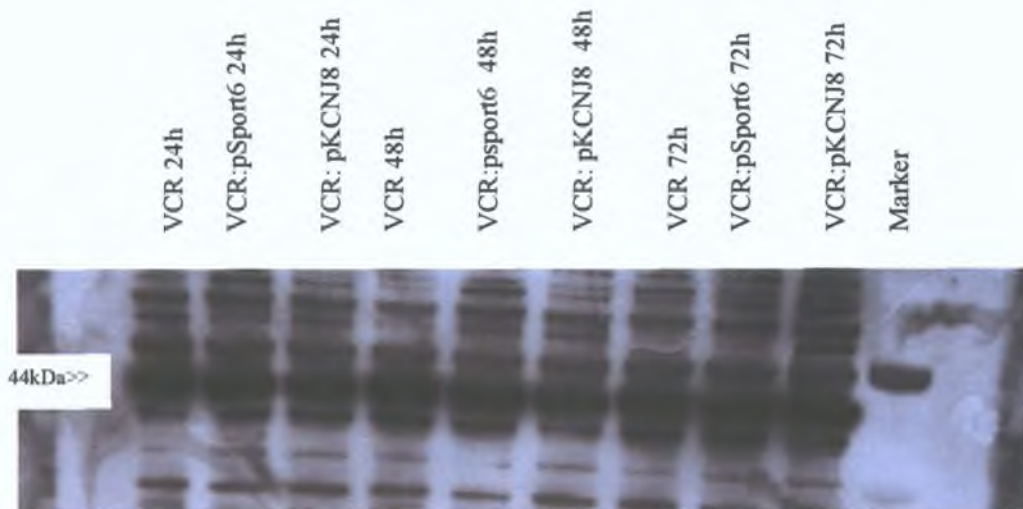


Figure 3.5.6.6 Western blot analysis of KCNJ8 cDNA transient transfection in VCR.

Blots were incubated using a 1/200 dilution of the CAF-1 antibody. The expected size of KCNJ8 is 44kDa. Due to the number of non-specific bands on the blot one cannot conclude that KCNJ8 cDNA transfection increased KCNJ8 protein expression in VCR. Ideally, this protocol would be optimised further.

3.5.6 4 Evaluation of KCNJ8 cDNA transient transfection on invasion

The effect of increasing KCNJ8 expression in the poorly invasive DLKP variants was examined. Invasion assay analysis was performed 72h post transfection, using commercial invasion assay kits containing inserts pre-coated with matrigel in conjunction with a serum gradient. The cells were incubated at 37°C for 24 hours after which, the underside of the inserts were stained with crystal violet and allowed to air dry. The inserts were then photographed using 10X magnification. Ten fields of view were counted per insert at 20X magnification and averaged. At least two inserts were used for the analysis of each condition. The counts per number of inserts used were then also averaged and this figure was used to generate graphs of relative invasive capacity per cell line per condition.

One set of representative photographs were included (Figure 3 5 6 7) in this section and do not clearly demonstrate any changes in the invasive capacities of TXT-1 or VCR in response to KCNJ8 cDNA transfection. These invasion assay results are also presented graphically (Figures 3 5 6 8). However, one cannot conclude that increasing KCNJ8 expression impacts on invasion since the increase in KCNJ8 protein expression was unconfirmed.

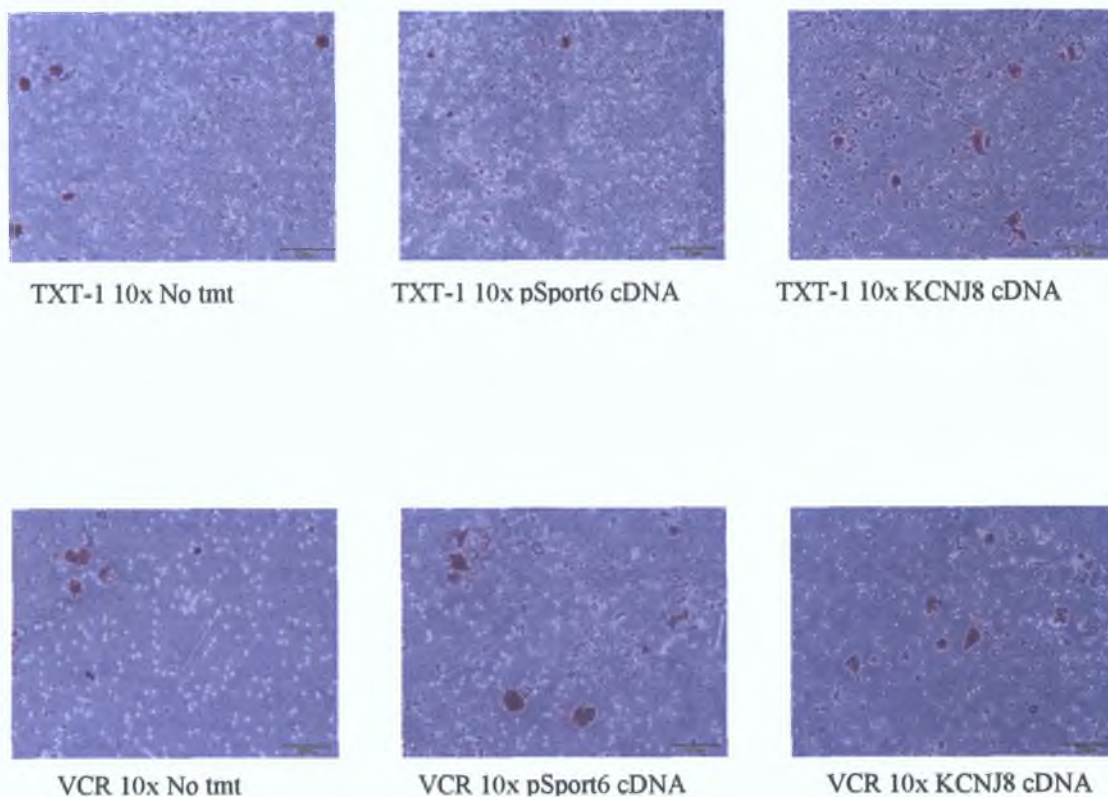


Figure 3.5.6.7 Photographic representation of invasion assay results 72h post KCNJ8 cDNA transfection.

The invasion assay was performed 72h post-transfection. Untransfected- and pSport6 empty vector transfected- cell lines are the controls for this experiment. Ten random fields were counted per insert at 20X. An increase in invasion was observed in the KCNJ8 cDNA transfected TXT-1 cell line ($P < 0.001$). No effect on invasion was observed in KCNJ8 cDNA transfected VCR cells compared with the empty vector and non-treated cells. This may be because there was no increase in KCNJ8 expression in KCNJ8 cDNA transfected VCR cell line, or that increased KCNJ8 expression is itself insufficient to induce an invasive phenotype in mildly invasive cells. This result is inconclusive.

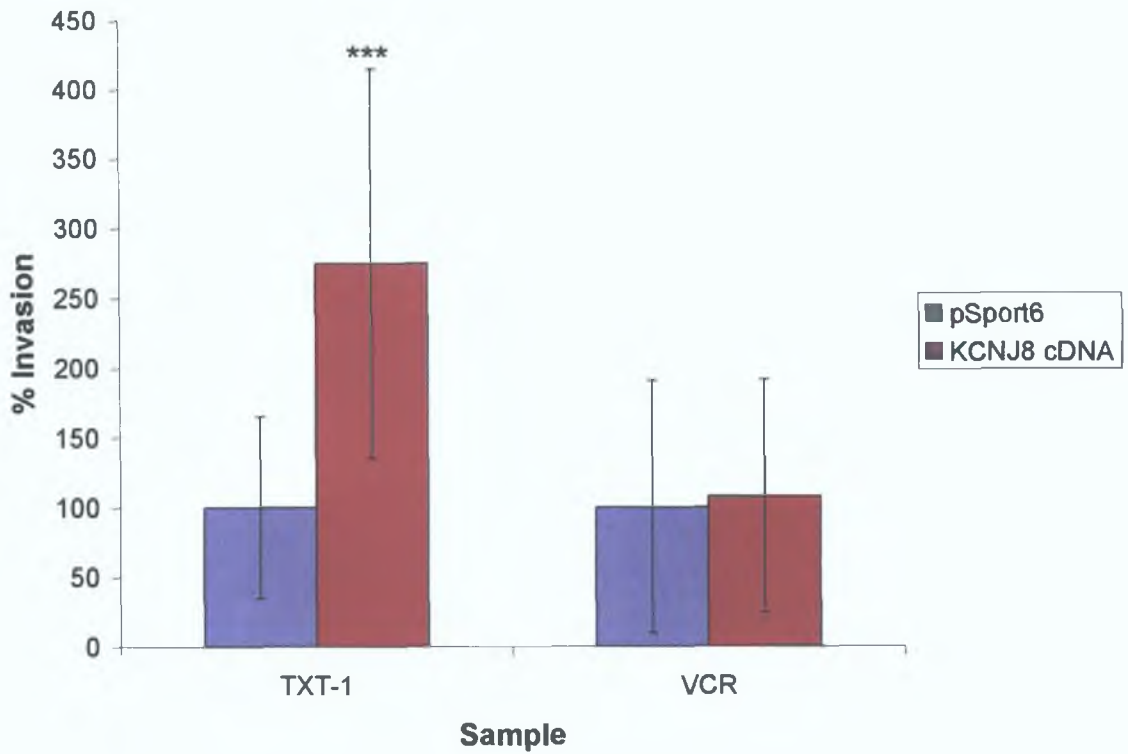


Figure 3.5.6.8 Graphic representation of invasion assay results 72 hrs post KCNJ8 cDNA transfection.

An increase in invasion was observed in the KCNJ8 cDNA transfected TXT-1 cell line ($P < 0.001$). No effect on invasion was observed in KCNJ8 cDNA transfected VCR cells compared with the empty vector control cells. This may potentially be attributed to poor transfection efficiency in this cell line. This result is inconclusive as no increase in KCNJ8 protein expression was confirmed by western blot.

3.6 Investigation into role of S100A13 in invasion in the DLKP variants

3.6.1 Aims of S100A13 experiments

S100A13 was identified as a gene potentially involved in invasion from the microarray analysis. The data indicated that S100A13 expression was increased in the more invasive cell lines compared with the poorly invasive DLKP variants. The aims of this set of experiments was as follows:

- 1 To confirm by PCR that S100A13 is differentially expressed between the DLKP cell lines
- 2 To decrease S100A13 expression by transfecting three independent siRNA sequences to S100A13 into the invasive cell lines DLKP-1, DLKP-2 and TXT-2
- 3 To demonstrate S100A13-specific siRNA knockdown at mRNA level
- 4 To evaluate the effect of S100A13 knockdown on proliferation
- 5 To evaluate the effect of decreased S100A13 expression on invasion
- 6 To increase S100A13 expression by transfecting a pSport6 plasmid containing the S100A13 sequence into the mildly invasive cell lines TXT-1 and VCR
- 7 To demonstrate an increase in S100A13 protein expression in cDNA transfected cells
- 8 To evaluate the effect of increasing S100A13 expression on invasion

To summarise the results detailed in this section, it was found that S100A13 was differentially expressed in the panel of cell lines studied, correlating with array data. Decreasing S100A13 expression had no effect on proliferation but did decrease invasion, as determined by *in vitro* invasion assays. Increasing S100A13 expression had no effect on invasion in the less/non-invasive cell lines, despite a measurable increase in protein expression following transient transfection.

3.6.2 RT-PCR validation of differential S100A13 mRNA expression

Semi-quantitative RT-PCR was used to confirm that S100A13 mRNA expression was higher in the invasive DLKP variants compared with the poorly invasive variants and were reflective of array data.

RNA from the duplicate array samples 2004 (Figure 3.6.2.1), RNA from a fresh set of cultures harvested separately to those for array analysis including RNA from three samples analysed on the Agilent array platform (Figure 3.6.2.2) were subject to this analysis. The Agilent data was not analysed further in this work. The aim of using different batches of RNA samples was to ensure that results from the array study matched to independent analysis of the cell lines.

β -actin was used as an endogenous control to normalise for RNA quantities added to each S100A13 PCR. The reactions were analysed by gel electrophoresis (GE) on a 2% agarose gel. The band size for S100A13 was 219bp. PCR negative controls consisted of consisted of PCR master mix to which no cDNA template was added. cDNA negative control (cDNA neg) contained PCR master mix with cDNA but without addition of Taq enzyme. Densitometric values were normalised by dividing S100A13 intensity values by β -actin intensity values and were graphed for each sample. The gels included in this section are representative of at least two independent repeats.

This analysis by semi-quantitative PCR demonstrates a trend towards higher S100A13 expression in the more invasive cell lines DLKP-2 and TXT-2, compared to the mildly invasive cell lines TXT-1 and VCR. This correlates with the results from the array data. DLKP-1 did not follow the expected trend.

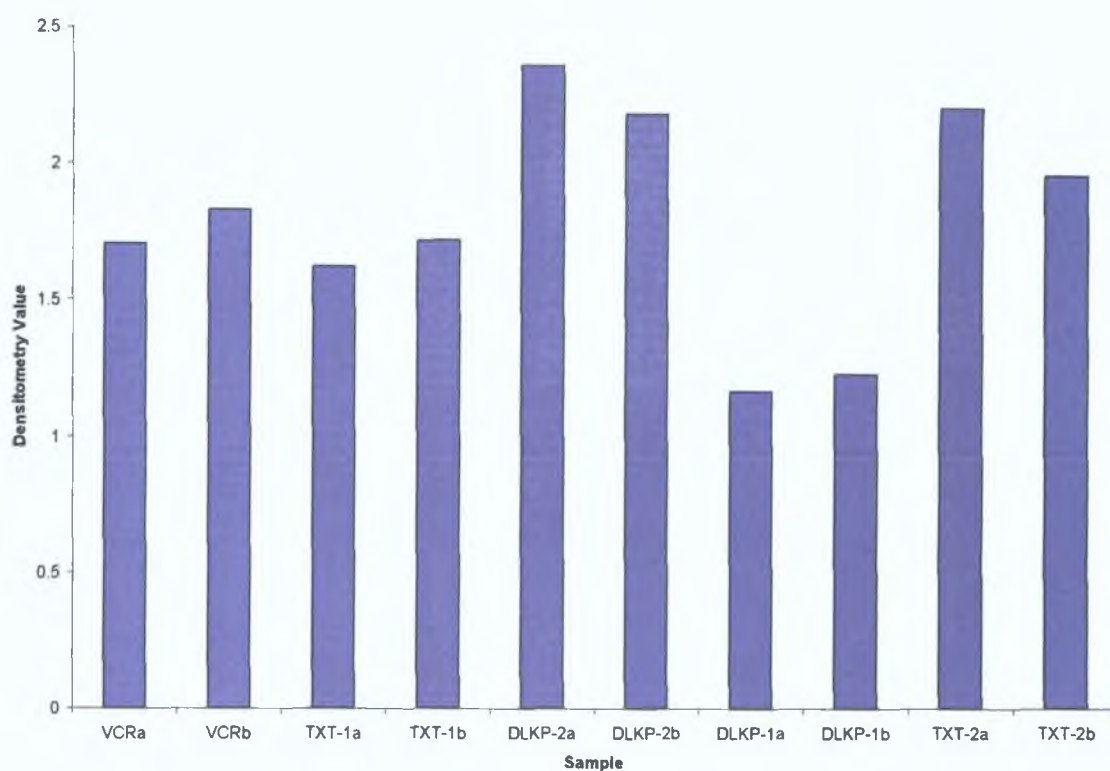


Figure 3.6.2.1 RT-PCR of S100A13 mRNA expression from RNA used in duplicate array samples 2004.

RNA for this reaction was analysed in the duplicate array analysis of the DLKP cell lines in 2004. β -actin was used as an endogenous control to normalise for RNA content in each reaction. The PCR was analysed by gel electrophoresis (GE) on a 2% agarose gel. PCR negative (PCR Neg was comprised of PCR master mix without cDNA template) and cDNA negative controls (cDNA neg consisted of PCR master mix with cDNA but without Taq) were included in the PCR. Densitometry was used to measure of band intensity. Densitometry values were normalised by dividing S100A13 intensity values by β -actin intensity values and were graphed for each sample. This PCR demonstrates increased S100A13 expression in the more invasive cell lines DLKP-2 and TXT-2, compared to the lesser invasive cell lines TXT-1 and VCR. Surprisingly, low S100A13 mRNA levels were obtained in DLKP-1.

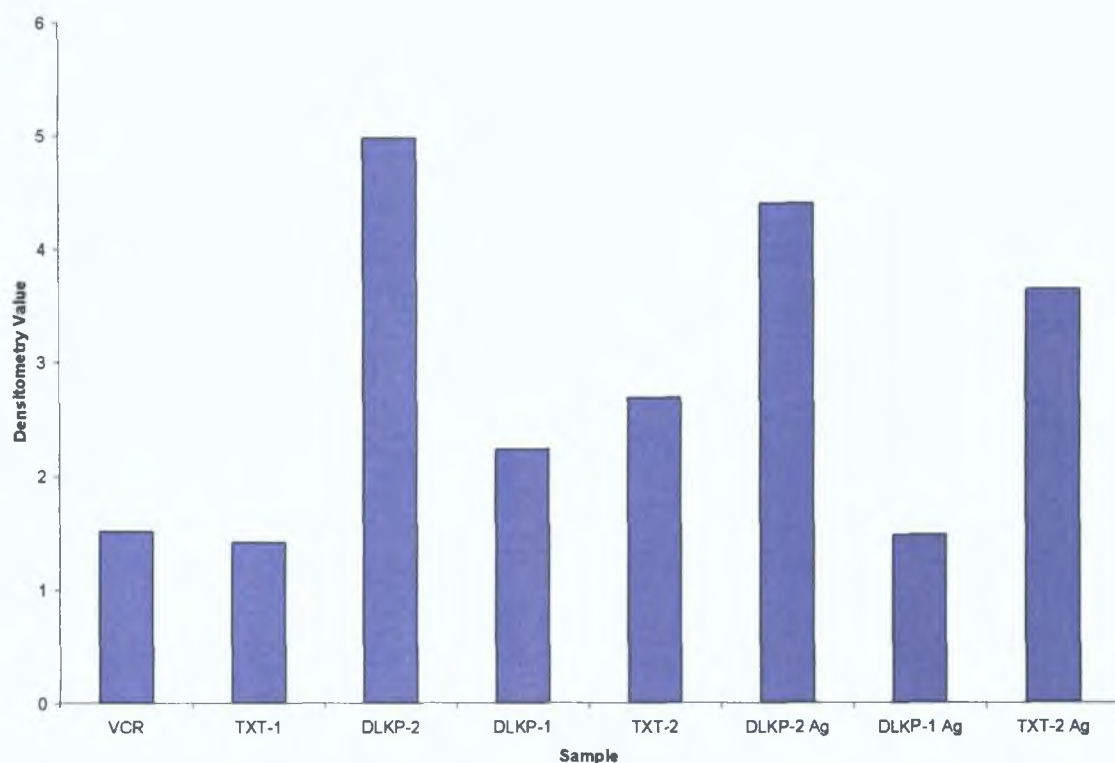


Figure 3.6.2.2 RT-PCR of S100A13 mRNA in a separate sample set and Agilent samples.

RNA for this analysis was from a separate batch of DLKP variant cultures not harvested or processed for Affymetrix array analysis. Also included were three samples analysed on the Agilent array platform but which were not investigated further. β -actin was used as an endogenous control to normalise for RNA content. The reaction was analysed by GE on a 2% agarose gel. Densitometry values were normalised by dividing S100A13 intensity values by β -actin intensity values and were graphed for each sample. This PCR demonstrates a trend towards increased S100A13 expression in the more invasive cell lines DLKP-1, DLKP-2 and TXT-2, compared to the lesser invasive cell lines TXT-1 and VCR. This result agrees with the array data.

3.6.3 S100A13 siRNA transfection in the invasive DLKP variants

3.6.3.1 Summary of S100A13 siRNA experimental plan

Array data and RT-PCR results indicated that S100A13 mRNA expression was higher in the invasive compared with the less invasive DLKP lines, thus it was decided to knockdown S100A13 expression using three independent siRNA sequences in the invasive cell lines DLKP-1, DLKP-2 and TXT-2 and determine any functional effect on invasion. Initial experiments were performed using S100A13 siRNA 1. A repeat was then performed using S100A13 siRNA 1 and the additional S100A13 siRNA 2 and S100A13 siRNA 3 sequences. 2µl of NeoFx transfection reagent per well of a 6-well plate was used to transfect 30nM of target siRNA into the cells. Transfections were performed according to the optimum procedures identified in Section 3.4.4.1. S100A13-specific knockdown was confirmed by qPCR and the effect S100A13 knockdown on proliferation and invasion investigated.

3.6.3.2 S100A13-specific siRNA decrease in mRNA levels

Three S100A13-specific siRNA sequences were transfected into the invasive DLKP cell lines and a decrease in mRNA expression examined by semi quantitative RT-PCR and qPCR respectively

Timecourse analysis of S100A13 knockdown was examined using RT-PCR (Figures 3 6 3 2 to 3 6 3 4) β -actin was included as an endogenous control to normalise for RNA content in each reaction. The PCRs were analysed by gel electrophoresis (GE) on a 2% agarose gel. The band size for S100A13 was 219bp. cDNA negative control (cDNA neg) consisted of PCR master mix with cDNA but without addition of Taq enzyme. PCR negative controls consisted of PCR master mix to which no cDNA template was added. Figures for the densitometry values were normalised by dividing S100A13 intensity values by β -actin intensity values and were plotted for each sample. The gels included in this timecourse study are representative of at least two independent repeats. These results demonstrate that RT-PCR is not sensitive enough to accurately monitor S100A13 expression but indicates an overall trend from the data that S100A13 siRNA transfection did affect S100A13 mRNA expression.

A commercial TaqMan probe to S100A13 was used to more accurately measure relative S100A13 mRNA expression. The data was normalised using β -actin as an endogenous control (Figure 3 6 3 1). An investigation into the timecourse of mRNA expression in S100A13 siRNA transfected samples was measured by qPCR (Figures 3 6 3 5 to 3 6 3 7). The results confirm that S100A13 knockdown was achieved at the mRNA level.

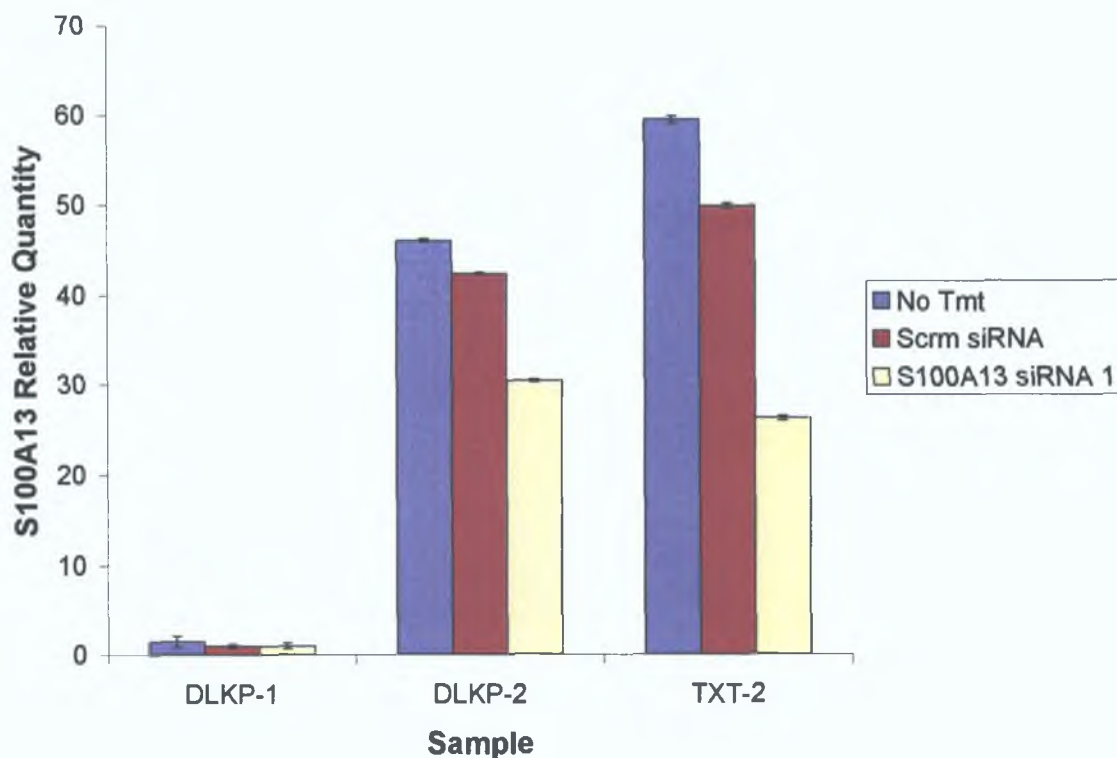


Figure 3.6.3.1 qPCR analysis of S100A13 siRNA experiment (I) at 24h.

S100A13 mRNA expression was examined by qRT-PCR using a commercial TaqMan S100A13 probe and normalised for RNA content using β -actin as an endogenous control. RNA was harvested 24h post-transfection and used to determine an S100A13-siRNA specific decrease in mRNA in response to siRNA transfection. The data represents S100A13 expression relative to DLKP-1 S100A13 siRNA, which was set to 1 for the analysis and was the lowest expresser in the qPCR data set. A decrease in S100A13 mRNA expression was observed in the DLKP-2 and TXT-2 S100A13 siRNA transfected samples. S100A13 expression in DLKP-1 was not decreased.



Densitometry of timecourse showing S100A13 mRNA knockdown in DLKP-1 (YL)

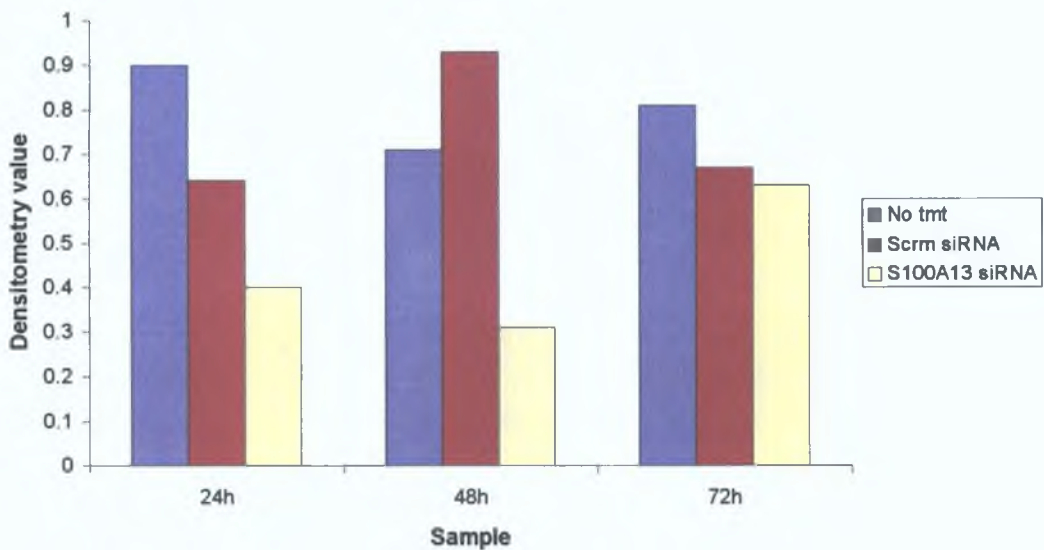
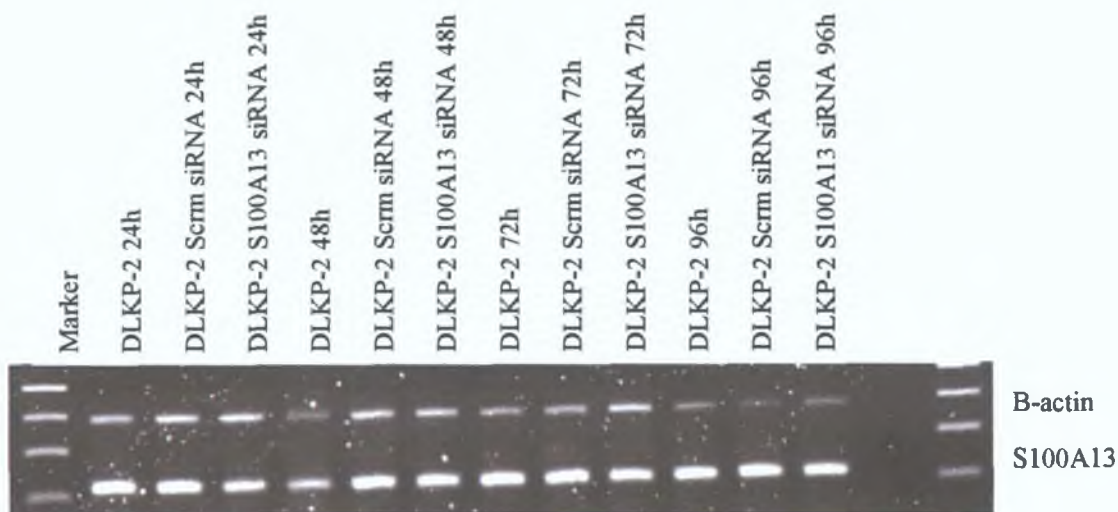


Figure 3.6.3.2 Timecourse analysis of S100A13 mRNA knockdown (I) by semi-quantitative RT-PCR in DLKP-1.

S100A13 siRNA was transfected into DLKP-1. RNA for the analysis of S100A13 mRNA was harvested at 24, 48, and 72h. β -actin was used to normalise for RNA content in each PCR. Figures representing the densitometry values graphed above were normalised by dividing S100A13 intensity values by β -actin intensity values. S100A13 mRNA levels were decreased at 24, 48 and 72h respectively, in comparison to the non-treated and scrambled siRNA transfected samples.



Densitometry of timecourse showing S100A13 mRNA knockdown in DLKP-2 (JC)

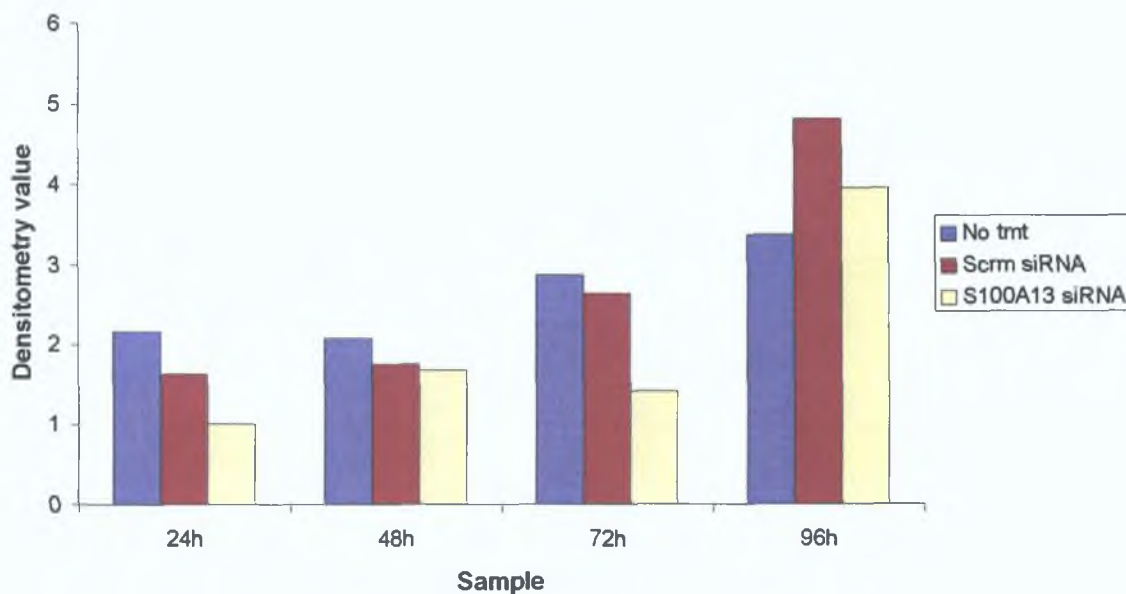
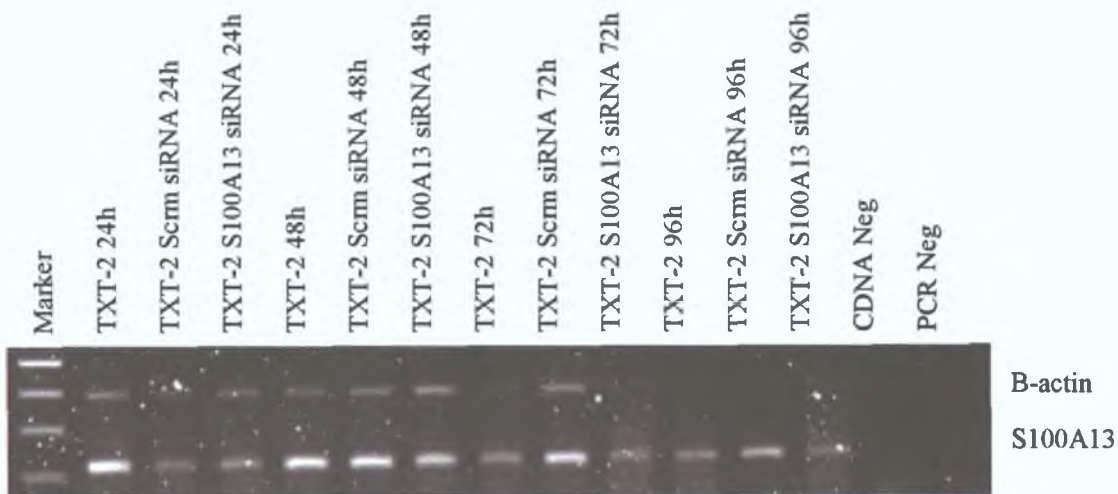


Figure 3.6.3.3 Timecourse analysis of S100A13 mRNA knockdown (I) by semi-quantitative RT-PCR in DLKP-2.

S100A13 siRNA was transfected into DLKP-2 and S100A13 mRNA expression analysed at 24, 48, 72 and 96h. β -actin was used as an endogenous control to normalise for RNA content in each PCR. Figures for the densitometry values were normalised by dividing S100A13 intensity values by β -actin intensity values and were graphed for each sample. S100A13 mRNA levels were decreased at 24, and 72h respectively, in comparison to the non-treated and scrambled siRNA transfected samples.



Densitometry of timecourse showing S100A13 mRNA knockdown in TXT-2 (RL)

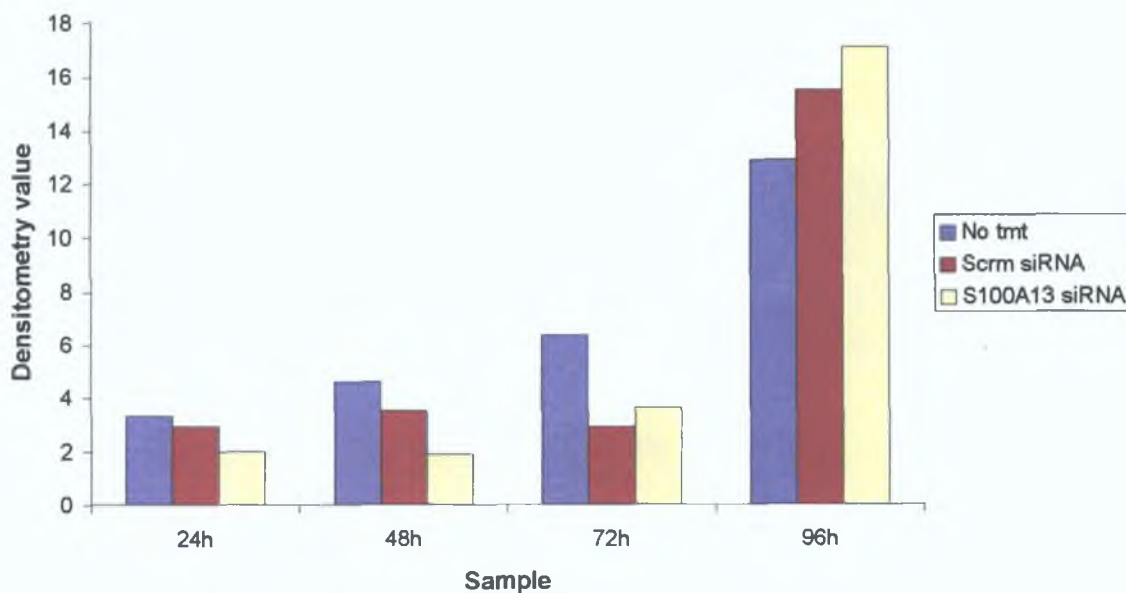


Figure 3.6.3.4 Timecourse analysis of S100A13 mRNA knockdown (I) by semi-quantitative RT-PCR in TXT-2.

S100A13 siRNA was transfected into TXT-2 and S100A13 mRNA expression measured at 24, 48, 72 and 96h. β -actin was used to normalise for RNA content in each PCR. Densitometric values were normalised by dividing S100A13 intensity values by β -actin intensity values and were graphed for each sample. S100A13 mRNA levels were decreased at 24, 48 and 72h respectively, in comparison to the non-treated and scrambled siRNA transfected samples.

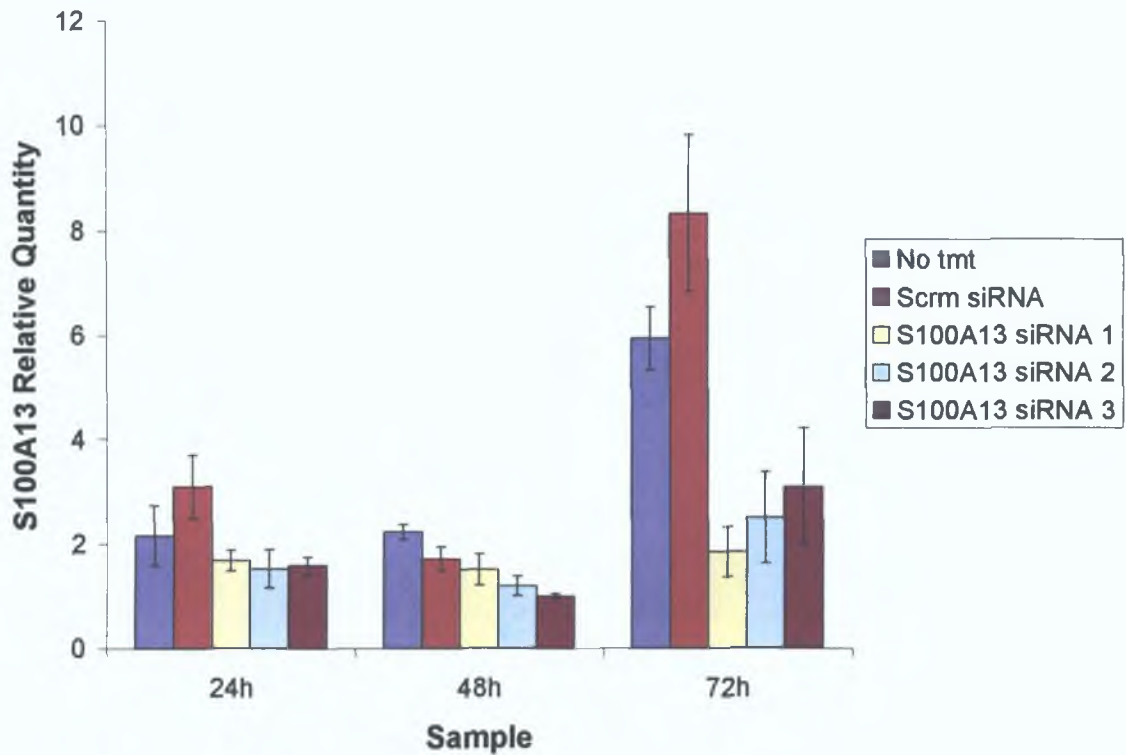


Figure 3.6.3.5 Timecourse analysis of S100A13 mRNA knockdown (II) in DLKP-1 by qPCR.

Three independent S100A13 siRNA sequences were transfected into DLKP-1. S100A13 mRNA expression in these samples was analysed by qPCR at 24, 48 and 72h using a commercial TaqMan probe to S100A13 and normalised for RNA content using β -actin as an endogenous control. The data represents S100A13 expression relative to the lowest S100A13 expresser in this data set, DLKP-1 S100A13 siRNA 3 48h sample, which was set to 1 for the analysis. A decrease in S100A13 mRNA expression was observed for all three siRNA's at 24 and 48h. This decrease was more pronounced at 72h.

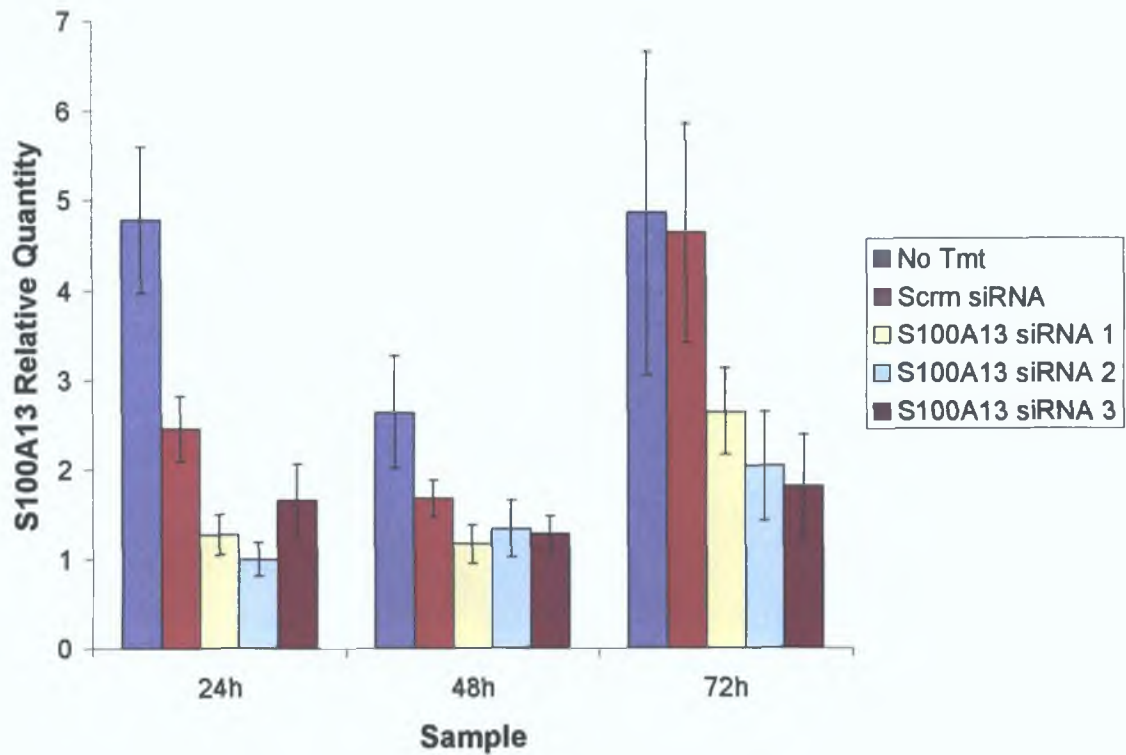


Figure 3.6.3.6 Timecourse analysis of S100A13 mRNA knockdown (II) in DLKP-2 by qPCR.

Three independent S100A13 siRNA sequences were transfected into DLKP-2. S100A13 mRNA expression in these samples was analysed by qPCR at 24, 48 and 72h. β -actin was used as an endogenous control. The data represents S100A13 expression relative the lowest S100A13 expresser in this data set, DLKP-2 S100A13 siRNA 2 24h sample, which was set to 1 for the analysis. S100A13 knockdown was observed for all three S100A13 siRNA's at all timepoints compared with the scrambled siRNA samples.

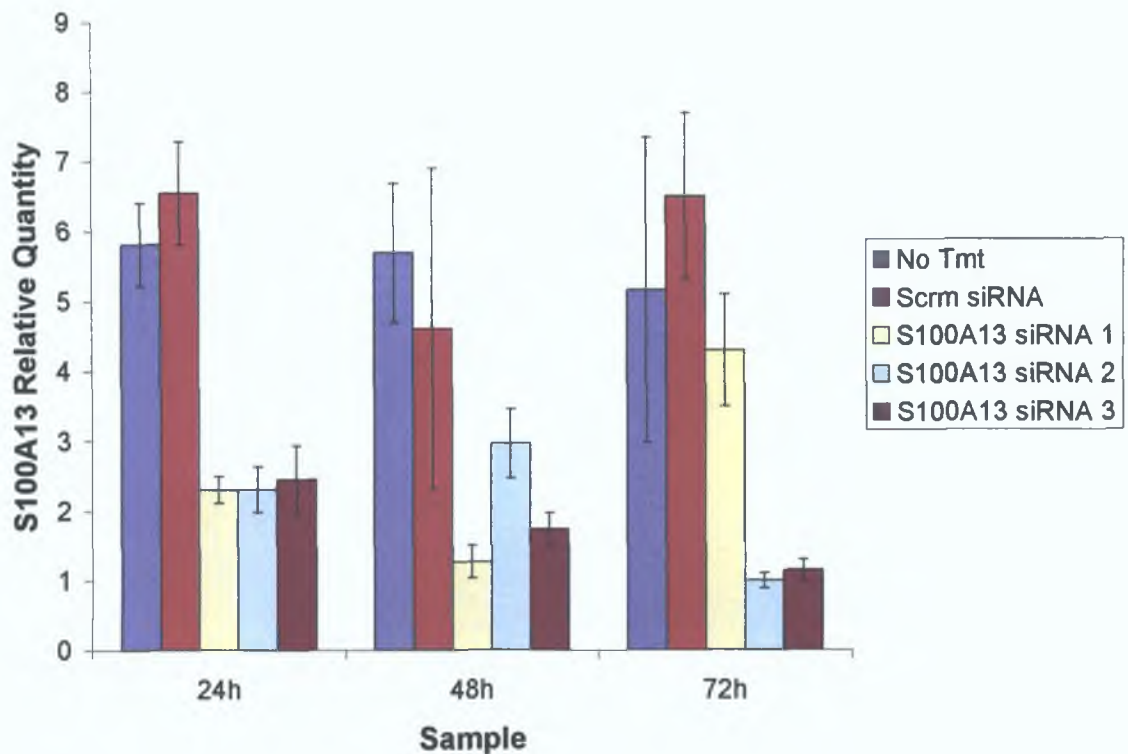


Figure 3.6.3.7 Timecourse analysis of S100A13 mRNA knockdown (II) in TXT-2 by qPCR.

Three independent S100A13 siRNA sequences were transfected into TXT-2. S100A13 mRNA expression in these samples was analysed by qPCR at 24, 48 and 72h using a commercial TaqMan S100A13 probe and normalised for RNA content using β -actin as an endogenous control. The data represents S100A13 expression relative to the lowest S100A13 expresser in this data set, TXT-2 S100A13 siRNA 2 72h sample, which was set to 1 for the analysis. S100A13 knockdown was observed for all three S100A13 siRNA's at all timepoints compared with the scrambled siRNA samples.

3.6.4 Evaluation of S100A13 siRNA effect on DLKP variant proliferation

The effect of transfecting S100A13 siRNA sequences on proliferation was investigated. Cells seeded at 3×10^5 cells/well of a 6-well plate (Figure 3.6.4.1), which was the cell number used to seed all the siRNA transfections in six-well plates. Relative cell number was determined using the acid phosphatase assay at 72h post transfection. Cell numbers were measured to determine what functional effect, if any, a decrease in S100A13 expression was having on proliferation.

Transfection with any of the siRNA sequences did not have a dramatic affect on proliferation compared with non-treated and scrambled siRNA transfected cells.

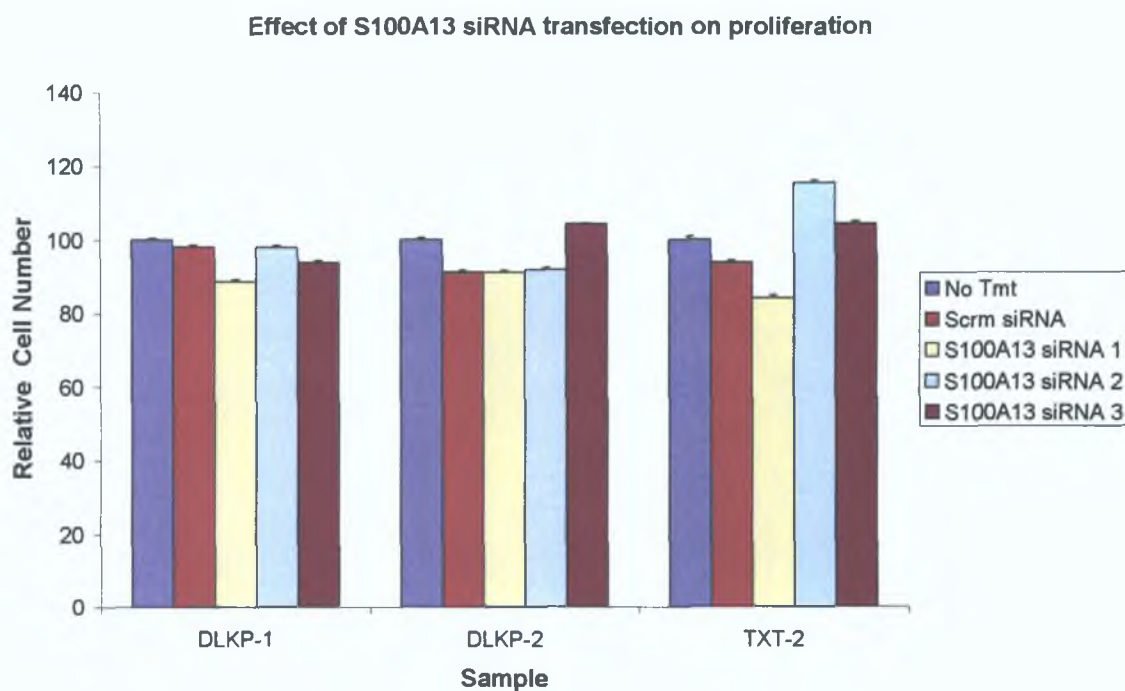


Figure 3.6.4.1 Effect of siRNA targeting S100A13 on DLKP variant cell number.

The cells were seeded at a 3×10^5 cells/well of a 6-well plate. Proliferation was measured by the acid phosphatase assay at 72h post transfection. There is a slight decrease in proliferation observed due to the transfection. S100A13 siRNA treatment does not appear to increase/decrease proliferation in any cell line.

3.6 5 Evaluation of S100A13 siRNA effect on DLKP variant invasion

The effect of decreasing S100A13 expression on DLKP variant invasion was investigated. Invasion assay analysis was performed 72h post transfection, to allow the cells to recover from the transfection procedure, using commercial invasion assay kits containing inserts pre-coated with matrigel in conjunction with a serum gradient. The cells were incubated at 37°C for 24h after which, the underside of the inserts were stained with crystal violet and allowed to air dry. The inserts were then photographed using 10X magnification. Ten fields of view were counted per insert at 20X magnification and averaged. At least two inserts were used for the analysis of each condition. The counts per number of inserts used were then also averaged and this figure was used to generate graphs of relative invasive capacity per cell line per condition.

One set of representative photographs was included (Figure 3 6 5 1) in this section and clearly demonstrate decreased invasion in S100A13 siRNA transfected cells. Invasion assay results are also presented graphically (Figures 3 6 5 2 and 3 6 5 3). Results for DLKP-2 are not included in Figure 3 6 5 1 and 3 6 5 2 due to a technical error, but are included in Figure 3 6 5 3.

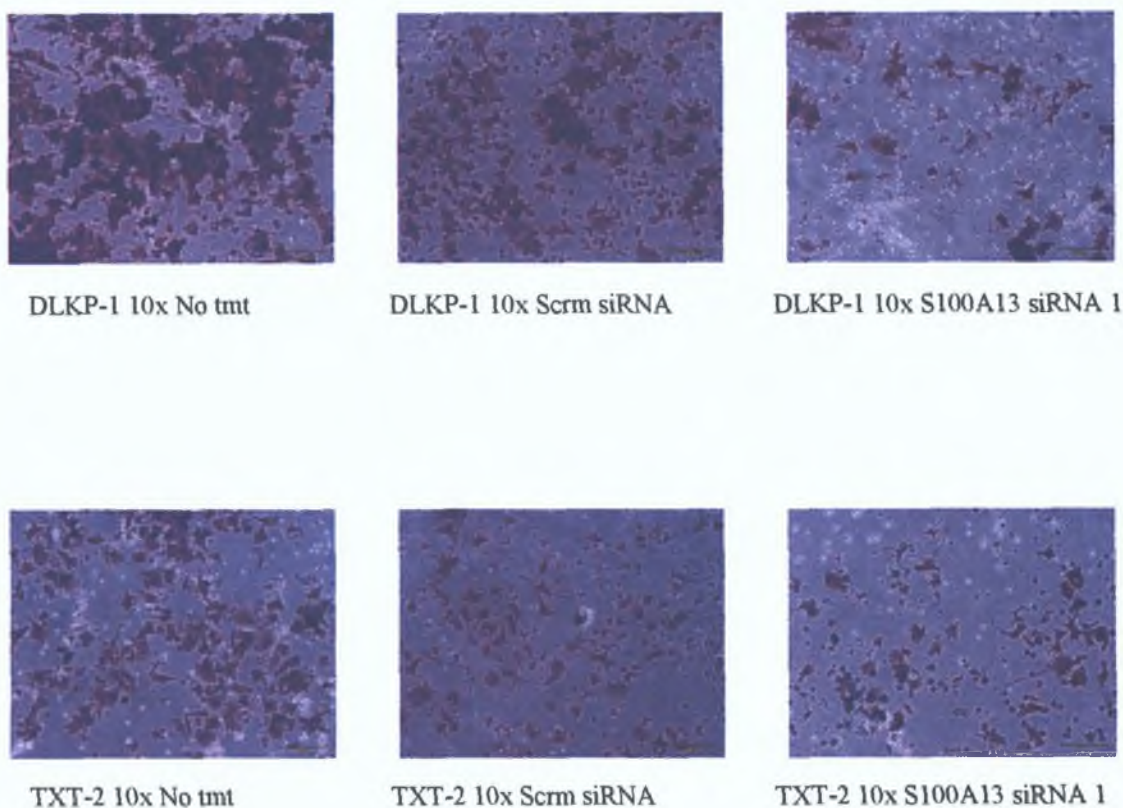


Figure 3.6.5.1 Photographic representation of invasion assay results 72h post S100A13 siRNA transfection (I).

The invasion assay was performed 72h post-transfection and was of 24h duration. Untransfected- and scrambled siRNA transfected- cell lines were the controls for this experiment. Representative photographs at 10X are shown above. Invasion was decreased in S100A13 siRNA transfected cells compared with the scrambled siRNA and non-treated cells ($P < 0.001$).

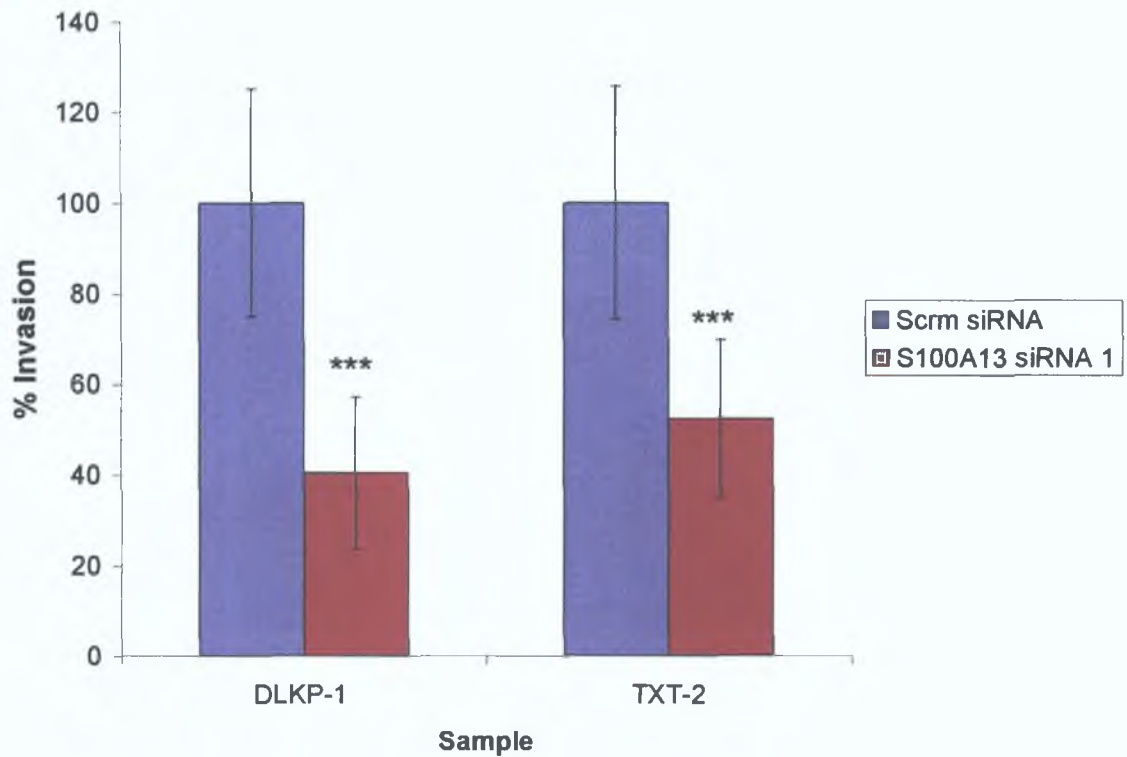


Figure 3.6.5.2 Graphic representation of invasion assay results 72h post S100A13 siRNA transfection (I).

The invasion assay was performed 72h post-transfection. Scrambled siRNA transfected- cell lines are the controls for this experiment. Ten random fields were counted at 20X. Each condition was examined using at least two invasion kit inserts. Counts per insert were averaged and plotted as percentage invasion normalised to the scrambled siRNA for each cell line. Invasion was decreased in S100A13 siRNA transfected cells compared with the scrambled siRNA control ($P < 0.001$).

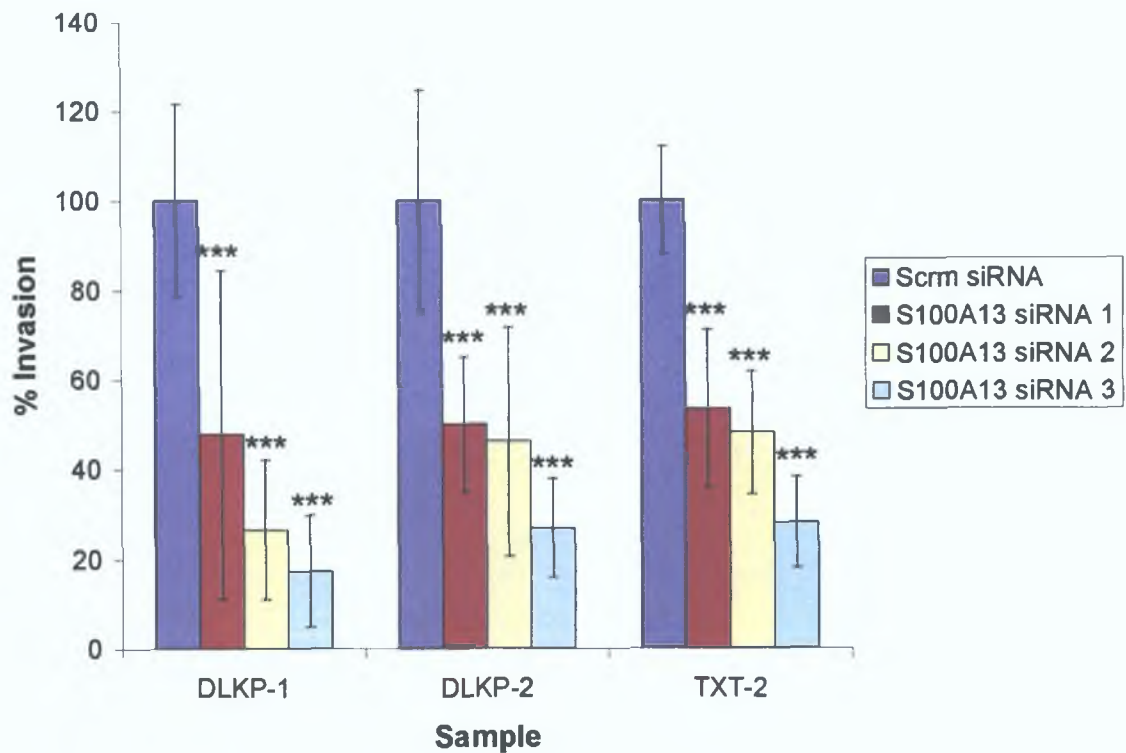


Figure 3.6.5.3 Graphic representation of invasion assay results 72h post S100A13 siRNA transfection (II).

The invasive cell lines DLKP-1, DLKP-2 and TXT-2 were transfected with scrambled siRNA and three independent siRNA sequences to S100A13. The effect of S100A13 expression knockdown on invasion was examined 72h post transfection. Scrambled siRNA transfected- cell lines were the controls for this experiment. Ten random fields were counted per insert at 20X. Each condition was examined using at least two invasion kit inserts. Counts per insert were averaged and plotted as percentage invasion normalised to the scrambled siRNA for each cell line. Invasion was decreased in S100A13 siRNA transfected cells compared with the scrambled siRNA control ($P < 0.001$).

3.6.6 S100A13 cDNA transfection in the non-invasive DLKP variants

3.6.6.1 Summary of S100A13 cDNA experimental plan

Array and RT-PCR results indicated that S100A13 mRNA expression was increased in the invasive compared with the poorly invasive DLKP lines, it was decided to overexpress S100A13 by transfecting the vector pSport6 containing the cDNA sequence to S100A13 into the mildly/non-invasive cell lines TXT-1 and VCR. This would help determine whether increasing S100A13 expression in poorly invasive cell lines could induce an invasive phenotype. Western blotting was used to confirm exogenous S100A13 expression in the cDNA transfected samples.

3.6.6.2 Western Blot analysis of S100A13 cDNA transient transfection

S100A13 protein expression in the poorly invasive DLKP cell lines and their S100A13 cDNA transfected counterparts was determined by western blotting. Cells were transfected with a pSport6 empty vector as a control to ensure that the transfection process did not affect S100A13 protein expression (Figures 3.6.6.1 and 3.6.6.2).

The polyclonal anti-S100A13 antibody used in these experiments was a gift from Prof. Claus Heizmann and was raised in rabbit. An 11kDa band is specific to S100A13. An α -tubulin antibody was used to demonstrate even loading between the samples. S100A13 protein expression was increased in response to S100A13 cDNA transient transfection in both TXT-1 and VCR.

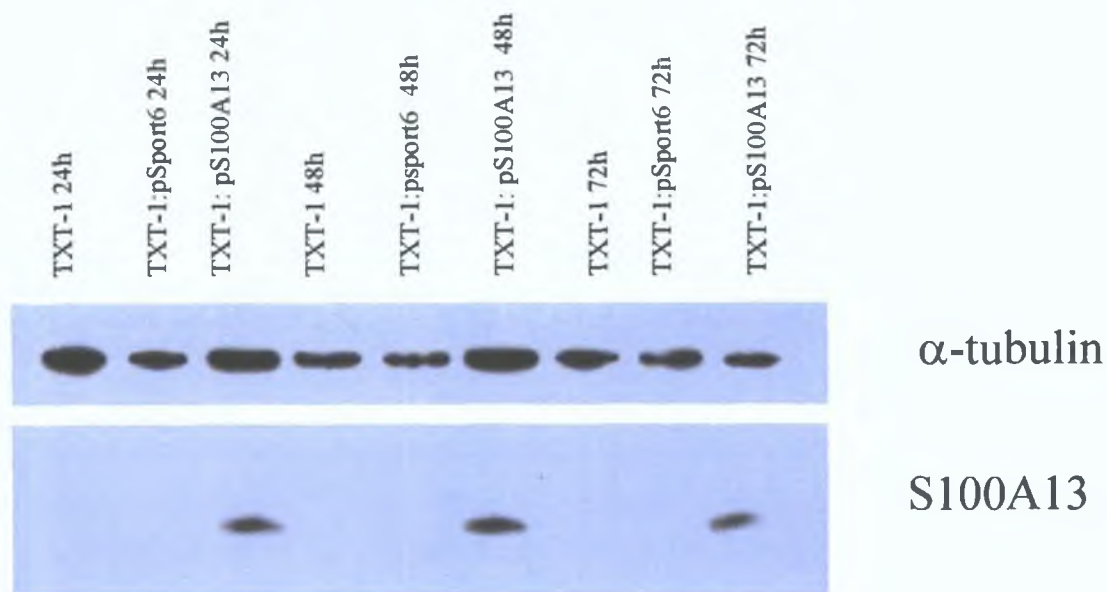


Figure 3.6.6.1 Western blot analysis of S100A13 cDNA transient transfection in TXT-1.

The polyclonal anti-S100A13 antibody used in this experiment was a gift from Prof. Claus Heizmann and was raised in rabbit. An 11kDa band is specific to S100A13. S100A13 expression is increased in S100A13 cDNA transfected samples in TXT-1 and was sustained over 72h.



Figure 3.6.6.2 Western blot analysis of S100A13 cDNA transient transfection in VCR.

The polyclonal anti-S100A13 antibody used in this experiment was a gift from Prof. Claus Heizmann and was raised in rabbit. An 11kDa band is specific to S100A13. S100A13 expression is increased in S100A13 cDNA transfected samples in VCR at all timepoints.

3.6.6.3 Evaluation of S100A13 cDNA transient transfection on invasion

The effect of overexpressing S100A13 in the poorly invasive DLKP variants was examined. Invasion assay analysis was performed 72h post transfection, using commercial invasion assay kits containing inserts pre-coated with matrigel in conjunction with a serum gradient. The cells were incubated at 37°C for 24h after which, the underside of the inserts were stained with crystal violet and allowed to air dry. The inserts were then photographed using 10X magnification. Ten fields of view were counted per insert at 20X magnification and averaged. At least two inserts were used for the analysis of each condition. The counts per number of inserts used were then also averaged and this figure was used to plot graphs of relative invasive capacity per cell line per condition.

One set of representative photographs were included (Figure 3.6.6.3) in this section and do not demonstrate any obvious alteration in the invasive capacities of TXT-1 or VCR in response to increased S100A13 expression. These invasion assay results are also presented graphically (Figures 3.6.6.4) and demonstrate a decrease in invasion in S100A13 cDNA transfected cells compared with the empty vector, however this decrease was significant for the TXT-1 S100A13 cDNA transfected cells ($P < 0.01$) only. This indicates that an increase in S100A13 expression is insufficient to induce an invasive phenotype in poorly or non-invasive cell lines.

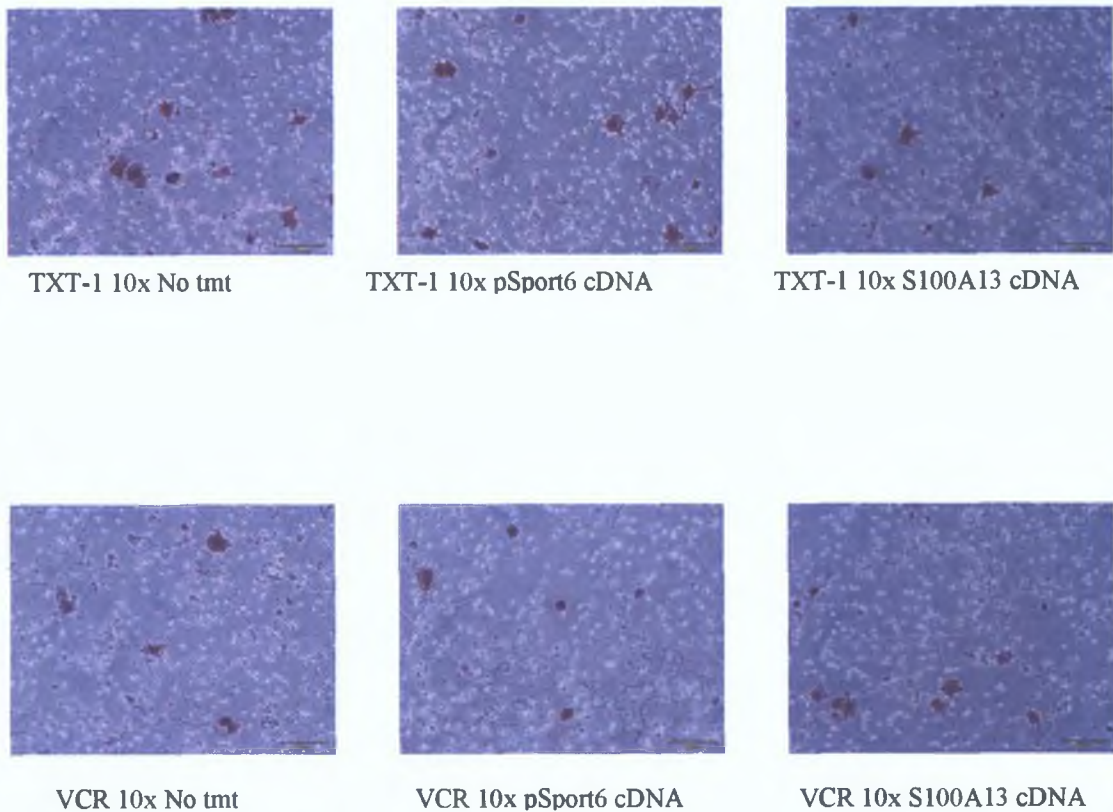


Figure 3.6.6.3 Photographic representation of invasion assay results 72h post S100A13 cDNA transfection.

The invasion assay was performed 72h post-transfection. Untransfected- and pSport6 empty vector transfected- cell lines are the controls for this experiment. Ten random fields were counted per insert at 20X. No effect on invasion was apparent in S100A13 cDNA transfected cells compared with the empty vector and non-treated cells. This indicates that increased S100A13 expression is itself insufficient to induce an invasive phenotype in mildly invasive cells. Surprisingly, when the counts were statistically examined, a decrease in invasion was observed in S100A13 cDNA transfected cells compared with the empty vector, however this decrease was significant for the TXT-1 S100A13 cDNA transfected cells ($P < 0.01$) only.

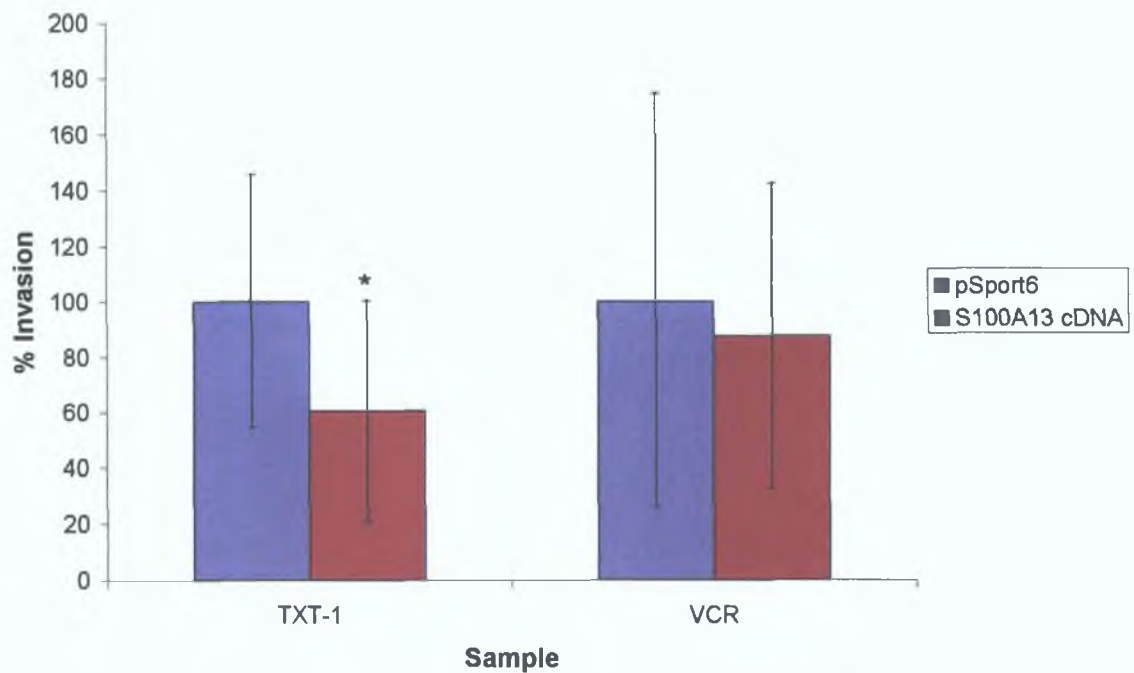


Figure 3.6.6.4 Graphic representation of invasion assay results 72h post S100A13 cDNA transfection.

The invasion assay was performed 72h post-transfection. pSport6 empty vector transfected- cell lines were the controls for this experiment. Ten random fields were counted at 20X. Counts per insert were averaged and plotted as percentage invasion normalised to the empty vector pSport6 cDNA for each cell line. A decrease in invasion was observed in S100A13 cDNA transfected cells compared with the empty vector, however this decrease was significant for the TXT-1 S100A13 cDNA transfected cells ($P < 0.01$) only. This indicates that increased S100A13 expression is itself insufficient to induce an invasive phenotype in lowly invasive cells.

3.7 Investigation into role of Stratifin (SFN) in invasion in the DLKP cell model

3.7.1 Aims of SFN experiments

SFN was identified being differentially expressed across the cell lines in our model of invasion by array expression analysis. Higher expression correlated with a greater degree of invasion. The aims of these experiments were as follows.

1. To confirm by PCR that SFN is differentially expressed across the DLKP cell line model of invasion.
2. To decrease SFN expression by transfecting an siRNA sequence to SFN using optimised transfection conditions into the invasive cell lines DLKP-1, DLKP-2 and TXT-2.
3. To demonstrate SFN-specific knockdown at mRNA level.
4. To evaluate the effect of decreased SFN expression on invasion.
5. To increase SFN expression by transfecting a pSport6 plasmid containing the SFN sequence into the poorly/non-invasive cell lines TXT-1 and VCR.
6. To demonstrate an increase in SFN protein expression in cDNA transfected cells.
7. To evaluate the effect of exogenous SFN expression on invasion.

To summarise the results detailed in this section, it was found that SFN was differentially expressed in the panel of cell lines studied where higher expression was associated with an increased capacity to invade. This correlated with array data. SFN knockdown was marginal in the DLKP-1 and DLKP-2 cell lines. The knockdown in TXT-2 was greater. Where knockdown was minimal no effect on invasion was observed. However, decreased SFN expression in TXT-2 increased invasion in this cell line. Overexpressing SFN had no effect on invasion in the less/non-invasive cell lines.

3.7.2 RT-PCR investigation of differential SFN mRNA expression

Semi-quantitative RT-PCR was used to confirm that SFN mRNA expression was higher in the invasive DLKP variants compared with the less invasive variants and were reflective of array data

To ensure that results from the array study matched to independent analyses of the cell lines, RNA samples from the preliminary Affymetrix array study by Dr Rasha Linehan in 2003 (Figure 3 7 2 1), RNA from the duplicate array samples 2004 (Figure 3 7 2 2), RNA from a fresh set of cultures harvested separately to those for array analysis including RNA from three samples analysed on the Agilent array platform (Figure 3 7 2 3) were included in this analysis. The Agilent data was not analysed further in this work

β -actin was used as an endogenous control to normalise for RNA content in each SFN PCR. The reactions were analysed by gel electrophoresis (GE) on a 2% agarose gel and visualised by ethidium bromide staining. The band size for SFN was 195bp. PCR negative controls consisted of PCR master mix to which no cDNA template was added. cDNA negative control (cDNA neg) contained PCR master mix with cDNA but without addition of Taq enzyme. Densitometry values were normalised by dividing SFN intensity values by β -actin intensity values and were plotted for each sample. The gels included in this section are representative of at least two independent repeats

This analysis by semi-quantitative PCR demonstrated a trend towards higher SFN expression in the more invasive cell lines DLKP-1 and TXT-2, compared to the less invasive cell lines TXT-1 and VCR. This correlates with the array data

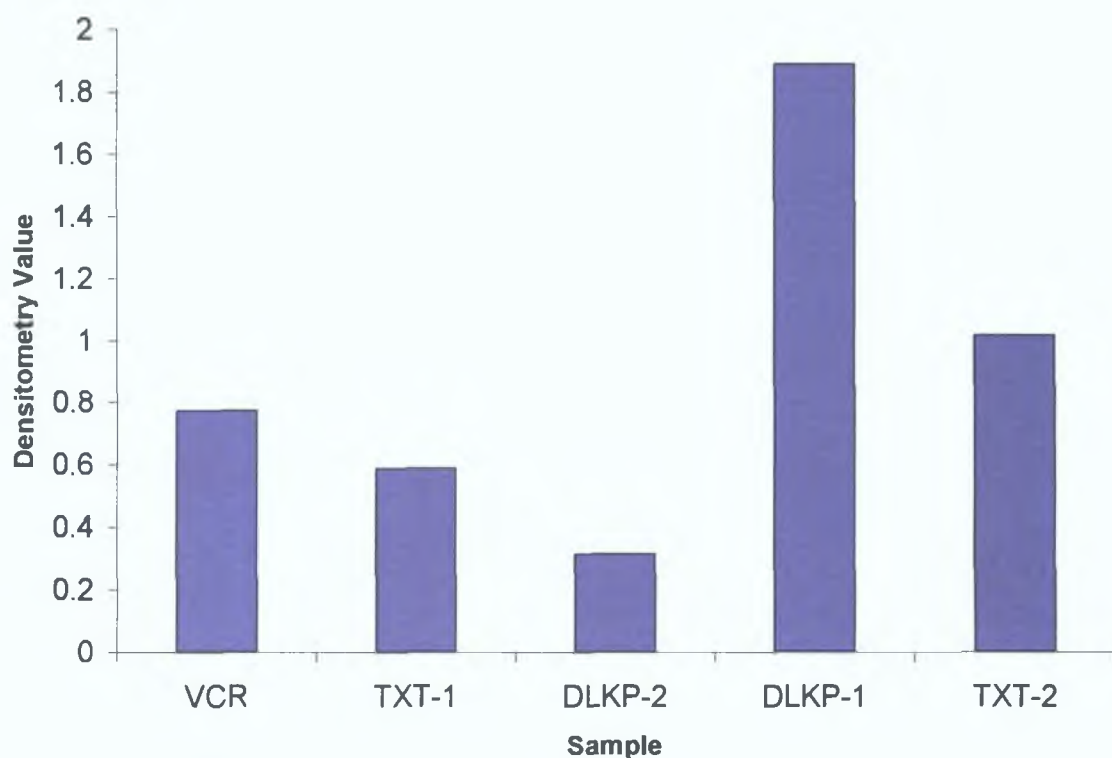


Figure 3.7.2.1 RT-PCR of SFN mRNA expression from RNA used in array samples 2003.

RNA used for this PCR was analysed on the 2003 arrays. β -actin was used as an endogenous control to normalise for RNA content in each reaction. The PCR was analysed by gel electrophoresis (GE) on a 2% agarose gel. A PCR Negative (PCR Neg) control was included in the analysis and consisted of PCR master mix to which no cDNA template was added. Densitometry values were normalised by dividing SFN intensity values by β -actin intensity values and were graphed for each sample. SFN mRNA expression is highest in the invasive DLKP-1 cell line followed by TXT-2. Surprisingly, SFN is expressed at low levels in DLKP-2.

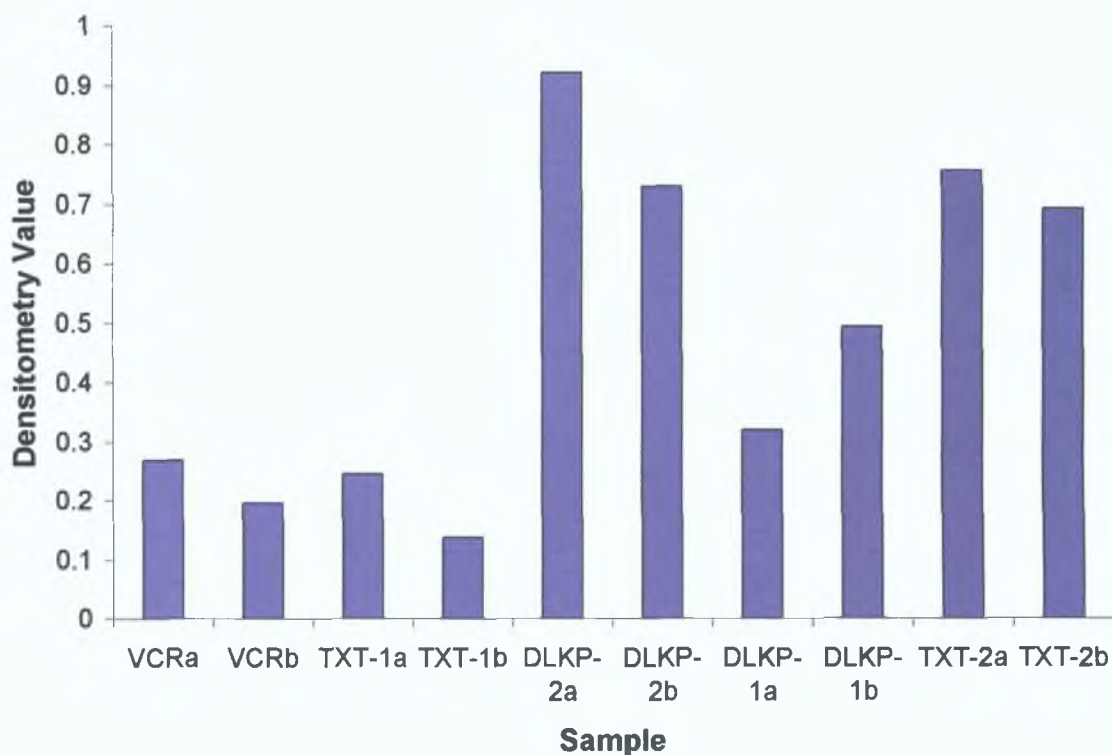


Figure 3.7.2.2 RT-PCR of SFN mRNA expression from RNA used in duplicate array samples 2004.

RNA for this reaction was analysed in the duplicate array analysis of the DLKP cell lines in 2004. β -actin was used as an endogenous control. A PCR negative (PCR Neg) control was included in the analysis. Densitometry values were normalised by dividing SFN intensity values by β -actin intensity values and were graphed for each sample. This PCR demonstrates higher SFN expression in the more invasive cell lines DLKP-1, DLKP-2 and TXT-2, compared to the poorly invasive cell lines TXT-1 and VCR. This result agrees with the array data.

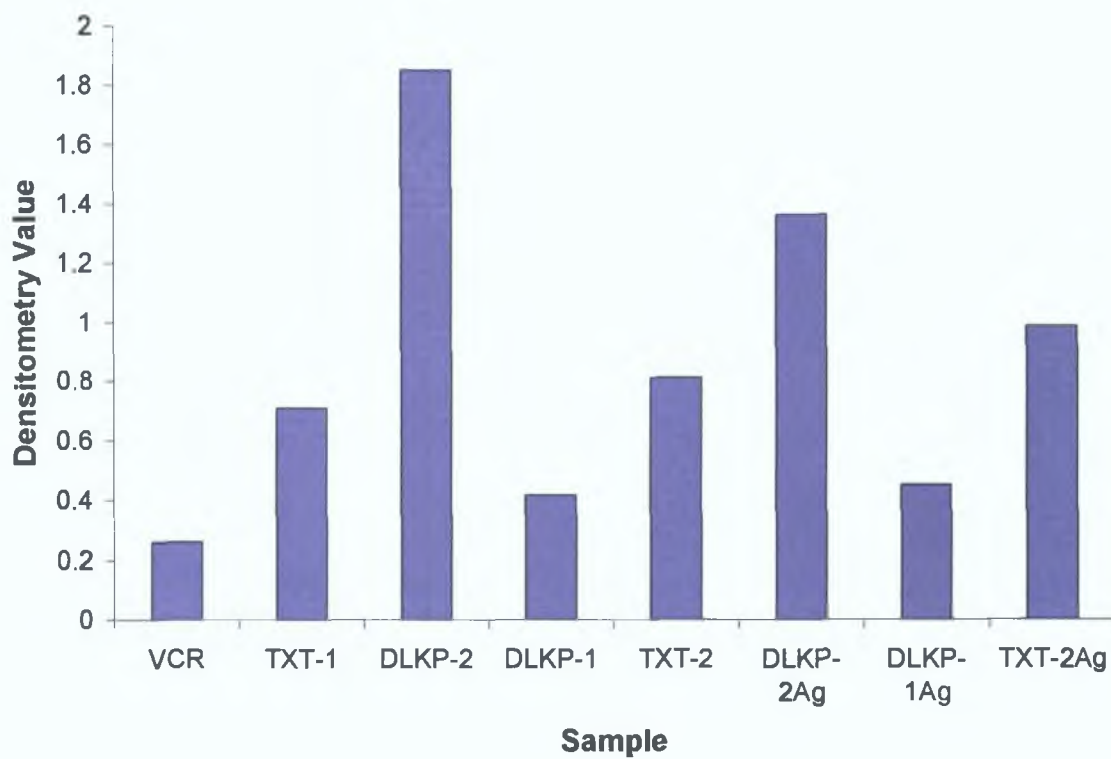


Figure 3.7.2.3 RT-PCR of SFN mRNA in a separate sample set and Agilent samples.

RNA for this analysis was from a separate batch of DLKP variant cultures not harvested or processed for Affymetrix array analysis. Also included were three samples analysed on the Agilent array platform but which were not investigated further. β -actin was used as an endogenous control. The reaction was analysed by GE on a 2% agarose gel. Densitometry values were normalised by dividing SFN intensity values by β -actin intensity values and were plotted for each sample. This PCR demonstrates increased SFN expression in DLKP-2 and TXT-2, with lower expression in TXT-1 and VCR. SFN mRNA levels were also low in DLKP-1 in this analysis.

3.7.3 SFN siRNA transfection in the invasive DLKP variants

3.7.3.1 Summary of SFN siRNA experimental plan

SFN was identified being differentially expressed across the cell lines in our model of invasion by array expression analysis. Higher expression correlated with a greater degree of invasion. This finding was confirmed by semi-quantitative RT-PCR, except in the case of DLKP-1. This correlation prompted us to investigate the impact of SFN knockdown using a commercial siRNA sequence on the invasive phenotype. Successful knockdown was confirmed by PCR and the phenotypic effect assessed by *in vitro* invasion assay. Western blot analysis of protein levels indicated that endogenous SFN levels were below the level of detection.

3.7.3.2 SFN-specific siRNA knockdown of mRNA levels

An SFN-specific siRNA sequence was transfected into the invasive DLKP cell lines and a decrease in mRNA expression examined by qPCR and semi-quantitative RT-PCR.

A commercial TaqMan probe to SFN was used to quantify relative SFN mRNA expression. The data was normalised using β -actin as an endogenous control (Figure 3.7.3.1). An siRNA-dependent decrease in SFN mRNA was observed for samples at 24h.

Timecourse analysis of SFN knockdown was examined by RT-PCR (Figures 3.7.3.2 to 3.7.3.4). β -actin was included as an endogenous control to normalise for RNA content in each reaction. The PCRs were analysed by gel electrophoresis (GE) on a 2% agarose gel and visualised with ethidium bromide staining. The band size for SFN was 195bp. cDNA negative control (cDNA neg) consisted of PCR master mix with cDNA but without addition of Taq enzyme. PCR negative controls consisted of PCR master mix to which no cDNA template was added. Densitometric values were normalised by dividing SFN intensity values by β -actin intensity values and were graphed for each sample. The gels included in this timecourse study are representative of at least two independent repeats. These results demonstrate the limited value of semi-quantitative RT-PCR timecourse analysis. However, the data does suggest an overall trend in that SFN siRNA transfection had a marginal effect on mRNA expression that warranted further investigation.

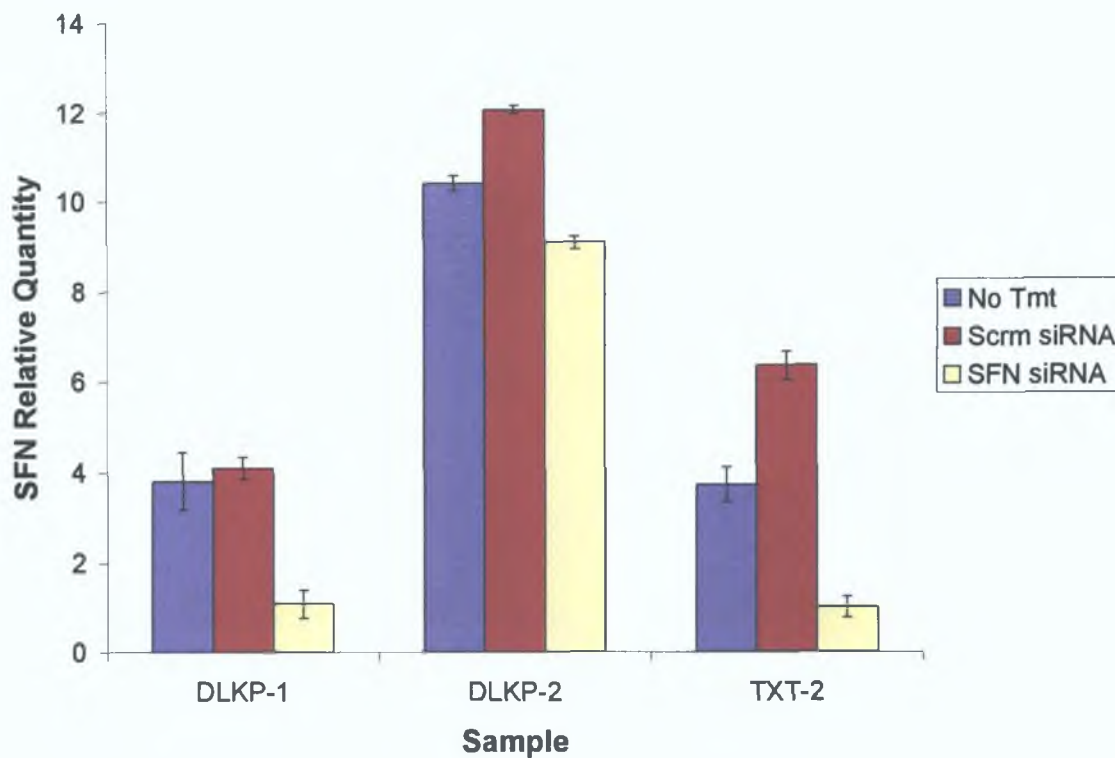


Figure 3.7.3.1 qPCR analysis of SFN siRNA experiment at 24h.

RNA was harvested 24h post-transfection and used to determine an SFN-siRNA specific decrease in mRNA in response to siRNA transfection. SFN mRNA expression was examined by qRT-PCR using a commercial TaqMan SFN probe and normalised for RNA content using β -actin as an endogenous control. The data represents SFN expression relative to TXT-2 SFN siRNA, which was set to 1 for the analysis and was the lowest expresser in the qPCR data set. A SFN siRNA specific decrease in mRNA was observed for all samples at 24h.



Densitometry of timecourse showing SFN mRNA knockdown in DLKP-1 (YL)

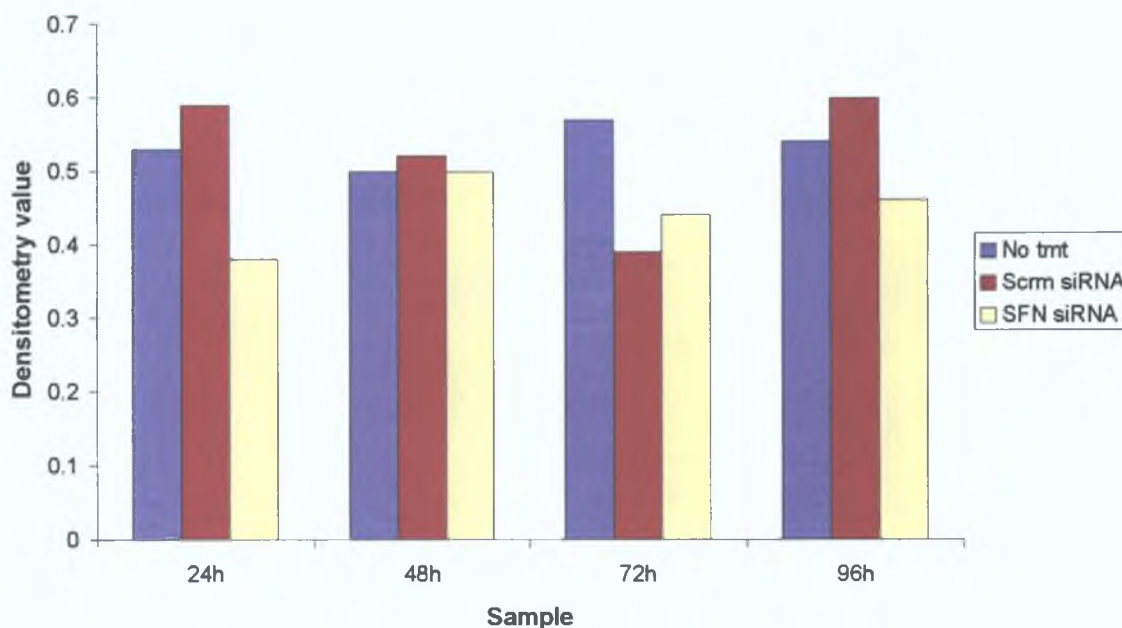
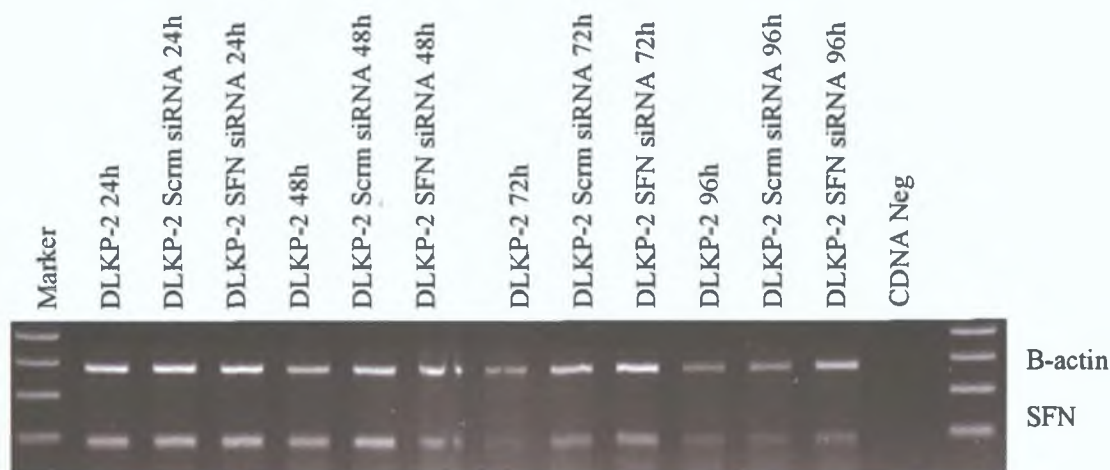


Figure 3.7.3.2 Timecourse analysis of SFN mRNA knockdown by semi-quantitative RT-PCR in DLKP-1.

SFN siRNA was transfected into DLKP-1. RNA for the analysis of SFN mRNA was harvested at 24, 48, 72 and 96h. β -actin was used to normalise for RNA content in each PCR. Densitometric values graphed above were normalised by dividing SFN intensity values by β -actin intensity values. The trend here indicates that SFN mRNA levels were marginally decreased at 24 and 96h respectively, in comparison to the non-treated and scrambled siRNA transfected samples.



Densitometry of timecourse showing SFN mRNA knockdown in DLKP-2 (JC)

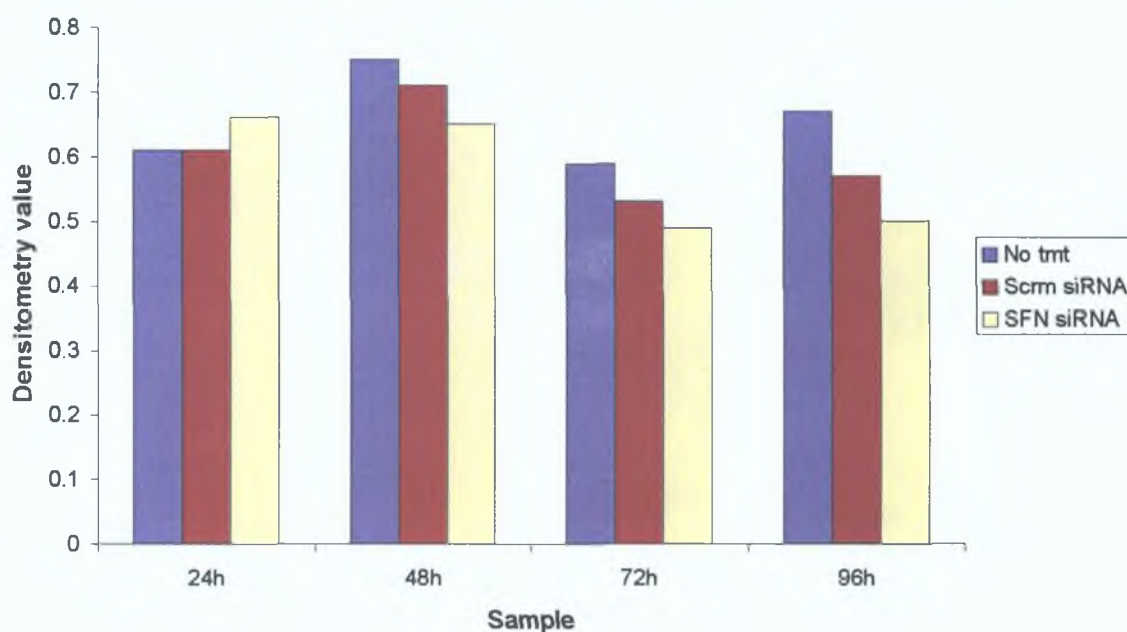
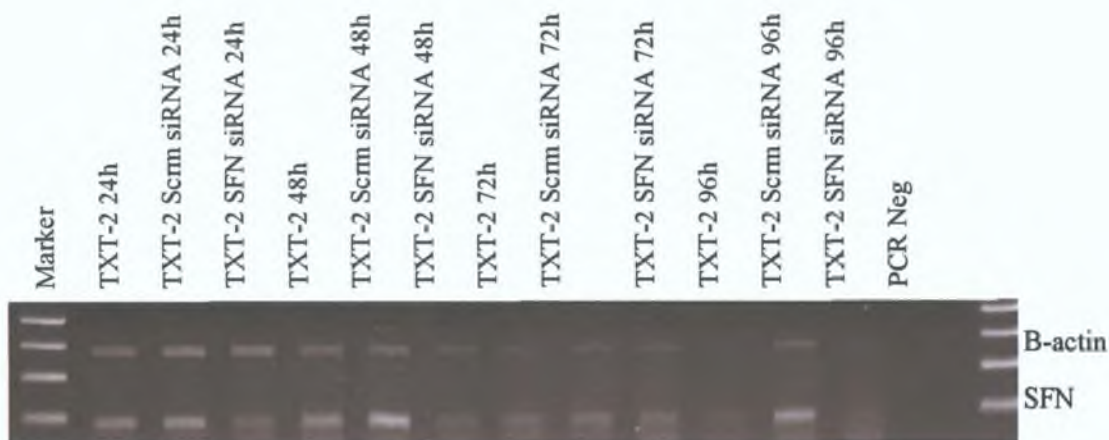


Figure 3.7.3.3 Timecourse analysis of SFN mRNA knockdown by semi-quantitative RT-PCR in DLKP-2.

A SFN siRNA sequence was transfected into DLKP-2 and SFN mRNA expression analysed at 24, 48, 72 and 96h. β -actin was used as an endogenous control to normalise for RNA content in each PCR. Figures for the densitometry values were normalised by dividing SFN intensity values by β -actin intensity values and were plotted for each sample. SFN mRNA levels were decreased, albeit slightly, at 48, 72 and 96h samples compared to the non-treated and scrambled transfected samples.



Densitometry of timecourse showing SFN mRNA knockdown in TXT-2 (RL)

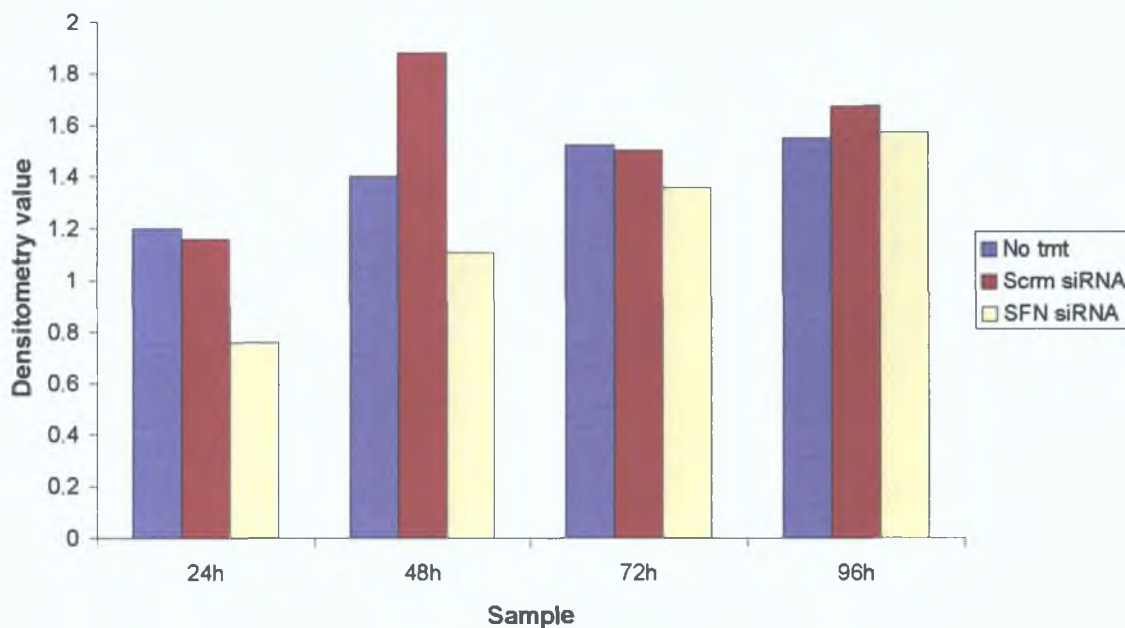


Figure 3.7.3.4 Timecourse analysis of SFN mRNA knockdown by semi-quantitative RT-PCR in TXT-2.

SFN siRNA was transfected into TXT-2 and SFN mRNA expression measured at 24, 48, 72 and 96h. β -actin was used to normalise for RNA content in each PCR. Figures for the densitometry values were normalised by dividing SFN intensity values by β -actin intensity values and were graphed for each sample. SFN mRNA levels were slightly decreased in the 24, 48 and 72h sample compared to the non-treated and scrambled transfected samples.

3.7 4 Evaluation of SFN siRNA effect on DLKP variant invasion

The impact of SFN knockdown on DLKP variant invasion was investigated. Invasion assay analysis was performed 72h post transfection, using commercial invasion assay kits containing inserts pre-coated with matrigel in conjunction with a serum gradient. The cells were incubated at 37°C for 24h after which, the underside of the inserts were stained with crystal violet and allowed to air dry. The inserts were then photographed using 10X magnification. Ten fields of view were counted per insert at 20X magnification and averaged. At least two inserts were used for the analysis of each condition. The counts per number of inserts used were then also averaged and this figure was used to plot graphs of relative invasive capacity per cell line per condition.

One set of representative photographs was included (Figure 3 7 4 1) in this section. Invasion assay results are also presented graphically (Figures 3 7 4 2). SFN knockdown had a negligible effect on the invasive capacity of DLKP-1. However, SFN knockdown in DLKP-2 and TXT-2 increased invasion ($P < 0.001$). These results do not clarify the potential role of SFN in invasion and require further investigation.

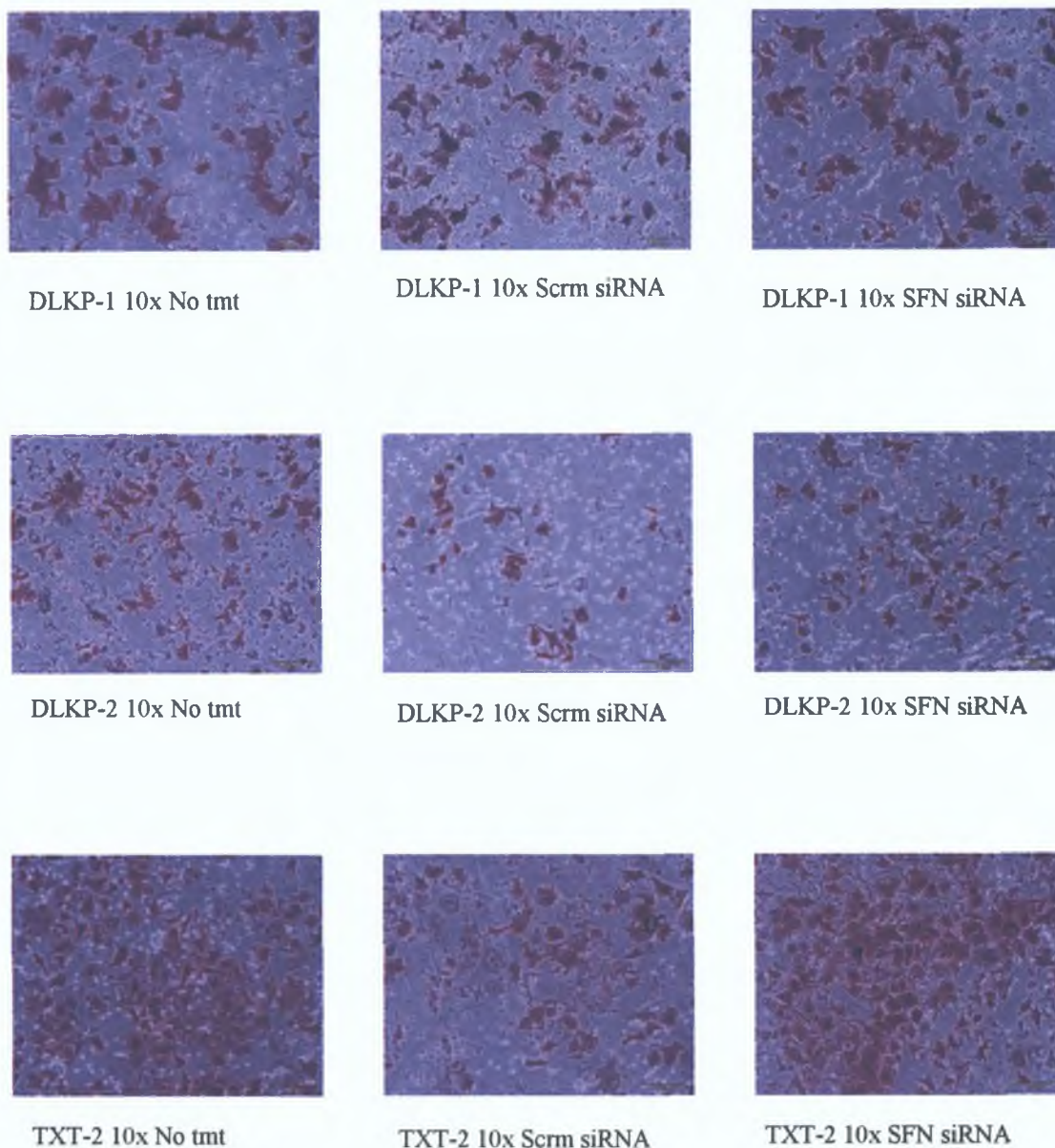


Figure 3.7.4.1 Photographic representation of invasion assay results 72h post SFN siRNA transfection.

The invasion assay was performed 72h post-transfection over 24h. Untransfected- and scrambled siRNA transfected- cell lines were the controls for this experiment. Representative photographs at 10X are shown above. Invasion was increased in SFN siRNA transfected cells in the DLKP-2 and TXT-2 cell lines compared with the scrambled siRNA and non-treated cells. No effect was observed in the DLKP-1 cell line.

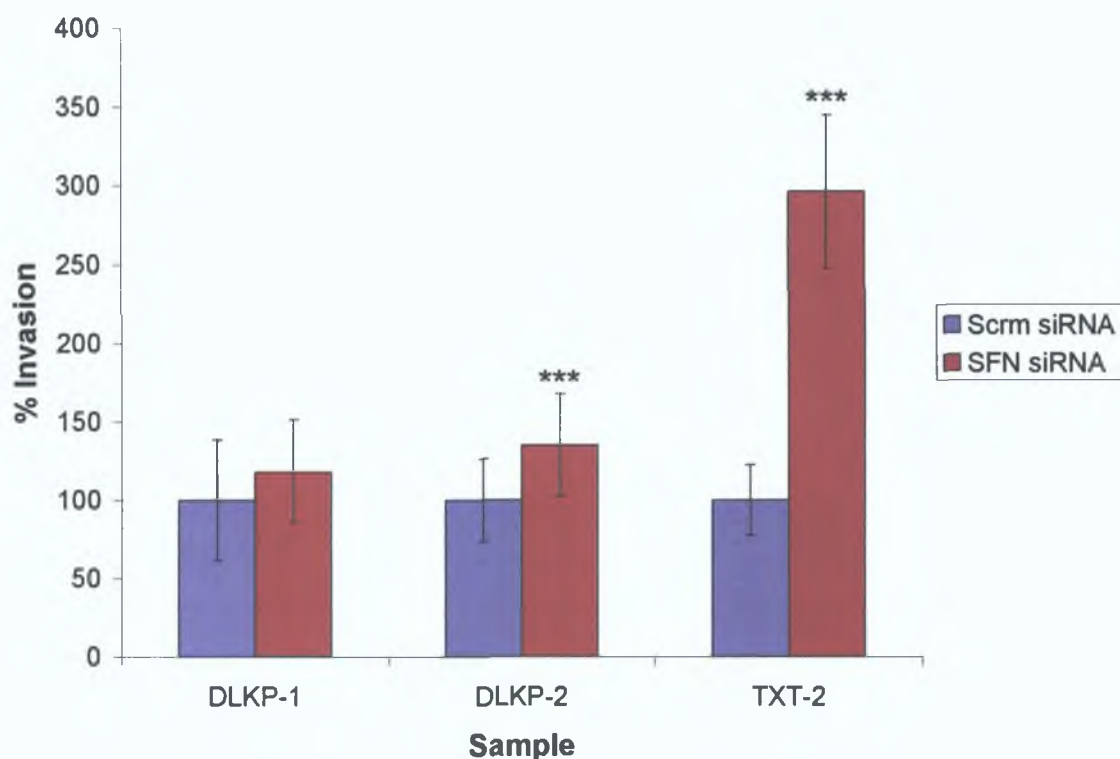


Figure 3.7.4.2 Graphic representation of invasion assay results 72h post SFN siRNA transfection

The invasion assay was performed 72h post-transfection over 24h. Untransfected- and scrambled siRNA transfected- cell lines were the controls for this experiment. Ten random fields were counted per insert at 20X. Each condition was examined using at least two invasion kit inserts. Counts per insert were averaged and plotted as percentage invasion normalised to the scrambled siRNA for each cell line. Invasion was increased in SFN siRNA transfected DLKP-2 and TXT-2 cells compared with the scrambled siRNA control ($P < 0.001$).

3.7.5 SFN cDNA transfection in the non-invasive DLKP variants

3.7.5.1 Summary of SFN cDNA experimental plan

Both microarray and RT-PCR analysis of SFN expression indicated an increase in SFN expression of invasive cell lines. To investigate the effect of overexpression of exogenous SFN on the invasive status of the cells we transiently transfected an expression vector containing the SFN cDNA sequence under the control of a strong viral promoter (pSport6). Transient transfection of this vector into the poorly/non-invasive cell lines TXT-1 and VCR resulted in SFN overexpression as determined by western blotting. However, this had no measurable effect on the invasive abilities of these cell lines.

3.7.5.2 Western Blot analysis of SFN cDNA transient transfection

SFN overexpression by transient transfection was confirmed by western blotting. Cells were transfected with a pSport6 empty vector as a control to ensure that the transfection process did not affect SFN protein expression (Figures 3.7.5.1 and 3.7.5.2).

A 30kDa band is specific to SFN. A α -tubulin antibody was used to demonstrate even loading between the samples. SFN protein expression was increased in response to SFN cDNA transient transfection in both TXT-1 and VCR.



Figure 3.7.5.1 Western blot analysis of SFN cDNA transient transfection in TXT-1.

A 30kDa band is specific to SFN. SFN expression is increased in SFN cDNA transfected samples over the 72h timecourse.

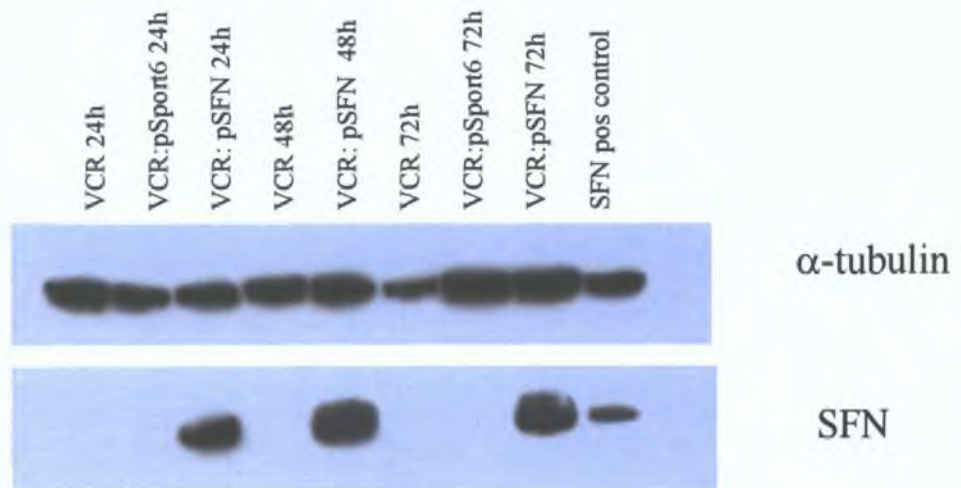


Figure 3.7.5.2 Western blot analysis of SFN cDNA transient transfection in VCR. A 30kDa band is specific to SFN. SFN expression is increased in SFN cDNA transfected samples in VCR over a 72h period.

3.7.6 Evaluation of SFN cDNA transient transfection on invasion

The effect of exogenously overexpressing SFN in the poorly invasive DLKP variants, TXT-1 and VCR was examined. Invasion assay analysis was performed 72h post transfection, using commercial invasion assay kits containing inserts pre-coated with matrigel in conjunction with a serum gradient, and was of 24h duration. After this time the underside of the inserts were stained with crystal violet and allowed to air-dry. The inserts were then photographed using 10X magnification. Ten fields of view were counted per insert at 20X magnification and averaged. At least two inserts were used for the analysis of each condition. The counts per number of inserts used were then also averaged and this figure was used to plot graphs of relative invasive capacity per cell line per condition.

One set of representative photographs were included (Figure 3.7.6.1) in this section and do not demonstrate any alteration in the invasive abilities of TXT-1 or VCR in response to increased SFN expression. These invasion assay results are also presented graphically (Figures 3.7.6.2). This indicates that exogenously increasing SFN expression is insufficient to induce an invasive phenotype in these poorly or non-invasive cell lines.

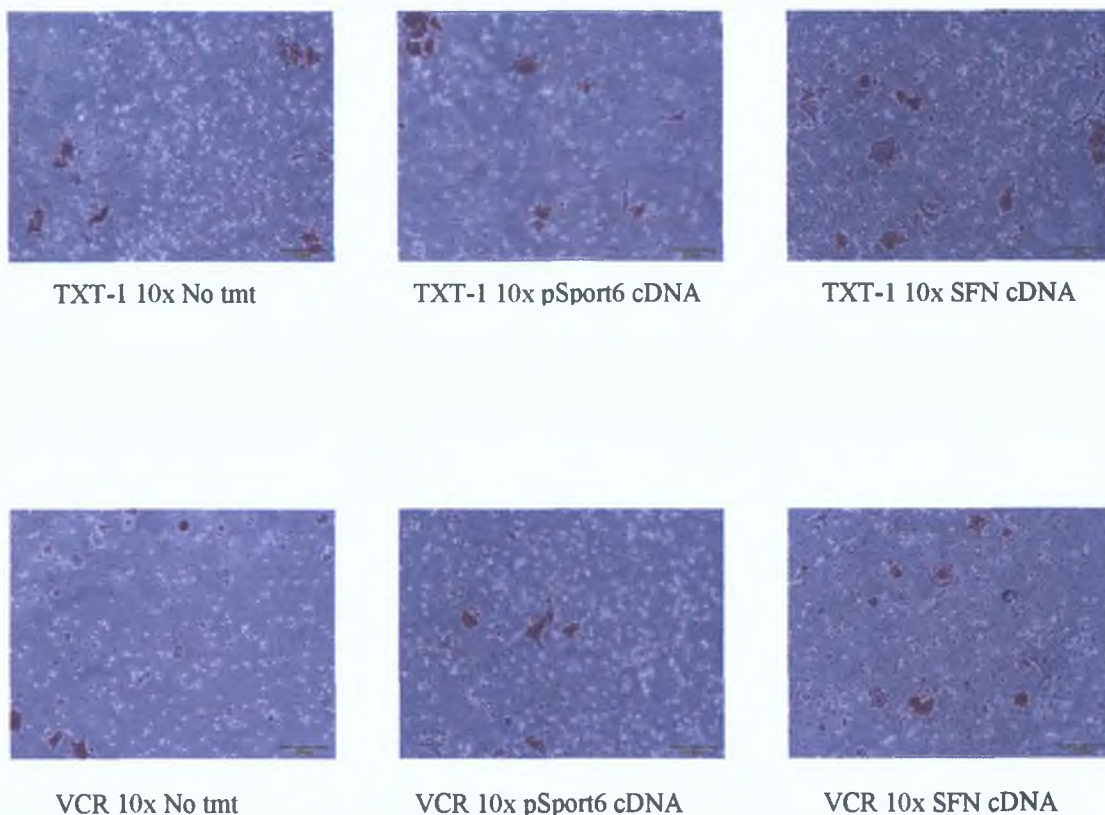


Figure 3.7.6.1 Photographic representation of invasion assay results 72h post SFN cDNA transfection.

The invasion assay was performed 72h post-transfection. Untransfected- and pSport6 empty vector transfected- cell lines were the controls for this experiment. Ten random fields were counted at 20X. No effect on invasion was observed in SFN cDNA transfected cells compared with the empty vector and non-treated cells. This indicates that increased SFN expression is itself insufficient to induce an invasive phenotype in poorly invasive cells.

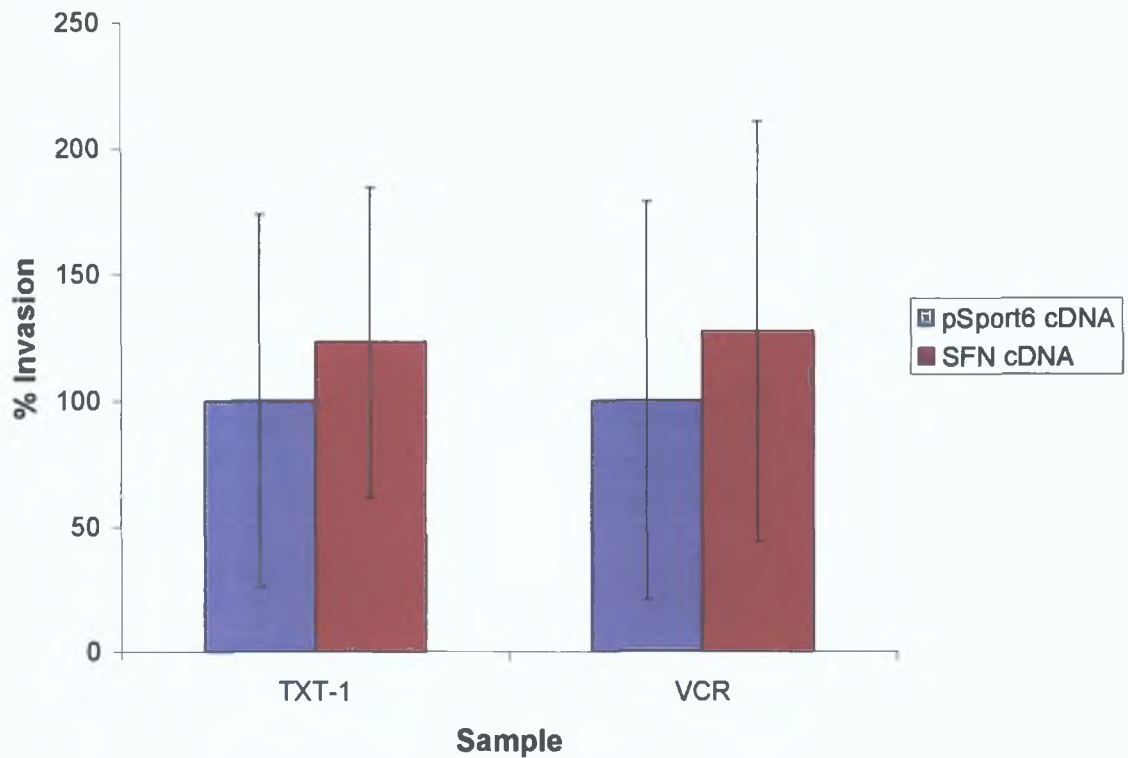


Figure 3.7.6.2 Graphic representation of invasion assay results 72h post SFN cDNA transfection.

Ten random fields were counted at 20X. Counts per insert were averaged and plotted as percentage invasion normalised to the pSport6 empty vector cDNA for each cell line. No effect on invasion was observed in SFN cDNA transfected cells compared with the empty vector transfected cells. This indicates that increasing SFN expression by transient transfection cannot induce an invasive phenotype in mildly invasive cells.

3.8 Investigation into role of Tissue Factor Pathway Inhibitor-2 (TFPI2) in invasion in the DLKP variants

3.8.1 Aims of TFPI2 experiments

TFPI2 was identified as a gene potentially involved in invasion as it was identified as being differentially expressed across the cell lines in our model of invasion by array expression analysis. The data showed that TFPI2 expression was lower in the invasive cell lines than the less/non-invasive cell lines. The aims of this set of experiments were as follows:

- 1 To confirm by PCR that TFPI2 is differentially expressed across the DLKP cell line model of invasion
- 2 To decrease TFPI2 expression by transfecting an independent siRNA sequence to TFPI2 into the non-invasive cell lines TXT-1 and VCR
- 3 To demonstrate TFPI2-specific siRNA knockdown at mRNA level
- 4 To evaluate the effect of decreased TFPI2 expression on invasion
- 5 To increase TFPI2 expression by transiently transfecting an expression vector containing the TFPI2 sequence into the invasive cell lines DLKP-1, DLKP-2 and TXT-2
- 6 To demonstrate an increase in TFPI2 protein expression in cDNA transfected cells by western blot
- 7 To evaluate the effect of TFPI2 cDNA transfection on proliferation
- 8 To evaluate the effect of increasing TFPI2 expression on invasion

To summarise the results detailed in this section, TFPI2 mRNA was differentially expressed in the panel of cell lines studied, with decreased invasive ability correlating with higher expression. This concurs with array data analysis. Decreasing TFPI2 expression had no effect on invasion in the non-invasive cell lines. Increasing TFPI2 expression exogenously by transient cDNA transfection had no effect on proliferation, but did decrease invasion dramatically.

3.8.2 RT-PCR investigation of differential TFPI2 mRNA expression

Semi-quantitative RT-PCR was used to confirm that TFPI2 mRNA expression was lower in the invasive DLKP variants compared with the poorly invasive variants and was reflective of array results.

To ensure that results from the array study matched to independent analysis of the cell lines, RNA samples from the preliminary Affymetrix array study by Dr. Rasha Linehan in 2003 (Figure 3.8.2.1), RNA from the duplicate array samples 2004 (Figure 3.8.2.2), RNA from a fresh set of cultures harvested separately to those for array analysis including RNA from three samples analysed on the Agilent array platform (Figure 3.8.2.3) were included in this analysis.

β -actin was used as an endogenous control to normalise for RNA content in each SFN PCR. The reactions were analysed by gel electrophoresis (GE) on a 2% agarose gel and visualised by ethidium bromide staining. The band size for TFPI2 was 183bp. cDNA negative control (cDNA neg) contained PCR master mix with cDNA but without addition of Taq enzyme. PCR negative controls consisted of PCR master mix to which no cDNA template was added. Densitometric values were normalised by dividing TFPI2 intensity values by β -actin intensity values and were graphed for each sample. The gels included in this section are representative of at least two independent repeats.

This analysis by semi-quantitative PCR demonstrates a trend of lower TFPI2 expression in the more invasive cell lines DLKP-1, DLKP-2 and TXT-2, compared to the less invasive cell lines TXT-1 and VCR. This correlates with the array data.

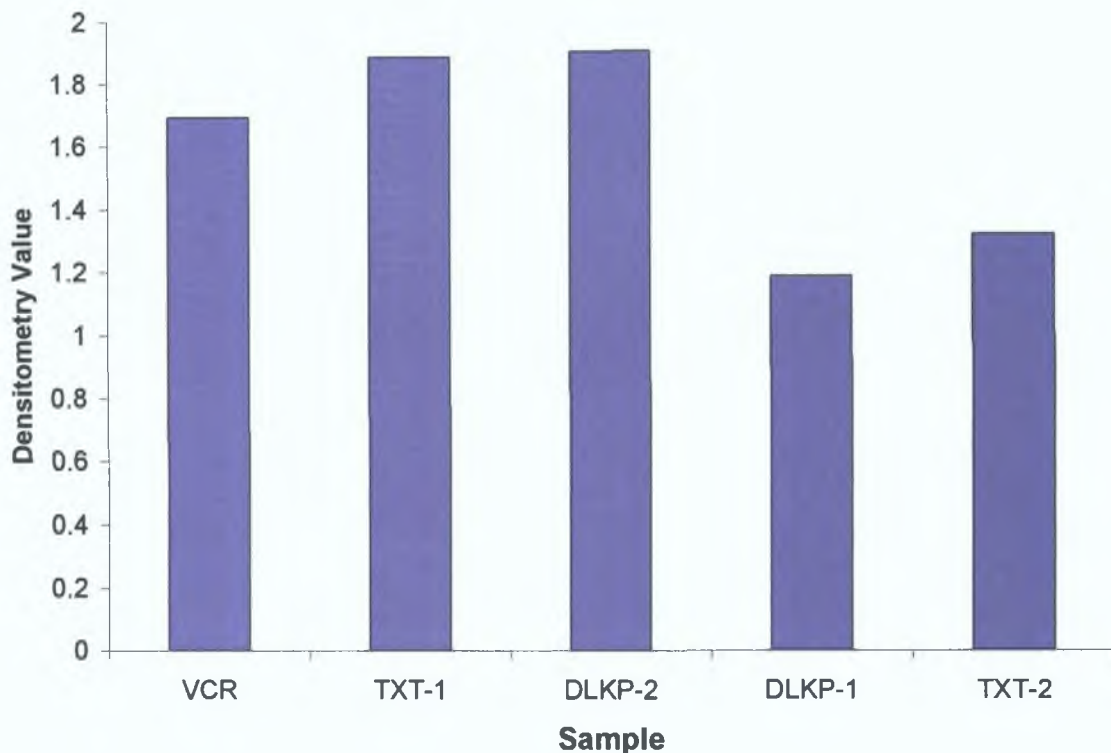


Figure 3.8.2.1 RT-PCR of TFPI2 mRNA expression from RNA used in array samples 2003.

RNA used for this PCR was analysed on the 2003 arrays. β -actin was used as an endogenous control to normalise for RNA content in each reaction. The PCR was analysed by gel electrophoresis (GE) on a 2% agarose gel and visualised by ethidium bromide staining. A PCR Negative (PCR Neg) control was included in the analysis and consisted of PCR master mix to which no cDNA template was added. Densitometry values were normalised by dividing TFPI2 intensity values by β -actin intensity values and were plotted for each sample. This PCR demonstrates increased TFPI2 expression in the mildly invasive cell lines TXT-1 and VCR, although there is high TFPI2 expression in DLKP-2 also. Considering that DLKP-2 is in the middle of the scale of invasion, it is not too surprising that TFPI-2 expression would be higher in this sample than DLKP-1 or TXT-2.

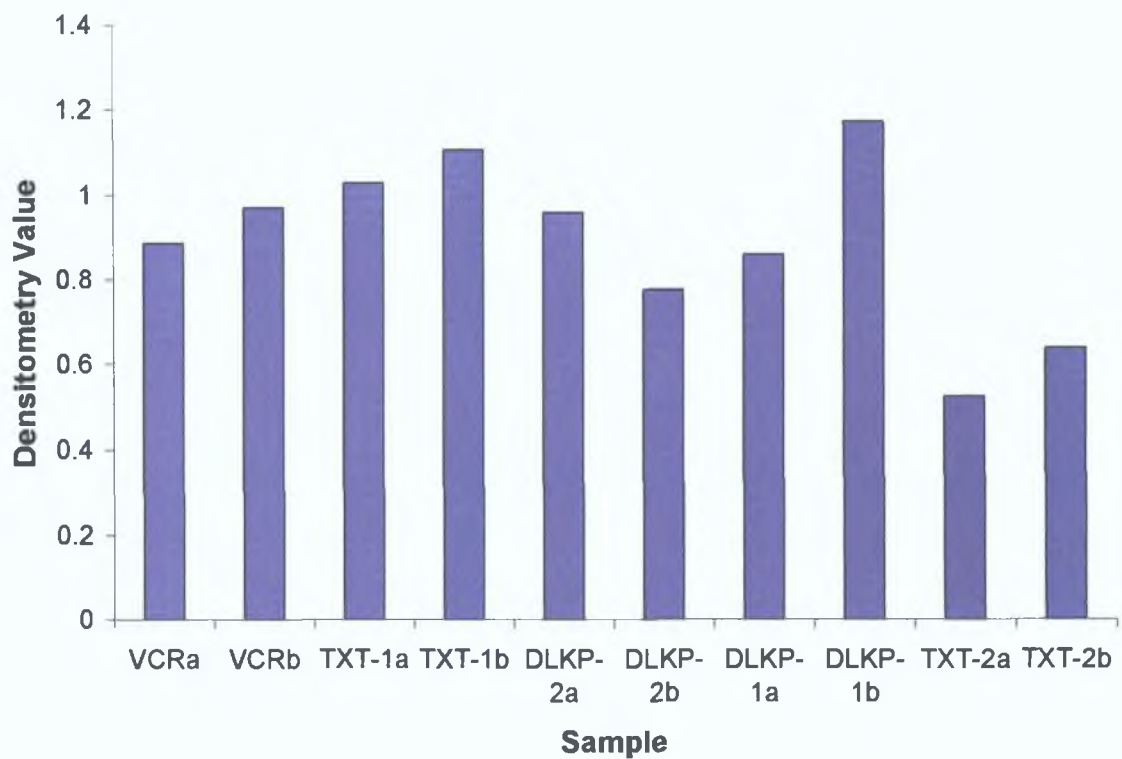


Figure 3.8.2.2 RT-PCR of TFPI2 mRNA expression from RNA used in duplicate array samples 2004.

RNA for this reaction was analysed in the duplicate array analysis of the DLKP cell lines in 2004. β -actin was used as an endogenous control. A PCR negative (PCR Neg) and cDNA negative (cDNA Neg) control was included in the analysis. Densitometry values were normalised by dividing TFPI2 intensity values by β -actin intensity values and were plotted for each sample. This PCR demonstrates high TFPI2 expression in the lesser invasive cell lines TXT-1 and VCR, although mRNA levels in DLKP-1 and DLKP-2 are also high. TFPI2 expression is lowest in the most invasive cell line TXT-2.

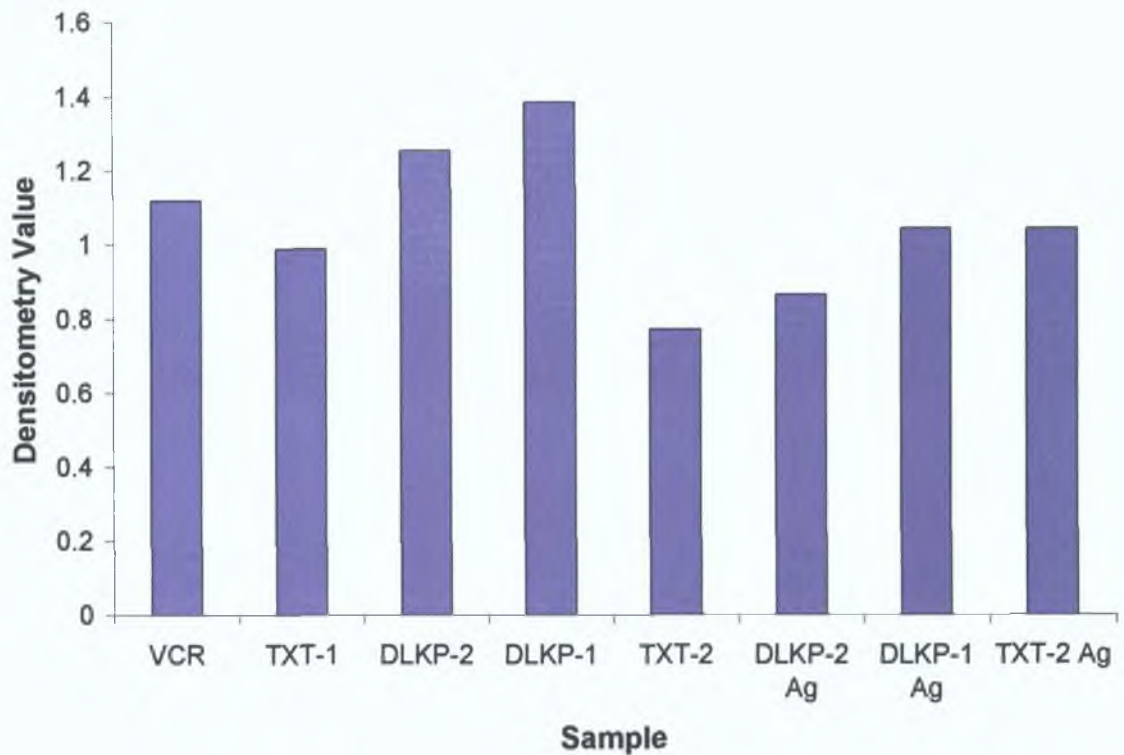


Figure 3.8.2.3 RT-PCR of TFPI2 mRNA in a separate sample set and Agilent samples.

RNA for this analysis was from a separate batch of DLKP variant cultures not harvested or processed for Affymetrix array analysis. Also included were three samples analysed on the Agilent array platform but which were not investigated further. β -actin was used as an endogenous control. The reaction was analysed by GE on a 2% agarose gel. Densitometry values were normalised by dividing TFPI2 intensity values by β -actin intensity values and were displayed graphically for each sample. This PCR demonstrates lowest TFPI2 mRNA expression in TXT-2, which is the most invasive cell line in the panel studied.

3.8.3 TFPI2 siRNA transfection in the non-invasive DLKP variants

3.8.3.1 Summary of TFPI2 siRNA experimental plan

TFPI2 was identified being differentially expressed across the cell lines in our model of invasion by array expression analysis. Lower TFPI2 expression correlated with a greater degree of invasion. This correlation was confirmed by RT-PCR though it was not as apparent. However, it was decided to examine the impact of TFPI2 knockdown using a commercial siRNA sequence on the less invasive phenotype. Successful knockdown was confirmed by PCR and the phenotypic effect assessed by *in vitro* invasion assay. Western blot analysis of protein levels indicated that endogenous TFPI2 levels were below the level of detection.

3.8.3.2 TFPI2 siRNA specific decrease in mRNA levels

An siRNA sequence to TFPI2 was transfected into the poorly invasive DLKP cell lines, TXT-1 and VCR. qPCR and semi quantitative RT-PCR was used to examine the effect of TFPI2 knockdown on mRNA expression.

A commercial TaqMan probe to TFPI2 was used to quantify relative TFPI2 mRNA expression. The data was normalised using β -actin as an endogenous control (Figure 3.8.3.1). Knockdown was achieved in VCR, but not to the same extent, at mRNA level, in TXT-1.

Timecourse analysis of TFPI2 knockdown was examined by RT-PCR (Figures 3.8.3.2 to 3.8.3.3). β -actin was included as an endogenous control to normalise for RNA content in each reaction. The PCRs were analysed by gel electrophoresis (GE) on a 2% agarose gel and visualised with ethidium bromide staining. The band size for TFPI2 was 183bp. cDNA negative control (cDNA neg) consisted of PCR master mix with cDNA but without addition of Taq enzyme. PCR negative controls consisted of PCR master mix to which no cDNA template was added. Densitometry values were normalised by dividing TFPI2 intensity values by β -actin intensity values and were visualised graphically for each sample. The gels included in this timecourse study are representative of at least two independent repeats. These results demonstrate the limited value of semi-quantitative RT-PCR timecourse analysis. However, it does suggest an overall trend from the data that TFPI2 siRNA transfection decreased mRNA expression in the VCR cell line but not to any great extent in TXT-1 cell line.

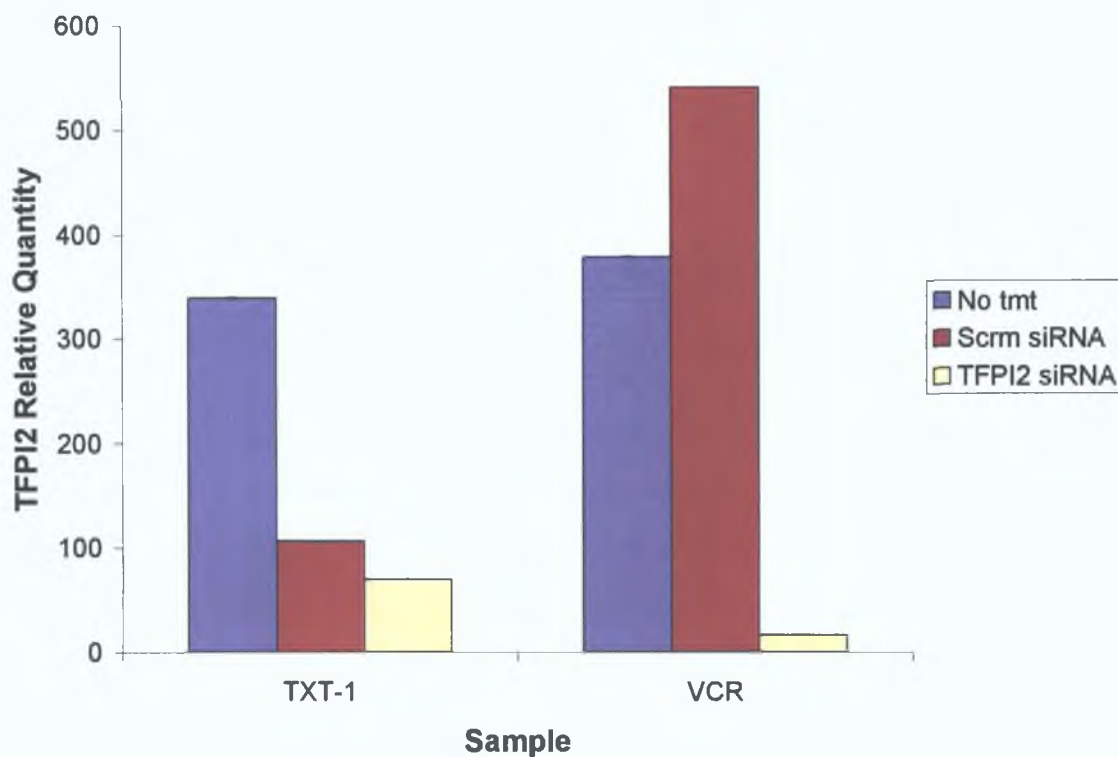
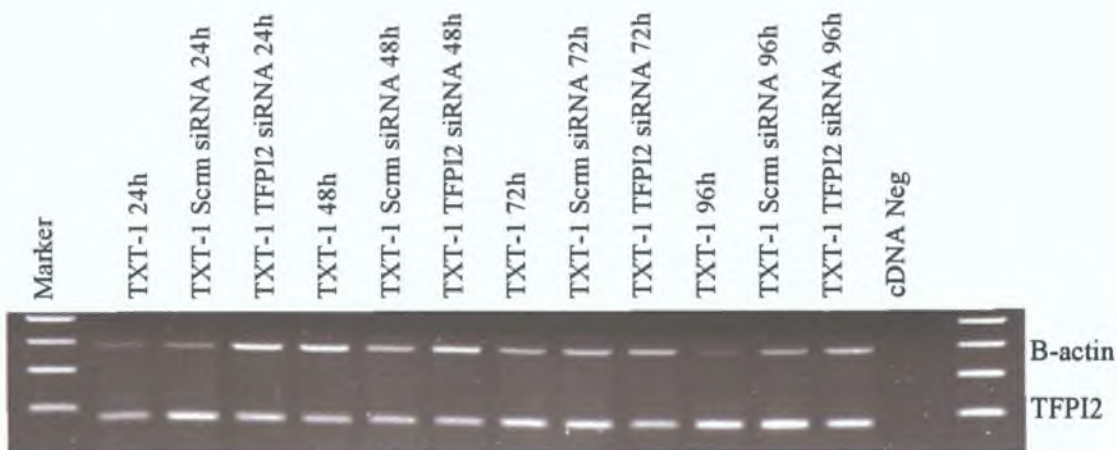


Figure 3.8.3.1 qPCR analysis of TFPI2 siRNA experiment at 24h.

RNA was harvested 24h post-transfection and used to determine a TFPI2-siRNA specific decrease in mRNA in response to siRNA transfection. TFPI2 mRNA expression was examined by qRT-PCR using a commercial TaqMan probe to TFPI2 was and normalised for RNA content using β -actin as an endogenous control. This graph is a composite of three biological repeats. The data represents TFPI2 expression relative to the VCR TFPI2 siRNA sample, which was set to 1 for the analysis and was the lowest expresser in the qPCR data set. A TFPI2 siRNA specific decrease in mRNA was observed for samples at 24h.



Densitometry of timecourse showing TFPI2 mRNA knockdown in TXT-1 (YL)

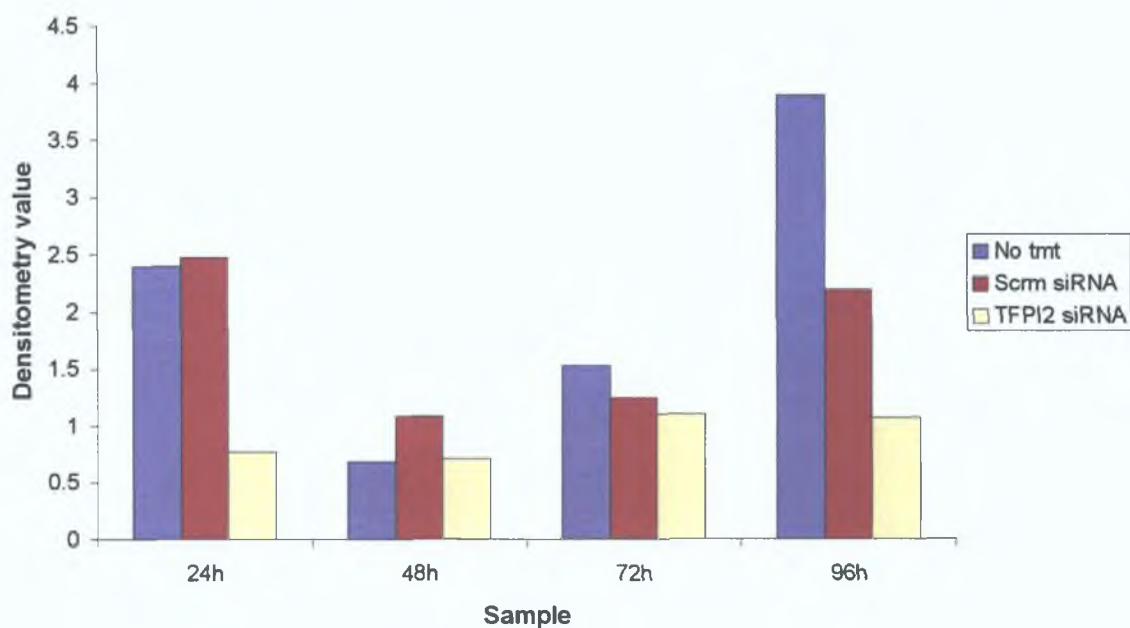
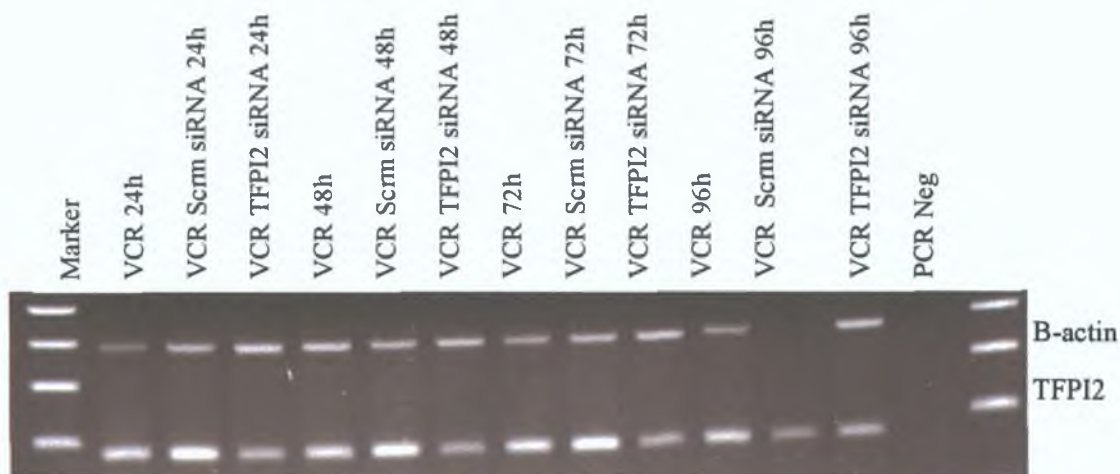


Figure 3.8.3.2 Timecourse analysis of TFPI2 mRNA knockdown by semi-quantitative RT-PCR in TXT-1.

TFPI2 siRNA was transfected into TXT-1. RNA for the analysis of TFPI2 mRNA was harvested at 24, 48, 72 and 96h. β -actin was used to normalise for RNA content in each PCR. Densitometric analysis assigned an arbitrary figure to each band as a measure of band intensity. Figures representing the densitometry values graphed above were calculated by dividing TFPI2 intensity values by β -actin intensity values.

TFPI2 mRNA levels were decreased at 24, 72 and 96h respectively, in comparison to the non-treated and scrambled siRNA transfected samples.



Densitometry of timecourse showing TFPI2 mRNA knockdown in VCR

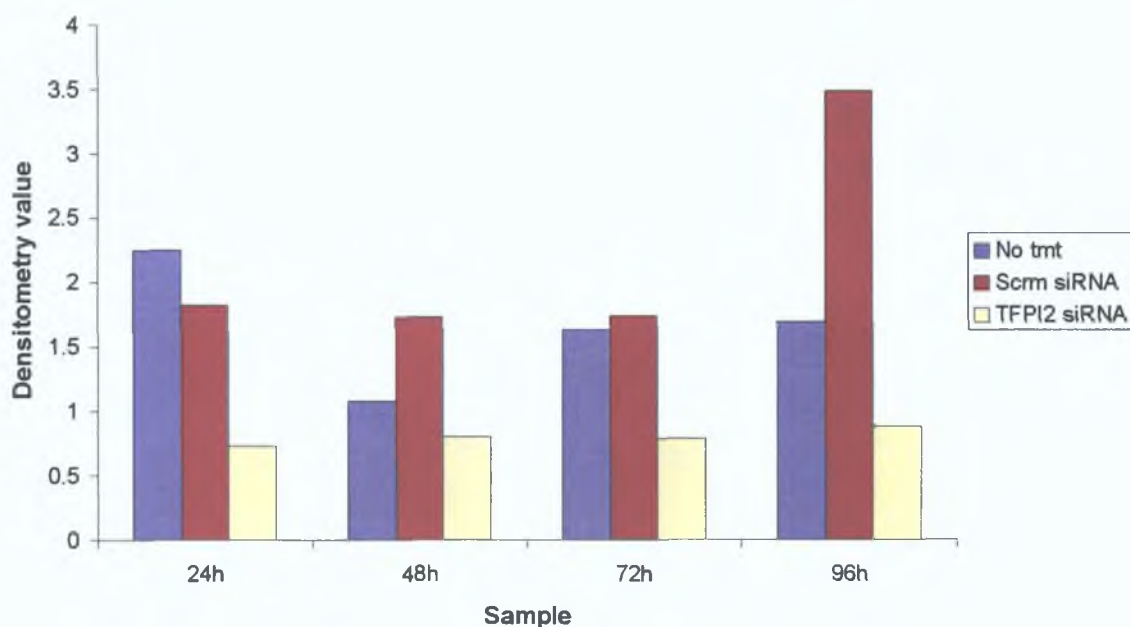


Figure 3.8.3.3 Timecourse analysis of TFPI2 mRNA knockdown by semi-quantitative RT-PCR in VCR.

TFPI2 siRNA was transfected into VCR. RNA for the analysis of TFPI2 mRNA was harvested at 24, 48, 72 and 96h. β -actin was used as an endogenous control to normalise for RNA content in each PCR. Figures for the densitometry values were normalised by dividing TFPI2 intensity values by β -actin intensity values and were plotted for each sample. TFPI2 mRNA levels were decreased at 24, 48, 72 and 96h respectively, in comparison to the non-treated and scrambled siRNA transfected samples.

3.8.4 Invasion assay analysis of TFPI2 siRNA transfection

The impact of TFPI2 knockdown on the invasive capacity of the poorly invasive DLKP variants was examined. Invasion assay analysis was performed 72h post transfection, using commercial invasion assay kits containing inserts pre-coated with matrigel in conjunction with a serum gradient. The cells were incubated at 37°C for 24 hours after which, the underside of the inserts were stained with crystal violet and allowed to air dry. The inserts were then photographed using 10X magnification. Ten fields of view were counted per insert at 20X magnification and averaged. At least two inserts were used for the analysis of each condition. The counts per number of inserts used were then also averaged and this figure was used to plot graphs of relative invasive capacity per cell line per condition.

One set of representative photographs was included (Figure 3.8.4.1) in this section. Invasion assay results are also presented graphically (Figures 3.8.4.2). TFPI2 knockdown did not impact the invasive capacity of TXT-1 and VCR. These results suggest that decreasing TFPI2 expression does not induce an invasive phenotype in poorly invasive cell lines.

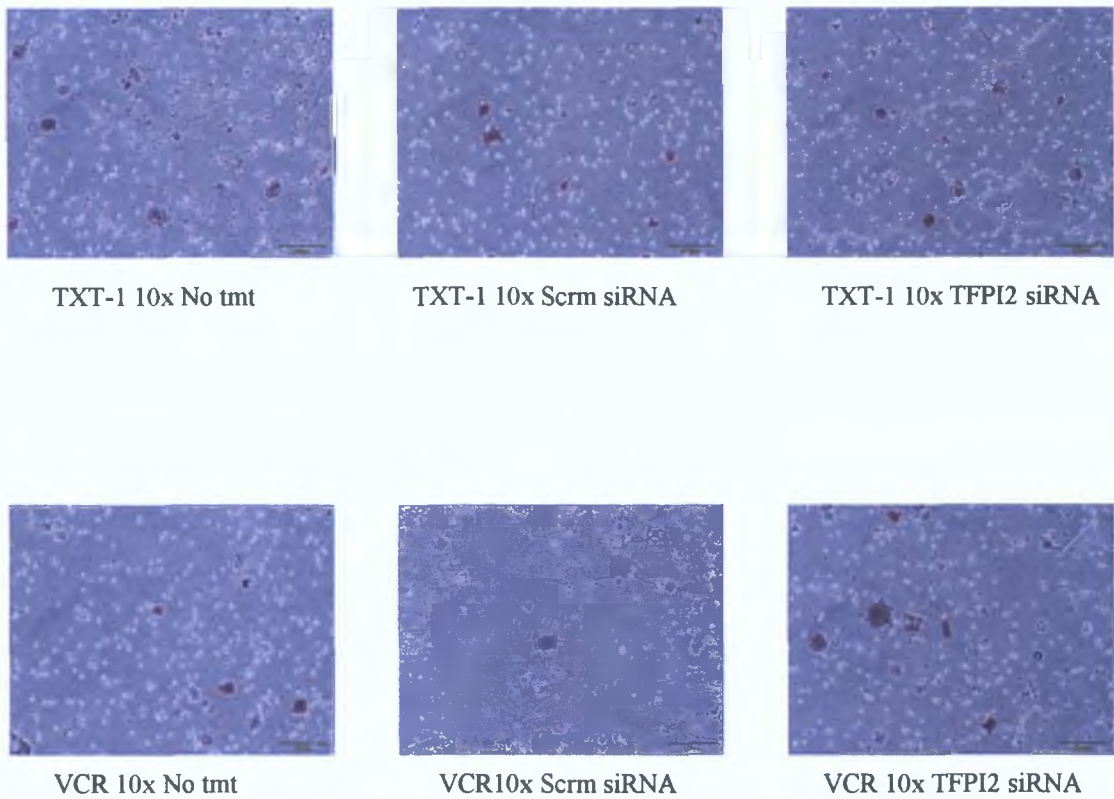


Figure 3.8.4.1 Photographic representation of invasion assay results 72h post TFPI2 siRNA transfection.

The invasion assay was performed 72h post-transfection. Untransfected- and scrambled siRNA transfected- cell lines are the controls for this experiment. Representative photographs at 10X are shown above. No obvious effect on invasion was observed in TFPI2 siRNA transfected cells compared with the scrambled siRNA transfected and non-treated cells. This indicates that decreased TFPI2 expression is itself insufficient to induce an invasive phenotype in mildly invasive cells.

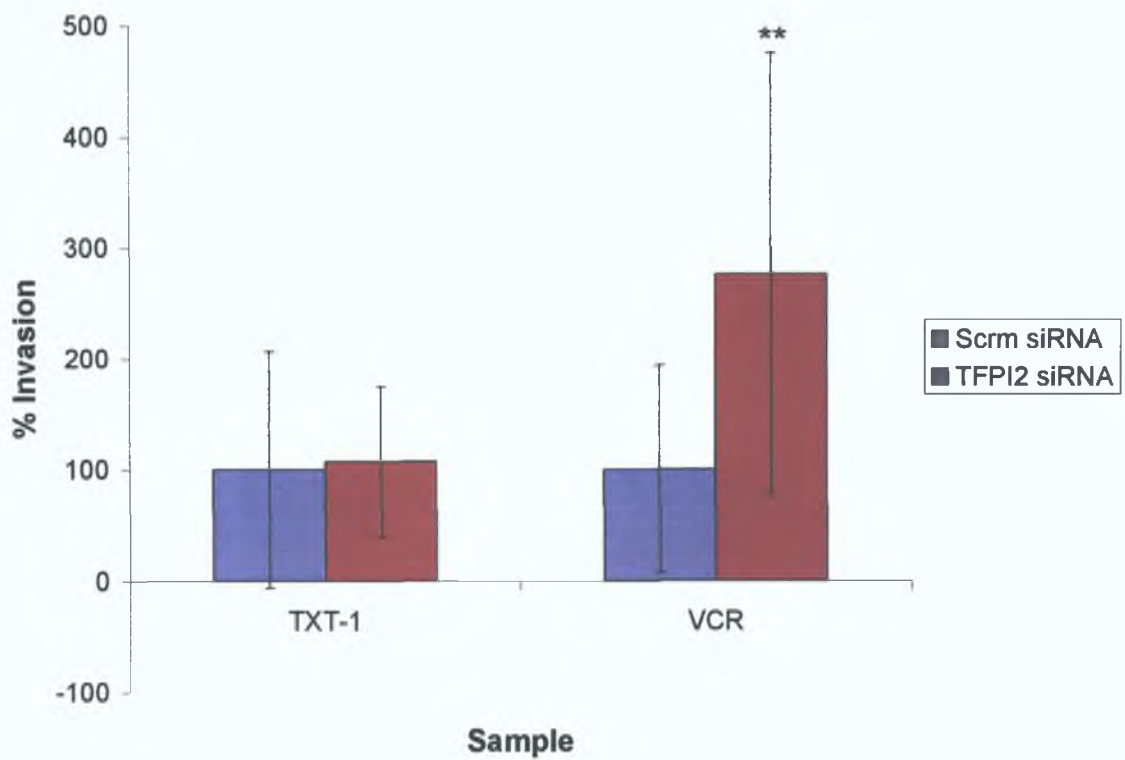


Figure 3.8.4.2 Graphic representation of invasion assay results 72h post TFPI2 siRNA transfection.

The invasion assay was performed 72h post-transfection. Scrambled siRNA transfected- cell lines were the controls for this experiment. Counts per insert were averaged and plotted as percentage invasion normalised to the scrambled siRNA for each cell line. Invasion was increased in TFPI2 siRNA transfected VCR cells compared with the scrambled siRNA control ($P < 0.005$). However, no effect on invasion was observed in TFPI2 siRNA transfected TXT-1 cells compared with the scrambled siRNA transfected control cells. These data indicate that decreased TFPI2 expression is itself insufficient to induce a highly invasive phenotype in mildly invasive cells.

3.8.5 TFPI2 cDNA transfection in the invasive DLKP variants

3.8.5.1 Summary of TFPI2 cDNA experimental plan

Array and RT-PCR results indicated that TFPI2 mRNA expression was increased in the poorly invasive compared with the invasive DLKP lines. To investigate the effect of overexpression of exogenous TFPI2 on the invasive status of the cells we transiently transfected the vector pSport6 containing the cDNA sequence to TFPI2 into the invasive cell lines DLKP-1, DLKP-2 and TXT-2. Transient transfection of this vector into the invasive cell lines increased TFPI2 protein expression as determined by western blotting. Exogenous overexpression of TFPI2 dramatically decreased the invasive capacities of the invasive DLKP variants.

3.8.5.2 Western Blot analysis of TFPI2 cDNA transient transfection

An increase in TFPI2 protein expression in response to TFPI2 cDNA transfection was determined by western blotting. Cells were transfected with a pSport6 empty vector as a control to ensure that the transfection process did not affect TFPI2 protein expression (Figures 3 8 5 1 to 3 8 5 3). Each blot in this section is representative of at least two independent repeats.

The polyclonal anti-TFPI2 antibody used in these experiments was a gift from Prof Walt Kisiel and was raised in rabbit. The bands specific for TFPI2 are a triplet of 33, 31 and 27kDa respectively. A α -tubulin antibody was used to demonstrate even loading between the samples. TFPI2 protein expression was increased in response to TFPI2 cDNA transient transfection in both TXT-1 and VCR.

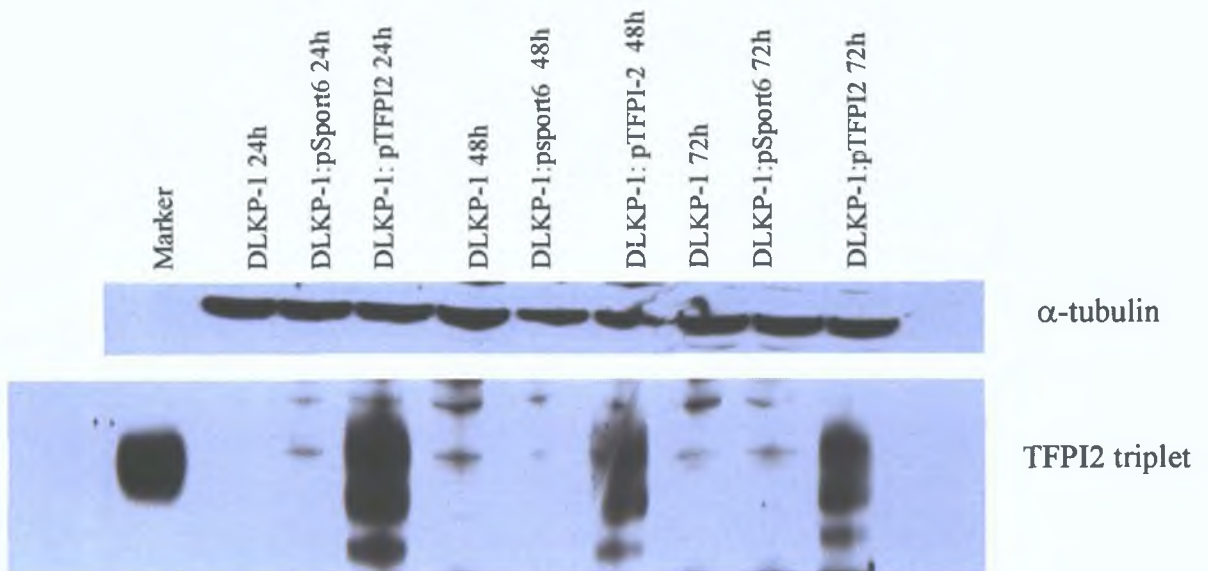


Figure 3.8.5.1 Western blot analysis of TFPI2 cDNA transient transfection in DLKP-1.

The polyclonal anti-TFPI2 antibody used in this experiment was a gift from Prof Walt Kisiel and was raised in rabbit. The bands specific for TFPI2 are a triplet of 33, 31 and 27kDa respectively. TFPI-2 protein expression is increased in response to TFPI-2 cDNA transfection over 72h in DLKP-1.

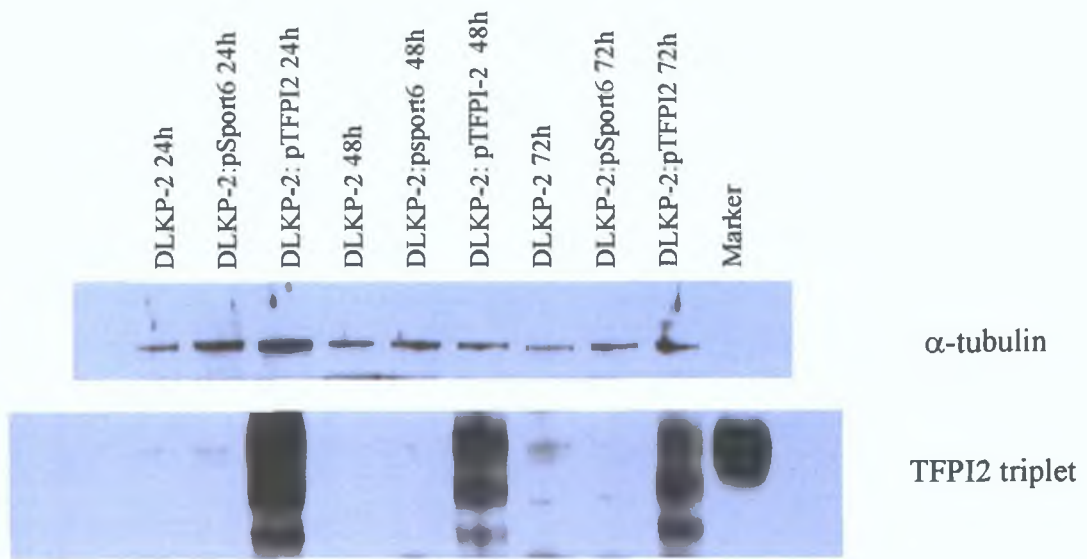


Figure 3.8.5.2 Western blot analysis of TFPI2 cDNA transient transfection in DLKP-2.

TFPI-2 protein expression is increased in DLKP-2 in response to TFPI-2 cDNA transfection over 72h.

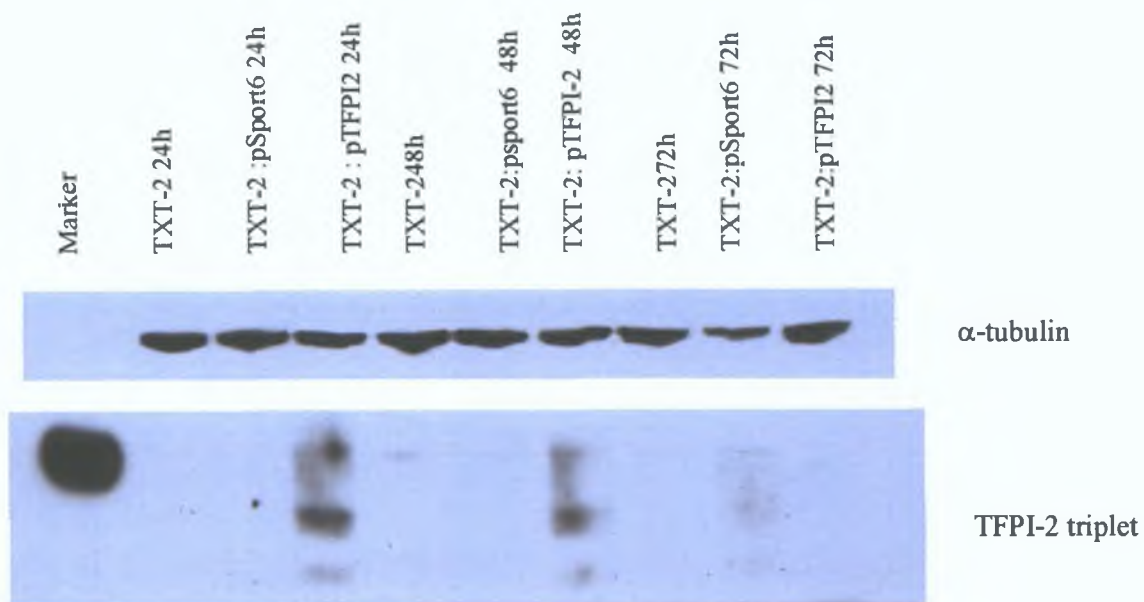


Figure 3.8.5.3 Western blot analysis of TFPI2 cDNA transient transfection in TXT-2.

TFPI-2 protein expression is increased in response to TFPI-2 cDNA transfection over 72h in TXT-2.

3.8.5.3 Investigation of effect of TFPI-2 cDNA transient transfection on proliferation.

The effect of increasing TFPI2 expression on proliferation was investigated. Cells seeded at 4×10^5 cells/well of a 6-well plate (Figure 3.8.5.4), which was the cell number used to seed all the cDNA transfections in six-well plates. Relative cell number was determined using the acid phosphatase assay at 72h post transfection. Cell numbers were measured to determine what functional effect, if any, an increase in TFPI2 expression was having on proliferation.

Exogenously TFPI2 expression did not have a dramatic affect proliferation compared with pSport6 empty vector –transfected and non-treated cells.

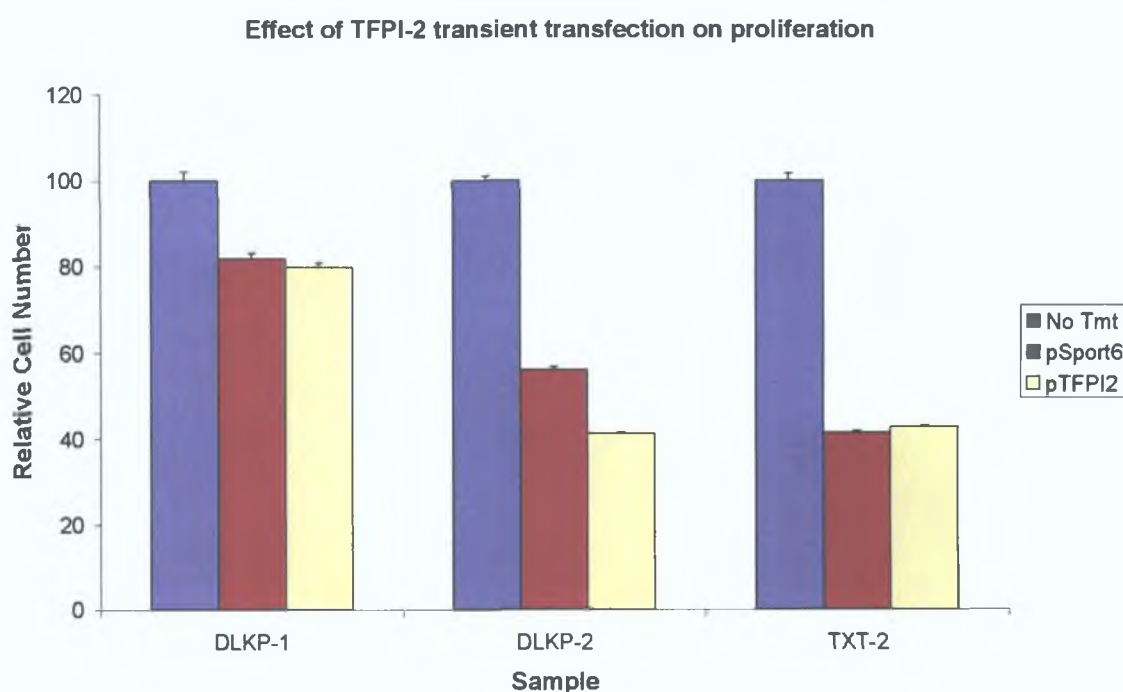


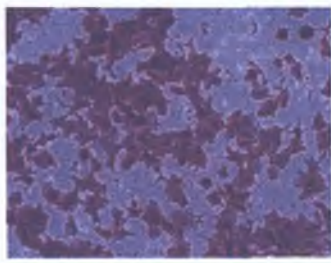
Figure 3.8.5.4 Effect of TFPI2 cDNA transfection on DLKP variant cell number.

The cells were seeded at a 4×10^5 cells/well of a 6-well plate. Proliferation was measured by the acid phosphatase assay at 72h post transfection. There is a decrease in proliferation observed due to the transfection. TFPI2 cDNA transfection does not appear to affect proliferation in the cell lines compared with the empty vector-pSport6 and non-transfected cells.

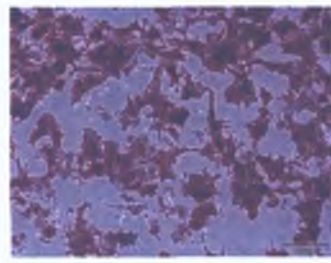
3.8.5.4 Evaluation of effect of TFPI2 cDNA transient transfection on DLKP variant invasion

The effect of exogenously increasing TFPI2 expression on the invasive abilities of the invasive DLKP variants was investigated. Invasion assay analysis was performed 72h post transfection, using commercial invasion assay kits containing inserts pre-coated with matrigel in conjunction with a serum gradient. The cells were incubated at 37°C for 24h after which, the underside of the inserts were stained with crystal violet and allowed to air dry. The inserts were then photographed using 10X magnification. Ten fields of view were counted per insert at 20X magnification and averaged. At least two inserts were used for the analysis of each condition. The counts per number of inserts used were then also averaged and this figure was used to generate graphs of relative invasive capacity per cell line per condition.

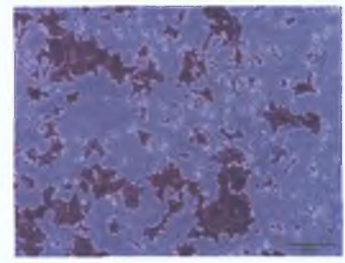
One set of representative photographs was included (Figure 3 8 5 5) in this section and clearly demonstrate decreased invasion in TFPI2 cDNA transfected cells. Invasion assay results are also presented graphically (Figures 3 8 5 6 and 3 8 5 7).



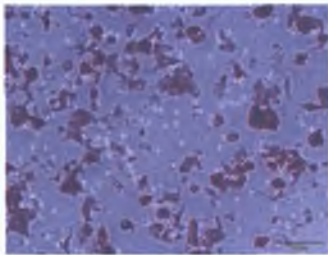
DLKP-1 10x No tmt



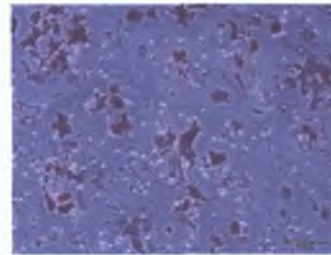
DLKP-1 10x pSport6 cDNA



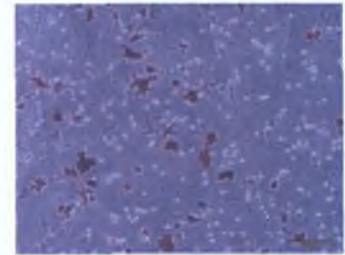
DLKP-1 10x TFPI2 cDNA



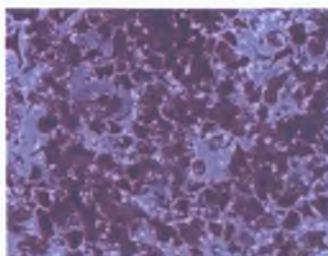
DLKP-2 10x No tmt



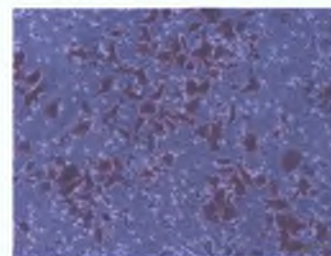
DLKP-2 10x pSport6 cDNA



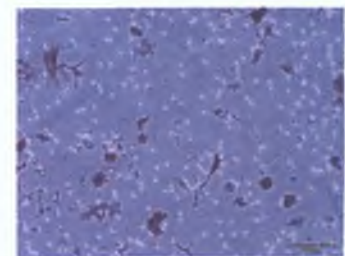
DLKP-2 10x TFPI2 cDNA



TXT-2 10x No tmt



TXT-2 10x pSport6 cDNA



TXT-2 10x TFPI2 cDNA

Figure 3.8.5.5 Photographic representation of invasion assay results 72h post TFPI2 cDNA transient transfection (I).

The invasion assay was performed 72h post-transfection. Untransfected- and empty vector pSport6 transfected- cell lines are the controls for this experiment. Representative photographs at 10X are shown above. Invasion was decreased in TFPI2 cDNA transfected cells compared with the empty vector and non-treated cells.

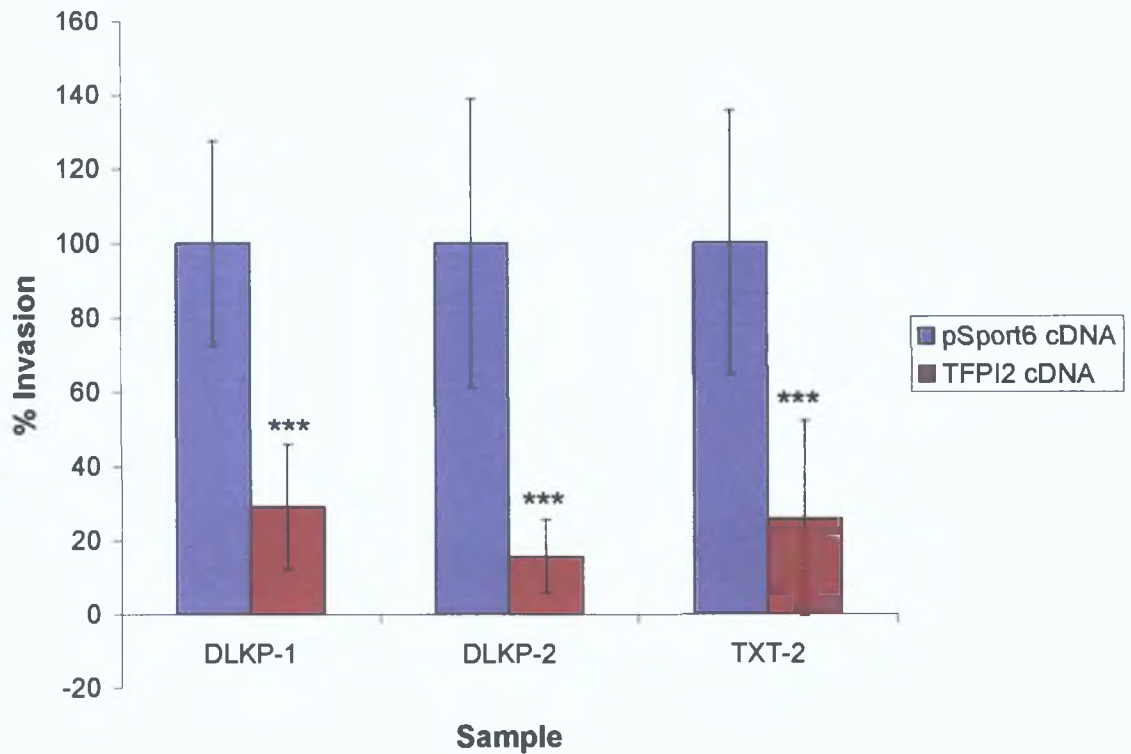


Figure 3.8.5.6 Graphic representation of invasion assay results 72h post TFPI2 cDNA transient transfection (I).

The invasion assay was performed 72h post-transfection. pSport6 empty vector transfected- cell lines were the controls for this experiment. Counts per insert were averaged and plotted as percentage invasion normalised to the empty vector transfected cells for each cell line. Invasion was decreased in TFPI2 cDNA transfected cells compared with the pSport6 empty vector control transfected cells ($P < 0.001$). A decrease of 50% or greater was observed in invasion in TFPI2 cDNA transfected samples compared with the empty vector controls.

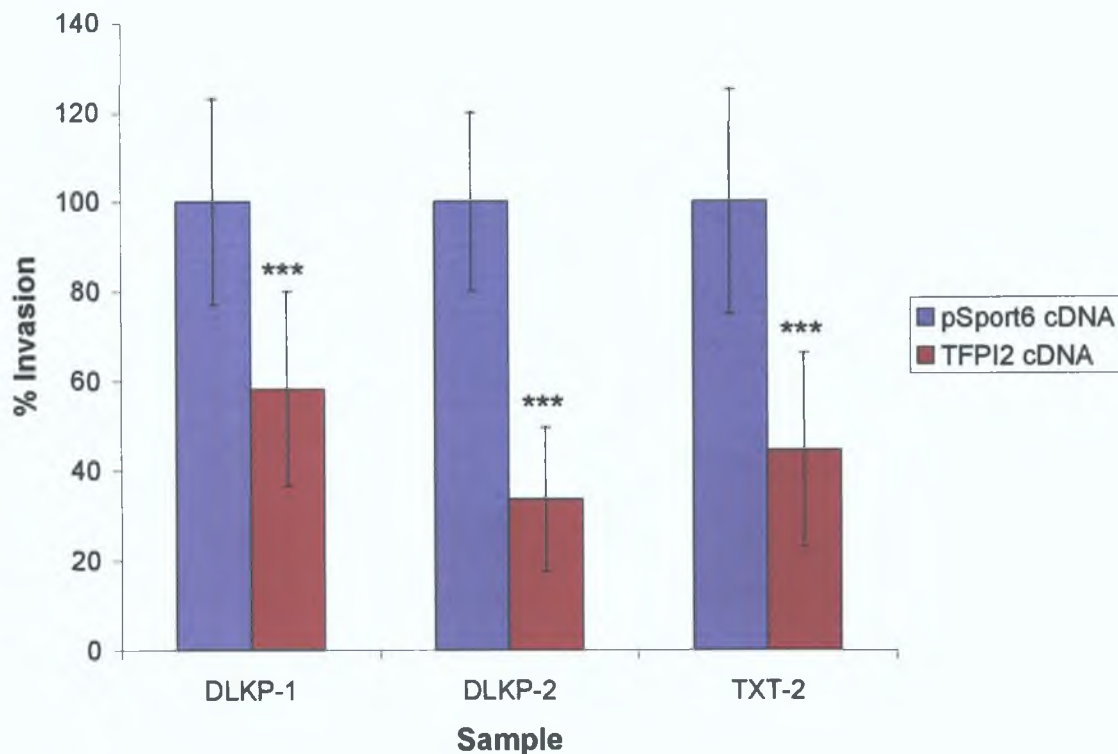


Figure 3.8.5.7 Graphic representation of invasion assay results 72h post TFPI2 cDNA transient transfection (II).

The invasion assay was performed 72h post-transfection. pSport6 empty vector transfected- cell lines were the controls for this experiment. Counts per insert were averaged and plotted as percentage invasion normalised to the empty vector transfected cells for each cell line. Invasion was decreased in TFPI2 cDNA transfected cells compared with the pSport6 empty vector control transfected cells ($P < 0.001$).

3.9 PCR analysis of cDNA transient transfections

Exogenous cDNA transfections were part of the functional investigations of the role of many of the targets in this study including KCNJ8, S100A13, SFN and TFPI2. The results in this section give an example of some of the challenges met when analysing the mRNA of cDNA transfected samples by RT-PCR.

RNA was harvested at 24, 48, 72 and 96h post cDNA transfection for each of the targets mentioned above and used to determine a target specific increase in mRNA in response to the cDNA transfection by PCR. Initial PCR analysis did not have a band for β -actin (endogenous control) in target cDNA transfected samples at any of the timepoints (Figure 3.9.1) this may possibly be attributed to competition for PCR components in the master mix. The result of this missing band for the endogenous control was that one could not definitively conclude that the increase in target band density was as a result of increased target expression and was possibly caused by cDNA carryover in the RT reaction.

To investigate the possibility of cDNA carryover affecting the RT reaction and consequently the PCR results, RT negative controls for the empty vector transfected and target cDNA transfected samples were included in the analysis. RT negative controls consisted of RNA, RT master mix but without the addition of MMLV enzyme. This identified cDNA carryover in the cDNA transfected samples. This cDNA carryover needed to be removed if an accurate increase in target mRNA due to transfection of target cDNA was to be measured.

To eliminate the cDNA carryover in the cDNA transfected samples we digested the cDNA in the RNA samples using Qiagen RNase free DNaseI (Figures 3.9.2 and 3.9.3). This digestion eliminated the cDNA carryover from the RT reaction. However, it also degraded the RNA in the process (Figure 3.9.4).

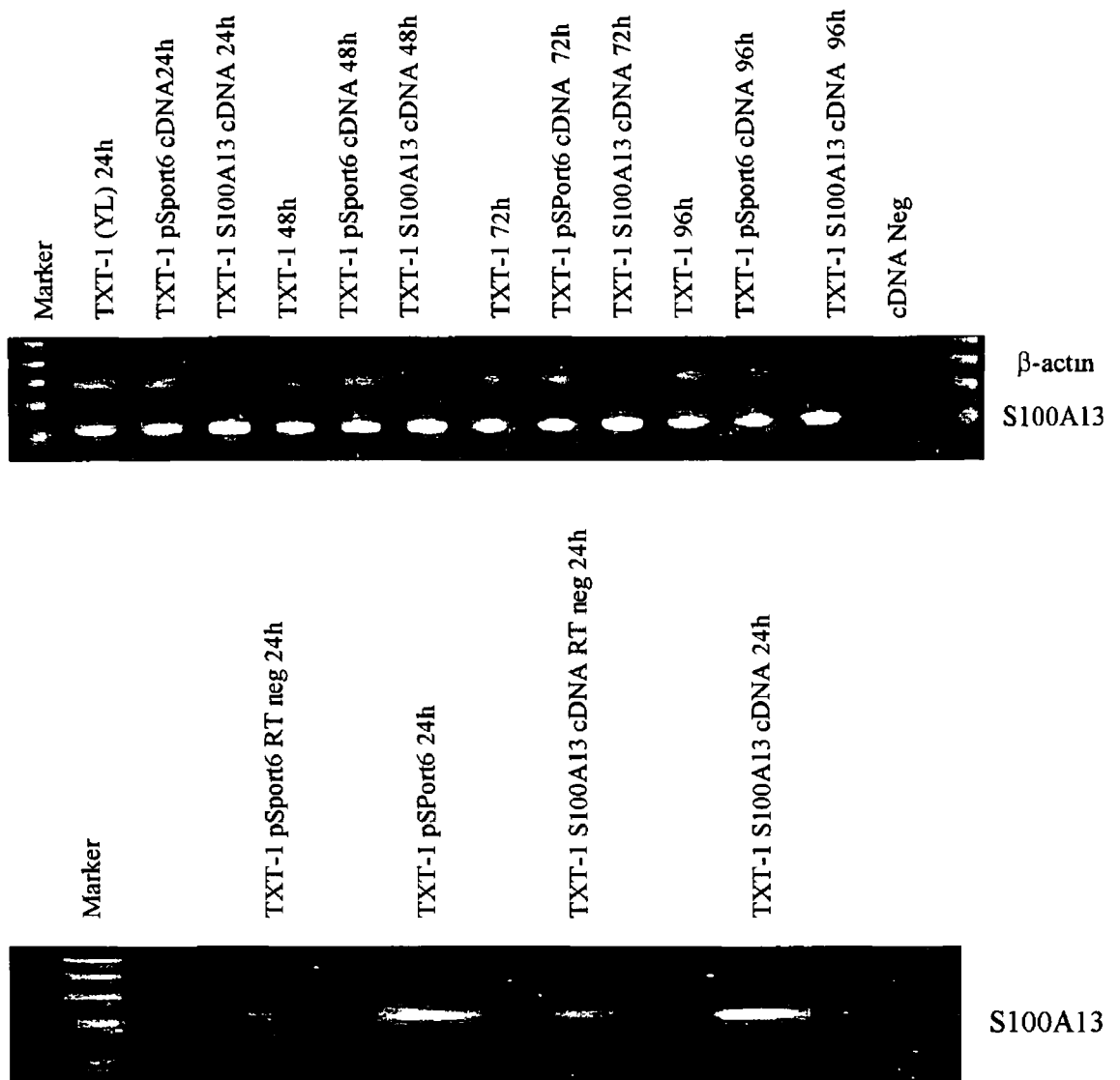


Figure 3 9 1 Timecourse analysis by semi-quantitative RT-PCR using S100A13 cDNA transient transfection in TXT-1 as an example.

S100A13 cDNA was transiently transfected into TXT-1 RNA for the analysis of S100A13 mRNA was harvested at 24, 48, 72 and 96h post transfection Negative RT controls, which consisted of mRNA, RT master mix, but no MMLV, were included in the PCR analysis of this transfection This showed that there was cDNA carryover from the transfection process biasing the results of the RT-PCR This cDNA carryover needed to be removed if an accurate increase in S100A13 mRNA due to transfection of S100A13 cDNA was to be measured

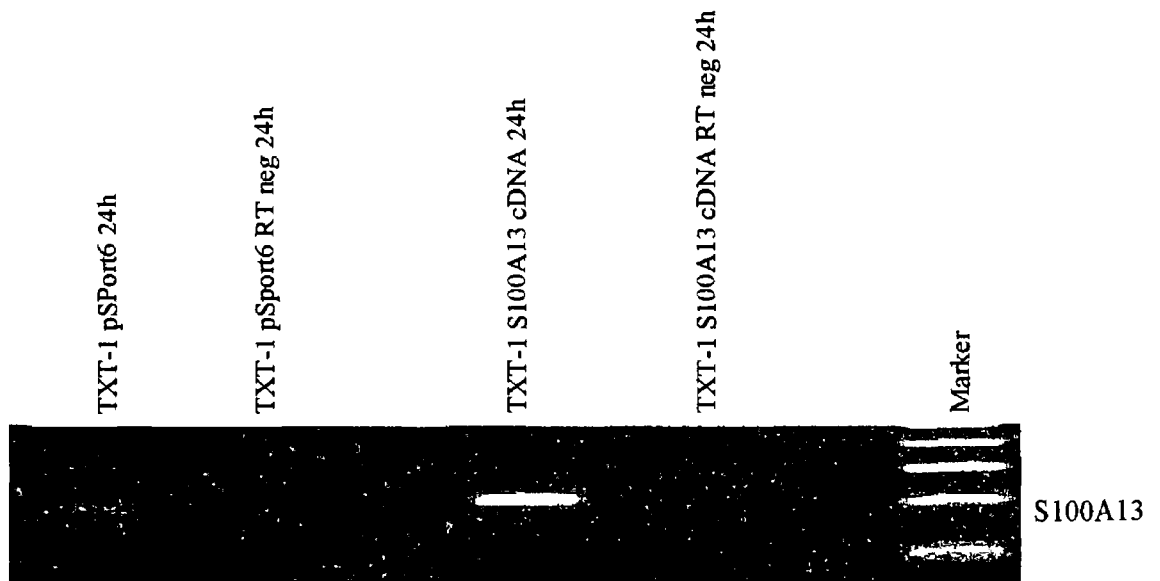


Figure 3 9 2 DNase I digestion of pSport6 empty vector and S100A13 cDNA transfected samples

2µg of pSport6 empty vector and S100A13 cDNA transfected RNA samples were subject to Qiagen RNase free DNase I digestion using 2U RNase free DNase I per µg RNA at 37⁰C for 30mins. These samples, including RT negative controls, were then analysed by RT-PCR. PCR analysis revealed that cDNA carryover in the RT reaction was eliminated following this procedure since RT negative controls showed no bands specific to S100A13.

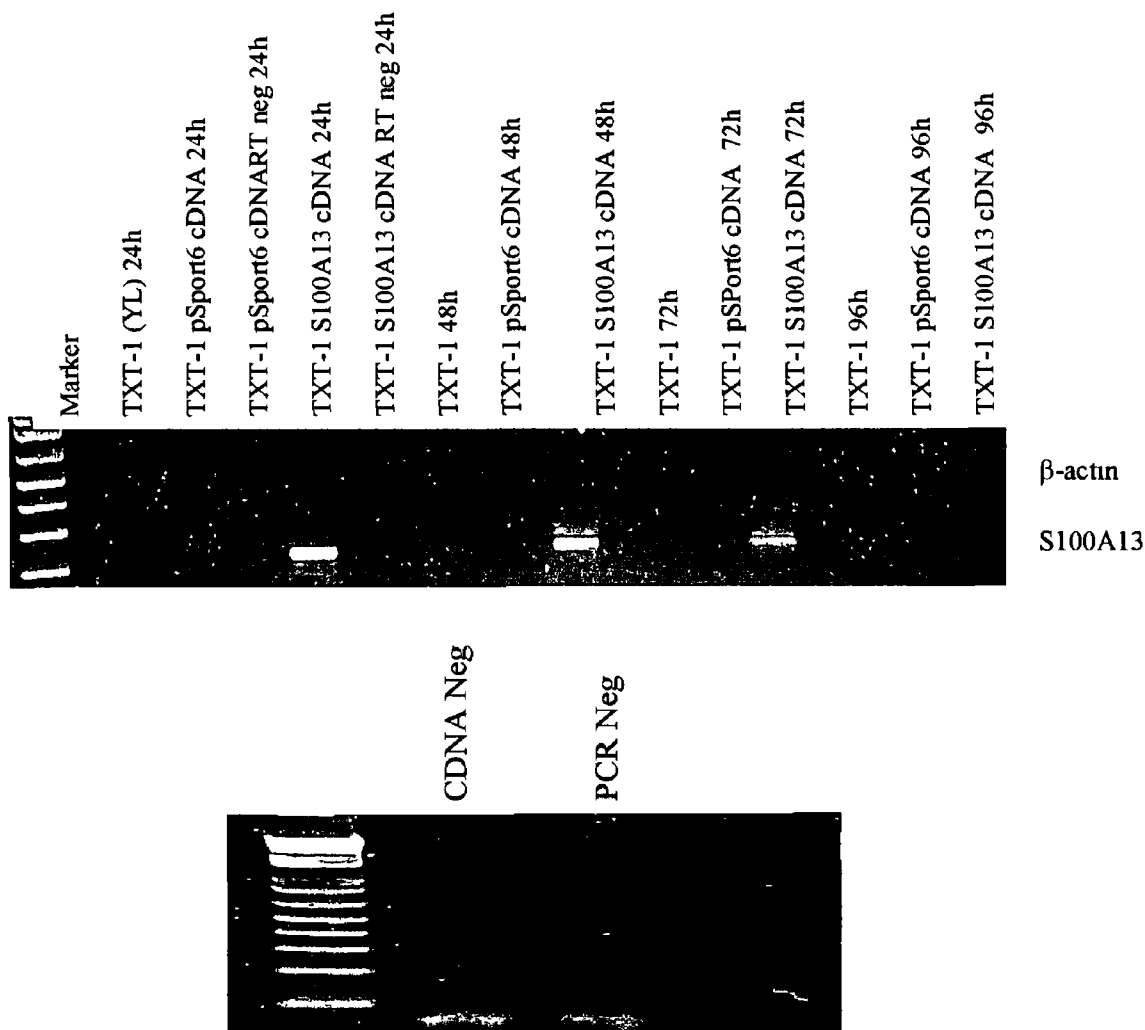


Figure 3.9 3 DNase I digestion of all samples from the S100A13 cDNA transient transfection

S100A13 cDNA was transiently transfected into TXT-1 RNA for the analysis of S100A13 mRNA was harvested at 24, 48, 72 and 96h 2µg of pSport6 empty vector and S100A13 cDNA transfected RNA samples were subject to Qiagen RNase free DNase I digestion using 2U RNase free DNase I per µg RNA at 37⁰C for 30mins PCR analysis revealed that cDNA carryover in the RT reaction was eliminated following this procedure since RT negative controls showed no bands specific to S100A13 However, while a strong band was obtained for the S100A13 transfected samples at 24, 48, 72 and 96h samples, no other band for S100A13 or β-actin was obtained

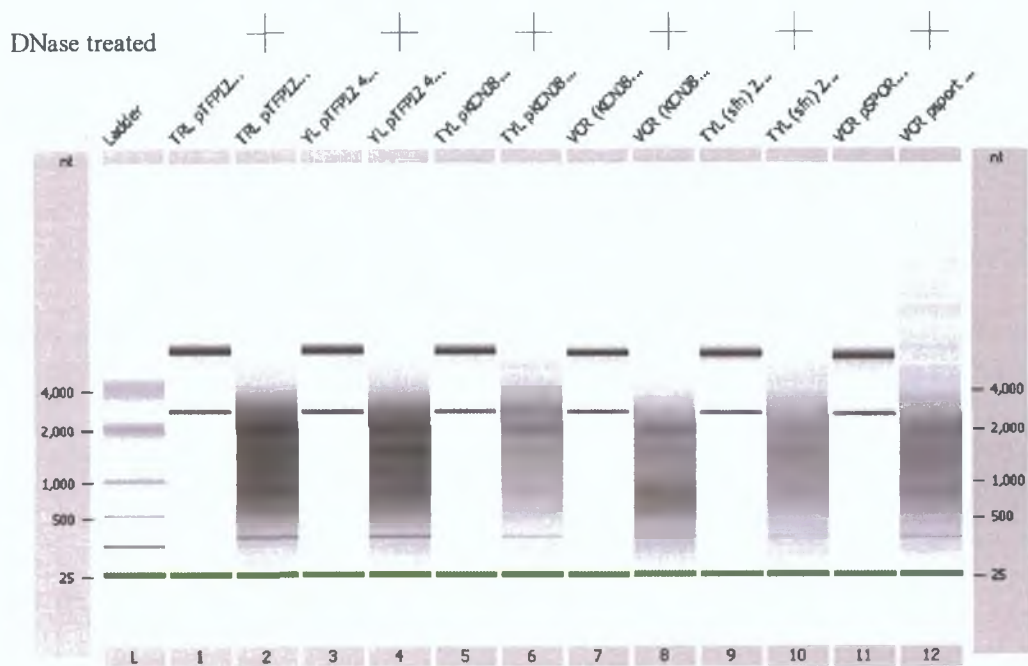


Figure 3.9.4 Analysis of RNA pre- and post- DNase I digestion using the Agilent Bioanalyser.

2 μ g of various cDNA transfected RNA samples were subject to Qiagen RNase free DNase I digestion using 2U RNase free DNase I per μ g RNA at 37 $^{\circ}$ C for 30mins. A sample of this RNA was also used for the analysis of RNA integrity pre-DNase I digestion. The Bioanalyser analysis of the RNA pre- and post- DNase I digestion revealed that RNA was degraded post digestion in all samples irrespective of the cDNA used in the transfection. This explains why RT-PCR analysis post DNase I digestion was unsuccessful.

Section 4.0: Discussion

The work described in this thesis was undertaken to increase our understanding of the molecular nature of invasion in human lung cancer cell lines using the following approaches

- 1 The gene-expression profiles of five human lung cancer cell lines with different invasive capacities (as determined by an *in vitro* invasion assay) were analysed using expression microarray methodology. Two invasive, parental DLKP cell lines (DLKP-1 and DLKP-2) were used along with an invasive Taxotere (TXT) resistant DLKP variant (TXT-2) and a poorly invasive TXT selected DLKP cell line that had lost its resistance to TXT (TXT-1). A Vincristine (VCR) resistant DLKP cell line that was less or non-invasive was included in the analysis. This provided us with a cell model to study *in vitro* invasion.
- 2 Bioinformatic analysis was performed on the raw microarray data that generated lists containing genes that potentially serve as a transcriptional signature for invasiveness in these cell lines.
- 3 An RT-PCR validation study was employed to confirm that the array results were a true reflection of gene expression in the cell lines studied.
- 4 The invasive abilities of each of the cell lines studied were validated by an *in vitro* invasion analysis of the cell lines over ten passages and using different invasion assay kit lot numbers. To further validate the invasion assay results RT-PCR was used to confirm that there was consistent differential gene expression between the invasive and non-invasive cell lines for the test genes over those ten passages.
- 5 siRNA technology was utilised to investigate the functional role of chosen genes from the microarray analysis.
- 6 cDNA transient transfection was also employed to investigate the functional role of the microarray gene targets in the invasive phenotype.

These results are discussed here in the context of previously published reports

4.1 Microarray analysis of DLKP and its invasive and chemotherapeutic resistant variants

A major obstacle in the use of chemotherapy for cancer treatment is the development of resistance. Consequently, a better understanding of the mechanisms of drug resistance would help to overcome this obstacle. Intrinsic and acquired drug resistance are believed to cause treatment failure in over 90% of patients with metastatic cancer (Longley & Johnston, 2005). Some tumours are initially sensitive to an anticancer agent and, over time, develop a resistance to it and this is referred to as acquired resistance. Whereas, other tumours are resistant before treatment and this is known as intrinsic resistance. One of the major factors leading to drug resistance is decreased drug accumulation. This is caused by decreased drug influx or enhanced drug efflux, both of which result in the chemotherapeutic agent not exerting its effect on the tumour. Drug resistance can also be caused by modified drug activation, drug inactivation, alterations in DNA repair mechanisms and altered response to apoptosis. Treatment with one agent can often lead to associated resistance to a number of unrelated agents. The development of resistance to a variety of unrelated chemotherapeutic drugs is called multiple drug resistance (MDR). MDR is caused by a variety of changes in the cancer cells and is almost always multifactorial.

Metastasis is the spread of cancer from a primary tumour to distant sites in the body. A distinguishing feature of malignant cells is their capacity to invade surrounding normal tissues and metastasise through the blood and lymphatic systems to distant organs. This process of metastasis is the most devastating aspect of cancer. Current therapies fail to eradicate metastasis for three major reasons. Firstly, when initially diagnosed, most tumours are well advanced and metastasis has already occurred. Secondly, specific organ environment can modify the response of a metastatic tumour cell to systemic therapy and alter the efficiency of anticancer agents. The third reason and the greatest obstacle to the success of therapy, is the heterogeneous composition of tumours, where highly metastatic cells can escape from the effect of therapeutic agents. Invading tumour cells appear to have lost the control mechanisms that which prevents normal cells from invading neighbouring tissue at inappropriate times and places. Thus, the fundamental difference between normal and malignant cells is

regulation. The difference must lie in the proteins that start, stop or maintain the invasion programme at times and places that are inappropriate for non-malignant cells. A major goal is to understand what signals and signal transduction pathways are perpetually activated or deregulated in malignant invasion (Kohn and Liotta, 1997)

Multidrug resistant (MDR) cells can survive chemotherapy and migrate to distant sites in the body, highly metastatic cells can evade the chemotherapeutic effect altogether. Cillo *et al*, (1987) demonstrated that some invasive/metastatic cells develop drug resistance more readily than their non-invasive counterparts. In 1994, Lucke-Huhle also found that some chemotherapeutic drug resistant cell lines were more invasive relative to non-resistant cells. Previously, studies of drug resistance and invasion proceeded along separate research pathways, however a better understanding of the relationship between chemotherapeutic drug resistance and invasion in cancer could lead to a more effective treatment for the disease (Liang *et al*, 2002)

Array technology can help answer increasingly complex questions and allow for more intricate experiments to be performed. It can be used, to infer probable functions of new genes based on similarities in expression patterns with those of known genes, to aid understanding of how genes coordinate and inter-relate, and to speed the identification of genes involved in the development of various diseases. Expression arrays can also aid the examination of the integration of gene expression and function at the cellular level, revealing how multiple gene products work together to produce physical and chemical responses to both static and changing cellular needs.

In a study by Ramaswamy *et al*, (2003) microarrays were utilised to identify a gene signature that would differentiate between various primary and metastatic adenocarcinomas. This group reported a metastasis-associated gene signature that contained eight up regulated and nine down-regulated genes. None of these acted as individual metastasis markers in their own right, rather the signature as a whole was of value in predicting metastatic spread in patients with primary tumours. The predictive value of this signature suggests that the clinical behaviour of solid tumours is, at the very least, partly determined by the intrinsic biological behaviour of the tumour cells and not simply by sensitivity to cancer therapies. Many different tumour types shared the metastatic signature identified in the study, which suggests the possibility that therapeutic targets could be developed that may be useful in different cancer types.

A study to identify genes involved in chemo-resistance in gastric cancers was conducted by Suganuma *et al* (2003) This group compared gene expression and drug resistance patterns in gastric cancer surgical specimen and, although they identified several resistance related candidate genes, they concluded that the mechanisms of resistance to chemotherapeutic agent are very complex In 2005, Rickardson *et al* compared the gene expression patterns of ten human tumour cell lines, including parental cells and resistant subtypes using cDNA microarray technology The resistant cells were selected for resistance to the cytotoxic effects of doxorubicin, temposide, melphalan and vincristine The drug activity of 66 cancer agents was determined in the cell lines and facilitated the calculation and ranking of correlations between drug activity and gene expression The group found that a number of apoptosis related genes including mitogen-activated protein kinase I (MAPK1) and focal adhesion kinase (FAK) were associated with drug resistance, while signal transducer of activator of transcription 5A (STAT 5A) was associated with general drug sensitivity

Orian-Rousseau *et al* , (2005) used suppression subtractive hybridisation to identify genes differentially expressed between the metastatic human colon cancer cell line HT29p and its non-metastatic counterpart HT29-MTX This led to the identification of fifty-eight genes with increased expression in the invasive cell line compared with the non-invasive line The majority of those genes had not been previously linked to the metastatic process While the study of clinical tumour samples using array methodology is useful to elucidate the mechanisms involved in tumour development, they can also generate data that is difficult to interpret This may be due to the complex nature of and the environmental impact on the samples for example, the age of the patient, smoker or non-smoker, effect of poor diet and so on The advantage of studying cancer progression using cell line models is that the samples can be cultured and processed using the same conditions, thereby eliminating any additional environmental impact on their gene expression, with the result that the transcriptional profile should reflect cancer development only

Therapeutic treatment of metastatic disease will need the development of biology-based approaches that will utilise the novel information on the molecular biology underlying metastasis to identify molecular targets that can interfere with expression

and thereby function (Brodt *et al*, 2000) Comparing the gene expression profiles of five lung cancer cell lines with different *in vitro* invasive abilities using DNA array methodology was the strategy employed to achieve this goal Two invasive parental DLKP cell lines (DLKP-1 and DLKP-2), an invasive Taxotere (TXT) resistant DLKP variant (TXT-2), a poorly invasive TXT selected DLKP cell line that had lost it's resistance to TXT (TXT-1) and a mildly invasive vincristine selected DLKP cell line (VCR) were used as a lung cancer cell model in this study The aim of this expression array analysis was to identify genes involved in the development of an invasive phenotype in lung cancer cell lines These cell lines with different invasive capacities (but from the same origin) offered a unique opportunity to study the less-well characterised mechanisms of invasion An important point to remember when considering this analysis is that there are potentially two ways to approach this data in that one could look at drug resistance and invasion In this study, the main focus was to analyse differences between the invasive and poorly invasive cell lines Theoretically however, any differentially expressed genes identified by the microarray analysis could relate to drug resistance and invasion

4.1.1 Genomatix analysis

The Genomatix analysis used in this study generated (Section 3.1.3) two promoter models each containing 5 elements involving three genes, VEGF, FSTL1 and FN1 (Figures 3.1.9 and 3.1.10). Genomatix would suggest that genes with the same promoter models are potentially co-regulated. To determine if these genes were in fact co-regulated, RT-PCR analysis was used to investigate VEGF, FSTL1 and FN1 mRNA expression in our DLKP cell model (Appendices). The RT-PCR results did not demonstrate differential expression of these genes with invasion thus were not subject to further investigation.

Although the promoter models in Figures 3.1.9 and 3.1.10 generated from Genomatix analysis did not identify co-regulated genes as suggested by RT-PCR results, a second vincristine-related analysis demonstrated the potential power of the software as a tool for data analysis. This work is not presented in the Results section as it is not focused on invasion but it does demonstrate the potential of this analytical approach. In this case the array data was mined to generate a vincristine related genelist by comparing the expression of DLKP-1, DLKP-2, TXT-1 and TXT-2 with VCR in the GeneSpring software. This generated a list of genes that theoretically related to vincristine resistance/treatment only.

The vincristine-related gene list divided was into the various Gene Ontology (GO) categories and weightings were assigned by the BiblioSphere software according to the over-, under-representation of genes in a given category (z-score) compared to what would be expected randomly. This gave some indication of the pathways, processes, cellular functions, etc being affected in VCR resistant cells. One category, Structural Molecule Activity received a high z-score and this group of genes was chosen for more detailed analysis.

The promoter sequences upstream of the genes were extracted from the El Dorado database hosted by Genomatix and analysed for the presence of common transcription factor (TF) binding sites. Potential promoter modules (two or more TF binding sites with defined spatial relationships) common to several of the input promoter sequences

were generated. Two of these modules were found to contain three common TF binding sites. As a measure of the specificity of the models and to identify other genes potentially regulated by these promoter modules, the entire human genome was searched for all occurrences of the models. One model was detected in the promoter sequences of several hundred other genes. These genes were grouped according to GO as before and the category with the highest z-score (>10) turned out to be genes associated with Sensory Perception of Taste or Smell. Though this did not initially appear to be of any significance, further investigation revealed that loss of sense of taste and smell is a well-documented physiological side effect experienced by patients undergoing a vincristine treatment regimen. As a further piece of corroborating evidence, the structural proteins identified in this analysis and in the microarray analysis are normally expressed in a tissue-specific manner - this usually indicates a co-regulatory mechanism. In particular, it was interesting to note that a subgroup is expressed in the olfactory bulb of the brain, a region involved in smell/taste perception. These findings provide multiple independent lines of evidence to support the probability of having identified a biologically relevant promoter module in this system.

4.2 Confirmation of array results by RT-PCR

Microarray data is quite accurate in terms of quantifying changes in mRNA abundance, however we felt it was important to confirm the trends observed, in a small panel of target genes, by an alternative quantification method. To this end a panel of genes were selected for RT-PCR analysis to validate the differential expression identified by array analysis by RT-PCR. This gave greater confidence in the significance of gene lists generated from array data mining and also functioned as a validation step before particular target genes were chosen for further investigation.

Twenty-eight genes were selected, based on information in the literature and on intuitive functions for a given gene, for RT-PCR analysis across the five DLKP cell lines. Tables 3.2.1 and 3.2.2, list the genes subject to RT-PCR analysis in the five cell lines comprising our cell model and give a summary of the PCR results. The actual gels representing each PCR are available for examination in the Appendices.

The ideal situation would be for the PCR results to reflect the array data for each gene both exactly and consistently. However, this was not always the case. For many genes, e.g. AKAP11 and NRG1 there were no significant expression differences across the panel of cell lines. It was less clear-cut for other genes e.g. TFPI-2 (Section 3.8.2). In this case the RT-PCR results, using various RNA samples as templates, did not always tally. The limitation of semi-quantitative RT-PCR must be considered here. Thirty and in some cases 35 cycles were used in the RT-PCR analysis so it is possible that the linear phase of target amplification was passed by the end of the last cycle. In this 'plateau' phase subtle differences become compressed - reflected in the intensities of the bands when analysed by gel electrophoresis and ethidium bromide staining.

The confirmatory RT-PCR analysis for IGF-1R (Section 3.4.2) correlated more closely with the array data, which demonstrated that IGF-1R expression was increased in the more invasive cell lines compared with the mildly invasive cell lines.

Subtle changes at mRNA level are more accurately detected by quantitative real time PCR (qPCR) This advantage of this technology was apparent when one compared the results of the siRNA timecourse experiments by RT-PCR and qPCR In this case RT-PCR gels displayed bands with little variation in target intensity, however knockdown was measured more sensitively and was more apparent in the qPCR results Thus gene expression should be measured using qPCR where possible Where more than one RT-PCR result for the various RNA samples matched the array data trend it was considered for future analysis as a target

4.3 Validation of invasion status of the DLKP cell lines used in this study

In order to establish defined conditions for the study of invasion using the DLKP cell model, fresh cell line stocks were thawed and analysed by *in vitro* invasion assays with increasing passage number to determine if cell characteristics were changing over time (Section 3.3.1). Commercial invasion assay kits were used throughout this study. In order to verify that that batch-to-batch variation was negligible between the commercial kits, cells with the same passage number and from the same cell suspension were applied to two different kits with different batch and lot numbers (Figure 3.3.1.2). The degrees of invasion for each of the DLKP variants were consistent between invasion assay kit batches.

The relative invasiveness of the sub-lines compared to each other remained constant over ten passages and this was the time frame used for all invasion analysis. This confirmed that the panel of DLKP cell lines described in this thesis represent robust, valuable models for the study of mechanisms of *in vitro* invasion.

Also, the invasion assay itself was optimised and performed using defined culture conditions. The inserts were placed in medium containing 5% serum. Cell suspensions were prepared in medium containing 1% serum and 100µl of a 1×10^6 cells/ml suspension was added to each insert. This provided serum gradient in the assay. The cells were incubated at 37°C for 24 hours. After this time, the underside of the insert stained with crystal violet and allowed to air dry. The definition of these assay protocols and culture boundaries gave confidence in the phenotypic changes observed following the deliberate manipulations of target molecules. The overall trend for the DLKP cell lines is as follows, starting from the most to least invasive, TXT-2 > DLKP-1 > DLKP-2 > TXT-1 > VCR.

The invasion assay validation studies also demonstrate that DLKP remains invasive over ten passages, which was the window in which subsequent studies involving selected array targets were performed.

To confirm that the differential invasive capacities of DLKP were matched with differential gene expression correlating with invasion, twelve genes that were differentially expressed in the invasive and less invasive cell lines were picked for analysis by RT-PCR. These included genes with a known role in invasion such as ICAM1, IGF-1R, EFNB2, VEGF-C, FN1, MMP3 and TFPI2. Genes whose expression pattern correlated with invasion status but that had unreported roles in invasion, including KCNJ8 and FSTL1, were also analysed. The SFN gene that has been both positively and negatively correlated with an invasive phenotype previously (Umbricht *et al* , 2001, Ide *et al* , 2004) was also investigated along with the transcription factors TCF4 and TLX1. The genes tabulated in 3.3.1 are those whose mRNA expression across the five DLKP cell lines correlated with invasion assay results with increasing passage number. EFNB2 was the only exception and was not selected for further study in any case. These results indicated reproducible correlation with the invasion assay results from the cell line validation study and highlight repeatable results over ten passages for the cell lines. They also confirmed the suitability of the cell lines, in conjunction with the optimised invasion assay, as a model system suitable for use in subsequent investigations into the molecular mechanisms of invasion.

4.4 Selection of Target genes for functional analysis

The results and discussion to this point demonstrate that the microarray comparison of the DLKP cell line variants is a suitable approach for the identification of genes involved in invasion. However, the challenge was that there are thousands of genes differentially expressed between the cell lines. It was only feasible to work with a small number of genes at a given time. The stringent filtering criteria used to narrow down gene lists to a manageable number inevitably meant discarding of potentially interesting genes.

Based on the compiled gene lists, and taking into account the results from the RT-PCR validation study, in addition to an extensive literature search, five genes were selected for further functional investigation in the context of our invasion model. These were, IGF-1R, KCNJ8, S100A13, SFN and TFPI2. Little is known about KCNJ8 and S100A13, particularly in relation to cancer and the development of an invasive phenotype. It was decided to investigate IGF-1R, KCNJ8, S100A13, SFN and TFPI2 as initial, high priority targets - which were considered a manageable number of experiments in the laboratory.

4 4 1 Experimental design for functional analysis of array targets

To study the individual role of IGF-1R, KCNJ8, S100A13, SFN and TFPI-2 in invasion in our cell model the following experimental plan was designed and is summarised in the table below

Table 4 1 1 Summary of experimental design to determine functional effect of array target genes in invasion in our cell model

Gene	IGF-1R	KCNJ8	TFPI2	S100A13	SFN
Cell lines used for siRNA transfection	DLKP-1 DLKP-2 TXT-1 TXT-2 VCR	DLKP-1 DLKP-2 TXT-2	TXT-1 VCR	DLKP-1 DLKP-2 TXT-2	DLKP-1 DLKP-2 TXT-2
Cell lines used for cDNA transfection	Sequence unavailable	TXT-1 VCR	DLKP-1 DLKP-2 TXT-2	TXT-1 VCR	TXT-1 VCR
PCR confirmation of increased/decreased expression	Y, by qRT-PCR	Y, RT-PCR & qRT-PCR for siRNA analysis	Y, RT-PCR & qRT-PCR	Y, RT-PCR & qRT-PCR for siRNA analysis	Y, RT-PCR & qRT-PCR for siRNA analysis
Confirmation by western	Yes	Western for over-expression study	Western for over-expression study	Western for over-expression study	Western for over-expression study

The functional effect of the above manipulations of target genes on invasion are summarised in the table below (4 1 2)

Table 4 1 2 Summary of functional effect of manipulation of array target genes on invasion, as determined by *in vitro* invasion assay, in our cell model

Gene	IGF-1R	KCNJ8	TFPI2	S100A13	SFN
Effect of siRNA transfection on Invasion (72hr)	Invasion was decreased in IGF-1R siRNA transfected cell lines (P<0 001)	Contrary to expectation, KCNJ8 knockdown increased invasion compared to controls* (P<0 001)	No effect of TFPI2 knockdown on non-invasive cell lines	S100A13 knockdown decreased invasion in all cell lines (P<0 001)	SFN knockdown increased invasion compared to controls* (P<0 001)
Effect of cDNA transfection on Invasion (72hr)		No effect on invasion was observed	Invasion was decreased compared to controls (P<0 001)	No effect on invasion was observed	No effect on invasion was observed

- *siRNA controls Non-treated cells and scrambled siRNA transfected cells
- *cDNA controls Non-treated cells and pSport6 empty vector transfected cells
- *Invasion assay controls RPMI-Mel and RPMI parent

4.5 Insulin-like growth factor-1 receptor (IGF-1R)

The IGF-1R is a receptor tyrosine kinase (RTK) that plays a critical role in signalling cell survival, regulation of the cell cycle, transformation, proliferation, motility and invasion. This heterotetrameric receptor is comprised of two 130-135kDa α - and two 90-95kDa β -chains, linked with many homo- and hetero-disulfide bridges. IGF-1R ligands include IGF-1, IGF-2 and insulin, but the receptor binds to IGF-1 with the highest affinity (Brodt *et al*, 2000). Regulation of IGF-1R gene expression is closely associated with the function of a variety of tumour suppressor genes and oncogenes.

IGF-1R was identified as a gene potentially involved in invasion in this microarray study. The data indicated that IGF-1R expression was increased in the more invasive cell lines compared with the mildly invasive cell lines. The aims of the experiments, the results of which are detailed in section 3.4, were as follows:

- 1 To confirm by PCR that IGF-1R is differentially expressed between the DLKP cell lines
- 2 To quantify endogenous IGF-1R levels in the cell model by qRT-PCR and western blot
- 3 To knockdown IGF-1R expression by transfecting a validated gene specific siRNA using optimised transfection conditions
- 4 To measure transfection efficiency of the siRNA using immunofluorescence
- 5 To demonstrate IGF-1R-specific siRNA knockdown at mRNA and protein level
- 6 To evaluate the effect of decreased IGF-1R knockdown on proliferation
- 7 To evaluate the effect of decreased IGF-1R knockdown on invasion
- 8 To compare the effect of treatment using an IGF-1R blocking antibody α IR3 on invasion, with the effect of IGF-1R siRNA knockdown on invasion

4.5.1 Endogenous IGF-1R expression in the DLKP variants

The array profile indicated that IGF-1R expression was increased in the more invasive cell lines than the lesser invasive cell lines. This agrees with a study by Jiang *et al*, (2004) who reported that strong IGF-1R expression in primary tumours correlated with an increased incidence of metastasis. The array data was confirmed using RT-PCR, qRT-PCR and western blot to investigate endogenous IGF-1R levels in the five DLKP variant cell lines (Sections 3.4.2 and 3.4.3). The RT-PCR validation of the array data did serve to demonstrate the predicted differential IGF-1R mRNA expression between the DLKP variants (Figures 3.4.2.1 and 3.4.2.2). However, there were incidences where the PCR trend differed slightly from the array prediction (Figure 3.4.2.3) and is most likely due to the semi-quantitative nature of the RT-PCR analysis, but in any case the least invasive cell line VCR consistently displayed lowest mRNA levels. qPCR provided a more accurate measure of IGF-1R mRNA expression.

Endogenous IGF-1R mRNA expression across the DLKP cell model was determined by qRT-PCR using a commercial TaqMan IGF-1R probe and normalised using β -actin (Figure 3.4.3.1). Expression levels were compared relative to DLKP-1, which was set to 1 for the analysis. This result, for the most part, correlates with the array results and demonstrated differential IGF-1R expression, with higher expression associated with the invasive cell lines, DLKP-2 and TXT-2 and lower expression in the mildly invasive cell line VCR. DLKP-1 and TXT-1, unexpectedly, have similar IGF-1R mRNA levels despite DLKP-1 being more invasive than TXT-1. There was no detectable IGF-1R mRNA in the VCR cell line.

Endogenous IGF-1R protein expression was determined by western blot (figure 3.4.3.2). α -tubulin and GAPDH antibodies were used to demonstrate even loading between the samples. This result correlated with the qPCR results, and demonstrated differential IGF-1R expression, with higher expression in the invasive cell lines, DLKP-2 and TXT-2 and lower expression in the poorly invasive cell line VCR. DLKP-1 and TXT-1, unexpectedly, have similar IGF-1R protein levels despite DLKP-1 being more invasive than TXT-1. To address this, one could speculate that although the IGF-1R may be present in both cell lines, that differences in the signalling

pathways activated may be responsible for either the presence or absence of invasive ability. This has previously been shown by Zhang *et al.* (2004) where MMP-2 (crucial in invasion) synthesis was regulated via PI 3-kinase/Akt/mTOR while the Raf/ERK pathway resulted in negative regulatory signals. Indeed the sub-cellular location and phosphorylation status of the IGF-1R can also impact on receptor function (Dupont and Le Roith, 2001), and the measurement of IGF-1R expression levels in these cell lines may not give the complete picture. A further point for discussion is the absence of detectable IGF-1R mRNA or protein in the VCR cell line, despite the parental cell line expressing the protein endogenously. This suggests that treatment of DLKP with Vincristine decreases endogenous IGF-1R expression or that cells that do not express IGF-1R are being selected by the treatment. This may have potential effects on cell motility, for example. It would be interesting to re-pulse a parental DLKP cell line with Vincristine and try to identify the point/points at which the drug affects IGF-1R levels and by which mechanism this occurs.

4.5.2 siRNA Transfection Optimisation for the DLKP variants

There were a number of different parameters that had to be determined to establish an optimised protocol for the siRNA transfection of DLKP and its variants. Initially, only the transfection protocol itself was considered. 2µl of NeoFx transfection reagent per well of a 6-well plate was used to transfect 30nM of target siRNA into the cells. The siRNA used for IGF-1R targeting was a commercial validated sequence from Ambion, which they guarantee to decrease IGF-1R expression. This was important since Bohula *et al.*, (2003) demonstrated that the efficiency of siRNA's to IGF-1R is influenced by secondary structure in the IGF-1R transcript, where poor IGF-1R knockdown was associated with poor accessibility of the siRNA to the IGF-1R transcript.

A protocol was also optimised for the analysis of a target siRNA specific effect on invasion. The invasion assays were initially performed 48h post-siRNA transfection (Figure 3.4.4.1). Non treated and scrambled siRNA transfected cell lines were the controls for these experiments. While a specific decrease in invasion can be attributed to the IGF-1R siRNA for DLKP-1, there was no related decrease in invasion in the

other four samples. Also, there was a considerable non-specific effect on invasion in the scrambled siRNA treated cells compared with the non-treated cells. One assumed that this was due to the transfection process and not the scrambled siRNA, since the scrambled siRNA was one of only three sequences that Ambion sells as a transfection control as they do not target any RNA sequence.

It was decided that allowing the cells to recover from the transfection for as long as possible before invasion analysis, could minimise the non-specific transfection effect on invasion. To this end invasion assays were performed 48 and 72 hours post-transfection on the invasive cell line TXT-2 and the mildly invasive TXT-1 (figure 3.4.4.2). Non treated and scrambled siRNA transfected cell lines were again included as the controls for this experiment. These results suggested that performing the invasion assay 72 hours post siRNA transfection allows more recovery time for the cells and decreases the non-specific transfection effect on invasion. It was not surprising that that exposure to NeoFx or a similar transfection reagent affects a mechanism such as invasion, given the impact on membrane integrity. The longer recovery time possibly facilitates the repair or renewal of damage caused by the transfection reagent. 72h post transfection was the time point at which further invasion analysis of siRNA transfected samples were performed. This data also suggests that the invasive capacity both the cell lines are decreased at 72h compared with the 48h analysis. The cells were more confluent at 72h with decreased nutrients in the medium, which may have decreased the capacity to invade.

siRNA transfection efficiency was evaluated using immunofluorescence and confocal microscopy (Figure 3.4.4.3 and 3.4.4.4). These immunofluorescence results demonstrate siRNA transfection efficiencies of 90%. The kinesin experiment (Figure 3.4.4.4) also provides a visual measure of excellent transfection efficiency.

4 5 3 Evaluation of IGF-1R siRNA targeting on mRNA and protein levels

RNA and protein were harvested 48 and 72h post-siRNA transfection respectively and used to determine an IGF-1R siRNA mediated decrease in mRNA and protein levels (Figures 3 4 4 5 and 3 4 4 6) Figure 3 4 4 5 illustrates an IGF-1R siRNA specific decrease in mRNA for samples at 48h, albeit a slight decrease. There is a noticeable increase in IGF-1R mRNA expression in the scrambled siRNA transfected DLKP-1, DLKP-2 and TXT-1 samples. This is surprising, as the scrambled siRNA sequences are not reported to affect target expression. However an explanation for this anomaly may be attributed to noise in the data i.e. that increases of one or two relative quantities when mRNA levels are low, impact on this data, whereas increases of one or two relative quantities would not impact on the data to such a great extent if the mRNA relative quantities were higher.

Figure 3 4 4 6 demonstrates that IGF-1R protein expression was almost completely silenced in siRNA transfected cells compared with scrambled and non-treated samples. This would indicate that the siRNA may be acting like a microRNA (miRNA) by not destroying mRNA but preventing its translation.

In the case of IGF-1R, endogenous protein levels were measurable by western blotting thus the decrease in protein expression in response to siRNA transfection was clear by western blotting. However, endogenous KCNJ8, S100A13, SFN and TFPI2 protein levels were below the detection limits of western blot. Consequently, the effect of siRNA transfection on protein levels could not be demonstrated. It may help immunoprecipitate the protein under investigation before western blot analysis to help visualise conclusively any potential decrease in protein expression in response to siRNA transfection.

4 5.4 Evaluation of IGF-1R siRNA targeting on proliferation

Many studies have reported that decreasing endogenous IGF-1R decreases cell/tumour growth. Galvan *et al*, (2003) state that IGF-1R binds to its ligand (IGF-1) and activates phosphoinositide 3-kinase (PI3K). This promotes cell proliferation by activating the MAPK cascade and simultaneously prevents apoptosis by inducing the

phosphorylation and inhibition of proapoptotic proteins such as BAD Remmuth *et al* , (2002) put forward a similar scenario Here, KM12L4 human colon cancer cells were transfected with a truncated dominant negative form of IGF-1R The transfected cells showed decreased growth and increased apoptosis and had decreased expression of VEGF at both the mRNA and protein levels Grzmil *et al* , (2004) report that using an antisense IGF-1R sequence in human PC-3 prostate cancer cells also decreased proliferation and increased spontaneous apoptosis by up to 17-fold Sekharam *et al* , (2003) transfected the human colon cancer cell line HCT116 with an expression plasmid containing the full length IGF-1R protein sequence Growth curve analysis in this study revealed a two-fold increase in proliferation in the IGF-1R transfected cells compared with the parental cells Resistance to serum deprivation induced apoptosis was also observed in the IGF-1R transfected cells

To study the effect of IGF-1R siRNA targeting on the DLKP variants, cells were seeded at both low (2.5×10^3 cells/well) and high (5×10^3 cells/well) densities in a 96-well plate format (Figures 3 4 4 7 and 3 4 4 8) Proliferation was measured using the acid phosphatase assay and an IGF-1R siRNA specific effect on cell proliferation was assessed by comparing with scrambled siRNA and non-treated cells An siRNA sequence to Kinesin was transfected as a positive control and acted by preventing cell doubling thus kinesin siRNA transfected cells did not increase in number compared with the non-treated, scrambled siRNA- and IGF-1R siRNA- transfected cells This is also visually demonstrated in Figure 3 4 4 4 Surprisingly, IGF-1R siRNA treatment did not appear to affect proliferation compared with the scrambled siRNA and non-treated cells

The IGF-1R siRNA treated DLKP variants, exhibited no decrease in proliferation Indeed, this is a major difference between this and other studies on IGF-1R It is possible that the decreased IGF-1R expression was compensated for (as regards proliferation) by the presence of epidermal growth factor receptor (EGFR) Personal communications within our laboratories have confirmed EGFR expression in all of the DLKP cell lines In a review by Adams *et al* , (2004) an overview is given of the interrelationship between IGF-1R and EGFR This is in agreement with the idea that cross talk between the IGF-1R and EGFR can significantly effect intracellular signalling in that EGFR expression can maintain DLKP cell growth despite decreasing

IGF-1R expression These experiments were carried out in the presence of serum, which contains a variety of growth factors, which may have compensated for IGF-1R silencing and maintained proliferation

When IGF-1R is silenced the proliferation is unaffected possibly due to the presence of other growth factors in the medium An indication of the pathway involved could be determined by serum starving the DLKP variants and re-feeding with either serum containing medium and serum free medium supplemented with IGF-1 only Following stimulation, levels of the relevant signalling molecules i.e phospho-PI3K, phospho-AKT, phospho-ERK could be measured and differences in the signalling identified This would also be a useful study in cells with the IGF-1R silenced by siRNA, and would provide a mechanistic explanation for the data presented Similarly, the result where proliferation in serum is maintained despite IGF-1R signalling should be investigated by silencing the IGF-1R and then growing the cells in SFM only supplemented with IGF-1 If only IGF-1 is present in the medium then proliferation should be reduced when IGF-1R is silenced, as there would be no other growth factor to signal cell growth

4.5.5 Evaluation of IGF-1R knockdown on invasion

Many studies have demonstrated that IGF-1R expression modulates metastatic potency In 1998 Long *et al* , found that lung carcinoma cells transfected with cDNA overexpressing IGF-1R had enhanced ability to invade and colonise the liver In addition to blocking tumour growth, IGF-1R antisense treatment has also been shown to inhibit metastasis (Chernicky *et al* , 2000, Scotlandi *et al* , 2002) Tanno *et al* , (2001) demonstrated that constitutively activated Akt or Src-activated Akt increased IGF-1R gene expression, and rendered pancreatic cancer cells more invasive Sekharam *et al* , (2003) found that injecting colon cancer cells overexpressing IGF-1R into mice resulted in the formation of bigger tumours which metastasised to distant organs, compared to mice injected with parental colon cancer cells Grzmil *et al* , (2004) report that using an antisense IGF-1R sequence in human PC-3 prostate cancer cells also decreased PC-3 invasive capacity and MMP-2 expression Furthermore, Jiang *et al* , (2004) examined IGF-1R expression in human gastric cancer and found

strong correlation with increased tumour angiogenesis and lymph node metastasis IGF-1R was expressed more strongly at the metastatic site

Two independent methods were employed in this study to decrease IGF-1R expression and investigate this effect on invasion. These included an siRNA to IGF-1R and an IGF-1R blocking antibody, α IR3. Sections 3.4.6 and 3.4.7 demonstrate the effect of IGF-1R siRNA transfection on DLKP variant invasion. The invasion assays were performed 72 hours post-transfection. Untransfected- and scrambled siRNA transfected- cell lines were the controls for this experiment. RPMI-Mel and RPMI-2650 are included as positive and negative invasion assay controls respectively. Counts per insert were averaged and plotted as percentage invasion normalised to the scrambled siRNA for each cell line. The invasive capacities of non-treated samples were not included graphically and were photographed to demonstrate the non-specific effect on the cells due to the transfection process. It was more statistically relevant to compare control (scrambled) siRNA transfected cells with target siRNA transfected cells.

Invasion was decreased in IGF-1R siRNA transfected cells compared with the scrambled siRNA and non-treated cells (Figure 3.4.4.9). In transfection I (Figure 3.4.4.10) invasion was decreased in IGF-1R siRNA transfected DLKP-2 ($P < 0.001$), TXT-1 and TXT-2 ($P < 0.005$) compared with the scrambled siRNA control. VCR does not express endogenous IGF-1R and is also non-invasive, so one would not expect an IGF-1R siRNA related effect on invasion in this cell line and the data concurs with this. However, only a slight IGF-1R siRNA related decrease in invasion was observed for DLKP-1. This may be accounted for by reduced transfection efficiency in this cell line, since results for transfection II (Figures 3.4.4.11 and 3.4.4.12) saw a 60% reduction in DLKP-1 ($P < 0.001$) IGF-1R invasion compared with scrambled siRNA transfected cells. Invasion was decreased by ~50% in IGF-1R siRNA treated DLKP-2, TXT-1 and TXT-2 in this transfection ($P < 0.001$). These results correlate with the studies outlined above and demonstrate that decreasing IGF-1R expression in DLKP variants using an IGF-1R siRNA decreases their capacity to invade.

An IGF-1R blocking antibody, α IR3 (Calbiochem, UK) was also used to achieve decreased IGF-1R expression by neutralising the ~130 kDa α and the ~90 kDa β subunits of IGF-I receptor. The effect of this α IR3 treatment on *in vitro* invasion was examined (Figure 3.4.4.13). The cell lines were seeded for invasion analysis with or without the addition of 1000ng/ml α IR3 monoclonal antibody over 24 hours. Only the invasive cell lines DLKP-1, DLKP-2 and TXT-2 were included in this experiment, since TXT-1 is only mildly invasive and VCR does not detectably express IGF-1R protein. The results demonstrate that a reduction in invasion of 50% or greater was achieved in α IR3 treated cells ($P < 0.001$). It would have been interesting to evaluate the amount of IGF-1R being blocked by the antibody. This could have been achieved by taking a sample of α IR3 treated and non-treated cells and using protein G sepharose to pull down the IGF-1R and compare the treated versus non-treated IGF-1R amounts. The decrease in IGF-1R amounts could then be correlated with the effect on invasion. Furthermore, it would be beneficial to include a control antibody in this experiment, to demonstrate the α IR3-specific effect on the IGF-1R activity and effect on invasion. Overall, it appears that employing either an IGF-1R specific siRNA sequence or an antibody to block IGF-1R expression yield comparable decreases in DLKP variant invasion.

The results above indicate the suitability of IGF-1R as a target for cancer therapy in that cancer spread can be decreased and/or maintained at a certain level. IGF-1R is also a suitable target for therapy, since inhibition causes a clinical response in a high proportion of IGF-1R bearing tumours, decreasing the requirement for other defined biomarkers to monitor response to therapy. A further aspect of this study would be to examine the effect of decreasing IGF-1R expression on DLKP variant sensitivity to chemotherapeutic drugs. One would hope that combining IGF-1R siRNA with chemotherapeutic drug treatment would result in an additive or synergistic effect. Sakuntala Warshamana-Greene *et al*, (2005) found that inhibition of IGF-1R signalling using a kinase inhibitor, NVP-ADW742 enhanced the sensitivity of small cell lung cancer cell lines to etoposide and carboplatin, which correlated with inhibition of PI3K-Akt activation. Another group, Camirand *et al*, (2005) found that combining the EGFR targeting drug, gefitinib with the IGF-1R specific inhibitor,

AG1024 had an additive to synergistic effect on cell growth inhibition on a panel of breast cancer cell lines

Mitsiades *et al* , (2004) studied the transcriptional and proteomic profile of NVP-ADW742 treated cancer cells and identified the antiproliferative and proapoptotic sequence that is triggered in response to this treatment They also found that NVP-ADW742 monotherapy or its combination with cytotoxic chemotherapy had significant antitumour activity in a mouse xenograft multiple myeloma model, proving the success *in vivo* of the use of selective IGF-1R inhibitors in cancer therapy Goetsch *et al* , (2005) treated nude mice bearing MCF-7 cells or A549 cells with a humanised anti-IGF-1R antibody, h7C10 An almost complete inhibition of A459 tumour growth was observed in mice treated with h7C10 combined with the chemotherapeutic agent, vinorelbine or the anti-EGFR antibody, 225 This study also highlights the potential of IGF-1R targeting in cancer therapy either with a chemotherapeutic agent or inhibitors of other growth factor receptors such as EGFR Obviously carefully designed clinical trials will be required to monitor the effect of IGF-1R inhibition on host glucose metabolism to avoid the induction of type I and type II diabetes through inhibition of the related insulin receptor (Yee, 2006) To this end, Macaulay (2004) used an array based screen to identify accessible IGF-1R mRNA regions to subsequently design an siRNA that silence IGF-1R without affecting the insulin receptor The Ambion validated siRNA against IGF-1R is known to be specific The clinical efficacy of IGF-1R targeting will be determined by the role of the receptor in established tumours, the extent to which IGF-1R expression can be decreased *in vivo* and the extent to which other signalling pathways compensate for IGF-1R silencing Naturally this therapy will have the usual difficulties associated with gene therapy, namely targeting and efficient delivery of a therapeutic dose to the site of action

4.6 Inwardly rectifying potassium channel J8 (KCNJ8)

KCNJ8 is of particular interest as its role in cancer and invasion has not been previously reported in the literature. K^+ channels are a diverse class of ion channels in the cytoplasmic membrane. Ion channels are pores in the cell membrane that allow the passage of specific ions. They are opened and closed by changes in membrane potential, ligand binding, intracellular calcium concentration and membrane tension (Laniado *et al*, 2001). There is accumulating evidence that various K^+ channels in tumour cells play important roles in regulating tumour cell proliferation and apoptosis. There is also increasing interest in the potential implications of K^+ channels as pharmacological targets for cancer therapy and for use as biomarkers to aid diagnosis (Wang, 2004). The potassium channels termed “inward rectifiers” of which KCNJ8 is included, pass currents over a hyperpolarized voltage range. They have an important role in the maintenance of resting membrane potential in many cell types. The gating of some inward rectifiers (including KCNJ8) is tightly regulated by intracellular ATP levels, thereby providing a link between cellular metabolism and membrane potential.

4.6.1 KCNJ8 expression in DLKP variants

Inagaki *et al*, (1995) identified a K_{ATP} channel, uK_{ATP-1} (KCNJ8/Kir6.1), which represented a new subfamily of the inwardly rectifying K^+ channel family. KCNJ8 was identified as a gene potentially involved in invasion in this microarray study. KCNJ8 expression was increased in the more invasive cell lines compared to less invasive cell lines. A study of KCNJ8 mRNA expression by RT-PCR (Section 3.5.2) confirmed increased expression in the invasive cell lines DLKP-1, DLKP-2 and TXT-2 compared with the less invasive cell lines TXT-1 and VCR. Inagaki *et al*, (1995) suggested that KCNJ8 might be involved in regulating cell membrane potential. Our novel results indicate that KCNJ8 contributes to the invasive phenotypes of the variants in the DLKP cell model. It is possible that this is achieved by regulation of cell membrane potential by KCNJ8. Laniado *et al*, (2001) also examined whether the activity of K^+ channels were different between cells with different invasive capacities, by testing strongly metastatic PC-3 and weakly metastatic LNCaP human prostate cancer cell

lines The group reported larger voltage-gated K^+ current density in LNCaP than PC-3 cells They also discovered that the K^+ currents in a PC-3 sub-population were sensitive to calcium ion levels These results were reflective of the different metastatic capabilities of the two cell lines, with PC-3 cells appearing potentially “more excitable”

Aguilar-Bryan *et al* , (1998) and Erginel-Unaltuna *et al* , (1998) dismissed the notion that KCNJ8 was a K^+ channel in its own right but rather that it encoded a subunit that forms a K_{ATP} channel when coexpressed with sulfonylurea receptors (SURs) SURs are part of the ABC transporter superfamily, and have greatest similarity with multidrug resistance proteins (MDRs) and multidrug resistance-associated protein (MRP) This association of KCNJ8 with the MDR- and MRP-like SUR proteins indicate that KCNJ8 may be involved, not only in invasion but also in drug resistance in our cell model Jirsch *et al* , (1993) compared K^+ channels in NCI-H69 cells with NCI-H69 derived MRP-1 overexpressing H69AR cells K^+ channels were undetected in NCI-H69 cells, but were present in the MRP-1 overexpressing cells In a contrasting study, Sakai *et al* , (2002) showed that a SCLC cell line, which did not express MRP-1 or MDR-1 had large inwardly rectifying K^+ currents present The association of KCNJ8 with drug resistance in our cell model has yet to be investigated

4.6.2 Evaluation of functional effects of KCNJ8 in DLKP variants

To define the role of KCNJ8 in metastatic lung cancer, two independent commercial KCNJ8 specific siRNA sequences were transfected into the invasive cell lines DLKP-1, DLKP-2 and TXT-2 and the effect of this decrease in KCNJ8 expression on both proliferation and invasion was examined. Conversely, KCNJ8 cDNA was transiently transfected into the non-invasive cell lines TXT-1 and VCR. It was hoped that decreasing KCNJ8 expression would decrease the invasive potential of the invasive cell lines and that a corresponding increase in invasion would be observed in response to an increase in KCNJ8 expression in the non-invasive cell lines.

4.6.2.1 KCNJ8 siRNA transfection

A decrease in KCNJ8 expression in response to KCNJ8 siRNA transfection was confirmed by PCR analysis (Section 3.5.3.2). The increased sensitivity of qPCR over semi-quantitative PCR is apparent in that small changes in expression can be precisely monitored. For the initial siRNA transfection (Figures 3.5.3.1-3.5.3.4) qPCR at 24h post transfection and a semi quantitative RT-PCR study over 96 hours was used to analyse the siRNA effect on KCNJ8 mRNA expression. For the second KCNJ8 siRNA transfection qPCR was used to analyse the effect of siRNA transfection over 72 hours (Figures 3.5.3.5-3.5.3.7). A marginal decrease in KCNJ8 mRNA was achieved in response to transfection of the KCNJ8 siRNA sequences.

The timecourse analyses by RT-PCR yielded interesting results (Figures 3.5.3.2 to 3.5.3.4). Taking DLKP-1 as an example (Figure 3.5.3.2), it appears there is an increase in KCNJ8 mRNA expression in the KCNJ8 siRNA 1-treated samples, at 48hours. A decrease is again observed at 72 hours, with expression increasing at 96 hours. This fluctuation in KCNJ8 mRNA levels in response to KCNJ8 siRNA transfection over time is most apparent in the DLKP-1 cell line, but also occurs in DLKP-2 and TXT-2. However, this data is less informative than the more sensitive qPCR timecourse analyses.

In the qPCR timecourse analysis in Figures 3.5.3.5 to 3.5.3.7 KCNJ8 mRNA knockdown is not achieved at 48h particularly for the KCNJ8 siRNA 1 transfected cell

lines This may be due to decreased transfection efficiency for this siRNA sequence What is also interesting is the fluctuation in KCNJ8 mRNA expression levels in non-treated samples over the 72h timecourse In figure 3 5 3 2 and 3 5 3 4 KCNJ8 mRNA expression is increased at 72h compared to expression at 24 and 48h This may indicate that KCNJ8 expression is increased when the cells become confluent possibly due to nutrient depletion There is a dramatic increase in KCNJ8 expression in the scrambled transfected siRNA DLKP-1 and DLKP-2 cells at 72h This is difficult to explain, as there are not supposed to be target effects attributed to scrambled siRNA transfection, although this is a controversial topic The exact role of KCNJ8 in maintenance of cell physiology is not defined in our model system as yet, but it is obviously of importance Miki *et al* (2002) demonstrate the importance of KCNJ8 physiologically, since KCNJ8 null mice die prematurely due to myocardial ischemia

Binggeli and Weinstein (1986) proposed that altered signalling of plasma membrane electric potential of cancer cells can contribute to tumour growth Bianchi *et al* , (1998) showed that plasma membrane electric potential in tumour cells is often modulated by the activity of K⁺ channels Zhou *et al* , (2003) found that a high concentration of a potent K_{ATP} inhibitor, Glibenclamide inhibited hepatocarcinoma cell adhesion and proliferation The effect of siRNA targeting KCNJ8 on proliferation is demonstrated in Figure 3 5 4 1 Unlike the study by Zhou *et al* (2003) decreasing KCNJ8 expression had no effect on proliferation However, by using Glibenclamide Zhou may also have inhibited Kir6 2 as well as KCNJ8 (Kir6 1) To qualify the role of KCNJ8 in cell growth or apoptosis in these cell lines one could use the H-Thymidine incorporation and TUNEL assays respectively

Stringer *et al* , (2001) used Representational Difference Analysis (RDA) to identify genes whose expressions are aberrantly increased in invasive breast carcinoma compared with adjacent normal breast tissue from the same person The group identified GIRK1, an inwardly rectifying K⁺ channel, whose expression correlated with lymph node metastasis, where the increase in GIRK1 expression was greatest in tumours with more than one positive lymph node The group postulate the use of this channel as a biomarker for breast cancer if correlated with the expression of other biomarkers Our array data and RT-PCR validation of KCNJ8 mRNA levels across the cell line panel indicated that KCNJ8 expression was associated with the invasive

compared with the lesser invasive cell lines included in this study. One would expect then, that decreasing KCNJ8 expression using siRNA would decrease the invasive capacity of the invasive cell lines DLKP-1, DLKP-2 and TXT-2. Figures 3.5.5.1 to 3.5.5.3 demonstrate the effect of decreasing KCNJ8 expression on *in vitro* invasion. As observed in our IGF-1R work, a slight decrease in mRNA expression was reflected in a substantial phenotypic effect suggesting that the siRNA sequences might be acting like miRNAs by inhibiting translation. Surprisingly, a decrease in KCNJ8 mRNA expression generated a substantial increase in invasion. Invasion was increased by between 45% to over 100% in KCNJ8 siRNA treated cell lines compared with scrambled siRNA transfected cell lines ($P < 0.001$). It is possible that the decrease in KCNJ8 expression generated a “compensation” response, whereby the expression of other proteins was increased to cause an additional increase in the invasive phenotype of these cell lines. This is merely hypothesis though and would require further investigation.

Ion channels can mediate cell migration as well as invasion. Liu *et al*, (2004) treated murine melanoma B-16 cells with endothelin-1 (ET-1) to decrease potassium channel current amplitude, thereby decreasing B-16 cell migration. Another study by Schwab *et al*, (1999) demonstrated that migration of transformed renal epithelial cells is a K^+ channel-dependent process. The group looked at migration of NIH3T3 fibroblasts and human melanoma cells using time-lapse photography in the presence and absence of a specific K^+ channel blocker Charybdotoxin (CTX). The treatment affected migration of both cell types in a dose dependent manner. The group also investigated whether blocking potassium channel activity could modulate melanoma cell invasion. In contrast to our novel finding above that decreasing KCNJ8 increased invasion, decreasing potassium channel activity in the Schwab study did not modulate the invasive capacity of melanoma cells.

4 6 2 2 KCNJ8 cDNA transfection

In 2004 Lastraioli *et al* , reported that the K⁺ channels from the HERG family are involved in the establishment of an invasive phenotype in colorectal cells *in vitro* and *in vivo* . With this in mind, we decided to investigate whether KCNJ8 overexpression could induce an invasive phenotype in the mildly invasive cell lines TXT-1 and VCR by transiently transfecting the expression vector pSport6 containing the KCNJ8 cDNA sequence . An increase in invasion was observed in the KCNJ8 cDNA transfected TXT-1 cell line (P<0 001) . No effect on invasion was observed in KCNJ8 cDNA transfected VCR cells compared with the empty vector control cells (Figures 3 5 6 7 and 3 5 6 8) . This may potentially be attributed to poor transfection efficiency in this cell line . This result is inconclusive, as an increase in KCNJ8 protein expression was not confirmed by western blot, as the protocol is not yet fully optimised (Figures 3 5 6 4 and 3 5 6 5) . To overcome this difficulty one could use a HA tag to optimise the western blot for this protein . A further optimisation strategy could include the development of an in-house antibody to KCNJ8 to aid more sensitive KCNJ8 protein detection, although Yoshida *et al* , (2004) demonstrated the difficulties in developing a specific and sensitive antibody to this protein . One could also speculate that an increase in KCNJ8 expression alone is insufficient to induce invasion in the non-invasive cell lines, however this theory remains inconclusive without confirmation of protein increases in response to the exogenous transfection by western or immunofluorescence . These results suggest that it is the deregulated expression of KCNJ8 that modulates cell line invasive capacity .

4 6 3 Assigning a function for KCNJ8

This work suggests a previously unreported role for KCNJ8 in lung cancer cell invasion . In fact, no cancer related function has ever been attributed to KCNJ8 . These experiments do not suggest a function for KCNJ8 in the regulation of proliferation or apoptosis . A further aspect of this study would be to examine the effect of decreasing KCNJ8 expression on DLKP variant sensitivity to chemotherapeutic drugs, as there are lines of evidence to suggest that KCNJ8 may also be involved in drug resistance . The mechanisms by which KCNJ8 specifically regulates the invasive phenotype remain unclear at present and warrant further investigation .

4.7 S100A13

S100 proteins are small EF hand Ca^{2+} binding proteins of variable length and sequence. There are a number of functions associated with S100 proteins, many associated with tumour development. In 1996, Wicki *et al* identified a new S100 member termed S100A13 by screening expressed sequence tags (EST) databases. The C-terminus of S100A13 protein ends with the motif RKK, which is also seen in the metastasis-associated protein S100A4 (Kim and Helfman, 2003) and S100A10. The results described in Section 3.6 describe a novel function for S100A13 in the modulation of an invasive phenotype.

4.7.1 S100A13 expression in the DLKP variants

S100A13 has been demonstrated to be overexpressed in brain tumours in concert with FGF-1 (Landriscina *et al*, 2002) and has been proven to be essential in the regulation and release of pro-angiogenic molecules FGF-1 and IL-1 α in a copper dependent manner (Madinova *et al*, 2003, and Landriscina *et al*, 2001). The array data indicated that S100A13 expression was increased in the more invasive cell lines in our model system. Analysis of S100A13 mRNA by RT-PCR (Section 3.6.2) confirmed increased expression in the invasive cell lines DLKP-1, DLKP-2 and TXT-2 compared with the poorly invasive cell lines TXT-1 and VCR. This data concurs with a study by Smirnov *et al*, (2005) who identified S100A13 as a novel predictor of metastasis following its detection in circulating tumour cells in blood. Section 3.6.2 demonstrates differences in S100A13 mRNA levels between the invasive cell lines DLKP-1 and TXT-2 and this was again evident in the qPCR analysis of the cell lines in Section 3.6.3.2. This data would suggest that although high S100A13 mRNA expression correlates with a more aggressive and invasive phenotype, that S100A13 mRNA expression cannot induce an invasive phenotype by itself, since S100A13 mRNA levels are low in the invasive cell line DLKP-1.

4 7 2 Evaluation of functional effects of S100A13 in DLKP variants

To help define the potential role of S100A13 in invasive lung cancer, we decided to transfect three independent Ambion S100A13 specific siRNA sequences in the invasive cell lines DLKP-1, DLKP-2 and TXT-2 and to examine the effect of this decrease in S100A13 expression on both proliferation and invasion. Additionally, S100A13 cDNA was transiently transfected into the non-invasive cell lines TXT-1 and VCR. It was theorised that decreasing S100A13 expression would decrease the invasive potential of the invasive cell lines and that a corresponding increase in invasion would be observed in response to an increase in S100A13 expression in the non-invasive cell lines.

An S100A13 siRNA-specific decrease in mRNA levels was confirmed by PCR analysis in Section 3 6 3 2. The siRNA's used in the IGF-1R and KCNJ8 work potentially acted like microRNA's by preventing mRNA translation into protein (Kim, 2003, Ke *et al*, 2003). In this experiment the clear reduction in mRNA is indicative of mRNA cleavage through RISC action (Hutvagner and Zamore, 2002). Endogenous S100A13 protein levels were below western blotting detection limits. A strategy to demonstrate S100A13 siRNA-specific knockdown would include the immunoprecipitation of S100A13 from the cell lines followed by western blot analysis. Alternatively one could pulse siRNA transfected cells with a radiolabelled amino acid for a defined length of time, using immuno-precipitation to pull down the protein of interest. The radiolabelled protein could then be counted and compared with a non-specific antibody to indicate new protein synthesis following siRNA knockdown.

In Figure 3 6 3 5 S100A13 expression in DLKP-1 is increased at 72h compared to the earlier timepoints in both non-treated, scrambled siRNA transfected and S100A13 siRNA transfected cells. This trend is again evident for DLKP-2 (Figure 3 6 3 6) but is not as obvious in TXT-2 (Figure 3 6 3 7). The changes involved are only 2-3 fold (see scale bar) and may be linked to increased confluency at 72h. Elevated S100A13 levels in the scrambled siRNA were evident in these qPCR analyses. The impact of these spikes is unclear, they were evident in the IGF-1R qPCR analysis also but western blotting demonstrated that IGF-1R protein levels remained unaffected in the scrambled siRNA samples.

S100 proteins can regulate progression through the cell cycle. For example, Breen and Tang (2003) used an antisense sequence to S100A6 and inhibited fibroblast proliferation. Figure 3.6.4.1 demonstrates that decreasing S100A13 expression had no obvious effect on DLKP variant proliferation thereby indicating no obvious role for S100A13 in cell growth or apoptosis in these cell lines, although more specific analysis such as H-thymidine incorporation assays and TUNEL assays would clarify this suggestion. Landriscina *et al.*, (2000) limited S100A13 availability through treatment with the anti-allergic drug Amlexanox. This resulted in non-apoptotic inhibition of cell migration and proliferation, by inducing tyrosine phosphorylation of cortactin, a Src substrate that regulates actin bundling. However, the decrease in proliferation in the study by Landriscina *et al.*, (2000) may also be attributed to the inhibition of FGF-1 release by Amlexanox and not simply the limited availability of S100A13.

The identification and characterisation of molecular markers that can identify patients at high risk for metastatic spread and improve clinical management, therapeutic outcome and patient survival is of paramount importance. S100 family members have been identified as molecular markers for metastatic potential. S100A2 is of prognostic significance in lung cancer in that it allows for the discrimination of high- and low-risk patients in the lymph node negative sub group. Clinically this translates as aggressive initial treatment of S100A2-negative patients thereby avoiding undertreatment. It also allows for the selection of S100A2-positive patients who would benefit from less aggressive treatment (Diederichs *et al.*, 2004). Komatsu *et al.*, (2002) associated S100A6 expression with human colorectal adenocarcinoma tumourigenesis and metastasis.

S100A13 has been recently implicated as a marker of angiogenesis in endometriosis (Hayrabyan *et al.*, 2005) and was identified as a novel predictor of metastasis following global gene expression profiling of circulating tumour cells by Smirnov *et al.*, (2005). The novel results in Section 3.6.5 show that decreasing S100A13 expression in invasive cell lines can reduce their invasive capacity by as much as 84% in siRNA treated cells compared with their scrambled siRNA transfected counterparts ($P < 0.001$). This is the first study to give causal evidence for the role of S100A13 in

invasion, since *in vitro* invasion can be inhibited by reduced S100A13 expression. However, the results from the S100A13 overexpression experiment (Figures 3.6.4) show that transient S100A13 expression (confirmed by western blotting) decreased invasion in S100A13 cDNA transfected cells compared with the empty vector, although this decrease was significant for the TXT-1 S100A13 cDNA transfected cells ($P < 0.01$) and not VCR S100A13 cDNA transfected cells. Stable transfection of S100A13 would help to elucidate further the role sustained increased S100A13 expression on invasion.

Given the impact of S100A13 knockdown on invasive capacity and the correlation of S100A13 mRNA expression with a more invasive phenotype, it is possible that S100A13 acts as a potential enhancer of metastasis given an already invasive background. To this end S100A13 may act in a similar manner to S100A4, whose expression is also increased in metastatic tumours but transgenic mice overexpressing S100A4 do not develop tumours. S100A4, like S100A13 can be secreted and once extracellular can affect angiogenesis (Kim and Helfman, 2003, Hayrabedian *et al*, 2005). Additionally, extracellular S100A4 can also affect cell differentiation and migration (Kim and Helfman, 2003) although a role for S100A13 has not been demonstrated in these processes at this point. S100A13 is involved in the secretion of the pro-angiogenic molecules FGF-1 and IL-1 α (Madinova *et al*, 2003, and Landriscina *et al*, 2001), S100A4 can also interact with other proteins both intra- and extra-cellular level. For example, S100A4 binds to myosin heavy chain IIA (MHC-IIA) and may modulate metastatic phenotype by regulating cellular motility and MHC-IIA function (Kim and Helfman, 2003, Garrett *et al*, 2005).

The results detailed here clearly show S100A13 is a novel regulator of invasion as measured by *in vitro* invasion assay. However, the way in which S100A13 regulates cellular functions remain to be determined, although preliminary indications are that it is not involved in the regulation of cell growth (Figure 3.6.4.1). The identification and characterisation of the molecular mechanisms by which S100A13 effects invasion will aid the understanding of the contribution of S100A13 to the metastatic process. A further aspect of this study would be to examine the effect of decreasing S100A13 expression on DLKP variant sensitivity to chemotherapeutic drugs. One would hope

that combining S100A13 siRNA with chemotherapeutic drug treatment would result in an additive or synergistic effect

The results here combined with the fact that S100A13 expression can help predict metastatic spread and is detectable from circulating tumour cells in blood indicate the suitability of S100A13 as a novel target for cancer therapy, in that cancer spread can be decreased and/or maintained at a certain level. S100A13 may also be of clinical value in the selection of patients for more aggressive chemotherapeutic regimens, or indeed drugs or siRNAs targeting S100A13 may act synergistically with other therapeutic drugs

4.8 Stratifin (SFN/14-3-3- σ)

SFN (or 14-3-3 protein sigma) belongs to the highly conserved 14-3-3 protein family, whose members play a role in the regulation of signal transduction pathways implicated in the control of cell proliferation, differentiation and survival. It has been described as a p53-induced inhibitor of G2/M progression (Taylor and Stark, 2001) although this mechanism has not yet fully described. In 2003, Yang *et al* , studied the link between SFN activities and p53 regulation. The group found that increased SFN expression stabilised p53 expression by antagonising the biological functions of Mdm2 and by blocking Mdm2-mediated p53 ubiquitination and nuclear export. SFN also enhanced the oligomerisation and transcriptional activity of p53 and appeared to have a positive feedback effect on p53 activity.

4.8.1 SFN expression in the DLKP variants

SFN repeatedly came through the various bioinformatic analyses of array data as a potential target for functional investigation. It was increased, in the invasive cell lines included in this study, as confirmed by PCR (Section 3.7.2). SFN has been found to be among the most differentially expressed genes in some gene expression profiling studies of human cancers (Iacobuzio-Donahue *et al* , 2003, Santin *et al* , 2004). The expression pattern for SFN identified by this study does not tally with the majority of published expression patterns for SFN. SFN is frequently inactivated in human cancers. Suzuki *et al* , (2000) reported that this is due to methylation of the 5' region. Umbricht *et al* , (2001) also found that SFN is frequently silenced in breast carcinomas due to hypermethylation and suggest that this occurs at an early stage in the progression to invasive breast cancer. This is in complete contrast to the preliminary finding that SFN expression is higher in the invasive cell lines compared with their mildly invasive counterparts.

In 2002, Osada *et al* , examined the DNA methylation status and expression level of SFN gene in 37 lung cancer cell lines and 30 primary lung tumour specimens. The group found that SCLC cell lines were frequently hypermethylated, which silenced stratifin expression (9 of 13 lines). Hypermethylation and silencing of SFN was also observed in 4 of 7 large cell lung cancer cell lines. However, in other NSCLC cell lines hypermethylation only occurred in 1 of 17 lines. In the primary specimens, all eight SCLC tumours had decreased SFN expression, while loss of expression was rare in primary NSCLC specimens. This demonstrates a possible role for SFN in lung tumorigenesis in a histological type-specific manner. In addition, Liu *et al* , (2004) examined the protein profiles of four different human NSCLC cell lines compared with normal bronchial epithelial cells by 2D-PAGE and MALDI-TOF mass spectrometry. They found a decrease in SFN expression and postulate that altered expression of SFN might be involved in lung carcinogenesis. Guweidhi *et al* , (2004) found that SFN mRNA levels were 54-fold higher in pancreatic adenocarcinoma in comparison with normal pancreatic samples and was localised in pancreatic cancer cells as determined by laser capture microdissection. High SFN expression was not indicative of maintenance of G(2)/M cell cycle checkpoint or apoptosis induction in the pancreatic cell lines. The group propose an important role of aberrant SFN downstream signalling in pancreatic cancer. Ide *et al* , (2004) found that hypermethylation of SFN was a rare event in colorectal cancers. They found by immunohistochemistry, that SFN was localised to the invasion-front of the tumour (i.e. the deep peripheral area of the tumour). They also demonstrated that SFN positive cases exhibited higher proliferative activity compared to cases with silenced SFN. The results detailed in Section 3.7 also indicate a role for deregulated SFN expression in lung cancer and do not suggest that SFN acts as a tumour suppressor gene.

Hermeking *et al* , (1997) reported that SFN expression is induced following exposure to DNA damaging agents and that this increase in SFN expression leads to G2 cell cycle arrest through p53 signalling, a finding supported by Chan *et al* , (1999), who propose that this occurs to prevent mitotic catastrophe following DNA damage.

4 8 2 Evaluation of functional effects of SFN in DLKP variants

A SFN siRNA-specific decrease in mRNA levels was confirmed by qPCR analysis at 24h in Figure 3 7 3 1. However the timecourse analysis of this knockdown by RT-PCR is of limited value and is quite subjective since the differences between SFN band intensities are so small (Figures 3 7 3 2 to 3 7 3 5). qPCR seems to give a more accurate representation of SFN knockdown.

Corresponding with a measurable knockdown in SFN expression at 24h, invasion was increased in SFN siRNA transfected DLKP-2 and TXT-2 cells compared with the scrambled siRNA control ($P < 0.001$) (Figure 3 7 4 1 and 3 7 4 2). Invasion was not significantly affected in SFN siRNA transfected DLKP-1 cells, this may be due to reduced transfection efficiency in this cell line. These data were unexpected in relation to the array data, however correlate with the view that SFN expression is decreased during the progression of a cancer phenotype (Umbricht *et al*, 2001, Osada *et al*, 2002, and Liu *et al*, 2004).

Zhang *et al*, (2004) reported SFN as a positive mediator of IGF-1R induced cell proliferation where treatment of MCF-7 cells with IGF-1 resulted in a four-fold increase in SFN mRNA and protein levels. Increased IGF-1R expression has already been demonstrated in the invasive cell lines included in this study and it is possible that the increased SFN levels observed in these cell lines are as a result of IGF-1 signalling through IGF-1R in a manner independent of p53. When SFN expression was reduced in MCF-7 cell lines it resulted in a reduction in cell proliferation and a delay in cell cycle progression (Zhang *et al*, 2004). It would be interesting to investigate the effect of SFN siRNA transfection on proliferation.

An investigation into SFN expression in thyroid neoplasms by Ito *et al*, (2003) revealed that normal follicles, follicular carcinomas and follicular adenomas did not express the protein. All of the papillary carcinomas studied expressed SFN with increased expression in advanced stage and poorly differentiated types. 21 of 23 anaplastic carcinomas expressed SFN at higher levels than those detected in papillary carcinomas. Huang *et al*, (2004) demonstrated by immunohistochemical analysis the nuclear localisation of SFN in higher Gleason grade prostate cancers relative to benign

glands Exogenous expression of SFN the poorly invasive cell lines TXT-1 and VCR did not result in any change in invasion (Figures 3 7 6 1 and 3 7 6 2) despite confirmation of increased SFN expression by western blot (Figures 3 7 5 1 and 3 7 5 2) This suggests that increasing SFN expression over a 72h period cannot induce invasion

There are many lines of evidence to suggest that SFN acts as a tumour suppressor gene (Mhaweche, 2005) This is not supported in this study Indeed it seems that higher SFN expression in the invasive DLKP variants may be a result of IGF-1 induction mediated by IGF-1R signalling Modulating SFN expression in the DLKP variants does not alter their *in vitro* invasion capacities

4.9 Tissue Factor Pathway Inhibitor 2 (TFPI2)

Human TFPI2 is a 32kDa serine protease inhibitor that is associated with the ECM. It has high homology to TFPI1, a regulator of the extrinsic blood coagulation pathway (Sprecher *et al* , 1994). TFPI2 inhibits the tissue factor VIIa complex and many serine proteases including trypsin and plasmin. However, it does not inhibit uPA and tPA (Petersen *et al* , 1996).

4.9.1 TFPI2 expression in the DLKP variants

Many studies have demonstrated the down regulation of TFPI2 in the development of an invasive phenotype in cancer. For example, Wojtukiewicz *et al* , (2003) used immunohistochemical procedures to examine TFPI2 expression in neoplastic cells of laryngeal, breast, gastric, colon, pancreatic, renal and endometrial cancer and in glial neoplasms. A higher staining intensity was observed in more differentiated tumours. This group also observed that TFPI2 expression decreased with increased malignancy. In a gene expression profile study of invasive cervical carcinomas versus normal cervical keratinocytes, TFPI2 expression was lower in the invasive carcinomas (Santin *et al* , 2005). The results in Section 3.8.2 agrees with these findings and demonstrates lower TFPI2 mRNA expression in the invasive cell lines, particularly in TXT-2, compared with the poorly invasive cell lines TXT-1 and VCR.

4.9.2 Evaluation of functional effects of TFPI2 in DLKP variants

To define the role of TFPI2 in a panel of lung cancer cell lines with different phenotypic levels of invasion, it was decided to transfect a TFPI2 specific siRNA sequence in the lesser-invasive cell lines TXT-1 and VCR and to examine the effect of this decrease in TFPI2 expression on invasion. Additionally, TFPI2 cDNA was transiently transfected into the invasive cell lines DLKP-1, DLKP-2 and TXT-2 and the effect on proliferation and *in vitro* invasion examined. It was theorised that increasing TFPI2 expression would decrease the invasive potential of the invasive cell

lines and that a corresponding increase in invasion would be observed in response to a silencing of TFPI2 expression in the mildly invasive cell lines.

A TFPI2 siRNA-specific decrease in mRNA levels was confirmed by PCR analysis in Figure 3.8.3.1 for VCR but not TXT-1. There was a dramatic knockdown of TFPI2 in VCR; this might indicate decreased transfection efficiency for the TXT-1 sample. This siRNA caused a substantial decrease in TFPI2 mRNA expression in VCR whereas the IGF-1R siRNA used in these studies did not exert their effects at mRNA level and potentially acted like microRNA's by preventing mRNA translation into protein.

A decrease in TFPI2 expression in response to siRNA transfection did not significantly increase invasion in the poorly invasive cell line TXT-1. It should be noted that in Figure 3.8.3.2 a decrease in TFPI2 mRNA expression was achieved in TXT-1 at 24h, however the invasion assays were not performed until 72h, hence the effect on TFPI2 knockdown on invasion may have been missed. Invasion assay analysis was performed at 72h to allow the cells to recover following the transfection process and this minimised the non-specific effect of the transfection reagent on the cells. However, invasion was increased in TFPI2 siRNA transfected VCR cells compared with the scrambled siRNA control. Invasion was increased in TFPI2 siRNA transfected VCR cells compared with the scrambled siRNA control ($P < 0.005$). (Figures 3.8.4.1 and 3.8.4.2). It is possible that there was a decreased efficiency of the TFPI2 siRNA transfection in the TXT-1 cell line. However, the decrease in TFPI2 mRNA expression in response to siRNA transfection in the VCR cell line and corresponding increase in invasion ($P < 0.005$) indicates that a decrease in TFPI2 expression can induce invasion. This result concurs with a study by Lakka *et al.*, (2000) who increased the invasiveness of A549, a lung cancer cell line expressing high TFPI2 levels, using an antisense cDNA to TFPI2. Decreasing TFPI2 expression in all of the cell lines could help to elucidate whether decreasing TFPI2 can further induce invasion given an already invasive background or determine if decreasing TFPI2 is itself insufficient to induce an invasive phenotype in poorly invasive cell lines.

TFPI2 is an ECM-associated serine protease inhibitor with a role in ECM degradation during tumour cell invasion and metastasis, wound healing and angiogenesis (Konduri *et al.*, 2000). An early study by Rao *et al.*, (1998) reported that recombinant TFPI2

inhibits plasmin that is bound to HT-1080 cells, preventing matrix degradation and invasion Eitzman *et al*, (1996), suggested that interfering with the plasminogen-activation system by inhibiting plasmin, rather than at the level of uPA and tPA may provide a more effective strategy for the inhibition of tumour cell invasion and metastasis As such increasing TFPI2 expression, thereby inhibiting plasmin, may be of therapeutic benefit in cancer therapy

In the present study, overexpression of TFPI2 following transient transfection in DLKP-1, DLKP-2 and TXT-2 was confirmed by western blot (Figures 3 8 5 2 to 3 8 5 3) This resulted in a reduction of invasive capacity for TFPI2 cDNA transfected cells ranging from 50% to 88% ($P < 0.001$) (Figures 3 8 5 5 to 3 8 5 7) as compared with the invasiveness of parental and empty vector transfected cells These results suggest that overexpression of TFPI2 inhibits *in vitro* invasion in the DLKP lung cancer cell lines In a similar study, Konduri *et al*, (2000) stably transfected a vector expressing TFPI2 in the melanoma cell line C-32 and also observed a decrease in invasion in TFPI2 transfected clones Sense and antisense vectors to TFPI2 were used in by Konduri *et al*, (2001) to examine the role of TFPI2 in human glioma invasiveness Sense clones were much less invasive compared to antisense clones *in vitro* and formed smaller tumours *in vivo* A study by Zhong *et al*, (2003) revealed that TFPI2 expression inhibited the invasive, but not the migratory, capability of ovarian tumour cells *in vitro* In 2004, Chand *et al*, put forward the theory that secretion of TFPI-2 by a highly metastatic tumour decreases its growth and metastasis *in vivo* by regulating ECM remodelling and angiogenesis The data presented in Section 3 8 4 support the former hypothesis

TFPI2 mRNA could not be detected in a high proportion of pancreatic cancer cell lines and in primary pancreatic ductal neoplasms (Sato *et al*, 2005) Loss of TFPI2 expression was attributed to hypermethylation of CpG islands in the promoter Phorbol 12-myristate 13-acetate (PMA) induced TFPI2 expression in cell lines with unmethylated or partially methylated TFPI2, but no induction was achieved in cell lines with fully methylated TFPI2 Restored TFPI2 expression in pancreatic cells resulted in decreased proliferation, migration and invasive potential *in vitro* (Sato *et al*, 2005) Unlike the study by Sato *et al*, (2005) restored TFPI2 expression had no obvious effect on invasive DLKP variant proliferation thereby indicating no obvious

role for TFPI2 in cell growth or apoptosis in these cell lines (Figure 3 8 5 4) and more specific assays can be employed to confirm this. Induction of TFPI2 was also achieved in epithelial cell lines (including HEK293, A549 and MCF7) using PMA. The PMA induction of TFPI2 was blocked with the MEK inhibitor, UO126 which indicated that the ERK/MAPK pathway regulates TFPI2 promoter activity (Kast *et al* , 2003). This may suggest that a signalling pathway other than the ERK/MAPK pathway mediates the increase in TFPI2 expression in cDNA transfected DLKP variants, since no effect on proliferation was observed.

Konduri *et al* , (2002) used TFPI2 promoter deletion constructs linked to a luciferase reporter gene to identify critical promoter regions that regulate TFPI2 expression in gliomas. The group demonstrated a region -312 to -81 upstream of the transcriptional start site as essential for the transcription of TFPI2 in glioma cells. This promoter region contained potential SP1 and AP1 binding motifs and did not have TATA and CAAT boxes immediately upstream of the transcriptional initiation site. A repressor region was found in -927 to -1181 and an enhancer region at -115 to -1181 upstream of the transcriptional initiation site (Konduri *et al* , 2002).

Hube *et al* , (2003) identified a complete CpG island spanning exon 1 and three transcription start sites in the TFPI2 promoter. They also demonstrated that treatment with 5'-aza-2'-deoxycytidine (5ac) restores TFPI2 transcription in JAR choriocarcinoma cells that have low TFPI2 expression levels. Thus transcriptional silencing of TFPI2 can be attributed (at least in part) to methylation of CpG islands (Hube *et al* , 2003). 5ac and Trichostatin A (TSA) (inhibitors of DNA methyltransferase and histone deacetylase respectively (HDAC)) were used to induce TFPI2 mRNA in SNB19 glioblastoma cells that have no detectable TFPI2 expression. An increase in mRNA and protein was observed with TSA being a more potent inducer than 5ac, although a 5ac and TSA combination proved highly synergistic (Konduri *et al* , 2003). It would be interesting to identify the mechanisms by which TFPI2 expression is silenced in the invasive DLKP variants. Comparison of TFPI2 expression levels following treatments with 5ac and TSA should indicate if the promoter is methylated and thus silenced or if histone deacetylation is involved.

A further interesting study by Yanamandra *et al*, (2005) in which a 0.8kb TFPI2 fragment was cloned into an adeno-associated viral vector (rAAV-TFPI2) and then transfected into SNB19 glioblastoma cells, resulted in decreased migration and invasion in a dose dependent manner. Angiogenesis, both *in vitro* and *in vivo* was also markedly decreased by the increase in TFPI2 expression. This study suggests that rAAV-TFPI2 mediated gene therapy could be used as a treatment for brain tumours.

The primary cause of therapeutic failure in the treatment of cancer is invasion. Proteolytic degradation of the ECM is considered an essential step in the invasion and metastasis of a malignant cell to distant sites. Protease inhibitors that could effectively protect the ECM from degradation by circulating tumour cells could be of use as therapeutic agents. The results discussed here clearly show that the serine protease inhibitor TFPI2, is a regulator of invasion as measured by *in vitro* invasion assay and has undoubted potential as a new therapy for cancer treatment. Increasing TFPI2 expression using rAAV or HDAC inhibitors in conjunction with chemotherapeutic drug treatment may potentially provide a more aggressive treatment for patients with metastatic cancer.

Section 5.0: Conclusions & Future work

5.1 Conclusions

Metastatic cancer is frequently unresponsive to chemotherapy, surgery and radiotherapy. Future treatment of metastatic disease will require the development of biology-based approaches that will utilise the novel information on the molecular mechanisms underlying metastasis in order to identify therapeutic targets whose expression, and thereby function, can be modified (Brodt *et al*, 2000).

In this study, the gene expression profiles of a panel of five, increasingly invasive, lung cancer cell lines were compared in order to identify molecules involved in this aspect of the metastatic process.

The results presented in this thesis identify molecules associated with a more aggressive invasive phenotype in lung cancer cell lines and demonstrate that altering the expression of these molecules can modulate the invasive capacity of these lung cancer cells.

5.1.1 Characterisation of a panel of lung cell lines with defined behaviour in an *in vitro* invasion assay

- The panel of DLKP cell lines described in this thesis represent robust, valuable models for the study of mechanisms of *in vitro* invasion. The relative invasiveness of the sub-lines compared to each other remained constant over ten passages and this was the time-frame used for all invasion analysis.
- The invasion assay itself was optimised and performed using defined culture conditions. The definition of these assay protocols and culture boundaries lends confidence to the phenotypic changes observed following the deliberate manipulations of target molecules.

5.1.2 Microarray profiling of a panel of invasive lung cancer cell lines

- This work generated many gene lists, some of which may potentially serve as molecular ‘signatures’ for invasiveness in lung cancer cell lines. These types of signatures may help provide earlier diagnosis and influence and individualise the therapies prescribed to cancer patients and thereby improve patient prognosis.

- Five genes were associated with changes in the invasive phenotype in the DLKP lung cancer cell lines. This was the first study within the NICB to apply this experimental approach with the workflow comprising microarray analysis, bioinformatic analysis, identification of targets and knock-up/down functional investigation. This was highly successful, given the challenges of using new technology and of becoming familiar with bioinformatic software for the microarray analysis. Indeed, the success of this study is reflected in the high “hit rate” whereby the experimental manipulation of all five targets studied caused a phenotypic functional effect in the cell line model. This project has yielded many interesting results that should be further investigated.

5.1.3 IGF-1R

Increased IGF-1R expression has been previously linked with tumour invasion (Grzmil *et al* , 2004, Jiang *et al* , 2004). The findings in this thesis concur with previous results in that decreasing IGF-1R expression decreases the *in vitro* invasiveness of the DLKP variants. Since decreasing IGF-1R expression did not affect growth one could postulate the suitability of IGF-1R as an adjuvant therapeutic target to inhibit/decrease cancer metastasis while killing the still actively growing primary tumour cells with conventional chemotherapeutic agents.

5.1.4 KCNJ8

This work identifies a previously unreported role for KCNJ8 in lung cancer cell invasion. In fact, no cancer related function has ever been attributed to KCNJ8. These experiments do not suggest a function for KCNJ8 in the regulation of proliferation or apoptosis. The association of KCNJ8 with the MDR- and MRP-like SUR proteins indicate that KCNJ8 may be involved, not only in invasion but also in drug resistance in our cell model. This has yet to be investigated. The mechanisms by which KCNJ8 specifically regulates the invasive phenotype remain unclear at present and warrant further investigation. Increasing KCNJ8 expression did not increase invasion in the poorly invasive cell lines TXT-1 and VCR. Decreasing KCNJ8 expression increased invasion in the invasive DLKP variants DLKP-1, DLKP-2 and TXT-2 ($P < 0.001$), suggesting that deregulated KCNJ8 expression can modulate the amplitude of invasion in invasive lung cancer cell lines.

5 1.5 S100A13

Possibly the most exciting results in this thesis, that decreasing S100A13 expression decreases the *in vitro* invasive capacity of invasive cell lines by up to 84% ($P < 0.001$), suggests S100A13 as a novel regulator of an invasive phenotype. Exogenously increasing S100A13 expression did not induce an invasive phenotype in poorly invasive cell lines, demonstrating that S100A13 on its own cannot induce an invasive phenotype in mildly or non-invasive cells. Preliminary indications are that S100A13 is not involved in cell survival or apoptosis, since decreasing S100A13 expression did not affect cell number. S100A13 may also be of value clinically in the selection of cancer patients for more aggressive therapy in a manner similar to the study of S100A2 expression in lung cancer patients (Diederichs *et al*, 2004). S100A13 may also have potential as a therapeutic target in its own right and may be suitable as a treatment to inhibit cancer spread in cancer patients who are undergoing chemotherapy. This may be especially beneficial since multidrug resistant cells can survive chemotherapy and migrate to distant sites in the body and highly metastatic cells can evade the chemotherapeutic effect altogether. Thus targeting S100A13 expression in conjunction with conventional chemotherapy may provide a more effective cancer treatment.

5 1.6 TFPI2

TFPI2 was differentially expressed across the cell line panel with lower expression of the gene correlating with increasing invasiveness. Decreased TFPI2 expression has been previously linked with the development of an invasive phenotype (Lakka *et al*, 2000, Yanamandra *et al*, 2005) and the results of this study concur with these findings. Overexpression of TFPI2 in invasive DLKP variants caused a decrease in the ability of these cells to traverse the matrigel inserts in our assay ($P < 0.001$).

We suggest that increasing TFPI2 expression may have real therapeutic potential in cancer to decrease metastatic spread. Indeed, this potential is already under serious consideration by other groups interested in targeting brain cancer. Our results demonstrate that it is also a powerful inhibitor of invasion in lung cancer-derived cells. In contrast, decreasing TFPI2 expression did not increase the invasive capacities of the poorly invasive cell lines TXT-1 and VCR, suggesting that a decrease in TFPI2 expression cannot independently induce or activate an invasive phenotype.

5 1 7 SFN

Stratifin was identified as being highly expressed in the invasive compared with the poorly invasive DLKP variants. Increased SFN expression is frequently correlated with good prognosis and many studies support the notion that it acts as a tumour suppressor gene through interaction with p53 in response to DNA damage. An siRNA-dependent decrease in SFN expression in this study was not definitively demonstrated. Western blots or immunohistochemistry would help to confirm the extent to which SFN expression was decreased by siRNA transfection thereby allowing much firmer conclusions to be made.

5.2 Future work

5.2.1 Microarray Analysis

- The panel of DLKP cell lines in this thesis represent valuable models for the study of mechanisms of *in vitro* invasion and also in the study of mechanisms of drug resistance. The microarray analysis in this thesis focused on the identification of molecules involved in invasion, however, similar analysis could be performed to identify targets that are involved in the development of resistance to taxotere and vincristine. The microarray data could be re-examined using the various bioinformatic tools available in the NICB and candidate genes for development of taxotere and/or vincristine resistance could be identified.
- The microarray analyses carried out in this thesis generated vast amounts of data. Only a fraction of the potential information contained within this dataset was mined. An alternative method of analysis, other than that used in this thesis might include examining the large gene lists generated by dChip in Pathway Analysis packages. Pathway analysis can help identify additional targets (that may not have been represented on the array or failed to pass the filters applied) based on their association with other genes in a common pathway. Biological association rather than correlation of expression levels drives this type of analysis.

5 2 2 IGF-1R

- We have established that decreasing IGF-1R expression can decrease *in vitro* invasion. To further this investigation it is planned to identify the pathway through which IGF-1R exerts its effect on proliferation. To date IGF-1R was silenced in serum-containing medium, which contains IGF, EGF, insulin and PDGF therefore proliferation was unaffected because of these other growth factors in the medium. By silencing IGF-1R in serum starved cells in serum free medium supplemented with IGF-1 one would expect to see a reduction in proliferation.
- It would also be interesting to examine the effect of IGF-1R silencing in DLKP variants on their sensitivity to chemotherapeutic drugs. One would hope to achieve an additive or synergistic effect to further prove the suitability of targeting IGF-1R as a cancer therapy, either alone or in combination with chemotherapeutic drug treatment.
- The VCR cell line did not express endogenous IGF-1R, despite endogenous expression in the parental DLKP cell lines. This is interesting in itself and suggests that development of resistance to vincristine may require loss of IGF-1R expression. It is hoped to re-pulse an invasive parental DLKP cell line with vincristine and attempt to identify the points at which the drug impacts IGF-1R levels and the cells lose their capacity to invade.

5.2.3 KCNJ8

- Given the novelty of the findings regarding KCNJ8's role in invasion, further effort will be applied to the optimisation of western blot and/or immunohistochemistry to accurately determine an increase or decrease in KCNJ8 expression in response to cDNA or siRNA transfection respectively
- The possibility that KCNJ8 may regulate both invasion and drug resistance will be examined. This will be achieved by investigating the effect of KCNJ8 over- or under- expression on drug sensitivity in the DLKP variants and possibly in other cell models
- KCNJ8 will be stably transfected into less/non-invasive DLKP variants in order to investigate the impact of sustained overexpression on the invasive characteristics of these cell lines. It may be that we did not witness any functional impact due to the transient approach reported in this work

5 2 4 S100A13

- S100A13 was identified as a functional regulator of *in vitro* invasion in the DLKP variants and further elucidation of the mechanism involved would be interesting. This might be achieved by examining the expression of FGF-1 and IL-1 α levels in S100A13 siRNA transfected cells. These molecules have been shown to be regulated by S100A13 in the process of angiogenesis and are co-expressed in brain tumours.
- Stably transfecting S100A13 into non-invasive cell lines may help to identify whether S100A13 can contribute to the development of an invasive phenotype over time. An invasive phenotype can be induced in cell lines by treatment with a chemotherapeutic drug over time (e.g. the TXT-2 cell line). It would be interesting to see whether S100A13 overexpressing cells were more or less susceptible to this induction.
- S100A13 has already been associated with angiogenesis and this work has now demonstrated a clear role in invasion. Invasion (in embryogenesis for example) is a normal part of new blood vessel formation, and rapidly growing tumours also require a blood supply. It would be interesting to investigate the effect of decreasing S100A13 expression on this panel of cell lines in an *in vitro* model of angiogenesis.

5.2 5 TFPI2

- Decreased TFPI2 expression has already been associated with a more aggressive/invasive cancer phenotype. It would be interesting to compare the mechanisms by which TFPI2 is silenced in lung cancer with that of brain cancer where promoter silencing by methylation/deacetylation has been demonstrated. There are many different lung cancer and brain cancer cell lines available in the NICB to facilitate this study. The application of 5ac or HDAC could help to identify whether the gene is silenced by methylation or histone deacetylation in the cell lines.
- The application of rAAV for the transduction of TFPI2 as a potential therapy for brain cancer has also been demonstrated. This methodology will shortly be available in the NICB and could be employed to examine the effect of rAAV-TFPI2 transfection on the invasive capacity of lung cell lines grown as spheroids in a 3D matrix, which would better represent the biology of tumours in the body.
- In addition, the effect of increasing TFPI2 expression on drug sensitivity should also be investigated with a view to the development of improved anti-metastatic therapy for cancer treatment (assuming there is any impact).

5 2 6 Other work

- Three other targets, ICAM-1, TLX-1 and TCF4 were identified in this study as potentially being involved in invasion. Functional studies similar to those detailed in this thesis should give an indication of the potential role in invasion and suggest whether or not they merit further investigation.
- It would also be of interest to investigate the expression of these targets in clinical samples.
- DLKP-1 is an interesting cell line, in that it is invasive but was an outlier in terms of the expression of the targets investigated in this thesis. Examination of the subcellular localisation of the targets and post-translational modification status could help to explain this anomaly.

Section 6.0: Bibliography

- Aalinkeel, R , Nair, M P N, Sufrin, G , Mahajan, S D , Chadha, K C , Chawda, R P and Schwartz, S A (2004) Gene expression of angiogenic factors with metastatic potential of prostate cancer cells *Cancer Res* **64**, 5311-21
- Abdul M, Santo A, Hoosein N (2003) Activity of potassium channel-blockers in breast cancer *Anticancer Res* **23**, 3347-51
- Adams, T E , McKern, N M and Ward, C W (2004) Signalling by the type I insulin-like growth factor receptor interplay with the epidermal growth factor receptor *Growth Factors* **22**, 89-95
- Aguilar-Bryan, L , Clement IV, J P , Gonzalez, G , Kunjilwar, K , Babenko, A and Bryan, J (1998) Toward understanding the assembly and structure of K_{ATP} channels *Physiological Rev* **78**, (227-245)
- Ahn, S J , Chung, K W , Lee, R A , Park, I A , Lee, S H , Park, D E and Noh, D Y (2003) Overexpression of β PIX-a in human breast cancer tissues *Cancer Lett* **193**, 99-107
- Albini A (1998) Tumor and endothelial cell invasion of basement membranes The matrigel chemoinvasion assay as a tool for dissecting molecular mechanisms *Pathol Oncol Res* **4**, 230-41
- Andre, F , Rigot, V , Thimonier, J *et al* (1999) Integrins and E-cadherin cooperate with IGF-1 to induce migration of epithelial colonic cells *Int J Cancer* **83**, 497-505
- Andreasen, P A , Kjoller, L , Christensen, L and Duffy, M J (1997) The urokinase-type plasminogen activator system in cancer metastasis A review *Int J cancer* **72**, 1-22
- Angiolillo, A L , Sgadari, C , Taub, D D , Liao, F , Farber, J M , Maheshwari, S , *et al* (1995) Human interferon-inducible protein 10 is a potent inhibitor of angiogenesis in vivo *J Exp Med* **182**, 155-62
- Aronin, N (2006) Target selectivity in mRNA silencing *Gene Therapy* **13**, 509-516
- Arya, M , Patel, H R H and Williamson, M (2003) Chemokines key players in cancer *Curr Med Res Opin* **19**, 557-564

- Baggiolini, M , Dewald, B , and Moser, B (1997) Human chemokines an update *Annu Rev Immunol* **15**, 675-705
- Baker, A H , Edwards, D R and Murphy, G (2002) Metalloproteinase inhibitors biological actions and therapeutic opportunities *J Cell Sci* **115**, 3719-27
- Bar-Eli, M (1999) Role of interleukin-8 in tumour growth and metastasis of human melanoma *Pathobiology* **67**, 12-18
- Basset, P , Bellocq, J P , Wolf, C , *et al* (1990) A novel metalloproteinase gene specifically sequestered in stromal cells of breast carcinomas *Nature* **348**, 699-704
- Behrens, J , von Kries, J P , Kuhl, M , Bruhn, L , Wedlich, D , Grosschedl, R , and Birchmeier, W (1996) Functional interaction of beta-catenin with the transcription factor LEF-1 *Nature* **382**, 638-642
- Bhatia, K , Siraj, A K , Hussain, A , Bu, R and Gutierrez, M I (2003) The tumour suppressor gene 14-3-3 σ is commonly methylated in normal and malignant lymphoid cells *Cancer Epid Biom Prev* **12**, 165-69
- Bianchi, L , Wible, B , Arcangeli, A , Taghialatela, M , Morra, F , Castalso, P , *et al* , (1998) *herg* encodes a K⁺ current highly conserved in tumours of different histogenesis a selective advantage for cancer cells? *Cancer Res* **58**, 815-822
- Binggeli, R and Weinstein, R C (1986) Membrane potentials and sodium channels hypotheses for growth regulation and cancer formation based on changes in sodium channels and gap junctions *J Theor Biol* **123**, 377-401
- Biswas, C , Zhang, Y , DeCastro, R , Gui, H , *et al* (1995) The human tumour cell derived collagenase stimulatory factor (renamed EMMPRIN) is a member of the immunoglobulin superfamily *Cancer Res* **55**, 434-9
- Bitko V, Musiyenko A, Shulyayeva O, Barik S (2005) Inhibition of respiratory viruses by nasally administered siRNA *Nat Med* **11**, 50-55

Bohula, E A , Salisbury, A J , Sohail, M , Playford, M P , Riedemann, J , Southern, E M and Macaulay, V M (2003) The efficacy of small interfering RNAs targeted to the Type I insulin-like growth factor receptor (IGFIR) is influenced by secondary structure in the IGFIR transcript *J Biol Chem* **278**, 15991-15997

Borghaei, R, C , Rawlings, P L Jr and Mochan, E (1998) Interleukin-4 suppression of interleukin-1 induced transcription of collagenase (MMP-1) and stromelysin 1 (MMP-3) in human synovial fibroblasts *Arthritis Rheum* **41**, 1398-1406

Bouzahzah, B , Albanese, C , Ahmed, F , Pixley, F , Lisanti, M P , Segall, J D *et al* (2001) Rho family GTPases regulate mammary epithelium cell growth and metastasis through distinguishable pathways *Mol Med* **7**, 816-30

Brabletz T, Jung A, Dag S, Reu S, Kirchner T (2000) beta-Catenin induces invasive growth by activating matrix metalloproteinases in colorectal carcinoma *Verh Dtsch Ges Pathol* **84**, 175-81

Brabletz, T , Jung, A , Dag, S , Hlubek, F and Kirchner, T (1999) Beta-catenin regulates the expression of the matrix metalloproteinase-7 in human colorectal cancer *Am J Pathol* **155**, 1033-38

Bradley, G , Naik, M and Ling, V (1989) P-glycoprotein expression in multidrug-resistant human ovarian cell lines *Cancer Res* **49**, 2790-2796

Brazma, A , Hingamp, P , Quackenbush, J , Sherlock, G , Spellman, P , Stoeckert, C , Aach, J , Ansorge, W , Ball, C A , Causton, H C , Gaasterland, T , Glemsson, P , Holstege, F C P , Kim, I F , Markowitz, V , Matese, J C , Parkinson, H , Robinson, A , Sarkans, U , Schulze-Kremer, S , Stewart, J , Taylor, R , Vilo, J , Vingron, M (2001) Minimum information about a microarray experiment (MIAME)-toward standards for microarray data *Nat Gene* , **29**, 365-371

Breen, E C and Tang, K (2003) Calcyclin (S100A6) regulates pulmonary fibroblast proliferation, morphology, and cytoskeletal organisation *in vitro* *J Cell Biochem* **88(4)**, 848-854

- Bridge, A J , Pebernard, S , Ducraux, A , Nicoulaz, A L , Iggo, R (2003) Induction of an interferon response by RNAi vectors in mammalian cells *Nat Genet* , **34**, 263-264
- Brod, P , Samani, A and Navab, R (2000) Inhibition of the type I insulin-like growth factor receptor expression and signalling Novel strategies for antimetastatic therapy *Biochem Pharmacol* **60**, 1101-1107
- Brooks, P C , Stromblad, S , Sanders, L C , *et al* (1996) Localisation of matrix metalloproteinase MMP-2 to the surface of invasive cells by interaction with integrin alpha v beta 3 *Cell* **85**, 683-93
- Brooks, R C , Clark, R A and Cheresch, D A (1994) Requirement of vascular integrin $\alpha 5\beta 3$ for angiogenesis *Science* **264**, 569-571
- Brooks, R C , Silletti, S , von Schalscha, T L , Friedlander, M and Cheresch, D A (1998) Disruption of angiogenesis by PEX, a noncatalytic metalloproteinase fragment with integrin binding activity *Cell* **92**, 391-400
- Bruchovsky, N , Owen, A A , Becker, A J and Till, J E (1965) *Effects* of vinblastine on the proliferative capacity of and their progress through the division cycle *Cancer Res* **25**, 1232-1237
- Cabral, F R , Brady, R C and Schibler, M J (1986) A mechanism of cellular resistance to drugs that interfere with microtubule assembly *Ann N Y Acad Sci* **466**, 745-756
- Cairns, R A , Khokha, R and Hill R P (2003) Molecular mechanisms of tumour invasion and metastasis an integrated view *Curr Mol Med* **3(7)**, 659-671
- Camirand, A , Zakikhani, M, Young, F and Pollak, M (2005) Inhibition of insulin-like growth factor-1 receptor signalling enhances growth-inhibitory and proapoptotic effects of gefitinib (Iressa) in human breast cancer cells *Breast Cancer Res* **7**, 570-579

Campo, E , Munoz, J , Miquel, R et al (1994) Cathepsin B expression in colorectal carcinomas correlates with tumour progression and shortened patient survival *Am J Pathol* **145**, 301-9

Cao Z, Fang J, Xia C, Shi X, Jiang BH (2004) trans-3,4,5'-Trihydroxystibene inhibits hypoxia-inducible factor 1 α and vascular endothelial growth factor expression in human ovarian cancer cells *Clin Cancer Res* **10**, 5253-63

Carreira, C M , LaVallee, T M , Tarantini, F , Jackson, A , Tait Lathrop, J , Hampton, B , Burgess, W H and Maciag, T (1998) S100A13 is involved in the regulation of fibroblast growth factor-1 and p40 synaptotagmin-1 release in vitro *J Biol Chem* **273**, 22224-31

Chambers, A F and Tuck, A B (1993) Ras-responsive genes and tumour metastasis *Crit Rev Oncol* **4**, 95-114

Chambers, A F , MacDonald, I C , Schmidt, E E , Koop, S , Morris, V L , Khokha, R , et al (1995) Steps in tumour metastasis new concepts from intravital videomicroscopy *Cancer Metastasis Rev* **14**, 279-301

Chan, T A , Hermeking, H , Lengauer, C , Kinzler, K W and Vogelstein, B (1999) 14-3-3- σ is required to prevent mitotic catastrophe after DNA damage *Nature letters* **401**, 616-620

Chand HS, Du X, Ma D, Inzunza HD, Kamei S, Foster D, Brodie S, Kisiel W (2004) The effect of human tissue factor pathway inhibitor-2 on the growth and metastasis of fibrosarcoma tumors in athymic mice *Blood* **103**, 1069-77

Chen KN, Gu ZD, Ke Y, Li JY, Shi XT, Xu GW (2005) Expression of 11 HOX genes is deregulated in esophageal squamous cell carcinoma *Clin Cancer Res* **11**, 1044-9

Chernicky, C L , Yi, L , Tan, H , Gan, S U and Ilan, J (2000) Treatment of human breast cancer cells with antisense RNA to the type I insulin-like growth factor receptor

inhibits cell growth, suppresses tumourigenesis, alters the metastatic potential and prolongs survival in vivo *Cancer Gene Ther* **7**, 384-95

Chi, J T , Chang, H Y , Wang, N N , Chang, D S , Dunphy, N , Brown, P O (2003) Genomewide view of gene silencing by small interfering RNAs *Proc Natl Acad Sci USA*, **100**, 6343-6346

Cillo, C , Dick, J E , Ling, V and Hill, R P (1987) Generation of drug-resistant variants in metastatic B16 mouse melanoma cell lines *Cancer Res*, **47**, 2604-2608

Clark, E A , Golub, T R , Lander, E S and Hynes, R O (2000) Genomic analysis of metastasis reveals an essential role for RhoC *Nature* **406**, 532-35

Condeelis, J (1993) Life at the leading edge, the formation of cell protrusions *Annu Rev Physiol* **9**, 411-444

Cook, D , Fry, M J , Hughes, K , Sumathipala, R , Woodgett, J R , and Dale, T C (1996) Wingless inactivates glycogen synthase kinase-3 via an intracellular signalling pathway which involves a protein kinase C *EMBO J* **15**, 4526-4536

Coussens, L M , Fingleton, B and Matrisian, L M (2002) Matrix metalloproteinase inhibitors and cancer trials and tribulations *Science* **295**, 2387-92

Culine, S , Kattan, J , Lhomme, C , Duvillard, P , Michel, G , Castaigne, D , Leclere, J , Pico, J and Droz, J P (1994) A phase II study of high-dose cisplatin, vinblastine, bleomycin and etoposide (PveBV regimen) in malignant nondysgerminomatous germ-cell tumours of the ovary *Gynecol* **54**, 47-53

Curran, S and Murry, G I (2000) Matrix metalloproteinases molecular aspects of their roles in tumour invasion and metastasis *Eur J Cancer* **36**, 1621-30

Debatin, K M (2000) Activation of apoptosis pathways by anticancer treatments *Toxicol Lett* , **112-113**, 41-48

DeClerck, Y A , Mercurio, A M , Sharon Stack, M , Chapman, H A , Zutter, M M , Muschel, R J *et al* (2004) Proteases, extracellular matrix and cancer *Am J Pathol* **164**, 1131-1139

Devroe, E , Silver, P A (2004) Therapeutic potential of retroviral RNAi vectors *Expert Opin Biol Ther* , **4**, 319-327

Diederichs, S , Bulk, E , Steffen, B , Ji, P , Tickenbrock, L , Lang, K *et al* (2004) S100 family members and trypsinogens are predictors of distant metastasis and survival in early-stage non-small cell lung cancer *Cancer Res* **64**, 5564-5569

Dong, J T , Lamb, P W , Rinker-Schaeffer, C W , Vukanovic, J , Ichikawa, T , Isaacs, J T *et al* (1995) KAI1, a metastasis suppressor gene for prostate cancer on human chromosome 11p11.2 *Science* **268**, 884-886

Duffy, M J (2002) Urokinase-type plasminogen activator a potent marker of metastatic potential in human cancers *Biochem Soc Trans* **30**, 207-210

Duffy, M J (2002b) Urokinase plasminogen activator and its inhibitor, PAI-1, as prognostic markers in breast cancer From pilot to level 1 evidence studies *Clin Chem* **48**, 1194-97

Dupont, J and Le Roith, D (2001) Insulin-like growth factor 1 and oestradiol promote cell proliferation of MCF-7 breast cancer cells new insights into their synergistic effects *Mol Pathol* **54(3)**, 149-54

Duval, A , Rolland, S , Tubacher, E , Bui, H , Thomas, G , and Hamelin, R (2000) The human T-cell transcription factor-4 gene Structure, extensive characterization of alternative splicings, and mutational analysis in colorectal cancer cell lines *Cancer Res* **60**, 3872-3879

Dykxhoorn D M , Palliser D and Lieberman J (2006) The silent treatment siRNAs as small molecule drugs *Gene Therapy* **13**, 541-552

Einhorn, E H (1997) Testicular cancer an oncological success story *Clin Cancer Res* **3**, 2630-2632

Eitzman, D T , Krauss, J C , Shen, T and Ginsburg, D (1996) Lack of plasminogen activator inhibitor-1 effect in a transgenic mouse model of metastatic melanoma *Blood* **87**, 4718-4722

Erginel-Unaltuna, N , Yang, W P and Blonar, M A (1998) Genomic organisation and expression of KCNJ8/Kir6 1, a gene encoding a subunit of an ATP-sensitive potassium channel *Gene* **211**, 71-78

Fearon, E R and Vogelstein, B (1990) A genetic model for colorectal tumorigenesis *Cell* **61**, 759-767

Fidler, I J (2002) The organ microenvironment and cancer metastasis *Differentiation* **70**, 498-505

Fidler, I J and Ellis, L M (1994) The implications of angiogenesis for the biology and therapy of cancer metastasis *Cell* **79**, 185-188

Fidler, I J and Kripke, M L (1977) Metastasis results from preexisting variant cells within a malignant tumour *Science* **197**, 893-895

Finzel, A H , Reinmger, A J , Bode, P A and Wurzinger, L J (2004) ICAM-1 supports adhesion of human small-cell lung carcinoma to endothelial cells *Clin Exp Metastasis* **21**, 185-9

Folkman, J , (1995) Angiogenesis in cancer, vascular, rheumatoid and other disease *Nature Med* **1**, 27-31

Fowlkes, J L , Thrailkill, K M m Serra, D M , Suzuki, K and Nagase, H (1995) Matrix metalloproteinases as insulin-like growth factor binding protein-degrading proteinases *Prog Growth factor Res* **6**, 255-63

Galvan V, Logvinova A, Sperandio S, Ichijo H, Bredesen DE (2003) Type 1 insulin-like growth factor receptor (IGF-IR) signaling inhibits apoptosis signal-regulating kinase 1 (ASK1) *J Biol Chem* **278**, 13325-32

Garrett, S C , Varney, K M , Weber, D J and Bresnick, A R (2005) S100A4 A mediator of metastasis *J Biol Chem Online* @ www.jbc.org/cgi/doi/10.1074/jbc.R500017200

Geyer, M and Wittinghofer, A (1997) GEFs, GAPs, GDIs and effectors taking a closer (3D) look at the regulation of Ras-related GTP-binding proteins *Curr Opin Struct Biol* **7**, 786-92

Ghahary A, Marcoux Y, Karimi-Busheri F, Li Y, Tredget EE, Kilani RT, Lam E, Weinfeld M (2005) Differentiated keratinocyte-releasable stratifin (14-3-3 sigma) stimulates MMP-1 expression in dermal fibroblasts *J Invest Dermatol* **124**, 170-7

Gilles C, Polette M, Mestdagt M, Nawrocki-Raby B, Ruggeri P, Birembaut P, Foidart JM (2003) Transactivation of vimentin by beta-catenin in human breast cancer cells *Cancer Res* **63**, 2658-64

Girnita, L , Girnita, A , Brodin, B , et al (2000) Increased expression of insulin-like growth factor I receptor in malignant cells expressing aberrant p53 functional impact *Cancer Res* **60**, 5278-83

Goetsch, L , Gonzalez, A, Leger, O , Beck, A , Pauwels, P J , Haeuw, J F and Corvaia, N (2005) A recombinant humanized anti-insulin-like growth factor receptor type I antibody (h7C10) enhances the antitumor activity of vinorelbine and anti-epidermal growth factor receptor therapy against human cancer xenografts *Int J Cancer* **113(2)**, 316-328

Gospodarowicz, D (1983) Growth factors and their action in vivo and in vitro *J Pathol* **141**, 201-33

Grier, D G , Thompson, A , Kwasniewka, A , McGonigle, G J , Halliday, H L and Lappin, T R (2005) The pathophysiology of HOX genes and their role in cancer *J Pathol* **205**, 154-71

Grosschedl, R , Giese, K , and Pagel, J (1994) HMG domain proteins Architectural elements in the assembly of nucleoprotein structures *Trends Genet* **10**, 94–100

Grzmil, M , Hemmerlein, B , Thelen, P , Schweyer, S and Burfeind, P (2004) Blockade of the type I IGF receptor expression in human prostate cancer cells inhibits proliferation and invasion, up-regulates IGF binding protein-3, and suppresses MMP-2 expression *J Pathol* **202**, 50-59

Guirguis, R , Marguiles, I , Taraboletti, G and Liotta, L A (1987) Cytokine-induced pseudopodial protrusion is coupled to tumour cell migration *Nature (Lond)* **329**, 2261-2263

Guvakova, M A and Surmacz, E (1999) The activated insulin-like growth factor I receptor induces depolarisation in breast epithelial cells characterised by actin filament disassembly and tyrosine phosphorylation of FAK, Cas and paxillin *Exp Cell Res* **251**, 244-55

Guvakova, M A , Boettiger, D and Adams, J C (2002) Induction of fascin spikes in breast cancer cells by activation of the insulin-like growth factor-I receptor *Int J Biochem Cell Biol* **34**, 685-98

Guweidhi, A , Kleeff, J , Giese, N , Fitori, J E , Ketterer, K , Giese, T , *et al* (2004) Enhanced expression of 14-3-3 sigma in pancreatic cancer and its role in cell cycle regulation and apoptosis *Carcinogenesis* **25**, 1575-85

Hagstrom J E , Hegge J, Zhang G, Noble M, Budker V, Lewis D L *et al* (2004) A facile nonviral method for delivering genes and siRNAs to skeletal muscle of mammalian limbs *Mol Ther* **10**,386–398

Hanahan D and Weinberg R A (2000) The hallmarks of cancer *Cell* **100**, 57-70

Harada, N , Tamai, Y , Ishikawa, T , Sauer, B , Takaku, K , Oshima, M , and Taketo, M M (1999) Intestinal polyposis in mice with a dominant stable mutation of the beta-catenin gene *EMBO J* **18**, 5935–5942

Hawley RG, Fong AZ, Reis MD, Zhang N, Lu M, Hawley TS (1997) Transforming function of the HOX11/TCL3 homeobox gene *Cancer Res* **57**, 337-45

Hayrabyan, S , Kyurkchiev, S and Kehayov, I (2005) Endoglin (cd105) and S100A13 as markers of active angiogenesis in endometriosis *Reproductive Biol* **5(1)**, 51-67

He, T C , Chan, T A , Vogelstein, B , and Kinzler, K W (1999) PPARdelta is an APC-regulated target of nonsteroidal anti-inflammatory drugs *Cell* **99**, 335–345

He, T C , Sparks, A B , Rago, C , Hermeking, H , Zawel, L , da Costa, L T , Morin, P J , Vogelstein, B , and Kinzler, K W (1998) Identification of c-MYC as a target of the APC pathway *Science* **281**, 1509–1512

Hecht, S S (2002) Cigarette smoking and lung cancer chemical mechanisms and approaches to prevention *Lancet Oncol* , **3**, 461-469

Hermeking, H , Lengauer, C , Polyak, K , He, T C , Zhang, L , Thiagalingam, S , Kinzler, K W and Vogelstein, B (1997) 14-3-3 sigma is a p53-regulated inhibitor of G2/M progression *Mol Cell* **1(1)**, 3-11

Hoffman, P C , Mauer, A M , Vokes, E E (2000) Lung cancer *The Lancet*, **355**, 479-485

Holmes, F A , Walters, R S , Theriault, R L , Forman, A D , Newton, L K , Raber, M N , Budzar, A U , Frye, D K and Hortobagyi, G N (1991) Phase II trial of taxol, an active drug in the treatment of metastatic breast cancer *J Natl Cancer Inst* **83**, 1797-1805

- Hood, J D and Cheresch, D A (2002) Role of integrins in cell invasion and migration *Nat Rev Cancer* **2**, 91-100
- Hornstein, I , Pikarsky, E , Groysman, M , Amir, G , Peylan-Ramu, N and Katzav, S (2003) The haematopoietic specific signal transducer Vav1 is expressed in a subset of human neuroblastomas *J Pathol* **199**, 526-533
- Hsieh, H L , Schafer, B W , Cox J A and Heizmann, C W (2002) S100A13 and S100A6 exhibit distinct translocation pathways in endothelial cells *J Cell Sci* **115**, 3149-58
- Hsieh, H L , Schafer, B W , Weigle, B and Heizmann, C W (2004) S100 protein translocation in response to extracellular S100 is mediated by receptor for advanced glycation endproducts in human endothelial cells *Biochem Biophys Res Comm* **316**, 949-59
- Huang, D , Liu, X , Plymate, S R , Idowu, M , Grimes, M , Best, A M , McKinney, J L and Ware, J L (2004) Proteomic identification of 14-3-3 sigma as a common component of the androgen receptor and the epidermal growth factor receptor signalling pathways of the human prostate epithelial cell line M12 *Oncogene* **23**, 6881-9
- Huang, W C , Chan, S T , Yang, T L , Tzeng, C C and Chen, C C (2004) Inhibition of ICAM-1 gene expression, monocyte adhesion and cancer cell invasion by targeting IKK complex molecular and functional study of novel alpha-methylene-gamma-butyrolactone derivatives *Carcinogenesis* **25**, 1925-34
- Hube F, Reverdiau P, Iochmann S, Rollin J, Cherpi-Antar C, Gruel Y (2003) Transcriptional silencing of the TFPI-2 gene by promoter hypermethylation in choriocarcinoma cells *Biol Chem* **384**, 1029-34
- Hunter, K (2006) Host genetics can influence tumour metastasis *Nat Reviews Cancer* **6**, 141-146

Hutvagner, G , Zamore, P D (2002) RNAi Nature abhors a double strand *Curr Op Gen Dev* , **12**, 225-232

Hynes, R O (1992) Integrins Versatility, modulation, and signalling in cell adhesion *Cell* **69**, 11-25

Iacobuzio-Donahue, C A , Ashfaq, R , Maitra, A , Adsay, N V , Shen-Ong, G L , Berg, K , *et al* (2003) Highly expressed genes in pancreatic ductal adenocarcinomas a comprehensive characterisation and comparison of the transcription profiles from three major technologies *Cancer Res* **63**, 8614-22

Ide, M , Nakajima, T , Asao, T and Kuwano, H (2004) Inactivation of 14-3-3 σ by hypermethylation is a rare event in colorectal cancers and its expression may correlate with cell cycle maintenance at the invasion front *Cancer Lett* **207**, 241-49

Inagaki, N , Inazawa, J and Seino, S (1995) cDNA sequence, gene structure, and chromosomal localization of the human ATP-sensitive potassium channel, uK_{ATP}-1, gene (KCNJ8) *Genomics* **30**, 102-104

Insuk SO, Chae MR, Choi JW, Yang DK, Sim JH, Lee SW (2003) Molecular basis and characteristics of KATP channel in human corporal smooth muscle cells *Int J Impot Res* **15**, 258-66

Ito, Y , Miyoshi, E , Uda, E , Yoshida, H , Uruno, T , Takamura, Y , *et al* (2003) 14-3-3 σ possibly plays a constitutive role in papillary carcinoma, but not in follicular tumour of the thyroid *Cancer Lett* **200**, 161-6

Jackson, A L , Bartz, S R , Schelter, J , Kobayashi, S V , Burchard, J , Mao, M , Li, B , Cavet, G , Linsley, P S (2003) Expression profiling reveals off-target gene regulation by RNAi *Nat Biotechnol* , **21**, 635-637

Jiang, Y , Wang, L , Gong, W , Wei, D , Le, X , Yao, J , Ajani, J , Abbruzzese, J L , Huang, S and Xie, K (2004) A high expression of insulin-like growth factor I receptor is associated with increased expression of transcription factor Sp1 and regional lymph node metastasis of human gastric cancer *Clinical Exp Mets* **21**, 755-764

Jirsch, J, Deeley, R G, Cole, S P C, Stewart, A J and Fedida, D (1993) Inwardly rectifying K channels and volume-regulated anion channels in multidrug-resistant small cell lung cancer cells *Cancer Res* **53**, 4156-4160

Karle C, Gehrig T, Wodopia R, Hoschele S, Kreye VA, Katus HA, Bartsch P, Mairbaurl H (2004) Hypoxia-induced inhibition of whole cell membrane currents and ion transport of A549 cells *Am J Physiol Lung Cell Mol Physiol* **286**, L1154-60

Kast C, Wang M, Whiteway M (2003) The ERK/MAPK pathway regulates the activity of the human tissue factor pathway inhibitor-2 promoter *J Biol Chem* **27**, 86787-94

Ke, X S, Liu, C M, Liu, D P, Liang, C C (2003) MicroRNAs key participants in gene regulatory networks *Curr Opin Chem Biol*, **7**, 516-523

Kealy, R J, Westwick, J K, Whitehead, I R, Der, C J and Parse, L V (1997) Cdc42 and Rac1 induce integrin-mediated cell motility and invasiveness through PI(3)K *Nature* **390**, 632-636

Kim, E J and Helfman, D M (2003) Characterisation of the metastasis-associated protein, S100A4 Roles of calcium binding and dimerisation in cellular localisation and interaction with myosin *J Biol Chem* **278**, 30063-73

Kim, V N (2003) RNA interference in functional genomics and medicine *J Korean Med Sci*, **18**, 309-318

Kinzler, K W and Vogelstein, B (1996) Lessons from hereditary colon cancer *Cell* **87**, 159-170

Kjoller, L and Hall, A (1999) Signalling to Rho GTPases *Exp Cell Res* **253**, 166-79

Klemke, R L *et al* (1997) Regulation of cell motility by mitogen activated protein kinase *J Cell Biol* **137**, 481-492

Klemke, R. L. *et al.* (1998). CAS/CRK coupling serves as a molecular switch for induction of cell migration. *J Cell Biol.* **140**, 961-972.

Knauper, V., Will, H., Lopez-Otin, C., *et al.* (1996). Cellular mechanisms for human procollagenase (MMP-13) activation. Evidence that MT1-MMP (MMP-14) and gelatinase A (MMP-2) are able to generate active enzyme. *J Biol Chem.* **271**, 17124-31.

Koblinski, J. E., Ahram, M. and Sloane, B. F. (2000). Unravelling the role of proteases in cancer. *Clinica Chimica Acta.* **291**, 113-135.

Koch, A. E., Polverini, P. J., Kunkel, S. L., Harlow, L. A., DiPietro, L. A., Elner, V. M., *et al.* (1992). Interleukin-8 as a macrophage-derived mediator of angiogenesis. *Science.* **258**, 1798-801.

Koh, T. J., Bulitta, C. J., Fleming, J. V., Dockray, G. J., Varro, A., and Wang, T. C. (2000). Gastrin is a target of the beta-catenin/TCF-4 growth-signaling pathway in a model of intestinal polyposis. *J. Clin. Invest.* **106**, 533-539.

Kohn, E. C. and Liotta, L. A. (1997). Molecular insights into cancer invasion: Strategies for prevention and intervention. *Perspectives in Cancer Res.* **55**, 1856-1862.

Komatsu, K., Murata, K., Kameyama, M., Ayaki, M., Mukai, M., Ishiguro, S., Miyoski, J., Tatsuta, M., Inoue, M. and Nakamura, H. (2002). Expression of S100A6 and S100A4 in matched samples of human colorectal mucosa, primary colorectal adenocarcinomas and liver metastases. *Oncology.* **63(2)**, 192-200.

Konduri SD, Osman FA, Rao CN, Srinivas H, Yanamandra N, Tasiou A, Dinh DH, Olivero WC, Gujrati M, Foster DC, Kisiel W, Kouraklis G, Rao JS. (2002). Minimal and inducible regulation of tissue factor pathway inhibitor-2 in human gliomas. *Oncogene.* **21**, 921-8.

Konduri SD, Rao CN, Chandrasekar N, Tasiou A, Mohanam S, Kin Y, Lakka SS, Dinh D, Olivero WC, Gujrati M, Foster DC, Kisiel W, Rao JS. (2001). A novel

function of tissue factor pathway inhibitor-2 (TFPI-2) in human glioma invasion
Oncogene **20**, 6938-45

Konduri SD, Srivenugopal KS, Yanamandra N, Dinh DH, Olivero WC, Gujrati M, Foster DC, Kisiel W, Ali-Osman F, Kondraganti S, Lakka SS, Rao JS (2003) Promoter methylation and silencing of the tissue factor pathway inhibitor-2 (TFPI-2), a gene encoding an inhibitor of matrix metalloproteinases in human glioma cells
Oncogene **22**, 4509-16

Konduri SD, Tasiou A, Chandrasekar N, Nicolson, G L and Rao, J S (2000) Role of tissue factor pathway inhibitor-2 (TFPI-2) in amelanotic melanoma (C-32) invasion
Clin Exp Metastasis **18**, 303-308

Koop, S , Khokha, R , Schmidt, E E MacDonald, I C , Morris, V L and Chambers A F (1994) Overexpression of metalloproteinase inhibitor in B16F10 cells does not affect extravasion but reduces tumour growth
Cancer Res **54**, 4791-5007

Korinek, V , Barker, N , Morin, P J , van Wichen, D , de Weger, R , Kinzler, K W , Vogelstein, B , and Clevers, H (1997) Constitutive transcriptional activation by a beta-catenin-Tcf complex in APC^{-/-} colon carcinoma
Science **275**, 1784-1787

Kramer, R H , Bensch, K G and Wong, J , (1986) Invasion of reconstituted basement membrane matrix by metastatic human tumour cells
Cancer Res **46**, 1980-9

Kusama, T , Mukai, M , Iwasaki, T , Tatsuta, M , Matsumoto, Y , Akedo, H and Nakamura, H (2001) Inhibition of epidermal growth factor-induced RhoA translocation and invasion of human pancreatic cancer cells by 3-hydroxy-3-methylglutaryl-coenzyme a reductase inhibitors
Cancer Res **61**, 4885-91

Lakka SS, Konduri SD, Mohanam S, Nicolson GL, Rao JS (2000) In vitro modulation of human lung cancer cell line invasiveness by antisense cDNA of tissue factor pathway inhibitor-2
Clin Exp Metastasis **18**, 239-44

Landriscina, M , Bagala, C , Mandinova, A , Soldi, R, Micucci, I , Bellum, S , Prudovsky, I and Maciag, T (2001) Copper induces the assembly of a multiprotein aggregate implicated in the release of fibroblast growth factor 1 in response to stress *J Biol Chem* **276**, 25549-57

Landriscina, M , Prudovsky, I , Carreira, C M , Soldi, R , Tarantini, F and Maciag, T (2000) Amlexanox reversibly inhibits cell migration and proliferation and induces the Src-dependent disassembly of actin stress fibres in vitro *J Biol Chem* **275**, 32753-62

Laniado, M E , Fraser, S P and Djamgoz, M B A (2001) Voltage-gated K⁺ channel activity in human prostate cancer cell lines of markedly different metastatic potential Distinguishing characteristics of PC-3 and LNCaP cells *The Prostate* **46**, 262-274

Lastraioli, E , Guasti, L , Crociani, O , Polvani S , Hofmann, G , Witchel, H , *et al* (2004) *herg1* gene and HERG1 protein are overexpressed in colorectal cancers and regulate cell invasion of tumour cells *Cancer Res* **64**, 606-611

Lee EJ, Mircean C, Shmulevich I, Wang H, Liu J, Niemisto A *et al* (2005) Insulin-like growth factor binding protein 2 promotes ovarian cancer cell invasion *Mol Cancer* **4**, 7

Lee, J H , Miele, M E , Hicks, D J , Philips, K K , Trent, J M , Weissman, B E , *et al* (1996) *Kiss-1*, a novel human malignant melanoma metastasis-suppressor gene *J Natl Cancer Inst* **88**, 1731-1737

Liang, Y , McDonnell, S and Clynes, M (2002) Examining the relationship between cancer invasion/metastasis and drug resistance *Curr Can Drug Targets* **2**, 257-277

Liang, Y , O'Driscoll, L , McDonnell, S , Doolan, P , Oglesby, I , Duffy, K , O'Connor, R , Clynes, M (2004) Enhanced *in vitro* invasiveness and drug resistance with altered gene expression patterns in a human lung carcinoma cell line after pulse selection with anticancer drugs *Int J Cancer*, **111**, 484-493

Lim, S C and Lee, M S (2002) Significance of E-cadherin/beta-catenin complex and cyclin D1 in breast cancer *Oncol Rep* **9**, 915-28

- Lin, R , Cerione, R A and Monor, D (1999) Specific contributions of the small GTPases Rho, Rac, and Cdc42 to Dbl transformation *J Biol Chem* **274**, 23633-41
- Liotta, L A , Klineran, J , Cataanzara, P and Rynbrandt, D Degradation of the basement membrane by murine tumour cells *J Natl Cancer Inst* **58**, 1427-1439
- Liotta, L A , Rao, C N and Barsky, S H (1983) Tumour invasion and the extracellular matrix *Lab Invest* **49**, 636-49
- Liu, L Y , Hu, C L , Ma, L J , Zhang, Z H and Mei, Y A (2004) ET-1 inhibits B-16 murine melanoma cell migration by decreasing K(+) currents *Cell Motil Cytoskeleton* **58 (2)** 127-136
- Liu, Y E , Wang, M , Greene, J , et al (1997) Preparation and characterization of recombinant tissue inhibitor of metalloproteinase-4 (TIMP-4) *J Biol Chem* **272**, 20479-83
- Liu, Y , Chen, Q and Zhang, J T (2004) Tumour suppressor gene 14-3-3 sigma is down-regulated whereas the proto-oncogene translation elongation factor 1delta is up-regulated in non-small cell lung cancers as identified by proteomic profiling *J Proteome Res* **3**, 728-35
- Lodygin, D , Yazdi, A S , Sander, C A , Herzinger, T and Hermeking, H (2003) Analysis of 14-3-3 sigma expression in hyperproliferative skin diseases reveals selective loss associated with CpG-methylation in basal cell carcinoma *Oncogene* **22**, 5519-24
- Long, L , Rubin, R and Brodt, P (1998) Enhanced invasion and liver colonization by lung carcinoma cells overexpressing the type I insulin-like growth factor receptor *Exp Cell Res* **238**, 116-121
- Longley, D B , Johnston, P G (2005) Molecular mechanisms of drug resistance *J Pathology*, **205**, 275-292

Lopez, T and Hanahan, D (2002) Elevated levels of IGF-1 receptor convey invasive and metastatic capability in a mouse model of pancreatic islet tumorigenesis *Cancer Cell* **1**, 39-53

Lucke-Huhle, C (1994) Permissivity for methotrexate-induced DHFR gene amplification correlates with the metastatic potential of rat adenocarcinoma cells *Carcinogenesis*, **15(4)**, 695-700

Macaulay, V M (2004) The IGF receptor as an anticancer treatment *Novartis Found Symp* **262**, 235-243

MacDonald, N J , de la Rosa, A and Steeg, P S (1995) The potential roles of nm23 in cancer metastasis and cellular differentiation *Eur J Cancer* **31A**, 1096-1100

Madhavan M, Srinivas P, Abraham E, Ahmed I, Vijayalekshmi NR, Balaram P (2002) Down regulation of endothelial adhesion molecules in node positive breast cancer possible failure of host defence mechanism *Pathol Oncol Res* **8**,125-8

Maeda K, Hamada J, Takahashi Y, Tada M, Yamamoto Y, Sugihara T, Moriuchi T (2005) Altered expressions of HOX genes in human cutaneous malignant melanoma *Int J Cancer* **114**, 436-41

Maione, T E , Gray, G S , Petro, J , Hunt, A J , Donner, A L , Bauer, S I , *et al* (1990) Inhibition of angiogenesis by recombinant human platelet factor-4 and related peptides *Science* **247**, 77-79

Makiyama K, Hamada J, Takada M, Murakawa K, Takahashi Y, Tada M, Tamoto E, Shindo G, Matsunaga A, Teramoto K, Komuro K, Kondo S, Katoh H, Koike T, Moriuchi T (2005) Aberrant expression of HOX genes in human invasive breast carcinoma *Oncol Rep* **13**, 673-9

Markman, M (2003) Management of toxicities associated with the administration of taxanes *Expert Opin Drug Saf* **2**, 141-6

- Marty, M , Espie, M , Cottu, P H , Cuvier, C and Lerebours, F (1999) Optimising chemotherapy for patients with advanced breast cancer *Oncology* **57**, Suppl 1 21-26
- Maryo, Y , Gochi, A , Kaihara, A , Shimamura, H , Yamada, T , Tanaka, N and Orita, K (2002) ICAM-1 expression and the soluble ICAM-1 level for evaluating the metastatic potential of gastric cancer *Int J Cancer* **100**, 486-90
- McManus, M T , Sharp, P A (2002) Gene silencing in mammals by small interfering RNAs *Nat Rev Genetics*, **3**, 737-747
- Metzner, B , Hofmann, C , Hememann, C , Zimpfer, U , Schraufstatter, I , Schopf, E , *et al* (1999) Overexpression of CXC-chemokines and CXC-chemokine receptor type II constitute an autocrine growth mechanism in the epidermoid carcinoma cells KB and A431 *Oncol Rep* **6**, 1405-10
- Mhawech, P (2005) 14-3-3 proteins – an update *Cell Research* **15(4)**, 228-236
- Mignatti, P and Rifkin, D B (1996) Plasminogen activators and matrix metalloproteinases in angiogenesis *Enzyme Protein* **49**, 117-7
- Miki, T , Suzuki, M , Shibusaki, T , Uemura, H , Sato, T , Yamaguchi, K , Koseki, H , Iwanaga, T , Nakaya, H and Seino, T (2002) Mouse model of Prinzmetal angina by disruption of the inward rectifier Kir6.1 *Nat Med* **8**, 466-472
- Minn AJ , Gupta GP , Siegel PM , Bos PD , Shu W , Giri D *et al* (2005) Genes that mediate breast cancer metastasis to lung *Nature* **436**, 518-524
- Mitsiades, C S , Mitsiades, N S , McMullan, C J , Poulaki, V , Shringarpure, R , Akiyama, M *et al* (2004) Inhibition of the insulin-like growth factor receptor-1 tyrosine kinase activity as a therapeutic strategy for multiple myeloma, other hematologic malignancies, and solid tumors *Cancer Cell* **5**, 221-230
- Mizejewski, G J (1999) Role of integrins in cancer survey of expression patterns *PSEBM* **222**, 124-138

Molenaar, M , van de Wetering, M , Oosterwegel, M , Peterson- Maduro, J , Godsave, S , Kornek, V , Roose, J , Destree, O , and Clevers, H (1996) Tcf-3 transcription factor mediates betacatenin-induced axis formation in *Xenopus* embryos *Cell* **86**, 391–399

Monteagudo, C , Merino, M J , San-Juan, J , Liotta, L A and Sterler-Stevnson, W G (1990) Immunohistochemical distribution of type IV collagenase in normal, benign, and malignant breast tissue *Am J Pathol* **136**, 585-592

Muller, A , Homey, B , Soto, H , Ge, N , Catron, D, Buchanan, M E *et al* (2001) Involvement of chemokine receptors in breast cancer metastasis *Nature* **410**, 50-56

Nagase, H (1996) Activation mechanisms of matrix metalloproteinases *Biol Chem Hoppe Seyler* **378**, 151-60

Nakajima, M , Morikawa, K , Fabra, A , Bucana, C D and Fidler, I J (1990) Influence of tumour microenvironment on extracellular matrix degradative activity and metastasis of human colon carcinoma cells *J Natl Cancer Inst* **82**, 1890-1898

Nakamura, K , Hongo, A , Kodama, J Miyagi, Y , Yoshinouchi, M, and Kudo, T (2000) Down-regulation of insulin-like growth factor I receptor by antisense RNA can reverse the transformed phenotype of human cervical cancer cell lines *Cancer Res* **60**, 760-65

Omatu T (1999) Overexpression of human homeobox gene in lung cancer A549 cells results in enhanced motile and invasive properties *Hokkaido Igaku Zasshi* **74**, 367-76

Orian-Rousseau, V , Sigrun, M , Mengwasser, J , HogenEsch, H , Guo, F , Thies, W-G , Hofmann, M , Herrlich, P and Helmut, P (2005) Genes upregulated in a metastasising human colon carcinoma cell line *Int J Cancer* **113**, 699-705

Osada, H , Tatematsu, Y , Yatabe, Y , Nakagawa, T , Konishi, H , Harano, T *et al* (2002) Frequent and histological type-specific inactivation of 14-3-3 sigma in human lung cancers *Oncogene* **21**, 2418-24

Ossowski, L and Aguirre-Ghiso, J A (2000) Urokinase receptor and integrin partnership Coordination of signalling for cell adhesion, migration and growth *Curr Opin Cell Biol* **12**, 613-20

Oursler, M J, Riggs, B L and Spelsberg, T C (1993) Glucocorticoid-induced activation of latent transforming growth factor β by normal human osteoblast-like cells *Endocrinology* **133**, 2187-96

Ozanne, B W, McGarry, L, Spence, H J, Johnston, I, Winnie, J, Meagher, L, *et al* (2000) Transcriptional regulation of cell invasion AP-1 regulation of multigenic invasion programme *Eur J Cancer* **36**, 1640-48

Pai S I, Lin Y-Y, Macaes B, Meneshian A, Hung C F and Wu T C (2006) Prospects of RNA interference therapy for cancer *Gene Therapy* **13**, 464-477

Pennisi, P A, Barr, V, Nunez, N P, Stannard, B and Le Roith, D (2002) Reduced expression of insulin-like growth factor-I receptors in MCF-7 breast cancer cells leads to a more metastatic phenotype *Cancer Res* **62**, 6529-37

Petersen LC, Sprecher CA, Foster DC, Blumberg H, Hamamoto T, Kisiel W (1996) Inhibitory properties of a novel human Kunitz-type protease inhibitor homologous to tissue factor pathway inhibitor *Biochemistry* **35**, 266-72

Polakis, P, Hart, M, and Rubinfeld, B (1999) Defects in the regulation of beta-catenin in colorectal cancer *Adv Exp Med Biol* **470**, 23-32

Polette, M, Gilles, G, Marchand, V, *et al* (1996) Tumour collagenase stimulatory factor (TCSF) expression and localisation in human lung and breast cancers *J Histochem Cytochem* **45**, 203-7

Polette, M, Nawrocki-Raby, B, Gilles, G, Clavel, C and Birembaut, P (2004) Tumour invasion and matrix metalloproteinases *Crit Rev Oncol Hemat* **49**, 179-186

- Poole, A R , Tiltman, K J , Recklies, A D and Stoker, T A M (1978) Differences in the secretion of the proteinase cathepsin B at the edges of human breast carcinomas and fibroadenomas *Nature* **273**, 545-7
- Powell, U C , Fingleton, B , Wilson, C L , Boothby, M , Matrisian, L M (1999) The metalloproteinase matrilysin proteolytically generates active soluble fas ligand and potentiates epithelial cell apoptosis *Curr Biol* **9**, 1441-7
- Pozzatti, R , Muschel , R , Williams, J , Padmanabhan, R , Howard, B , Liotta, L and Khoury, G (1986) Primary rat embryo cells transformed by one or two oncogenes show different metastatic potentials *Science (Washington DC)* **232**, 223-227
- Pratt, W B , Ruddon, R W , Ensminger, W D and Maybaum, J (1994) *The Anticancer drugs* (second edition)
- Price, L S and Collard, J G (2001) Regulation of the cytoskeleton by Rho-family GTPases implications for tumour cell invasion *Semin Cancer Biol* **11**, 167-73
- Prudovsky, I , Mandinova, A , Soldi, R , Bagala, C , Graziani, I , Landriscina, M , Tarantini, F , *et al* (2003) The non-classical export routes FGF-1 and IL-1 α point the way *J Cell Sci* **116**, 4871-81
- Ramaswamy, S , Ross, K N , Lander, E S and Golub, T R (2003) A molecular signature of metastasis in primary solid tumors *Nature Genetics* **33**, 49-54
- Rao, C N , Cook, B , Liu, Y , Chilukuri, K , Stack, M S , Foster, D C , Kisiel, W and Woodly, D T (1998) HT-1080 fibrosarcoma cell matrix degradation and invasion are inhibited by the matrix-associated serine protease inhibitor TFPI-2/33kDa MSPI *Int J Cancer* **76**, 749-756
- Reinmuth, N , Liu, W , Fan, F *et al* (2002) Blockade of insulin-like growth factor I receptor function inhibits growth and angiogenesis of colon cancer *Clin Cancer Res* **8**, 3259-69
- Rommelink M , Mijatovic T , Gustin, A , Mathieu A , Rombaut, K , Kiss R , Salmon I and Decaestecker C (2005) Identification by means of cDNA microarray analyses of

gene expression modifications in squamous non-small cell lung cancers as compared to normal bronchial epithelial tissue *Int J Oncol* **1**, 247-258

Ren, X D , Kiosses, W B and Schwartz, M A (1999) Regulation of the small GTP-binding protein Rho by cell adhesion and cytoskeleton *EMBO J* **18**, 578-585

Ren, X D , Kiosses, W B , Sieg, D J , Otey, C A , Schlaepfer, D D and Schwartz, M A (2000) Focal adhesion kinase suppresses Rho activity to promote focal adhesion turnover *J Cell Sci* **113**, 3673-78

Ren, X O , Kiosses, W B and Schwartz, M A (1999) Regulation of the small GTP-binding protein Rho by cell adhesion and the cytoskeleton *EMBO J* **18**, 578-585

Rickardson, L , Fryknas, M , Dhar, S , Lovborg, H , Gullbo, J , Rydåker, M , Nygren, P , Gustafsson, M G , Larsson, R and Isaksson, A (2005) Identification of molecular mechanisms for cellular drug resistance by combining drug activity and gene expression profiles *B J Cancer* **93**, 483-492

Ridinger, K , Schafer, B W , Durussel, I , Cox J A and Heizmann, C W (2000) S100A13 Biochemical characterisation and subcellular localisation in different cell lines *J Biol Chem* **275**, 8686-94

Ridley, A J (2004) Rho proteins and cancer *Breast Cancer Res Treat*, **84**, 13-19

Roose, J , Huls, G , van Beest, M , Moerer, P , van der, H K , Goldschmeding, R , Logtenberg, T , and Clevers, H (1999) Synergy between tumor suppressor APC and the beta-catenin-Tcf4 target Tcf1 *Science* **285**, 1923-1926

Rosic-Kablar S, Chan K, Reis MD, Dube ID, Hough MR (2000) Induction of tolerance to immunogenic tumor antigens associated with lymphomagenesis in HOX11 transgenic mice *Proc Natl Acad Sci USA* **97**, 13300-5

Rowinsky, E K , Cazenave, L A and Donehower, R C (1990) Taxol a novel investigational antimicrotubule agent *J Natl Cancer Inst* **82**, 1247-1259

Sahi, E (2005) Mechanisms of cancer cell invasion *Curr Opin Genetics and Dev* **15**, 87-96

Sakai H, Shimizu T, Hori K, Ikaru A, Asano S, Takeguchi N (2002) Molecular and pharmacological properties of inwardly rectifying K⁺ channels of human lung cancer cells *Eur J Pharmacol* **435**, 125-33

Sakuntala Warshamana-Greene, G, Litz, J, Buchdunger, E, Garcia-Echeverria, C, Hofmann, F and Krystal, G W (2005) The insulin-like growth factor I receptor kinase inhibitor, NVP-ADW742, sensitizes small cell lung cancer cell lines to the effects of chemotherapy, *Clin Can Res* **11**, 1563-1571

Santin AD, Zhan F, Bignotti E, Siegel ER, Cane S, Bellone S, Palmieri M, Anfossi S, Thomas M, Burnett A, Kay HH, Roman JJ, O'Brien TJ, Tian E, Cannon MJ, Shaughnessy J Jr, Pecorelli S (2005) Gene expression profiles of primary HPV16- and HPV18-infected early stage cervical cancers and normal cervical epithelium identification of novel candidate molecular markers for cervical cancer diagnosis and therapy *Virology* **331**, 269-91

Santin, A D, Zhan, F, Bellone, S, Palmieri, M, Cane, S, Bignotti, E, et al (2004) Gene expression profiles in primary ovarian serous papillary tumours and normal ovarian epithelium identification of candidate molecular markers for ovarian cancer diagnosis and therapy *Int J Cancer* **112**, 14-25

Sato N, Parker AR, Fukushima N, Miyagi Y, Iacobuzio-Donahue CA, Eshleman JR, Goggins M (2005) Epigenetic inactivation of TFPI-2 as a common mechanism associated with growth and invasion of pancreatic ductal adenocarcinoma *Oncogene* **24**, 850-8

Savagner, P (2001) Leaving the neighbourhood molecular mechanisms involved during epithelial-mesenchymal transition *Bioessays* **23**, 912-923

Saxena, S , Jonsson, Z O , Dutta, A (2003) Small RNAs with imperfect match to endogenous mRNA repress translation Implications for off-target activity of small inhibitory RNA in mammalian cells *J Biol Chem* , **278**, 44312-44319

Schadendorf, D , Moller, A , Algermissen, B , Worm, M , Sticherling, M and Czarnetzki, B M (1993) IL-8 produced by human malignant melanoma cells in vitro is an essential autocrine growth factor *J Immunol* **151**, 2267-75

Schafer, B W and Heizmann, C W (1996) The S100 family of EF-hand calcium-binding proteins functions and pathology *Trends Biochem Sci* **21**, 134-140

Schibler, M J and Cabral, F (1986) Taxol-dependent mutants of Chinese hamster ovary cells with alterations in alpha- and beta-tubulin *J Cell Biol* **102**, 1522-1531

Schiller, J H (2001) Current standards of care in small-cell and non-small-cell lung cancer *Oncology* **61**, 3-13

Schmitt, M , Harbeck, N , Thomssen, C , Wilhelm, O , Magdolen, V , Reuning, U , *et al* (1997) Clinical impact of the plasminogen activation system in tumour invasion and metastasis Prognostic relevance and target for therapy *Thromb Haemost* **78**, 285-96

Schuette, W (2001) Chemotherapy as treatment of primary and recurrent small cell lung cancer *Lung Cancer* **33**, S99-S107 (Abstract)

Schwab, A , Reinhardt, J , Schneider, S W , Gassner, B and Schuricht, B (1999) K (+) channel-dependent migration of fibroblasts and human melanoma cells *Cell Physiol Biochem* **9**, 126-32

Scotlandi, K , Maim, C , Manara, M C , *et al* (2002) Effectiveness of insulin-like growth factor I receptor antisense strategy against Ewing's sarcoma cells *Cancer Gene Ther* **9**, 296-307

Sekharam, M , Zhao, H , Sun, M , Fang, Q , Zhang, Q , Yuan, Z , Dan, H , Boulware, D , Cheng, J Q and Coppola, D (2003) Insulin-like growth factor I receptor enhances invasion and induces resistance to apoptosis of colon cancer cells through the Akt/Bcl- χ_L pathway *Cancer Res* **63**, 7708-7716

Semizarov, D , Frost, L , Sarthy, A , Kroeger, P , Halbert, D N , Fesik, S W (2003) Specificity of short interfering RNA determined through gene expression signatures *Proc Natl Acad Sci USA*, **100**, 6347-6352

Sharma, S , Stolina, M , Luo, J , Strieter, R M, Burdick, M , Zhu, L X *et al* (2000) Secondary lymphoid tissue cheokine mediated T cell-dependent antitumour responses in vivo *J Immunol* **164**, 4558-63

Shen, C , Buck, A K , Liu, X , Winkler, M , Reske, S N (2003) Gene silencing by adenovirus-delivered siRNA *FEBS Lett* , **539**, 111-114

Shimura, T , Tanenaka, Y , Tsutsumi, S , Hogan, V , Kikuchi, A and Raz, A (2004) Galectin-3, a novel binding partner of β -catenin *Cancer Res* **64**, 6363-67

Shishibori, T , Oyama, Y , Matsushita, O , Yamashita, K , Furuichi, H , Okabe, A , *et al* (1999) Three distinct anti-allergic drugs, amlexanox, cromolyn and tranilast, bind to S100A12 and S100A13 of the S100 protein family *J Biochem* **338**, 583-589

Sledz, C A , Holko, M , de Veer, M J , Silverman, R H , Williams, B R (2003) Activation of the interferon system by short-interfering RNAs *Nat Cell Biol* , **5**, 834-839

Smirnov, D A , Zweitzig, D R , Foulk, B W , Craig Miller, M , Doyle, G V , Pienta, K J , Meropol, N J , Weiner, L M , Cohen, S J , Moreno, J G , Connelly, M C , Terstappen, L W M M and O' Hara, S M (2005) Global gene expression profiling of circulating tumour cells *Cancer Res* **65(12)** 4993-4887

Song, S W , Fuller, G N , Khan, A , Kong, S , Shen, W , Taylor, E , *et al* (2003) Iip45, an insulin-like growth factor binding protein 2 (IGFBP-2) binding protein, antagonizes IGFBP-2 stimulation of glioma cell invasion *PNAS* **100**, 13970-75

Spratt, J S , Greenberg, R A and Heuser, L S (1986) Geometry, growth rates and duration of cancer and carcinoma in situ of the breast before detection by screening *Cancer Res* **46**, 970-974

Sprecher CA, Kisiel W, Mathewes S, Foster DC (1994) Molecular cloning, expression, and partial characterization of a second human tissue-factor-pathway inhibitor *Proc Natl Acad Sci USA* **91**, 3353-7

Sprenger, A , Schardt, C , Rotsch, M , Zehrer, M , Wolf, M , Havemann, K and Heymanns, J (1997) Soluble intercellular adhesion molecule-1 in patients with lung cancer and benign lung diseases *J Cancer Res Clin Oncol* **123**, 632-8

Stewart, S A , Dykxhoorn, D M , Palliser, D , Mizuno, H , Yu, E Y , An, D S , Sabatmi, D M , Chen, I S , Hahn, W C , Sharp, P A , Weinberg, R A , Novina, C D (2003) Lentivirus-delivered stable gene silencing by RNAi in primary cells *RNA*, **9**, 493-501

Strieter, R M , Polverini, P J , Kunkel, S L , Arenberg, D A , Burdick, M D , Kasper, J *et al* (1995) The functional role of the ELR motif in CXC chemokine-mediated angiogenesis *J Biol Chem* **270**, 27348-57

Stringer, B K , Cooper, A G and Shepard, S B (2001) Overexpression of the G-protein inwardly rectifying potassium channel 1 (GIRK1) in primary breast carcinomas correlates with axillary lymph node metastasis *Cancer Res* **61**, 582-88

Suganuma, K , Kubota, T , Saikawa, Y , Abe, S , Otani, Y , Furukawa, T , Kumai, K , Hasegawa, H , Watanabe, M , Kitajima, M , Nakayama, H , Okabe, H (2003) Possible chemoresistance-related genes for gastric cancer detected by cDNA microarray *Cancer Sci* , **94**, 355-359

Sui, G., Soohoo, C., Affar, B., Gay, F., Shi, Y., Forrester, W.C., Shi, Y. (2002). A DNA vector-based RNAi technology to suppress gene expression in mammalian cells. *Proc. Natl. Acad. Sci. USA*, **99**, 5515-5520.

Sukoh, N., Abe, S., Ogura, S. *et al.* (1994). Immunohistochemical study of cathepsin B. Prognostic significance in human lung cancer. *Cancer*. **74**, 46-51.

Sun, J. J., Zhou, X. D., Liu, Y. K., Tang, Z. Y., Feng, J. X., Zhou, G., Xue, Q and Chen, J. (1999). Invasion and metastasis of liver cancer: expression of intercellular adhesion molecule 1. *J Cancer Res Clin Oncol*. **125**, 28-34.

Suzuki, H., Itoh, F., Toyota, M., Kikuchi, T. and Imai, K. (2000). Inactivation of the 14-3-3 sigma gene is associated with 5' CpG island hypermethylation in human cancers. *Cancer Res*. **60**, 4353-7.

Symons, M. and Settleman, J. (2000). Rho family GTPases: more than simple switches. *Trends Cell Biol*. **10**, 415-19.

Sympson, C. J., Bissell, M. J. and Werb, Z. (1995). Mammary gland tumour formation in transgenic mice overexpressing stromelysin-1. *Semin Cancer Biol*. **6**, 159-63.

Taguchi, O., Gabazza, E. C., Kobayashi, T., Yoshida, M., Yasui, H. and Kobayashi, H. (1997). Circulating intercellular adhesion molecule-1 in patients with lung cancer. *Intern Med*. **36**, 14-8.

Talhok, R. S., Bisell, M. J. and Werb, Z. (1992). Coordinated expression of extracellular matrix degrading proteinases and their inhibitors regulate mammary epithelial function during involution. *J Cell Biol*. **118**, 1271-1282.

Talmadge, J. E., Wolman, S. R. and Fidler, I. J. (1982). Evidence for the clonal origin of spontaneous metastasis. *Science*. **217**, 361-363.

Tanno, S., Mitsuuchi, Y., Altomare, D. A., Xiao, G. H. and Testa, J. R. (2001). AKT activation up-regulates insulin-like growth factor I receptor expression and promotes invasiveness of human pancreatic cancer cells. *Cancer Res*. **61**, 589-93.

Taylor, W R and Stark, G R (2001) Regulation of the G2/M transition by p53
Oncogene **20**, 1803-15

Tetsu, O , and McCormick, F (1999) Beta-catenin regulates expression of cyclin D1
in colon carcinoma cells *Nature* **398**, 422–426

Tiscornia, G , Singer, O , Ikawa, M , Verma, I M (2003) A general method for gene
knockdown in mice by using lentiviral vectors expressing small interfering RNA
Proc Natl Acad Sci USA, **100**, 1844-1848

Tompkins S M , Lo C Y , Tumpey T M , and Epstein S L (2004) Protection against
lethal influenza virus challenge by RNA interference *in vivo* *Proc Natl Acad Sci USA*
101, 8682–8686

Tong X, O'Kelly J, Xie D, Mori A, Lemp N, McKenna R, Miller CW, Koeffler HP
(2004) Cyr61 suppresses the growth of non-small-cell lung cancer cells via the beta-
catenin-c-myc-p53 pathway *Oncogene* **23**, 4847-55

Tuck, A B , Wilson, S M , Khokha, R and Chambers, A F (1991a) Different
patterns of gene expression in ras-resistant and ras-sensitive cells *J Natl Cancer Inst*
83(7), 485-491

Tuck, A B , Wilson, S M , Sergovich , F R and Chambers, A F (1991b) Gene
expression and metastasis of somatic cell hybrids between murine fibroblast cell lines
of different malignant potential *Somat Cell Mol Genet* **17(4)**, 377-389

Umbricht, C B , Evron, E , Gabrielson, E , Ferguson, A, Marks, J and Sukumar, S
(2001) Hypermethylation of 14-3-3 sigma (stratifin) is an early event in breast cancer
Oncogene **20**, 3348-53

Van't Veer L J , Dai, H , van de Vijver M J , He Y D , Hart A A M , Mao M ,
Peterse H L , van der Koo K , Marton M J *et al* (2002) Gene expression profiling
predicts clinical outcome of breast cancer *Nature* **415**, 530-536

Van't Veer, L J and Weigelt, B (2003) Road map to metastasis *Nat Med* **9(8)**, 999-1000

Vicari, A P , Ait-Yahia, S , Chemin, K , Mueller, A , Zlotnik, A and Caux, C (2000) Antitumour effects of the mouse chemokine 6Ckine/SLC through angiostatic and immunological mechanisms *J Immunol* **165**, 1992-2000

Wang, W , Wyckoff, J B , Frohlich, V C , Oleynikov, Y , Huttelmaier, S , Zavadil, J *et al* (2002) Single cell behaviour in metastatic primary mammary tumours correlated with gene expression patterns revealed by molecular profiling *Cancer Res* **62**, 6278-88

Wang, Z (2004) Roles of K⁺ channels in regulating tumour cell proliferation and apoptosis *Pflugers Arch* **448**, 274-86

Wani, M C , Taylor, H L , Wall, M E , Coggon, P and McPhail, A T (1971) Plant anti-tumour agents VI The isolation and structure of taxol, a novel antileukemic and anti tumour agent from *taxus brevifolia* *J Am Chem Soc* **93**, 2325

Wary, K K , Manero, F, Isakoff, S J , Mercantonio, E E and Giancosti, F G (1996) The adaptor protein Shc couples a class of integrins to the control of cell cycle progression *Cell* **87**, 733-743

Watt PM, Kumar R, Kees UR (2000) Promoter demethylation accompanies reactivation of the HOX11 proto-oncogene in leukemia *Genes Chromosomes Cancer* **29**, 371-7

Weigelt B , Hu Z , He X , Livasy C , Carey L A , Ewend M G , Glas A M , Peron C M and Van't Veer, L J (2005) Molecular portraits and 70-gene prognosis signature are preserved through the molecular process of breast cancer *Cancer Res* **65(20)**, 9155-9158

Werner, H , Karnieli, E , Rauscher, F J and LeRoith, D (1996) Wild-type and mutant p53 differentially regulate transcription of the insulin-like growth factor I receptor gene *Proc Natl Acad Sci USA* **93**, 8318-23

Wicki, R , Schafer, B W , Erne, P and Heizmann, C W (1996) Characterisation of the human and mouse cDNAs coding for S100A13, a new member of the S100 protein family *Biochem Biophys Res Comm* **227**, 594-99

Wilson, C L , Heppner, K J , Labosky, P A , Hogan, B L and Matrisian, L M (1997) Intestinal tumourigenesis is suppressed in mice lacking the metalloproteinase matrilysin *Proc Natl Acad Sci USA* **94**, 1402-7

Wilson, L , Creswell, K M and Chin, D (1975) The mechanism of action of vinblastine Binding of [acetyl-3H]vinblastine to embryonic chick brain tubulin and tubulin from sea urchin sperm tail outer doublet microtubules *Biochemistry* **14**, 5586

Wojtukiewicz MZ, Sierko E, Zimnoch L, Kozłowski L, Kisiel W (2003) Immunohistochemical localization of tissue factor pathway inhibitor-2 in human tumor tissue *Thromb Haemost* **90**, 140-6

Yanamandra N, Kondraganti S, Gondi CS, Gujrati M, Olivero WC, Dinh DH, Rao JS (2005) Recombinant adeno-associated virus (rAAV) expressing TFPI-2 inhibits invasion, angiogenesis and tumor growth in a human glioblastoma cell line *Int J Cancer* 2005 Feb 18, [Epub ahead of print]

Yang, H Y , Wen, Y Y , Chen, C H , Lozano, G and Lee M H (2003) 14-3-3 sigma positively regulates p53 and suppresses tumour growth *Mol Cell Biol* **23**, 7096-107

Yano, S , Muguruma, H , Matsumori, Y , Goto, H , Nakataki, E , Edakuni, N *et al* (2005) Antitumour vascular strategy for controlling experimental metastatic spread of human small cell lung cancer cells with ZD6474 in natural killer cell-depleted severe combined immunodeficient mice *Clin Can Res* **11(24)**, 8789-8798

Yee, D (2006) Targeting insulin-like growth factor pathways *B J Cancer* **94**, 465-468

Yost, C , Torres, M , Miller, J R , Huang, E , Kimelman, D , and Moon, R T (1996) The axis-inducing activity, stability, and subcellular distribution of beta-catenin is

regulated in *Xenopus* embryos by glycogen synthase kinase 3 *Genes Dev* **10**, 1443–1454

Yu, D , Shi, D , Scanlon, M and Hung, M C (1993) Reexpression of neu-encoded oncoprotein counteracts the tumour-suppressing but not the metastasis-suppressing function of E1A *Cancer Res* **53**, 5784-5790

Yu, Q and Stamenkovic, I (2000) Cell surface-localised matrix metalloproteinase-9 proteolytically activates TGF-beta and promotes tumour invasion and angiogenesis *Genes Dev* **14**, 163-76

Yurcheno, R D and Schittny, J C (1990) Molecular architecture of basement membranes *FAESB J* **4**, 1577

Zeng, Y , Yi, R , Cullen, B R (2003) MicroRNAs and small interfering RNAs can inhibit mRNA expression by similar mechanisms *Proc Natl Acad Sci USA* , **100**, 9779-9784

Zhang N, Gong ZZ, Minden M, Lu M (1993) The HOX-11 (TCL-3) homeobox proto-oncogene encodes a nuclear protein that undergoes cell cycle-dependent regulation *Oncogene* **8**, 3265-70

Zhang N, Shen W, Hawley RG, Lu M (1999) HOX11 interacts with CTF1 and mediates hematopoietic precursor cell immortalization *Oncogene* **18**, 2273-9

Zhang X, Shan P, Jiang D, Noble P W , Abraham N G , Kappas A *et al* (2004) Small interfering RNA targeting heme oxygenase-1 enhances ischemia-reperfusion-induced lung apoptosis *J Biol Chem* **279**, 10677–10684

Zhang, Y , Karas, M , Zhao, H , Yakar, S and LeRoith, D (2004) 14-3-3 σ mediation of cell cycle progression is p53-independent in response to insulin-like growth factor-1 receptor activation *J Biol Chem* **279**, 34353-60

Zhao, D H , Hong, J J , Guo, S Y , Yang, R L , Yuan, J , Wen, C J , Zhou, K Y , and Li, C J (2004) Aberrant expression and function of TCF4 in the proliferation of hepatocellular carcinoma cell line BEL-7402 *Cell Research* **14**, 74-80

Zheng Z H , Sun X J , Zhou H T , Shang C Ji H and Sun K L (2005) Analysis of metastasis suppressing function of E-cadherin in gastric cancer cells by RNAi *World J Gastroenterol* **11(13)**, 2000-2003

Zhong R, Huang RB, Song SJ (2003) Role of tissue factor pathway inhibitor-2 in ovarian tumor migration and invasion *Ai Zheng* **22**, 1038-41

Zhou Q, Kwan HY, Chan HC, Jiang JL, Tam SC, Yao X (2003) Blockage of voltage-gated K⁺ channels inhibits adhesion and proliferation of hepatocarcinoma cells *Int J Mol Med* **11**, 261-6

Yoshida H, Feig JE, Morrissey A, Ghu IA, Artman M, Coetzee WA (2004) KATP channels of primary human coronary artery endothelial cells consist of a heteromultimeric complex of Kir6 1, Kir6 2, and SUR2B subunits *J Mol Cell Cardiology* **37**, 857-869

Section 7.0: Appendices

7.1 Appendix 1 – RT-PCR investigation of genes with increased expression in the invasive DLKP variants from microarray analysis

Semi quantitative RT-PCR was used to confirm that expression changes in the array data were reflected in the cell lines studied

To ensure that results from the array study matched to independent analysis of the cell lines, RNA samples from the preliminary Affymetrix array study by Dr Rasha Linehan in 2003, RNA from the duplicate array samples 2004, RNA from a fresh set of cultures harvested separately to those for array analysis including RNA from three samples analysed on the Agilent array platform and RNA from cells with increasing passage number were included in this analysis. The Agilent data was not analysed further in this work

In all of the PCRs in this section β -actin was used as an endogenous control to normalise for RNA quantities added to each reaction. The reactions were analysed by gel electrophoresis (GE) on a 2% agarose gel. cDNA negative control (cDNA neg) consisted of PCR master mix with cDNA but without addition of Taq enzyme. PCR negative controls consisted of PCR master mix to which no cDNA template was added. Densitometric values were normalised by dividing target intensity values by β -actin intensity values and were graphed for each sample. The gels included in this section are representative of at least two independent repeats

7.1.1 AKAP11

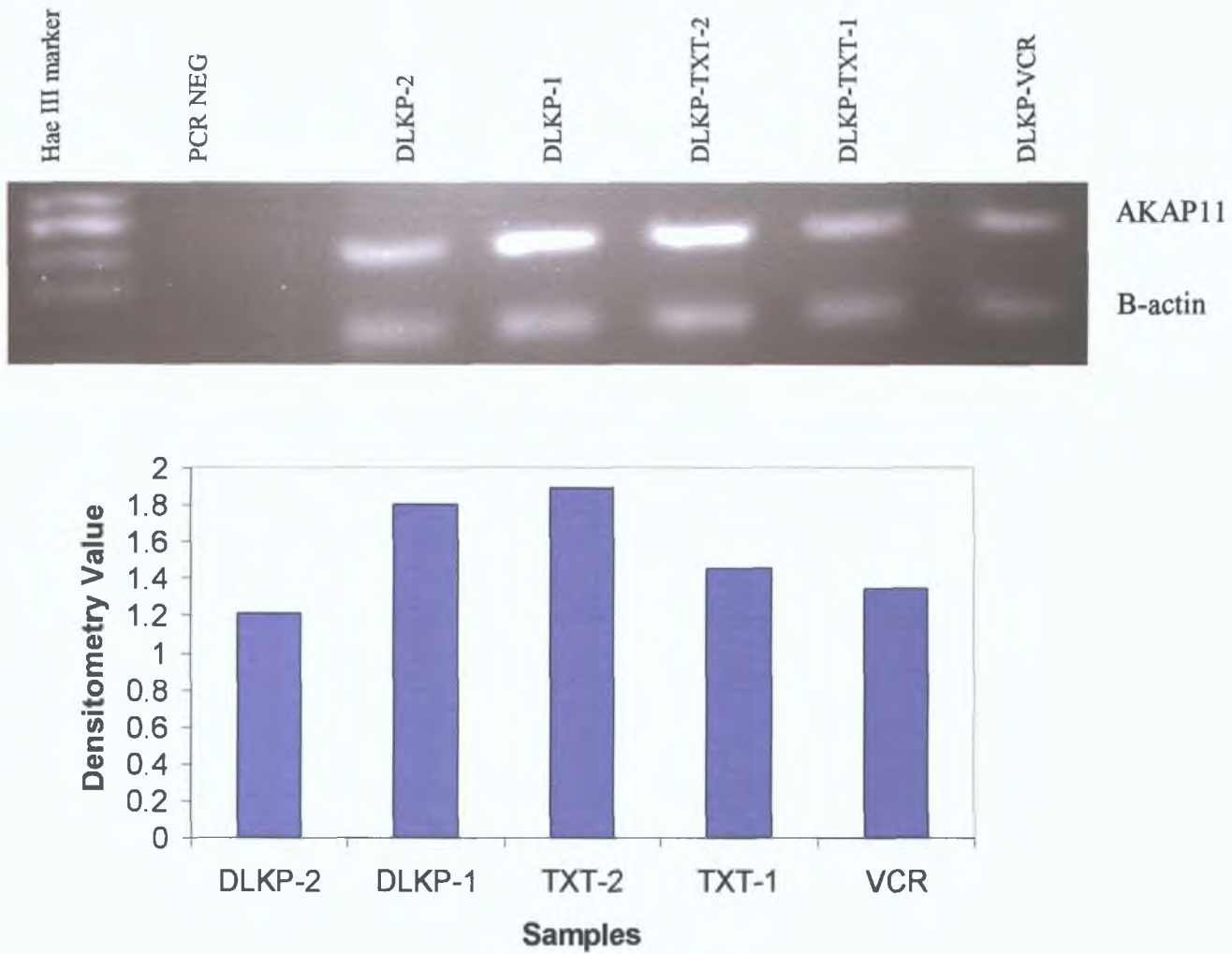


Figure 7.1.1.1 RT-PCR of AKAP11 expression from RNA used in array samples 2003.

The band size for AKAP11 was 233bp.

7.1.2 BCHE

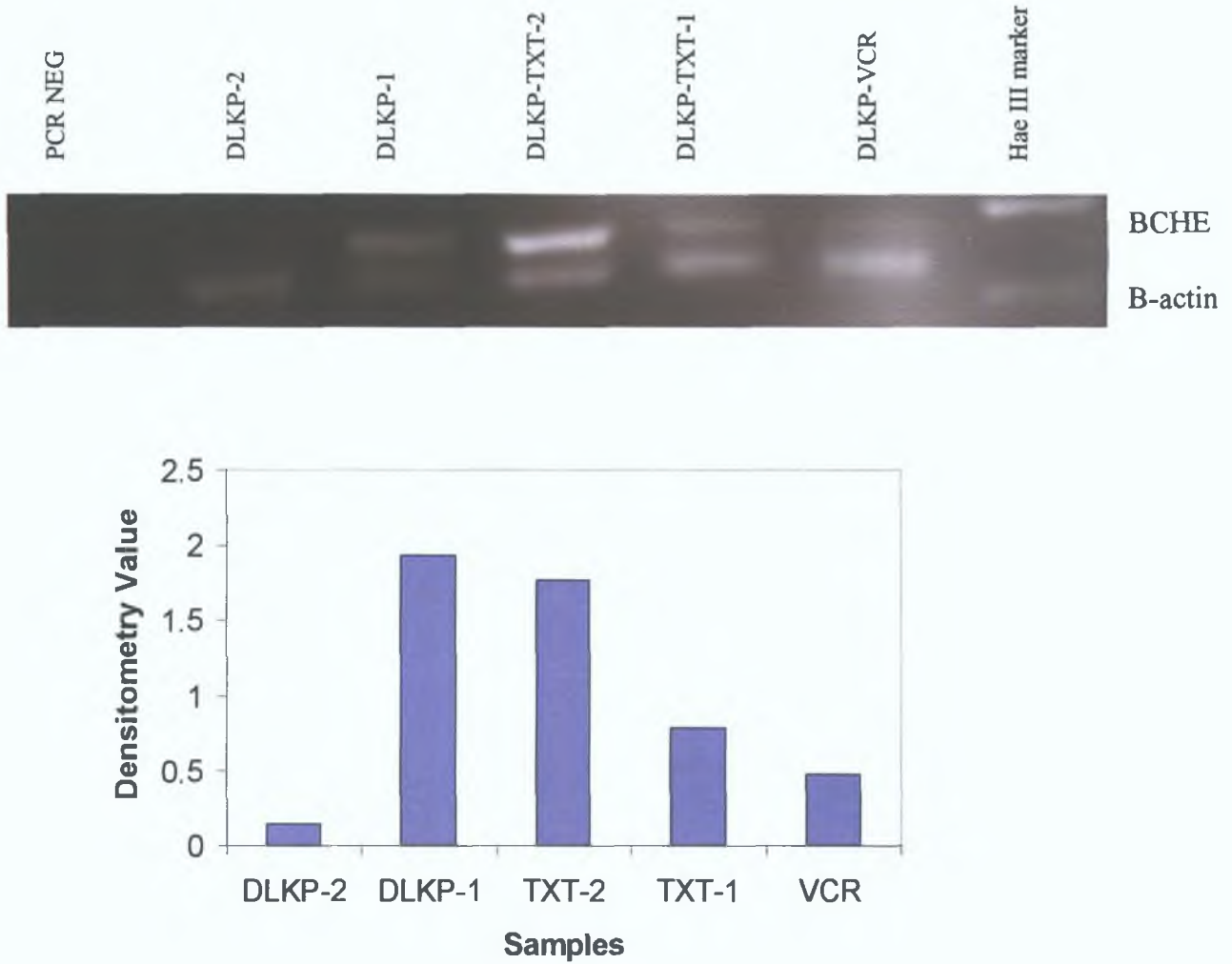


Figure 7.1.2.1 RT-PCR of BCHE expression from RNA used in array samples 2003.

The band size for BCHE was 180bp.

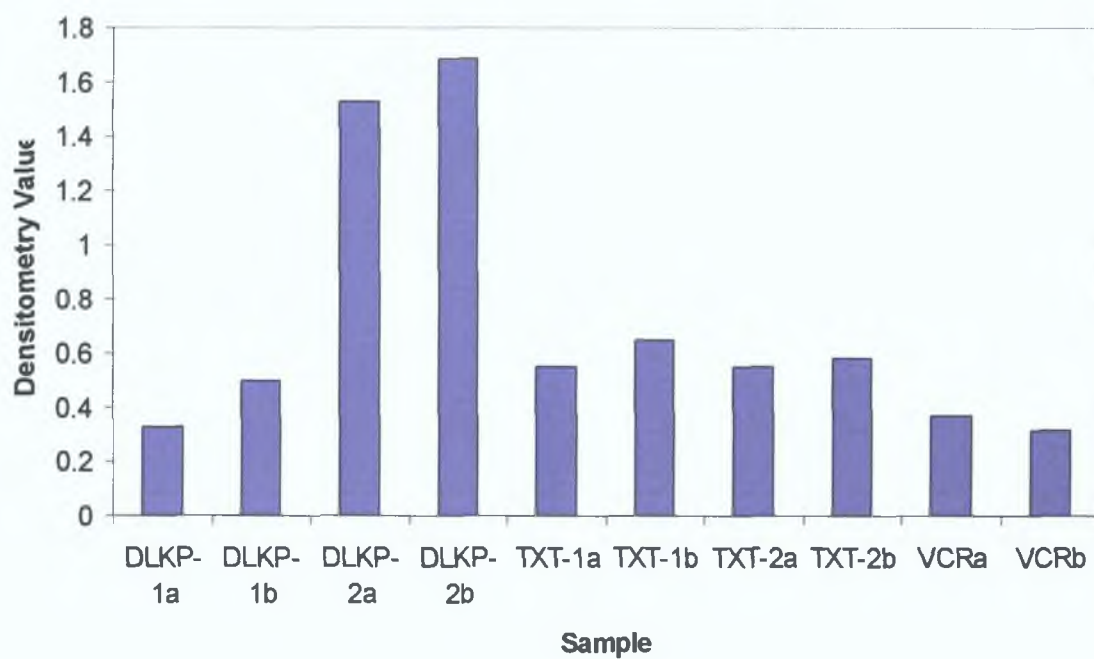
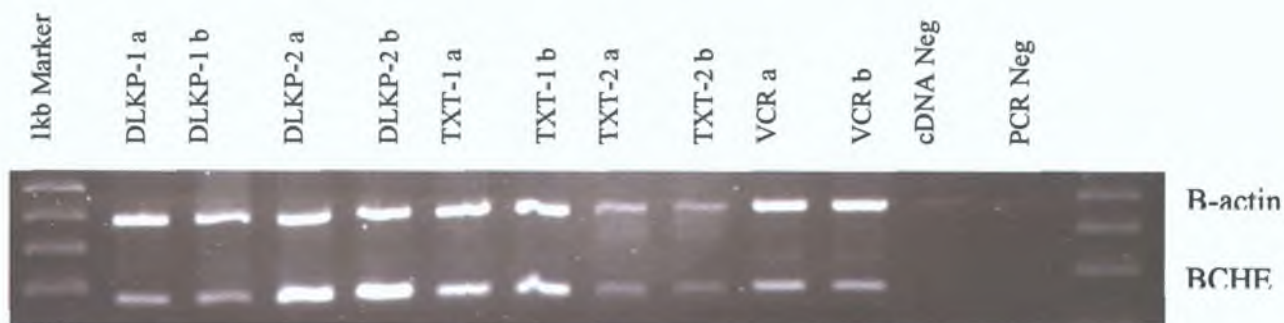


Figure 7.1.2.2 RT-PCR of BCHE mRNA expression from RNA used in duplicate array samples 2004.

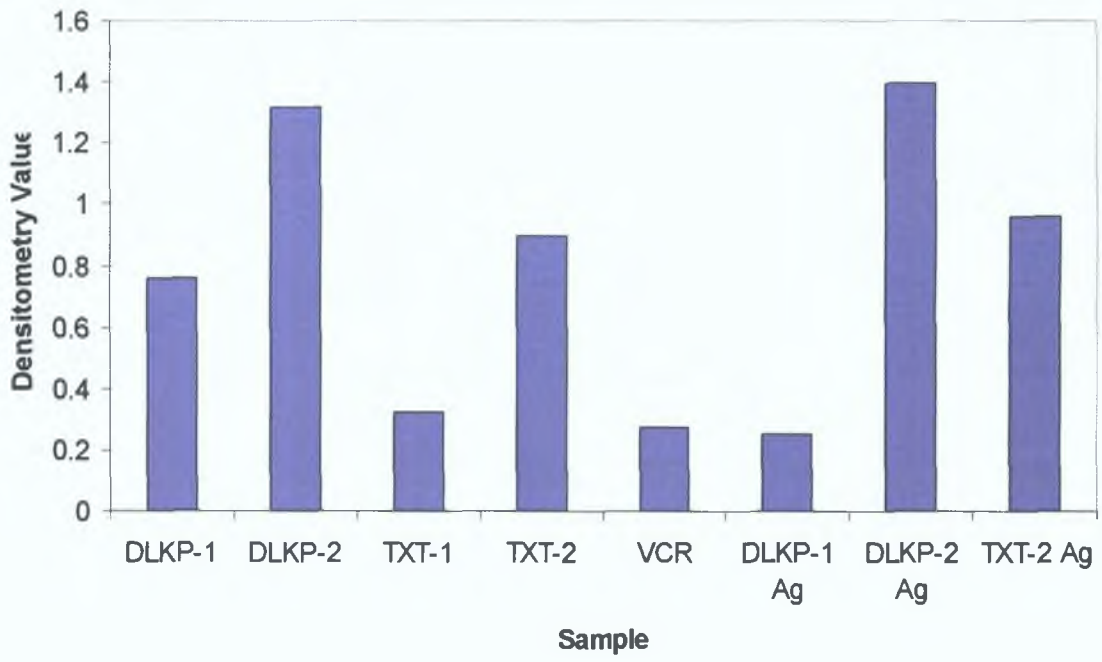


Figure 7.1.2.3 RT-PCR of BCHE mRNA in a separate sample set and Agilent samples.

7.1.3 CYB5R2

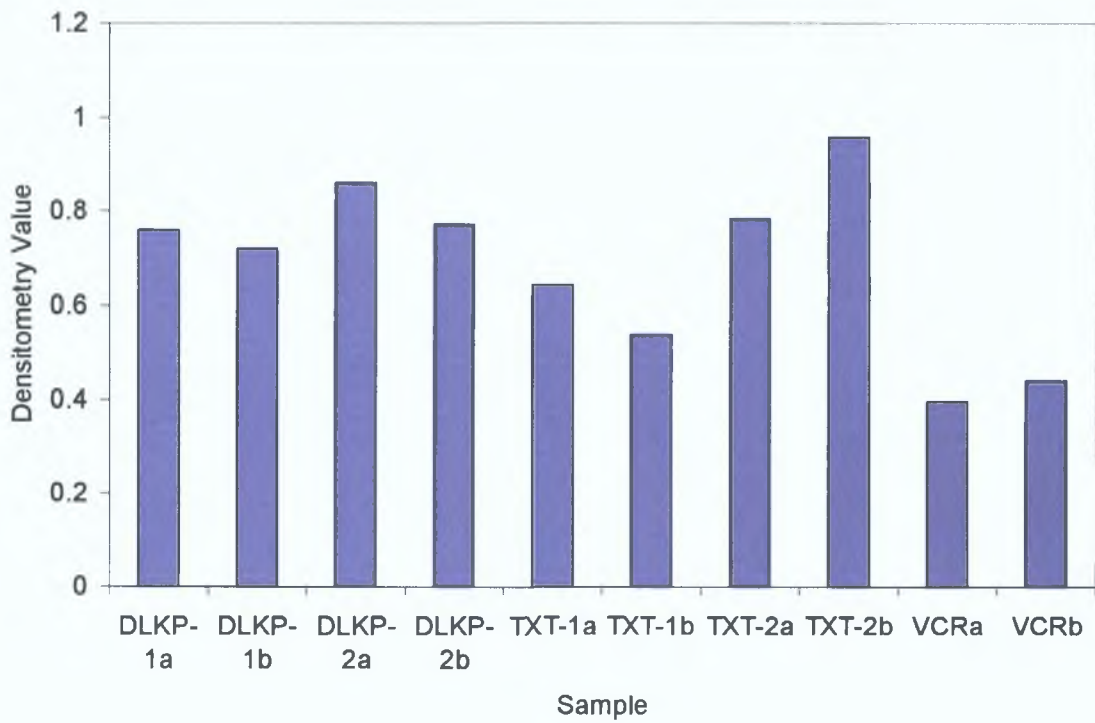
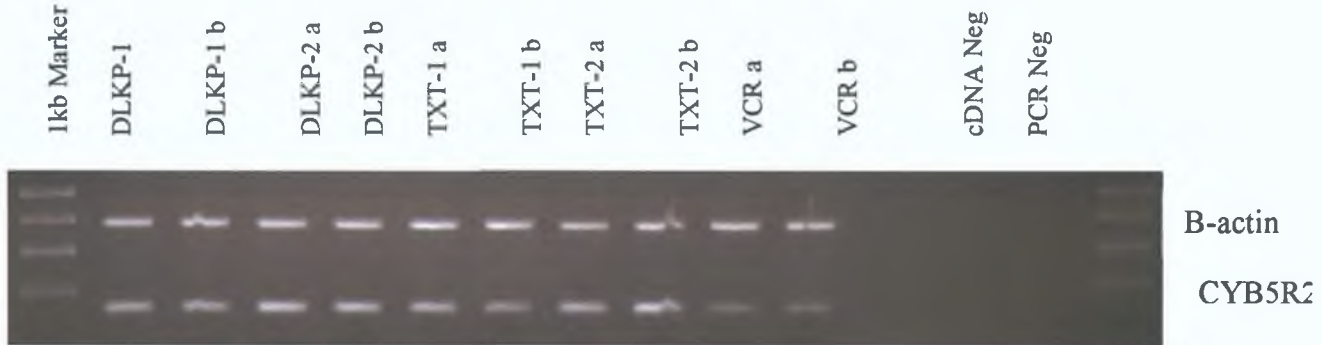


Figure 7.1.3.1 RT-PCR of CYB5R2 mRNA expression from RNA used in duplicate array samples 2004.

The band size size for CYB5R2 is 172bp.

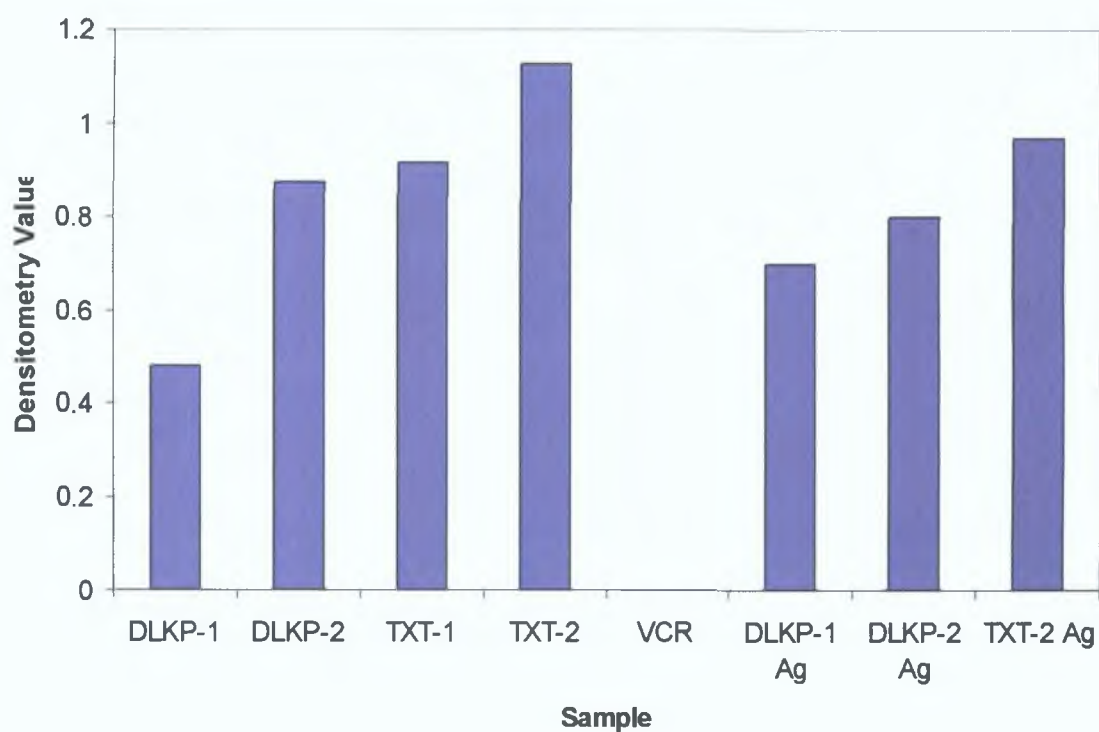


Figure 7.1.3.2 RT-PCR of CYB5R2 mRNA in a separate sample set and Agilent samples.

7.1.4 EFNB2

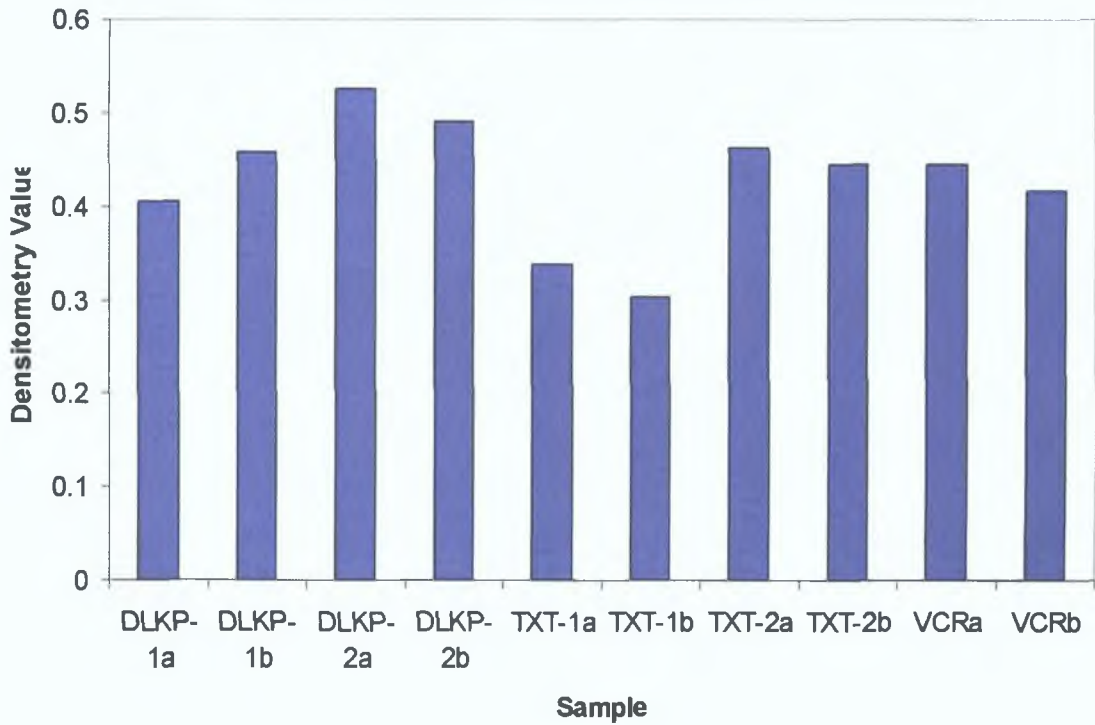
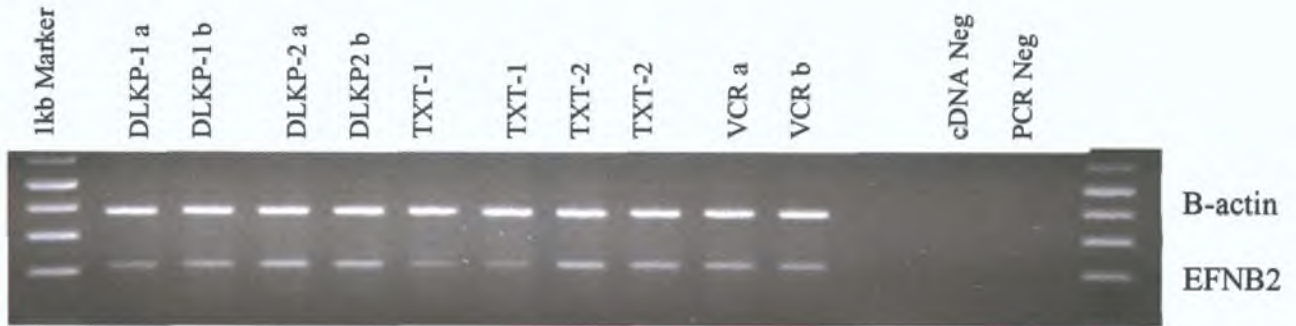


Figure 7.1.4.1 RT-PCR of EFNB2 mRNA expression from RNA used in duplicate array samples 2004.

The band size size for EFNB2 is 220bp.

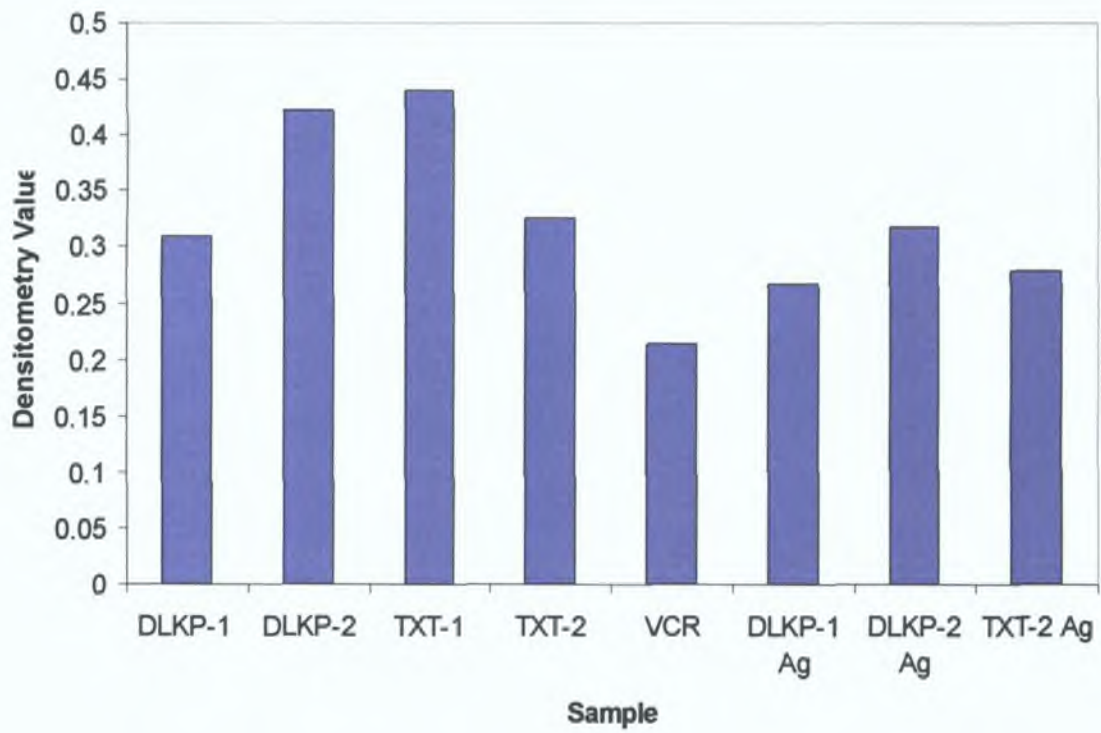
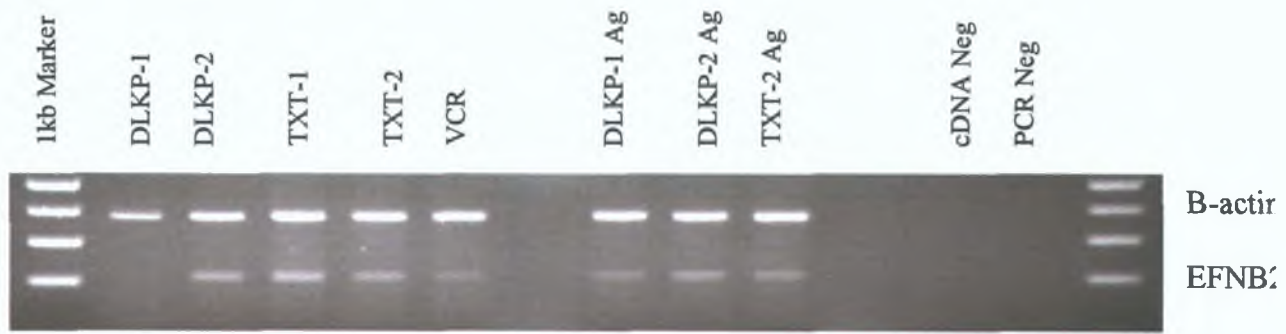


Figure 7.1.4.2 RT-PCR of EFNB2 mRNA in a separate sample set and Agilent samples.

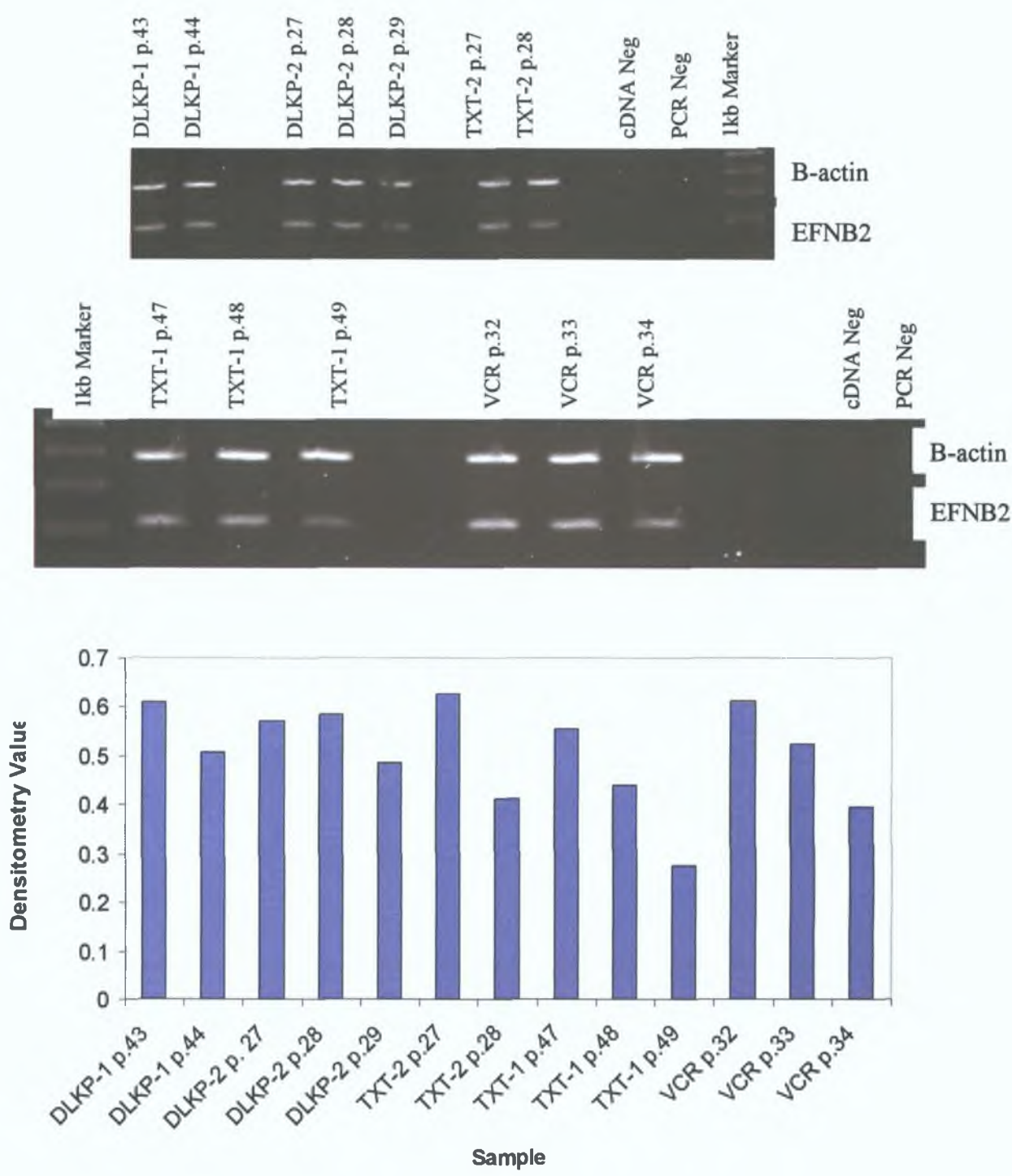


Figure 7.1.4.3 RT-PCR of EFNB2 mRNA in samples with increasing passage number.

7.1.5 GLP1R

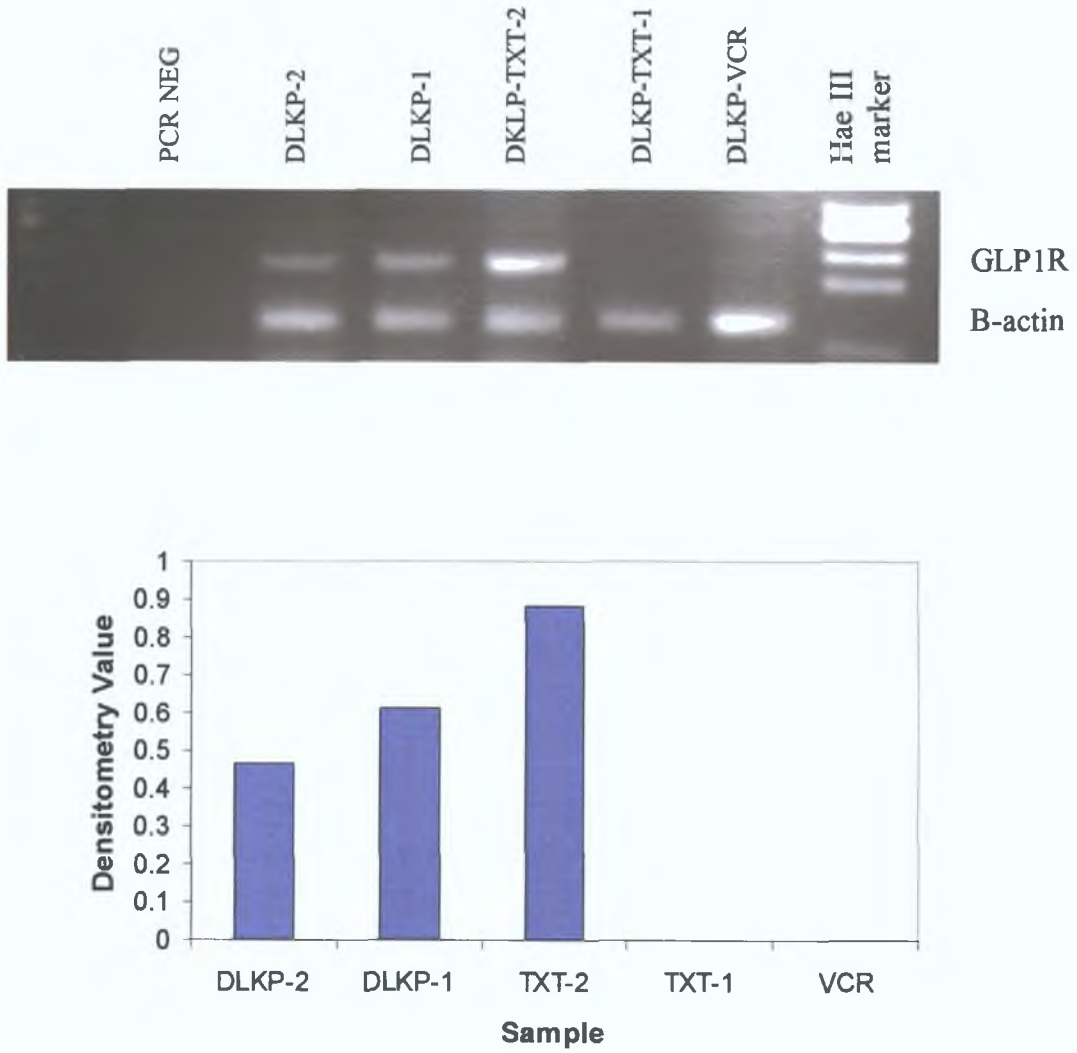


Figure 7.1.5.1 RT-PCR of GLP1R expression from RNA used in array samples 2003.

The band size for GLP1R was 228bp.

7.1.6 ICAM1

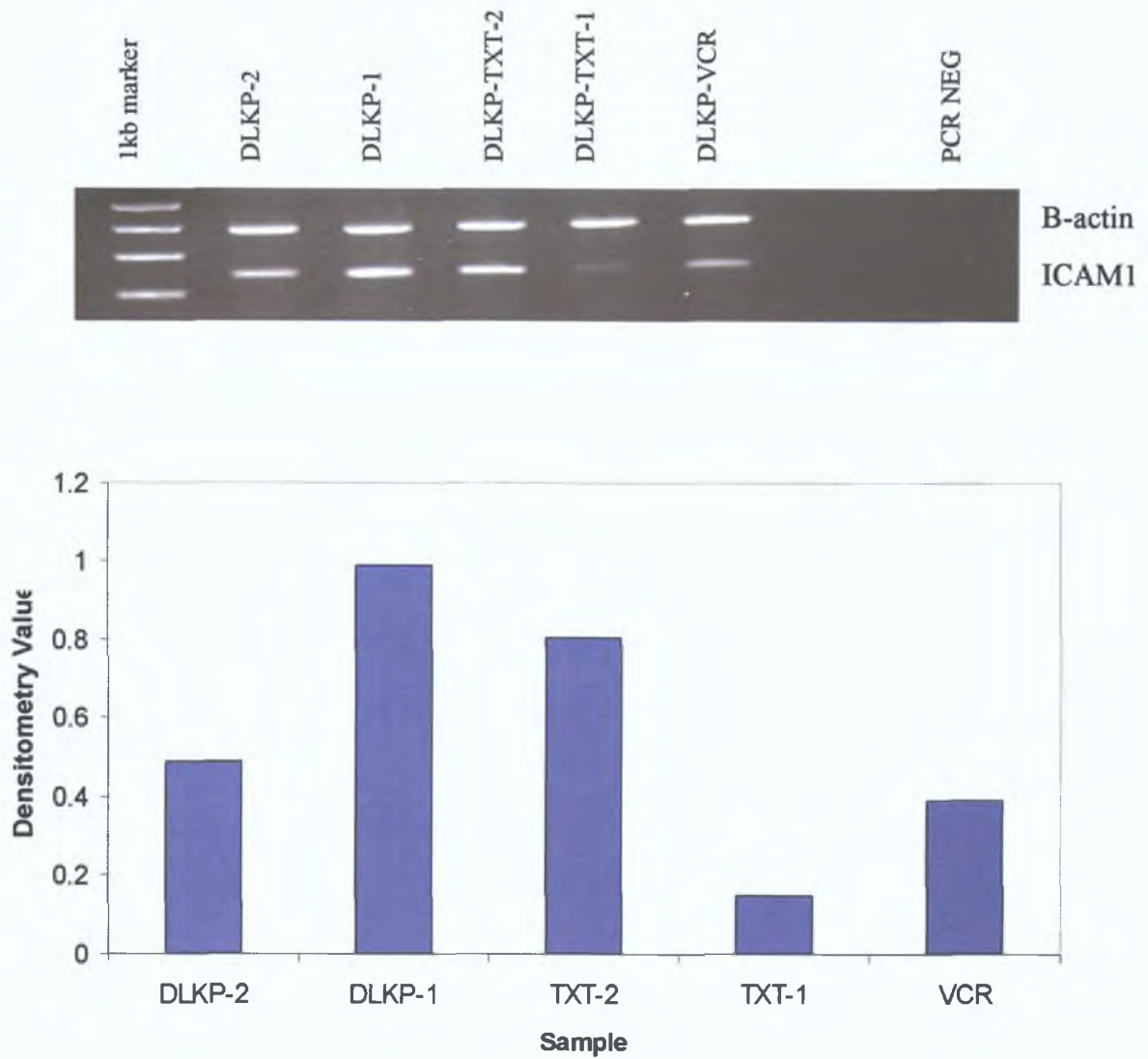


Figure 7.1.6.1 RT-PCR of ICAM1 expression from RNA used in array samples 2003.

The band size for ICAM1 was 245bp.

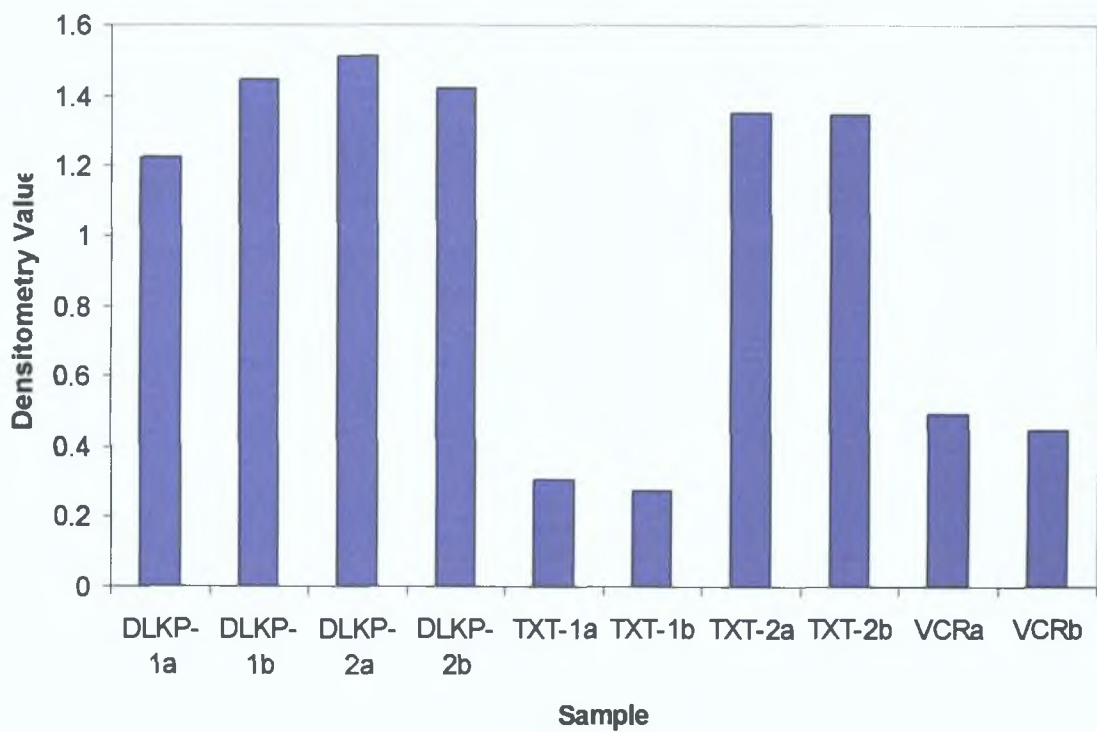


Figure 7.1.6.2 RT-PCR of ICAM1 mRNA expression from RNA used in duplicate array samples 2004.

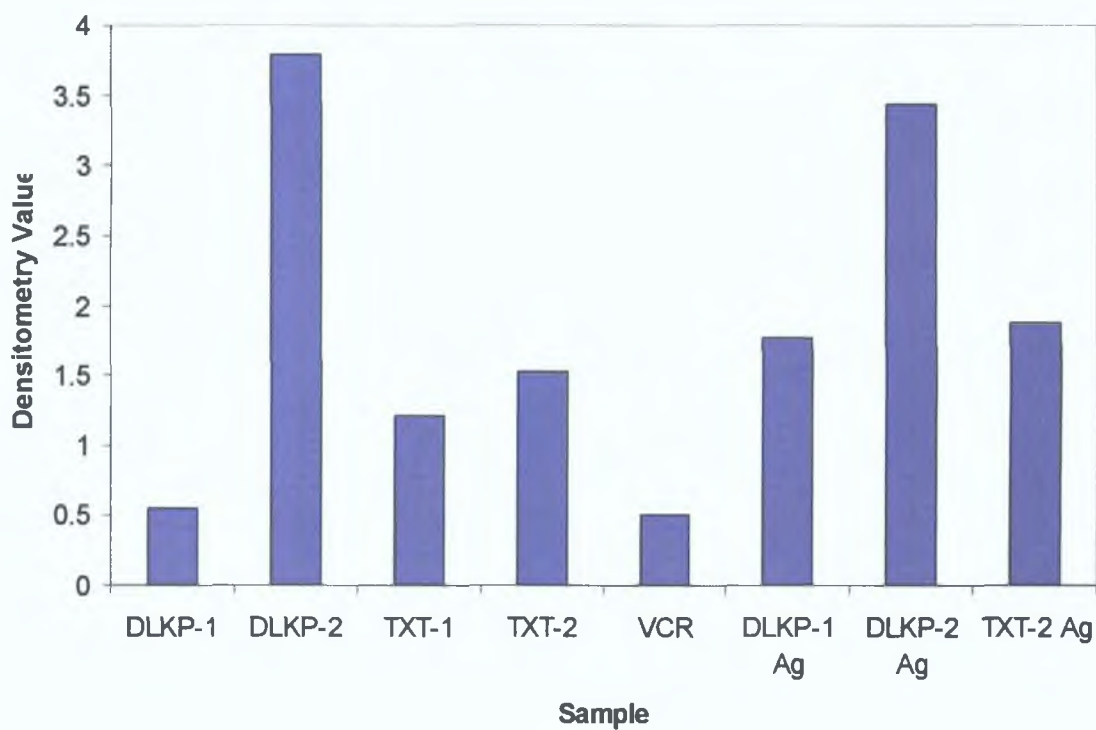


Figure 7.1.6.3 RT-PCR of ICAM1 mRNA in samples in a separate sample set and Agilent samples.

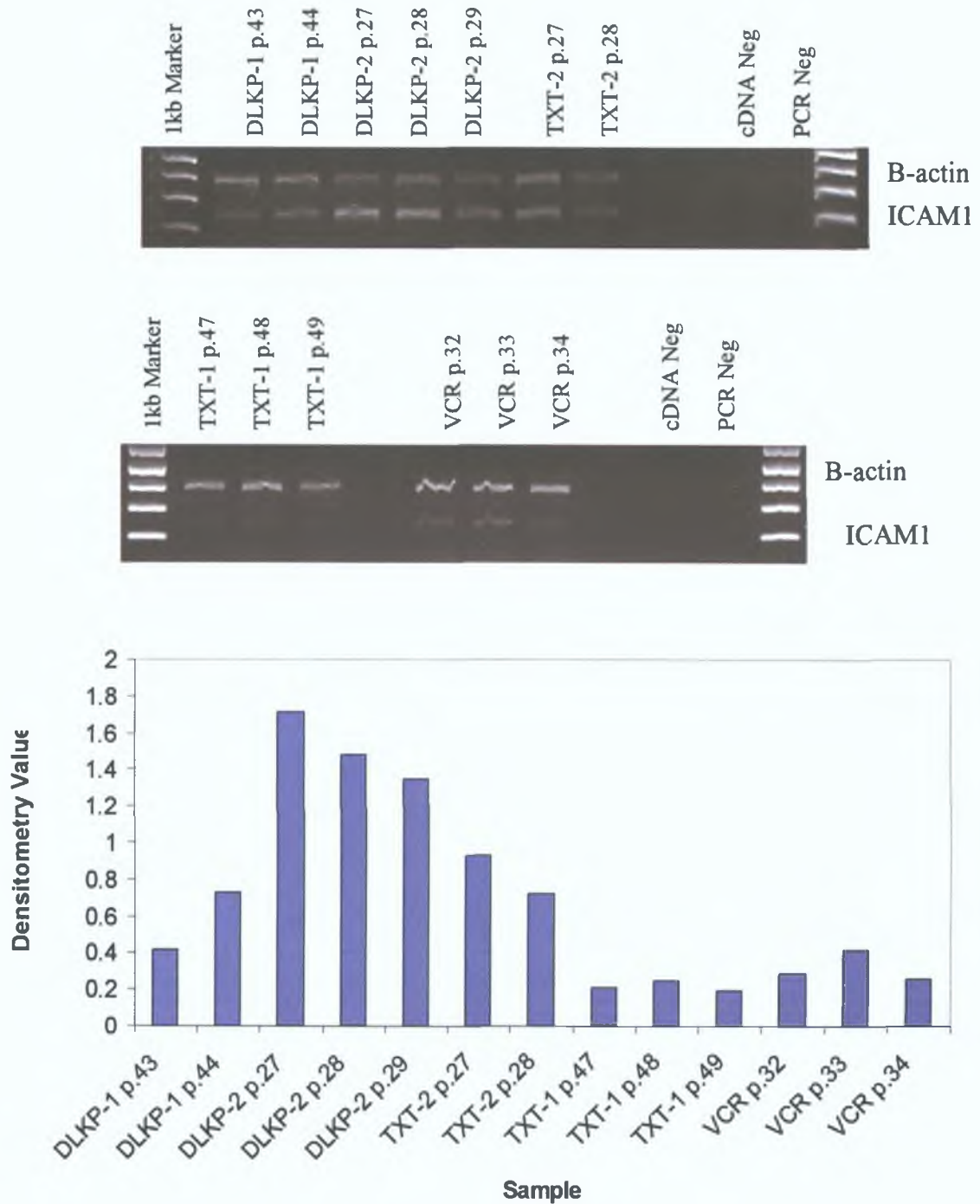


Figure 7.1.6.4 RT-PCR of ICAM1 mRNA in samples with increasing passage number.

7.1.7 IGF1R

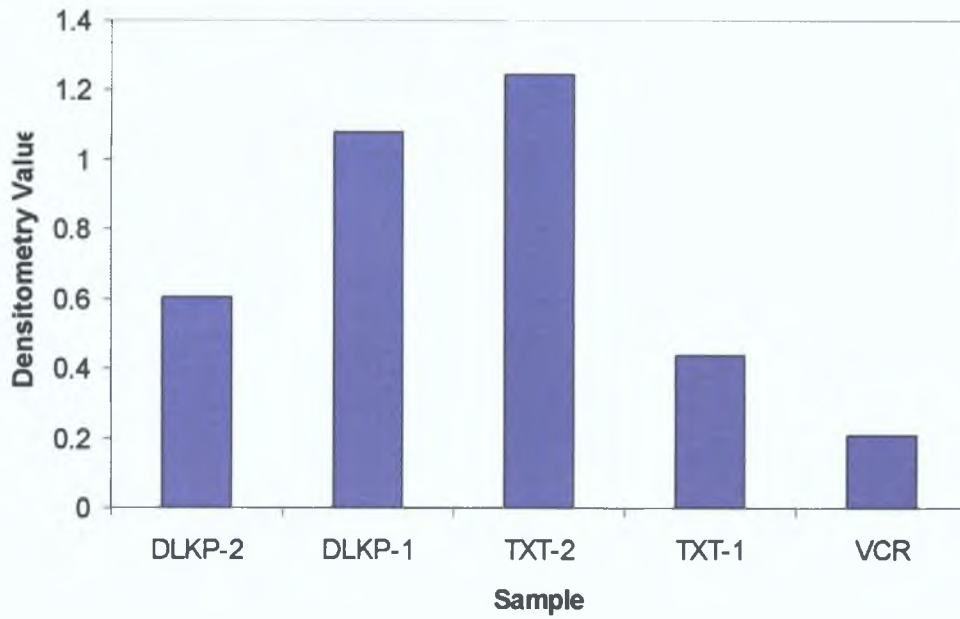
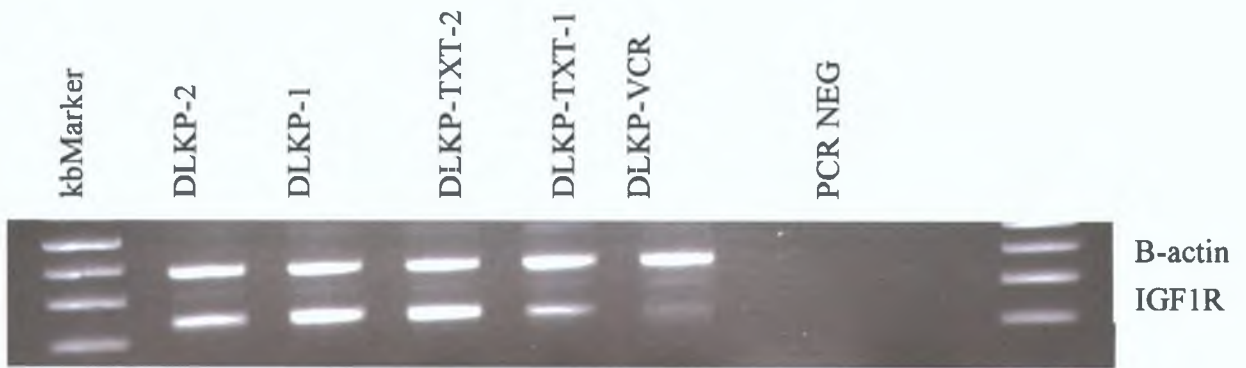


Figure 7.1.7.1 RT-PCR of IGF-1R expression from RNA used in array samples 2003.

The band size for IGF-1R was 241bp.

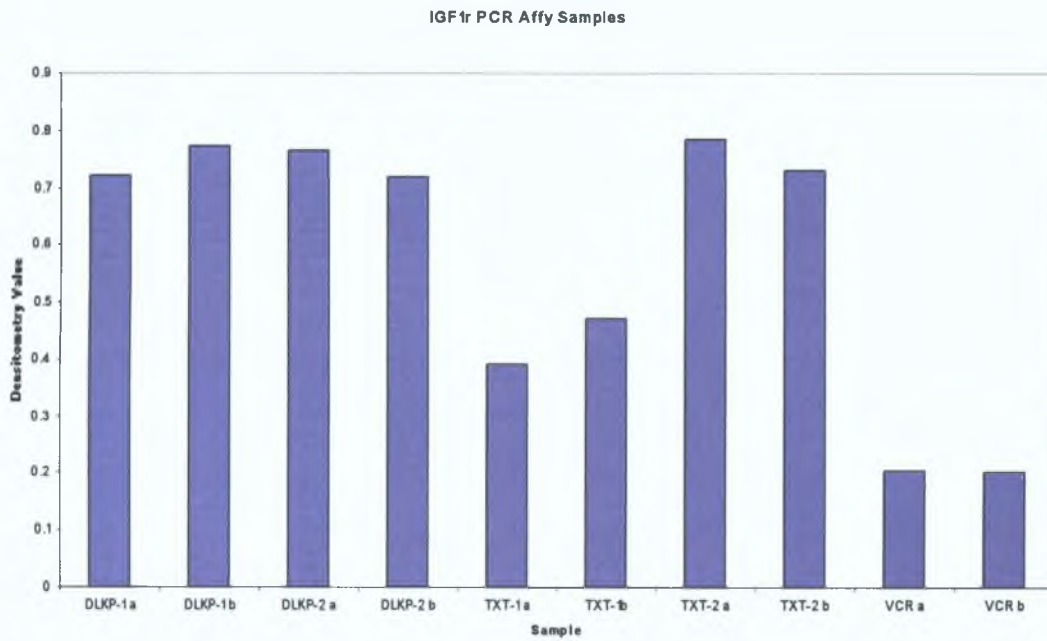
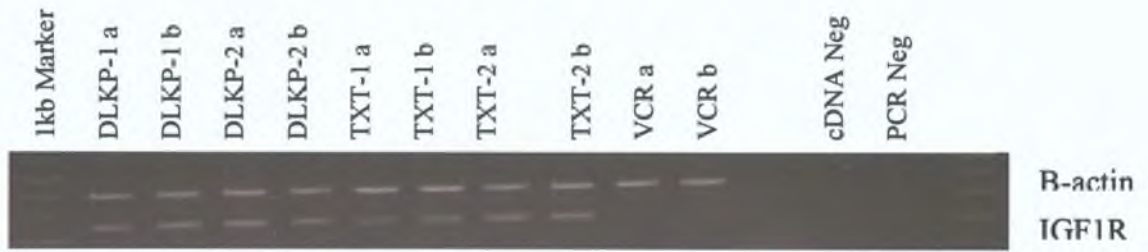


Figure 7.1.7.2 RT-PCR of IGF-1R mRNA expression from RNA used in duplicate array samples 2004.

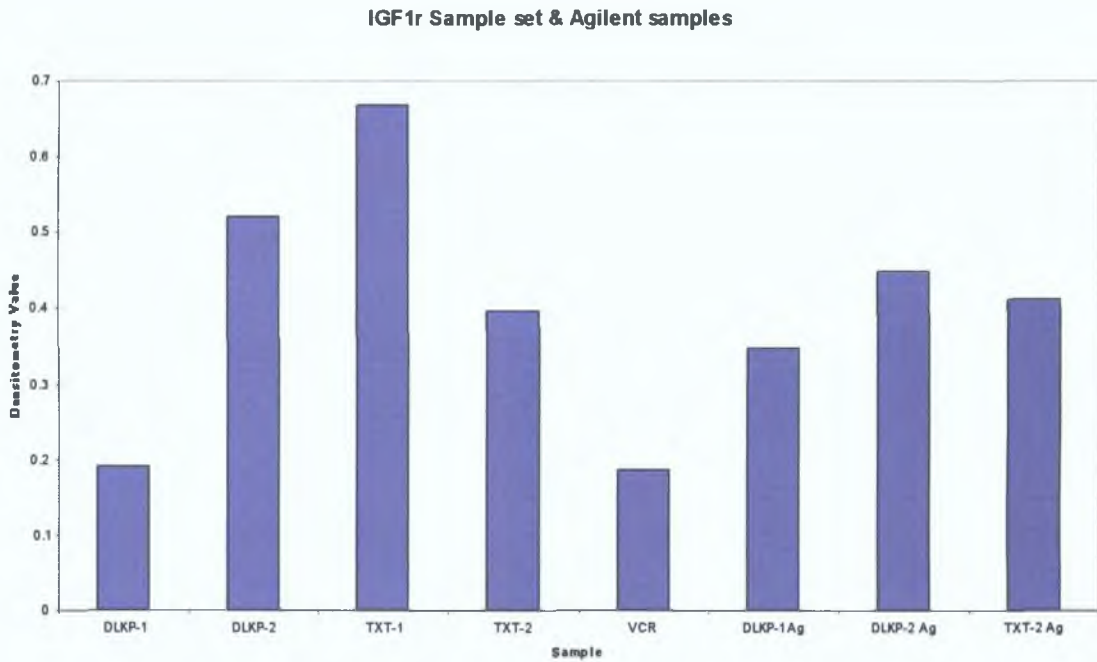
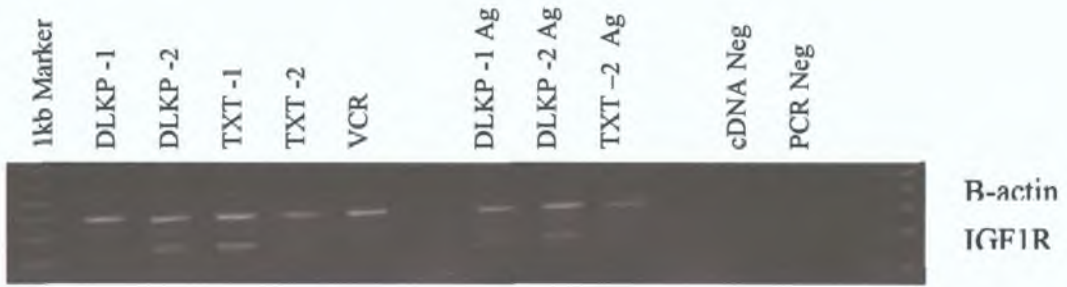


Figure 7.1.7.3 RT-PCR of IGF-1R mRNA in samples in a separate sample set and Agilent samples.

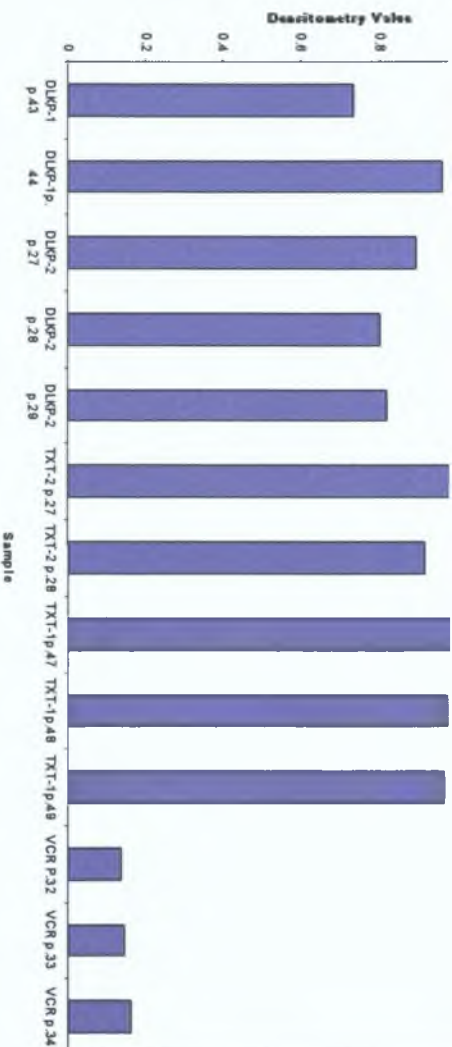
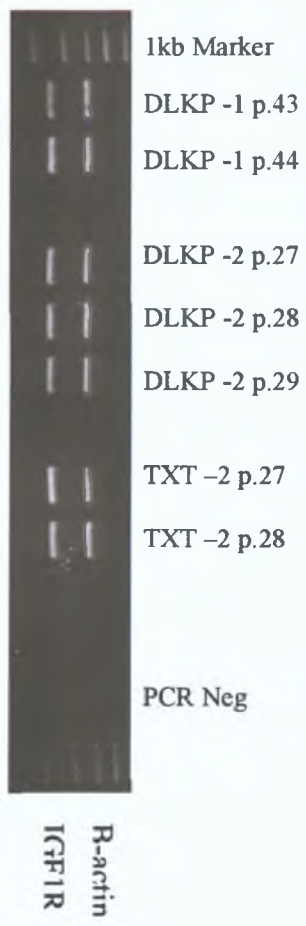
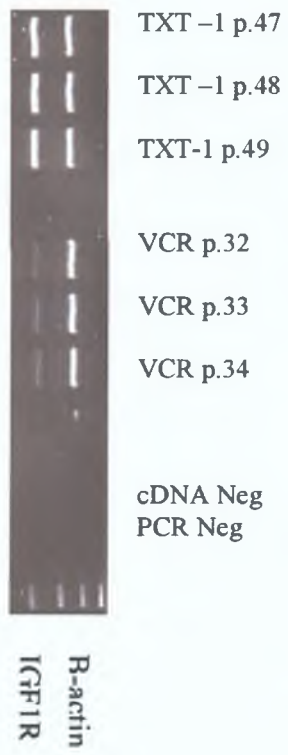


Figure 7.1.7.4.RT-PCR of IGF-1R mRNA in samples with increasing passage number.



7.1.8 KCNJ8

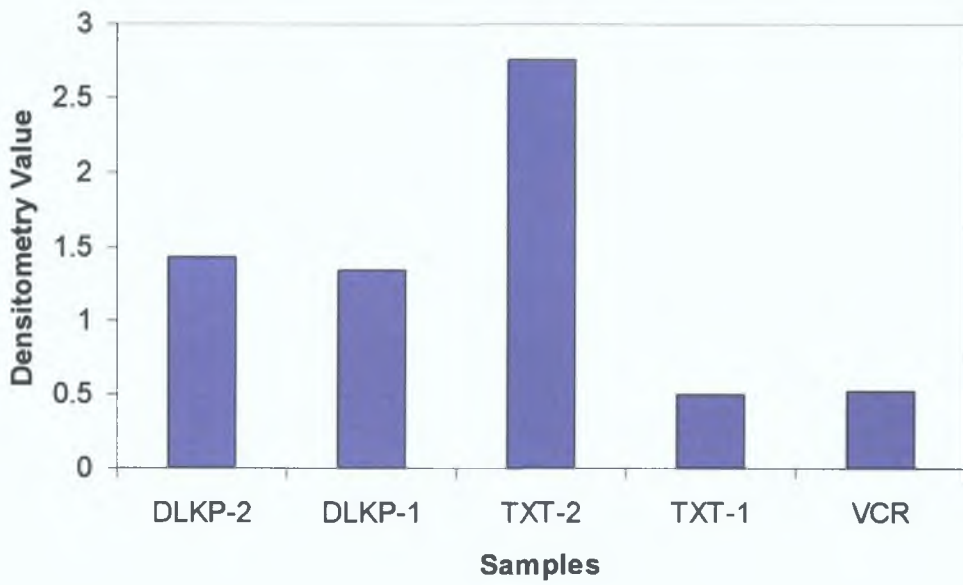


Figure 7.1.8.1 RT-PCR of KCNJ8 expression from RNA used in array samples 2003.

The band size for KCNJ8 was 210bp.

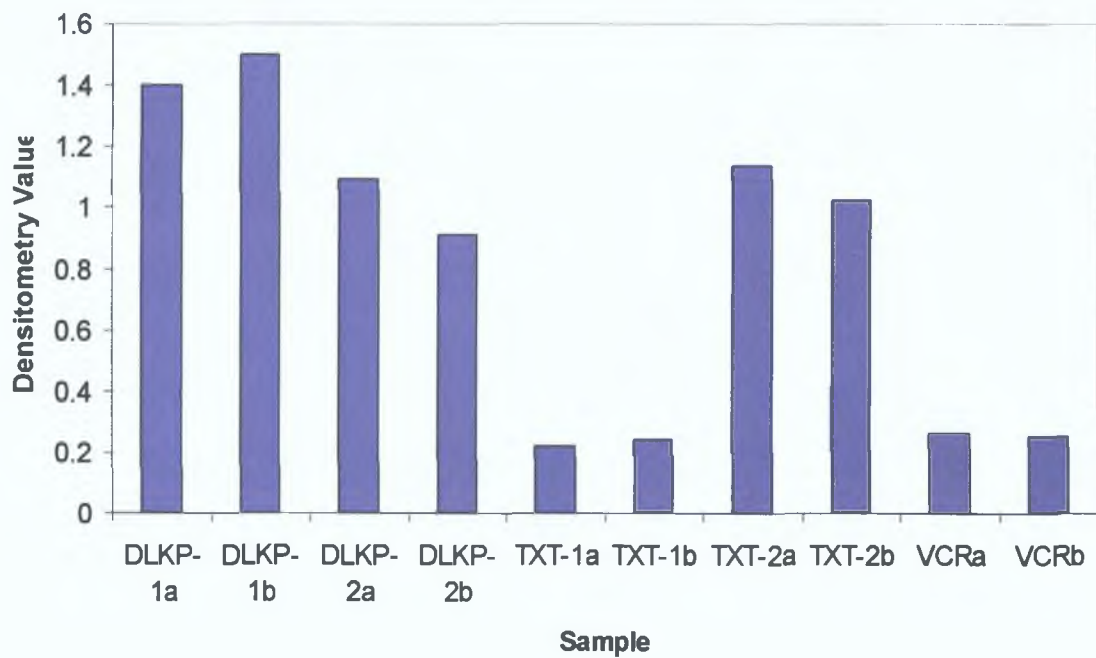
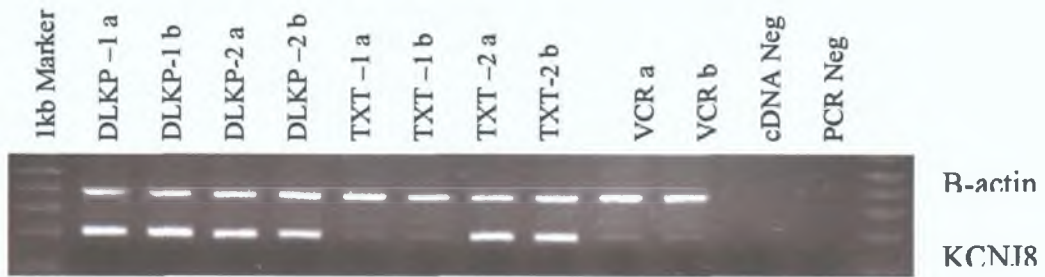


Figure 7.1.8.2 RT-PCR of KCNJ8 mRNA expression from RNA used in duplicate array samples 2004.

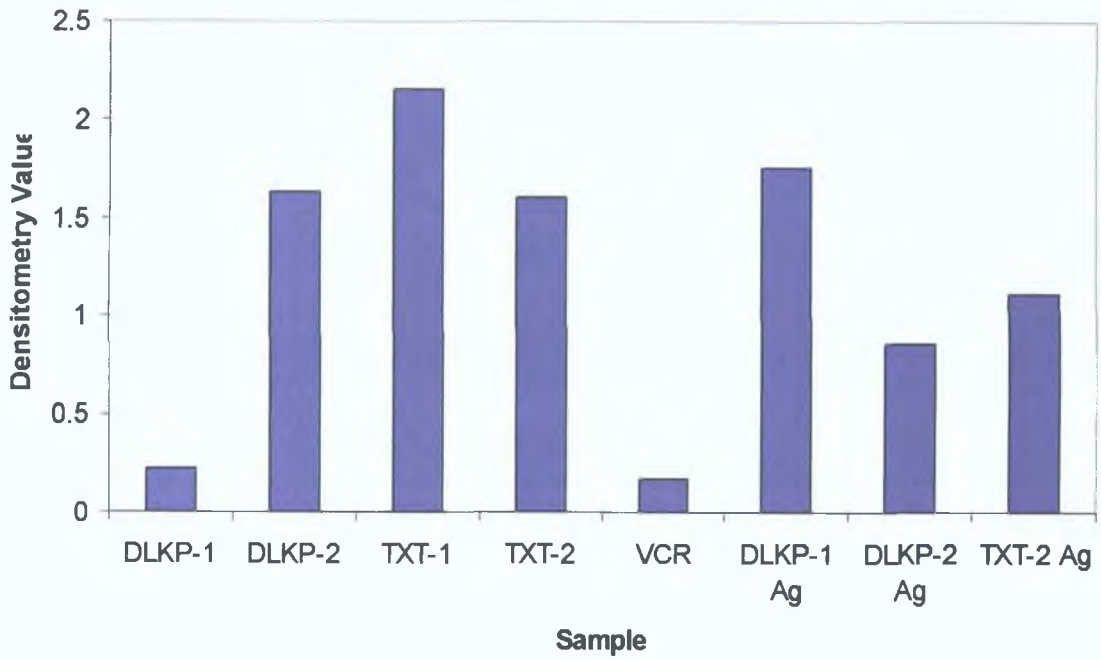


Figure 7.1.8.3 RT-PCR of KCNJ8 mRNA in samples in a separate sample set and Agilent samples.

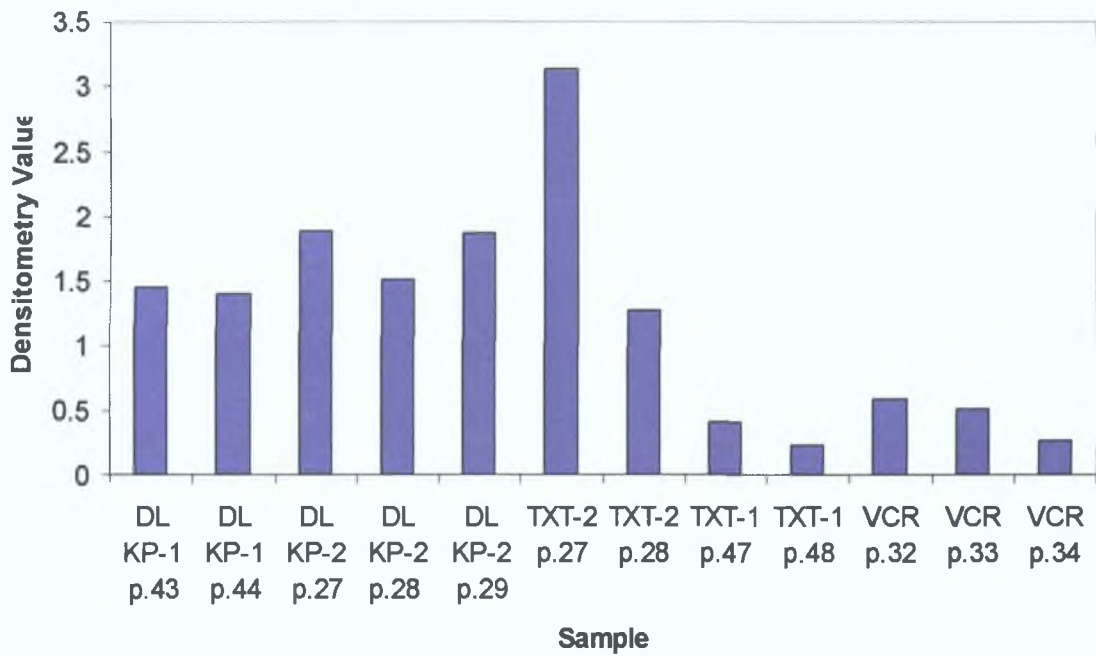
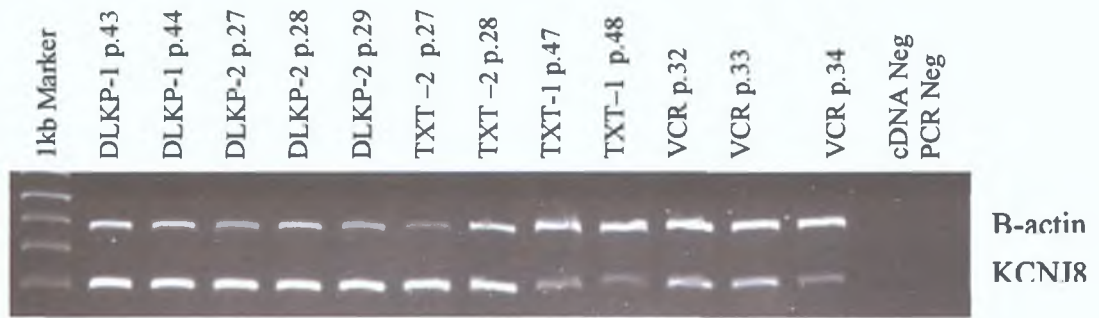


Figure 7.1.8.4 RT-PCR of KCNJ8 mRNA in samples with increasing passage number.

7.1.9 LOC5119

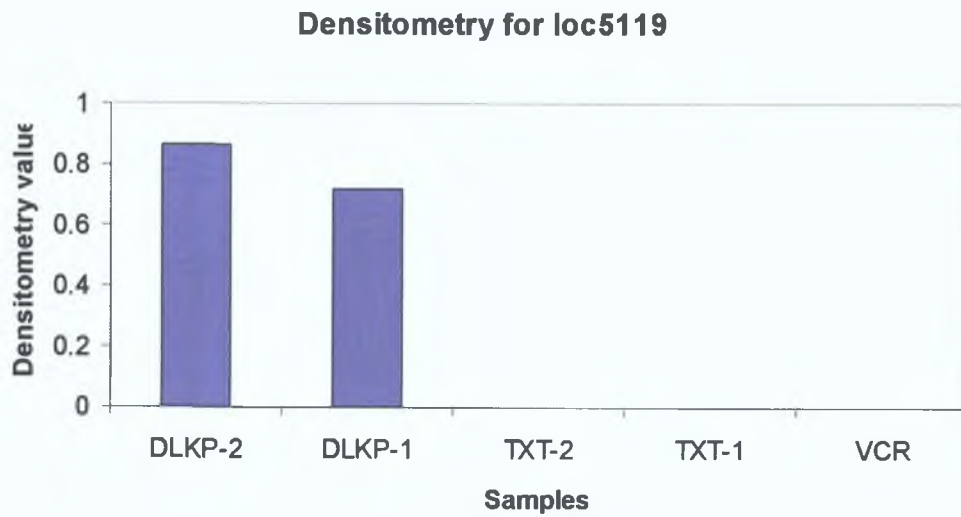
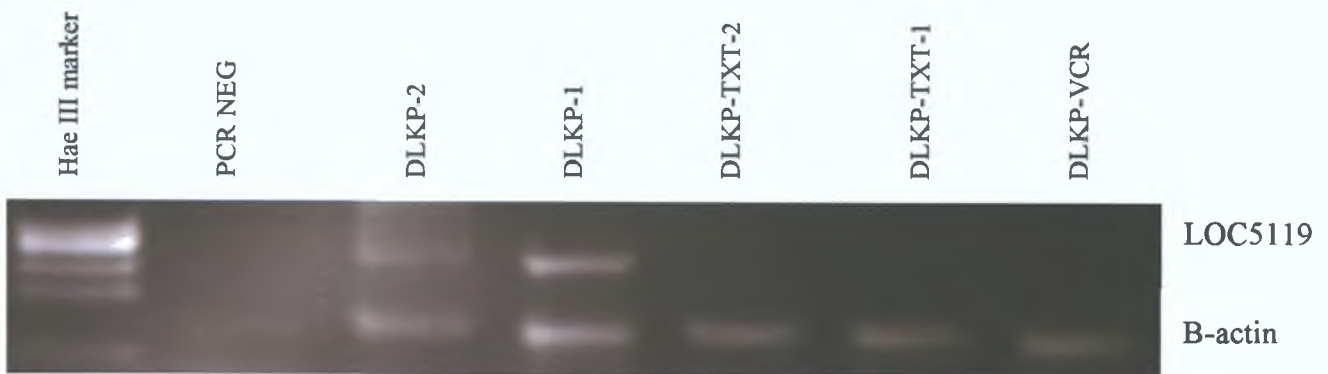


Figure 7.1.9.1 RT-PCR of LOC5119 expression from RNA used in array samples 2003.

The band size for LOC5199 was 249bp.

7.1.10 MFAP2

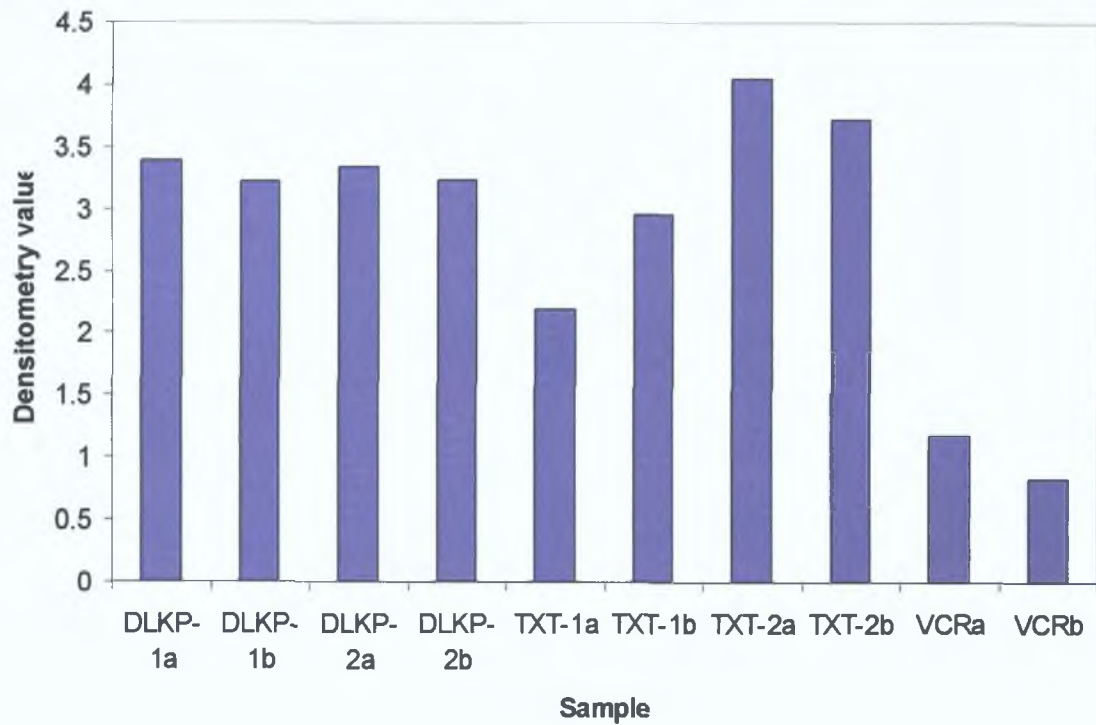
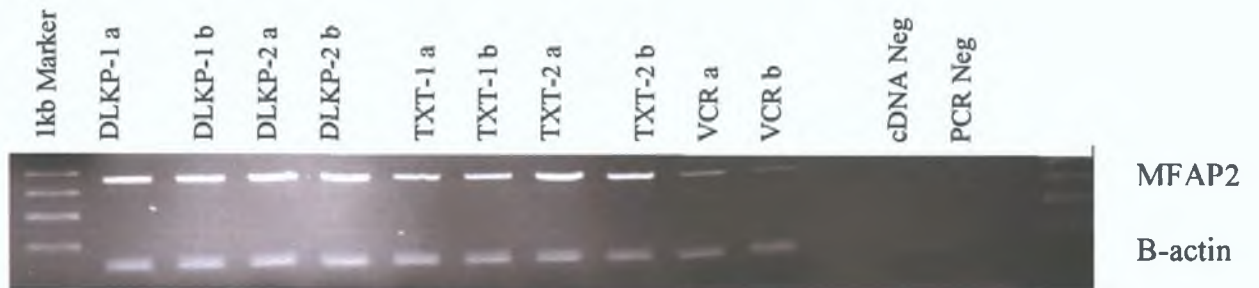


Figure 7.1.10.1 RT-PCR of MFAP2 mRNA expression from RNA used in duplicate array samples 2004.

The band size for MFAP2 was 422bp.

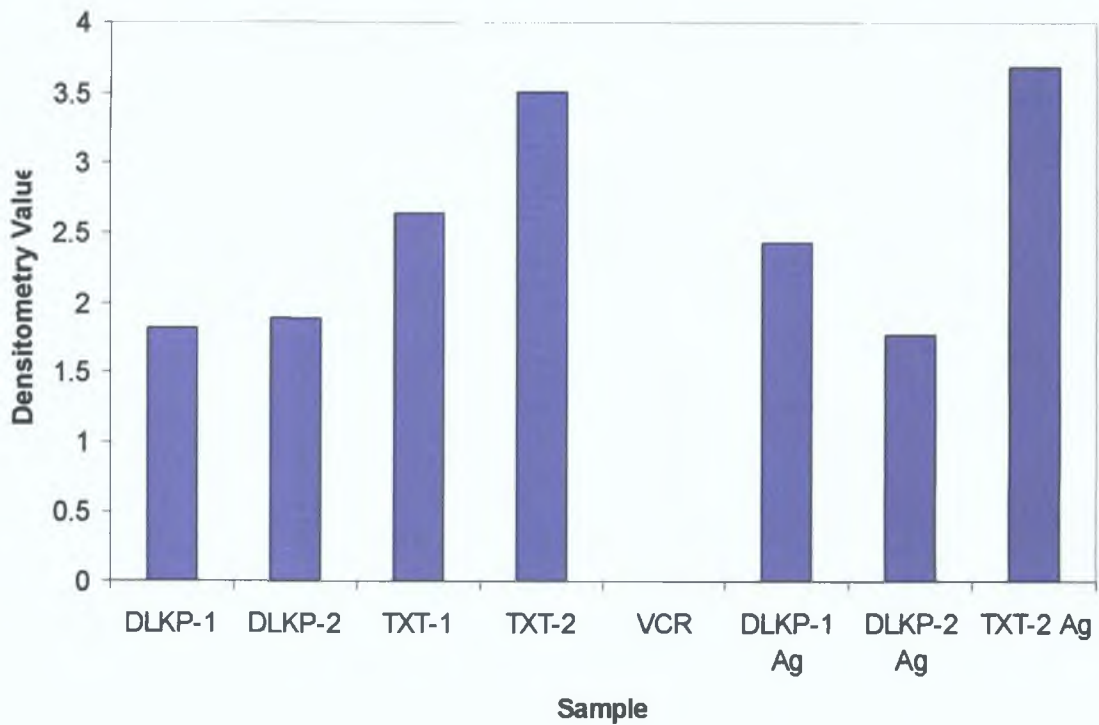


Figure 7.1.10.2 RT-PCR of MFAP2 mRNA in samples in a separate sample set and Agilent samples.

7.1.11 MGC3900

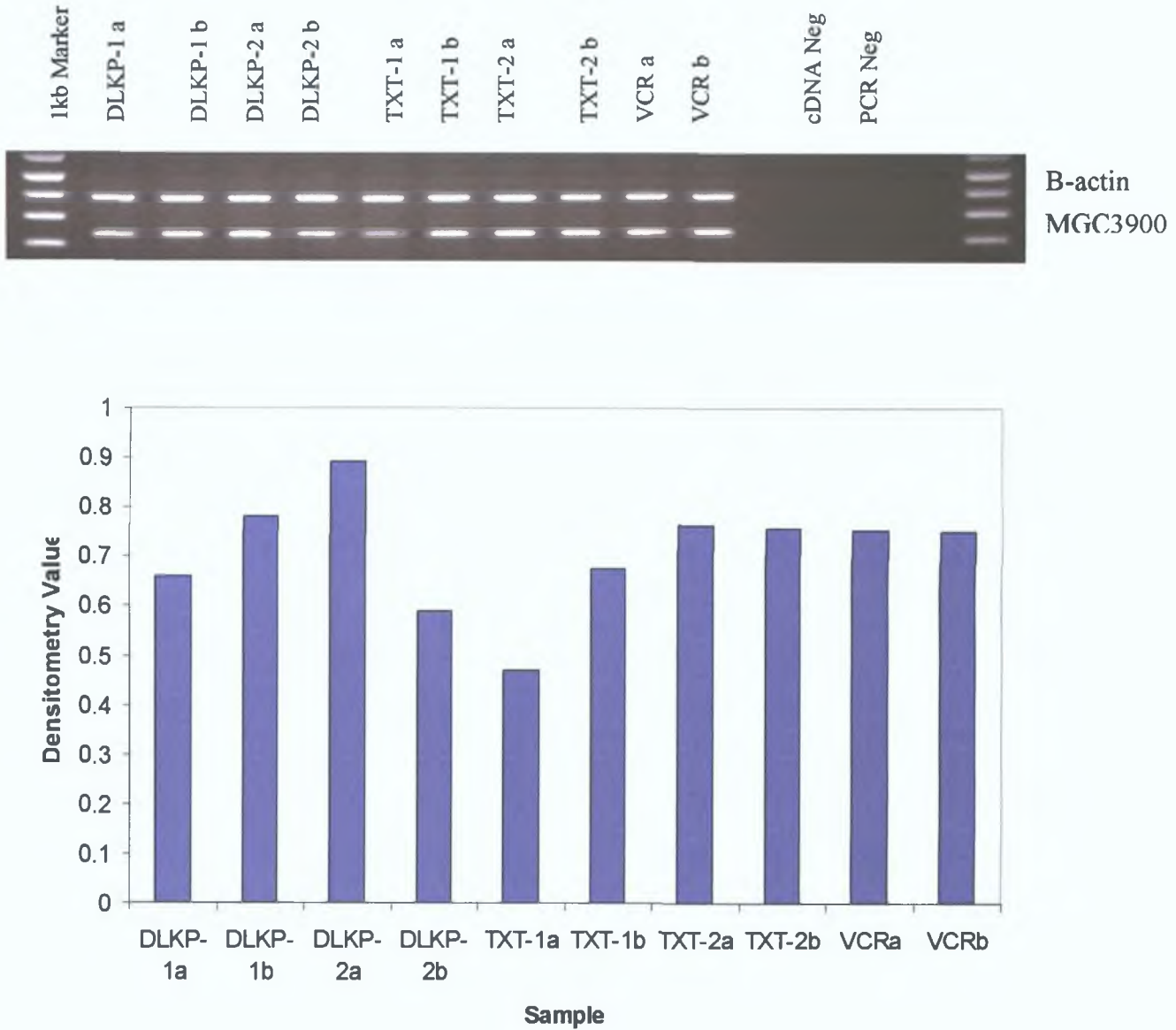


Figure 7.1.11.1 RT-PCR of MGC3900 mRNA expression from RNA used in duplicate array samples 2004.

The band size for MFAP2 was 219bp.

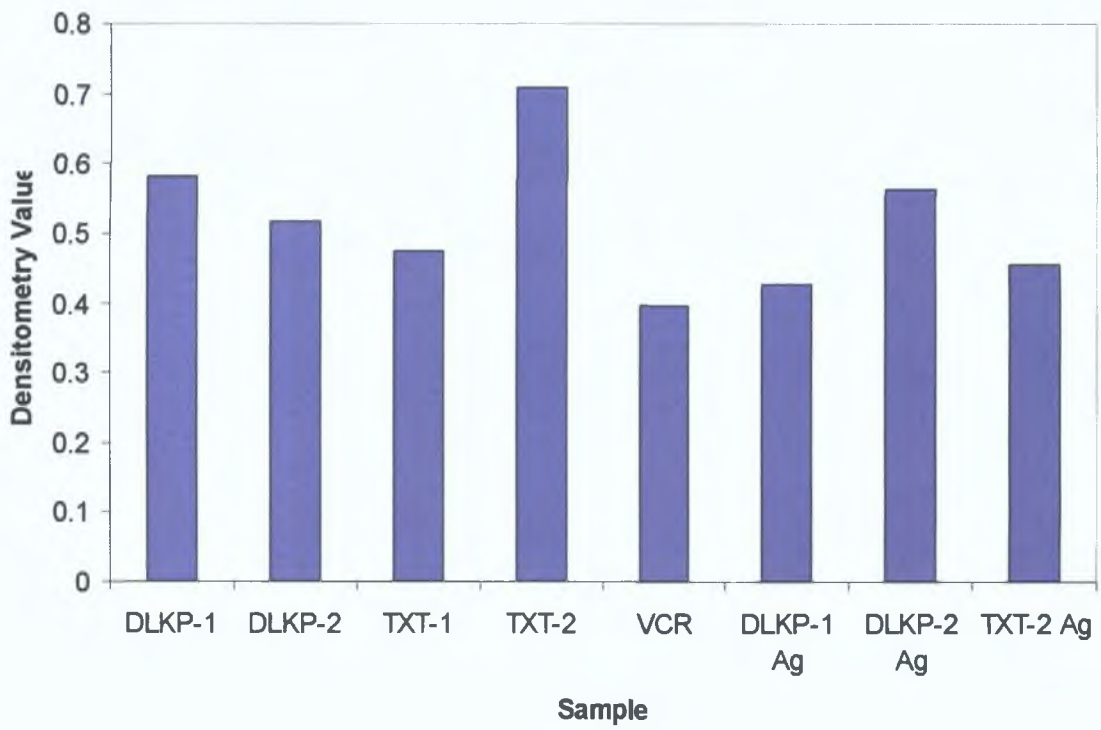


Figure 7.1.11.2 RT-PCR of MGC3900 mRNA in samples in a separate sample set and Agilent samples.

7.1.12 MMP3

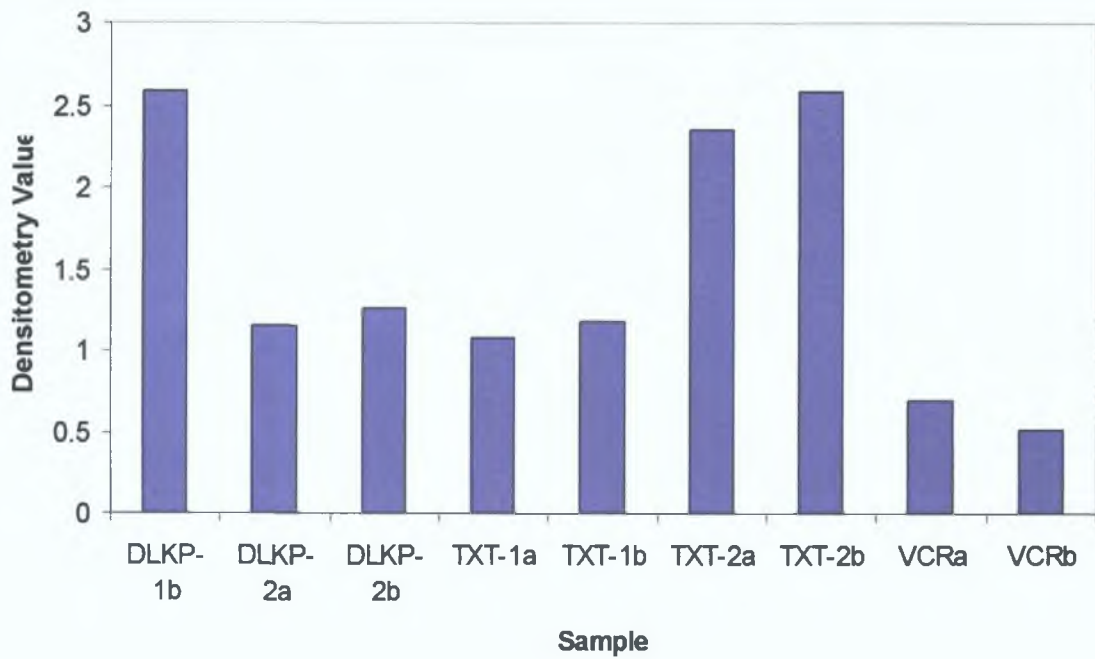
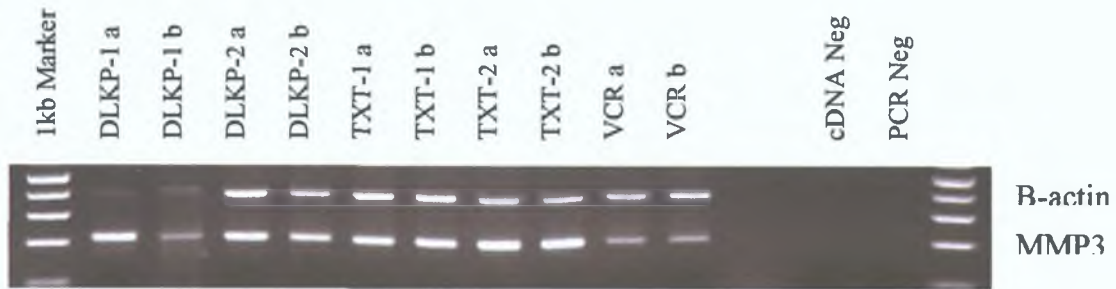


Figure 7.1.12.1 RT-PCR of MMP3 mRNA expression from RNA used in duplicate array samples 2004.

The band size for MMP3 was 241bp.

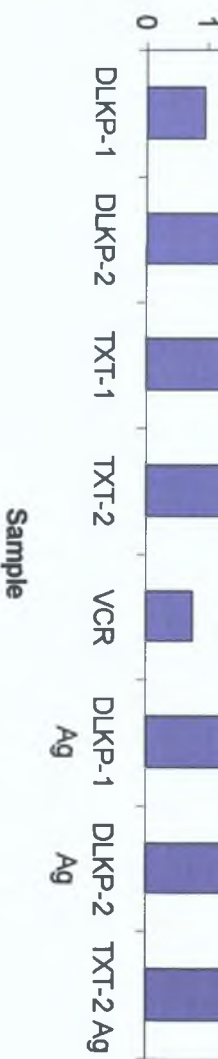
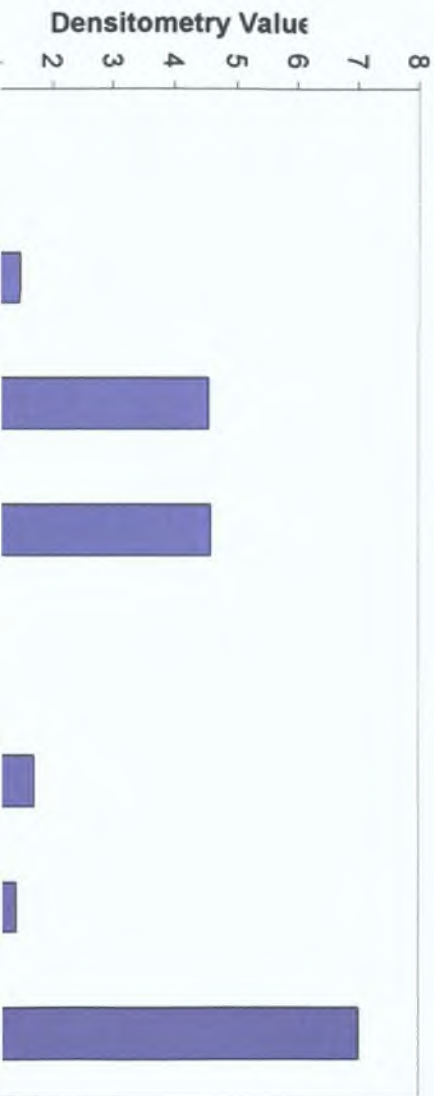


Figure 7.1.12.2 RT-PCR of MMP3 mRNA in samples in a separate sample set and Agilent samples.



1kb Marker
 DLKP-1
 DLKP-2
 TXT-1
 TXT-2
 VCR
 DLKP-1 Ag
 DLKP-2 Ag
 TXT-2 Ag
 cDNA Neg
 PCR Neg

R-actin
 MMP3

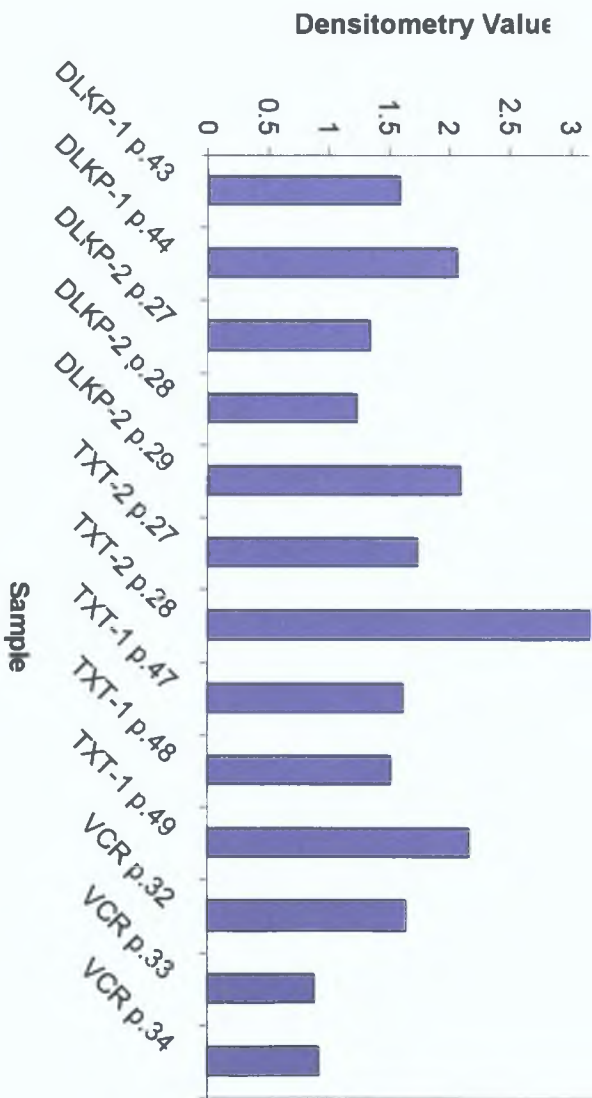
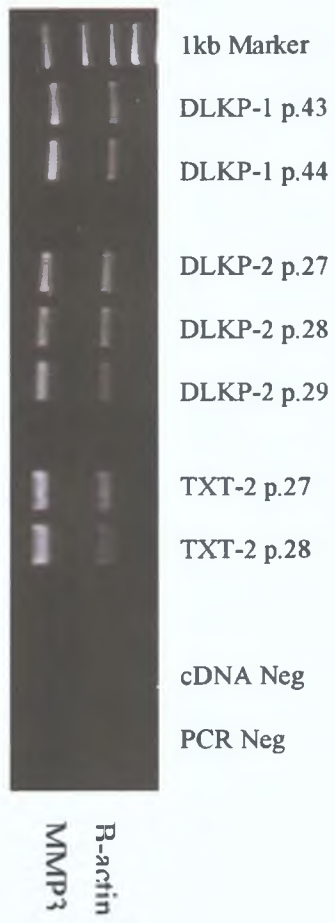
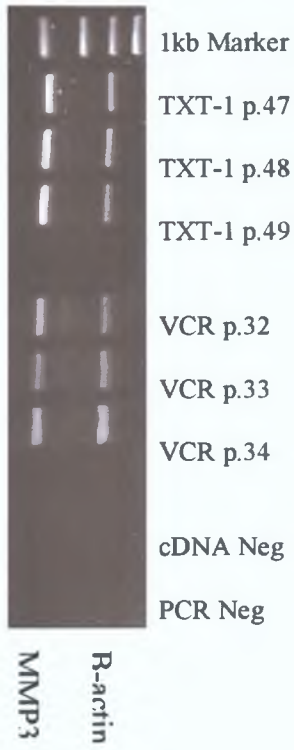


Figure 7.1.12.3a RT-PCR of MMP3 mRNA in samples with increasing passage number.



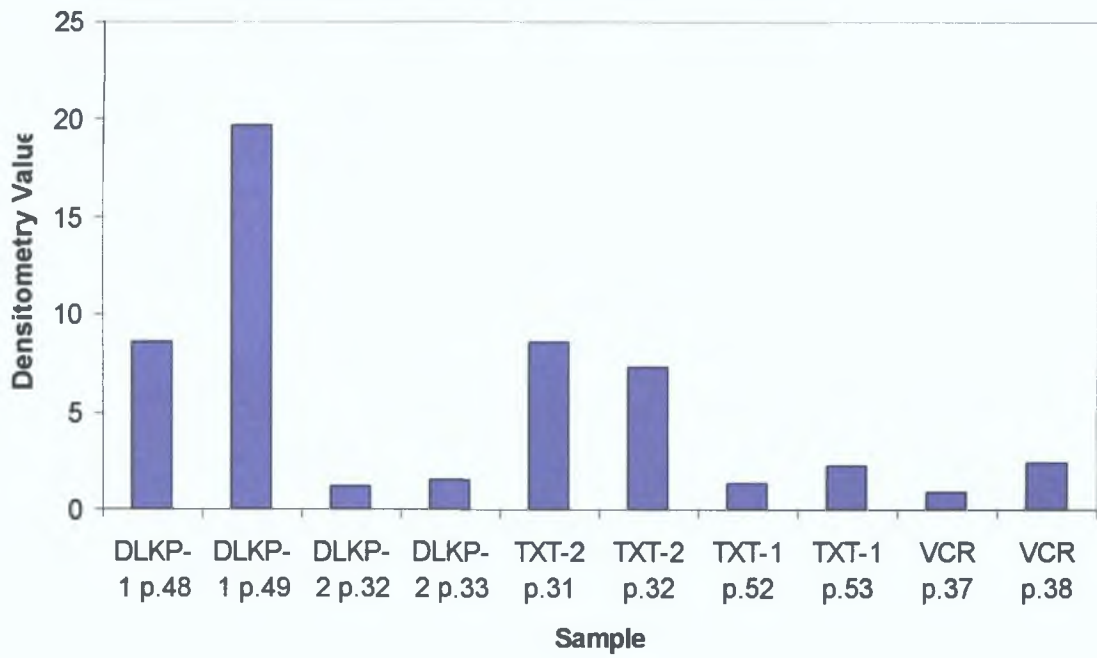
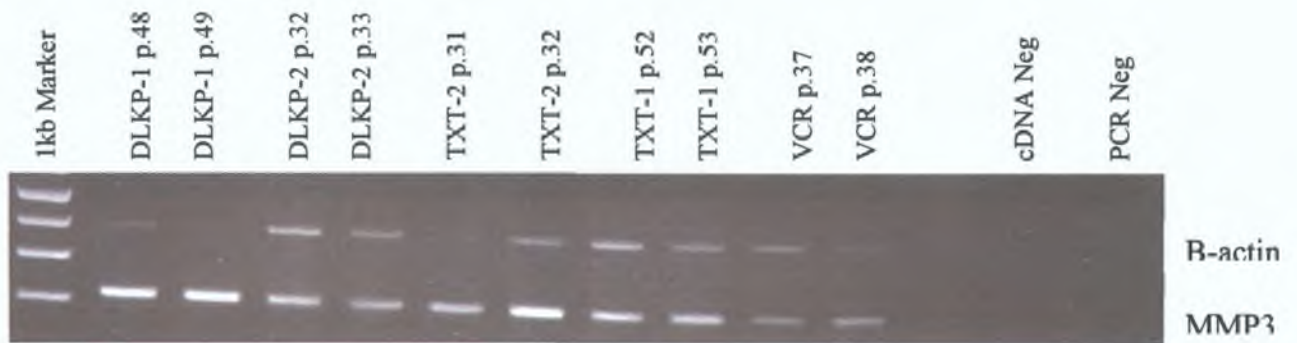


Figure 7.1.12.3b RT-PCR of MMP3 mRNA in samples with increasing passage number.

7.1.13 S100A13

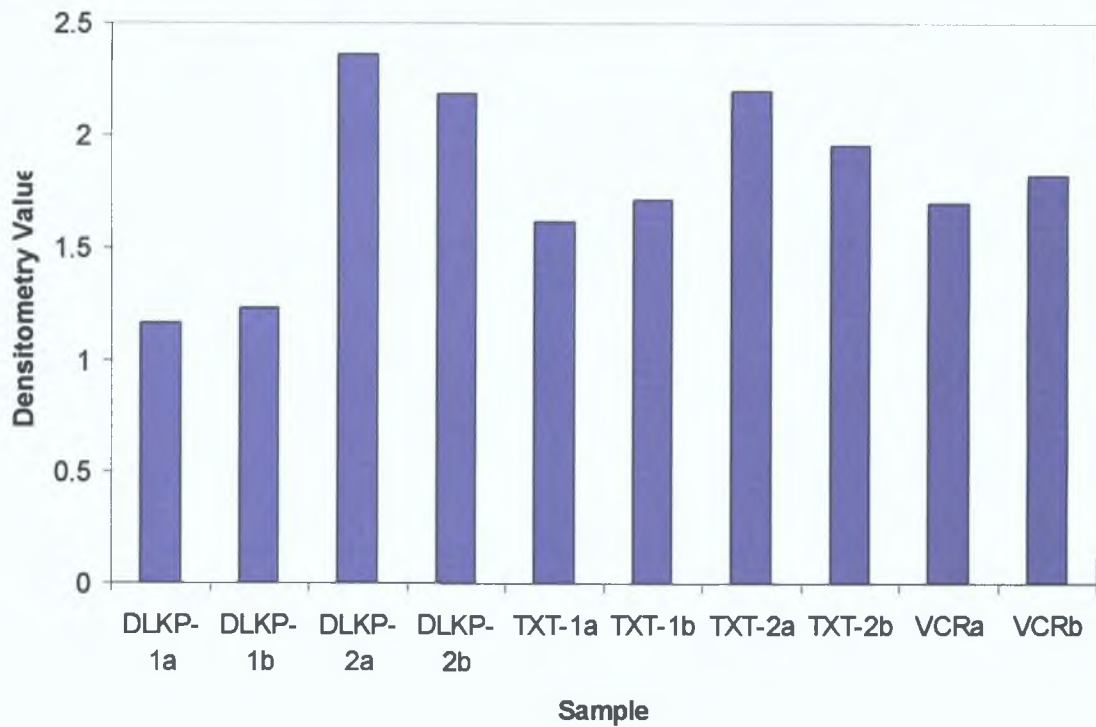
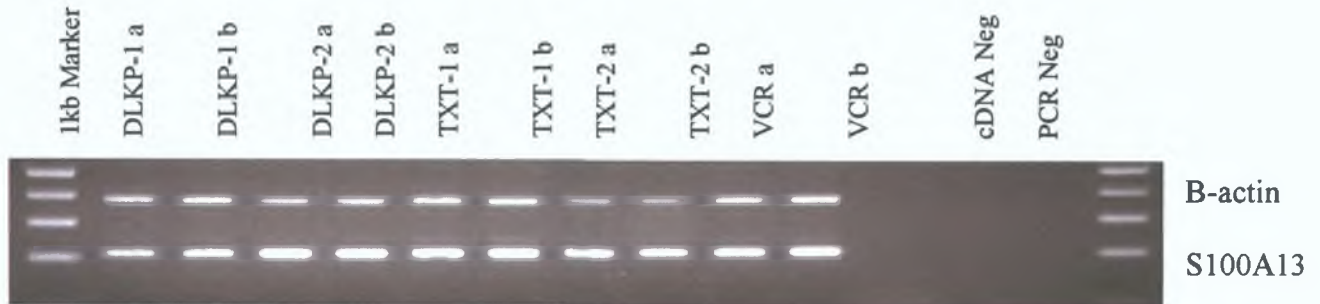


Figure 7.1.13.1 RT-PCR of S100A13 mRNA expression from RNA used in duplicate array samples 2004.

The band size for S100A13 was 219bp.

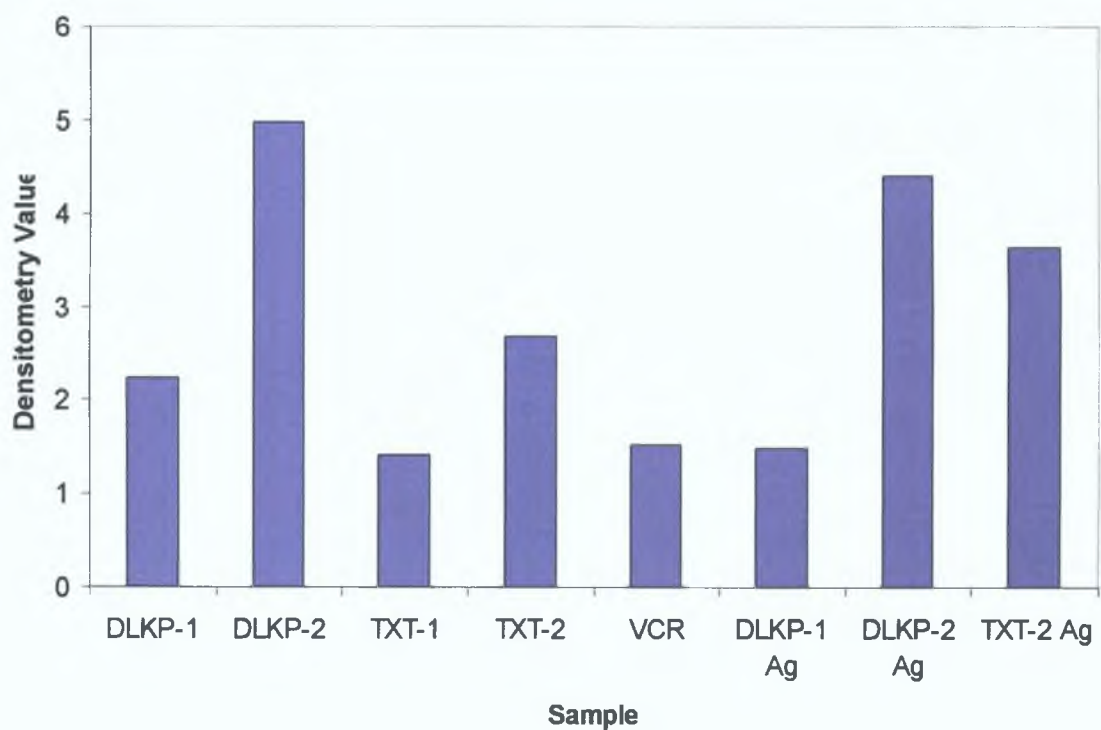


Figure 7.1.13.2 RT-PCR of S100A13 mRNA in samples in a separate sample set and Agilent samples.

7.1.14 SFN

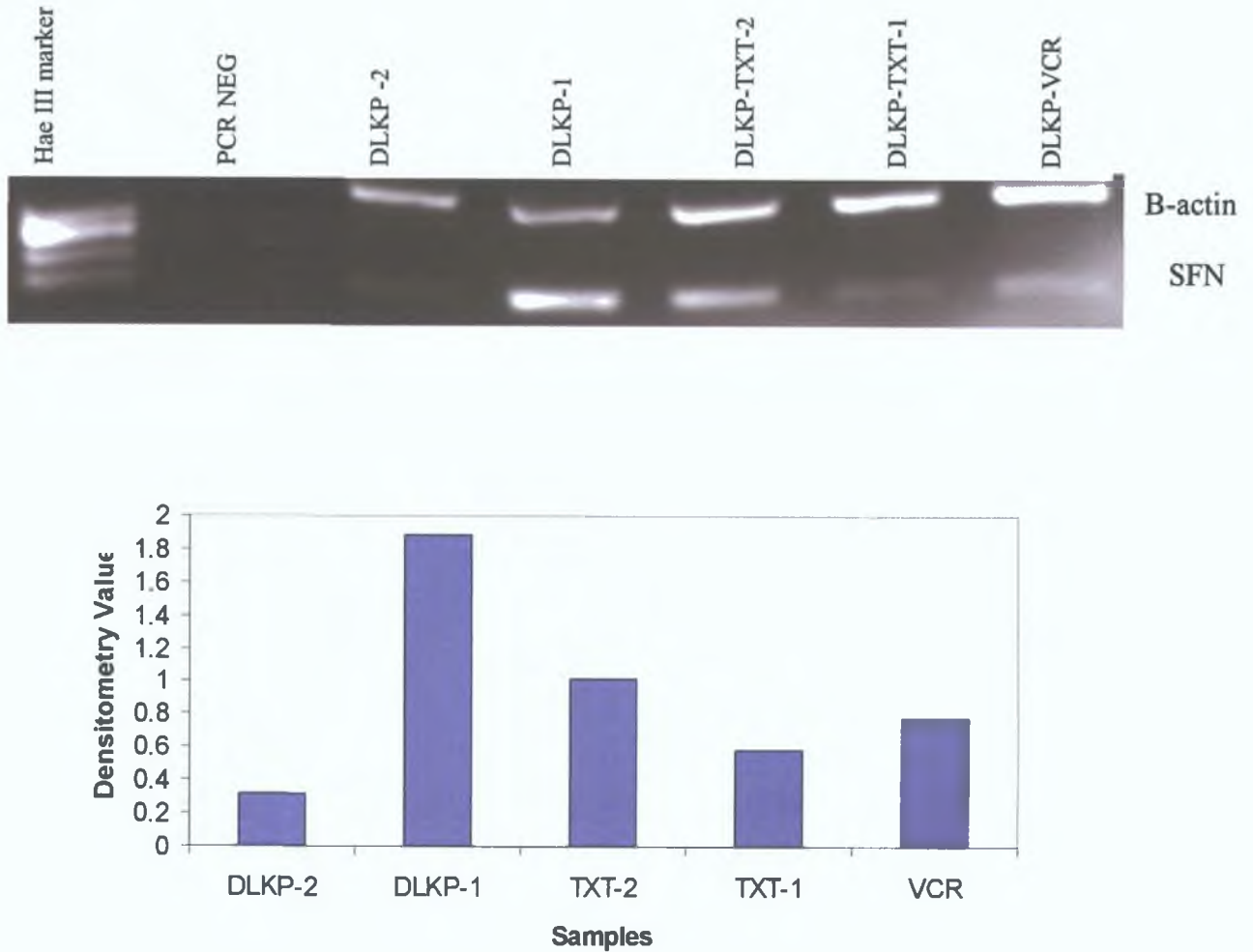


Figure 7.1.14.1 RT-PCR of SFN expression from RNA used in array samples 2003.

The band size for SFN was 195bp.

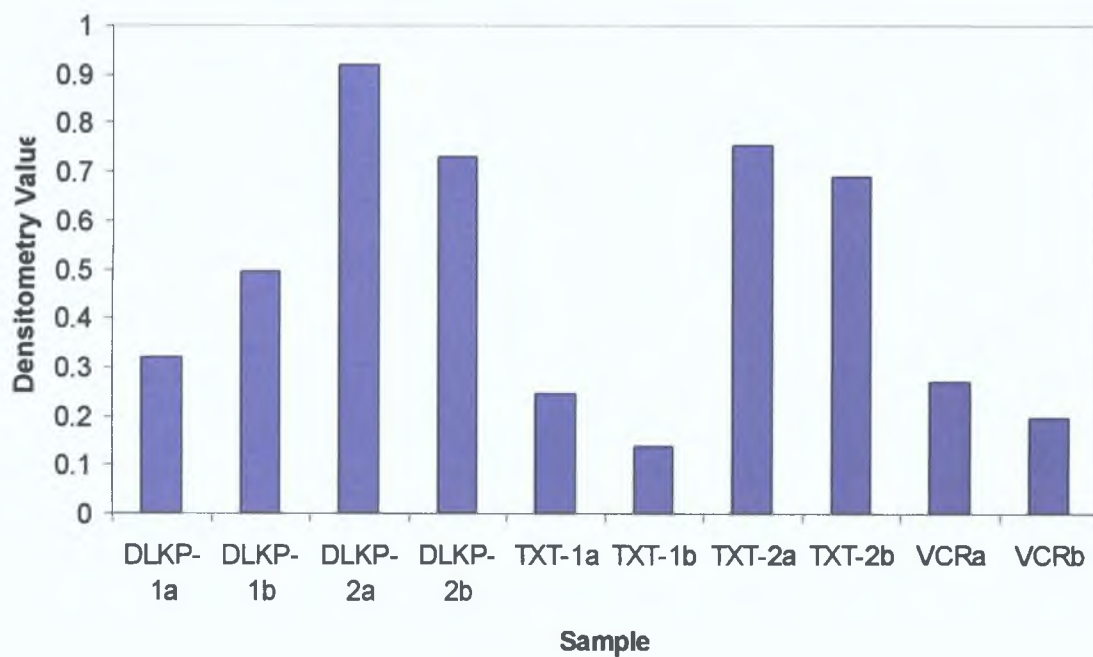
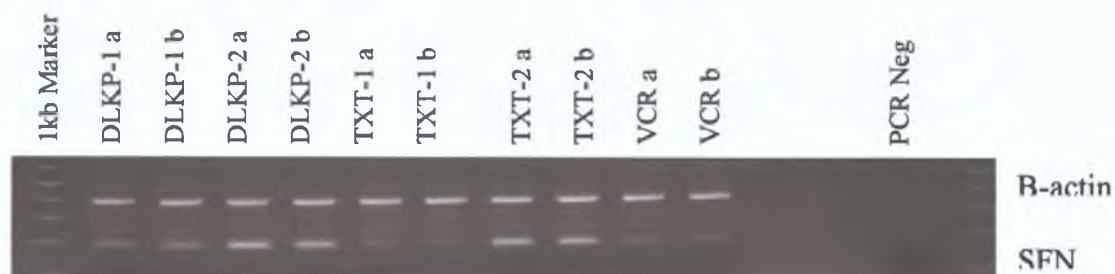


Figure 7.1.14.2 RT-PCR of SFN mRNA expression from RNA used in duplicate array samples 2004.

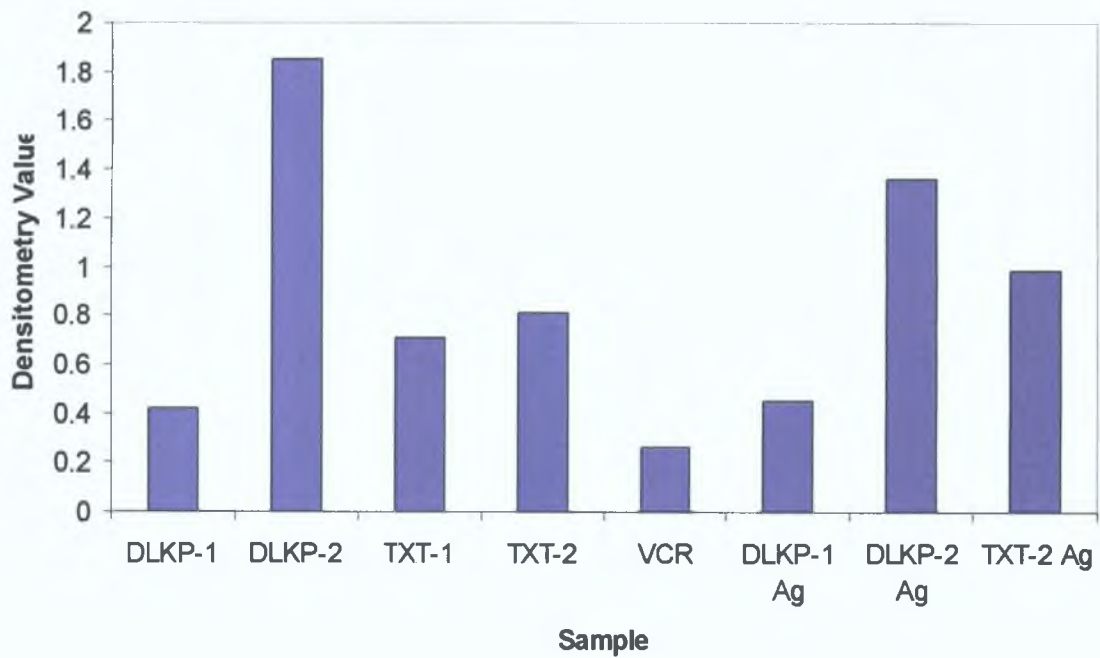


Figure 7.1.14.3 RT-PCR of SFN mRNA in samples in a separate sample set and Agilent samples.

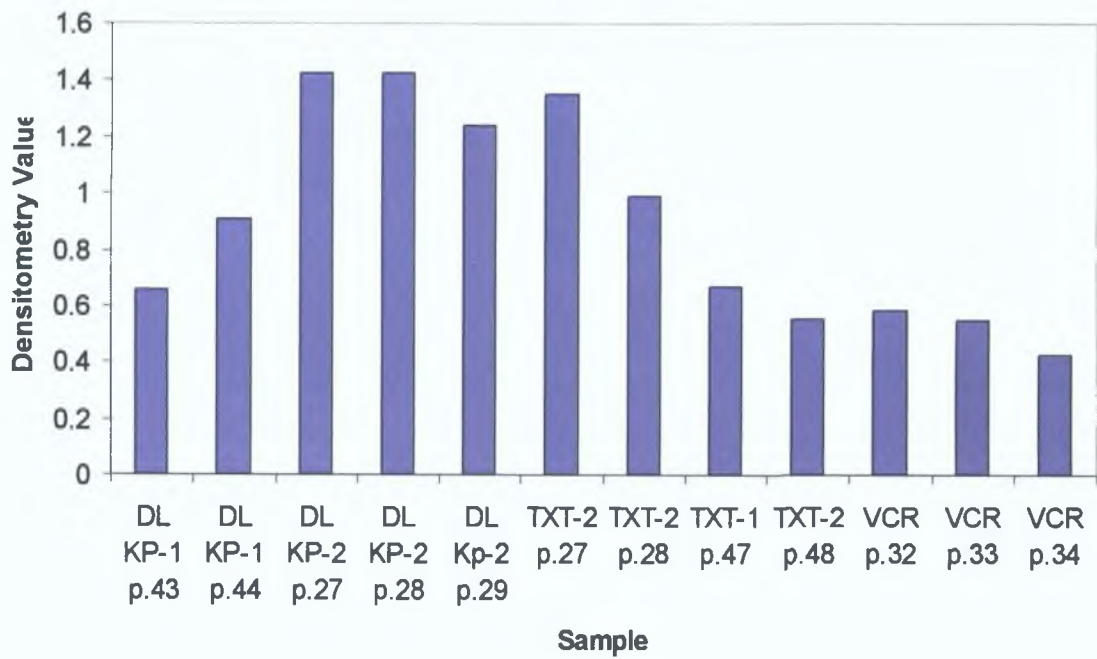
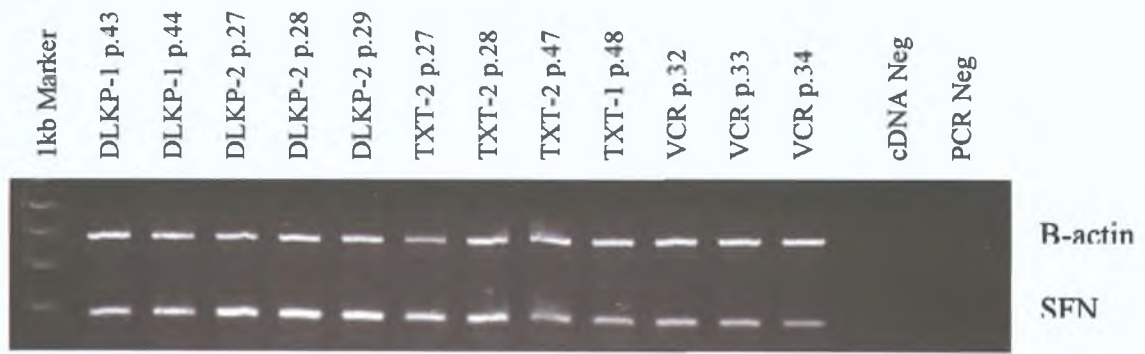


Figure 7.1.14.4a RT-PCR of SFN mRNA in samples with increasing passage number.

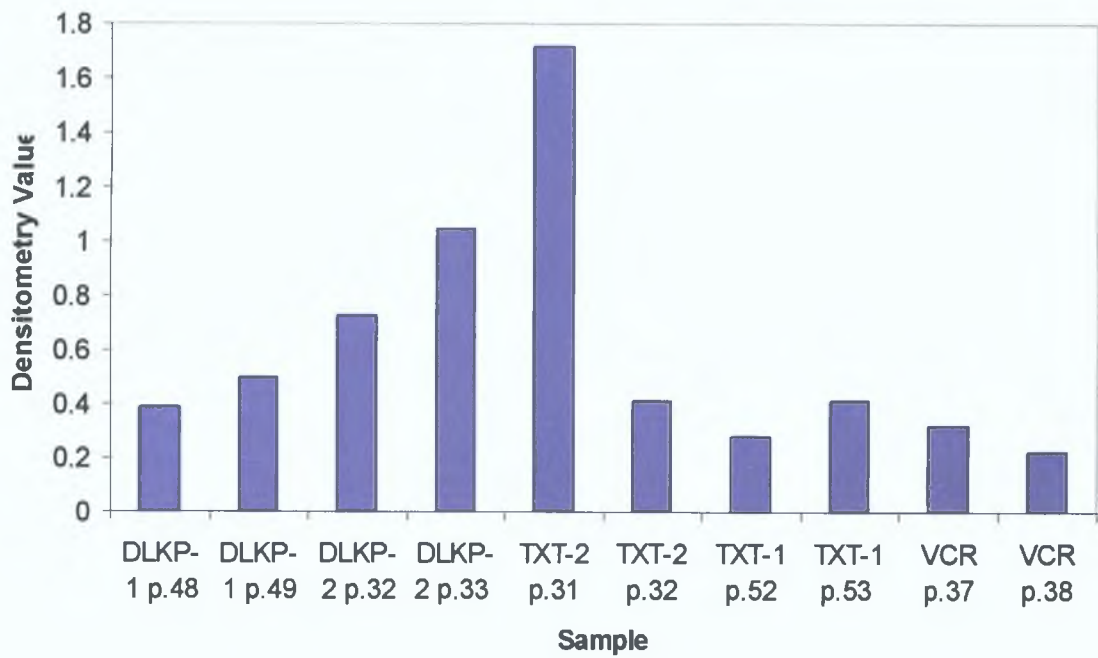
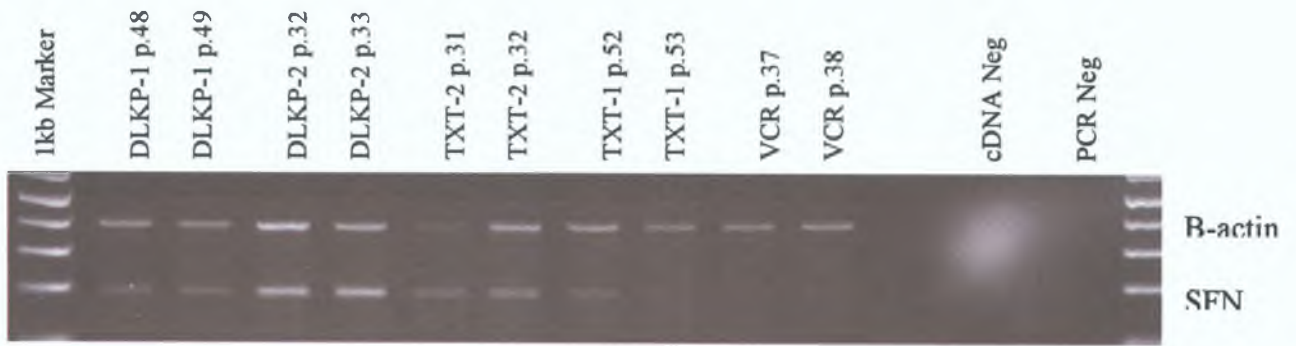


Figure 7.1.14.4b RT-PCR of SFN mRNA in samples with increasing passage number.

7.1.15 TCF4

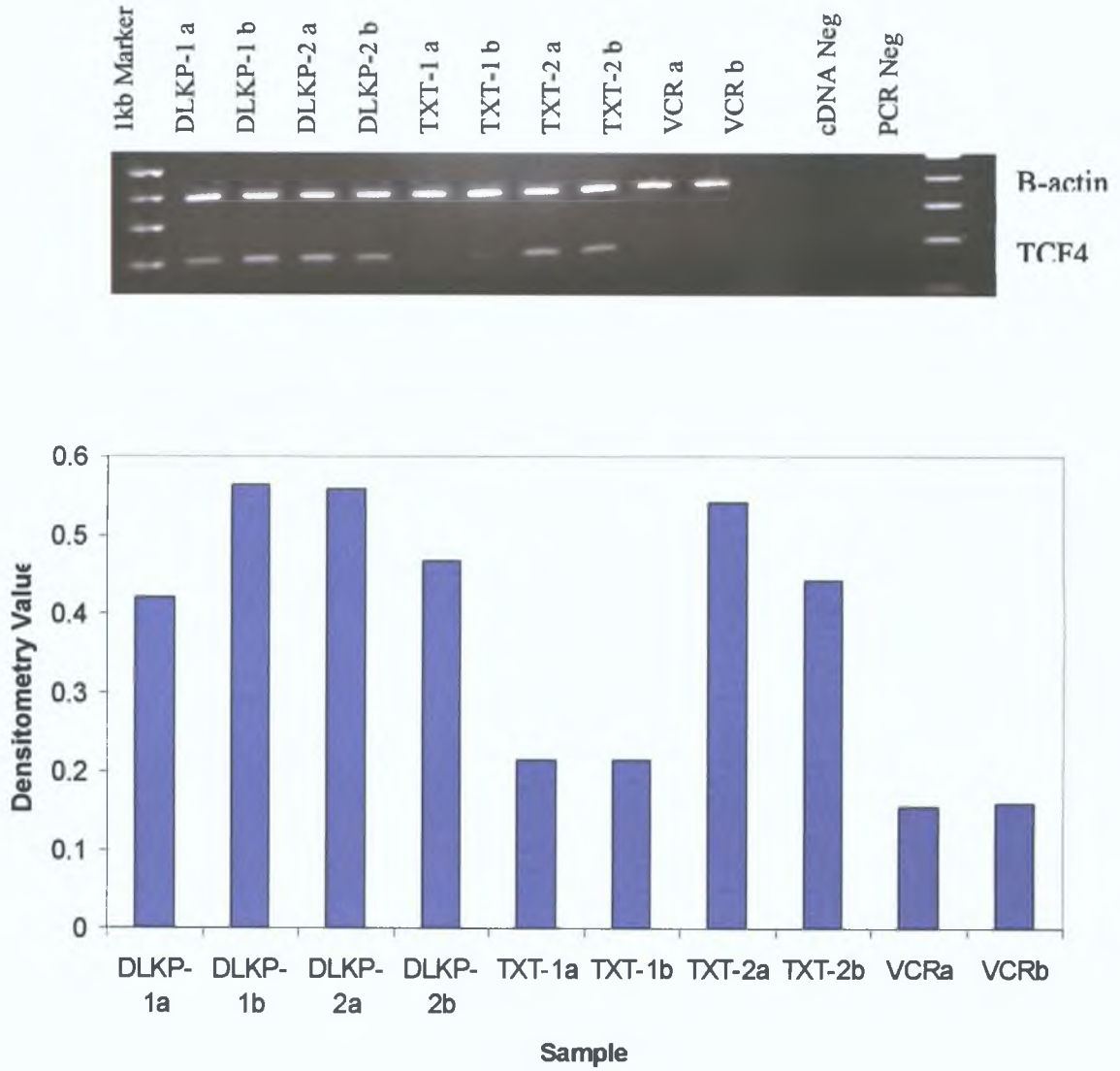


Figure 7.1.15.1 RT-PCR of TCF4 mRNA expression from RNA used in duplicate array samples 2004.

The band size for TCF4 is 204bp.

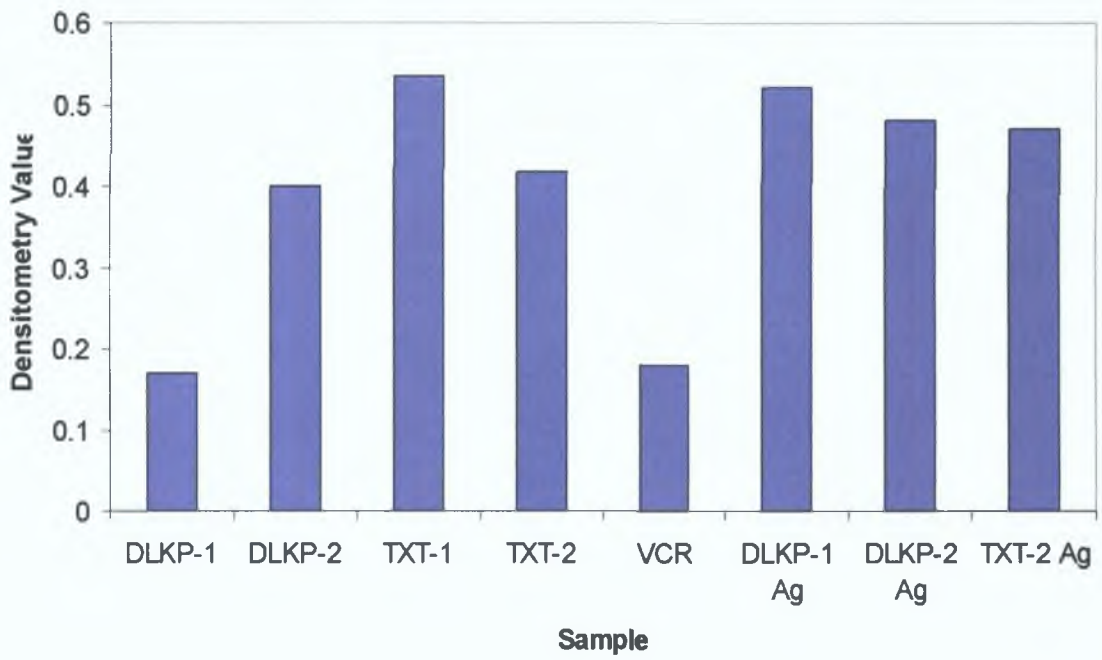


Figure 7.1.15.2 RT-PCR of TCF4 mRNA in samples in a separate sample set and Agilent samples.

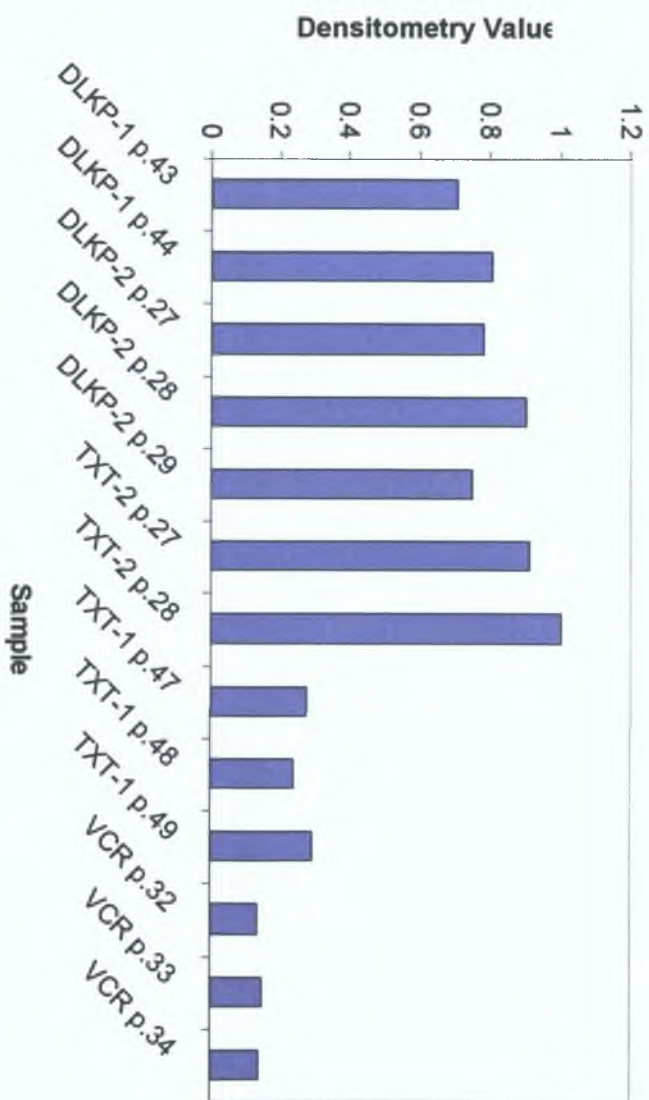
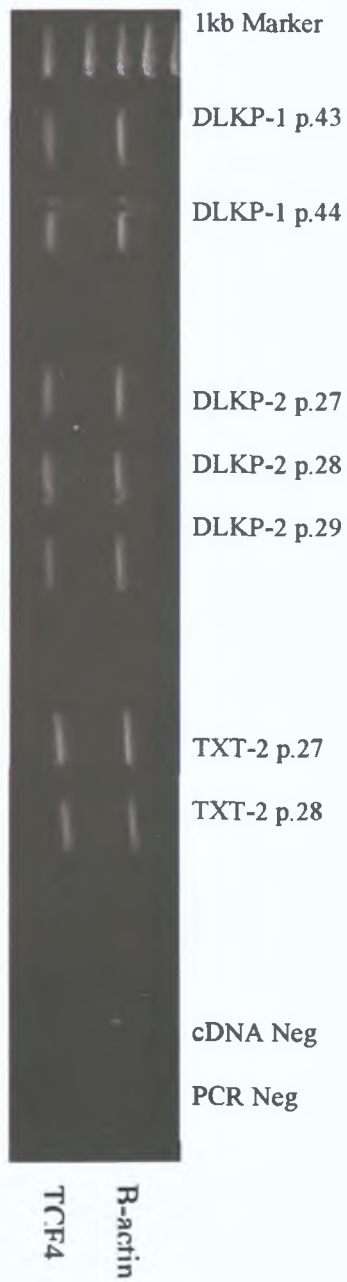
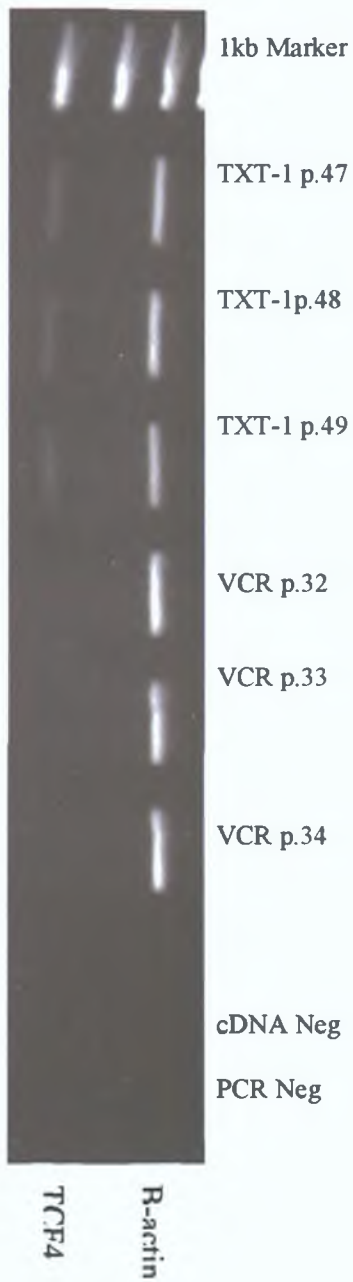


Figure 7.1.15.3 RT-PCR of TCF4 mRNA in samples with increasing passage number.



7.1.16 TEM7

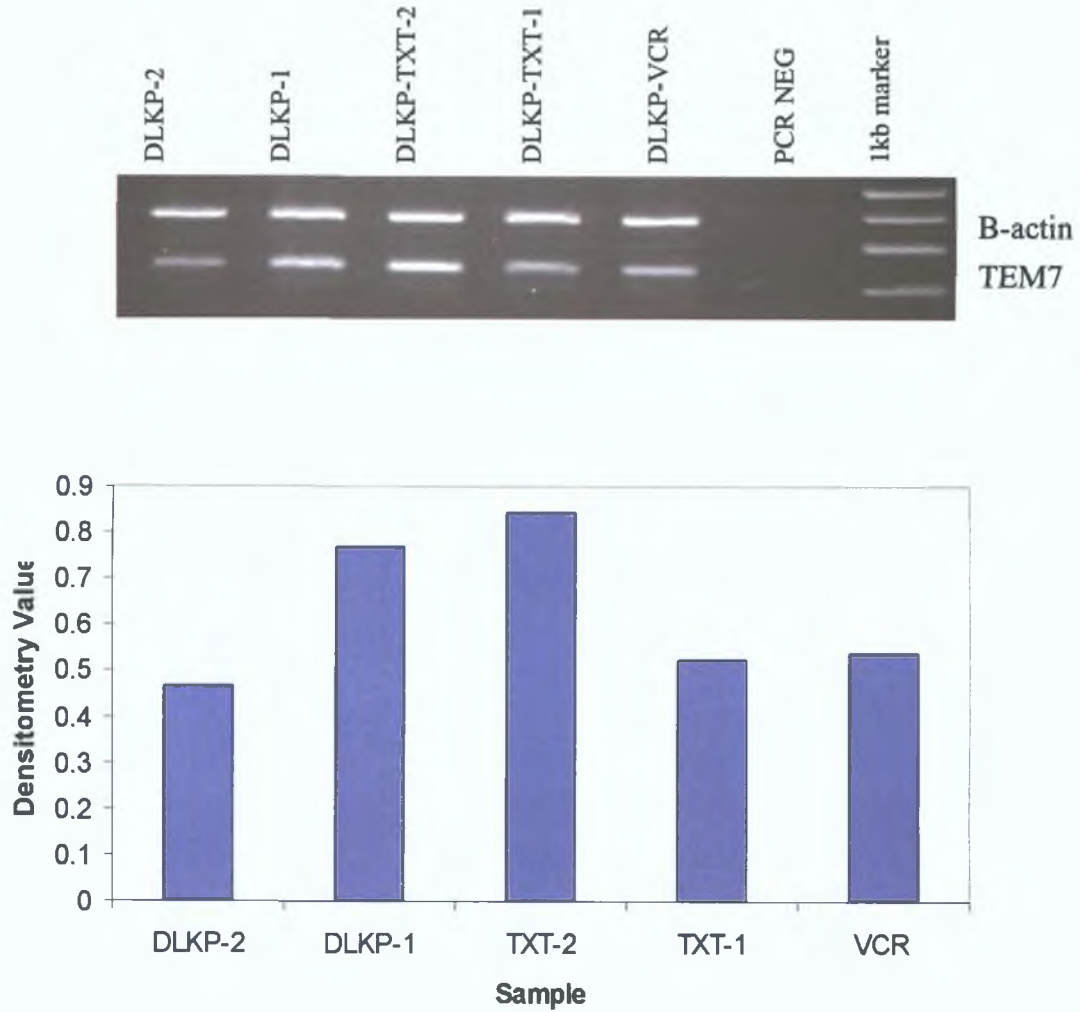


Figure 7.1.16.1 RT-PCR of TEM7 expression from RNA used in array samples 2003.

The band size for TEM7 was 239bp.

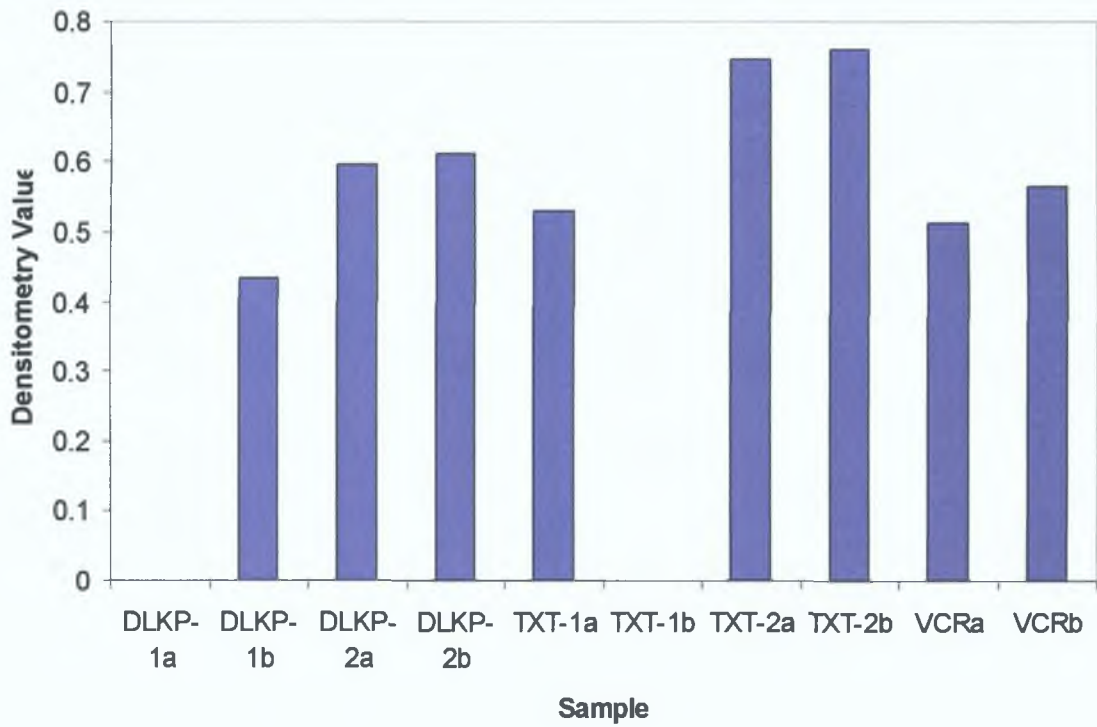
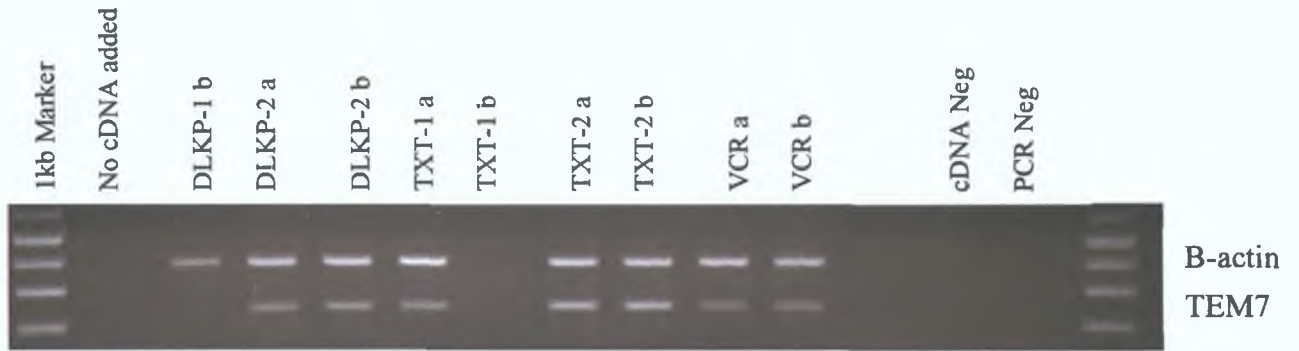


Figure 7.1.16.2 RT-PCR of TEM7 mRNA expression from RNA used in duplicate array samples 2004.

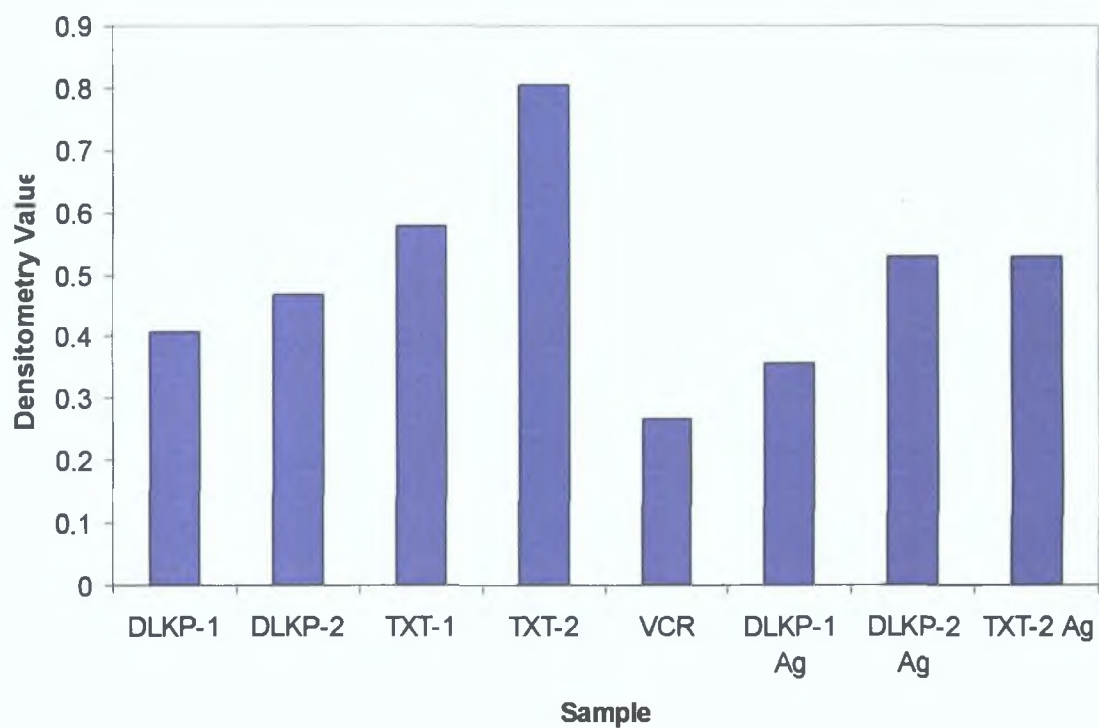
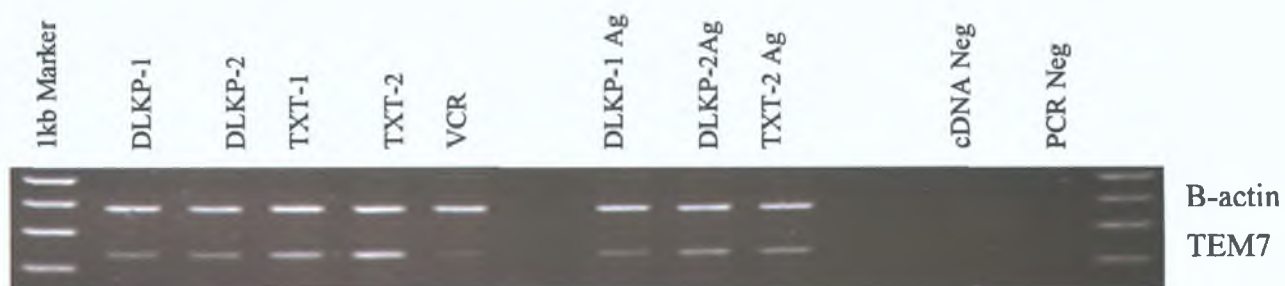


Figure 7.1.16.3 RT-PCR of TEM7 mRNA in samples in a separate sample set and Agilent samples.

7.1.17 TLX1

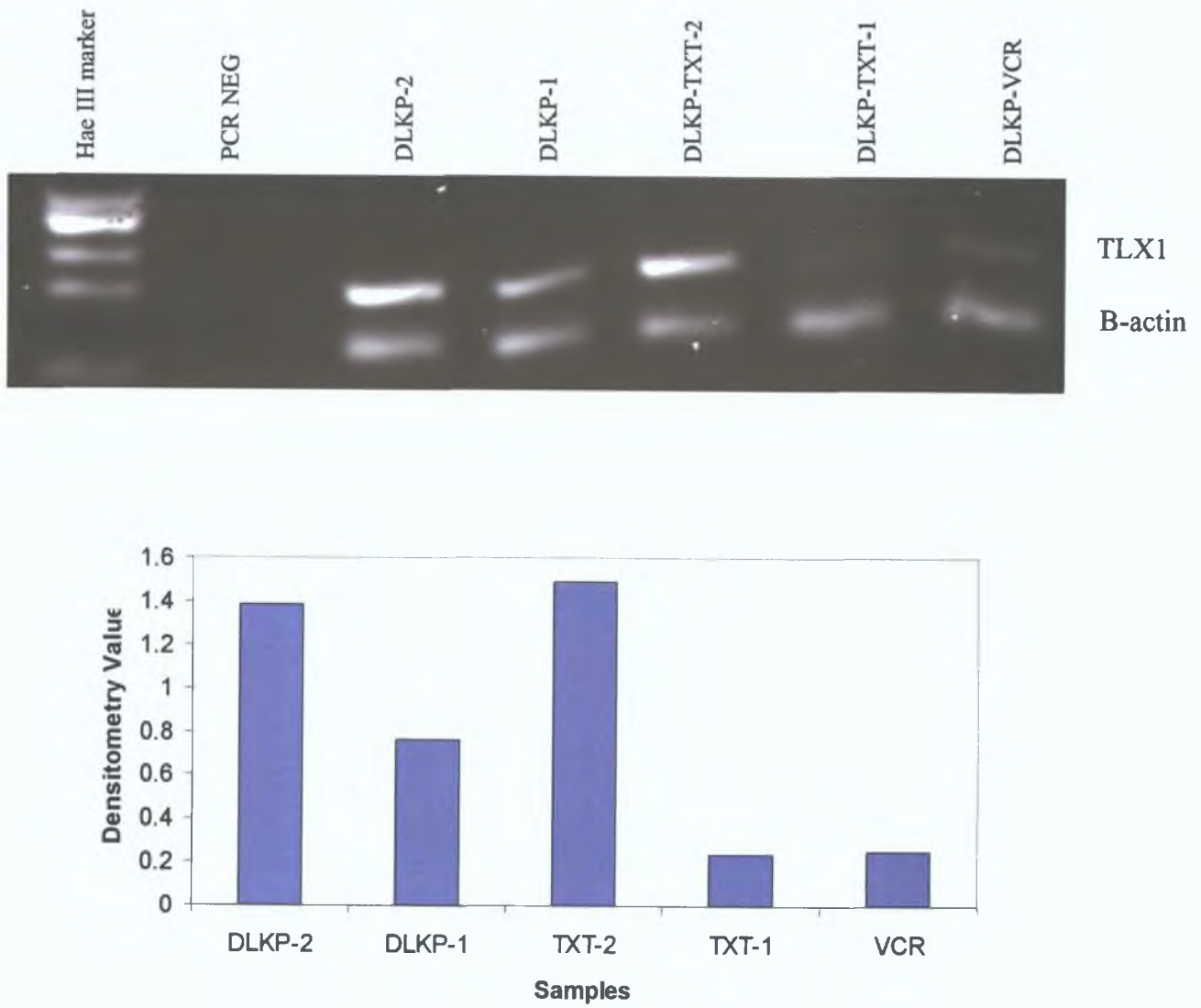


Figure 7.1.17.1 RT-PCR of TLX1 expression from RNA used in array samples 2003.

The band size for TLX1 was 201bp.

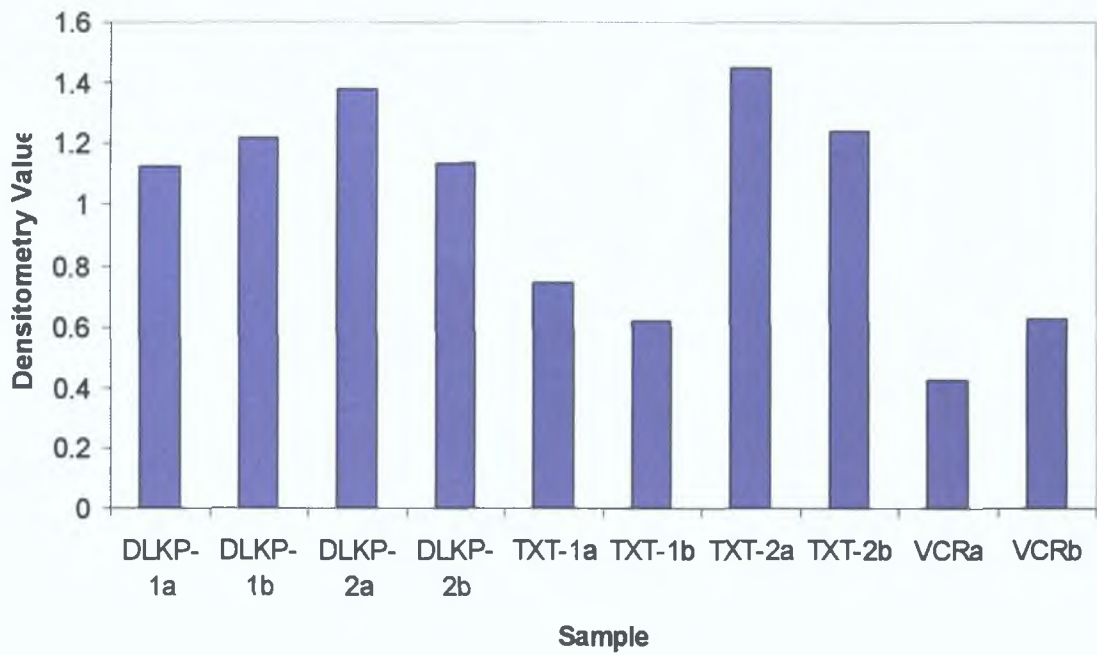
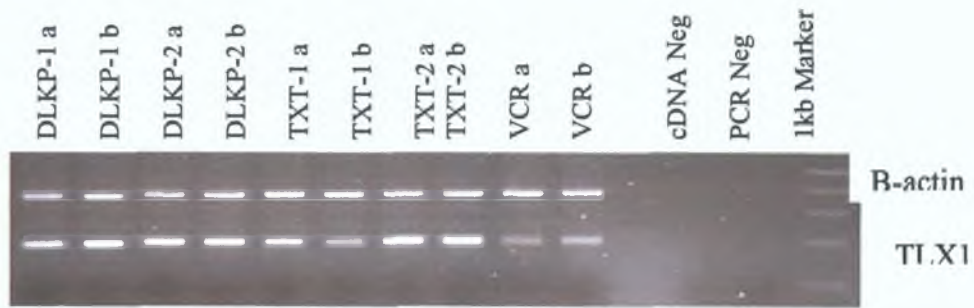


Figure 7.1.18.2 RT-PCR of TLX1 mRNA expression from RNA used in duplicate array samples 2004.

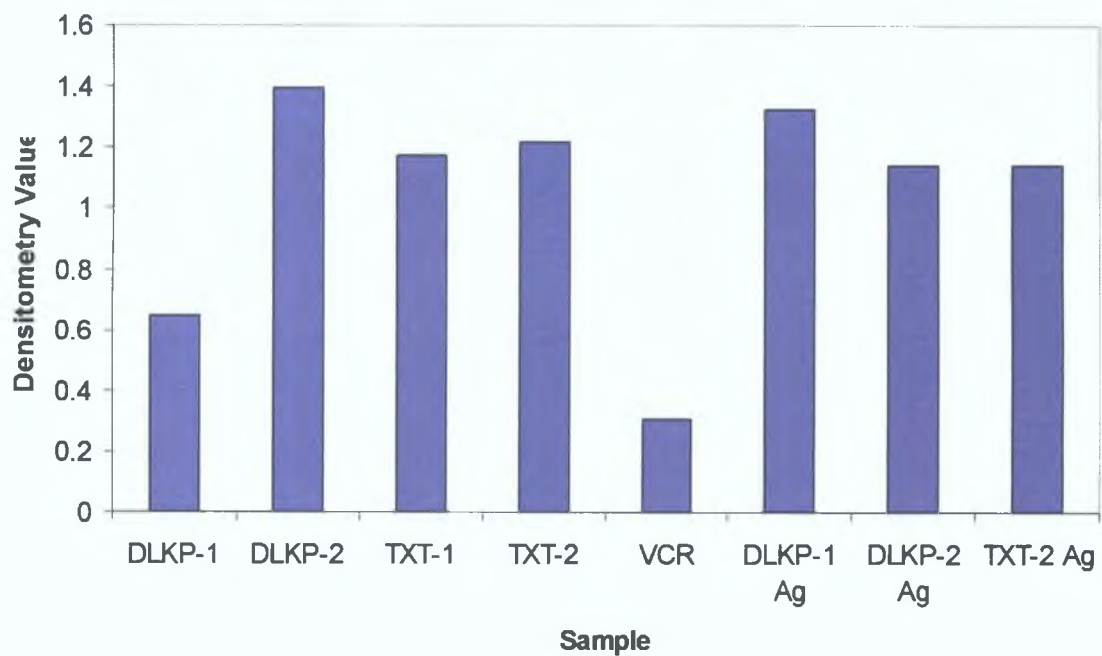


Figure 7.1.18.3 RT-PCR of TLX1 mRNA in samples in a separate sample set and Agilent samples.

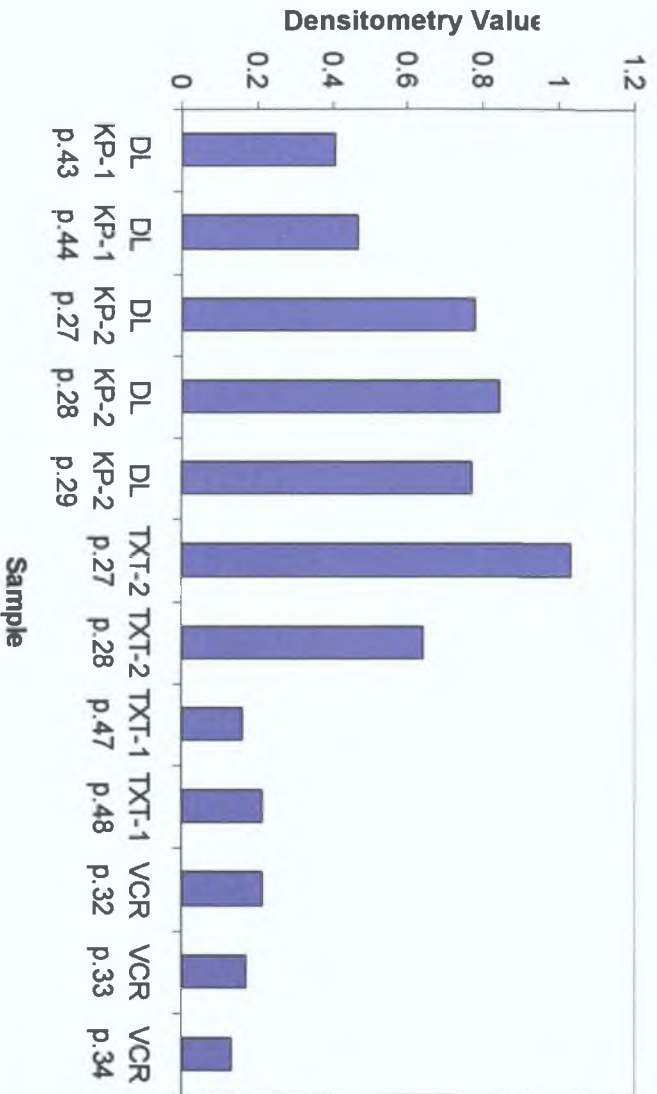
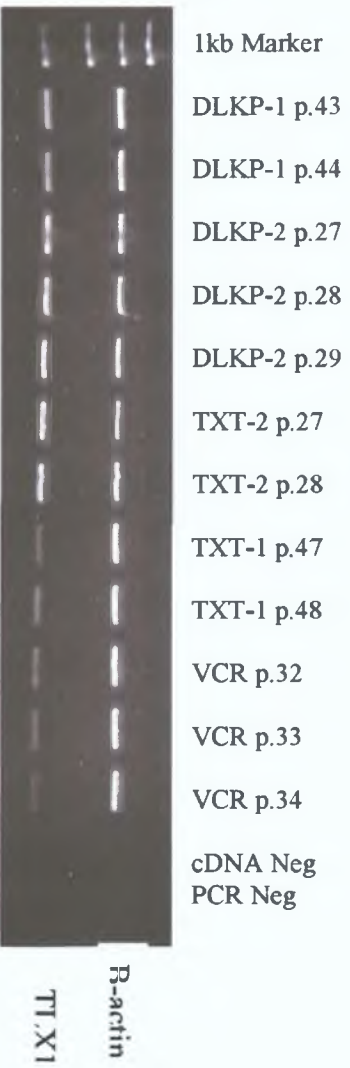


Figure 7.1.18.4a RT-PCR of TLX1 mRNA in samples with increasing passage number.

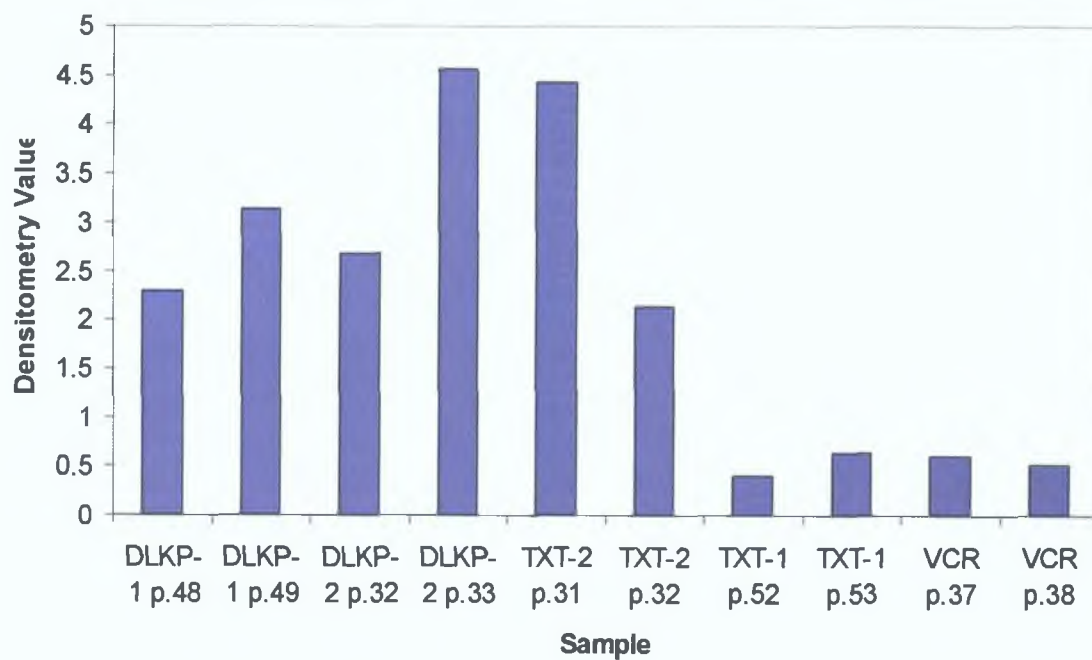
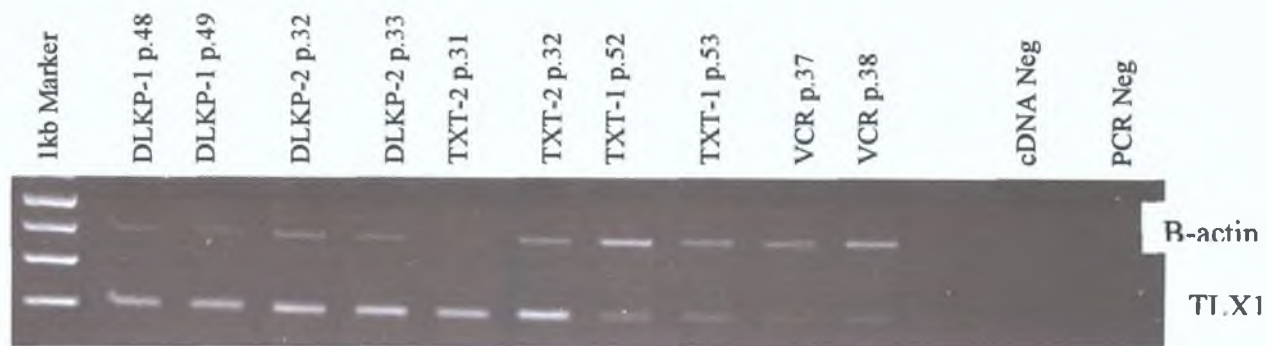


Figure 7.1.18.4b RT-PCR of TLX1 mRNA in samples with increasing passage number.

7.1.19 VEGF-A

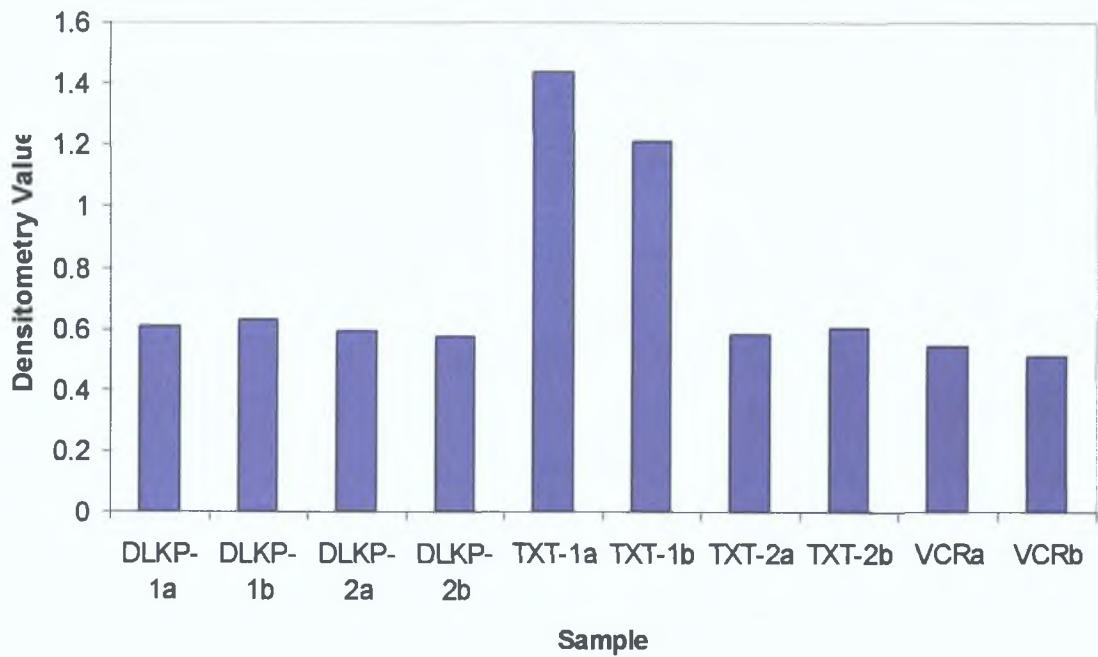
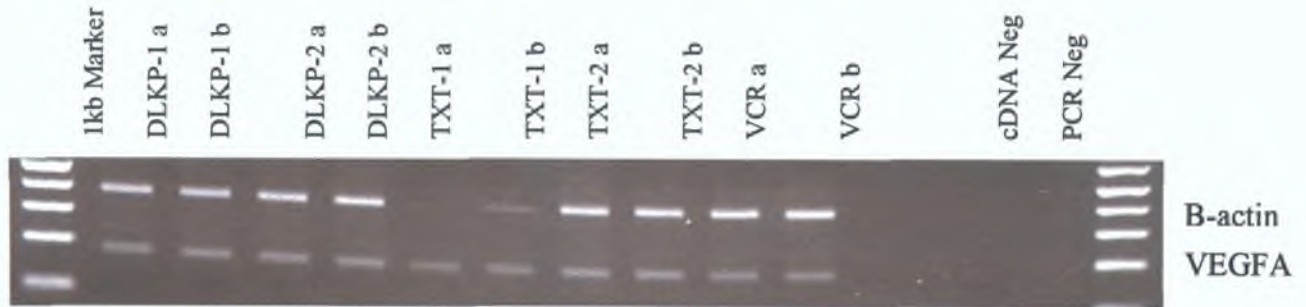


Figure 7.1.19.1 RT-PCR of VEGF-A mRNA expression from RNA used in duplicate array samples 2004.

The band size for VEGF-A was 186bp.

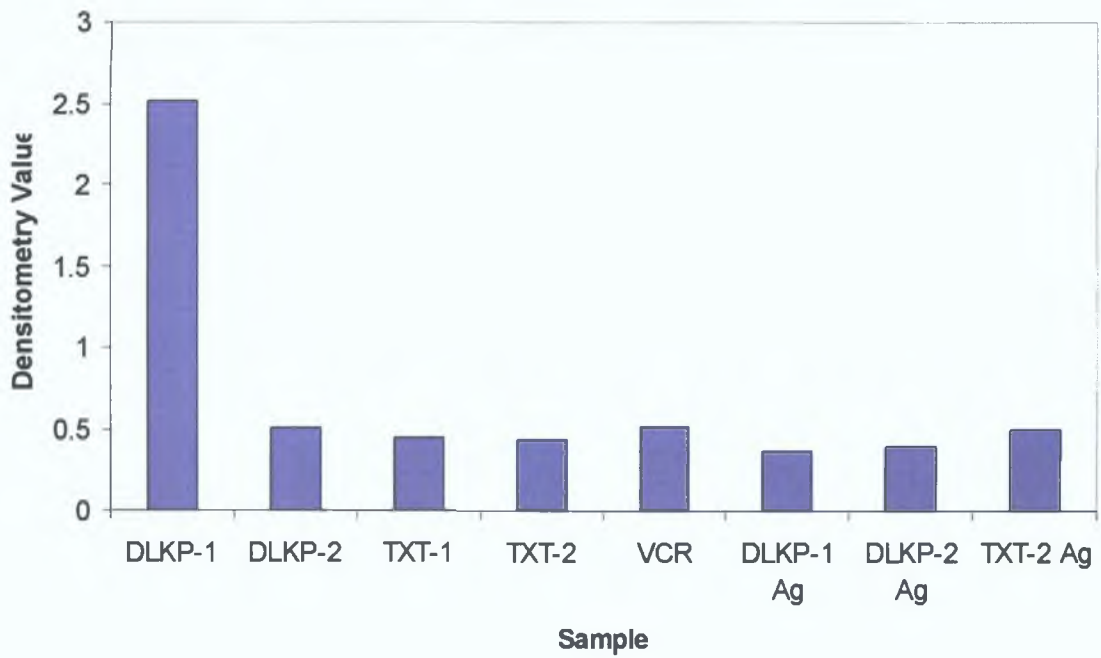
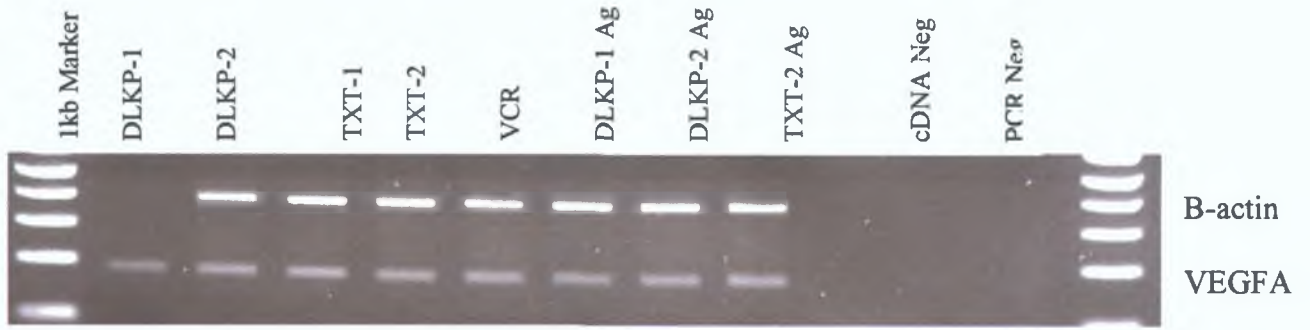


Figure 7.1.19.2 RT-PCR of VEGF-A mRNA in samples in a separate sample set and Agilent samples.

7.1.20 VEGF-C

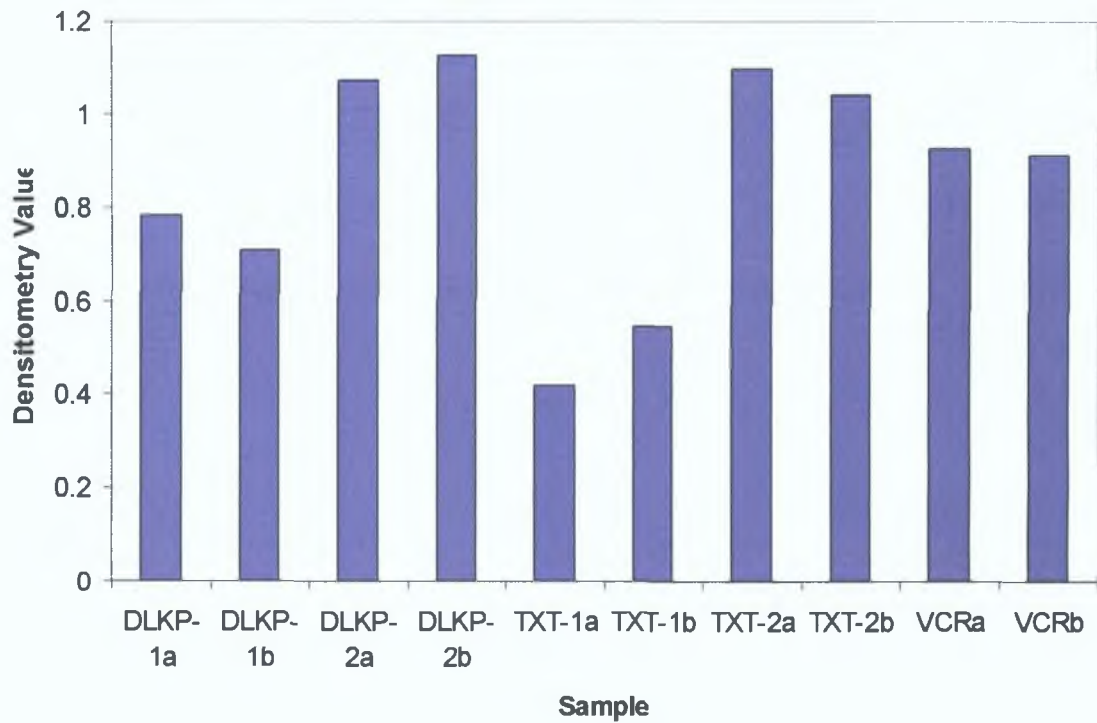
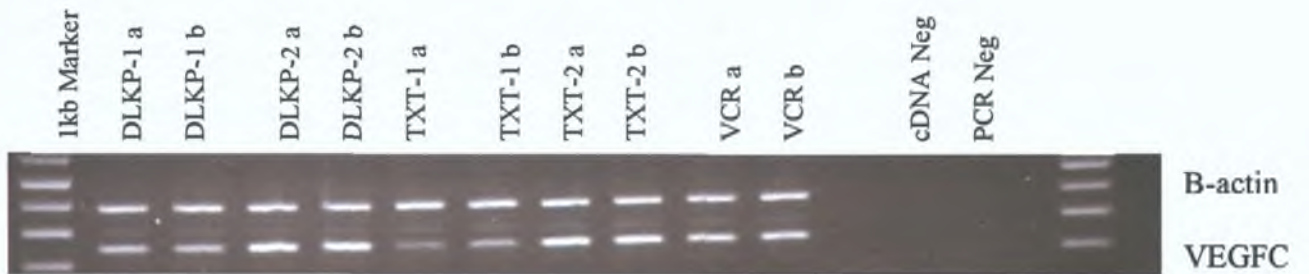


Figure 7.1.20.1 RT-PCR of VEGF-C mRNA expression from RNA used in duplicate array samples 2004.

The band size for VEGF-A was 249bp.

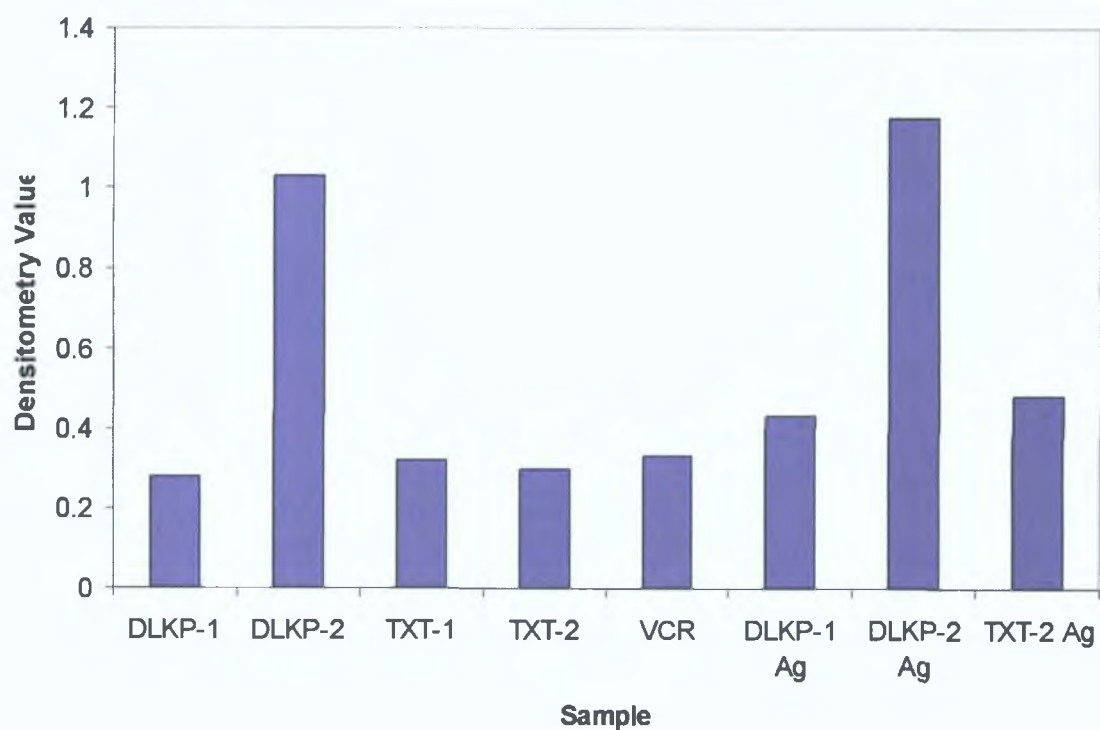
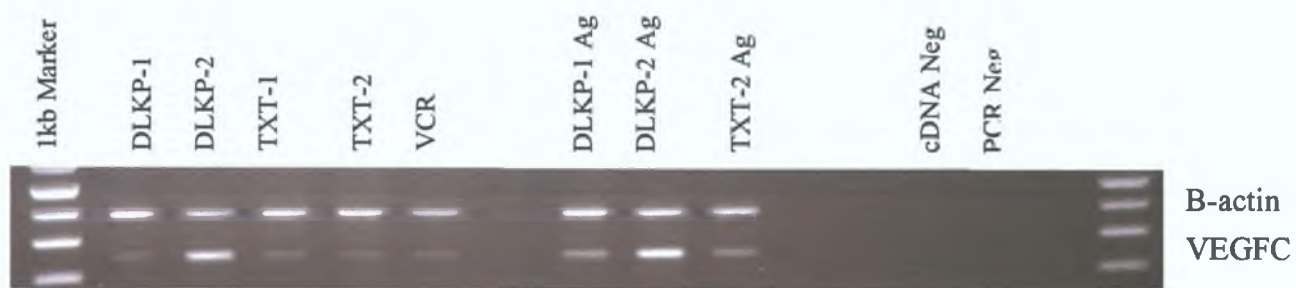


Figure 7.1.20.2 RT-PCR of VEGF-C mRNA in samples in a separate sample set and Agilent samples.

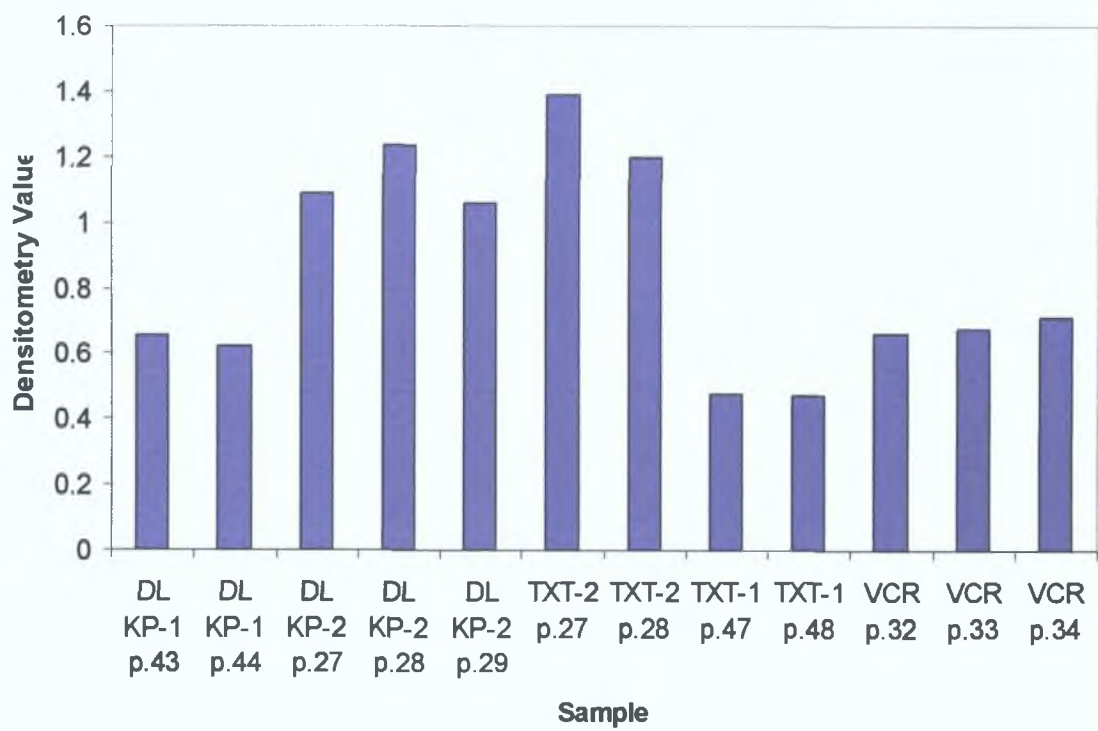
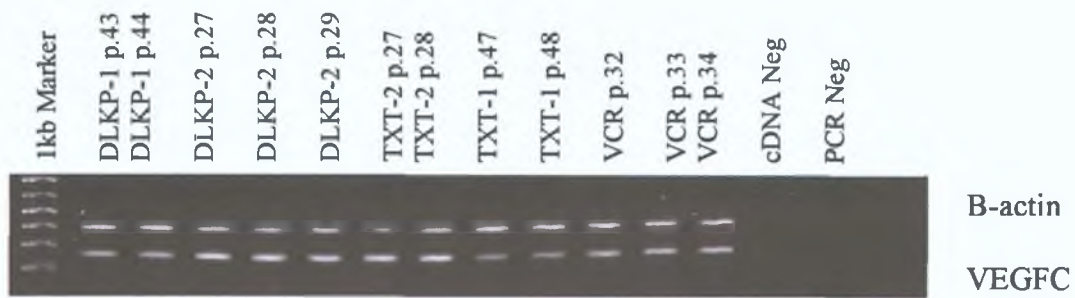


Figure 7.1.20.3 RT-PCR of VEGF-C mRNA in samples with increasing passage number.

7.2 Appendix 2 – RT-PCR investigation of genes with decreased expression in the invasive DLKP variants from microarray analysis

Semi quantitative RT-PCR was used to confirm that expression changes in the array data were reflected in the cell lines studied

To ensure that results from the array study matched to independent analysis of the cell lines, RNA samples from the preliminary Affymetrix array study by Dr Rasha Linehan in 2003, RNA from the duplicate array samples 2004, RNA from a fresh set of cultures harvested separately to those for array analysis including RNA from three samples analysed on the Agilent array platform and RNA from cells with increasing passage number were included in this analysis. The Agilent data was not analysed further in this work.

In all of the PCRs in this section β -actin was used as an endogenous control to normalise for RNA quantities added to each reaction. The reactions were analysed by gel electrophoresis (GE) on a 2% agarose gel. cDNA negative control (cDNA neg) consisted of PCR master mix with cDNA but without addition of Taq enzyme. PCR negative controls consisted of PCR master mix to which no cDNA template was added. Densitometric values were normalised by dividing target intensity values by β -actin intensity values and were graphed for each sample. The gels included in this section are representative of at least two independent repeats.

7.2.1 FN1

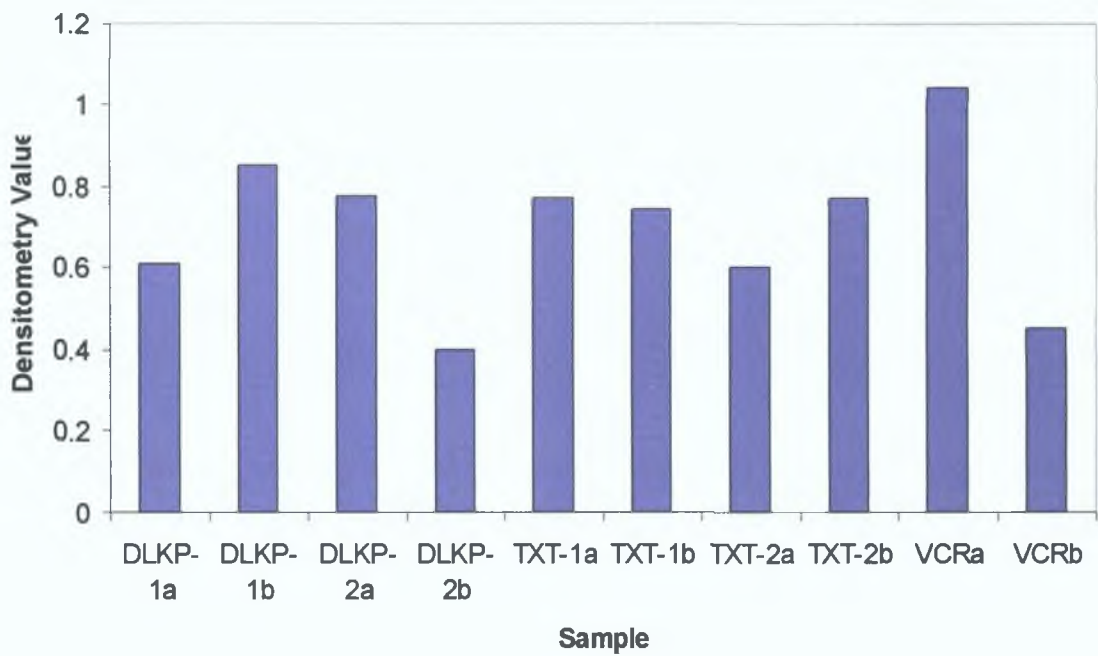
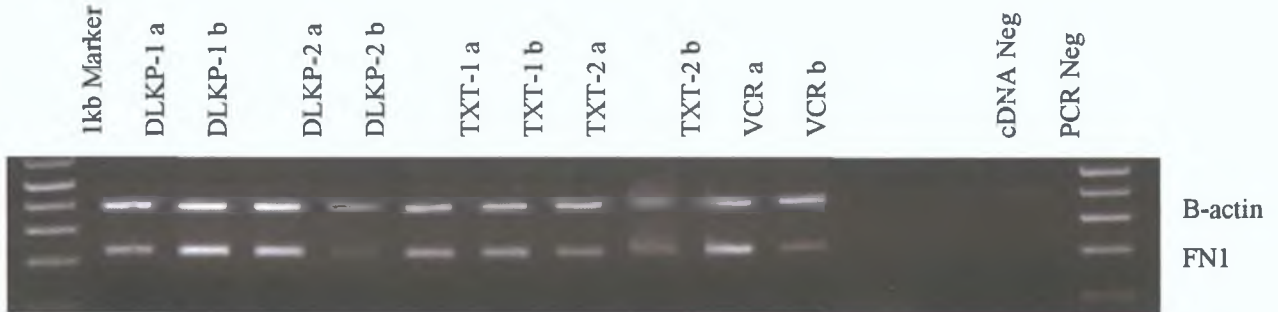


Figure 7.2.1.1 RT-PCR of FN1 mRNA expression from RNA used in duplicate array samples 2004.

The band size for FN1 was 230bp.

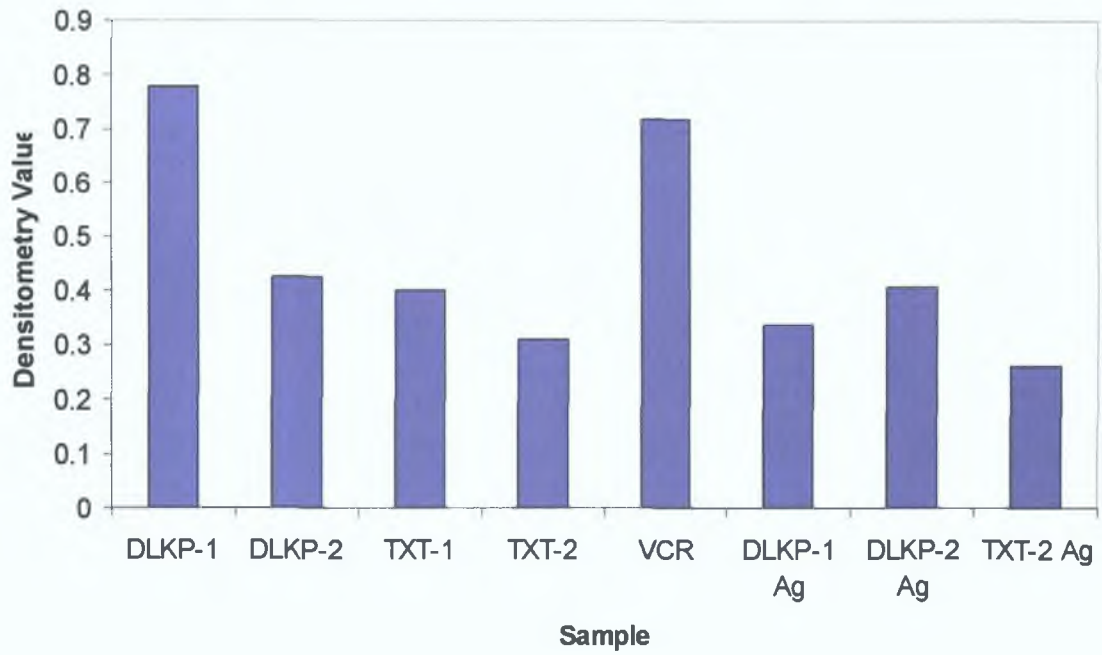


Figure 7.2.1.2 RT-PCR of FN1 mRNA in a separate sample set and Agilent samples.

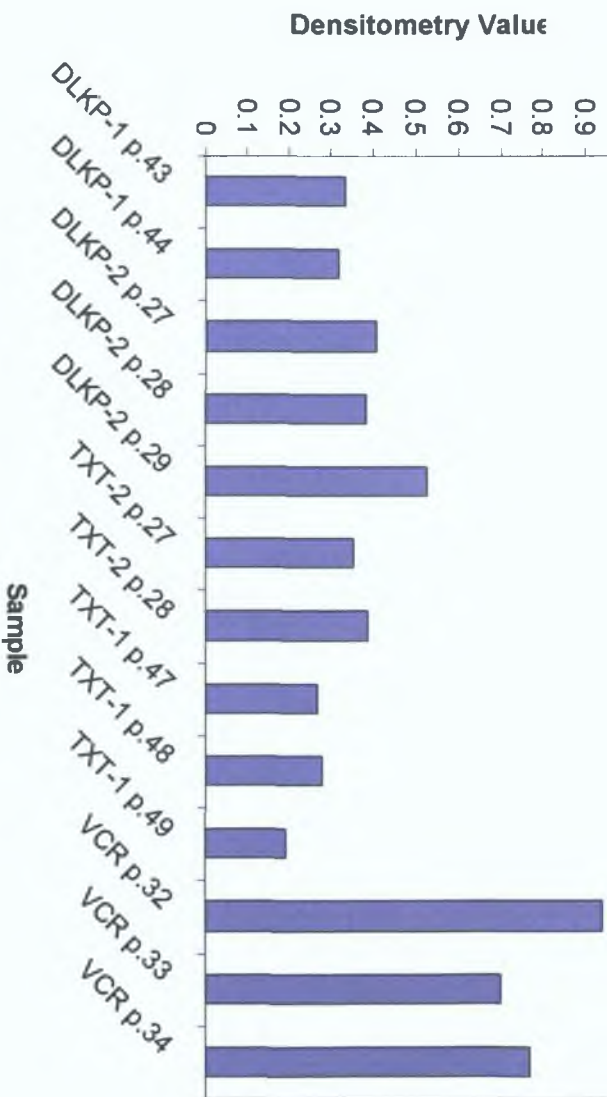
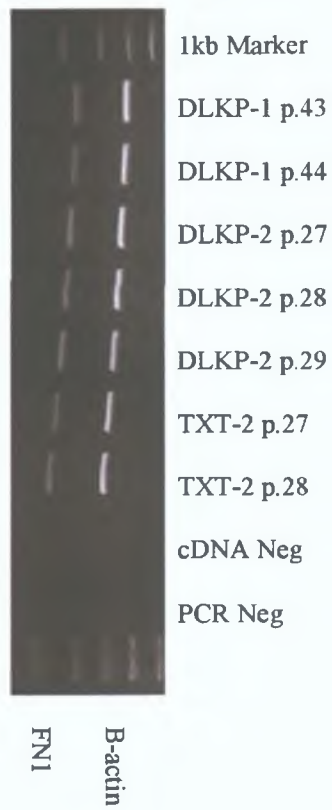
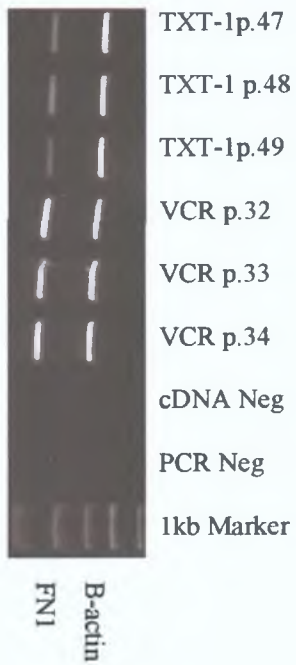


Figure 7.2.1.3a RT-PCR of FNI mRNA in samples with increasing passage number.



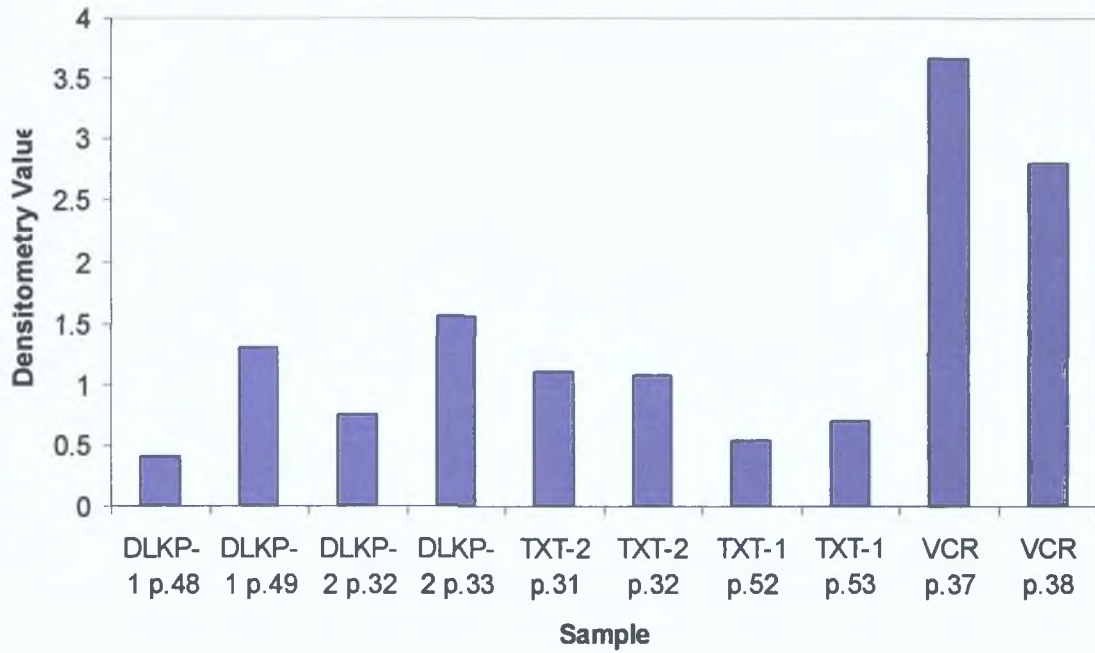
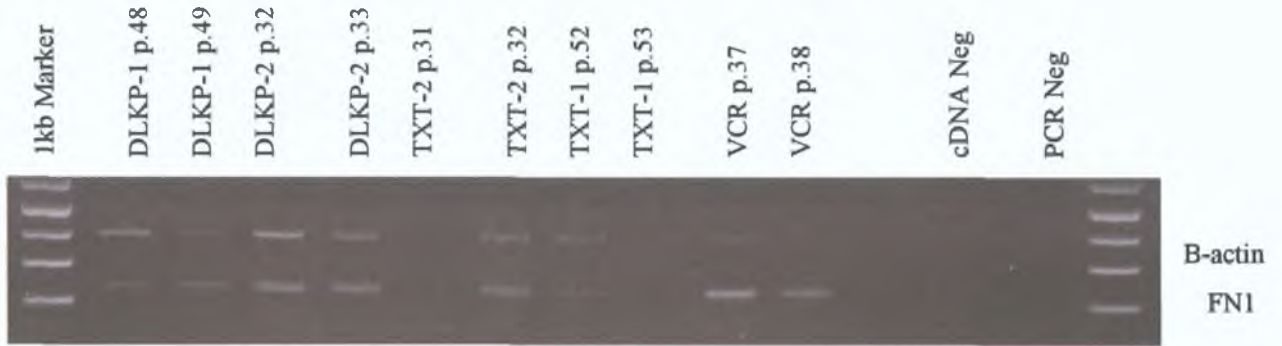


Figure 7.2.1.3b RT-PCR of FN1 mRNA in samples with increasing passage number.

7.2.2 FSTL1

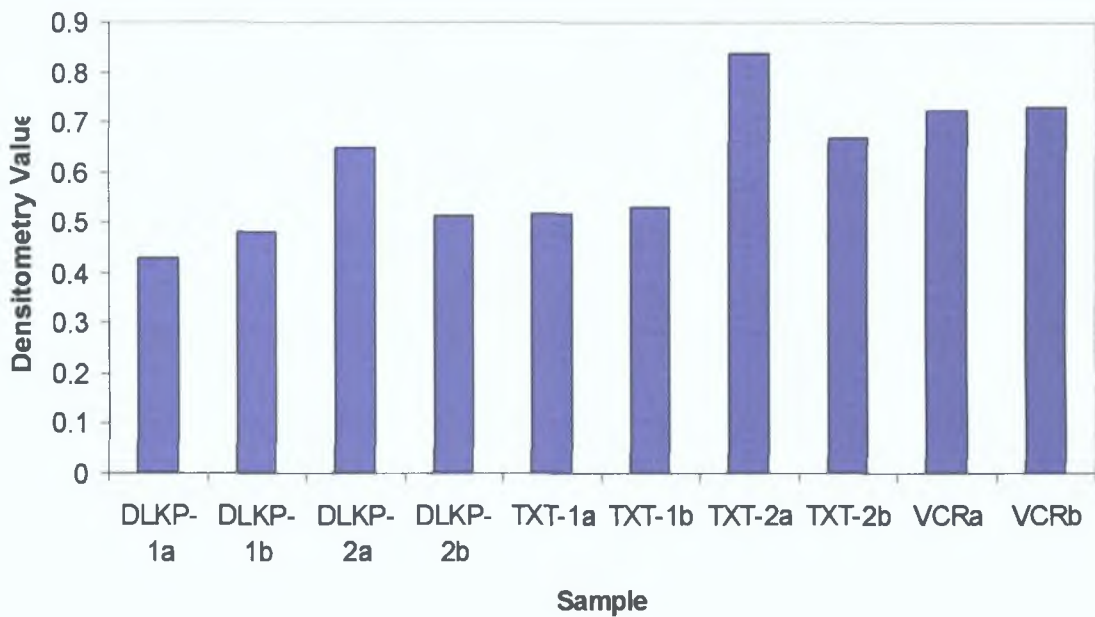
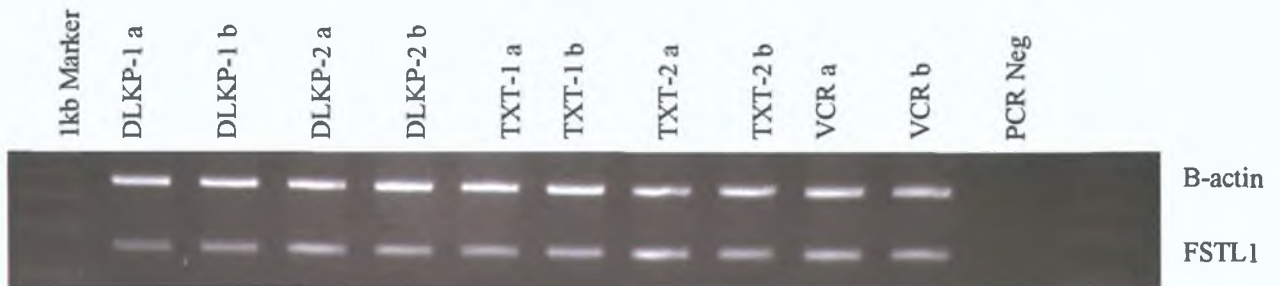


Figure 7.2.2.1 RT-PCR of FSTL1 mRNA expression from RNA used in duplicate array samples 2004.

The band size for FSTL1 was 242bp.

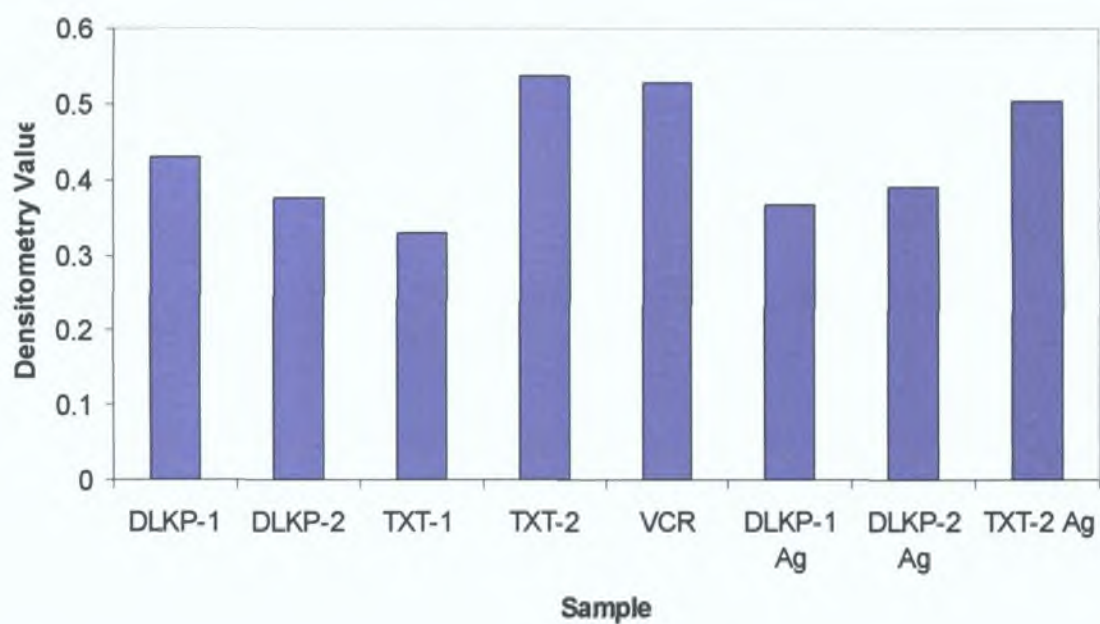
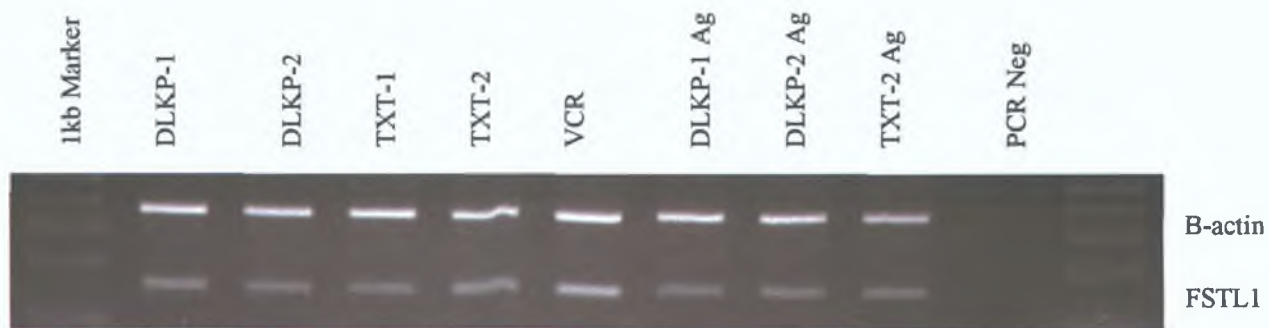


Figure 7.2.2.2 RT-PCR of FSTL1 mRNA in a separate sample set and Agilent samples.

7.2.3 MAP3K12

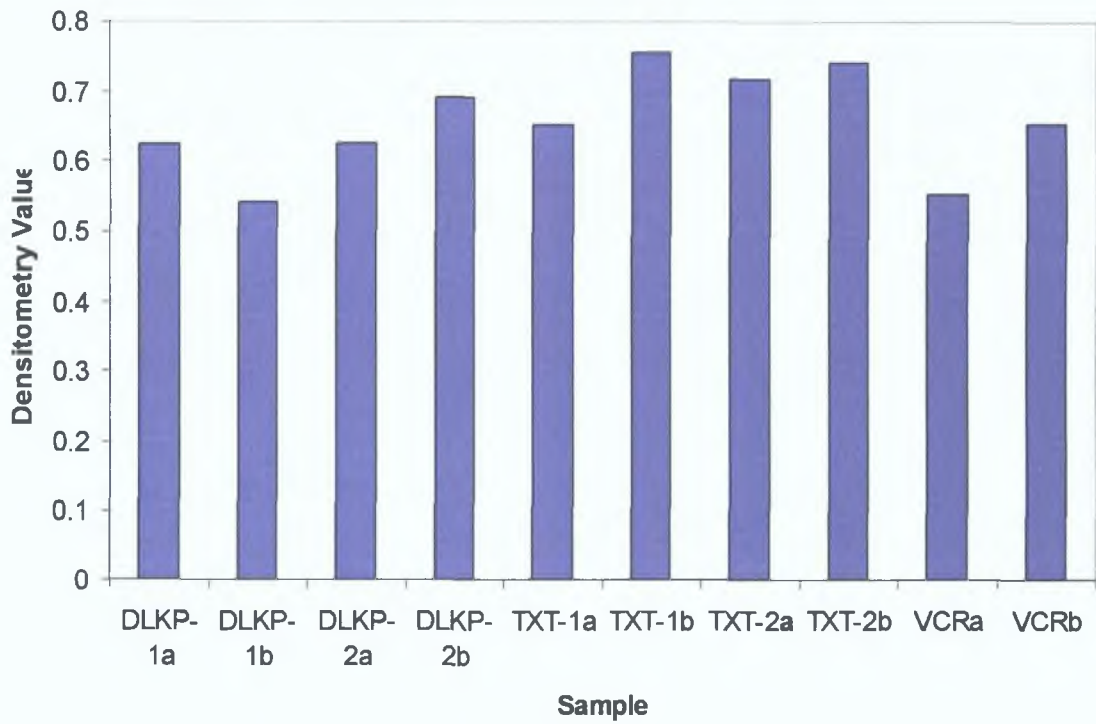
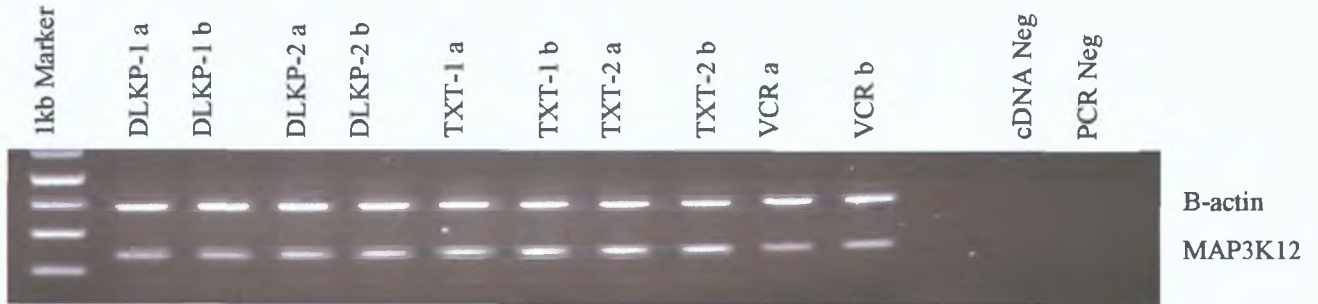


Figure 7.2.3.1 RT-PCR of MAP3K12 mRNA expression from RNA used in duplicate array samples 2004.

The band size for MAP3K12 was 240bp.

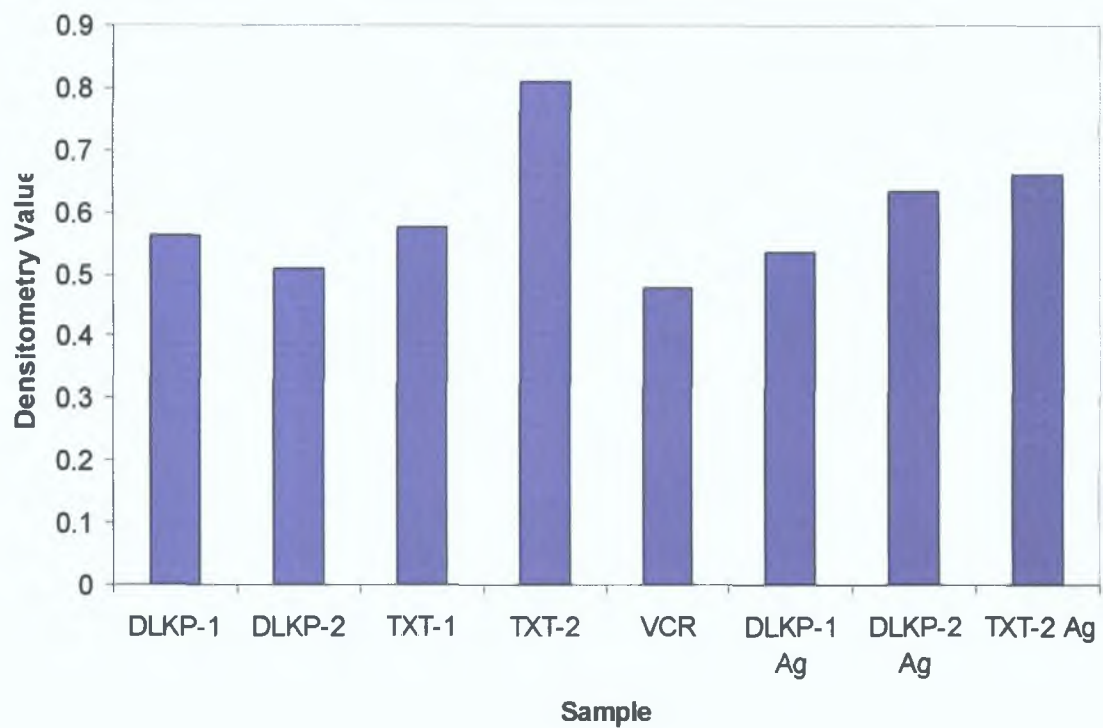


Figure 7.2.3.2 RT-PCR of MAP3K12 mRNA in a separate sample set and Agilent samples.

7.2.4 NRG1

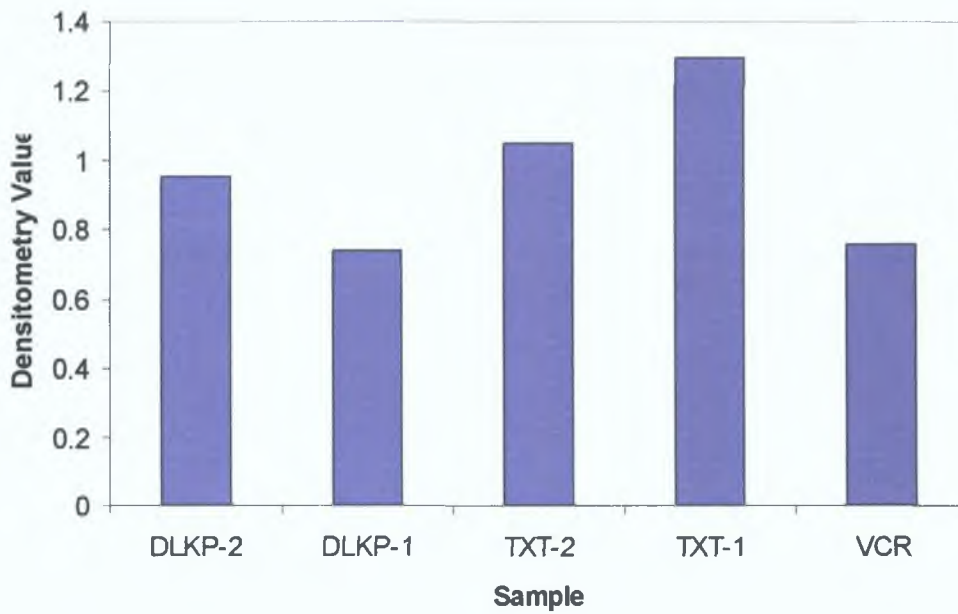


Figure 7.1.4.1 RT-PCR of NRG1 expression from RNA used in array samples 2003.

The band size for NRG1 was 190bp.

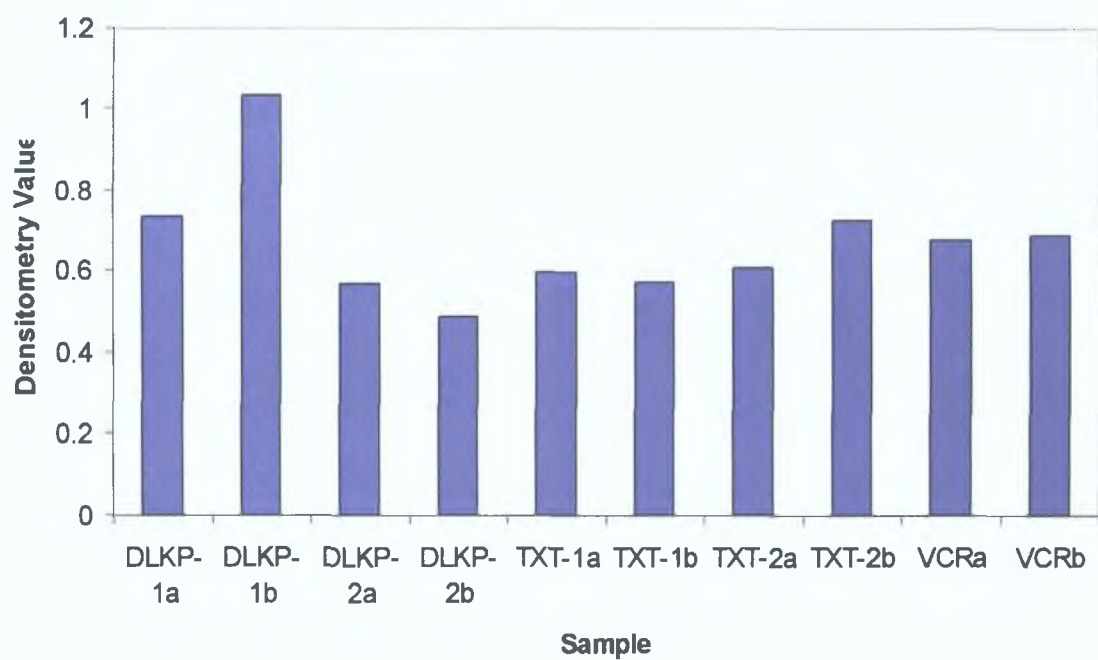
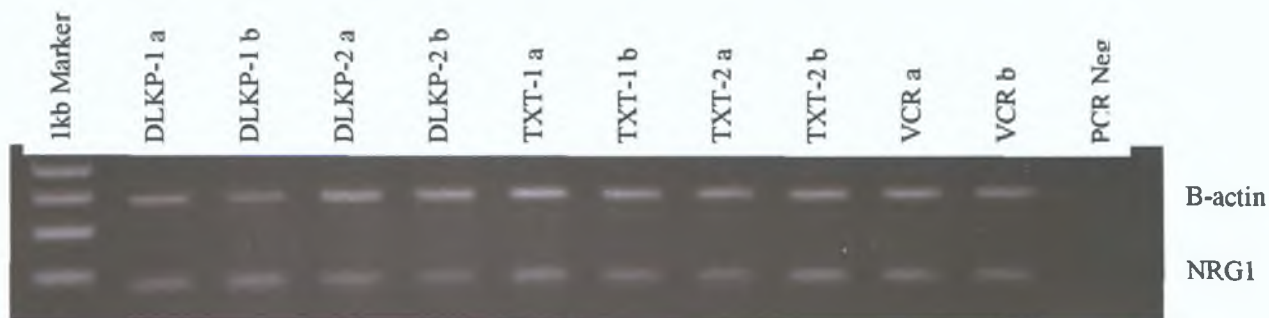


Figure 7.2.4.2 RT-PCR of NRG1 mRNA expression from RNA used in duplicate array samples 2004.

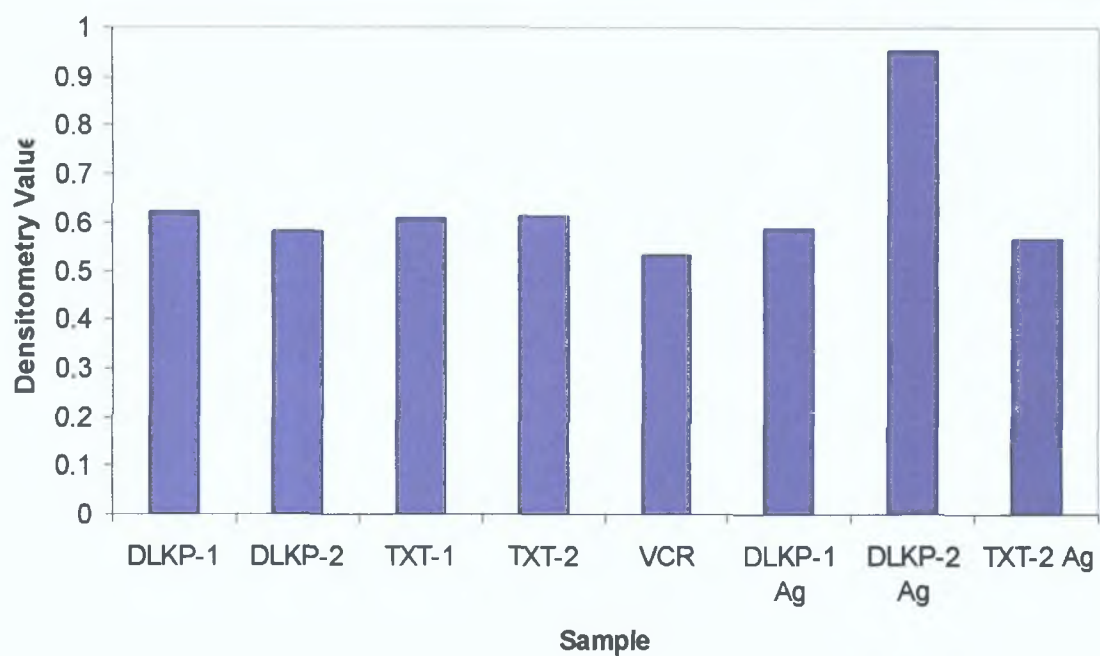
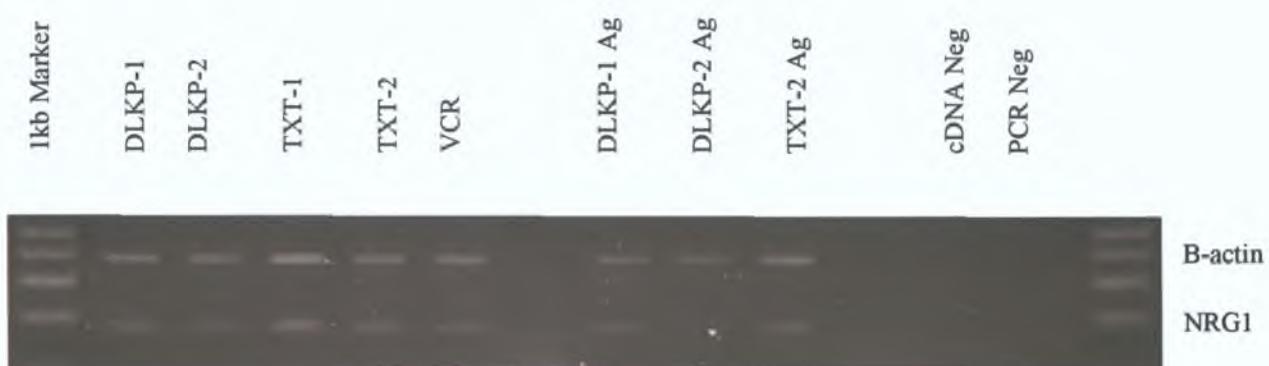


Figure 7.2.4.2 RT-PCR of NRG1 mRNA in a separate sample set and Agilent samples.

7.2.5 RANBP2

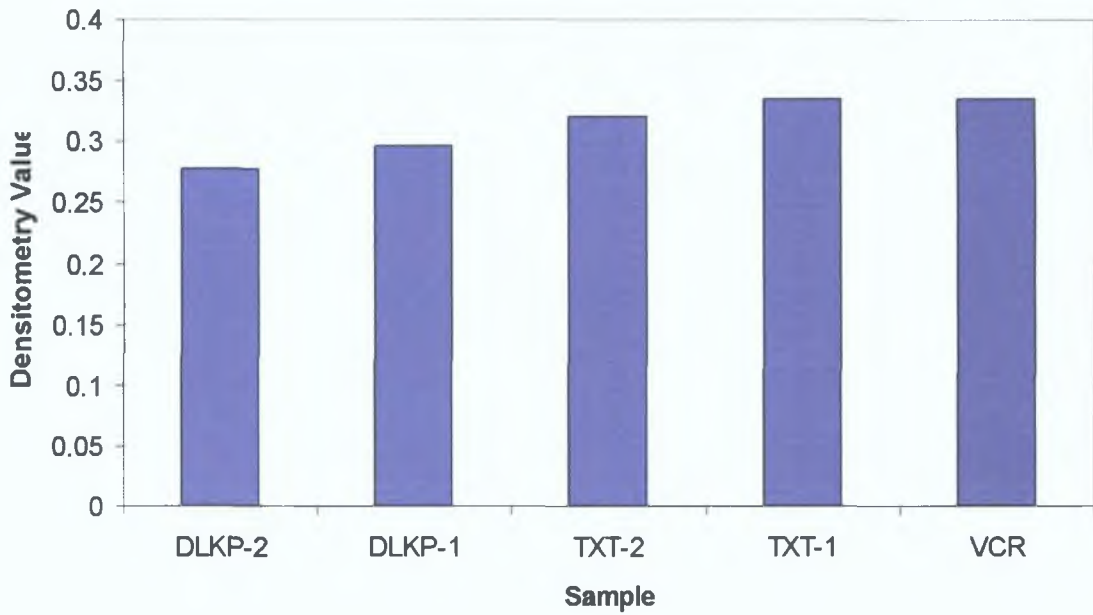


Figure 7.2.5.1 RT-PCR of RANBP2 expression from RNA used in array samples 2003.

The band size for RANBP2 was 218bp.

7.2.6 SCHIP1

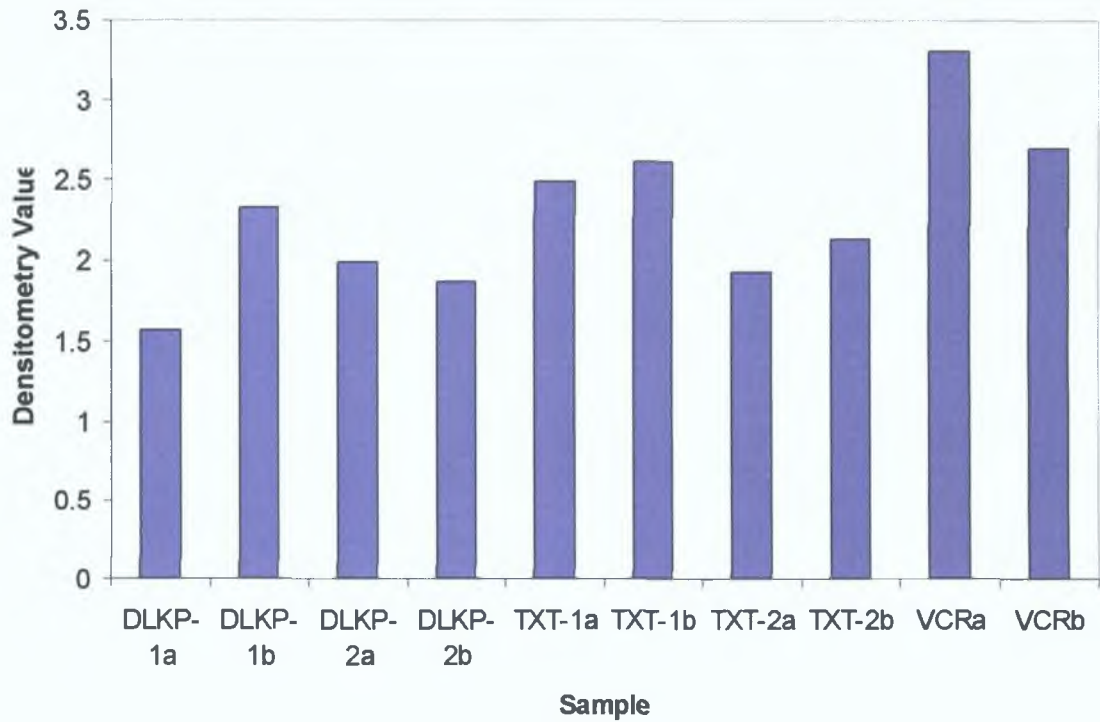
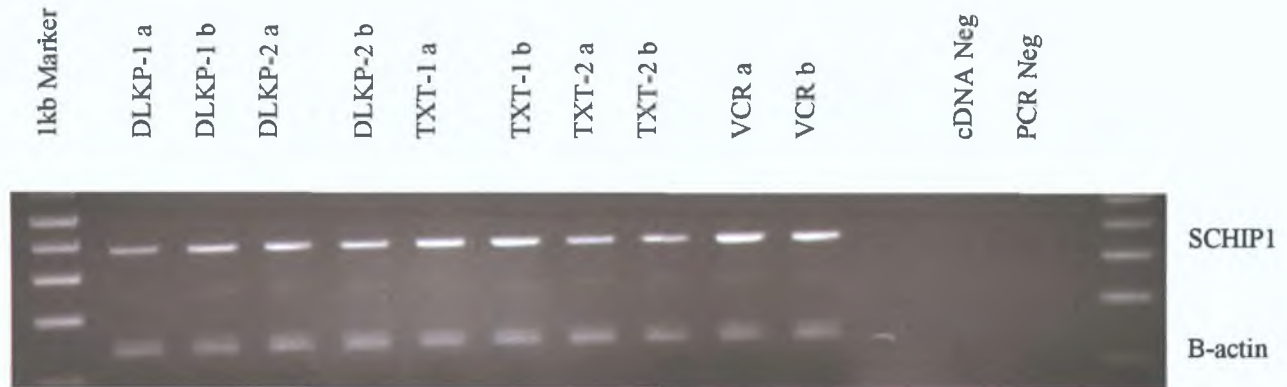


Figure 7.2.6.1 RT-PCR of SCHIP1 mRNA expression from RNA used in duplicate array samples 2004.

The band size for SCHIP1 was 355bp.

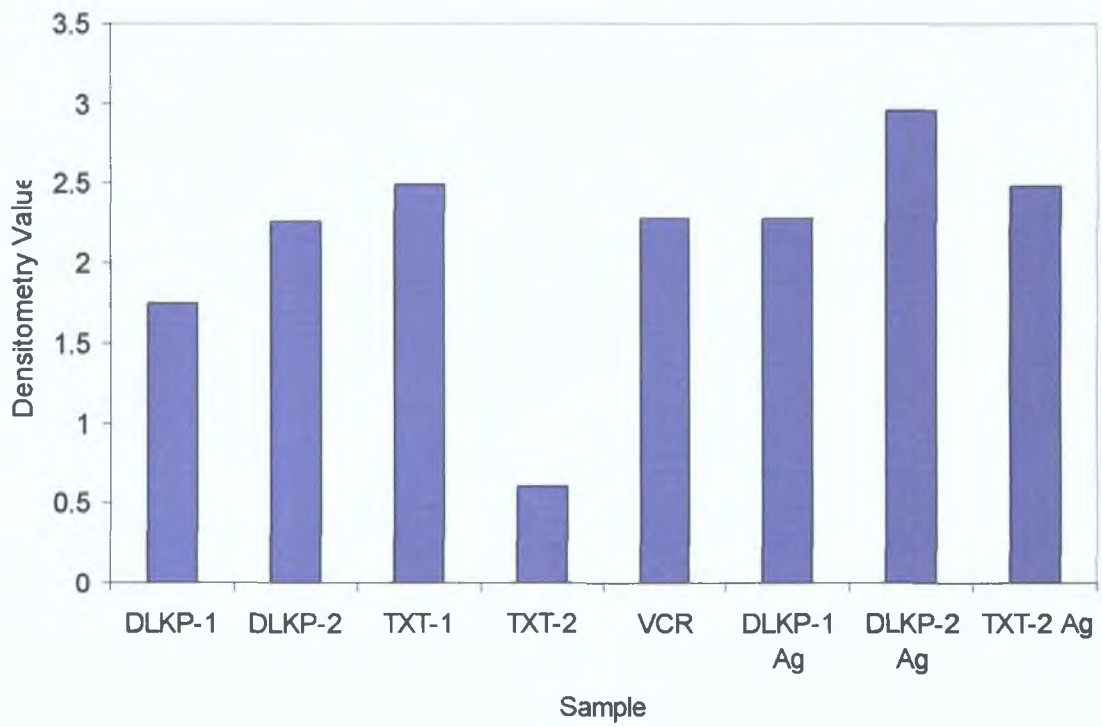
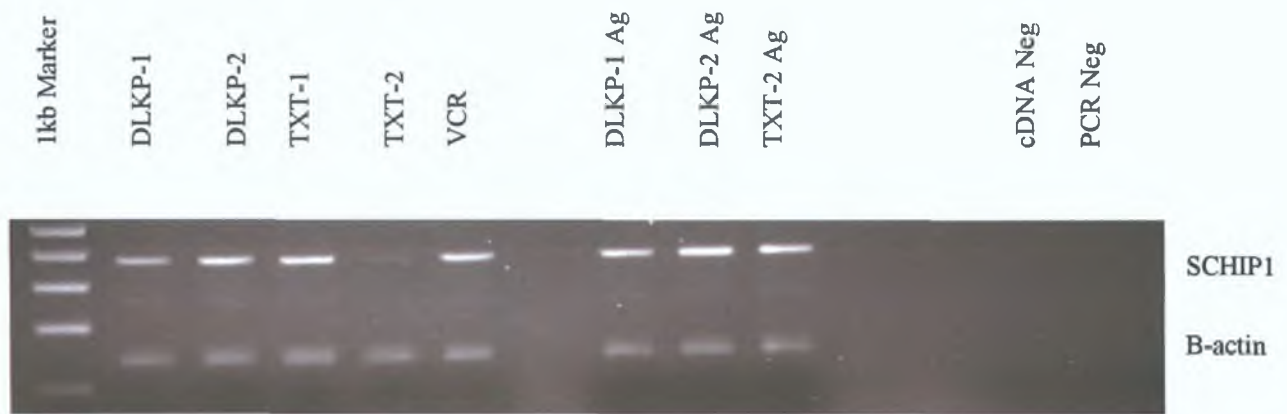


Figure 7.2.6.2 RT-PCR of SCHIP1 mRNA in a separate sample set and Agilent samples.

7.2.7 SPP1

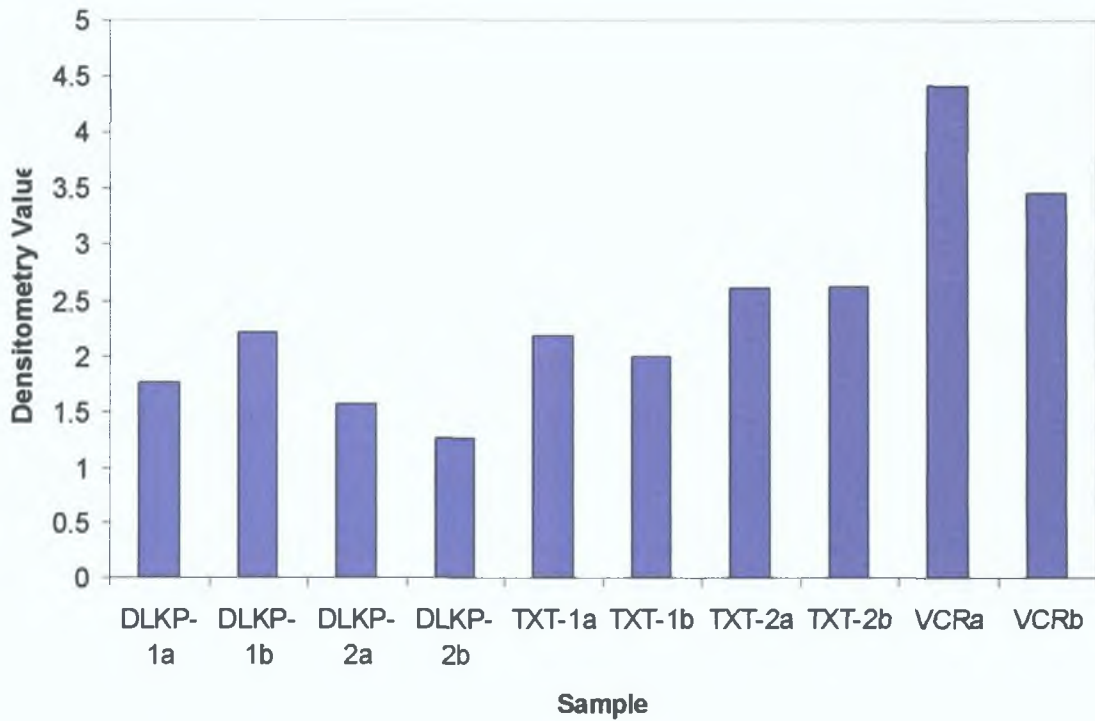
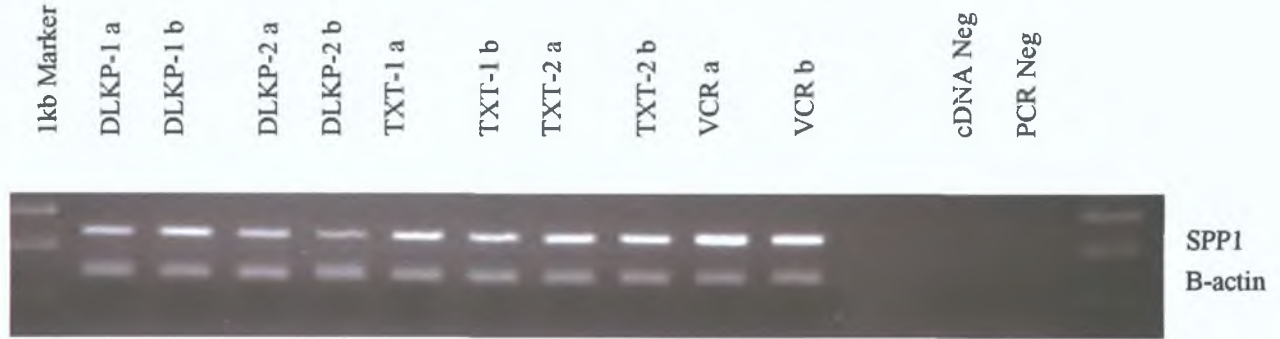


Figure 7.2.7.1 RT-PCR of SPP1 mRNA expression from RNA used in duplicate array samples 2004.

The band size for SPP1 was 244bp.

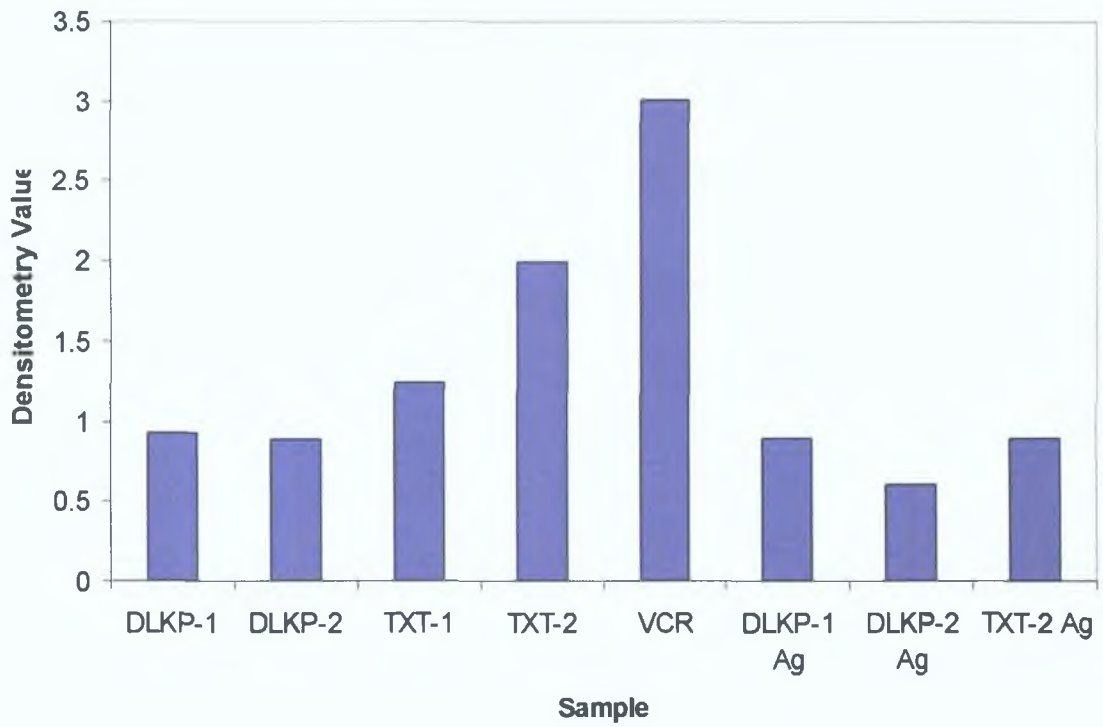
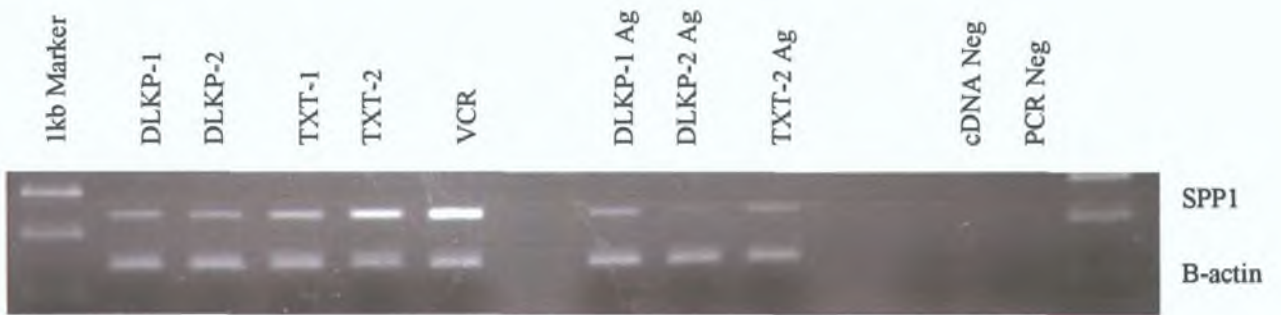


Figure 7.2.7.2 RT-PCR of SPP1 mRNA in a separate sample set and Agilent samples.

7.2.8 TEM6

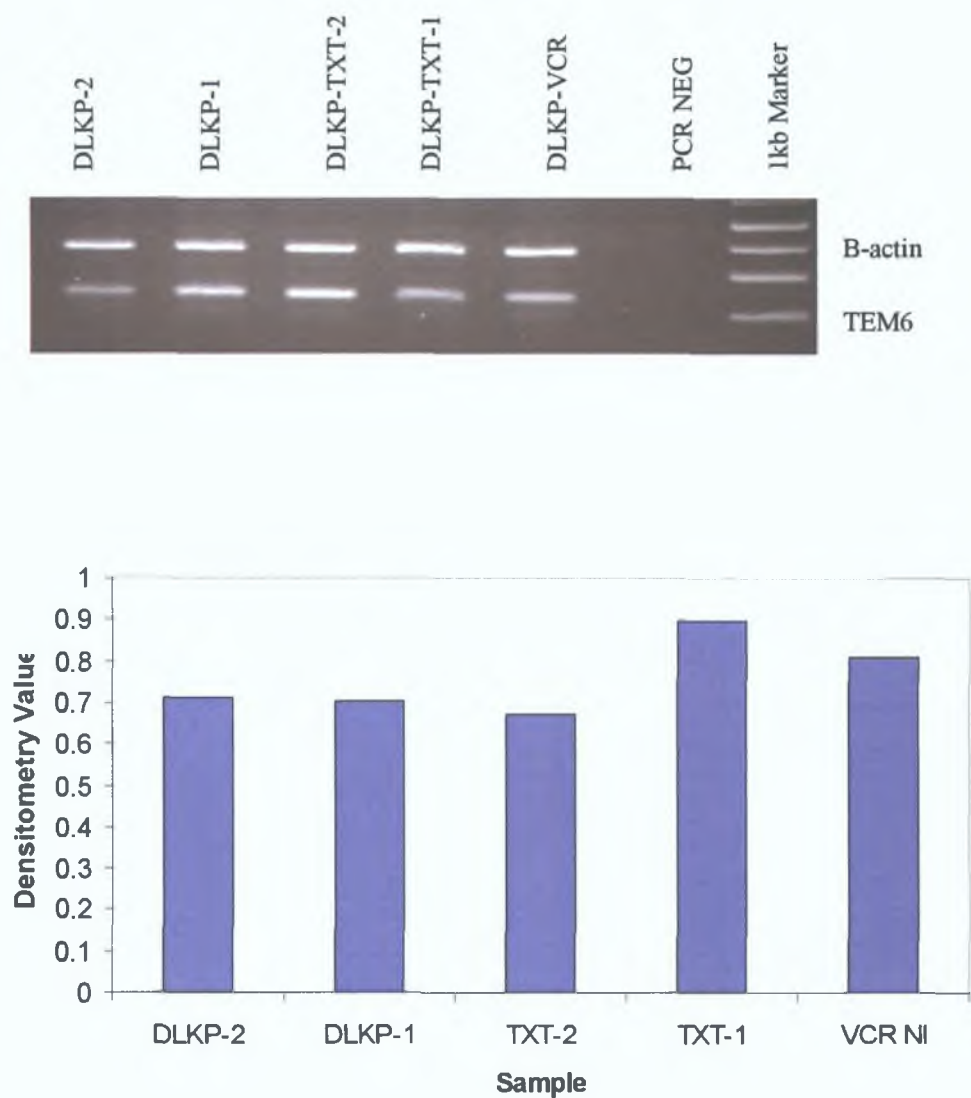


Figure 7.2.8.1 RT-PCR of TEM6 expression from RNA used in array samples 2003.

The band size for TEM6 was 199bp.

7.2.9 TFPI2

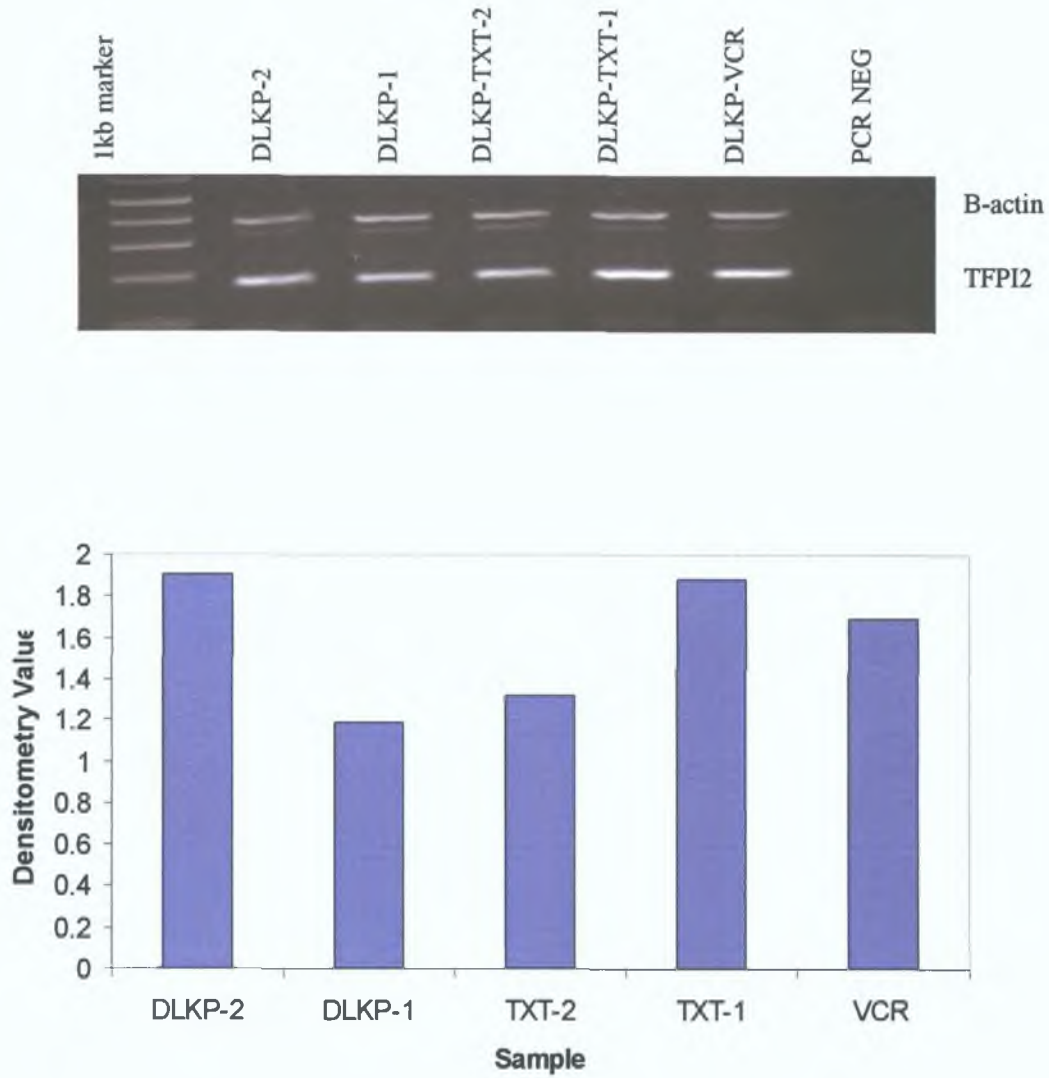


Figure 7.2.9.1 RT-PCR of TFPI2 expression from RNA used in array samples 2003.

The band size for TFPI2 was 183bp.

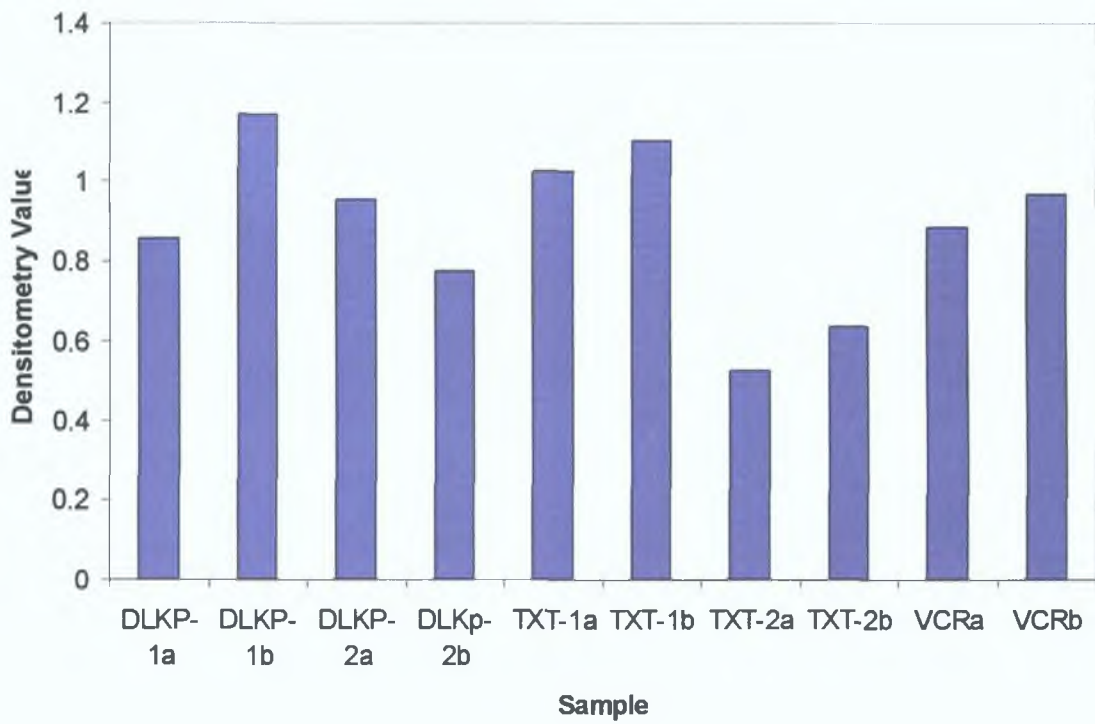
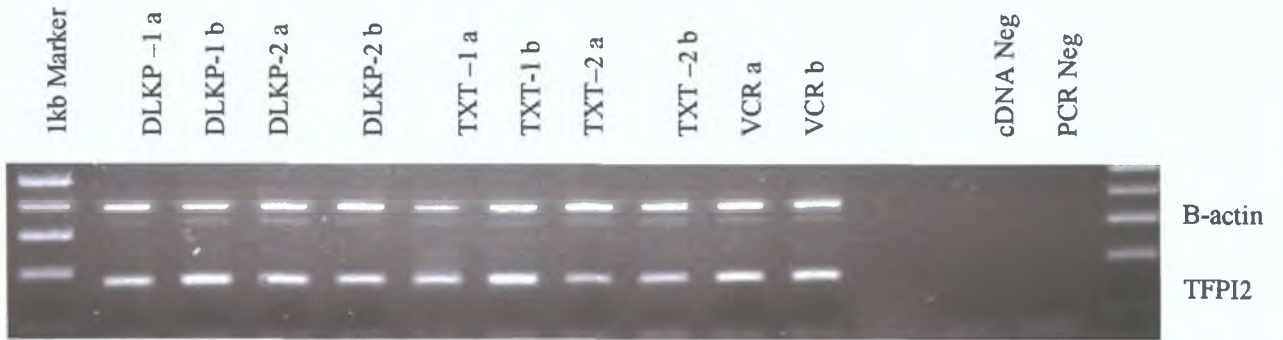


Figure 7.2.9.2 RT-PCR of TFPI2 mRNA expression from RNA used in duplicate array samples 2004.

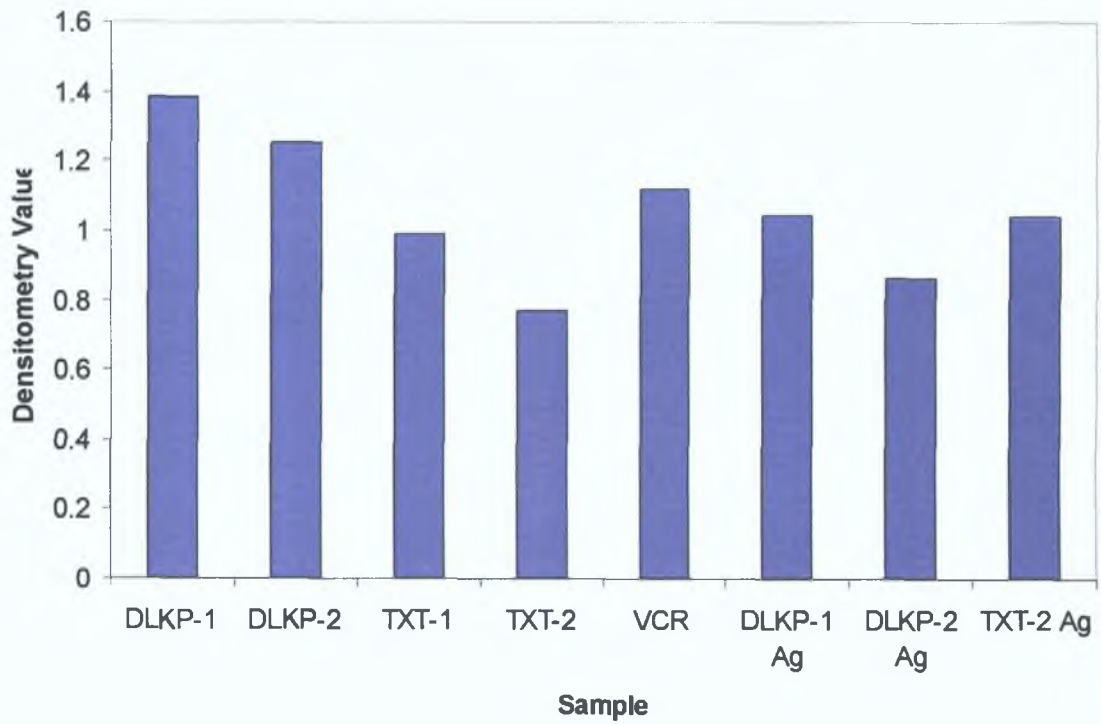


Figure 7.2.9.3 RT-PCR of TFPI2 mRNA in a separate sample set and Agilent samples.

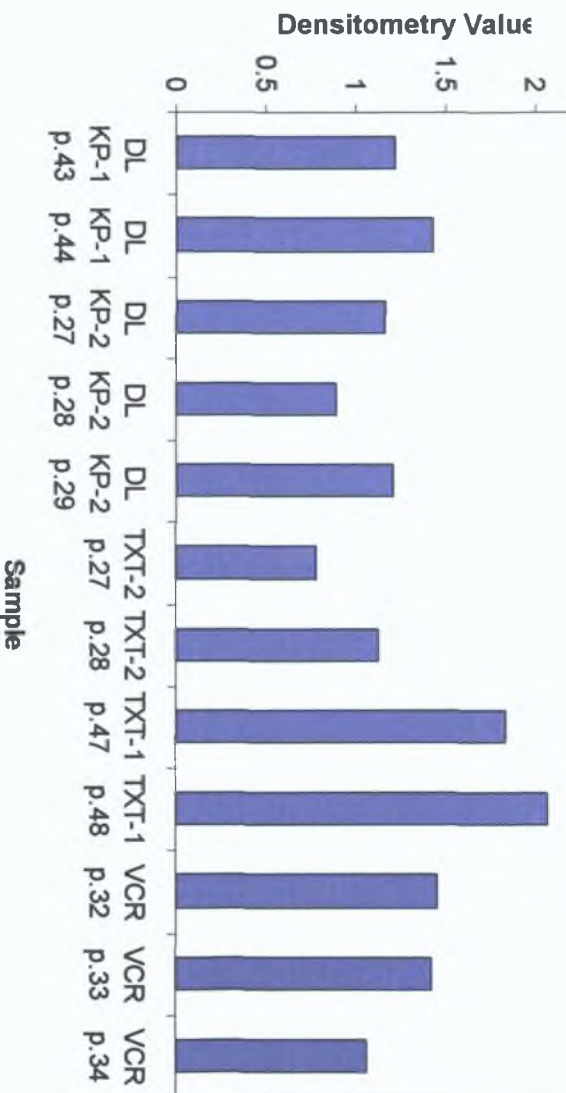


Figure 7.2.9.4 RT-PCR of TFP12 mRNA in samples with increasing passage number.



1kb Marker

DLKP-1p.43

DLKP-1p.44

DLKP-2 p.27

DLKP-2 p.28

DLKP-2 p.29

TXT-2 p.27

TXT-2 p.28

TXT-1 p.47

TXT-1 p.48

VCR p.32

VCR p.33

VCR p.34

cDNA Neg

PCR Neg

TFPI2

B-actin

7.3 Appendix 3 – Table of PCR primers used in this study

Name	Supplier	Band size (bp)	Primer Sequences
AKAP11	Sigma	233	AAG GGC ACA AAC ATG GAA AG (s) AGC TGG AGT ACA GCC TCC AA (as)
BCHE	Sigma	180	AAG CTG GCC TGT CTT CAA AA (s) TGG AAT CCT GCT TTC CAC TC (as)
CYB5R2	Sigma	172	CCCAGGACATGATTTTCACC (s) CACCCAAAAGAGGAGAACCA (as)
EFNB2	Sigma	220	TCCATGGGTAATCCGTTTCAT (s) TCAGCAAAACCAAAGTGCTG (as)
GLP1R	Sigma	228	GTTCCCCTGCTGTTTGTGT (s) CTTGGCAAGTCTGCATTTGA (as)
KCNJ8	Sigma	210	AGTTGGTGAAACCCAGATCG (s) CGACAGACAAAGCGAATGAA (as)
LOC5119	Sigma	249	CAATGGTTCTGGGGATATGG (s) CCCTTTGGATTCTGAAGCAC (as)
MFAP2	Sigma	422	GCAGTGAACGGAGTCACAAA (s) GTCTGGGTTGTCGATCTGGT (as)
MGC3900	Sigma	219	CTCAGTCAAACCACGAAGCA (s) AAGTGGAGCTCTGGAGGTGA (as)
MMP3	MWG Biotech	214	GCAGTTTGCTCAGCCTATCC (s) GAGTGTCGGAGTCCAGCTTC (as)
S100A13	Sigma	219	TAATGGCAGCAGAACCACTG (s) TTGAGCTCCGAGTCCTGATT (as)
SFN	Sigma	195	GGATCCCACTCTTCTTG CAG (s) CTGTCCAGTTCTCAGCCACA (as)
TCF4	MWG Biotech	204	GCAGAGTCTCCTTG GAGGTG (s) GTGCTTGCTGATGGAGCATA (as)
TEM7	Sigma	239	GTCCTCCAGAGATGCTCCAG (s)

TLX1	Sigma	201	GGTCAGGGGTGACACAGACT (s) TGGGCTGCATTTATGTGAAA (as)
VEGF-A	MWG Biotech	186	CCCACTGAGGAGTCCAACAT (s) TTTCTTGCGCTTTCGTTTTT (as)
VEGF-C	Sigma	249	GGAAAGAAGTTCCACCACCA (s) TTTGTTAGCATGGACCCACA (as)
FN1	MWG Biotech	230	ACCAACCTACGGATGACTCG (s) GCTCATCATCTGGCCATTTT (as)
FSTL1	MWG Biotech	242	GCACAGGCAACTGTGAGAAA (s) CATAGTGTCCAAGGGCTGGT (as)
MAP3K12	Sigma	240	AGAAGGTGCGAGACCTCAAA (s) TCTTGTGCAGGTGCAGGTAG (as)
SCHIP1	Sigma	355	ATGCTGTTGCTAAAGGTGGC (s) ACATATTACGGAGAGCTACA (as)
SPP1	Sigma	244	CCCACAGACCCTTCCAAGTA (s) GGGGACAACCTGGAGTGAAAA (as)